Published in Journals: Fractal and Fractional, Axioms,
Mathematical and Computational Applications,
Mathematics and Symmetry

Topic Reprint

Fractional Calculus

Theory and Applications
Volume II

Edited by
António Lopes, Alireza Alfi, Liping Chen and Sergio Adriani David

mdpi.com/topics

MDPI

Fractional Calculus: Theory and Applications—Volume II

Fractional Calculus: Theory and Applications—Volume II

Editors

António Lopes
Alireza Alfi
Liping Chen
Sergio Adriani David

MDPI

Basel • Beijing • Wuhan • Barcelona • Belgrade • Novi Sad • Cluj • Manchester

Editors

António Lopes
University of Porto
Porto
Portugal

Alireza Alfi
Shahrood University of Technology
Shahrood
Iran

Liping Chen
Hefei University of Technology
Hefei
China

Sergio Adriani David
University of São Paulo
Pirassununga
Brazil

Editorial Office
MDPI
St. Alban-Anlage 66
4052 Basel, Switzerland

This is a reprint of articles from the Topic published online in the open access journals *Fractal and Fractional* (ISSN 2504-3110), *Axioms* (ISSN 2075-1680), *Mathematical and Computational Applications* (ISSN 2297-8747), *Mathematics* (ISSN 2227-7390), and *Symmetry* (ISSN 2073-8994) (available at: https://www.mdpi.com/topics/Fractional_Calculus).

For citation purposes, cite each article independently as indicated on the article page online and as indicated below:

Lastname, A.A.; Lastname, B.B. Article Title. *Journal Name* **Year**, *Volume Number*, Page Range.

Volume II
ISBN 978-3-7258-1147-2 (Hbk)
ISBN 978-3-7258-1148-9 (PDF)
doi.org/10.3390/books978-3-7258-1148-9

Set
ISBN 978-3-7258-1143-4 (Hbk)
ISBN 978-3-7258-1144-1 (PDF)

Contents

Preface

Fractional calculus (FC) generalizes the operations of differentiation and integration to non-integer orders. FC has emerged as an important tool for the study of dynamical systems since fractional order operators are non-local and capture the history of dynamics. Moreover, FC and fractional processes have become one of the most useful approaches to dealing with the particular properties of (long) memory effects in a myriad of applied sciences. Linear, nonlinear, and complex dynamical systems have attracted researchers from many areas of science and technology, involved in systems modelling and control, with applications to real-world problems. Despite the extraordinary advances in FC, addressing both systems' modelling and control, new theoretical developments and applications are still needed in order to accurately describe or control many systems and signals characterized by chaos, bifurcations, criticality, symmetry, memory, scale invariance, fractality, fractionality, and other rich features. This reprint focuses on new and original research results on fractional calculus in science and engineering. Manuscripts address fractional calculus theory, methods for fractional differential and integral equations, nonlinear dynamical systems, advanced control systems, fractals and chaos, complex dynamics, and other topics of interest within FC.

António Lopes, Alireza Alfi, Liping Chen, and Sergio Adriani David
Editors

fractal and fractional

MDPI

Article

Left Riemann–Liouville Fractional Sobolev Space on Time Scales and Its Application to a Fractional Boundary Value Problem on Time Scales

Xing Hu and Yongkun Li *

Department of Mathematics, Yunnan University, Kunming 650091, China; huxing@mail.ynu.edu.cn
* Correspondence: yklie@ynu.edu.cn

Abstract: First, we show the equivalence of two definitions of the left Riemann–Liouville fractional integral on time scales. Then, we establish and characterize fractional Sobolev space with the help of the notion of left Riemann–Liouville fractional derivative on time scales. At the same time, we define weak left fractional derivatives and demonstrate that they coincide with the left Riemann–Liouville ones on time scales. Next, we prove the equivalence of two kinds of norms in the introduced space and derive its completeness, reflexivity, separability, and some embedding. Finally, as an application, by constructing an appropriate variational setting, using the mountain pass theorem and the genus properties, the existence of weak solutions for a class of Kirchhoff-type fractional p-Laplacian systems on time scales with boundary conditions is studied, and three results of the existence of weak solutions for this problem is obtained.

Keywords: Riemann–Liouvillederivatives; time scales; left fractional Sobolev's spaces; boundary value problems; mountain pass theorem; genus properties

Citation: Hu, X.; Li, Y. Left Riemann–Liouville Fractional Sobolev Space on Time Scales and Its Application to a Fractional Boundary Value Problem on Time Scales. *Fractal Fract.* **2022**, *6*, 268. https://doi.org/10.3390/fractalfract6050268

Academic Editors: António M. Lopes, Alireza Alfi, Liping Chen and Sergio Adriani David

Received: 3 April 2022
Accepted: 11 May 2022
Published: 15 May 2022

1. Introduction

To unify the discrete analysis and continuous analysis, and allow a simultaneous treatment of differential and difference equations, Stefan Hilger [1] proposed the time scale theory and established its related basic theory [2,3]. To date, the study of dynamic equations on time scales has attracted attention worldwide.

It is well known that Sobolev space theory was established to study modern differential equation theory and many problems in the field of mathematical analysis. It has become an integral part of analytical mathematics. In order to study the solvability of boundary value problems of dynamic equations on time scales, Sobolev space theory on time scales is studied in [4–7].

On the one hand, the classical derivatives are local in nature; i.e., using classical derivatives, we can describe changes in the neighborhood of a point, but using fractional derivatives we can describe changes in an interval. Namely, fractional derivatives are non-local in nature. Fractional derivatives are non-local, so the $\frac{1}{2}$ derivative cannot have a local meaning such as tangent or curvature but would have to take into account the properties of the curve to a large extent (boundary conditions). This property makes these derivatives suitable to simulate more physical phenomena such as earthquake vibrations, polymers, etc. The geometrical meaning of ordinary derivatives is simple and intuitive: for the smooth function f, which is differentiable at x, it shows local behavior of f around point x. A simple definition can be provided directly from the geometrical meaning: one can expect that the fractional derivative could give a nonlinear (power law) approximation of the local behavior of non-differentiable functions. Fractional order derivatives are related to memory. No other physical meaning can be attached to them at present, although the theory is old. Fractional order derivatives are related to memory and hereditary properties of various real materials [8–13]. In the past few decades, fractional calculus and fractional differential

equations have attracted widespread attention in the field of differential equations, as well as in applied mathematics and science. In addition to true mathematical interest and curiosity, this trend is also driven by interesting scientific and engineering applications that have produced fractional differential equation models to better describe (time) memory effects and (space) non-local phenomena [14–19]. There are various definitions of the fractional derivative [20–23]. Wang et al. introduced the theory of fractional Sobolev spaces on time scales by conformable fractional derivatives on time scales in [6]. The rise in these applications gives new vitality to the field of fractional calculus and fractional differential equations and calls for further research in this field.

On the other hand, recently, based on the concept of the fractional derivative of Riemann–Liouville on time scales [24], the authors of [7] established the fractional Sobolev space on time scales. However, in a recent work, the authors of [25] pointed out that the definition of fractional integral on time scales proposed in [24] is not the natural one on time scales. Furthermore, they developed a new notion of Riemann–Liouville fractional integral on time scales, which can effectively unify the discrete fractional calculus [26,27] and its continuous counterpart [28].

Motivated by the above discussion, in order to fix this defect in the fractional Sobolev space on time scales established in [7], in this paper, we want to contribute with the development of this new area in terms of theories of fractional differential equations on time scales. More precisely, we first show that the concept of the Riemann–Liouville fractional integral on time scales from [7] coincides with the ones from [29], which is significant as it allows us to prove the semigroup properties of the Riemann–Liouville fractional integral on time scales. Next, the left fractional Sobolev space in the sense of weak Riemann–Liouville derivatives on time scales was constructed and characterized via Riemann–Liouville derivatives on time scales. Then, as an application of our new theory, we study the solvability of a class of Kirchhoff-type fractional p-Laplacian systems on time scales with boundary conditions by using variational methods and the critical point theory. As far as we know, no one has studied this problem using other methods.

The rest of present paper is organized as follows: In Section 2, we review some symbols, basic notions and basic results of time-scale calculus that will be used in this paper and provide the definitions of fractional integrals and derivatives on time scales. In Section 3, we study some basic properties of left Riemann–Liouville fractional integral and differential operators on time scales, including the equivalence between fractional integrals and fractional derivatives on time scales defined by fractional integrals and fractional derivatives on time scales defined by the Laplace transform and the inverse Laplace transform. In Section 4, we provide the definition of left fractional Sobolev spaces on time scales and study some of their important properties. In Section 5, as an application of the results of this paper, we study the solvability of Kirchhoff-type fractional p-Laplacian systems on time scales by using the mountain pass theorem and the genus properties. In Section 6, we give a concise conclusion.

2. Preliminaries

In this section, we briefly collect some basic known notations, definitions, and results that will be used later.

A time scale $\mathbb{T}$ is an arbitrary nonempty closed subset of the real set $\mathbb{R}$ with the topology and ordering inherited from $\mathbb{R}$. Throughout this paper, we denote by $\mathbb{T}$ a time scale.

Definition 1 ([2]). *For $t \in \mathbb{T}$, we define the forward jump operator $\sigma : \mathbb{T} \to \mathbb{T}$ by $\sigma(t) := \inf\{s \in \mathbb{T} : s > t\}$, while the backward jump operator $\rho : \mathbb{T} \to \mathbb{T}$ is defined by $\rho(t) := \sup\{s \in \mathbb{T} : s < t\}$.*

We will use the following notations: $J_{\mathbb{R}}^0 = [a, b)$, $J_{\mathbb{R}} = [a, b]$, $J^0 = J_{\mathbb{R}}^0 \cap \mathbb{T}$, $J = J_{\mathbb{R}} \cap \mathbb{T}$, $J^k = [a, \rho(b)] \cap \mathbb{T}$.

Remark 1 ([2]). (1) *In Definition 1, we put* $\inf\emptyset = \sup\mathbb{T}$ *(i.e.,* $\sigma(t) = t$ *if* $\mathbb{T}$ *has a maximum t) and* $\sup\emptyset = \inf\mathbb{T}$ *(i.e.,* $\rho(t) = t$ *if* $\mathbb{T}$ *has a minimum t), where* $\emptyset$ *denotes the empty set.*
(2) *If* $\sigma(t) > t$*, we say that t is right-scattered, while if* $\rho(t) < t$*, we say that t is left-scattered. Points that are right-scattered and left-scattered at the same time are called isolated.*
(3) *If* $t < \sup\mathbb{T}$ *and* $\sigma(t) = t$*, we say that t is right-dense, while if* $t > \inf\mathbb{T}$ *and* $\rho(t) = t$*, we say that t is left-dense. Points that are right-dense and left-dense at the same time are called dense.*
(4) *The graininess function* $\mu : \mathbb{T} \to [0, \infty)$ *is defined by* $\mu(t) := \sigma(t) - t$*.*
(5) *The derivative makes use of the set* $\mathbb{T}^k$*, which is derived from the time scale* $\mathbb{T}$ *as follows: If* $\mathbb{T}$ *has a left-scattered maximum M, then* $\mathbb{T}^k := \mathbb{T}\backslash\{M\}$*; otherwise,* $\mathbb{T}^k := \mathbb{T}$*.*

Definition 2 ([2]). *Assume that* $f : \mathbb{T} \to \mathbb{R}$ *is a function and let* $t \in \mathbb{T}^k$*. Then we define* $f^\Delta(t)$ *to be the number (provided it exists) with the property that given any* $\varepsilon > 0$*, there is a neighborhood U of t (i.e,* $U = (t - \delta, t + \delta) \cap \mathbb{T}$ *for some* $\delta > 0$*) such that*

$$|f(\sigma(t)) - f(s) - f^\Delta(t)(\sigma(t) - s)| \leq \varepsilon|\sigma(t) - s|$$

for all $s \in U$*. We call* $f^\Delta(t)$ *the delta (or Hilger) derivative of f at t. Moreover, we say that f is delta (or Hilger) differentiable (or in short, differentiable) on* $\mathbb{T}^k$ *provided* $f^\Delta(t)$ *exists for all* $t \in \mathbb{T}^k$*. The function* $f^\Delta : \mathbb{T}^k \to \mathbb{R}$ *is then called the (delta) derivative of f on* $\mathbb{T}^k$*.*

Definition 3 ([2]). *A function* $f : \mathbb{T} \to \mathbb{R}$ *is called rd-continuous provided it is continuous at right-dense points in* $\mathbb{T}$ *and its left-sided limits exist (finite) at left-dense points in* $\mathbb{T}$*. The set of rd-continuous functions* $f : \mathbb{T} \to \mathbb{R}$ *will be denoted by* $C_{rd} = C_{rd}(\mathbb{T}) = C_{rd}(\mathbb{T}, \mathbb{R})$*. The set of functions* $f : \mathbb{T} \to \mathbb{R}$ *that are differentiable and whose derivative is rd-continuous is denoted by* $C^1_{rd} = C^1_{rd}(\mathbb{T}) = C^1_{rd}(\mathbb{T}, \mathbb{R})$*.*

Theorem 1 ([3]). *If* $a, b \in \mathbb{T}$ *and* $f, g \in C_{rd}(\mathbb{T})$*, then*

$$\int_{J^0} f^\sigma(t) g^\Delta(t) \Delta t = (fg)(b) - (fg)(a) - \int_{J^0} f^\Delta(t) g(t) \Delta t.$$

Theorem 2 ([3]). *If f is* Δ*-integrable on* $a, b \in \mathbb{T}$*, then so is* $|f|$*, and*

$$\left| \int_a^b f(t) \Delta t \right| \leq \int_a^b |f(t)| \Delta t.$$

Definition 4 ([24]). *Let J denote a closed bounded interval in* $\mathbb{T}$*. A function* $F : J \to \mathbb{R}$ *is called a delta antiderivative of function* $f : J \to \mathbb{R}$ *provided F is continuous on J, delta-differentiable at J, and* $F^\Delta(t) = f(t)$ *for all* $t \in J$*. Then, we define the* Δ*-integral of f from a to b by* $\int_a^b f(t) \Delta t := F(b) - F(a)$*.*

Theorem 3 ([30]). *The convolution is commutative and associative, that is, for* $f, g, h \in \mathcal{F}$*,*

$$f * g = g * f, \quad (f * g) * h = f * (g * h).$$

Proposition 1 ([31]). *f is an increasing continuous function on J. If F is the extension of f to the real interval* $J_{\mathbb{R}}$ *given by*

$$F(s) := \begin{cases} f(s), & if\ s \in \mathbb{T}, \\ f(t), & if\ s \in (t, \sigma(t)) \notin \mathbb{T}, \end{cases}$$

then $\int_a^b f(t) \Delta t \leq \int_a^b F(t) dt$*.*

Theorem 4 ([32]). *$y(t,s) = h_{n-1}(t,\sigma(s))$ is the Cauchy function of $y^{\Delta^n} = 0$, where*

$$h_0(t,s) = 1, \quad h_n(t,s) = \int_s^t h_{n-1}(\tau,s)\Delta\tau, \quad n \in \mathbb{N}.$$

Theorem 5 ([32]). *For all $n \in \mathbb{N}_0$, we have*

$$\mathcal{L}_{\mathbb{T}}(h_n(x,0))(z) = \frac{1}{z^{n-1}}, \quad x \in \mathbb{T}_0,$$

for all $z \in \mathbb{C}\backslash\{0\}$ such that $1 + z\mu(x) \neq 0$, $x \in \mathbb{T}_0$, and

$$\lim_{x\to\infty}(h_n(x,0)e_{\ominus z}(x,0)) = 0.$$

Definition 5 ([32], shift (delay) of a function). *For a given function $f : [t_0,\infty) \to \mathbb{C}$, the solution of the shifting problem*

$$u^{\Delta_t}(t,\sigma(s)) = -u^{\Delta_s}(t,s), \quad t,s \in \mathbb{T}, \quad t \geq t \geq s \geq t_0,$$
$$u(t,t_0) = f(t), \quad t \in \mathbb{T}, \quad t \geq t_0,$$

is denoted by $\hat{f}$ and is called the shift or delay of f.

Definition 6 ([32], Δ power function). *Suppose that $\alpha \in \mathbb{R}$; we define the generalized Δ-power function $h_\alpha(t,t_0)$ on $\mathbb{T}$ as follows:*

$$h_\alpha(t,t_0) = \mathcal{L}_{\mathbb{T}}^{-1}\left(\frac{1}{z^{\alpha+1}}\right)(t), \quad t \geq t_0,$$

for all $z \in \mathbb{C}\backslash\{0\}$ such that $\mathcal{L}_{\mathbb{T}}^{-1}$ exists, $t \geq t_0$. The fractional generalized Δ power function $h_\alpha(t,s)$ on $\mathbb{T}$, $t \geq s \geq t_0$ is defined as the shift of $h_\alpha(t,t_0)$, i.e.,

$$h_\alpha(t,s) = \widehat{h_\alpha(\cdot,t_0)}(t,s), \quad t,s \in \mathbb{T}, \quad t \geq s \geq t_0.$$

Definition 7 ([25,33], fractional integral on time scales). *Suppose h is an integrable function on J. Let $0 < \alpha \leq 1$. Then, the left fractional integral of order α of h is defined by*

$${}_a^{\mathbb{T}}I_t^\alpha h(t) := \int_a^t \frac{(t-\sigma(s))^{\alpha-1}}{\Gamma(\alpha)}h(s)\Delta s. \tag{1}$$

The right fractional integral of order α of h is defined by

$${}_t^{\mathbb{T}}I_b^\alpha h(t) := \int_t^b \frac{(s-\sigma(t))^{\alpha-1}}{\Gamma(\alpha)}h(s)\Delta s,$$

where Γ is the gamma function.

Definition 8 ([25,33], Riemann–Liouville fractional derivative on time scales). *Let $t \in \mathbb{T}$, $0 < \alpha \leq 1$, and $h : \mathbb{T} \to \mathbb{R}$. The left Riemann–Liouville fractional derivative of order α of h is defined by*

$${}_a^{\mathbb{T}}D_t^\alpha h(t) := \left({}_a^{\mathbb{T}}I_t^{1-\alpha}h(t)\right)^\Delta = \frac{1}{\Gamma(1-\alpha)}\left(\int_a^t (t-\sigma(s))^{-\alpha}h(s)\Delta s\right)^\Delta. \tag{2}$$

Actually, ${}_a^{\mathbb{T}}D_t^{\alpha}h(t)$ *can be rewritten as* $\Delta \circ {}_a^{\mathbb{T}}I_t^{1-\alpha}h(t)$. *The right Riemann–Liouville fractional derivative of order* α *of* h *is defined by*

$$ {}_t^{\mathbb{T}}D_b^{\alpha}h(t) := -\left({}_t^{\mathbb{T}}I_b^{1-\alpha}h(t)\right)^{\Delta} = \frac{-1}{\Gamma(1-\alpha)}\left(\int_t^b (s-\sigma(t))^{-\alpha}h(s)\Delta s\right)^{\Delta}. $$

Definition 9 ([25,33], Caputo fractional derivative on time scales)**.** *Let* $t \in \mathbb{T}$, $0 < \alpha \leq 1$ *and* $h : \mathbb{T} \to \mathbb{R}$. *The left Caputo fractional derivative of order* α *of* h *is defined by*

$$ {}_a^{\mathbb{T}C}D_t^{\alpha}h(t) := {}_a^{\mathbb{T}}I_t^{1-\alpha}h^{\Delta}(t) = \frac{1}{\Gamma(1-\alpha)}\int_a^t (t-\sigma(s))^{-\alpha}h^{\Delta}(s)\Delta s. $$

The right Caputo fractional derivative of order α *of* h *is defined by*

$$ {}_t^{\mathbb{T}C}D_b^{\alpha}h(t) := -{}_t^{\mathbb{T}}I_b^{1-\alpha}h^{\Delta}(t) = \frac{-1}{\Gamma(1-\alpha)}\int_t^b (s-\sigma(t))^{-\alpha}h^{\Delta}(s)\Delta s. $$

Definition 10 ([34])**.** *For* $f : \mathbb{T} \to \mathbb{R}$, *the time scale or generalized Laplace transform of* f, *denoted by* $\mathcal{L}_{\mathbb{T}}\{f\}$ *or* $F(z)$, *is given by*

$$ \mathcal{L}_{\mathbb{T}}\{f\}(z) = F(z) := \int_0^{\infty} f(t)g^{\sigma}(t)\Delta t, $$

where $g(t) = e_{\ominus z}(t, 0)$.

Theorem 6 ([34], Inversion formula of the Laplace transform)**.** *Suppose that* $F(z)$ *is analytic in the region* $Re_{\mu}(z) > Re_{\mu}(c)$ *and* $F(z) \to 0$ *uniformly as* $|z| \to \infty$ *in this region. Suppose* $F(z)$ *has finitely many regressive poles of finite order* $\{z_1, z_2, \ldots, z_n\}$ *and* $\widetilde{F}_{\mathbb{R}}(z)$ *is the transform of the function* $\widetilde{f}(t)$ *on* $\mathbb{R}$ *that corresponds to the transform* $F(z) = F_{\mathbb{T}}(z)$ *of* $f(t)$ *on* $\mathbb{T}$, *If*

$$ \int_{c-i\infty}^{c+i\infty} |\widetilde{F}_{\mathbb{R}}(z)||dz| < \infty, $$

then

$$ f(t) = \sum_{i=1}^{n} Res_{z=z_i} e_z(t, 0)F(z), $$

has transform $F(z)$ *for all* z *with* $Re(z) > c$.

Definition 11 ([29], Riemann–Liouville fractional integral on time scales)**.** *Let* $\alpha > 0$, $\mathbb{T}$ *be a time scale, and* $f : \mathbb{T} \to \mathbb{R}$. *The left Riemann–Liouville fractional integral of* f *of order* α *on the time scale* $\mathbb{T}$, *denoted by* $I_{\mathbb{T}}^{\alpha}f$, *is defined by*

$$ I_{\mathbb{T}}^{\alpha}f(t) = \mathcal{L}_{\mathbb{T}}^{-1}\left[\frac{F(z)}{z^{\alpha}}\right](t). $$

Theorem 7 ([25], Cauchy result on time scales)**.** *Let* $n \in \{1, 2\}$, $\mathbb{T}$ *be a time scale with* $a, t_1, \ldots, t_n \in \mathbb{T}$, $t_i > a$, $i = 1, \ldots, n$, *and* f *an integrable function on* $\mathbb{T}$. *Then,*

$$ \int_a^{t_n} \ldots \int_a^{t_1} f(t_0)\Delta t_0 \ldots \Delta t_{n-1} = \frac{1}{(n-1)!}\int_a^{t_n} (t_n - \sigma(s))^{n-1}\Delta s. $$

Theorem 8 ([5]). *A function $f : J \to \mathbb{R}^N$ is absolutely continuous on J iff f is Δ-differentiable $\Delta-a.e.$ on J^0 and*

$$f(t) = f(a) + \int_{[a,t)_{\mathbb{T}}} f^{\Delta}(s)\Delta s, \quad \forall t \in J.$$

Theorem 9 ([35]). *A function $f : \mathbb{T} \to \mathbb{R}$ is absolutely continuous on $\mathbb{T}$ iff the following conditions are satisfied:*

(i) f is Δ-differentiable $\Delta-a.e.$ on J^0 and $f^{\Delta} \in L^1(\mathbb{T})$.
(ii) The equality

$$f(t) = f(a) + \int_{[a,t)_{\mathbb{T}}} f^{\Delta}(s)\Delta s$$

holds for every $t \in \mathbb{T}$.

Theorem 10 ([36]). *A function $q : J_{\mathbb{R}} \to \mathbb{R}^m$ is absolutely continuous iff there exist a constant $c \in \mathbb{R}^m$ and a function $\varphi \in L^1$ such that*

$$q(t) = c + (I^1_{a^+}\varphi)(t), \quad t \in J_{\mathbb{R}}.$$

In this case, we have $q(a) = c$ and $q'(t) = \varphi(t)$, $t \in J_{\mathbb{R}}$ a.e.

Theorem 11 ([5], integral representation). *Let $\alpha \in (0,1)$ and $q \in L^1$. Then, q has a left-sided Riemann–Liouville derivative $D^{\alpha}_{a^+}q$ of order α iff there exist a constant $c \in \mathbb{R}^m$ and a function $\varphi \in L^1$ such that*

$$q(t) = \frac{1}{\Gamma(\alpha)}\frac{c}{(t-a)^{1-\alpha}} + (I^{\alpha}_{a^+}\varphi)(t), \quad t \in J_{\mathbb{R}} \quad a.e..$$

In this case, we have $I^{1-\alpha}_{a^+}q(a) = c$ and $(D^{\alpha}_{a^+}q)(t) = \varphi(t)$, $t \in J_{\mathbb{R}}$ a.e.

Lemma 1 ([4]). *Let $f \in L^1_{\Delta}(J^0)$. Then, the following*

$$\int_{J^0} (f \cdot \varphi^{\Delta})(s)\Delta s = 0, \quad for\ every\ \varphi \in C^1_{0,rd}(J^k)$$

holds iff there exists a constant $c \in \mathbb{R}$ such that

$$f \equiv c \quad \Delta-a.e.\ on\ J^0.$$

Definition 12 ([4]). *Let $p \in \bar{\mathbb{R}}$ be such that $p \geq 1$ and $u : J \to \bar{\mathbb{R}}$. Say that u belongs to $W^{1,p}_{\Delta}(J)$ iff $u \in L^p_{\Delta}(J^0)$ and there exists $g : J^k \to \bar{\mathbb{R}}$ such that $g \in L^p_{\Delta}(J^0)$ and*

$$\int_{J^0} (u \cdot \varphi^{\Delta})(s)\Delta s = -\int_{J^0} (g \cdot \varphi^{\sigma})(s)\Delta s, \quad \forall \varphi \in C^1_{0,rd}(J^k),$$

with

$$C^1_{0,rd}(J^k) := \left\{ f : J \to \mathbb{R} : f \in C^1_{rd}(J^k),\ f(a) = f(b) \right\},$$

where $C^1_{rd}(J^k)$ is the set of all continuous functions on J such that they are Δ-differential on J^k and their Δ-derivatives are $rd-$continuous on J^k.

Theorem 12 ([4]). *Let $p \in \bar{\mathbb{R}}$ be such that $p \geq 1$. Then, the set $L^p_\Delta(J^0)$ is a Banach space together with the norm defined for every $f \in L^p_\Delta(J^0)$ as*

$$\|f\|_{L^p_\Delta} := \begin{cases} \left[\int_{J^0} |f|^p(s)\Delta s\right]^{\frac{1}{p}}, & if\ p \in \mathbb{R}, \\ \inf\{C \in \mathbb{R} : |f| \leq C\,\Delta - a.e.\ \text{on}\ J^0\}, & if\ p = +\infty. \end{cases}$$

Moreover, $L^2_\Delta(J^0)$ is a Hilbert space together with the inner product given for every $(f,g) \in L^2_\Delta(J^0) \times L^2_\Delta(J^0)$ by

$$(f,g)_{L^2_\Delta} := \int_{J^0} f(s) \cdot g(s)\Delta s.$$

Theorem 13 ([28]). *Fractional integration operators are bounded in $L^p(J_\mathbb{R})$; i.e., the following estimate*

$$\|I^\alpha_{a^+}\varphi\|_{L^p(a,b)} \leq \frac{(b-a)^{Re\alpha}}{Re\alpha|\Gamma(\alpha)|}\|\varphi\|_{L^p(J_\mathbb{R})}, \quad Re\alpha > 0$$

holds.

Proposition 2 ([4]). *Suppose $p \in \bar{\mathbb{R}}$ and $p \geq 1$. Let $p' \in \bar{\mathbb{R}}$ be such that $\frac{1}{p'} + \frac{1}{p'} = 1$. Then, if $f \in L^p_\Delta(J^0)$ and $g \in L^{p'}_\Delta(J^0)$, then $f \cdot g \in L^1_\Delta(J^0)$ and*

$$\|f \cdot g\|_{L^1_\Delta} \leq \|f\|_{L^p_\Delta} \cdot \|g\|_{L^{p'}_\Delta}.$$

This expression is called Hölder's inequality and Cauchy–Schwarz's inequality whenever $p = 2$.

Theorem 14 ([3]). *(the first mean value theorem) . Let f and g be bounded and integrable functions on J, and let g be nonnegative (or nonpositive) on J. Let us set*

$$m = \inf\{f(t) : t \in J^0\} \quad and \quad M = \sup\{f(t) : t \in J^0\}.$$

Then, there exists a real number Λ satisfying the inequalities $m \leq \Lambda \leq M$ such that

$$\int_{J^0} f(t)g(t)\Delta t = \Lambda \int_{J^0} g(t)\Delta t.$$

Corollary 1 ([3]). *Let f be an integrable function on J, and let m and M be the infimum and supremum, respectively, of f on J^0. Then, there exists a number Λ between m and M such that $\int_{J^0} f(t)\Delta t = \Lambda(b-a)$.*

Theorem 15 ([3]). *Let f be a function defined on J and let $c \in \mathbb{T}$ with $a < c < b$. If f is Δ-integrable from a to c and from c to b, then f is Δ-integrable from a to b and*

$$\int_{J^0} f(t)\Delta t = \int_a^c f(t)\Delta t + \int_c^b f(t)\Delta t.$$

Lemma 2 ([3]). *Assume that $a, b \in \mathbb{T}$. Every constant function $f : \mathbb{T} \to \mathbb{R}$ is Δ-integrable from a to b and*

$$\int_{J^0} c\Delta t = c(b-a).$$

Lemma 3 ([37], A time-scale version of the Arzela–Ascoli theorem)**.** *Let X be a subset of $C(J,\mathbb{R})$ satisfying the following conditions:*

(i) *X is bounded;*
(ii) *For any given $\epsilon > 0$, there exists $\delta > 0$ such that $t_1, t_2 \in J$, $|t_1 - t_2| < \delta$ implies $|f(t_1) - f(t_2)| < \epsilon$ for all $f \in X$.*

Then, X is relatively compact.

3. Some Fundamental Properties of Left Riemann–Liouville Fractional Operators on Time Scales

Inspired by [38], we can obtain the consistency of Definitions 7 and 11 by using the above theory of the Laplace transform on time scales and the inverse Laplace transform on time scales.

Theorem 16. *Let $\alpha > 0$, $\mathbb{T}$ be a time scale, J be an interval of $\mathbb{T}$, and f be an integrable function on J. Then, $\left({}^{\mathbb{T}}_{a}I^{\alpha}_{t}f\right)(t) = I^{\alpha}_{\mathbb{T}}f(t)$.*

Proof. Using the Laplace transform on time scale $\mathbb{T}$ for (1), in view of Definitions 6, 7, Theorem 5, the proof of Theorem 4.14 in [32], and Definition 10, we have

$$\begin{aligned}
&\mathcal{L}_{\mathbb{T}}\left\{\left({}^{\mathbb{T}}_{a}I^{\alpha}_{t}f\right)(t)\right\}(z)\\
&= \mathcal{L}_{\mathbb{T}}\left\{\frac{1}{\Gamma(\alpha)}\int_a^t (t-\sigma(s))^{\alpha-1}f(s)\Delta s\right\}(z)\\
&= \mathcal{L}_{\mathbb{T}}(h_{\alpha-1}(\cdot,a) * f)(t)(z)\\
&= \mathcal{L}_{\mathbb{T}}(h_{\alpha-1}(\cdot,a))(z)\mathcal{L}_{\mathbb{T}}(f)(t)(z)\\
&= \frac{1}{z^{\alpha}}\mathcal{L}_{\mathbb{T}}\{f\}(z)\\
&= \frac{F(z)}{z^{\alpha}}(t).
\end{aligned} \tag{3}$$

Taking the inverse Laplace transform on time scales for (3), with an eye to Definition 11, one arrives at

$$\left({}^{\mathbb{T}}_{a}I^{\alpha}_{t}f\right)(t) = \mathcal{L}^{-1}_{\mathbb{T}}\left[\frac{F(z)}{z^{\alpha}}\right](t) = I^{\alpha}_{\mathbb{T}}f(t).$$

The proof is complete. □

Combining [24,29] with Theorem 16, we see that Propositions 15–17, Corollary 18, and Theorems 20 and 21 from [24] remain intact under the new Definition 7.

Proposition 3. *Let h be Δ-integrable on J and $0 < \alpha \leq 1$. Then ${}^{\mathbb{T}}_{a}D^{\alpha}_{t}h(t) = \Delta \circ {}^{\mathbb{T}}_{a}I^{1-\alpha}_{t}h(t)$.*

Proof. Let $h : \mathbb{T} \to \mathbb{R}$. In view of (1) and (2), we obtain

$$\begin{aligned}
{}^{\mathbb{T}}_{t}D^{\alpha}_{b}h(t) =& \frac{1}{\Gamma(1-\alpha)}\left(\int_a^t (t-\sigma(s))^{-\alpha}h(s)\Delta s\right)^{\Delta}\\
=& \left({}^{\mathbb{T}}_{a}I^{1-\alpha}_{t}h(t)\right)^{\Delta}\\
=& \Delta \circ {}^{\mathbb{T}}_{a}I^{1-\alpha}_{t}h(t).
\end{aligned}$$

The proof is complete. □

Proposition 4. *For any function h that is integrable on J, the Riemann–Liouville Δ-fractional integral satisfies ${}^{\mathbb{T}}_{a}I^{\alpha}_{t} \circ {}^{\mathbb{T}}_{a}I^{\beta}_{t} = {}^{\mathbb{T}}_{a}I^{\alpha+\beta}_{t} = {}^{\mathbb{T}}_{a}I^{\beta}_{t} \circ {}^{\mathbb{T}}_{a}I^{\alpha}_{t}$ for $\alpha > 0$ and $\beta > 0$.*

Proof. Combining with Proposition 3.4 in [29] and Theorem 16, one obtains

$$ {}_a^{\mathbb{T}}I_t^{\alpha} \circ {}_a^{\mathbb{T}}I_t^{\beta} = {}_a^{\mathbb{T}}I_t^{\alpha+\beta}. $$

In a similarly way, one arrives at

$$ {}_a^{\mathbb{T}}I_t^{\beta} \circ {}_a^{\mathbb{T}}I_t^{\alpha} = {}_a^{\mathbb{T}}I_t^{\alpha+\beta}. $$

Consequently, we obtain that

$$ {}_a^{\mathbb{T}}I_t^{\alpha} \circ {}_a^{\mathbb{T}}I_t^{\beta} = {}_a^{\mathbb{T}}I_t^{\alpha+\beta} = {}_a^{\mathbb{T}}I_t^{\beta} \circ {}_a^{\mathbb{T}}I_t^{\alpha}. $$

The proof is complete. □

Proposition 5. *For any function h that is integrable on J one has ${}_a^{\mathbb{T}}D_t^{\alpha} \circ {}_a^{\mathbb{T}}I_t^{\alpha} h = h$.*

Proof. Taking account of Propositions 3 and 4, one can get

$$ {}_a^{\mathbb{T}}D_t^{\alpha} \circ {}_a^{\mathbb{T}}I_t^{\alpha} h(t) = \left({}_a^{\mathbb{T}}I_t^{1-\alpha} ({}_a^{\mathbb{T}}I_t^{\alpha}(h(t))) \right)^{\Delta} = \left({}_a^{\mathbb{T}}I_t h(t) \right)^{\Delta} = h. $$

The proof is complete. □

Corollary 2. *For $0 < \alpha \leq 1$, we have ${}_a^{\mathbb{T}}D_t^{\alpha} \circ {}_a^{\mathbb{T}}D_t^{-\alpha} = Id$ and ${}_a^{\mathbb{T}}I_t^{-\alpha} \circ {}_a^{\mathbb{T}}I_t^{\alpha} = Id$, where Id denotes the identity operator.*

Proof. In view of Proposition 5, we have

$$ {}_a^{\mathbb{T}}D_t^{\alpha} \circ {}_a^{\mathbb{T}}D_t^{-\alpha} = {}_a^{\mathbb{T}}D_t^{\alpha} \circ {}_a^{\mathbb{T}}I_t^{\alpha} = Id \quad \text{and} \quad {}_a^{\mathbb{T}}I_t^{-\alpha} \circ {}_a^{\mathbb{T}}I_t^{\alpha} = {}_a^{\mathbb{T}}D_t^{\alpha} \circ {}_a^{\mathbb{T}}I_t^{\alpha} = Id. $$

The proof is complete. □

Theorem 17. *Let $f \in C(J)$ and $\alpha > 0$, then $f \in {}_a^{\mathbb{T}}I_t^{\alpha}(J)$ iff*

$$ {}_a^{\mathbb{T}}I_t^{1-\alpha} f \in C^1(J) \tag{4} $$

and

$$ \left({}_a^{\mathbb{T}}I_t^{1-\alpha} f(t) \right)\Big|_{t=a} = 0, \tag{5} $$

where ${}_a^{\mathbb{T}}I_t^{\alpha}(J)$ denotes the space of functions that can be represented by the left Riemann–Liouville Δ-integral of order α of a $C(J)-$function.

Proof. Suppose $f \in {}_a^{\mathbb{T}}I_t^{\alpha}(J)$, $f(t) = {}_a^{\mathbb{T}}I_t^{\alpha} g(t)$ for some $g \in C(J)$, and

$$ {}_a^{\mathbb{T}}I_t^{1-\alpha}(f(t)) = {}_a^{\mathbb{T}}I_t^{1-\alpha}({}_a^{\mathbb{T}}I_t^{\alpha} g(t)). $$

In view of Proposition 4, one gets

$$ {}_a^{\mathbb{T}}I_t^{1-\alpha}(f(t)) = {}_a^{\mathbb{T}}I_t g(t) = \int_a^t g(s)\Delta s. $$

As a result, ${}_a^{\mathbb{T}}I_t^{1-\alpha} f \in C(J)$ and

$$ \left({}_a^{\mathbb{T}}I_t^{1-\alpha} f(t) \right)\Big|_{t=a} = \int_a^a g(s)\Delta s = 0. $$

Inversely, suppose that $f \in C(J)$ satisfies (4) and (5). Then, by applying Taylor's formula to function ${}_a^{\mathbb{T}}I_t^{1-\alpha} f$, we obtain

$$ {}_a^{\mathbb{T}}I_t^{1-\alpha} f(t) = \int_a^t \frac{\Delta}{\Delta s} {}_a^{\mathbb{T}}I_s^{1-\alpha} f(s)\Delta s, \quad \forall t \in J. $$

Let $\varphi(t) = \frac{\Delta}{\Delta t} {}_a^{\mathbb{T}}I_t^{1-\alpha} f(t)$. Note that $\varphi \in C(J)$ by (4). Now by Proposition 4, one sees that

$$ {}_a^{\mathbb{T}}I_t^{1-\alpha}(f(t)) = {}_a^{\mathbb{T}}I_t^{1}\varphi(t) = {}_a^{\mathbb{T}}I_t^{1-\alpha}[{}_a^{\mathbb{T}}I_t^{\alpha}\varphi(t)] $$

and hence

$$ {}_a^{\mathbb{T}}I_t^{1-\alpha}(f(t)) - {}_a^{\mathbb{T}}I_t^{1-\alpha}[{}_a^{\mathbb{T}}I_t^{\alpha}\varphi(t)] \equiv 0. $$

Therefore, we have

$$ {}_a^{\mathbb{T}}I_t^{1-\alpha}[f(t) - {}_a^{\mathbb{T}}I_t^{\alpha}\varphi(t)] \equiv 0. $$

From the uniqueness of the solution to Abel's integral Equation ([39]), this implies that $f - {}_a^{\mathbb{T}}I_t^{\alpha}\varphi \equiv 0$. Hence, $f = {}_a^{\mathbb{T}}I_t^{\alpha}\varphi$ and $f \in {}_a^{\mathbb{T}}I_t^{\alpha}(J)$. The proof is complete. □

Theorem 18. *Let $\alpha > 0$ and $f \in C(J)$ satisfy the condition in Theorem 17. Then,*

$$ ({}_a^{\mathbb{T}}I_t^{\alpha} \circ {}_a^{\mathbb{T}}D_t^{\alpha})(f) = f. $$

Proof. Combining Theorem 17 with Proposition 5, we can see that

$$ {}_a^{\mathbb{T}}I_t^{\alpha} \circ {}_a^{\mathbb{T}}D_t^{\alpha} f(t) = {}_a^{\mathbb{T}}I_t^{\alpha} \circ {}_a^{\mathbb{T}}D_t^{\alpha}({}_a^{\mathbb{T}}I_t^{\alpha}\varphi(t)) = {}_a^{\mathbb{T}}I_t^{\alpha}\varphi(t) = f(t). $$

The proof is complete. □

Theorem 19. *Let $\alpha > 0$, $p, q \geq 1$, and $\frac{1}{p} + \frac{1}{q} \leq 1 + \alpha$, where $p \neq 1$ and $q \neq 1$ in the case when $\frac{1}{p} + \frac{1}{q} = 1 + \alpha$. Moreover, let*

$$ {}_a^{\mathbb{T}}I_t^{\alpha}(L^p) := \left\{ f : f = {}_a^{\mathbb{T}}I_t^{\alpha} g, g \in L^p(J) \right\} $$

and

$$ {}_t^{\mathbb{T}}I_b^{\alpha}(L^p) := \left\{ f : f = {}_t^{\mathbb{T}}I_b^{\alpha} g, g \in L^p(J) \right\}, $$

then the following integration by part formulas hold.

(*a*) *If $\varphi \in L^p(J)$ and $\psi \in L^q(J)$, then*

$$ \int_{J^0} \varphi(t) \left({}_a^{\mathbb{T}}I_t^{\alpha}\psi \right)(t)\Delta t = \int_{J^0} \psi(t) \left({}_t^{\mathbb{T}}I_b^{\alpha}\varphi \right)(t)\Delta t. $$

(*b*) *If $g \in {}_t^{\mathbb{T}}I_b^{\alpha}(L^p)$ and $f \in {}_a^{\mathbb{T}}I_t^{\alpha}(L^q)$, then*

$$ \int_{J^0} g(t) \left({}_a^{\mathbb{T}}D_t^{\alpha} f \right)(t)\Delta t = \int_{J^0} f(t) \left({}_t^{\mathbb{T}}D_b^{\alpha} g \right)(t)\Delta t. $$

(*c*) *For Caputo fractional derivatives, if* $g \in {}_{t}^{\mathbb{T}}I_{b}^{\alpha}(L^{p})$ *and* $f \in {}_{a}^{\mathbb{T}}I_{t}^{\alpha}(L^{q})$, *then*

$$\int_{J^0} g(t)\left({}_{a}^{\mathbb{T}C}D_{t}^{\alpha}f\right)(t)\Delta t = \left[{}_{t}^{\mathbb{T}}I_{b}^{1-\alpha}g(t)\cdot f(t)\right]\Big|_{t=a}^{b} + \int_{J^0} f(\sigma(t))\left({}_{t}^{\mathbb{T}}D_{b}^{\alpha}g\right)(t)\Delta t.$$

and

$$\int_{J^0} g(t)\left({}_{t}^{\mathbb{T}C}D_{b}^{\alpha}f\right)(t)\Delta t = \left[{}_{a}^{\mathbb{T}}I_{t}^{1-\alpha}g(t)\cdot f(t)\right]\Big|_{t=a}^{b} + \int_{J^0} f(\sigma(t))\left({}_{a}^{\mathbb{T}}D_{t}^{\alpha}g\right)(t)\Delta t.$$

Proof. (*a*) It follows from Definition 7 and Fubini's theorem on time scales that

$$\begin{aligned}
&\int_{J^0} \varphi(t)\left({}_{a}^{\mathbb{T}}I_{t}^{\alpha}\psi\right)(t)\Delta t\\
&= \int_{J^0} \varphi(t)\left(\int_{a}^{t}\frac{(t-\sigma(s))^{\alpha-1}}{\Gamma(\alpha)}\psi(s)\Delta s\right)\Delta t\\
&= \int_{J^0} \psi(s)\int_{s}^{b}\frac{(t-\sigma(s))^{\alpha-1}}{\Gamma(\alpha)}\varphi(t)\Delta t\Delta s\\
&= \int_{J^0} \psi(t)\int_{t}^{b}\frac{(s-\sigma(t))^{\alpha-1}}{\Gamma(\alpha)}\varphi(s)\Delta s\Delta t\\
&= \int_{J^0} \psi(t)\left({}_{t}^{\mathbb{T}}I_{b}^{\alpha}\varphi\right)(t)\Delta t.
\end{aligned}$$

(*b*) It follows from Definition 8 and Fubini's theorem on time scales that

$$\begin{aligned}
&\int_{J^0} g(t)\left({}_{a}^{\mathbb{T}}D_{t}^{\alpha}f\right)(t)\Delta t\\
&= \int_{J^0} g(t)\left(\frac{1}{\Gamma(1-\alpha)}\left(\int_{a}^{t}(t-\sigma(s))^{-\alpha}f(s)\Delta s\right)^{\Delta}\right)\Delta t\\
&= \int_{J^0} f(s)\left(\frac{1}{\Gamma(1-\alpha)}\left(\int_{s}^{b}(t-\sigma(s))^{-\alpha}g(t)\Delta t\right)^{\Delta}\right)\Delta s\\
&= \int_{J^0} f(t)\left(\frac{1}{\Gamma(1-\alpha)}\left(\int_{t}^{b}(s-\sigma(t))^{-\alpha}g(s)\Delta s\right)^{\Delta}\right)\Delta t\\
&= \int_{J^0} g(t)\left({}_{t}^{\mathbb{T}}D_{b}^{\alpha}f\right)(t)\Delta t.
\end{aligned}$$

(c) It follows from Definition 9, Fubini's theorem on time scales and Theorem 1 that

$$\begin{aligned}
&\int_{J^0} g(t)\left({}_a^{\mathbb{T}}{}^{C}D_t^{\alpha} f\right)(t)\Delta t \\
&= \int_{J^0} g(t)\left(\frac{1}{\Gamma(1-\alpha)}\int_a^t (t-\sigma(s))^{-\alpha} f^{\Delta}(s)\Delta s\right)\Delta t \\
&= \int_{J^0} f^{\Delta}(s)\left(\frac{1}{\Gamma(1-\alpha)}\int_s^b (t-\sigma(s))^{-\alpha} g(t)\Delta t\right)\Delta s \\
&= \int_{J^0} f^{\Delta}(t)\left(\frac{1}{\Gamma(1-\alpha)}\int_t^b (s-\sigma(t))^{-\alpha} g(s)\Delta s\right)\Delta t \\
&= \left[{}_t^{\mathbb{T}}I_b^{1-\alpha} g(t)\cdot f(t)\right]\Big|_{t=a}^{b} - \int_{J^0} f(\sigma(t))\left(\frac{1}{\Gamma(1-\alpha)}\int_t^b (s-\sigma(t))^{-\alpha} g(s)\Delta s\right)^{\Delta} \\
&= \left[{}_t^{\mathbb{T}}I_b^{1-\alpha} g(t)\cdot f(t)\right]\Big|_{t=a}^{b} + \int_{J^0} f(\sigma(t))\left(\frac{-1}{\Gamma(1-\alpha)}\int_t^b (s-\sigma(t))^{-\alpha} g(s)\Delta s\right)^{\Delta} \\
&= \left[{}_t^{\mathbb{T}}I_b^{1-\alpha} g(t)\cdot f(t)\right]\Big|_{t=a}^{b} + \int_{J^0} f(\sigma(t))\left({}_t^{\mathbb{T}}D_b^{\alpha} g\right)(t)\Delta t.
\end{aligned}$$

The second relation is obtained in a similar way. The proof is complete.
□

4. Fractional Sobolev Spaces on Time Scales and Their Properties

In this section, we present and prove some lemmas, propositions, and theorems, which are of utmost significance for our main results.

In the following, let $0 < a < b$. Inspired by Theorems 8–11, we give the following definition.

Definition 13. *Let $0 < \alpha \leq 1$. By $AC^{\alpha,1}_{\Delta,a^+}(J,\mathbb{R}^N)$ we denote the set of all functions $f : J \to \mathbb{R}^N$ that have the representation*

$$f(t) = \frac{1}{\Gamma(\alpha)}\frac{c}{(t-a)^{1-\alpha}} + {}_a^{\mathbb{T}}I_t^{\alpha}\varphi(t), \quad t \in J \quad \Delta - a.e. \tag{6}$$

with $c \in \mathbb{R}^N$ and $\varphi \in L^1_{\Delta}$.

Then, we have the following result.

Theorem 20. *Let $0 < \alpha \leq 1$ and $f \in L^1_{\Delta}$. Then, function f has the left Riemann–Liouville derivative ${}_a^{\mathbb{T}}D_t^{\alpha} f$ of order α on the interval J iff $f \in AC^{\alpha,1}_{\Delta,a^+}(J,\mathbb{R}^N)$; that is, f has the representation* (6)*. In such a case,*

$$({}_a^{\mathbb{T}}I_t^{1-\alpha} f)(a) = c, \quad ({}_a^{\mathbb{T}}D_t^{\alpha} f)(t) = \varphi(t), \quad t \in J \quad \Delta - a.e.$$

Proof. Let us assume that $f \in L^1_{\Delta}$ has a left-sided Riemann–Liouville derivative ${}_a^{\mathbb{T}}D_t^{\alpha} f$. This means that ${}_a^{\mathbb{T}}I_t^{1-\alpha} f$ is (identified to) an absolutely continuous function. From the integral representation of Theorems 8 and 10, there exists a constant $c \in \mathbb{R}^N$ and a function $\varphi \in L^1_{\Delta}$ such that

$$({}_a^{\mathbb{T}}I_t^{1-\alpha} f)(t) = c + ({}_a^{\mathbb{T}}I_t^{1}\varphi)(t), \quad t \in J, \tag{7}$$

with $({}_a^{\mathbb{T}}I_t^{1-\alpha} f)(a) = c$ and $\left(({}_a^{\mathbb{T}}I_t^{1-\alpha} f)(t)\right)^{\Delta} = {}_a^{\mathbb{T}}D_t^{\alpha} f(t) = \varphi(t), t \in J \quad \Delta - a.e..$

By Proposition 4 and applying ${}^{\mathbb{T}}_{a}I^{\alpha}_{t}$ to (7), we obtain

$$({}^{\mathbb{T}}_{a}I^{1}_{t}f)(t) = ({}^{\mathbb{T}}_{a}I^{\alpha}_{t}c)(t) + ({}^{\mathbb{T}}_{a}I^{1}_{t}{}^{\mathbb{T}}_{a}I^{\alpha}_{t}\varphi)(t), \quad t \in J \quad \Delta - a.e.. \tag{8}$$

The result follows from the Δ-differentiability of (8).

Conversely, let us assume that (6) holds true. From Proposition 4 and applying ${}^{\mathbb{T}}_{a}I^{1-\alpha}_{t}$ to (6), we obtain

$$({}^{\mathbb{T}}_{a}I^{1-\alpha}_{t}f)(t) = c + ({}^{\mathbb{T}}_{a}I^{1}_{t}\varphi)(t), \quad t \in J \quad \Delta - a.e.$$

and then, ${}^{\mathbb{T}}_{a}I^{1-\alpha}_{t}f$ has an absolutely continuous representation. Further, f has a left-sided Riemann–Liouville derivative ${}^{\mathbb{T}}_{a}D^{\alpha}_{t}f$. This completes the proof. □

Remark 2. (i) *By* $AC^{\alpha,p}_{\Delta,a^+}$ $(1 \le p < \infty)$ *we denote the set of all functions* $f : J \to \mathbb{R}^N$ *possessing representation* (6) *with* $c \in \mathbb{R}^N$ *and* $\varphi \in L^p_\Delta$.

(ii) *It is easy to see that Theorem 20 implies that for any* $1 \le p < \infty$, f *has the left Riemann–Liouville derivative* ${}^{\mathbb{T}}_{a}D^{\alpha}_{t}f \in L^p_\Delta$ *iff* $f \in AC^{\alpha,p}_{\Delta,a^+}$; *that is,* f *has the representation* (6) *with* $\varphi \in L^p_\Delta$.

Definition 14. *Let* $0 < \alpha \le 1$ *and let* $1 \le p < \infty$. *By left Sobolev space of order* α *we will mean the set* $W^{\alpha,p}_{\Delta,a^+} = W^{\alpha,p}_{\Delta,a^+}(J,\mathbb{R}^N)$ *given by*

$$W^{\alpha,p}_{\Delta,a^+} := \left\{ u \in L^p_\Delta;\ \exists\, g \in L^p_\Delta,\ \forall \varphi \in C^\infty_{c,rd} \text{ such that } \int_{J^0} u(t)\cdot {}^{\mathbb{T}}_{t}D^{\alpha}_{b}\varphi(t)\Delta t = \int_{J^0} g(t)\cdot\varphi(t)\Delta t \right\}.$$

Remark 3. *A function* g *given in Definition 16 will be called the weak left fractional derivative of order* $0 < \alpha \le 1$ *of* u; *let us denote it by* ${}^{\mathbb{T}}u^{\alpha}_{a^+}$. *The uniqueness of this weak derivative follows from [4].*

We have the following characterization of $W^{\alpha,p}_{\Delta,a^+}$.

Theorem 21. *If* $0 < \alpha \le 1$ *and* $1 \le p < \infty$, *then* $W^{\alpha,p}_{\Delta,a^+} = AC^{\alpha,p}_{\Delta,a^+} \cap L^p_\Delta$.

Proof. On the one hand, if $u \in AC^{\alpha,p}_{\Delta,a^+} \cap L^p_\Delta$, then from Theorem 20 it follows that u has derivative ${}^{\mathbb{T}}_{a}D^{\alpha}_{t}u \in L^p_\Delta$. Theorem 19 implies that

$$\int_{J^0} u(t)\,{}^{\mathbb{T}}_{t}D^{\alpha}_{b}\varphi(t)\Delta t = \int_{J^0} ({}^{\mathbb{T}}_{a}D^{\alpha}_{t}u)(t)\,\varphi(t)\Delta t$$

for any $\varphi \in C^\infty_{c,rd}$. So, $u \in W^{\alpha,p}_{\Delta,a^+}$ with ${}^{\mathbb{T}}u^{\alpha}_{a^+} = g = {}^{\mathbb{T}}_{a}D^{\alpha}_{t}u \in L^p_\Delta$.

On the other hand, if $u \in W^{\alpha,p}_{\Delta,a^+}$, then $u \in L^p_\Delta$ and there exists a function $g \in L^p_\Delta$ such that

$$\int_{J^0} u(t){}^{\mathbb{T}}_{t}D^{\alpha}_{b}\varphi(t)\Delta t = \int_{J^0} g(t)\varphi(t)\Delta t \tag{9}$$

for any $\varphi \in C^\infty_{c,rd}$. To show that $u \in AC^{\alpha,p}_{\Delta,a^+} \cap L^p_\Delta$, it suffices to check (Theorem 20 and definition of $AC^{\alpha,p}_{\Delta,a^+}$) that u possesses the left Riemann–Liouville derivative of order α, which belongs to L^p_Δ; that is, ${}^{\mathbb{T}}_{a}I^{1-\alpha}_{t}u$ is absolutely continuous on J and its delta derivative of α order (existing $\Delta - a.e.$ on J) belongs to L^p_Δ.

In fact, let $\varphi \in C^{\infty}_{c,rd}$, then $\varphi \in {}^{\mathbb{T}}_{t}D^{\alpha}_{b}(C_{rd})$ and ${}^{\mathbb{T}}_{t}D^{\alpha}_{b}\varphi = -({}^{\mathbb{T}}_{t}I^{1-\alpha}_{b})^{\Delta}$. From Theorem 19, it follows that

$$\begin{aligned}\int_{J^0} u(t)\,{}^{\mathbb{T}}_{t}D^{\alpha}_{b}\varphi(t)\Delta t &= \int_{J^0} u(t)(-{}^{\mathbb{T}}_{t}I^{1-\alpha}_{b}\varphi)^{\Delta}(t)\Delta t\\ &= \int_{J^0} ({}^{\mathbb{T}}_{a}D^{1-\alpha}_{t}\,{}^{\mathbb{T}}_{a}I^{1-\alpha}_{t}u)(t)(-{}^{\mathbb{T}}_{t}I^{1-\alpha}_{b}\varphi)^{\Delta}(t)\Delta t\\ &= \int_{J^0} ({}^{\mathbb{T}}_{a}I^{1-\alpha}_{t}u)(t)(-\varphi)^{\Delta}(t)\Delta t\\ &= -\int_{J^0} ({}^{\mathbb{T}}_{a}I^{1-\alpha}_{t}u)(t)\varphi^{\Delta}(t)\Delta t. \end{aligned} \tag{10}$$

In view of (9) and (10), we obtain

$$\int_{J^0} ({}^{\mathbb{T}}_{a}I^{1-\alpha}_{t}u)(t)\varphi^{\Delta}(t)\Delta t = -\int_{J^0} g(t)\varphi(t)\Delta t$$

for any $\varphi \in C^{\infty}_{c,rd}$. So, ${}^{\mathbb{T}}_{a}I^{1-\alpha}_{t}u \in W^{1,p}_{\Delta,a^+}$. Consequently, ${}^{\mathbb{T}}_{a}I^{1-\alpha}_{t}u$ is absolutely continuous and its delta derivative is equal $\Delta - a.e.$ on $[a,b]_{\mathbb{T}}$ to $g \in L^{p}_{\Delta}$. The proof is complete. □

From the proof of Theorem 21 and the uniqueness of the weak fractional derivative, the following theorem follows.

Theorem 22. *If $0 < \alpha \leq 1$ and $1 \leq p < \infty$, then the weak left fractional derivative ${}^{\mathbb{T}}u^{\alpha}_{a^+}$ of a function $u \in W^{\alpha,p}_{\Delta,a^+}$ coincides with its left Riemann–Liouville fractional derivative ${}^{\mathbb{T}}_{a}D^{\alpha}_{t}u$ $\Delta - a.e.$ on J.*

Remark 4. (1) *If $0 < \alpha \leq 1$ and $(1-\alpha)p < 1$, then $AC^{\alpha,p}_{\Delta,a^+} \subset L^{p}_{\Delta}$ and, consequently,*

$$W^{\alpha,p}_{\Delta,a^+} = AC^{\alpha,p}_{\Delta,a^+} \cap L^{p}_{\Delta} = AC^{\alpha,p}_{\Delta,a^+}.$$

(2) *If $0 < \alpha \leq 1$ and $(1-\alpha)p \geq 1$, then $W^{\alpha,p}_{\Delta,a^+} = AC^{\alpha,p}_{\Delta,a^+} \cap L^{p}_{\Delta}$ is the set of all functions belong to $AC^{\alpha,p}_{\Delta,a^+}$ that satisfy the condition $({}^{\mathbb{T}}_{a}I^{1-\alpha}_{t}f)(a) = 0$.*

By using the definition of $W^{\alpha,p}_{\Delta,a^+}$ with $0 < \alpha \leq 1$ and Theorem 22, one can easily prove the following result.

Theorem 23. *Let $0 < \alpha \leq 1, 1 \leq p < \infty$ and $u \in L^{p}_{\Delta}$. Then $u \in W^{\alpha,p}_{\Delta,a^+}$ iff there exists a function $g \in L^{p}_{\Delta}$ such that*

$$\int_{J^0} u(t)\,{}^{\mathbb{T}}_{t}D^{\alpha}_{b}\varphi(t)\Delta t = \int_{J^0} g(t)\varphi(t)\Delta t, \quad \varphi \in C^{\infty}_{c,rd}.$$

In such a case, there exists the left Riemann–Liouville derivative ${}^{\mathbb{T}}_{a}D^{\alpha}_{t}u$ of u and $g = {}^{\mathbb{T}}_{a}D^{\alpha}_{t}u$.

Remark 5. *Function g will be called the weak left fractional derivative of $u \in W^{\alpha,p}_{\Delta,a^+}$ of order α. Its uniqueness follows from [4]. From the above theorem it follows that it coincides with an appropriate Riemann–Liouville derivative.*

Let us fix $0 < \alpha \leq 1$ and consider in the space $W^{\alpha,p}_{\Delta,a^+}$ a norm $\|\cdot\|_{W^{\alpha,p}_{\Delta,a^+}}$ given by

$$\|u\|^{p}_{W^{\alpha,p}_{\Delta,a^+}} = \|u\|^{p}_{L^{p}_{\Delta}} + \|{}^{\mathbb{T}}_{a}D^{\alpha}_{t}u\|^{p}_{L^{p}_{\Delta}}, \quad u \in W^{\alpha,p}_{\Delta,a^+}.$$

(Here $\|\cdot\|^p_{L_\Delta}$ denotes the delta norm in L^p_Δ (Theorem 12)).

Lemma 4. *Let $0 < \alpha \le 1$ and $1 \le p < \infty$. For any $f \in L^p_\Delta(J, \mathbb{R}^N)$, we have*

$$\|{}^{\mathbb{T}}_a I^\alpha_\xi f\|_{L^p_\Delta([a,t]_{\mathbb{T}})} \le \frac{(t-a)^\alpha}{\Gamma(\alpha+1)}\|f\|_{L^p_\Delta([a,t]_{\mathbb{T}})}, \quad \text{for } \xi \in [a,t]_{\mathbb{T}},\ t \in J. \tag{11}$$

That is to say, the fractional integration operator is bounded in L^p_Δ.

Proof. Inspired by Theorem 13 and the proof of Lemma 3.1 of [40], we can prove (11).

In fact, if $p = 1$, in light of Definition 7, Theorem 2, Fubini's theorem on time scales, and Proposition 1, we have

$$\begin{aligned}
&\|{}^{\mathbb{T}}_a I^\alpha_\xi f\|_{L^1_\Delta([a,t]_{\mathbb{T}})} \\
&= \int_a^t |{}^{\mathbb{T}}_a I^\alpha_\xi f|\Delta\xi \\
&= \frac{1}{\Gamma(\alpha)}\int_a^t \left|\int_a^\xi (\xi - \sigma(\tau))^{\alpha-1} f(\tau)\right|\Delta\tau\Delta\xi \\
&\le \frac{1}{\Gamma(\alpha)}\int_a^t \int_a^\xi (\xi - \sigma(\tau))^{\alpha-1}|f(\tau)|\Delta\tau\Delta\xi \\
&= \frac{1}{\Gamma(\alpha)}\int_a^t |f(\tau)|\Delta\tau \int_\tau^t (\xi - \sigma(\tau))^{\alpha-1}\Delta\xi \\
&\le \frac{1}{\Gamma(\alpha)}\int_a^t |f(\tau)|\Delta\tau \int_\tau^t (\xi - \tau)^{\alpha-1} d\xi \\
&= \frac{1}{\Gamma(\alpha)}\int_a^t |f(\tau)|(t-\tau)^\alpha\Delta\tau \\
&\le \frac{(t-a)^\alpha}{\Gamma(\alpha+1)}\|f\|_{L^1_\Delta([a,t]_{\mathbb{T}})}, \quad \text{for } t \in J.
\end{aligned} \tag{12}$$

Now, suppose that $1 < p < \infty$ and $g \in L^q_\Delta(J, \mathbb{R}^N)$, where $\frac{1}{p} + \frac{1}{q} = 1$. In consideration of Theorems 2 and 3, Fubini's theorem on time scales, and Propositions 1 and 2, one arrives at

$$\begin{aligned}
&\left|\int_a^t g(\xi)\int_a^\xi (\xi - \sigma(\tau))^{\alpha-1} f(\tau)\Delta\tau\Delta\xi\right| \\
&= \left|\int_a^t g(\xi)\int_a^\xi \tau^{\alpha-1} f(\xi - \sigma(\tau))\Delta\tau\Delta\xi\right| \\
&\le \int_a^t |g(\xi)|\int_a^\xi \tau^{\alpha-1}|f(\xi - \sigma(\tau))|\Delta\tau\Delta\xi \\
&\le \int_a^t \tau^{\alpha-1}\Delta\tau\int_\tau^t |g(\xi)||f(\xi - \sigma(\tau))|\Delta\xi \\
&\le \int_a^t \tau^{\alpha-1}\Delta\tau\left(\int_\tau^t |g(\xi)|^q\Delta\xi\right)^{\frac{1}{q}}\left(\int_\tau^t |f(\xi - \sigma(\tau))|^p\Delta\xi\right)^{\frac{1}{p}} \\
&\le \int_a^t \tau^{\alpha-1}d\tau\|g\|_{L^q_\Delta([a,t]_{\mathbb{T}})}\|f\|_{L^p_\Delta([a,t]_{\mathbb{T}})} \\
&= \frac{(t-a)^\alpha}{\alpha}\|f\|_{L^p_\Delta([a,t]_{\mathbb{T}})}\|g\|_{L^q_\Delta([a,t]_{\mathbb{T}})}, \quad \text{for } t \in J.
\end{aligned} \tag{13}$$

For any fixed $t \in J$, consider the functional $H_{\xi * f} : L^q_\Delta(J, \mathbb{R}^N) \to \mathbb{R}$

$$H_{\xi*f}(g) = \int_a^t \left[\int_a^\xi (\xi - \sigma(\tau))^{\alpha-1} f(\tau) \Delta\tau \right] g(\xi) \Delta\xi \tag{14}$$

According to (13), it is obvious that $H_{\xi*f} \in \left(L^q_\Delta(J, \mathbb{R}^N) \right)^*$, where $\left(L^q_\Delta(J, \mathbb{R}^N) \right)^*$ denotes the dual space of $L^q_\Delta(J, \mathbb{R}^N)$. Therefore, by (13) and (14) and the Riesz representation theorem, there exists $h \in L^p_\Delta(J, \mathbb{R}^N)$ such that

$$\int_a^t h(\xi) g(\xi) \Delta\xi = \int_a^t \left[\int_a^\xi (\xi - \sigma(\tau))^{\alpha-1} f(\tau) \Delta\tau \right] g(\xi) \Delta\xi \tag{15}$$

and

$$\|h\|_{L^p_\Delta([a,t]_\mathbb{T})} = \|H_{\xi*f}\|_{L^p_\Delta([a,t]_\mathbb{T})} \leq \frac{(t-a)^\alpha}{\alpha} \|f\|_{L^p_\Delta([a,t]_\mathbb{T})} \tag{16}$$

for all $g \in L^q_\Delta(J, \mathbb{R}^N)$. Hence, we have by (15) and Definition 7

$$\frac{1}{\Gamma(\alpha)} h(\xi) = \frac{1}{\Gamma(\alpha)} \int_a^\xi (\xi - \sigma(\tau))^{\alpha-1} f(\tau) \Delta\tau = {}^{\mathbb{T}}_{a} I^\alpha_\xi f(\xi), \quad \text{for } \xi \in [a,t]_\mathbb{T},$$

which means that

$$\|{}^{\mathbb{T}}_{a} I^\alpha_\xi f\|_{L^p_\Delta([a,t]_\mathbb{T})} = \frac{1}{\Gamma(\alpha)} \|h\|_{L^p_\Delta([a,t]_\mathbb{T})} \leq \frac{(t-a)^\alpha}{\Gamma(\alpha+1)} \|f\|_{L^p_\Delta([a,t]_\mathbb{T})} \tag{17}$$

according to (16). Combining this with (12) and (17), we obtain inequality (11). The proof is complete. □

Theorem 24. *If* $0 < \alpha \leq 1$, *then the norm* $\|\cdot\|_{W^{\alpha,p}_{\Delta,a^+}}$ *is equivalent to the norm* $\|\cdot\|_{a,W^{\alpha,p}_{\Delta,a^+}}$ *given by*

$$\|u\|^p_{a,W^{\alpha,p}_{\Delta,a^+}} = |{}^{\mathbb{T}}_{a} I^{1-\alpha}_t u(a)|^p + \|{}^{\mathbb{T}}_{a} D^\alpha_t u\|^p_{L^p_\Delta}, \quad u \in W^{\alpha,p}_{\Delta,a^+}.$$

Proof. (1) Assume that $(1-\alpha)p < 1$. On the one hand, in view of Remarks 2 and 4, for $u \in W^{\alpha,p}_{\Delta,a^+}$, we can write it as

$$u(t) = \frac{1}{\Gamma(\alpha)} \frac{c}{(t-a)^{1-\alpha}} + {}^{\mathbb{T}}_{a} I^\alpha_t \varphi(t)$$

with $c \in \mathbb{R}^N$ and $\varphi \in L^p_\Delta$. Since $(t-a)^{(\alpha-1)p}$ is an increasing monotone function, by using Proposition 1, we can write that $\int_{J^0} (t-a)^{(\alpha-1)p} \Delta t \leq \int_{J^0_\mathbb{R}} (t-a)^{(\alpha-1)p} dt$. Furthermore, taking into account Lemma 4, we have

$$\begin{aligned}
\|u\|^p_{L^p_\Delta} &= \int_{J^0} \left| \frac{1}{\Gamma(\alpha)} \frac{c}{(t-a)^{1-\alpha}} + {}^{\mathbb{T}}_{a} I^\alpha_t \varphi(t) \right|^p \Delta t \\
&\leq 2^{p-1} \left(\frac{|c|^p}{\Gamma^p(\alpha)} \int_{J^0} (t-a)^{(\alpha-1)p} \Delta t + \|{}^{\mathbb{T}}_{a} I^\alpha_t \varphi\|^p_{L^p_\Delta} \right) \\
&\leq 2^{p-1} \left(\frac{|c|^p}{\Gamma^p(\alpha)} \int_{J^0_\mathbb{R}} (t-a)^{(\alpha-1)p} dt + \|{}^{\mathbb{T}}_{a} I^\alpha_t \varphi\|^p_{L^p_\Delta} \right) \\
&\leq 2^{p-1} \left(\frac{|c|^p}{\Gamma^p(\alpha)} 1(\alpha-1)p + 1(b-a)^{(\alpha-1)p+1} + K^p \|\varphi\|^p_{L^p_\Delta} \right),
\end{aligned}$$

where $K = \frac{(b-a)^\alpha}{\Gamma(\alpha+1)}$. Noting that $c = {}_a^{\mathbb{T}}I_t^{1-\alpha}u(a)$, $\varphi = {}_a^{\mathbb{T}}D_t^\alpha u$, one can obtain

$$\begin{aligned}\|u\|_{L_\Delta^p}^p \leq & L_{\alpha,0}(|c|^p + \|\varphi\|_{L_\Delta^p}^p)\\ \leq & L_{\alpha,0}\left(|{}_a^{\mathbb{T}}I_t^{1-\alpha}u(a)|^p + \|{}_a^{\mathbb{T}}D_t^\alpha u\|_{L_\Delta^p}^p\right)\\ = & L_{\alpha,0}\|u\|_{a,W_{\Delta,a^+}^{\alpha,p}}^p,\end{aligned}$$

where

$$L_{\alpha,0} = 2^{p-1}\left(\frac{(b-a)^{1-(1-\alpha)p}}{\Gamma^p(\alpha)(1-(1-\alpha)p)} + K^p\right).$$

Consequently,

$$\begin{aligned}\|u\|_{W_{\Delta,a^+}^{\alpha,p}}^p = & \|u\|_{L_\Delta^p}^P + \|{}_a^{\mathbb{T}}D_t^\alpha u\|_{L_\Delta^p}^p\\ \leq & L_{\alpha,1}\|u\|_{a,W_{\Delta,a^+}^{\alpha,p}}^p,\end{aligned}$$

where $L_{\alpha,1} = L_{\alpha,0} + 1$.

On the other hand, we will prove that there exists a constant $M_{\alpha,1}$ such that

$$\|u\|_{a,W_{\Delta,a^+}^{\alpha,p}}^p \leq M_{\alpha,1}\|u\|_{W_{\Delta,a^+}^{\alpha,p}}^p, \quad u \in W_{\Delta,a^+}^{\alpha,p}. \tag{18}$$

Indeed, let $u \in W_{\Delta,a^+}^{\alpha,p}$ and consider coordinate functions $({}_a^{\mathbb{T}}I_t^{1-\alpha}u)^i$ of ${}_a^{\mathbb{T}}I_t^{1-\alpha}u$ with $i \in \{1,\ldots,N\}$. Lemma 4, Theorem 14 and Corollary 1 imply that there exist constants

$$\Lambda_i \in \left[\inf_{t\in[a,b)_{\mathbb{T}}}({}_a^{\mathbb{T}}I_t^{1-\alpha}u)^i(t), \sup_{t\in[a,b)_{\mathbb{T}}}({}_a^{\mathbb{T}}I_t^{1-\alpha}u)^i(t)\right], \quad (i = 1,2,\ldots,N)$$

such that

$$\Lambda_i = \frac{1}{b-a}\int_a^b ({}_a^{\mathbb{T}}I_t^{1-\alpha}u)^i(s)\Delta s.$$

Hence, for a fixed $t_0 \in J^0$, if $({}_a^{\mathbb{T}}I_t^{1-\alpha}u)^i(t_0) \neq 0$ for all $i = 1,2,\ldots,N$, then we can take constants θ_i such that

$$\theta_i({}_a^{\mathbb{T}}I_t^{1-\alpha}u)^i(t_0) = \Lambda_i = \frac{1}{b-a}\int_a^b ({}_a^{\mathbb{T}}I_t^{1-\alpha}u)^i(s)\Delta s.$$

Therefore, we have

$$({}_a^{\mathbb{T}}I_t^{1-\alpha}u)^i(t_0) = \frac{\theta_i}{b-a}\int_a^b ({}_a^{\mathbb{T}}I_t^{1-\alpha}u)^i(s)\Delta s.$$

From the absolute continuity (Theorem 9) of $({}_a^{\mathbb{T}}I_t^{1-\alpha}u)^i$ it follows that

$$({}_a^{\mathbb{T}}I_t^{1-\alpha}u)^i(t) = ({}_a^{\mathbb{T}}I_t^{1-\alpha}u)^i(t_0) + \int_{[t_0,t)_{\mathbb{T}}}\left[({}_a^{\mathbb{T}}I_t^{1-\alpha}u)^i(s)\right]^\Delta \Delta s$$

for any $t \in J$. Consequently, combining with Proposition 3 and Lemma 4, we see that

$$
\begin{aligned}
|({}_a^{\mathbb{T}}I_t^{1-\alpha}u)^i(t)| =& \left|({}_a^{\mathbb{T}}I_t^{1-\alpha}u)^i(t_0) + \int_{[t_0,t)_{\mathbb{T}}} \left[({}_a^{\mathbb{T}}I_t^{1-\alpha}u)^i(s)\right]^{\Delta}\Delta s\right| \\
\leq& \frac{|\theta_i|}{b-a}\|{}_a^{\mathbb{T}}I_t^{1-\alpha}u\|_{L^1_\Delta} + \int_{[t_0,t)_{\mathbb{T}}} |({}_a^{\mathbb{T}}D_t^{\alpha}u)(s)|\Delta s \\
\leq& \frac{|\theta_i|}{b-a}\|{}_a^{\mathbb{T}}I_t^{1-\alpha}u\|_{L^1_\Delta} + \|{}_a^{\mathbb{T}}D_t^{\alpha}u\|_{L^1_\Delta} \\
\leq& \frac{|\theta_i|}{b-a}\frac{(b-a)^{1-\alpha}}{\Gamma(2-\alpha)}\|u\|_{L^1_\Delta} + \|{}_a^{\mathbb{T}}D_t^{\alpha}u\|_{L^1_\Delta}
\end{aligned}
$$

for $t \in J$. In particular,

$$
|({}_a^{\mathbb{T}}I_t^{1-\alpha}u)^i(a)| \leq \frac{|\theta_i|}{b-a}\frac{(b-a)^{1-\alpha}}{\Gamma(2-\alpha)}\|u\|_{L^1_\Delta} + \|{}_a^{\mathbb{T}}D_t^{\alpha}u\|_{L^1_\Delta}.
$$

So,

$$
\begin{aligned}
|({}_a^{\mathbb{T}}I_t^{1-\alpha}u)(a)| \leq& N\left(\frac{|\theta|(b-a)^{-\alpha}}{\Gamma(2-\alpha)} + 1\right)\left(\|u\|_{L^1_\Delta} + \|{}_a^{\mathbb{T}}D_t^{\alpha}u\|_{L^1_\Delta}\right) \\
\leq& NM_{\alpha,0}(b-a)^{\frac{p-1}{p}}\left(\|u\|_{L^p_\Delta} + \|{}_a^{\mathbb{T}}D_t^{\alpha}u\|_{L^p_\Delta}\right),
\end{aligned}
$$

where $|\theta| = \max_{i\in\{1,2,\ldots,N\}}|\theta_i|$ and $M_{\alpha,0} = \frac{|\theta|(b-a)^{-\alpha}}{\Gamma(2-\alpha)} + 1$. Thus,

$$
|({}_a^{\mathbb{T}}I_t^{1-\alpha}u)(a)|^p \leq N^pM_{\alpha,0}^p(b-a)^{p-1}2^{p-1}\left(\|u\|^p_{L^p_\Delta} + \|{}_a^{\mathbb{T}}D_t^{\alpha}u\|^p_{L^p_\Delta}\right),
$$

and, consequently,

$$
\begin{aligned}
\|u\|^p_{a,W^{\alpha,p}_{\Delta,a^+}} =& |{}_a^{\mathbb{T}}I_t^{1-\alpha}u(a)|^p + \|{}_a^{\mathbb{T}}D_t^{\alpha}u\|^p_{L^p_\Delta} \\
\leq& \left(N^pM_{\alpha,0}^p(b-a)^{p-1}2^{p-1} + 1\right)\left(\|u\|^p_{L^p_\Delta} + \|{}_a^{\mathbb{T}}D_t^{\alpha}u\|^p_{L^p_\Delta}\right) \\
=& M_{\alpha,1}\|u\|^p_{W^{\alpha,p}_{\Delta,a^+}},
\end{aligned}
$$

where $M_{\alpha,1} = N^pM_{\alpha,0}^p(b-a)^{p-1}2^{p-1} + 1$.

If $({}_a^{\mathbb{T}}I_t^{1-\alpha}u)^i(t_0) = 0$ for i belongs to some subset of $\{1,2,\ldots,N\}$, from the above argument process one can easily see that there exists a constant $M_{\alpha,1}$ such that (18) holds.

(2) When $(1-\alpha)p \geq 1$, then (Remark 4) $W^{\alpha,p}_{\Delta,a^+} = AC^{\alpha,p}_{\Delta,a^+} \cap L^p_\Delta$ is the set of all functions belonging to $AC^{\alpha,p}_{\Delta,a^+}$ that satisfy the condition $({}_a^{\mathbb{T}}I_t^{1-\alpha}u)(a) = 0$. Hence, in the same way as in the case of $(1-\alpha)p < 1$ (putting $c = 0$), we obtain the inequality

$$
\|u\|^p_{W^{\alpha,p}_{\Delta,a^+}} \leq L_{\alpha,1}\|u\|^p_{a,W^{\alpha,p}_{\Delta,a^+}}, \quad \text{with some } L_{\alpha,1} > 0.
$$

The inequality

$$
\|u\|^p_{a,W^{\alpha,p}_{\Delta,a^+}} \leq M_{\alpha,1}\|u\|^p_{W^{\alpha,p}_{\Delta,a^+}}, \quad \text{with some } M_{\alpha,1} > 0
$$

is obvious (it is sufficient to put $M_{\alpha,1} = 1$ and use the fact that $({}_a^{\mathbb{T}}I_t^{1-\alpha}u)(a) = 0$).

The proof is complete. □

Now, we are in a position to prove some basic properties of the space $W^{\alpha,p}_{\Delta,a^+}$.

Theorem 25. *The space $W^{\alpha,p}_{\Delta,a^+}$ is complete with respect to each of the norms $\|\cdot\|_{W^{\alpha,p}_{\Delta,a^+}}$ and $\|\cdot\|_{a,W^{\alpha,p}_{\Delta,a^+}}$ for any $0<\alpha\leq 1$, $1\leq p<\infty$.*

Proof. In view of Theorem 24, we only need to show that $W^{\alpha,p}_{\Delta,a^+}$ with the norm $\|\cdot\|_{a,W^{\alpha,p}_{\Delta,a^+}}$ is complete. Let $\{u_k\}\subset W^{\alpha,p}_{\Delta,a^+}$ be a Cauchy sequence with respect to this norm. The sequences $\{{}^{\mathbb{T}}_{a}I^{1-\alpha}_{t}u_k(a)\}$ and $\{{}^{\mathbb{T}}_{a}D^{\alpha}_{t}u_k\}$ are Cauchy sequences in $\mathbb{R}^N$ and L^p_Δ, respectively.

Let $c\in\mathbb{R}^N$ and $\varphi\in L^p_\Delta$ be the limits of the above two sequences in $\mathbb{R}^N$ and L^p_Δ, respectively. Then the function

$$u(t)=\frac{c}{\Gamma(\alpha)}(t-a)^{\alpha-1}+{}^{\mathbb{T}}_{a}I^{\alpha}_{t}\varphi(t),\quad t\in J\quad \Delta-a.e.$$

belongs to $W^{\alpha,p}_{\Delta,a^+}$ and it is the limit of $\{u_k\}$ in $W^{\alpha,p}_{\Delta,a^+}$ with respect to $\|\cdot\|_{a,W^{\alpha,p}_{\Delta,a^+}}$. The proof is complete. □

The proof method of the following two theorems is inspired by the method used in the proof of Proposition 8.1 $(b),(c)$ in [41].

Theorem 26. *The space $W^{\alpha,p}_{\Delta,a^+}$ is reflexive with respect to the norm $\|\cdot\|_{W^{\alpha,p}_{\Delta,a^+}}$ for any $0<\alpha\leq 1$ and $1<p<\infty$.*

Proof. Let us consider $W^{\alpha,p}_{\Delta,a^+}$ with the norm $\|\cdot\|_{W^{\alpha,p}_{\Delta,a^+}}$ and define a mapping

$$\lambda: W^{\alpha,p}_{\Delta,a^+}\ni u\mapsto \left(u,\,{}^{\mathbb{T}}_{a}D^{\alpha}_{t}u\right)\in L^p_\Delta\times L^p_\Delta.$$

It is obvious that

$$\|u\|_{W^{\alpha,p}_{\Delta,a^+}}=\|\lambda u\|_{L^p_\Delta\times L^p_\Delta},$$

where

$$\|\lambda u\|_{L^p_\Delta\times L^p_\Delta}=\left(\sum_{i=1}^{2}\|(\lambda u)_i\|^p_{L^p_\Delta}\right)^{\frac{1}{p}},\quad \lambda u=\left(u,\,{}^{\mathbb{T}}_{a}D^{\alpha}_{t}u\right)\in L^p_\Delta\times L^p_\Delta,$$

which means that the operator $\lambda: u\mapsto\left(u,\,{}^{\mathbb{T}}_{a}D^{\alpha}_{t}u\right)$ is a isometric isomorphic mapping and the space $W^{\alpha,p}_{\Delta,a^+}$ is isometric isomorphic to the space $\Omega=\left\{\left(u,\,{}^{\mathbb{T}}_{a}D^{\alpha}_{t}u\right):\forall u\in W^{\alpha,p}_{\Delta,a^+}\right\}$, which is a closed subset of $L^p_\Delta\times L^p_\Delta$ as $W^{\alpha,p}_{\Delta,a^+}$ is closed.

Since L^p_Δ is reflexive, the Cartesian product space $L^p_\Delta\times L^p_\Delta$ is also a reflexive space with respect to the norm $\|v\|_{L^p_\Delta\times L^p_\Delta}=\left(\sum\limits_{i=1}^{2}\|v_i\|^p_{L^p_\Delta}\right)^{\frac{1}{p}}$, where $v=(v_1,v_2)\in L^p_\Delta\times L^p_\Delta$.

Thus, $W^{\alpha,p}_{\Delta,a^+}$ is reflexive with respect to the norm $\|\cdot\|_{W^{\alpha,p}_{\Delta,a^+}}$. The proof is complete. □

Theorem 27. *The space $W^{\alpha,p}_{\Delta,a^+}$ is separable with respect to the norm $\|\cdot\|_{W^{\alpha,p}_{\Delta,a^+}}$ for any $0<\alpha\leq 1$ and $1\leq p<\infty$.*

Proof. Let us consider $W^{\alpha,p}_{\Delta,a^+}$ with the norm $\|\cdot\|_{W^{\alpha,p}_{\Delta,a^+}}$ and the mapping λ defined in the proof of Theorem 26. Obviously, $\lambda(W^{\alpha,p}_{\Delta,a^+})$ is separable as a subset of separable space $L^p_\Delta\times L^p_\Delta$. Since λ is the isometry, $W^{\alpha,p}_{\Delta,a^+}$ is also separable with respect to the norm $\|\cdot\|_{W^{\alpha,p}_{\Delta,a^+}}$. The proof is complete. □

Proposition 6. *Let $0 < \alpha \leq 1$ and $1 < p < \infty$. For all $u \in W^{\alpha,p}_{\Delta,a^+}$, if $1-\alpha \geq \frac{1}{p}$ or $\alpha > \frac{1}{p}$, then*

$$\|u\|_{L^p_\Delta} \leq \frac{b^\alpha}{\Gamma(\alpha+1)} \left\| {}^{\mathbb{T}}_{a}D^{\alpha}_{t} u \right\|_{L^p_\Delta}; \tag{19}$$

if $\alpha > \frac{1}{p}$ and $\frac{1}{p} + \frac{1}{q} = 1$, then

$$\|u\|_\infty \leq \frac{b^{\alpha-\frac{1}{p}}}{\Gamma(\alpha)((\alpha-1)q+1)^{\frac{1}{q}}} \left\| {}^{\mathbb{T}}_{a}D^{\alpha}_{t} u \right\|_{L^p_\Delta}. \tag{20}$$

Proof. In view of Remark 4 and Theorem 18, in order to prove inequalities (19) and (20), we only need to prove that

$$\left\| {}^{\mathbb{T}}_{a}I^{\alpha}_{t}({}^{\mathbb{T}}_{a}D^{\alpha}_{t} u) \right\|_{L^p_\Delta} \leq \frac{b^\alpha}{\Gamma(\alpha+1)} \left\| {}^{\mathbb{T}}_{a}D^{\alpha}_{t} u \right\|_{L^p_\Delta} \tag{21}$$

for $1-\alpha \geq \frac{1}{p}$ or $\alpha > \frac{1}{p}$, and that

$$\left\| {}^{\mathbb{T}}_{a}I^{\alpha}_{t}({}^{\mathbb{T}}_{a}D^{\alpha}_{t} u) \right\|_{\infty} \leq \frac{b^{\alpha-\frac{1}{p}}}{\Gamma(\alpha)((\alpha-1)q+1)^{\frac{1}{q}}} \left\| {}^{\mathbb{T}}_{a}D^{\alpha}_{t} u \right\|_{L^p_\Delta} \tag{22}$$

for $\alpha > \frac{1}{p}$ and $\frac{1}{p} + \frac{1}{q} = 1$.

Note that ${}^{\mathbb{T}}_{a}D^{\alpha}_{t} u \in L^p_\Delta(J, \mathbb{R}^N)$, and the inequality (21) follows directly from Lemma 4.

We are now in a position to prove (22). For $\alpha > \frac{1}{p}$, choose q such that $\frac{1}{p} + \frac{1}{q} = 1$. For all $u \in W^{\alpha,p}_{\Delta,a^+}$, since $(t-s)^{(\alpha-1)q}$ is an increasing monotone function, by using Proposition 1, we find that $\int_a^t (t-\sigma(s))^{(\alpha-1)q}\Delta s \leq \int_a^t (t-s)^{(\alpha-1)q} ds$. Taking into account of Proposition 2, we have

$$\begin{aligned}
\left| {}^{\mathbb{T}}_{a}I^{\alpha}_{t}({}^{\mathbb{T}}_{a}D^{\alpha}_{t} u(t)) \right| =& \frac{1}{\Gamma(\alpha)} \left| \int_a^t (t-\sigma(s))^{\alpha-1} {}^{\mathbb{T}}_{a}D^{\alpha}_{t} u(s)\Delta s \right| \\
\leq& \frac{1}{\Gamma(\alpha)} \left(\int_a^t (t-\sigma(s))^{(\alpha-1)q}\Delta s \right)^{\frac{1}{q}} \| {}^{\mathbb{T}}_{a}D^{\alpha}_{t} u \|_{L^p_\Delta} \\
\leq& \frac{1}{\Gamma(\alpha)} \left(\int_a^t (t-s)^{(\alpha-1)q} ds \right)^{\frac{1}{q}} \| {}^{\mathbb{T}}_{a}D^{\alpha}_{t} u \|_{L^p_\Delta} \\
\leq& \frac{b^{\frac{1}{q}+\alpha-1}}{\Gamma(\alpha)((\alpha-1)q+1)^{\frac{1}{q}}} \left\| {}^{\mathbb{T}}_{a}D^{\alpha}_{t} u \right\|_{L^p_\Delta} \\
=& \frac{b^{\alpha-\frac{1}{p}}}{\Gamma(\alpha)((\alpha-1)q+1)^{\frac{1}{q}}} \left\| {}^{\mathbb{T}}_{a}D^{\alpha}_{t} u \right\|_{L^p_\Delta}.
\end{aligned}$$

The proof is complete. □

Remark 6. (*i*) *According to* (19)*, we can consider $W^{\alpha,p}_{\Delta,a^+}$ with respect to the norm*

$$\|u\|^p_{W^{\alpha,p}_{\Delta,a^+}} = \| {}^{\mathbb{T}}_{a}D^{\alpha}_{t} u\|^p_{L^p_\Delta} = \left(\int_{J^0} \left| {}^{\mathbb{T}}_{a}D^{\alpha}_{t} u(t) \right|^p \Delta t \right)^{\frac{1}{p}} \tag{23}$$

in the following analysis.

(*ii*) *It follows from* (19) *and* (20) *that $W^{\alpha,p}_{\Delta,a^+}$ is continuously immersed into $C(J, \mathbb{R}^N)$ with the natural norm $\|\cdot\|_\infty$.*

Proposition 7. *Let $0 < \alpha \leq 1$ and $1 < p < \infty$. Assume that $\alpha > \frac{1}{p}$ and the sequence $\{u_k\} \subset W^{\alpha,p}_{\Delta,a^+}$ converges weakly to u in $W^{\alpha,p}_{\Delta,a^+}$. Then, $u_k \to u$ in $C(J,\mathbb{R}^N)$, i.e., $\|u - u_k\|_\infty = 0$, as $k \to \infty$.*

Proof. If $\alpha > \frac{1}{p}$, then by (20) and (30), the injection of $W^{\alpha,p}_{\Delta,a^+}$ into $C(J,\mathbb{R}^N)$, with its natural norm $\|\cdot\|_\infty$, is continuous, i.e., $u_k \to u$ in $W^{\alpha,p}_{\Delta,a^+}$, then $u_k \to u$ in $C(J,\mathbb{R}^N)$.

Since $u_k \rightharpoonup u$ in $W^{\alpha,p}_{\Delta,a^+}$, it follows that $u_k \rightharpoonup u$ in $C(J,\mathbb{R}^N)$. In fact, for any $h \in \left(C(J,\mathbb{R}^N)\right)^*$, if $u_k \to u$ in $W^{\alpha,p}_{\Delta,a^+}$, then $u_k \to u$ in $C(J,\mathbb{R}^N)$, and thus $h(u_k) \to h(u)$. Therefore, $h \in \left(W^{\alpha,p}_{\Delta,a^+}\right)^*$, which means that $\left(C(J,\mathbb{R}^N)\right)^* \subset \left(W^{\alpha,p}_{\Delta,a^+}\right)^*$. Hence, if $u_k \rightharpoonup u$ in $W^{\alpha,p}_{\Delta,a^+}$, then for any $h \in \left(C(J,\mathbb{R}^N)\right)^*$, we have $h \in \left(W^{\alpha,p}_{\Delta,a^+}\right)^*$, and thus $h(u_k) \to h(u)$, i.e., $u_k \rightharpoonup u$ in $C(J,\mathbb{R}^N)$.

By the Banach–Steinhaus theorem, $\{u_k\}$ is bounded in $W^{\alpha,p}_{\Delta,a^+}$ and, hence, in $C(J,\mathbb{R}^N)$. Now, we prove that the sequence $\{u_k\}$ is equicontinuous. Let $\frac{1}{p} + \frac{1}{q} = 1$ and $t_1, t_2 \in J$ with $t_1 \leq t_2$, for all $f \in L^p_\Delta(J,\mathbb{R}^N)$, by using Proposition 2, Proposition 1, and Theorem 15, and noting $\alpha > \frac{1}{p}$, we have

$$
\begin{aligned}
&\left|{}^{\mathbb{T}}_{a}I^{\alpha}_{t_1}f(t_1) - {}^{\mathbb{T}}_{a}I^{\alpha}_{t_2}f(t_2)\right| \\
&= \frac{1}{\Gamma(\alpha)}\left|\int_a^{t_1}(t_1-\sigma(s))^{\alpha-1}f(s)\Delta s - \int_a^{t_2}(t_2-\sigma(s))^{\alpha-1}f(s)\Delta s\right| \\
&\leq \frac{1}{\Gamma(\alpha)}\left|\int_a^{t_1}(t_1-\sigma(s))^{\alpha-1}f(s)\Delta s - \int_a^{t_1}(t_2-\sigma(s))^{\alpha-1}f(s)\Delta s\right| \\
&\quad + \frac{1}{\Gamma(\alpha)}\left|\int_{t_1}^{t_2}(t_2-\sigma(s))^{\alpha-1}f(s)\Delta s\right| \\
&\leq \frac{1}{\Gamma(\alpha)}\int_a^{t_1}\left((t_1-\sigma(s))^{\alpha-1} - (t_2-\sigma(s))^{\alpha-1}\right)|f(s)|\Delta s \\
&\quad + \frac{1}{\Gamma(\alpha)}\int_{t_1}^{t_2}(t_2-\sigma(s))^{\alpha-1}|f(s)|\Delta s \\
&\leq \frac{1}{\Gamma(\alpha)}\left(\int_a^{t_1}\left((t_1-\sigma(s))^{\alpha-1} - (t_2-\sigma(s))^{\alpha-1}\right)^q\Delta s\right)^{\frac{1}{q}}\|f\|_{L^p_\Delta} \\
&\quad + \frac{1}{\Gamma(\alpha)}\left(\int_{t_1}^{t_2}(t_2-\sigma(s))^{(\alpha-1)q}\Delta s\right)^{\frac{1}{q}}\|f\|_{L^p_\Delta} \\
&\leq \frac{1}{\Gamma(\alpha)}\left(\int_a^{t_1}\left((t_1-\sigma(s))^{(\alpha-1)q} - (t_2-\sigma(s))^{(\alpha-1)q}\right)\Delta s\right)^{\frac{1}{q}}\|f\|_{L^p_\Delta} \\
&\quad + \frac{1}{\Gamma(\alpha)}\left(\int_{t_1}^{t_2}(t_2-\sigma(s))^{(\alpha-1)q}\Delta s\right)^{\frac{1}{q}}\|f\|_{L^p_\Delta} \\
&\leq \frac{1}{\Gamma(\alpha)}\left(\int_a^{t_1}\left((t_1-s)^{(\alpha-1)q} - (t_2-s)^{(\alpha-1)q}\right)ds\right)^{\frac{1}{q}}\|f\|_{L^p_\Delta} \\
&\quad + \frac{1}{\Gamma(\alpha)}\left(\int_{t_1}^{t_2}(t_2-s)^{(\alpha-1)q}ds\right)^{\frac{1}{q}}\|f\|_{L^p_\Delta} \\
&= \frac{\|f\|_{L^p_\Delta}}{\Gamma(\alpha)(1+(\alpha-1)q)^{\frac{1}{q}}}\left(t_1^{(\alpha-1)q+1} - t_2^{(\alpha-1)q+1} + (t_2-t_1)^{(\alpha-1)q+1}\right)^{\frac{1}{q}} \\
&\quad + \frac{\|f\|_{L^p_\Delta}}{\Gamma(\alpha)(1+(\alpha-1)q)^{\frac{1}{q}}}\left((t_2-t_1)^{(\alpha-1)q+1}\right)^{\frac{1}{q}} \\
&\leq \frac{2\|f\|_{L^p_\Delta}}{\Gamma(\alpha)(1+(\alpha-1)q)^{\frac{1}{q}}}(t_2-t_1)^{\alpha-1+\frac{1}{q}} \\
&= \frac{2\|f\|_{L^p_\Delta}}{\Gamma(\alpha)(1+(\alpha-1)q)^{\frac{1}{q}}}(t_2-t_1)^{\alpha-\frac{1}{p}}.
\end{aligned}
\tag{24}
$$

Therefore, the sequence $\{u_k\}$ is equicontinuous since, for $t_1, t_2 \in J$, $t_1 \leq t_2$, by applying (24) and (30), we have

$$\begin{aligned}
|u_k(t_1) - u_k(t_2)| =& \left| {}_a^{\mathbb{T}}I_{t_1}^{\alpha}({}_a^{\mathbb{T}}D_{t_1}^{\alpha}u_k(t_1)) - {}_a^{\mathbb{T}}I_{t_2}^{\alpha}({}_a^{\mathbb{T}}D_{t_2}^{\alpha}u_k(t_2)) \right| \\
\leq& \frac{2(t_2-t_1)^{\alpha-\frac{1}{p}}}{\Gamma(\alpha)(1+(\alpha-1)q)^{\frac{1}{q}}} \|{}_a^{\mathbb{T}}D_t^{\alpha}u_k\|_{L_{\Delta}^p} \\
=& \frac{2(t_2-t_1)^{\alpha-\frac{1}{p}}}{\Gamma(\alpha)(1+(\alpha-1)q)^{\frac{1}{q}}} \|{}_a^{\mathbb{T}}D_t^{\alpha}u_k\|_{L_{\Delta}^p} \\
\leq& \frac{2(t_2-t_1)^{\alpha-\frac{1}{p}}}{\Gamma(\alpha)((\alpha-1)q+1)^{\frac{1}{q}}} \left\|{}_a^{\mathbb{T}}D_t^{\alpha}u\right\|_{L_{\Delta}^p} \\
=& \frac{2(t_2-t_1)^{\alpha-\frac{1}{p}}}{\Gamma(\alpha)((\alpha-1)q+1)^{\frac{1}{q}}} \|u_k\|_{W_{\Delta,a^+}^{\alpha,p}} \\
\leq& C(t_2-t_1)^{\alpha-\frac{1}{p}},
\end{aligned}$$

where $\frac{1}{p} + \frac{1}{q} = 1$ and $C \in \mathbb{R}^+$ is a constant. By the Ascoli–Arzela theorem on time scales (Lemma 3), $\{u_k\}$ is relatively compact in $C(J, \mathbb{R}^N)$. By the uniqueness of the weak limit in $C(J, \mathbb{R}^N)$, every uniformly convergent subsequence of $\{u_k\}$ converges uniformly on J to u. The proof is complete. □

Remark 7. *It follows from Proposition 7 that $W_{\Delta,a^+}^{\alpha,p}$ is compactly immersed into $C(J, \mathbb{R}^N)$ with the natural norm $\|\cdot\|_{\infty}$.*

Theorem 28. *Let $1 < p < \infty$, $\frac{1}{p} < \alpha \leq 1$, $\frac{1}{p} + \frac{1}{q} = 1$, $L : J \times \mathbb{R}^N \times \mathbb{R}^N \to \mathbb{R}$, $(t, x, y) \mapsto L(t, x, y)$ satisfies*

(i) for each $(x, y) \in \mathbb{R}^N \times \mathbb{R}^N$, $L(t, x, y)$ is Δ-measurable in t;
(ii) for Δ, almost every $t \in J$, $L(t, x, y)$ is continuously differentiable in (x, y).

If there exist $m_1 \in C(\mathbb{R}^+, \mathbb{R}^+)$, $m_2 \in L_{\Delta}^1(J, \mathbb{R}^+)$ and $m_3 \in L_{\Delta}^q(J, \mathbb{R}^+)$, $1 < q < \infty$, such that, for Δ a.e. $t \in J$ and every $(x, y) \in \mathbb{R}^N \times \mathbb{R}^N$, one has

$$\begin{aligned}
|L(t, x, y)| &\leq m_1(|x|)(m_2(t) + |y|^p), \\
|D_x L(t, x, y)| &\leq m_1(|x|)(m_2(t) + |y|^p), \\
|D_y L(t, x, y)| &\leq m_1(|x|)(m_3(t) + |y|^{p-1}).
\end{aligned}$$

Then the functional χ defined by

$$\chi(u) = \int_{J^0} L(t, u(t), {}_a^{\mathbb{T}}D_t^{\alpha}u(t))\Delta t$$

is continuously differentiable on $W_{\Delta,a^+}^{\alpha,p}$, and $\forall\, u, v \in W_{\Delta,a^+}^{\alpha,p}$, one has

$$\langle \chi'(u), v \rangle = \int_{J^0} \left[\left(D_x L(t, u(t), {}_a^{\mathbb{T}}D_t^{\alpha}u(t), v(t) \right) + \left(D_y L(t, u(t), {}_a^{\mathbb{T}}D_t^{\alpha}u(t), {}_a^{\mathbb{T}}D_t^{\alpha}v(t) \right) \right] \Delta t. \tag{25}$$

Proof. It suffices to prove that χ has, at every point u, a directional derivative $\chi'(u) \in (W_{\Delta,a^+}^{\alpha,p})^*$ given by (25) and that the mapping

$$\chi' : W_{\Delta,a^+}^{\alpha,p} \ni u \mapsto \chi'(u) \in (W_{\Delta,a^+}^{\alpha,p})^*$$

is continuous. The rest of proof is similar to the proof of Theorem 1.4 in [42]. We will omit it here. The proof is complete. □

5. An Application

As an application of the concepts we introduced and the results obtained in Section 3, in this section we will use critical point theory to study the solvability of a class of boundary value problems on time scales. More precisely, our goal is to study the following Kirchhoff-type fractional p-Laplacian system on time scales with boundary condition (KFBVP$_{\mathbb{T}}$ for short):

$$\begin{cases} \left(\beta + \varrho \int_{J^0} |{}_a^{\mathbb{T}}D_t^{\alpha} u(t)|^p \Delta t\right)^{p-1} {}_t^{\mathbb{T}}D_b^{\alpha} \phi_p({}_a^{\mathbb{T}}D_t^{\alpha} u(t)) = \lambda(t) \nabla G(t, u(t)), \quad \Delta - a.e.\ t \in J, \\ u(a) = u(b) = 0, \end{cases} \tag{26}$$

where $\beta, \varrho > 0$ and $p > 1$ are constants, $\lambda \in L_{\Delta}^{\infty}(J, \mathbb{R}^+)$ with $ess \sup_{t \in J} \lambda(t) := \lambda^0 > \lambda_0 := ess \inf_{t \in J} \lambda(t) > 0$, ${}_t^{\mathbb{T}}D_b^{\alpha}$ and ${}_a^{\mathbb{T}}D_t^{\alpha}$ are the right and the left Riemann–Liouville fractional derivative operators of order α defined on $\mathbb{T}$, respectively, and $\phi_p : \mathbb{R} \to \mathbb{R}$ is the p-Laplacian ([43]) defined by

$$\phi_p(y) = \begin{cases} |y|^{p-2} y, & if\ y \neq 0, \\ 0, & if\ y = 0. \end{cases}$$

Furthermore, $\nabla G \in C(J \times \mathbb{R}, \mathbb{R})$ denotes the gradient of $G(t, x)$ in x. When $\mathbb{T} = \mathbb{R}$, FBVP$_{\mathbb{T}}$ (26) reduces to the following Kirchhoff-type fractional p-Laplacian system

$$\begin{cases} \left(\beta + \varrho \int_{J_{\mathbb{R}}} |{}_aD_t^{\alpha} u(t)|^p dt\right)^{p-1} {}_tD_b^{\alpha} \phi_p({}_aD_t^{\alpha} u(t)) = \lambda(t) \nabla G(t, u(t)), \quad a.e.\ t \in J_{\mathbb{R}}, \\ u(a) = u(b) = 0. \end{cases}$$

When $\mathbb{T} = \mathbb{R}$ and $\lambda(t) = \lambda \in (0, +\infty)$, FBVP$_{\mathbb{T}}$ (26) reduces to the following Kirchhoff-type fractional p-Laplacian system

$$\begin{cases} \left(\beta + \varrho \int_{J_{\mathbb{R}}} |{}_aD_t^{\alpha} u(t)|^p dt\right)^{p-1} {}_tD_b^{\alpha} \phi_p({}_aD_t^{\alpha} u(t)) = \lambda \nabla G(t, u(t)), \quad a.e.\ t \in J_{\mathbb{R}}, \\ u(a) = u(b) = 0. \end{cases}$$

When $\mathbb{T} = \mathbb{R}$, $\lambda(t) = 1$, our results further reduce to the following problem

$$\begin{cases} \left(\beta + \varrho \int_{J_{\mathbb{R}}} |{}_aD_t^{\alpha} u(t)|^p dt\right)^{p-1} {}_tD_b^{\alpha} \phi_p({}_aD_t^{\alpha} u(t)) = \nabla G(t, u(t)), \quad a.e.\ t \in J_{\mathbb{R}}, \\ u(a) = u(b) = 0, \end{cases}$$

which has been studied by [44]. So, in short, our results are improved and generalized [44].

Definition 15 ([42]). *Let E be a real Banach space and $\varphi \in C^1(E, \mathbb{R})$. If any sequence $\{u_k\} \subset E$ for which $\varphi(u_k)$ is bounded and $\varphi'(u_k) \to 0$ as $k \to \infty$ possesses a convergent subsequence in E, then we say that φ satisfies the (PS) condition.*

Lemma 5 ([45]). *Let E be a real Banach space and $\varphi \in C^1(E, \mathbb{R})$ satisfying the (PS) condition. Assume that $\varphi(0) = 0$ and the following conditions:*

(A_1) there are constants $\rho, \sigma > 0$ such that $\varphi|_{\partial B_\rho(0)} \geq \sigma$;

(A_2) there exists an $e \in E \setminus \overline{B_\rho(0)}$ such that $\varphi(e) \leq 0$.

Then, φ possesses a critical value $c \geq \sigma$. Furthermore, c can be characterized as

$$c = \inf_{\nu \in \Gamma} \max_{s \in [0,1]} \varphi(\nu(s)),$$

where

$$\Gamma = \{\nu \in C([0,1], E) | \nu(0) = 0, \nu(1) = e\}.$$

Lemma 6 ([42]). *Let E be a real Banach space and $\varphi \in C^1(E, \mathbb{R})$ satisfying the (PS) condition. If φ is bounded from below, then $c = \inf_E \varphi$ is a critical value of φ.*

For the sake of the infinitely many critical points of φ, one introduces the genus properties as follows. First, we let

$$\begin{aligned} \Xi &= \{A \subset E - \{0\} | A \text{ is closed in } E \text{ and symmetric with respect to } 0\}, \\ K_c &= \{u \in E | \varphi(u) = c, \varphi'(u) = 0\}, \\ \varphi^c &= \{u \in E | \varphi(u) \leq c\}. \end{aligned}$$

Definition 16 ([45]). *For $A \in \Xi$, we say that the genus of A is n denoted by $\gamma(A) = n$ if there is an odd map $P \in C(A, \mathbb{R}^N \setminus \{0\})$ and n is the smallest integer with this property.*

Lemma 7 ([45]). *Let φ be an even C^1 functional on E and satisfy the (PS) condition. For any $n \in \mathbb{N}$, set*

$$\begin{aligned} \Xi_n &= \{A \in \Xi | \gamma(A) \geq n\}, \\ c_n &= \inf_{A \in \Xi_n} \sup_{u \in A} \varphi(u). \end{aligned}$$

(i) If $\Xi_n \neq 0$ and $c_n \in \mathbb{R}$, then c_n is a critical value of φ.
(ii) If there exists $l \in \mathbb{N}$ such that $c_n = c_{n+1} = \cdots = c_{n+l} = c \in \mathbb{R}$ and $c \neq \varphi(0)$, then $\gamma(K_c) \geq l + 1$.

Remark 8 ([45]). *In view of Remark 7.3 in [45], one sees that if $K_c \in \Xi$ and $\gamma(K_c)$ contains infinitely many distinct points. In other words, φ has infinitely many distinct critical points in E.*

There have been many results using critical point theory to study boundary value problems of fractional differential equations [46–52] and dynamic equations on time scales [53–57], but results using critical point theory to study boundary value problems of fractional dynamic equations on time scales are still rare [6]. This section will explain that critical point theory is an effective way to deal with the existence of solutions of (26) on time scales.

In this section, we let $N = 1$. For the purpose of the presence and proof of our main results, let us first define the functional $\varphi : W^{\alpha,p}_{\Delta,a^+} \to \mathbb{R}$ by

$$\varphi(u) = \frac{1}{\varrho p^2} \left(\beta + \varrho \int_{J^0} |{}^{\mathbb{T}}_{a} D^{\alpha}_{t} u(t)|^p \Delta t \right)^p - \int_{J^0} \lambda(t) G(t, u(t)) \Delta t - \frac{\beta^p}{\varrho p^2}. \tag{27}$$

It is easy to note from (19), condition (G_1) (will be stated in Theorem 29) and $g \in C(J \times \mathbb{R}, \mathbb{R})$, that the functional φ is well defined on $W^{\alpha,p}_{\Delta,a^+}$ and $\varphi \in C(W^{\alpha,p}_{\Delta,a^+}, \mathbb{R})$. Moreover, for $\forall u, v \in W^{\alpha,p}_{\Delta,a^+}$, one obtains

$$\langle \varphi'(u), v \rangle = (\beta + \varrho \|u\|^p)^{p-1} \int_{J^0} \phi_p({}^{\mathbb{T}}_{a} D^{\alpha}_{t} u(t)) {}^{\mathbb{T}}_{a} D^{\alpha}_{t} v(t) \Delta t - \int_{J^0} \lambda(t) \nabla G(t, u(t)) v(t) \Delta t, \tag{28}$$

which yields

$$\langle \varphi'(u), u\rangle = (\beta + \varrho\|u\|^p)^{p-1}\|u\|^p - \int_{J^0} \lambda(t)\nabla G(t,u(t))u(t)\Delta t. \tag{29}$$

Now, it is time for us to present and prove our main results as follows:

Theorem 29. *Let $\alpha \in \left(\frac{1}{p}, 1\right]$, and suppose that G satisfies the following conditions:*

(G_1) *$G(t,x)$ is $\Delta-$ measurable and continuously differentiable in x for $t \in J$ and there exist $a \in C(\mathbb{R}^+, \mathbb{R}^+)$, $b \in L^1_\Delta(J, \mathbb{R}^+)$ such that*

$$|G(t,x)| \le a(|x|)b(t), \quad |\nabla G(t,x)| \le a(|x|)b(t) \tag{30}$$

for all $x \in \mathbb{R}$ and $t \in J$.

(G_2) *There are two constants $\mu > p^2$, $M > 0$ such that*

$$0 < \mu\, G(t,x) \le x\, \nabla G(t,x), \quad \forall t \in J \text{ and } |x| \ge M.$$

(G_3) *$\nabla G(t,x) = o(|x|^{p-1})$ as $|x| \to 0$ uniformly for $t \in J$.*

Then, KFBVP$_\mathbb{T}$ (26) has at least one nontrivial weak solution.

Proof. It is clear that $\varphi(0) = 0$, $\varphi \in C^1(W^{\alpha,p}_{\Delta,a^+}, \mathbb{R})$, where $W^{\alpha,p}_{\Delta,a^+}$ is a real Banach space from Theorem 25. Therefore, we are now in a position to prove, using Mountain pass theorem (Lemma 5), that

step 1. φ satisfies the (PS) condition in $W^{\alpha,p}_{\Delta,a^+}$. The argument is as follows: Let $\{u_k\} \subset W^{\alpha,p}_{\Delta,a^+}$ be a sequence such that

$$\begin{aligned} |\varphi(u_k)| &\le K, \\ \varphi'(u_k) &\to 0 \quad \text{as } k \to \infty, \end{aligned} \tag{31}$$

where $K > 0$ is a constant. We first prove that $\{u_k\}$ is bounded in $W^{\alpha,p}_{\Delta,a^+}$. From the continuity of $\mu G(t,x) - xg(t,x)$, we obtain that there is a constant $c > 0$ such that

$$G(t,x) \le \frac{1}{\mu} x\nabla G(t,x) + c, \quad \forall t \in J,\ |x| \le M$$

Combining with (G_2), we obtain that

$$G(t,x) \le \frac{1}{\mu} x\nabla G(t,x) + c, \quad \forall (t,x) \in J \times \mathbb{R}. \tag{32}$$

Hence, taking account of (27), (29)–(32), and Lemma 2, we have

$$\begin{aligned} & K \\ \ge\ & \varphi(u_k) \\ =\ & \frac{1}{\varrho p^2}\left(\beta + \varrho \int_{J^0} |{}^{\mathbb{T}}_a D^\alpha_t u_k(t)|^p \Delta t\right)^p - \int_{J^0} \lambda(t) G(t, u_k(t))\Delta t - \frac{\beta^p}{\varrho p^2} \\ =\ & \frac{1}{\varrho p^2}(\beta + \varrho\|u_k\|^p)^p - \int_{J^0} \lambda(t) G(t, u_k(t))\Delta t - \frac{\beta^p}{\varrho p^2} \\ \ge\ & \frac{1}{\varrho p^2}(\beta + \varrho\|u_k\|^p)^p - \int_{J^0} \left[\frac{1}{\mu} u_k(t)\nabla G(t, u_k(t)) + c\right]\Delta t - \frac{\beta^p}{\varrho p^2} \\ =\ & \frac{1}{\varrho p^2}(\beta + \varrho\|u_k\|^p)^p + \frac{1}{\mu}\langle \varphi'(u_k), u_k\rangle - \frac{1}{\mu}(\beta + \varrho\|u_k\|^p)^{p-1} - c(b-a) - \frac{\beta^p}{\varrho p^2} \\ \ge\ & (\beta + \varrho\|u_k\|^p)^{p-1}\left[\left(\frac{1}{p^2} - \frac{1}{\mu}\right)\|u_k\|^p + \frac{\beta}{\varrho p^2}\right] - \frac{1}{\mu}\|\varphi'(u_k)\|_{(W^{\alpha,p}_{\Delta,a^+})^*}\|u_k\| \\ & - cb - \frac{\beta^p}{\varrho p^2}, \end{aligned} \tag{33}$$

which together with $\varphi'(u_k) \to 0$ as $k \to \infty$ yields

$$K \geq (\beta + \varrho\|u_k\|^p)^{p-1}\left[\left(\frac{1}{p^2} - \frac{1}{\mu}\right)\|u_k\|^p + \frac{\beta}{\varrho p^2}\right] - \|u_k\| - cb - \frac{\beta^p}{\varrho p^2}. \tag{34}$$

Then, combining with $\mu > p^2$ and proof by contradiction, we know that $\{u_k\}$ is bounded in $W^{\alpha,p}_{\Delta,a^+}$.

Because $W^{\alpha,p}_{\Delta,a^+}$ is a reflexive Banach space (Theorems 25 and 26), going if necessary to a subsequence, we can assume $u_k \rightharpoonup u$ in $W^{\alpha,p}_{\Delta,a^+}$. As a result, in view of $\varphi'(u_k) \to 0$ as $k \to \infty$ and the definition of weak convergence, one sees

$$\begin{aligned}\langle \varphi'(u_k) - \varphi'(u), u_k - u\rangle =& \langle \varphi'(u_k), u_k - u\rangle - \langle \varphi'(u), u_k - u\rangle\\ \leq& \|\varphi'(u_k)\|_{(W^{\alpha,p}_{\Delta,a^+})^*}\|u_k - u\| - \langle \varphi'(u), u_k - u\rangle\\ \leq& \|\varphi'(u_k)\|_{(W^{\alpha,p}_{\Delta,a^+})^*}(\|u_k\| + \|u\|) - \langle \varphi'(u), u_k - u\rangle\\ \to& 0, \quad \text{as } k \to \infty.\end{aligned} \tag{35}$$

Furthermore, it follows from (20), (30), and Remark 7 that $\{u_k\}$ is bounded in $C(J, \mathbb{R})$ and $\|u_k - u\|_\infty \to 0$, as $k \to \infty$. Therefore, there is a constant $c_1 > 0$ such that

$$|\nabla G(t, u_k(t)) - \nabla G(t, u(t))| \leq c_1, \quad \forall t \in J, \tag{36}$$

which yields

$$\begin{aligned}&\left|\int_{J^0}(\nabla G(t, u_k(t)) - \nabla G(t, u(t)))(u_k(t) - u(t))\Delta t\right|\\ \leq\ & c_1 b\|u_k - u\|_\infty\\ \to\ & 0, \quad \text{as } k \to \infty.\end{aligned} \tag{37}$$

Furthermore, it follows from the boundedness of $\{u_k\}$ in $W^{\alpha,p}_{\Delta,a^+}$ that

$$\begin{aligned}&\left[(\beta + \varrho\|u_k\|^p)^{p-1} - (\beta + \varrho\|u\|^p)^{p-1}\right]\int_{J^0}\phi_p({}^{\mathbb{T}}_a D^\alpha_t u(t))({}^{\mathbb{T}}_a D^\alpha_t u_k(t) - {}^{\mathbb{T}}_a D^\alpha_t u(t))\Delta t\\ =\ & \left[(\beta + \varrho\|u_k\|^p)^{p-1} - (\beta + \varrho\|u\|^p)^{p-1}\right]\left\langle \frac{1}{p}\int_{J^0}|{}^{\mathbb{T}}_a D^\alpha_t u(t)|^p\Delta t, u_k - u\right\rangle\\ \to\ & 0, \quad \text{as } k \to \infty.\end{aligned} \tag{38}$$

In consideration of (28), one obtains

$$\begin{aligned}&\langle \varphi'(u_k) - \varphi'(u), u_k - u\rangle + \int_{J^0}\lambda(t)(\nabla G(t, u_k(t)) - \nabla G(t, u(t)))(u_k(t) - u(t))\Delta t\\ =\ & (\beta + \varrho\|u_k\|^p)^{p-1}\int_{J^0}\phi_p({}^{\mathbb{T}}_a D^\alpha_t u_k(t))({}^{\mathbb{T}}_a D^\alpha_t u_k(t) - {}^{\mathbb{T}}_a D^\alpha_t u(t))\Delta t\\ &-(\beta + \varrho\|u\|^p)^{p-1}\int_{J^0}\phi_p({}^{\mathbb{T}}_a D^\alpha_t u(t))({}^{\mathbb{T}}_a D^\alpha_t u_k(t) - {}^{\mathbb{T}}_a D^\alpha_t u(t))\Delta t\\ =\ & (\beta + \varrho\|u_k\|^p)^{p-1}\int_{J^0}(\phi_p({}^{\mathbb{T}}_a D^\alpha_t u_k(t)) - \phi_p({}^{\mathbb{T}}_a D^\alpha_t u(t)))({}^{\mathbb{T}}_a D^\alpha_t u_k(t) - {}^{\mathbb{T}}_a D^\alpha_t u(t))\Delta t\\ &+\left[(\beta + \varrho\|u_k\|^p)^{p-1} - (\beta + \varrho\|u\|^p)^{p-1}\right]\\ &\times\int_{J^0}(\phi_p({}^{\mathbb{T}}_a D^\alpha_t u(t))({}^{\mathbb{T}}_a D^\alpha_t u_k(t) - ({}^{\mathbb{T}}_a D^\alpha_t u(t))\Delta t,\end{aligned} \tag{39}$$

which together with (35)–(39) yields

$$\int_{J^0}(\phi_p({}_a^{\mathbb{T}}D_t^\alpha u_k(t))-\phi_p({}_a^{\mathbb{T}}D_t^\alpha u(t)))({}_a^{\mathbb{T}}D_t^\alpha u_k(t)-{}_a^{\mathbb{T}}D_t^\alpha u(t))\Delta t\to 0,\quad \text{as } k\to\infty. \tag{40}$$

Considering (2.10) in [58], we can find two positive constants c_2, c_3 such that

$$\begin{aligned}&\int_{J^0}(\phi_p({}_a^{\mathbb{T}}D_t^\alpha u_k(t))-\phi_p({}_a^{\mathbb{T}}D_t^\alpha u(t)))({}_a^{\mathbb{T}}D_t^\alpha u_k(t)-{}_a^{\mathbb{T}}D_t^\alpha u(t))\Delta t\\ &\geq\begin{cases}c_2\int_{J^0}|{}_a^{\mathbb{T}}D_t^\alpha u_k(t)-{}_a^{\mathbb{T}}D_t^\alpha u(t)|^p\Delta t, & p\geq 2,\\ c_3\int_{J^0}\frac{|{}_a^{\mathbb{T}}D_t^\alpha u_k(t)-{}_a^{\mathbb{T}}D_t^\alpha u(t)|^2}{(|{}_a^{\mathbb{T}}D_t^\alpha u_k(t)|+|{}_a^{\mathbb{T}}D_t^\alpha u(t)|)^{p-2}}\Delta t, & 1<p<2.\end{cases}\end{aligned} \tag{41}$$

When $1<p<2$, with an eye to Proposition 2 and $(|x|+|y|)^p\leq 2^{p-1}(|x|^p+|y|^p)(\ \forall x,y\in\mathbb{R},\ p>0)$, one obtains

$$\begin{aligned}&\int_{J^0}|{}_a^{\mathbb{T}}D_t^\alpha u_k(t)-{}_a^{\mathbb{T}}D_t^\alpha u(t)|^p\Delta t\\ &=\int_{J^0}\frac{|{}_a^{\mathbb{T}}D_t^\alpha u_k(t)-{}_a^{\mathbb{T}}D_t^\alpha u(t)|^p}{(|{}_a^{\mathbb{T}}D_t^\alpha u_k(t)|+|{}_a^{\mathbb{T}}D_t^\alpha u(t)|)^{\frac{p(2-p)}{2}}}(|{}_a^{\mathbb{T}}D_t^\alpha u_k(t)|+|{}_a^{\mathbb{T}}D_t^\alpha u(t)|)^{\frac{p(2-p)}{2}}\Delta t\\ &\leq\left\{\int_{J^0}\left[\frac{|{}_a^{\mathbb{T}}D_t^\alpha u_k(t)-{}_a^{\mathbb{T}}D_t^\alpha u(t)|^p}{(|{}_a^{\mathbb{T}}D_t^\alpha u_k(t)|+|{}_a^{\mathbb{T}}D_t^\alpha u(t)|)^{\frac{p(2-p)}{2}}}\right]^{\frac{2}{p}}\Delta t\right\}^{\frac{p}{2}}\\ &\quad\times\left\{\int_{J^0}\left[(|{}_a^{\mathbb{T}}D_t^\alpha u_k(t)|+|{}_a^{\mathbb{T}}D_t^\alpha u(t)|)^{\frac{p(2-p)}{2}}\right]^{\frac{2}{2-p}}\Delta t\right\}^{\frac{2-p}{2}}\\ &=\left[\int_{J^0}\frac{|{}_a^{\mathbb{T}}D_t^\alpha u_k(t)-{}_a^{\mathbb{T}}D_t^\alpha u(t)|^2}{(|{}_a^{\mathbb{T}}D_t^\alpha u_k(t)|+|{}_a^{\mathbb{T}}D_t^\alpha u(t)|)^{2-p}}\Delta t\right]^{\frac{p}{2}}\\ &\quad\times\left[\int_{J^0}(|{}_a^{\mathbb{T}}D_t^\alpha u_k(t)|+|{}_a^{\mathbb{T}}D_t^\alpha u(t)|)^p\Delta t\right]^{\frac{2-p}{2}}\\ &\leq\left[\int_{J^0}\frac{|{}_a^{\mathbb{T}}D_t^\alpha u_k(t)-{}_a^{\mathbb{T}}D_t^\alpha u(t)|^2}{(|{}_a^{\mathbb{T}}D_t^\alpha u_k(t)|+|{}_a^{\mathbb{T}}D_t^\alpha u(t)|)^{2-p}}\Delta t\right]^{\frac{p}{2}}\\ &\quad\times\left[\int_{J^0}2^{p-1}(|{}_a^{\mathbb{T}}D_t^\alpha u_k(t)|^p+|{}_a^{\mathbb{T}}D_t^\alpha u(t)|^p)\Delta t\right]^{\frac{2-p}{2}}\\ &=\left[\int_{J^0}\frac{|{}_a^{\mathbb{T}}D_t^\alpha u_k(t)-{}_a^{\mathbb{T}}D_t^\alpha u(t)|^2}{(|{}_a^{\mathbb{T}}D_t^\alpha u_k(t)|+|{}_a^{\mathbb{T}}D_t^\alpha u(t)|)^{2-p}}\Delta t\right]^{\frac{p}{2}}2^{\frac{(p-1)(2-p)}{2}}(\|u_k\|^p+\|u\|^p)^{\frac{2-p}{2}}.\end{aligned} \tag{42}$$

Therefore, we have

$$\begin{aligned}&\int_{J^0}\frac{|{}_a^{\mathbb{T}}D_t^\alpha u_k(t)-{}_a^{\mathbb{T}}D_t^\alpha u(t)|^2}{(|{}_a^{\mathbb{T}}D_t^\alpha u_k(t)|+|{}_a^{\mathbb{T}}D_t^\alpha u(t)|)^{2-p}}\Delta t\\ &\geq\left[\frac{1}{2^{\frac{(p-1)(2-p)}{2}}(\|u_k\|^p+\|u\|^p)^{\frac{2-p}{2}}}\|u_k-u\|^p\right]^{\frac{2}{p}}\\ &=2^{\frac{(p-1)(p-2)}{p}}(\|u_k\|^p+\|u\|^p)^{\frac{p-2}{p}}\|u_k-u\|^2,\end{aligned} \tag{43}$$

which together with (41) implies

$$\begin{aligned}
&\int_{J^0}(\phi_p({}_a^{\mathbb{T}}D_t^{\alpha}u_k(t))-\phi_p({}_a^{\mathbb{T}}D_t^{\alpha}u(t)))({}_a^{\mathbb{T}}D_t^{\alpha}u_k(t)-{}_a^{\mathbb{T}}D_t^{\alpha}u(t))\Delta t\\
\geq\ & c_3\int_{J^0}\frac{|{}_a^{\mathbb{T}}D_t^{\alpha}u_k(t)-{}_a^{\mathbb{T}}D_t^{\alpha}u(t)|^2}{(|{}_a^{\mathbb{T}}D_t^{\alpha}u_k(t)|+|{}_a^{\mathbb{T}}D_t^{\alpha}u(t)|)^{p-2}}\Delta t\\
\geq\ & c_3 2^{\frac{(p-1)(p-2)}{p}}(\|u_k\|^p+\|u\|^p)^{\frac{p-2}{p}}\|u_k-u\|^2,\quad 1<p<2. \qquad (44)
\end{aligned}$$

When $p>2$, taking (41) into account, one obtains

$$\begin{aligned}
&\int_{J^0}(\phi_p({}_a^{\mathbb{T}}D_t^{\alpha}u_k(t))-\phi_p({}_a^{\mathbb{T}}D_t^{\alpha}u(t)))({}_a^{\mathbb{T}}D_t^{\alpha}u_k(t)-{}_a^{\mathbb{T}}D_t^{\alpha}u(t))\Delta t\\
\geq\ & c_2\|u_k-u\|^p,\quad p>2. \qquad (45)
\end{aligned}$$

As a consequence, combining with (40), (44) and (45), one sees

$$\|u_k-u\|\to 0,\quad \text{as } k\to\infty. \qquad (46)$$

Therefore, φ satisfies the (PS) condition in $W^{\alpha,p}_{\Delta,a^+}$.

step 2. φ satisfies the (A_1) condition in Lemma 5, which can be explained by the following: Taking (G_3) into account, we can find two positive constants $\varepsilon'\in(0,1)$ and δ such that

$$G(t,x)\leq\frac{(1-\varepsilon')\beta^{p-1}}{\lambda^0 p\frac{b^{\alpha p}}{\Gamma^p(\alpha+1)}}|x|^p,\quad \forall\, t\in J,\ \text{with } |x|\leq\delta. \qquad (47)$$

Let $\rho=\frac{\delta}{\frac{b^{\alpha-\frac{1}{p}}}{\Gamma(\alpha)((\alpha-1)q+1)^{\frac{1}{q}}}}$ and $\delta=\frac{\varepsilon'\beta^{p-1}\rho^p}{p}$. Hence, taking (30) into consideration, one has

$$\|u\|_\infty\leq\frac{b^{\alpha-\frac{1}{p}}}{\Gamma(\alpha)((\alpha-1)q+1)^{\frac{1}{q}}}\|u\|,\quad \forall\, u\in W^{\alpha,p}_{\Delta,a^+},\ \text{with } \|u\|=\rho, \qquad (48)$$

which together with (19), (30), (27), and (47) implies

$$\begin{aligned}
\varphi(u)=&\frac{1}{\varrho p^2}\left(\beta+\varrho\int_{J^0}|{}_a^{\mathbb{T}}D_t^{\alpha}u(t)|^p\Delta t\right)^p-\int_{J^0}\lambda(t)G(t,u(t))\Delta t-\frac{\beta^p}{\varrho p^2}\\
=&\frac{1}{\varrho p^2}(\beta+\varrho\|u\|^p)^p-\int_{J^0}\lambda(t)G(t,u(t))\Delta t-\frac{\beta^p}{\varrho p^2}\\
\geq&\frac{\beta^{p-1}}{p}\|u\|^p-\lambda^0\frac{(1-\varepsilon')\beta^{p-1}}{\lambda^0 p\frac{b^{\alpha p}}{\Gamma^p(\alpha+1)}}\int_{J^0}|u(t)|^p\Delta t\\
\geq&\frac{\beta^{p-1}}{p}\|u\|^p-\lambda^0\frac{(1-\varepsilon')\beta^{p-1}}{\lambda^0 p\frac{b^{\alpha p}}{\Gamma^p(\alpha+1)}}\frac{b^{\alpha p}}{\Gamma^p(\alpha+1)}\|{}_a^{\mathbb{T}}D_t^{\alpha}u\|^p_{L^p_\Delta}\\
=&\frac{\beta^{p-1}}{p}\|u\|^p-\lambda^0\frac{(1-\varepsilon')\beta^{p-1}}{\lambda^0 p}\|u\|^p\\
=&\frac{\varepsilon'\beta^{p-1}}{p}\|u\|^p\\
=&\sigma,\quad \forall\, u\in W^{\alpha,p}_{\Delta,a^+},\ \text{with } \|u\|=\rho, \qquad (49)
\end{aligned}$$

which means that the (A_1) condition in Lemma 5 is satisfied.

step 3. φ satisfies the (A_2) condition in Lemma 5. Here are some reasons why:

For $s \in \mathbb{R}$, $|x| \geq M$ and $t \in J$, let

$$F(s) = G(t, sx), \qquad H(s) = F'(s) - \frac{\mu}{s} F(s). \tag{50}$$

In view of (G_2), when $s \geq \frac{M}{|x|}$, one obtains

$$H(s) = \frac{\nabla G(t, sx)sx - \mu G(t, sx)}{s} \geq 0.$$

In addition, taking the expressions of $F(\cdot)$ and $H(\cdot)$ in (50) into account, we can easily obtain the result that $F(s)$ satisfies

$$F'(s) = H(s) + \frac{\mu}{s} F(s).$$

Therefore, when $s \geq \frac{M}{|x|}$, we have

$$G(t, sx) = s^{\mu} \left[G(t, x) + \int_1^s \tau^{-\mu} H(\tau) d\tau \right].$$

So, for $|x| \geq M$ and $t \in J$, together with (G_1), one obtains

$$\left(\frac{M}{|x|} \right)^{\mu} G(t, x) \leq G\left(t, x \frac{M}{|x|} \right) \leq \max_{|x| \leq M} a(|x|) b(t),$$

which implies that

$$G(t, x) \leq \frac{|x|^{\mu}}{M^{\mu}} \max_{|x| \leq M} a(|x|) b(t).$$

So, one gets

$$G(t, x) \geq \frac{|x|^{\mu}}{M^{\mu}} \min_{|x| \leq M} a(|x|) b(t). \tag{51}$$

Therefore, for any $u \in W^{\alpha,p}_{\Delta,a^+} \setminus \{0\}$, $\xi \in \mathbb{R}^+$, it follows from (27), (30), (51), and $\mu > p^2$ that

$$\begin{aligned}
\varphi(\xi u) =& \frac{1}{\varrho p^2} \left(\beta + \varrho \int_{J^0} |{}_a^{\mathbb{T}} D_t^{\alpha}(\xi u)(t)|^p \Delta t \right)^p - \int_{J^0} \lambda(t) G(t, \xi u(t)) \Delta t - \frac{\beta^p}{\varrho p^2} \\
=& \frac{1}{\varrho p^2} (\beta + \varrho \|\xi u\|^p)^p - \int_{J^0} \lambda(t) G(t, \xi u(t)) \Delta t - \frac{\beta^p}{\varrho p^2} \\
\leq& \frac{1}{\varrho p^2} (\beta + \varrho \|\xi u\|^p)^p - \frac{\lambda_0 \min\limits_{|\xi x| \leq M} a(|\xi x|)}{M^{\mu}} |\xi|^{\mu} \|u\|_{\infty}^{\mu} \int_{J^0} b(t) \Delta t - \frac{\beta^p}{\varrho p^2} \\
=& \frac{1}{\varrho p^2} (\beta + \varrho \|\xi u\|^p)^p - \frac{\lambda_0 \min\limits_{|\xi x| \leq M} a(|\xi x|) \|b\|_{L^1_{\Delta}} \|u\|_{\infty}^{\mu}}{M^{\mu}} |\xi|^{\mu} - \frac{\beta^p}{\varrho p^2} \\
\to& -\infty, \quad \text{as } \xi \to \infty.
\end{aligned} \tag{52}$$

Therefore, taking ξ_0 large enough and letting $e = \xi_0 u$, we have $\varphi(e) \leq 0$. As a consequence, φ also satisfies the (A_2) condition in Lemma 5.

As a result, we get a critical point u^* of φ satisfying $\varphi(u^*) \geq \sigma > 0$, and so u^* is a nontrivial solution of KFBVP$_{\mathbb{T}}$ (26). All in all, Theorem is proved by *Step* 1–*Step* 3. □

Theorem 30. *Let $\alpha \in \left(\frac{1}{p}, 1\right]$, and suppose that G satisfies (G_1) and the following conditions:*

(G_4) *There are a constant $1 < r_1 < p^2$ and a function $d \in L^1_\Delta(J, \mathbb{R}^+)$ such that*

$$|\nabla G(t,x)| \leq r_1 d(t)|x|^{r_1-1}, \quad \forall (t,x) \in J \times \mathbb{R}.$$

(G_5) *There is an open interval $\mathbb{I} \subset J$ and three constants $\eta, \delta > 0$, $1 < r_2 < p^2$ such that*

$$G(t,x) \geq \eta |x|^{r_2}, \quad \forall (t,x) \in \mathbb{I}_{\mathbb{T}} \times |-\delta, \delta|.$$

Then, KFBVP$_{\mathbb{T}}$ (26) has at least one nontrivial weak solution.

Proof. It is obvious that $\varphi(0) = 0$, $\varphi \in C^1(W^{\alpha,p}_{\Delta,a^+}, \mathbb{R})$, where $W^{\alpha,p}_{\Delta,a^+}$ is a real Banach space from Theorem 25. Next, we will finish our proof with the help of Lemma 6.

(1) φ is bounded from below in $W^{\alpha,p}_{\Delta,a^+}$, which can be explained by the following:
Taking account of (G_4), (20) and (30), we get

$$\begin{aligned}
\varphi(u) =& \frac{1}{\varrho p^2}\left(\beta + \varrho \int_{J^0} |{}^{\mathbb{T}}_a D^\alpha_t u(t)|^p \Delta t\right)^p - \int_{J^0} \lambda(t) G(t, u(t)) \Delta t - \frac{\beta^p}{\varrho p^2} \\
=& \frac{1}{\varrho p^2}(\beta + \varrho \|u\|^p)^p - \int_{J^0} \lambda(t) G(t, u(t)) \Delta t - \frac{\beta^p}{\varrho p^2} \\
\geq& \frac{1}{\varrho p^2}(\beta + \varrho \|u\|^p)^p - \lambda^0 \int_{J^0} d(t)|u(t)|^{r_1} \Delta t - \frac{\beta^p}{\varrho p^2} \\
\geq& \frac{1}{\varrho p^2}(\beta + \varrho \|u\|^p)^p - \lambda^0 \|d\|_{L^1_\Delta} \|u\|^{r_1}_\infty - \frac{\beta^p}{\varrho p^2} \\
\geq& \frac{1}{\varrho p^2}(\beta + \varrho \|u\|^p)^p - \frac{\lambda^0 \|d\|_{L^1_\Delta} b^{r_1(\alpha - \frac{1}{p})}}{\Gamma^{r_1}(\alpha)((\alpha-1)q+1)^{\frac{r_1}{q}}} \|u\|^{r_1} - \frac{\beta^p}{\varrho p^2}.
\end{aligned} \tag{53}$$

Since $1 < r_1 < p^2$, (53) yields $\varphi(u) \to \infty$ as $\|u\| \to \infty$. Consequently, φ is bounded from below in $W^{\alpha,p}_{\Delta,a^+}$.

(2) φ satisfies the (PS) condition in $W^{\alpha,p}_{\Delta,a^+}$. The argument is as follows:
Let $\{u_k\} \subset W^{\alpha,p}_{\Delta,a^+}$ be a sequence such that (31) holds. So, together with the proof by contradiction and (53), we can easily see that $\{u_k\} \subset W^{\alpha,p}_{\Delta,a^+}$ is bounded in $W^{\alpha,p}_{\Delta,a^+}$. The remainder of proof is similar to the proof of Step 1 in Proof of Theorem 29. We omit the details.
Consequently, combining with Lemma 6, (1) and (2) in Proof of Theorem 30, one gets $c = \inf\limits_{W^{\alpha,p}_{\Delta,a^+}} \varphi(u)$, which is a critical value of φ. In other words, there is a critical point $u^* \in W^{\alpha,p}_{\Delta,a^+}$ such that $\varphi(u^*) = c$.

(3) $u^* \neq 0$, for the following reasons:
Let $u_0 \in (W^{1,2}_{\Delta,T}(\mathbb{I}, \mathbb{R}) \cap W^{\alpha,p}_{\Delta,a^+}) \setminus \{0\}$ [5], and $\|u_0\|_\infty = 1$, it follows from (27), (30), (G_5) and (19) that

$$\begin{aligned}
\varphi(\varsigma u_0) =& \frac{1}{\varrho p^2}\left(\beta + \varrho \int_{J^0} |{}^{\mathbb{T}}_a D^\alpha_t (\varsigma u_0)(t)|^p \Delta t\right)^p - \int_{J^0} \lambda(t) G(t, \varsigma u_0(t)) \Delta t - \frac{\beta^p}{\varrho p^2} \\
\leq& \frac{1}{\varrho p^2}(\beta + \varrho \|\varsigma u_0\|^p)^p - \int_{\mathbb{I}} \lambda(t) G(t, \varsigma u_0(t)) \Delta t - \frac{\beta^p}{\varrho p^2} \\
\leq& \frac{1}{\varrho p^2}(\beta + \varrho \|\varsigma u_0\|^p)^p - \lambda_0 \eta \varsigma^{r_2} \int_{\mathbb{I}} |u_0(t)|^{r_2} \Delta t - \frac{\beta^p}{\varrho p^2}, \quad 0 < s \leq \delta.
\end{aligned} \tag{54}$$

Because of $1 < r_2 < p^2$, (54) implies $\varphi(\varsigma u_0) < 0$ for $s > 0$ that is small enough. Therefore, $u^* \neq 0$.

All in all, $u^* \in W^{\alpha,p}_{\Delta,a^+}$ is a nontrivial critical point of φ, and consequently, u^* is a nontrivial solution of KFBVP$_{\mathbb{T}}$ (26). Hence, we complete the proof of Theorem 30. □

Theorem 31. *Let $\alpha \in \left(\frac{1}{p}, 1\right]$, and suppose that G satisfies (G_1), (G_4), (G_5) and the following conditions:*

(G_6) *There are a constant $1 < r_1 < p^2$ and a function $d \in L^1_\Delta(J, \mathbb{R}^+)$ such that*

$$\nabla G(t,x) = \nabla G(t,-x), \quad \forall (t,x) \in J \times \mathbb{R}.$$

Then, KFBVP$_{\mathbb{T}}$ (26) possesses infinitely many nontrivial weak solutions.

Proof. Lemma 7 is a powerful tool for us to clarify our conclusion.

Considering (1) and (2) in Proof of Theorem 30, we see that $\varphi \in C^1(W^{\alpha,p}_{\Delta,a^+}, \mathbb{R})$ is bounded from below and satisfies the (PS) condition. Furthermore, it follows from (27) and (G_6) that φ is even and $\varphi(0) = 0$.

Fixing $n \in \mathbb{N}$, we take n disjoint open intervals $\mathbb{I}_i$ such that $\bigcup_{i=1}^{n} \mathbb{I}_i \subset \mathbb{I}$.

Let $u_i \in (W^{1,2}_{\Delta,T}(\mathbb{I}_i, \mathbb{R}) \cap W^{\alpha,p}_{\Delta,a^+}) \setminus \{0\}$ and $\|u_i\| = 1$, and

$$\begin{aligned} W_n &= \operatorname{span}\{u_1, u_2, \cdots, u_n\}, \\ D_n &= \{u \in W_n \,|\, \|u\| = 1\}. \end{aligned} \tag{55}$$

For $u \in W_n$, there are $\kappa_i \in \mathbb{R}$ such that

$$u(t) = \sum_{i=1}^{n} \kappa_i u_i(t), \quad \forall\, t \in J. \tag{56}$$

Consequently, one obtains

$$\begin{aligned} \|u\|^p &= \int_{J^0} |{}^{\mathbb{T}}_{a}D^{\alpha}_{t} u(t)|^p \Delta t \\ &= \sum_{i=1}^{n} |\kappa_i|^p \int_{J^0} |{}^{\mathbb{T}}_{a}D^{\alpha}_{t} u_i(t)|^p \Delta t \\ &= \sum_{i=1}^{n} |\kappa_i|^p \|u_i\|^p \\ &= \sum_{i=1}^{n} |\kappa_i|^p, \quad \forall\, u \in W_n. \end{aligned} \tag{57}$$

In consideration of (20), (30), (27), and (G_5), for $0 < \iota \leq \dfrac{\delta}{\frac{b^{\alpha-\frac{1}{p}}}{\Gamma(\alpha)((\alpha-1)q+1)^{\frac{1}{q}}} \max\limits_{i=1,2,\cdots,n} |\kappa_i|}$ and $u \in D_n$, we obtain

$$\begin{aligned} \varphi(\iota u) =& \frac{1}{\varrho p^2}\left(\beta + \varrho \int_{J^0} |{}^{\mathbb{T}}_{a}D^{\alpha}_{t}(\iota u)(t)|^p \Delta t\right)^p - \int_{J^0} \lambda(t) G(t, \iota u(t)) \Delta t - \frac{\beta^p}{\varrho p^2} \\ =& \frac{1}{\varrho p^2}(\beta + \varrho \|\iota u\|^p)^p - \sum_{i=1}^{n} \int_{\mathbb{I}_i} \lambda(t) G(t, \iota \kappa_i u_i(t)) \Delta t - \frac{\beta^p}{\varrho p^2} \\ \leq& \frac{1}{\varrho p^2}(\beta + \varrho \|\iota u_0\|^p)^p - \lambda_0 \eta \iota^{r_2} \sum_{i=1}^{n} \kappa_i^{r_2} \int_{\mathbb{I}_i} |u_i(t)|^{r_2} \Delta t - \frac{\beta^p}{\varrho p^2}. \end{aligned} \tag{58}$$

Since $1 < r_2 < p^2$, together with (58), there are two positive constants ϵ, σ such that

$$\varphi(\sigma u) < -\epsilon, \quad \forall\, u \in D_n. \tag{59}$$

Set

$$D_n^\sigma = \{\sigma u | u \in D_n\},$$
$$\Pi = \left\{ (\kappa_1, \kappa_2, \cdots, \kappa_n) \in \mathbb{R}^n \middle| \sum_{i=1}^{n} |\kappa_i|^p < \sigma^p \right\}. \tag{60}$$

Hence, in view of (59), one has

$$\varphi(u) < -\epsilon, \quad \forall\, u \in D_n^\sigma. \tag{61}$$

Together with the fact of φ is even and $\varphi(0) = 0$, we obtain

$$D_n^\sigma \subset \varphi^{-\epsilon} \subset \Xi. \tag{62}$$

By (57), we see that the mapping $(\kappa_1, \kappa_2, \cdots, \kappa_n) \to \sum_{i=1}^{n} \kappa_i u_i(t)$ from $\partial\Pi$ to D_n^σ is odd and homeomorphic. As a result, combining with Propositions 7.5 and 7.7 in [45], one gets

$$\gamma(\varphi^{-\epsilon}) \geq \gamma(D_n^\sigma) = n. \tag{63}$$

Hence, $\varphi^{-\epsilon} \in \Xi_n$ and so $\Xi_n \neq 0$. Let

$$c_n = \inf_{A \in \Xi_n} \sup_{u \in A} \varphi(u). \tag{64}$$

It follows from the fact that φ is bounded from below that $-\infty < c_n \leq -\epsilon < 0$. In other words, for any $n \in \mathbb{N}$, c_n is a real negative number.

Consequently, considering Lemma 7, we see that φ admits infinitely many nontrivial critical points, and so, KFBVP$_\mathbb{T}$ (26) possesses infinitely many nontrivial weak solutions. The proof of Theorem 31 is complete. □

6. Conclusions

In present paper, a class of fractional Sobolev spaces on time scales is established with the help of the weak Riemann–Liouville fractional derivative on time scales, and some basic properties of them are obtained. As an application, we study a class of Kirchhoff-type fractional p-Laplace boundary value problems on time scales. The existence and multiplicity of nontrivial weak solutions are obtained by using the Mountain path theorem and genus properties. The methods of this paper can also be used to study the solvability of other boundary value problems on time scales. Nowadays, the notions of fractional derivative on time scales in different senses are constantly being put forward. Therefore, our future direction is to study the theory and application of fractional Sobolev spaces on time scales introduced by fractional derivatives in other senses on time scales such as the Caputo, Hadamard, and so on.

Author Contributions: Conceptualization, Y.L.; methodology, Y.L.; formal analysis, X.H. and Y.L.; investigation, X.H. and Y.L.; writing—original draft preparation, X.H. and Y.L.; writing—review and editing, X.H. and Y.L.; supervision, Y.L.; project administration, Y.L.; funding acquisition, Y.L. All authors have read and agreed to the published version of the manuscript.

Funding: This work is supported by the National Natural Science Foundation of China under Grant No. 11861072.

Institutional Review Board Statement: Not applicable.

Informed Consent Statement: Not applicable.

Data Availability Statement: Not applicable.

Conflicts of Interest: The authors declare no conflict of interest.

References

1. Hilger, S. Analysis on measure chains—A unified approach to continuous and discrete calculus. *Results Math.* **1990**, *18*, 18–56. [CrossRef]
2. Bohner, M.; Peterson, A. *Dynamic Equations on Time Scales: An Introduction With Applications*; Birkhäuser: Boston, MA, USA, 2001.
3. Bohner, M.; Peterson, A. *Advances in Dynamic Equations on Time Scales*; Birkhäuser: Boston, MA, USA, 2003.
4. Agarwal, R.P.; Otero-Espinar, V.; Perera, K.; Vivero, D.R. Basic properties of Sobolev's spaces on time scales. *Adv. Diff. Equ.* **2006**, *2006*, 38121. [CrossRef]
5. Zhou, J.; Li, Y. Sobolev's spaces on time scales and its application to a class of second order Hamiltonian systems on time scales. *Nonlinear Anal.* **2010**, *73*, 1375–1380. [CrossRef]
6. Wang, Y.; Zhou, J.; Li, Y. Fractional Sobolev's spaces on time scales via conformable fractional calculus and their application to a fractional differential equation on time scales. *Adv. Math. Phys.* **2016**, *2016*, 9636491. [CrossRef]
7. Hu, X.; Li, Y. Fractional Sobolev space on time scales and its application to a fractional boundary value problem on time scales. *J. Funct. Spaces* **2022**, *2022*, 7149356. [CrossRef]
8. Anatoly, K.; Yuri, L. *Handbook of Fractional Calculus with Applications*; De Gruyter: Berlin, Germany, 2019.
9. Tarasov, V.E. Geometric interpretation of fractional-order derivative. *Fract. Calc. Appl. Anal.* **2016**, *19*, 1200–1221. [CrossRef]
10. Tavassoli, M.H.; Tavassoli, A.; Ostad Rahimi, M.R. The geometric and physical interpretation of fractional order derivatives of polynomial function. *Differ. Geom. Dyn. Syst.* **2013**, *15*, 93–104.
11. Du, M.; Wang, Z.; Hu, H. Measuring memory with the order of fractional derivative. *Sci. Rep.* **2013**, *3*, 3431. [CrossRef]
12. Podlubny, I. Geometric and physical interpretation of fractional integration and fractional differentiation. *Fract. Calc. App. Anal.* **2002**, *5*, 367–386.
13. Rutman, R.S. On physical interpretations of fractional integration and differentiation. *Theor. Math. Phys.* **1995**, *105*, 1509–1519. [CrossRef]
14. Du, Q. *Nonlocal Modeling, Analysis, and Computation*; SIAM: Philadelphia, PA, USA, 2019.
15. Guo, B.; Pu, X.; Huang, F. *Fractional Partial Differential Equations and Their Numerical Solutions*; World Scientific Publishing Co.: London, UK, 2015.
16. Hilfer, R. *Applications of Fractional Calculus in Physics*; World Scientific Publishing Co.: London, UK, 2000.
17. Kilbas, A.A.; Srivastava, H.M.; Trujillo, J.J. *Theory and Applications of Fractional Differential Equations*; Elsevier: Amsterdam, The Netherlands, 2006.
18. Meerschaert, M.; Sikorskii, A. *Stochastic Models for Fractional Calculus*; De Gruyter: Boston, MA, USA, 2012.
19. Wang, J.; Zhou, Y.; Fečkan, M. On recent developments in the theory of boundary value problems for impulsive fractional differential equations. *Comput. Math. Appl.* **2012**, *64*, 3008–3020. [CrossRef]
20. Kimeu, J.M. Fractional Calculus : Definitions and Applications. Master's Thesis, Western Kentucky University, Bowling Green, KY, USA, 2012.
21. Abdelrahman, M.A.E.; Hassan, S.Z.; Alomair, R.A.; Alsaleh, D.M. Fundamental solutions for the conformable time fractional Phi-4 and space-time fractional simplified MCH equations. *AIMS Math.* **2021**, *6*, 6555–6568. [CrossRef]
22. Abdelrahman, M.A.E.; Sohaly, M.A.; Alharbi, Y.F. Fundamental stochastic solutions for the conformable fractional NLSE with spatiotemporal dispersion via exponential distribution. *Phys. Scr.* **2021**, *96*, 125223. [CrossRef]
23. Wang, K.J.; Wang, G.D.; Zhu, H.W. A new perspective on the study of the fractal coupled Boussinesq-Burger equation in shallow water. *Fractals* **2021**, *29*, 2150122. [CrossRef]
24. Benkhettou, N.; Hammoudi, A.; Torres, D.F.M. Existence and uniqueness of solution for a fractional Riemann−Liouville initial value problem on time scales. *J. King Saud Univ. Sci.* **2016**, *28*, 87–92. [CrossRef]
25. Torres, D.F.M. Cauchy's formula on nonempty closed sets and a new notion of Riemann−Liouville fractional integral on time scales. *Appl. Math. Lett.* **2021**, *121*, 107407. [CrossRef]
26. Bastos, N. Fractional Calculus on Time Scales. Ph.D. Thesis, University of Aveiro, Aveiro, Portugal, 2012.
27. Goodrich, A.C. Peterson, C. *Discrete Fractional Calculus*; Springer: Cham, Switzerland, 2015.
28. Samko, S.G.; Kilbas, A.A.; Marichev, O.I. *Fractional Integrals and Derivatives-Theory and Applications*; Gordonand Breach Science Publishers: Amsterdam, The Netherlands, 1993.
29. Bastos, N.R.O.; Mozyrska, D.; Torres, D.F.M. Fractional derivatives and integrals on time scales via the inverse generalized Laplace transform. *Int. J. Math. Comput.* **2011**, *11*, 1–9.
30. Bohner, M.; Guseinov, G.S. The convolution on time scales. *Abstr. Appl. Anal.* **2007**, *2007*, 058373. [CrossRef]
31. Ahmadkhanlu, A.; Jahanshahi, M. On the existence and uniqueness of solution of initial value problem for fractional order differential equations on time scales. *Bull. Iranian Math. Soc.* **2012**, *38*, 241–252. [CrossRef]
32. Georgiev, S.G. *Fractional Dynamic Calculus and Fractional Dynamic Equations on Time Scales*; Springer: Cham, Switzerland, 2018.
33. Hu, X.; Li, Y. Right fractional Sobolev Space via Riemann–Liouville derivatives on time scales and an application to fractional boundary value problem on time scales. *Fractal Fract.* **2021**, *6*, 121. [CrossRef]

34. Davis, J.M.; Gravagne, I.A.; Jackson, B.J.; Marks, R.J.; Ramos, A.A. The Laplace transform on time scales revised. *J. Math. Anal. Appl.* **2007**, *33*, 1291–1307. [CrossRef]
35. Cabada, A.; Vivero, D.R. Criterions for absolute continuity on time scales. *J. Diff. Equ. Appl.* **2005**, *11*, 1013–1028. [CrossRef]
36. Bourdin, L.; Idczak, D. Fractional fundamental lemma and fractional integration by parts formula−applications to critical points of Bolza functionals and to linear boundary value problems. *Adv. Differ. Equ.* **2014**, *20*, 213–232.
37. Agarwal, R.P.; Bohner, M.; Řehák, P. Half−Linear dynamic equations. In *Nonlinear Analysis and Applications to V. Lakshmikantham on His 80th Birthday*; Agarwal, R.P., O'Regan, D., Eds.; Kluwer Academic Publishers: Dordrecht, The Netherlands, 2003; pp. 1–57.
38. Carpinteri, A.; Mainardi, F. *Fractals and Fractional Calculus in Continuum Mechanics*; Springer: Vienna, Austria, 1997.
39. Jahanshahi, S.; Babolian, E.; Torres, D.F.M.; Vahidi, A. Solving Abel integral equations of first kind via fractional calculus. *J. King Saud Univ. Sci.* **2015**, *27*, 161–167. [CrossRef]
40. Jiao, F.; Zhou, Y. Existence of solutions for a class of fractional boundary value problems via critical point theory. *Comput. Math. Appl.* **2011**, *62*, 1181–1199. [CrossRef]
41. Brezis, H. *Analyse Fonctionnelle, Theorie et Applications*; Masson: Paris, France, 1983.
42. Mawhin, J.; Willem, M. *Critical Point Theory and Hamiltonian Systems*; Springer: Berlin/Heidelberg, Germany, 1989.
43. Leibenson, L.S. General problem of the movement of a compressible fluid in a porous medium. *Izvestiia Akademii Nauk Kirgizsko SSSR* **1983**, *9*, 7–10.
44. Jiao, F.; Zhou, Y. Nontrivial solutions of the Kirchhoff-Type fractional p-Laplacian Dirichlet problem. *J. Funct. Space.* **2020**, *2020*, 8453205. [CrossRef]
45. Rabinowitz, P.H. *Minimax Methods in Critical Point Theory with Applications to Differential Equations*; American Mathematical Society: Providence, RI, USA, 1989.
46. Bahaa, G.M.; Torres, D.F.M. To study existence of at least three weak solutions to a system of over-determined Fredholm fractional integro−differential equations. *Commun. Nonlinear Sci. Numer. Simulat.* **2021**, *101*, 105892. [CrossRef]
47. Liang, S.; Pu, H.; Rădulescu, V.D. High perturbations of critical fractional Kirchhoff equations with logarithmic nonlinearity. *Appl. Math. Lett.* **2021**, *116*, 107027. [CrossRef]
48. He, X.; Rădulescu, V.D. Small linear perturbations of fractional Choquard equations with critical exponent. *J. Differ. Equ.* **2021**, *282*, 481–540. [CrossRef]
49. Mugnai, D.; Lippi, E.P. Linking over cones for the Neumann fractional p-Laplacian. *J. Differ. Equ.* **2021**, *271*, 797–820. [CrossRef]
50. Fall, M.M.; Feulefack, P.A.; Temgoua, R.Y.; Weth, T. Morse index versus radial symmetry for fractional Dirichlet problems. *Adv. Math.* **2021**, *384*, 107728. [CrossRef]
51. Jeelani, M.B.; Saeed, A.M.; Abdo, M.S.; Shah, K. Positive solutions for fractional boundary value problems under a generalized fractional operator. *Math. Meth. Appl. Sci.* **2021**, *44*, 9524–9540. [CrossRef]
52. Ghanmi, A.; Zhang, Z. Nehari manifold and multiplicity results for a class of fractional boundary value problems with p-Laplacian. *Bull. Korean Math. Soc.* **2019**, *56*, 1297–1314. [CrossRef]
53. Heidarkhani, S.; Bohner, M.; Caristi, G.; Ayazi, F. A critical point approach for a second-order dynamic Sturm−Liouville boundary value problem with p-Laplacian. *Appl. Math. Comput.* **2021**, *409*, 125521. [CrossRef]
54. Barilla, D.; Bohner, M.; Heidarkhani, S.; Moradi, S. Existence results for dynamic Sturm–Liouville boundary value problems via variational methods. *Appl. Math. Comput.* **2021**, *409*, 125614. [CrossRef]
55. Zhou, J.; Li, Y. Variational approach to a class of second order Hamiltonian systems on time scales. *Acta Appl. Math.* **2012**, *117*, 47–69. [CrossRef]
56. Su, Y.H.; Feng, Z. A non-autonomous Hamiltonian system on time scales. *Nonlinear Anal.* **2012**, *75*, 4126–4136. [CrossRef]
57. Zhou, J.; Li, Y.; Wang, Y. An application of variational approach to delay hamiltonian systems on time scales with impulses. *Bull. Malays. Math. Sci. Soc.* **2017**, *40*, 1523–1543. [CrossRef]
58. Simon, J. Régularité de la solution dun problème aux limites non linéaires. *Ann. Fac. Sci. Toulouse Math.* **1981**, *3*, 247–274. [CrossRef]

mathematics

MDPI

Article

Complex Dynamic Behaviour of Food Web Model with Generalized Fractional Operator

Ajay Kumar [1], Sara Salem Alzaid [2], Badr Saad T. Alkahtani [2] and Sunil Kumar [1,2,3,4,*]

[1] Department of Mathematics, National Institute of Technology, Jamshedpur 831014, Jharkhand, India; ajaychauhanmsctech@gmail.com
[2] Department of Mathematics, College of Science, King Saud University, P.O. Box 1142, Riyadh 11989, Saudi Arabia; sarsalzaid@ksu.edu.sa (S.S.A.); balqahtani1@ksu.edu.sa (B.S.T.A.)
[3] Nonlinear Dynamics Research Center (NDRC), Ajman University, Ajman P.O. Box 346, United Arab Emirates
[4] Department of Mathematics, University Centre for Research and Development, Chandigarh University, Gharuan, Mohali 140413, Punjab, India
* Correspondence: skiitbhu28@gmail.com or skumar.math@nitjsr.ac.in; Tel.: +91-787-010-2516

Abstract: We apply a new generalized Caputo operator to investigate the dynamical behaviour of the non-integer food web model (FWM). This dynamical model has three population species and is nonlinear. Three types of species are considered in this population: prey species, intermediate predators, and top predators, and the top predators are also divided into mature and immature predators. We calculated the uniqueness and existence of the solutions applying the fixed-point hypothesis. Our study examines the possibility of obtaining new dynamical phase portraits with the new generalized Caputo operator and demonstrates the portraits for several values of fractional order. A generalized predictor–corrector (P-C) approach is utilized in numerically solving this food web model. In the case of the nonlinear equations system, the effectiveness of the used scheme is highly evident and easy to implement. In addition, stability analysis was conducted for this numerical scheme.

Keywords: food web model (FWM); dynamical behaviour; generalized Caputo operator; uniqueness; stability; existence; generalized P-C numerical algorithm

MSC: 45D05

Citation: Kumar, A.; Alzaid, S.S.; Alkahtani, B.S.T.; Kumar, S. Complex Dynamic Behaviour of Food Web Model with Generalized Fractional Operator. *Mathematics* **2022**, *10*, 1702. https://doi.org/10.3390/math10101702

Academic Editors: António M. Lopes, Alireza Alfi, Liping Chen, Sergio Adriani David and Christopher Goodrich

Received: 1 March 2022
Accepted: 11 April 2022
Published: 16 May 2022

1. Introduction

Energy and materials follow one path between species in a food chain model, whereas food webs are more complex because they connect many food chains. Different trophic levels are found in a food web. There are various categories of organisms within the trophic levels, including producers, consumers, and decomposers. The structure of a food web is typically represented by a lattice arrangement. Using a system of differential equations, it is possible to design food chains and food webs. Food chains, in ecology, are a chain of organisms feeding on the organism next to them, while food webs are a collection of food chains joined together. It has been of interest to several researchers to analyse the dynamical behaviour of the food chain model and the web model [1–4]. A modular food web theory, which studies the structural and functional properties of low-species-based food webs, aims to determine how the structure and interactions mediate ecosystem stability [5,6]. Several species in nature have life cycles that are divided into at least two stages: mature and immature. These stages have different characteristics. Food web models (FWMs) depicting a stage structure have been extensively studied [7,8]. The impact of cannibalism on ecological systems has been studied extensively over the past few decades. Aquatic, as well as terrestrial food webs have cannibalistic populations. This subject has been addressed by several studies [9–12]. Stage-structured populations frequently engage in

cannibalism, whether in the wild or in watery food webs. The cannibalism model was examined and investigated by Diekmann et al. [13]. A watery food chain in which a predator cannibalizes was studied by Bhattacharyya and Pal [14]. The dynamics of the system are therefore influenced by cannibalism in a very significant way. Fishes, birds, mammals, and others are among the animals that have cannibalistic natures.

There are over 300 years of development behind fractional calculus, and today, this is still an important concept of studying real-world problems [15–20]. The literature of fractional calculus has introduced a variety of fractional derivatives, including Caputo [21], Atangana–Baleanu [22], and Caputo–Fabrizio [23], which are the most widely used derivatives. Fractional differential equations can describe dynamic processes within biological and ecological systems with a higher degree of accuracy and reliability since most biological and ecological mathematical models have long-term memories. An understanding of fractional species systems can provide new possibilities for describing the dynamic behaviours of multi-species food web ecosystems, given the complexity and existence of nonlinear effects [24]. In addition, fractional-order forms have a number of advantages, such as a meticulous illustration and an accurate interpretation of operation rules. In order to further explore the dynamics of systems with competition, predation, and parasitism, classical integer differential equations of ecosystems are replaced with fractional differential equations. The literature contains a variety of nonlocal operators, which are used extensively in applied mathematics. An integral and fractional derivative introduced by Katugampola in 2014 generalizes both Riemann–Liouville and Hadamard integrals and derivatives [25,26]. The generalized Caputo operator was recently constructed by Odibat et al. [27]. In the literature, the generalized Caputo operator has been applied in various ways. A recent study by Rubayyi T. Alqahtani et al. [28] utilized a generalized Caputo operator to model bioethanol production. The new generalized Caputo operator was used to analyse the COVID-19 model [29]. In the paper [30], the author investigated irregular meshes with finite difference methods to determine the error estimates when the Caputo operator of the solution of the FDEs has a low smoothness. The paper [31] developed the asymptotic expansion formula for the trapezoidal approximation of the fractional integral, and the author applied the expansion formula to calculate approximations for fractional integrals of orders $\alpha, \alpha+1, \alpha+2, \alpha+3$, and $\alpha+4$.

In this paper, we extend the classical integer-order food web model (FWM) to a non-integer food web model through a generalized Caputo operator. Moreover, we discuss a generalized predictor–corrector numerical solution that is a generalization of the P-C numerical scheme [32,33] to study the complexity of the food web model's behaviour, and we analyse the stability of this scheme. With the generalized Caputo operator, a non-uniform grid is used in the P-C scheme instead of the uniform grid in the Caputo operator. φ and ρ are the only parameters needed to generalize the Caputo integral operator, which provides a great deal of theoretical and numerical equipment for fractional mathematical modelling. There are numerous applications of this P-C technique in various fields of FDEs. In this study, we analysed the behaviour of the food web model on various different fractional orders and on another parameter of the derivative, which gives us different dynamic phase diagrams of this food web model.

Due to Caputo derivatives describing better certain physical problems involving memory effects, we defined the generalized fractional derivatives in a Caputo form. This Caputo version of generalized fractional derivatives would prove useful for researchers interested in describing real-world phenomena using fractional operators. Finally, by noticing that $\lim_{\rho\to 0}\left(\frac{x^\rho - a^\rho}{\rho}\right) = In\left(\frac{x}{a}\right)$ and $\lim_{\rho\to 0}\left(\frac{b^\rho - x^\rho}{\rho}\right) = In\left(\frac{b}{x}\right)$ lead to Hadamard and Caputo–Hadamard results, we saw that the limiting case as $\rho \to 0$ leads to those results. Furthermore, when $\rho \to 1$, the fractional derivatives of Riemann–Liouville and of Caputo were obtained.

Outline of the Paper

We divided this whole work into the following sections: Section 2 represents the description of the food web model. The preliminaries of fractional calculus (FC) are covered in Section 3. The existence of solutions is demonstrated in Section 4. Solution uniqueness is demonstrated in Section 5. Section 6 presents generalized predictor–corrector numerical algorithms for fractional-order food web models using the generalized Caputo operator. Section 7 contains simulations and discussions of the numerical results. A conclusion is given in Section 8.

2. Description of the Food Web Model

Our study proposes and analyses a three-species FWM that includes cannibalism and a stage structure within top predator species. Predators at the top are generally divided into immature and mature stages. Initial stage individuals are unable to hunt or reproduce, as they are dependent on their mature parents for survival. Additionally, we constructed an ecological model that includes stage cannibalism and structure in the top predators as part of a three-species food web model.

A food web model can be constructed using the above considerations [34].

$$\begin{aligned}
\frac{dx(t)}{dt} &= rx(t)\left(1-\frac{x(t)}{\mathcal{H}}\right)-a_1x(t)y(t),\\
\frac{dy(t)}{dt} &= a_1e_1x(t)y(t)-a_2y(t)z(t)-d_1y(t),\\
\frac{dz(t)}{dt} &= a_2e_2y(t)z(t)+a_3e_3z(t)u(t)+cu(t)-d_2z(t),\\
\frac{du(t)}{dt} &= bz(t)-cu(t)-a_3z(t)u(t)-d_3u(t).
\end{aligned} \tag{1}$$

Prey density (lower level species) at time t is denoted by $x(t)$; intermediate predator density (middle-level species) at time t is denoted by $y(t)$; top predator density (mature and immature of higher-level species) at time t is denoted by $z(t)$, $u(t)$. With an intrinsic growth rate r and carrying capacity $\mathcal{H}$, the prey grows logistically. Based on the Lotka–Volterra functional response, the intermediate predator consumes the prey at the lowest level, with an attack rate a_1 and a conversion rate e_1. In the absence of their food source, it continues to decay exponentially as a result of natural mortality rate d_1. There are two kinds of top predators: mature and immature. Immature populations are assumed to grow exponentially along with their parents denoted by the mature population with growth rate b, while a part grows up to become a mature population with growth rate c. Additionally, both the mature and immature populations face natural death with mortality rates of d_2 and d_3, respectively. With maximum attack rate a_3 and conversion rate e_2, the mature top predator attacks the intermediate predator using the Lotka–Volterra response functional. When the availability of their preferred food becomes rare, they cannibalise the immature top predator based on the Lotka–Volterra functional response with maximum attack rate a_3 and conversion rate e_3.

Equilibrium Points of the Food Web Model

In the part of this section, we calculate the equilibrium points corresponding to the food web model. The steady-state conditions for the model are as follows:

- $\mathbf{E}_0 = (0,0,0,0)$ is the trivial equilibrium point that always exists.
- $\mathbf{E}_1 = (\mathcal{H},0,0,0)$ is the axial equilibrium point.
- $\mathbf{E}_2 = (\check{x},\check{y},0,0) = \left(\frac{d_1}{a_1e_1}, \frac{r}{a_1}\left(1-\frac{d_1}{a_1e_1\mathcal{H}}\right),0,0\right)$ is the top predator free equilibrium point. If the condition $\mathcal{H} > \frac{d_1}{a_1e_1}$ holds, then it exists.

- $\mathbf{E}_3 = (\ddot{x}, \ddot{y}, \ddot{z}, \ddot{u}) = \left(\ddot{x}, \frac{r}{a_1}\left(1 - \frac{\ddot{x}}{\mathcal{H}}\right), \frac{a_1 e_1 \ddot{x} - d_1}{a_2}, \frac{b(a_1 e_1 \ddot{x} - d_1)}{a_2(c+d_3)+a_3(a_1 e_1 \ddot{x} - d_1)}\right)$ is the interior equilibrium point. The characteristic equation for $\ddot{x}$ is as follows:

$$\gamma_1 \ddot{x}^3 + \gamma_2 \ddot{x}^2 + \gamma_3 \ddot{x} + \gamma_4 = 0. \tag{2}$$

where

$$\begin{aligned}
\gamma_1 &= -a_1^2 a_2 a_3 e_1^2 e_2 r < 0.\\
\gamma_2 &= a_1 e_1 [a_2 e_2 r(d_1 a_3 - a_2(c+d_3)) + a_1^2 a_3 e_1 \mathcal{H}(be_3 - d_2) + a_2 a_3 r(a_1 e_1 e_2 \mathcal{H} + d_1)]\\
\gamma_3 &= a_2^2 r(c+d_3)(a_1 e_1 e_2 \mathcal{H} + 2d_1) - 2\mathcal{H} a_1 a_3 e_1 d_1 (r a_2 e_2 - a_1 d_2)\\
&- \mathcal{H} e_1 a_1^2 a_2 (d_2 d_3 + c(d_2 - b)) - b\mathcal{H} e_1 a_1^2 d_1 (a_3 e_3 + 1) - r a_2 a_3 d_1.\\
\gamma_4 &= r\mathcal{H} a_2 e_2 d_1 (a_3 d_1 - a_2(c+d_3)) + \mathcal{H} a_1 a_3 d_1^2 (be_3 - d_2) + \mathcal{H} a_1 d_1 (a_2 d_2 (c+d_3) - bc).
\end{aligned}$$

Thus, a simple computation shows that this exists only if and only if the following is true:

$$\check{x} < \ddot{x} < \mathcal{H}, \tag{3}$$

with one set condition ($\gamma_2 < 0$ and $\gamma_4 < 0$) or ($\gamma_3 > 0$ and $\gamma_4 > 0$).

3. Preliminaries

Definition 1. *The non-integer-order Riemann–Liouville (RL) integral of a function f(t) is described as*

$$\begin{aligned}
{}^{RL}_{a}\mathcal{J}^{\varphi}_{t}[f(t)] &= \frac{1}{\Gamma(\varphi)} \int_a^t f(\varsigma)(t-\varsigma)^{\varphi-1} d\varsigma.\\
{}^{RL}_{a}\mathcal{J}^{0}_{t}[f(t)] &= f(t).
\end{aligned} \tag{4}$$

Definition 2. *Consider $f(t) \in H^1$ to be a differentiable function in the interval $(a, b), a < b$, and $\varphi \in [0, 1]$, then we define the Caputo non-classical operator as*

$${}^{C}_{a}\mathcal{D}^{\varphi}_{t} f(t) = \begin{cases} \frac{1}{\Gamma(n-\varphi)} \int_a^t f^{(n)}(\varsigma)(t-\varsigma)^{(n-\varphi-1)} d\varsigma, & \text{if} \quad n-1 < \varphi < n, \\ \frac{d^n f(t)}{dt^n}, & \text{if} \quad \varphi = n, \end{cases} \tag{5}$$

Gamma functions are represented by $\Gamma(.)$. Here is the definition of the gamma function:

$$\Gamma(x) = \int_0^{+\infty} \Omega^{x-1} e^{-\Omega} d\Omega, \quad (Re(x) > 0). \tag{6}$$

Definition 3. *Here, the order of derivative $\varphi > 0$ and $\rho > 0$, and the generalized non-classical integral ${}^{GC}\mathcal{J}^{\varphi,\rho}_{a+}$ of a function f(t) is defined (assuming it exists) as*

$${}^{GC}\mathcal{J}^{\varphi,\rho}_{a+}[f(t)] = \frac{\rho^{1-\varphi}}{\Gamma(\varphi)} \int_a^t \varsigma^{\rho-1} f(\varsigma)(t^\rho - \varsigma^\rho)^{\varphi-1} d\varsigma, \qquad t > a. \tag{7}$$

Definition 4. *Here, the order of derivative $\varphi > 0$ $(m-1 < \varphi < m)$ and $\rho > 0$. For a function f(t), the generalized Riemann-type non-classical derivative ${}^{GRL}\mathcal{D}^{\varphi,\rho}_{a+}$ is defined as*

$${}^{GRL}\mathcal{D}^{\varphi,\rho}_{a+}[f(t)] = \frac{\rho^{\varphi-m+1}}{\Gamma(m-\varphi)} \left(t^{1-\rho}\frac{d}{dt}\right) \int_a^t \varsigma^{\rho-1} f(\varsigma)(t^\rho - \varsigma^\rho)^{\varphi-1} d\varsigma, \qquad t > a \geq 0. \tag{8}$$

Definition 5. *Here, the order of derivative $\varphi > 0$, $\rho > 0$ and $m = \lceil \varphi \rceil$. For a function f(t), the generalized Caputo-type non-classical derivative ${}^{GC}\mathcal{D}^{\varphi,\rho}_{a+}$ is defined as*

$${}^{GC}\mathcal{D}^{\varphi,\rho}_{a+}[f(t)] = \left({}^{GRL}\mathcal{D}^{\varphi,\rho}_{a+}\left[f(x) - \sum_{n=0}^{m-1} \frac{f(n)(a)}{n!}(x-a)^n\right]\right)(t), \qquad t > a \geq 0. \tag{9}$$

Definition 6. *Here, the order of derivative $\varphi > 0$ $(m-1 < \varphi < m)$ and $\rho > 0$. For a function f(t), the generalized Caputo-type non-classical derivative ${}^{GC}\mathcal{D}_{a+}^{\varphi,\rho}$ is defined as*

$$ {}^{GC}\mathcal{D}_{a+}^{\varphi,\rho}[f(t)] = \frac{\rho^{\varphi-m+1}}{\Gamma(m-\varphi)} \int_a^t \varsigma^{\rho-1} f(\varsigma)(t^\rho - \varsigma^\rho)^{\varphi-1} \left(\varsigma^{1-\rho}\frac{d}{d\varsigma}\right) d\varsigma, \qquad t > a \geq 0. \tag{10} $$

- The relation between the Riemann–Liouville and the generalized non-classical integral from the substitution $\chi^\rho \to \chi$ is as follows

$$ {}_a^{GC}\mathcal{J}_t^{\varphi,\rho}[f(t)] = \rho^{-\varphi}\, {}_{a^\rho}^{RL}\mathcal{J}_{t^\rho}^{\varphi}[f(t^{1/\rho})]. \tag{11} $$

When the lower limit is zero $a = 0$, the relation is

$$ {}_0^{GC}\mathcal{J}_t^{\varphi,\rho}[f(t)] = \rho^{-\varphi}\, {}_0^{RL}\mathcal{J}_{t^\rho}^{\varphi}[f(t^{1/\rho})]. \tag{12} $$

4. Existence of Solutions

The fixed-point assumption is used to investigate the existence of a solution for the fractional food web mathematical model. Now, a non-integer food web mathematical model can be described as follows.

$$ \begin{aligned} {}^{GC}\mathcal{D}_{0+}^{\varphi,\rho}[x(t)] &= rx(t)\left(1-\frac{x(t)}{\mathcal{H}}\right) - a_1 x(t)y(t), \\ {}^{GC}\mathcal{D}_{0+}^{\varphi,\rho}[y(t)] &= a_1 e_1 x(t)y(t) - a_2 y(t)z(t) - d_1 y(t), \\ {}^{GC}\mathcal{D}_{0+}^{\varphi,\rho}[z(t)] &= a_2 e_2 y(t)z(t) + a_3 e_3 z(t)u(t) + cu(t) - d_2 z(t), \\ {}^{GC}\mathcal{D}_{0+}^{\varphi,\rho}[u(t)] &= bz(t) - cu(t) - a_3 z(t)u(t) - d_3 u(t). \end{aligned} \tag{13} $$

The initial conditions of a mathematical model of a food web are as follows:

$$ x(0) = x_0, \qquad y(0) = y_0, \qquad z(0) = z_0, \qquad u(0) = u_0. \tag{14} $$

Using the generalized Caputo-type non-classical integral, we have

$$ \begin{aligned} x(t) - x(0) &= \frac{\rho^{1-\varphi}}{\Gamma(\varphi)} \int_0^t \left\{ rx(t)\left(1-\frac{x(t)}{\mathcal{H}}\right) - a_1 x(t)y(t) \right\} \varsigma^{\rho-1}(t^\rho - \varsigma^\rho)^{(\varphi-1)} d\varsigma, \\ y(t) - y(0) &= \frac{\rho^{1-\varphi}}{\Gamma(\varphi)} \int_0^t \{a_1 e_1 x(t)y(t) - a_2 y(t)z(t) - d_1 y(t)\} \varsigma^{\rho-1}(t^\rho - \varsigma^\rho)^{(\varphi-1)} d\varsigma, \\ z(t) - z(0) &= \frac{\rho^{1-\varphi}}{\Gamma(\varphi)} \int_0^t \{a_2 e_2 y(t)z(t) + a_3 e_3 z(t)u(t) + cu(t) - d_2 z(t)\} \varsigma^{\rho-1}(t^\rho - \varsigma^\rho)^{(\varphi-1)} d\varsigma, \\ u(t) - u(0) &= \frac{\rho^{1-\varphi}}{\Gamma(\varphi)} \int_0^t \{bz(t) - cu(t) - a_3 z(t)u(t) - d_3 u(t)\} \varsigma^{\rho-1}(t^\rho - \varsigma^\rho)^{(\varphi-1)} d\varsigma. \end{aligned} \tag{15} $$

In order to simplify, we determine

$$ \begin{aligned} \mho_1(t,x) &= rx(t)\left(1-\frac{x(t)}{\mathcal{H}}\right) - a_1 x(t)y(t), \\ \mho_2(t,y) &= a_1 e_1 x(t)y(t) - a_2 y(t)z(t) - d_1 y(t), \\ \mho_3(t,z) &= a_2 e_2 y(t)z(t) + a_3 e_3 z(t)u(t) + cu(t) - d_2 z(t), \\ \mho_4(t,u) &= bz(t) - cu(t) - a_3 z(t)u(t) - d_3 u(t). \end{aligned} \tag{16} $$

Theorem 1. *When $0 \leq \mho_1, \mho_2, \mho_3, \mho_4 < 1$, then the kernels $\mho_l, \mho_2, \mho_3, \mho_4$ satisfy the Lipschitz condition.*

Proof of Theorem 1. Then, if $\mho_1(t,x) = rx(t)\left(1-\frac{x(t)}{k}\right) - a_1x(t)y(t)$ is the kernel and $x(t)$ and $x_1(t)$ are two function, we can find

$$\begin{aligned}
\|\mho_1(t,x) - \mho_1(t,x_1)\| &= \left\| rx(t)\left(1-\frac{x(t)}{\mathcal{H}}\right) - a_1x(t)y(t) - \left(rx(t)\left(1-\frac{x(t)}{\mathcal{H}}\right) - a_1x(t)y(t)\right)\right\|,\\
&= \left\| \left(r\left(1-\frac{x(t)+x_1(t)}{\mathcal{H}}\right) - a_1y(t)\right)(x(t)-x_1(t))\right\|,\\
&\leq \left\| r\left(1-\frac{x(t)+x_1(t)}{\mathcal{H}}\right) - a_1y(t)\right\|\|x(t)-x_1(t)\|,\\
&\leq \left(r\left(1-\frac{\|x(t)\|+\|x_1(t)\|}{k}\right) - a_1\|y(t)\|\right)\|x(t)-x_1(t)\|,\\
&\leq \left(r\left(1-\frac{2q_1}{\mathcal{H}}\right) - a_1q_2\right)\|x(t)-x_1(t)\|,\\
&\leq \amalg_1\|x(t)-x_1(t)\|.
\end{aligned} \tag{17}$$

By putting $\amalg_1 = \left(r\left(1-\frac{2q_1}{\mathcal{H}}\right) - a_1q_2\right)$, $\|x(t)\| \leq q_1$, $\|y(t)\| \leq q_2$, $\|z(t)\| \leq q_3$, and $\|u(t)\| \leq q_4$ are the bounded functions; furthermore, we have □

$$\|\mho_1(t,x) - \mho_1(t,x_1)\| \leq \amalg_1\|x(t)-x_1(t)\|. \tag{18}$$

Therefore, the Lipschitz condition holds for $\mho_1$ if the inequality $0 \leq \mho_1 < 1$ is the contraction of $\mho_1$. As we apply the same procedure to kernels $\mho_2$, $\mho_3$, and $\mho_4$, the following results emerge:

$$\begin{aligned}
\|\mho_2(t,y) - \mho_2(t,y_1)\| &\leq \amalg_2\|y(t)-y_1(t)\|,\\
\|\mho_3(t,z) - \mho_3(t,z_1)\| &\leq \amalg_3\|z(t)-z_1(t)\|,\\
\|\mho_4(t,u) - \mho_4(t,u_1)\| &\leq \amalg_4\|u(t)-u_1(t)\|.
\end{aligned} \tag{19}$$

Kernels $\mho_1$, $\mho_2$, $\mho_3$, and $\mho_4$ are determined by Equation (16). Afterwards, we determine the associated integrals:

$$\begin{aligned}
x(t) &= x(0) + \frac{\rho^{1-\varphi}}{\Gamma(\varphi)}\int_0^t \mho_1(\varsigma,x)\varsigma^{\rho-1}(t^\rho-\varsigma^\rho)^{(\varphi-1)}d\varsigma,\\
y(t) &= y(0) + \frac{\rho^{1-\varphi}}{\Gamma(\varphi)}\int_0^t \mho_2(\varsigma,y)\varsigma^{\rho-1}(t^\rho-\varsigma^\rho)^{(\varphi-1)}d\varsigma,\\
z(t) &= z(0) + \frac{\rho^{1-\varphi}}{\Gamma(\varphi)}\int_0^t \mho_3(\varsigma,z)\varsigma^{\rho-1}(t^\rho-\varsigma^\rho)^{(\varphi-1)}d\varsigma,\\
u(t) &= u(0) + \frac{\rho^{1-\varphi}}{\Gamma(\varphi)}\int_0^t \mho_4(\varsigma,u)\varsigma^{\rho-1}(t^\rho-\varsigma^\rho)^{(\varphi-1)}d\varsigma;
\end{aligned} \tag{20}$$

furthermore, we obtain

$$\begin{aligned}
x_n(t) &= x(0) + \frac{\rho^{1-\varphi}}{\Gamma(\varphi)}\int_0^t \mho_1(\varsigma,x_{n-1})\varsigma^{\rho-1}(t^\rho-\varsigma^\rho)^{(\varphi-1)}d\varsigma,\\
y_n(t) &= y(0) + \frac{\rho^{1-\varphi}}{\Gamma(\varphi)}\int_0^t \mho_2(\varsigma,y_{n-1})\varsigma^{\rho-1}(t^\rho-\varsigma^\rho)^{(\varphi-1)}d\varsigma,\\
z_n(t) &= z(0) + \frac{\rho^{1-\varphi}}{\Gamma(\varphi)}\int_0^t \mho_3(\varsigma,z_{n-1})\varsigma^{\rho-1}(t^\rho-\varsigma^\rho)^{(\varphi-1)}d\varsigma,\\
u_n(t) &= u(0) + \frac{\rho^{1-\varphi}}{\Gamma(\varphi)}\int_0^t \mho_4(\varsigma,u_{n-1})\varsigma^{\rho-1}(t^\rho-\varsigma^\rho)^{(\varphi-1)}d\varsigma,
\end{aligned} \tag{21}$$

and the initial condition is

$$x(0) = x_0, \qquad y(0) = y_0, \qquad z(0) = z_0, \qquad u(0) = u_0. \tag{22}$$

When we subtract consecutive terms, we obtain

$$\begin{aligned}
\Xi_n(t) = x_n(t) - x_{n-1}(t) &= \frac{\rho^{1-\varphi}}{\Gamma(\varphi)} \int_0^t (\mho_1(\varsigma, x_{n-1}) - \mho_1(\varsigma, x_{n-2}))\varsigma^{\rho-1}(t^\rho - \varsigma^\rho)^{(\varphi-1)} d\varsigma, \\
\Delta_n(t) = y_n(t) - y_{n-1}(t) &= \frac{\rho^{1-\varphi}}{\Gamma(\varphi)} \int_0^t (\mho_2(\varsigma, y_{n-1}) - \mho_2(\varsigma, y_{n-2}))\varsigma^{\rho-1}(t^\rho - \varsigma^\rho)^{(\varphi-1)} d\varsigma, \\
\aleph_n(t) = z_n(t) - z_{n-1}(t) &= \frac{\rho^{1-\varphi}}{\Gamma(\varphi)} \int_0^t (\mho_3(\varsigma, z_{n-1}) - \mho_3(\varsigma, z_{n-2}))\varsigma^{\rho-1}(t^\rho - \varsigma^\rho)^{(\varphi-1)} d\varsigma, \\
\beth_n(t) = u_n(t) - u_{n-1}(t) &= \frac{\rho^{1-\varphi}}{\Gamma(\varphi)} \int_0^t (\mho_4(\varsigma, u_{n-1}) - \mho_4(\varsigma, u_{n-2}))\varsigma^{\rho-1}(t^\rho - \varsigma^\rho)^{(\varphi-1)} d\varsigma.
\end{aligned} \tag{23}$$

Take the following

$$x_n(t) = \sum_{j=1}^{n} \Xi_n(t), \quad y_n(t) = \sum_{j=1}^{n} \Delta_n(t), \quad z_n(t) = \sum_{j=1}^{n} \aleph_n(t), \quad u_n(t) = \sum_{j=1}^{n} \beth_n(t). \tag{24}$$

Equation (23) is found using the triangular and norm properties.

$$\begin{aligned}
\|\Xi_n(t)\| &= \|x_n(t) - x_{n-1}(t)\| \\
&\leq \frac{\rho^{1-\varphi}}{\Gamma(\varphi)} \left\| \int_0^t (\mho_1(\varsigma, x_{n-1}) - \mho_1(\varsigma, x_{n-2}))\varsigma^{\rho-1}(t^\rho - \varsigma^\rho)^{(\varphi-1)} d\varsigma \right\|,
\end{aligned} \tag{25}$$

and under the Lipschitz condition, the Kernels will exhibit the following outcomes:

$$\begin{aligned}
\|x_n(t) - x_{n-1}(t)\| &\leq \frac{\rho^{1-\varphi}}{\Gamma(\varphi)} \int_0^t \|\mho_1(\varsigma, x_{n-1}) - \mho_1(\varsigma, x_{n-2})\| \varsigma^{\rho-1}(t^\rho - \varsigma^\rho)^{(\varphi-1)} d\varsigma, \\
&\leq \frac{\amalg_1 \rho^{1-\varphi}}{\Gamma(\varphi)} \int_0^t \|x_{n-1} - x_{n-2}\| \varsigma^{\rho-1}(t^\rho - \varsigma^\rho)^{(\varphi-1)} d\varsigma.
\end{aligned} \tag{26}$$

Therefore, we obtain the following:

$$\|\Xi_n(t)\| \leq \frac{\amalg_1 \rho^{1-\varphi}}{\Gamma(\varphi)} \int_0^t \|\Xi_n(\varsigma)\| \varsigma^{\rho-1}(t^\rho - \varsigma^\rho)^{(\varphi-1)} d\varsigma. \tag{27}$$

We obtain the same results for $\Delta_n(t)$, $\aleph_n(t)$, and $\beth_n(t)$ when we follow the same procedure:

$$\begin{aligned}
\|\Delta_n(t)\| &\leq \frac{\amalg_2 \rho^{1-\varphi}}{\Gamma(\varphi)} \int_0^t \|\Delta_n(\varsigma)\| \varsigma^{\rho-1}(t^\rho - \varsigma^\rho)^{(\varphi-1)} d\varsigma, \\
\|\aleph_n(t)\| &\leq \frac{\amalg_3 \rho^{1-\varphi}}{\Gamma(\varphi)} \int_0^t \|\aleph_n(\varsigma)\| \varsigma^{\rho-1}(t^\rho - \varsigma^\rho)^{(\varphi-1)} d\varsigma, \\
\|\beth_n(t)\| &\leq \frac{\amalg_4 \rho^{1-\varphi}}{\Gamma(\varphi)} \int_0^t \|\beth_n(\varsigma)\| \varsigma^{\rho-1}(t^\rho - \varsigma^\rho)^{(\varphi-1)} d\varsigma.
\end{aligned} \tag{28}$$

Following the above conclusion, we can prove the new theorem.

Theorem 2. *The generalized Caputo-type non-classical-order food web mathematical model has a unique solution if t_{max} fulfills the following criteria.*

$$\frac{\amalg_1}{\Gamma(1+\varphi)} \left(\frac{t_{max}^\rho}{\rho} \right)^\varphi < 1. \tag{29}$$

Proof of Theorem 2. By assuming that $x(t)$, $y(t)$, $z(t)$, and $u(t)$ are bounded functions and considering that we have already shown that the kernels possess the Lipschitz condition, the following relation is then given:

$$\begin{aligned}
\|\Xi_n(t)\| &\leq \|x(0)\|\left[\frac{\mathrm{II}_1}{\Gamma(1+\varphi)}\left(\frac{t^{\rho}_{max}}{\rho}\right)^{\varphi}\right]^n,\\
\|\Delta_n(t)\| &\leq \|y(0)\|\left[\frac{\mathrm{II}_2}{\Gamma(1+\varphi)}\left(\frac{t^{\rho}_{max}}{\rho}\right)^{\varphi}\right]^n,\\
\|\aleph_n(t)\| &\leq \|z(0)\|\left[\frac{\mathrm{II}_3}{\Gamma(1+\varphi)}\left(\frac{t^{\rho}_{max}}{\rho}\right)^{\varphi}\right]^n,\\
\|\beth_n(t)\| &\leq \|z(0)\|\left[\frac{\mathrm{II}_4}{\Gamma(1+\varphi)}\left(\frac{t^{\rho}_{max}}{\rho}\right)^{\varphi}\right]^n,
\end{aligned} \tag{30}$$

Considering that all the above functions exist and are smooth, we prove that these functions are the solution to the food web mathematical model. Hence, we assume

$$\begin{aligned}
x(t) - x(0) &= x_n(t) - \mathcal{A}_n(t),\\
y(t) - y(0) &= y_n(t) - \mathcal{B}_n(t),\\
z(t) - z(0) &= z_n(t) - \mathcal{C}_n(t).\\
u(t) - u(0) &= u_n(t) - \mathcal{D}_n(t).
\end{aligned} \tag{31}$$

When $n \to 0$ is taken as the limit in Equation (31), we obtain

$$\begin{aligned}
\|\mathcal{A}_n(t)\| &\leq \frac{\rho^{1-\varphi}}{\Gamma(\varphi)}\left\|\int_0^t(\mho_1(\varsigma,x)-\mho_1(\varsigma,x_{n-1}))\varsigma^{\rho-1}(t^{\rho}-\varsigma^{\rho})^{(\varphi-1)}d\varsigma\right\|,\\
&\leq \frac{\rho^{1-\varphi}}{\Gamma(\varphi)}\int_0^t\|\mho_1(\varsigma,x)-\mho_1(\varsigma,x_{n-1})\|\varsigma^{\rho-1}(t^{\rho}-\varsigma^{\rho})^{(\varphi-1)}d\varsigma,\\
&\leq \frac{\mathrm{II}_1\rho^{1-\varphi}}{\Gamma(\varphi)}\int_0^t\|x-x_{n-1}\|\varsigma^{\rho-1}(t^{\rho}-\varsigma^{\rho})^{(\varphi-1)}d\varsigma,\\
&\leq \frac{\mathrm{II}_1}{\Gamma(1+\varphi)}\left(\tfrac{t^{\rho}}{\rho}\right)^{\varphi}\|x-x_{n-1}\|.
\end{aligned} \tag{32}$$

A recursive process leads to the following equation:

$$\|\mathcal{A}_n(t)\| \leq \|x(0)\|\left[\frac{1}{\Gamma(1+\varphi)}\left(\frac{t^{\rho}}{\rho}\right)^{\varphi}\right]^{n+1}\mathrm{II}_1^n\,\mathcal{F}, \tag{33}$$

then, for t_{max}, we obtain:

$$\|\mathcal{A}_n(t)\| \leq \|x(0)\|\left[\frac{1}{\Gamma(1+\varphi)}\left(\frac{t^{\rho}_{max}}{\rho}\right)^{\varphi}\right]^{n+1}\mathrm{II}_1^n\,\mathcal{F}. \tag{34}$$

We can obtain $\|\mathcal{A}_n(t)\| \to 0$ at $n \to \infty$ by taking the limits of both sides of the above equation, and $\|\mathcal{B}_n(t)\| \to 0$, $\|\mathcal{C}_n(t)\| \to 0$ and $\|\mathcal{D}_n(t)\| \to 0$ can also be obtained by taking the limits of both sides. Therefore, the proof is complete. □

5. Find the Uniqueness of the Solution

In this segment of the food web mathematical model, unique solutions are presented. Consider $x_1(t)$, $y_1(t)$, $z_1(t)$, and $u_1(t)$ to be the other solutions of the proposed system, then we have

$$x(t) - x_1(t) = \frac{\rho^{1-\varphi}}{\Gamma(\varphi)} \int_0^t (\mho_1(\varsigma, x) - \mho_1(\varsigma, x_1))\varsigma^{\rho-1}(t^\rho - \varsigma^\rho)^{(\varphi-1)} d\varsigma. \tag{35}$$

When the norm is applied to each side of Equation (35), the following result is obtained:

$$\|x(t) - x_1(t)\| \leq \frac{\rho^{1-\varphi}}{\Gamma(\varphi)} \int_0^t \|\mho_1(\varsigma, x) - \mho_1(\varsigma, x_1)\|\varsigma^{\rho-1}(t^\rho - \varsigma^\rho)^{(\varphi-1)} d\varsigma. \tag{36}$$

The Lipschitz condition applied to the kernel yields

$$\begin{aligned} \|x(t) - x_1(t)\| &\leq \frac{\mho_1 \rho^{1-\varphi}}{\Gamma(\varphi)} \int_0^t \|x - x_1\|\varsigma^{\rho-1}(t^\rho - \varsigma^\rho)^{(\varphi-1)} d\varsigma, \\ &\leq \frac{\amalg_1}{\Gamma(1+\varphi)} \left(\frac{t^\rho}{\rho}\right)^\varphi \|x - x_{n-1}\|. \end{aligned} \tag{37}$$

In addition, we obtain the following:

$$\|x(t) - x_1(t)\| \left(1 - \frac{\amalg_1}{\Gamma(1+\varphi)} \left(\frac{t^\rho}{\rho}\right)^\varphi\right) \leq 0, \tag{38}$$

$$\|x(t) - x_1(t)\| = 0 \Rightarrow x(t) = x_1(t). \tag{39}$$

According to the above, the first differential equation of the financial model has a unique solution. Similarly, we show that $y(t)$, $z(t)$, and $u(t)$ have unique solutions.

6. Generalized Predictor–Corrector Technique

We converted the model into a fractional Volterra type in order to obtain numerical solutions. We propose a P-C scheme with a generalized Caputo operator to solve the food web system.

Consider the Volterra integral form of the first equation of the food web system:

$$x(t) = x(0) + \frac{1}{\Gamma(\varphi)} \int_0^t \mathbb{A}_1(\varsigma, x, y, z, u) \left(\frac{(t^\rho - \varsigma^\rho)}{\rho}\right)^{(\varphi-1)} \frac{d\varsigma}{\varsigma^{1-\rho}}; \tag{40}$$

we can write the above equation as follows:

$$x(t) = x(0) + \frac{\rho^{1-\varphi}}{\Gamma(\varphi)} \int_0^t \mathbb{A}_1(\varsigma, x, y, z, u)\varsigma^{\rho-1}(t^\rho - \varsigma^\rho)^{\varphi-1} d\varsigma. \tag{41}$$

In order to simplify, we write $\mathbb{A}_1(\varsigma, x(\varsigma))$ instead of $\mathbb{A}_1(\varsigma, x, y, z, u)$. The interval [0, T] is divided into N subintervals $\{[t_r, t_{r+1}], r = 0, 1, 2, \ldots, N-1\}$ with the mesh points as follows:

$$\begin{cases} t_0 = 0, \\ t_{n+1} = (t_n^\rho + h)^{1/\rho}, \qquad n = 0, 1, \ldots, N-1, \end{cases} \tag{42}$$

Here, $h = \frac{T^\rho}{N}$. The approximate solution $x_{n+1} \approx x(t_{n+1})$ of Equation (41) can be calculated as follows:

$$x(t_{n+1}) = x(0) + \frac{\rho^{1-\varphi}}{\Gamma(\varphi)} \int_0^{t_{n+1}} \mathbb{A}_1(\varsigma, x(\varsigma))\varsigma^{\rho-1}(t_{n+1}^\rho - \varsigma^\rho)^{\varphi-1} d\varsigma. \tag{43}$$

Let $k = \varsigma^{\rho}$; therefore, the above equation becomes:

$$x(t_{n+1}) = x(0) + \frac{\rho^{-\varphi}}{\Gamma(\varphi)} \int_0^{t_{n+1}^{\rho}} \mathbb{A}_1(k^{\frac{1}{\rho}}, x(k^{\frac{1}{\rho}}))(t_{n+1}^{\rho} - k)^{\varphi-1} dk. \tag{44}$$

The integral can now be discretized as follows:

$$x(t_{n+1}) = x(0) + \frac{\rho^{-\varphi}}{\Gamma(\varphi)} \sum_{r=0}^{n} \int_{t_r^{\rho}}^{t_{r+1}^{\rho}} \mathbb{A}_1(k^{\frac{1}{\rho}}, x(k^{\frac{1}{\rho}}))(t_{n+1}^{\rho} - k)^{\varphi-1} dk. \tag{45}$$

Using the trapezoidal rule, the right-hand side of (45) is evaluated relative to the weight function $(t_{n+1}^{\rho} - k)^{\varphi-1}$. We can replace $\mathbb{A}_1(k^{\frac{1}{\rho}}, x(k^{\frac{1}{\rho}}))$ with its piecewise linear interpolant by choosing nodes at $t_r^{\rho} (r = 0, 1, 2, \ldots, n+1)$. Then, we have:

$$\begin{aligned} \int_{t_r^{\rho}}^{t_{r+1}^{\rho}} \mathbb{A}_1(k^{\frac{1}{\rho}}, x(k^{\frac{1}{\rho}}))(t_{n+1}^{\rho} - k)^{\varphi-1} dk &= \frac{h^{\varphi-1}}{\varphi\Gamma(\varphi+1)} \big[((n-r)^{\varphi+1} - (n-r-\varphi)(n-r+1)^{\varphi}) \\ &\times \mathbb{A}_1(t_r, x(t_r)) + (n-r+1)\varphi - (n-r+1+\varphi)(n-r)^{\varphi} \\ &\times \mathbb{A}_1(t_{r+1}, x(t_{r+1}))\big]. \end{aligned} \tag{46}$$

The corrector expression for $x(t_{n+1}), n = 0, 1, 2, \ldots, N-1$ is as follows if the above term is substituted into (45):

$$x(t_{n+1}) = x(0) + \frac{\rho^{-\varphi} h^{\varphi}}{\Gamma(\varphi+2)} \sum_{r=0}^{n} \Delta_{r,n+1} \mathbb{A}_1(t_r, x(t_r)) + \frac{\rho^{-\varphi} h^{\varphi}}{\Gamma(\varphi+2)} \mathbb{A}_1(t_{n+1}, x(t_{n+1})), \tag{47}$$

where

$$\Delta_{r,n+1} = \begin{cases} n^{\varphi+1} - (n-\varphi)(n+1)^{\varphi}, & \text{if} \quad r = 0, \\ (n-r+2)^{(\varphi+1)} + (n-r)^{(\varphi+1)} - 2(n-r+1)^{(\varphi+1)}, & \text{if} \quad 1 \le r \le n. \end{cases} \tag{48}$$

Using the Adams–Bashforth method, we determine the predictor value $x^p(t_{n+1})$ for integral (44). We replace $\mathbb{A}_1(k^{\frac{1}{\rho}}, x(k^{\frac{1}{\rho}}))$ with $\mathbb{A}_1(t_r, x(t_r))$ at each integral in Equation (45) to obtain the following:

$$x^p(t_{n+1}) = x(0) + \frac{\rho^{-\varphi}}{\Gamma(\varphi)} \sum_{r=0}^{n} \int_{t_r^{\rho}}^{t_{r+1}^{\rho}} \mathbb{A}_1(t_r, x(t_r))(t_{n+1}^{\rho} - k)^{\varphi-1} dk. \tag{49}$$

Thus, we can conclude that:

$$x^p(t_{n+1}) = x(0) + \frac{\rho^{-\varphi} h^{\varphi}}{\Gamma(\varphi+2)} \sum_{r=0}^{n} [(n+1-r)^{\varphi} - (n-r)^{\varphi}] \mathbb{A}_1(t_r, x(t_r)). \tag{50}$$

We now approximate $x(t_{n+1}) \approx x_{n+1}$ to develop the P-C algorithm by replacing $x^p(t_{n+1})$ with $x(t_{n+1})$ in Equation (47), as follows:

$$x_{n+1} = x(0) + \frac{\rho^{-\varphi} h^{\varphi}}{\Gamma(\varphi+2)} \sum_{r=0}^{n} \Delta_{r,n+1} \mathbb{A}_1(t_r, x_r) + \frac{\rho^{-\varphi} h^{\varphi}}{\Gamma(\varphi+2)} \mathbb{A}_1(t_{n+1}, x_{n+1}^p). \tag{51}$$

We developed a P-C scheme specified in (50) and (51). In this case, the P-C algorithm for the whole model can be written as follows:

$$\begin{aligned}
x_{n+1} &= x(0)+\frac{\rho^{-\varphi}h^{\varphi}}{\Gamma(\varphi+2)}\sum_{r=0}^{n}\Delta_{r,n+1}\mathbb{A}_1(t_r,x_r)+\frac{\rho^{-\varphi}h^{\varphi}}{\Gamma(\varphi+2)}\mathbb{A}_1(t_{n+1},x_{n+1}^{p}),\\
y_{n+1} &= y(0)+\frac{\rho^{-\varphi}h^{\varphi}}{\Gamma(\varphi+2)}\sum_{r=0}^{n}\Delta_{r,n+1}\mathbb{A}_2(t_r,y_r)+\frac{\rho^{-\varphi}h^{\varphi}}{\Gamma(\varphi+2)}\mathbb{A}_2(t_{n+1},y_{n+1}^{p}),\\
z_{n+1} &= z(0)+\frac{\rho^{-\varphi}h^{\varphi}}{\Gamma(\varphi+2)}\sum_{r=0}^{n}\Delta_{r,n+1}\mathbb{A}_3(t_r,z_r)+\frac{\rho^{-\varphi}h^{\varphi}}{\Gamma(\varphi+2)}\mathbb{A}_3(t_{n+1},z_{n+1}^{p}),\\
u_{n+1} &= u(0)+\frac{\rho^{-\varphi}h^{\varphi}}{\Gamma(\varphi+2)}\sum_{r=0}^{n}\Delta_{r,n+1}\mathbb{A}_4(t_r,u_r)+\frac{\rho^{-\varphi}h^{\varphi}}{\Gamma(\varphi+2)}\mathbb{A}_4(t_{n+1},u_{n+1}^{p});
\end{aligned} \tag{52}$$

here, $h=\frac{T^{\rho}}{N}$ and $x_{n+1}^{p}, y_{n+1}^{p}, z_{n+1}^{p}$, and u_{n+1}^{p} are defined as follows:

$$\begin{aligned}
x^{p}(t_{n+1}) &= x(0)+\frac{\rho^{-\varphi}h^{\varphi}}{\Gamma(\varphi+2)}\sum_{r=0}^{n}[(n+1-r)^{\varphi}-(n-r)^{\varphi}]\mathbb{A}_1(t_r,x_r),\\
y^{p}(t_{n+1}) &= y(0)+\frac{\rho^{-\varphi}h^{\varphi}}{\Gamma(\varphi+2)}\sum_{r=0}^{n}[(n+1-r)^{\varphi}-(n-r)^{\varphi}]\mathbb{A}_2(t_r,y_r),\\
z^{p}(t_{n+1}) &= z(0)+\frac{\rho^{-\varphi}h^{\varphi}}{\Gamma(\varphi+2)}\sum_{r=0}^{n}[(n+1-r)^{\varphi}-(n-r)^{\varphi}]\mathbb{A}_3(t_r,z_r),\\
u^{p}(t_{n+1}) &= u(0)+\frac{\rho^{-\varphi}h^{\varphi}}{\Gamma(\varphi+2)}\sum_{r=0}^{n}[(n+1-r)^{\varphi}-(n-r)^{\varphi}]\mathbb{A}_4(t_r,u_r),
\end{aligned} \tag{53}$$

where $\mathbb{A}_1, \mathbb{A}_2$ and $\mathbb{A}_3$ are defined as follows:

$$\begin{aligned}
\mathbb{A}_1(t,x) &= rx(t)\left(1-\frac{x(t)}{\mathcal{H}}\right)-a_1x(t)y(t),\\
\mathbb{A}_2(t,y) &= a_1e_1x(t)y(t)-a_2y(t)z(t)-d_1y(t),\\
\mathbb{A}_3(t,z) &= a_2e_2y(t)z(t)+a_3e_3z(t)u(t)+cu(t)-d_2z(t),\\
\mathbb{A}_4(t,u) &= bz(t)-cu(t)-a_3z(t)u(t)-d_3u(t).
\end{aligned} \tag{54}$$

Remark 1. *The comparison of our adaptive P-C formula with that of [12], based on the product integration methods described in [30], shows that the error should behave in this way:*

$$\max_{r=0,1,..N}|x(t_r)-x_r| = O\left(\left(\frac{h}{\rho}\right)^{p}\right). \tag{55}$$

where $p=min\{2,1+\varphi\}$.

Theorem 3. *(P-C stability) Suppose* $\mathbb{A}_1(t,x(t))$ *fulfills the Lipschitz condition and* $S_e(e=1,2,3,\ldots,i+1)$ *is a solution of Systems (53) and (54). Consequently, the P-C numerical algorithm is conditionally stable.*

Proof of Theorem 3. Consider $\hat{x}_0$, $\hat{x}_e(e=0,1,2,\ldots,i+1)$, and $\hat{x}_{i+1}^{p}(i=0,1,2,\ldots,N-1)$ to be perturbations of x_0, x_e and x_{i+1}^{p}. Equations (52) and (53) become

$$\hat{x}_{i+1}^{p} = \hat{x}(0)+\frac{\rho^{-\varphi}h^{\varphi}}{\Gamma(\varphi+1)}\sum_{e=0}^{i}\Theta_{e,i+1}[\mathbb{A}_1(t_e,x_e+\hat{x}_e)-\mathbb{A}_1(t_e,x_e)], \tag{56}$$

where $\Theta_{e,i+1}=[(i+1-e)^{\varphi}-(i-e)^{\varphi}]$. Therefore,

$$\begin{aligned}
\hat{x}_{i+1} &= \hat{x}(0)+\frac{\rho^{-\varphi}h^{\varphi}}{\Gamma(\varphi+2)}\left[\mathbb{A}_1(t_{i+1},x_{i+1}^{p}+\hat{x}_{i+1}^{p})-\mathbb{A}_1(t_{i+1},x_{i+1}^{p})\right]\\
&+ \frac{\rho^{-\varphi}h^{\varphi}}{\Gamma(\varphi+2)}\sum_{e=0}^{i}\Pi_{e,i+1}[\mathbb{A}_1(t_e,x_e+\hat{x}_e)-\mathbb{A}_1(t_e,x_e)],
\end{aligned} \tag{57}$$

and we use the Lipschitz property of $\mathbb{A}_1(t, x(t))$, then we can have

$$|\hat{x}_{i+1}| \leq \mathbb{T}_0 + \frac{\rho^{-\varphi} h^{\varphi} \psi_1}{\Gamma(\varphi+2)} \left\{ \left| \hat{x}_{i+1}^{p} \right| + \sum_{e=1}^{i} \Pi_{e,i+1} |\hat{x}_e| \right\}. \tag{58}$$

where $\mathbb{T}_0 = \max_{0 \leq i \leq N} \left\{ |\hat{x}_0| + \frac{\rho^{-\varphi} h^{\varphi} \psi_1 \Pi_{i,0}}{\Gamma(\varphi+2)} |\hat{x}_0| \right\}$. The following equation can also be easily derived:

$$\left| \hat{x}_{i+1}^{p} \right| \leq \mathbb{S}_0 + \frac{\rho^{-\varphi} h^{\varphi} \psi_1}{\Gamma(\varphi+1)} \left\{ \sum_{e=1}^{i} \Theta_{e,i+1} |\hat{x}_e| \right\}. \tag{59}$$

where $\mathbb{S}_0 = \max_{0 \leq i \leq N} \left\{ |\hat{x}_0| + \frac{\rho^{-\varphi} h^{\varphi} \psi_1 \Theta_{i,0}}{\Gamma(\varphi+1)} |\hat{x}_0| \right\}$. Now, substituting $\left| \hat{x}_{i+1}^{p} \right|$ from Equation (59) into (58), we obtain:

$$\begin{aligned} |\hat{x}_{i+1}| &\leq \mathbb{R}_0 + \frac{\rho^{-\varphi} h^{\varphi} \psi_1}{\Gamma(\varphi+2)} \left\{ \frac{\rho^{-\varphi} h^{\varphi} \psi_1}{\Gamma(\varphi+1)} \sum_{e=1}^{i} \Theta_{e,i+1} |\hat{x}_e| + \sum_{e=1}^{i} \Pi_{e,i+1} |\hat{x}_e| \right\}, \\ &\leq \mathbb{R}_0 + \frac{\rho^{-\varphi} h^{\varphi} \psi_1}{\Gamma(\varphi+2)} \sum_{e=1}^{i} \left\{ \frac{\rho^{-\varphi} h^{\varphi} \psi_1}{\Gamma(\varphi+1)} \Theta_{e,i+1} + \Pi_{e,i+1} \right\} |\hat{x}_e|, \\ &\leq \mathbb{R}_0 + \frac{\rho^{-\varphi} h^{\varphi} \psi_1 \mathfrak{D}_{\varphi,2}}{\Gamma(\varphi+2)} \sum_{e=1}^{i} \{i+1-e\}^{\varphi-1} |\hat{x}_e|. \end{aligned} \tag{60}$$

Here, $\mathbb{R}_0 = max \left\{ \mathbb{T}_0 + \frac{\rho^{-\varphi} h^{\varphi} \psi_1 \Pi_{i+1,i+1}}{\Gamma(\varphi+2)} \mathbb{S}_0 \right\}$ and a constant $\mathfrak{D}_{\varphi,2} > 0$ is determined by φ. It follows that $|\hat{x}_{i+1}| \leq \mathfrak{D} \mathbb{R}_0$. □

7. Numerical Results and Discussion

For the numerical simulation of the food web mathematical model, we propose a predictor–corrector (P-C) algorithm involving a generalized Caputo operator. Our numerical solution for the food web generalized Caputo derivative model illustrates the applicability and efficiency of the proposed algorithm. MATLAB was used to perform the simulations. The proposed algorithms should be beneficial for the simulation of non-integer models. The dynamical behaviours of the food web model were examined in our analysis. We considered the following parameter values and initial values in Table 1.

Table 1. Representation and numerical values of the assumed parameters.

Parameters	Numerical Values	Description	References
r	1	Intrinsic growth rate	[34]
$\mathcal{H}$	100	Carrying capacity	[34]
a_1	1.0	Maximum attack rate	[34]
a_2	0.25	Maximum attack rate	[34]
a_3	0.1	Maximum attack rate	[34]
d_1	0.01	Natural mortality rate	[34]
d_2	0.2	Natural mortality rate	[34]
d_3	0.01	Natural mortality rate	[34]
c	0.15	Growth rate	[34]
b	0.15	Growth rate	[34]
e_1	0.65	Conversion rate	[34]
e_2	0.5	Conversion rate	[34]
e_3	0.5	Conversion rate	[34]

Generalized Caputo-type fractional derivatives also possess the same properties as Caputo-type derivatives. In order to solve the fractional IVP efficiently, consistently, and accurately, the predictor–corrector (PC) scheme is one of the best available. We solved the projected model using the modified PC scheme in the current study. According to the generalized Caputo algorithm, adaptive PC schemes use a nonuniform grid, which differs from the derivative Caputo PC algorithm. In fractional calculus applications, the generalized

fractional integral operator is a valuable tool for controlling and building mathematical models due to the effect of its parameters φ and ρ. This new generalized Caputo fractional derivative has extra features over the other fractional derivatives such as Caputo, Caputo–Fabrizio, and Atangana–Baleanu. There is another parameter ρ that is very helpful to graphical simulations when it comes to true data, in addition to the fractional-order parameter φ. Changing the parameter value ρ allows us to see more kinds of graphs.

Figures 1 and 2 illustrate the three-dimensional and two-dimensional dynamic phase portrait of the fractional food web system with the generalized Caputo derivative, respectively, when $\varphi = 1$ and $\rho = 1.1$. Figure 3 exhibits the state variables $x(t)$, $y(t)$ $z(t)$, and $u(t)$ of the proposed model when $\varphi = 1$ and $\rho = 1.1$. It can be seen that the value of ρ strongly influences the characteristics of the fractional derivative, and this provides a different way of approaching control applications. Figures 4 and 5 illustrate the three-dimensional and two-dimensional dynamic phase portrait of the fractional food web system with the generalized Caputo derivative, respectively, when $\varphi = 1$ and $\rho = 1.1$. Figure 6 exhibits the state variables $x(t)$, $y(t)$ $z(t)$, and $u(t)$ of the proposed model when $\varphi = 1$ and $\rho = 1.2$. At fixed ρ, depending on the fractional-order value, our fractional food web system displays the complexity of the chaotic phase portrait. Hence, Figures 7–9 are the graphical illustrations of the proposed system at different fractional-order $\varphi = 1, 0.95, 0.90$ and fixed ρ. Further, we took the different values of ρ and φ to be fixed, then the fractional food web system exhibits different phase portraits, which are shown in Figures 10–12. During the simulation of models with two fractional parameters, we observed chaos, and we noticed that the dynamics became more complex.

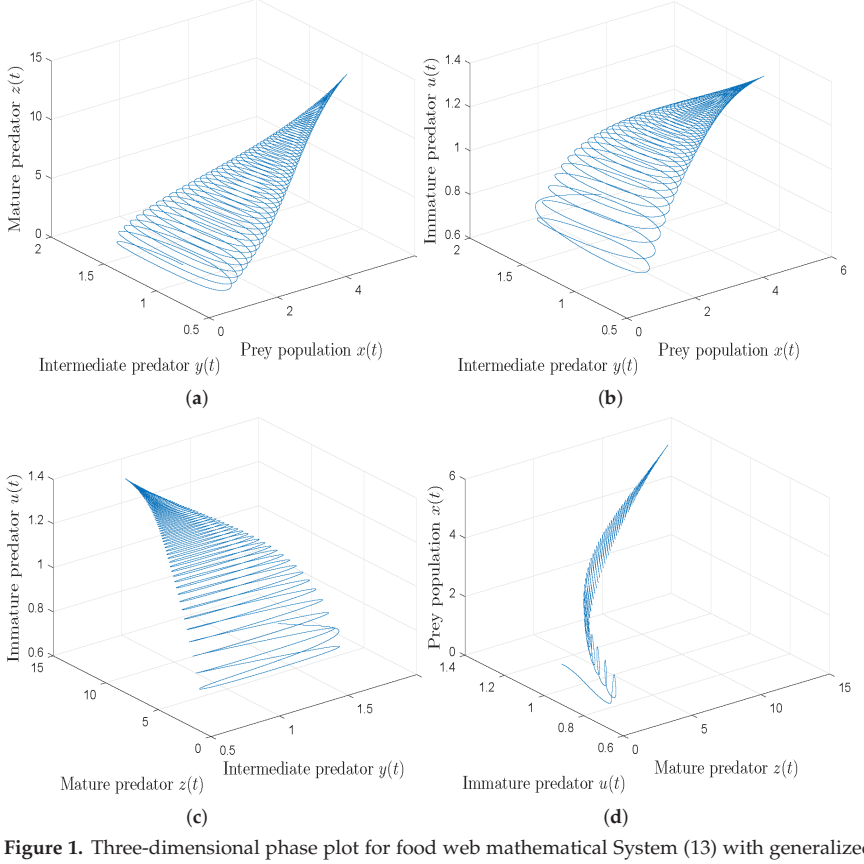

Figure 1. Three-dimensional phase plot for food web mathematical System (13) with generalized Caputo fractional operator when $\varphi = 1$ and $\rho = 1.1$.

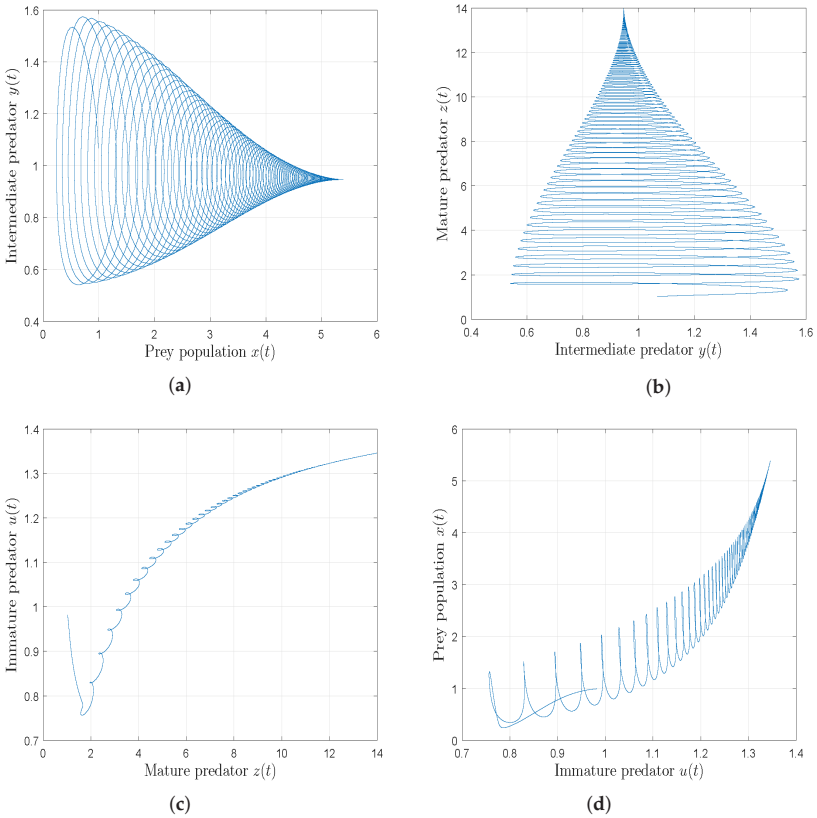

Figure 2. Two-dimensional phase plot for food web mathematical System (13) with generalized Caputo fractional operator when $\varphi = 1$ and $\rho = 1.1$.

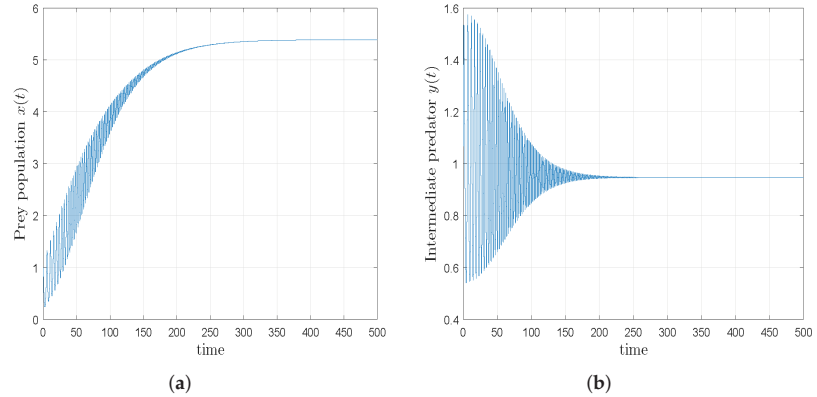

Figure 3. *Cont.*

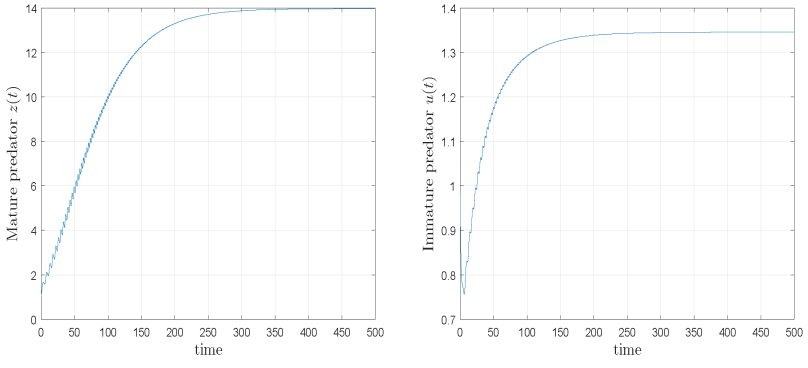

(**c**) (**d**)

Figure 3. State variables $x(t)$, $y(t)$ $z(t)$, and $u(t)$ plots of food web mathematical System (13) with generalized Caputo fractional operator when $\varphi = 1$ and $\rho = 1.1$.

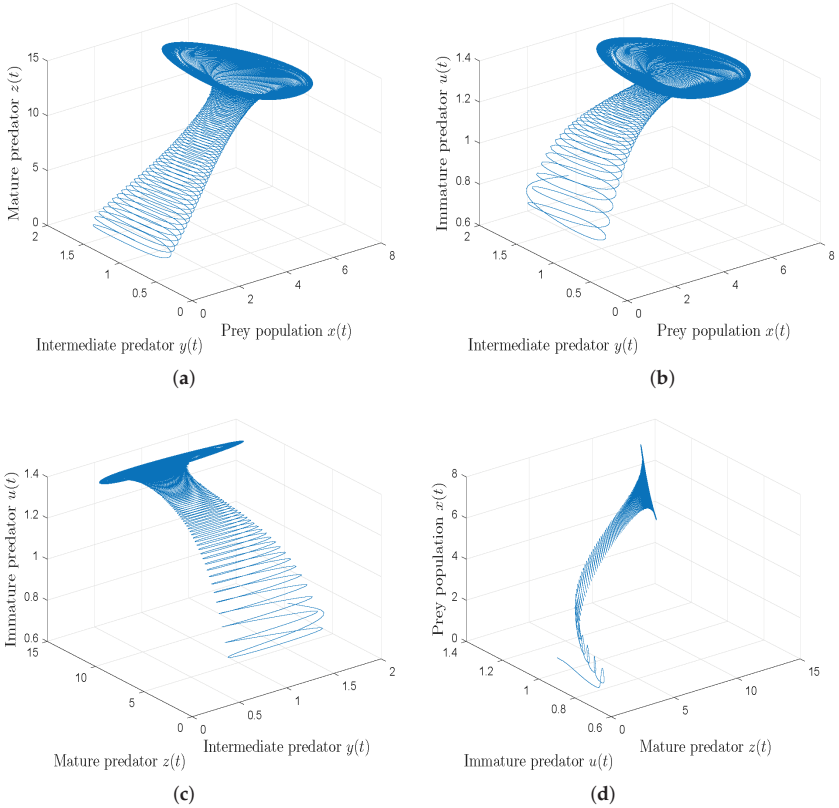

(**a**) (**b**)

(**c**) (**d**)

Figure 4. Three-dimensional chaotic phase plot for food web mathematical System (13) with generalized Caputo fractional operator when $\varphi = 1$ and $\rho = 1.2$.

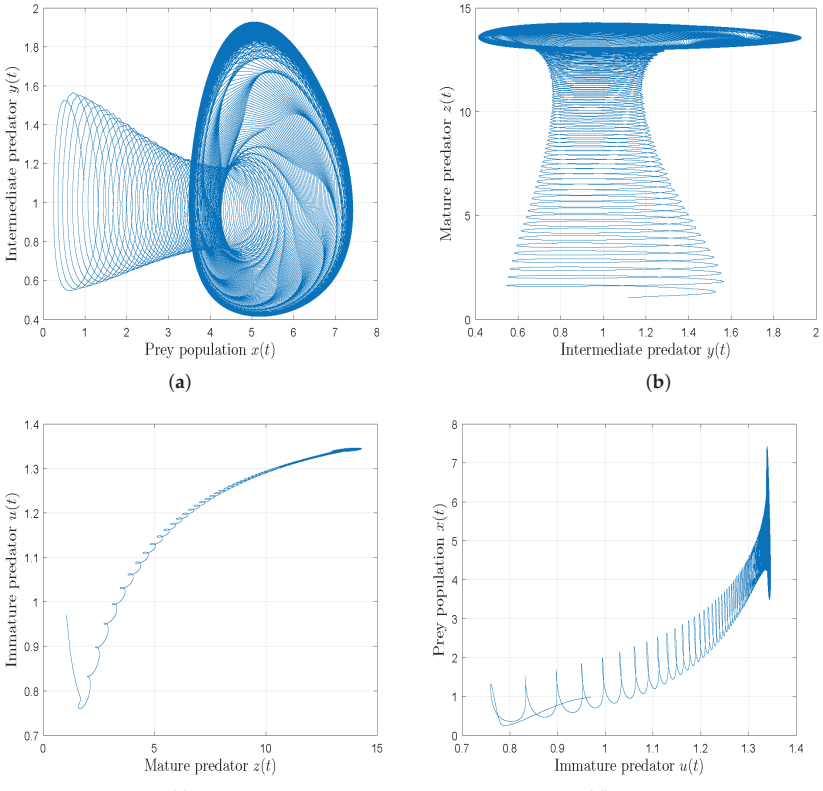

Figure 5. Two-dimensional chaotic phase plot for food web mathematical System (13) with generalized Caputo fractional operator when $\varphi = 1$ and $\rho = 1.2$.

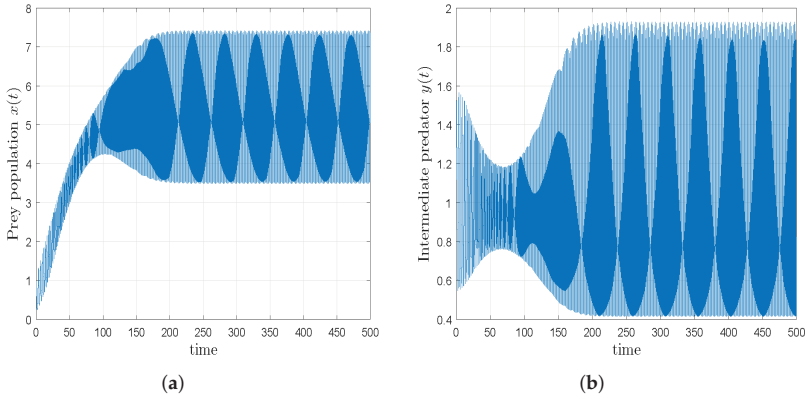

Figure 6. *Cont.*

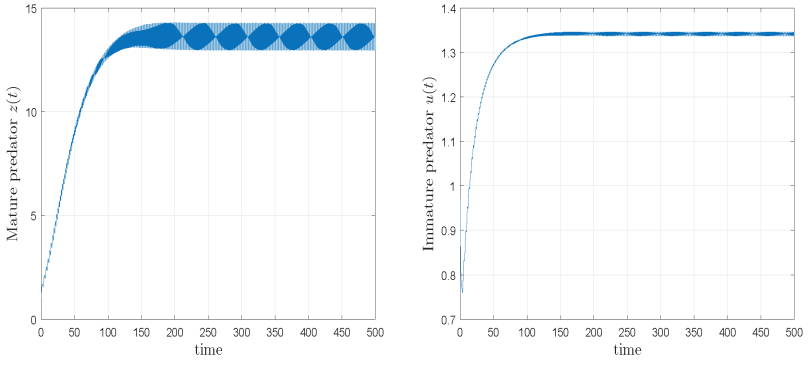

(**c**) (**d**)

Figure 6. State variables $x(t)$, $y(t)$ $z(t)$, and $u(t)$ plots of food web mathematical System (13) with generalized Caputo fractional operator when $\varphi = 1$ and $\rho = 1.2$.

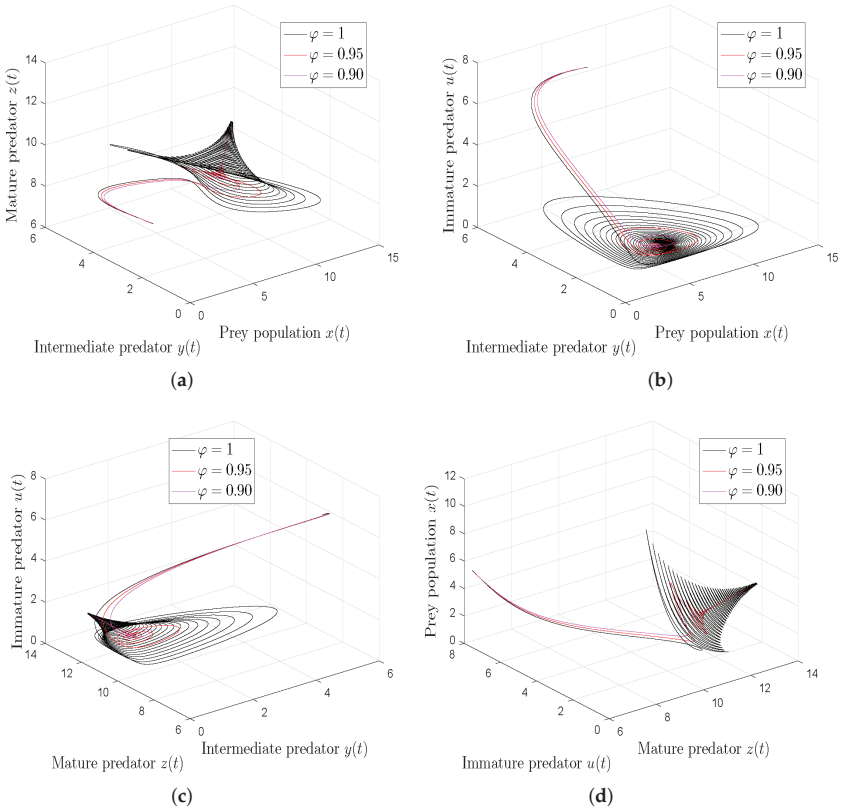

(**a**) (**b**)

(**c**) (**d**)

Figure 7. Three-dimensional chaotic phase plot for food web mathematical System (13) with generalized Caputo fractional operator when $\rho = 0.80$.

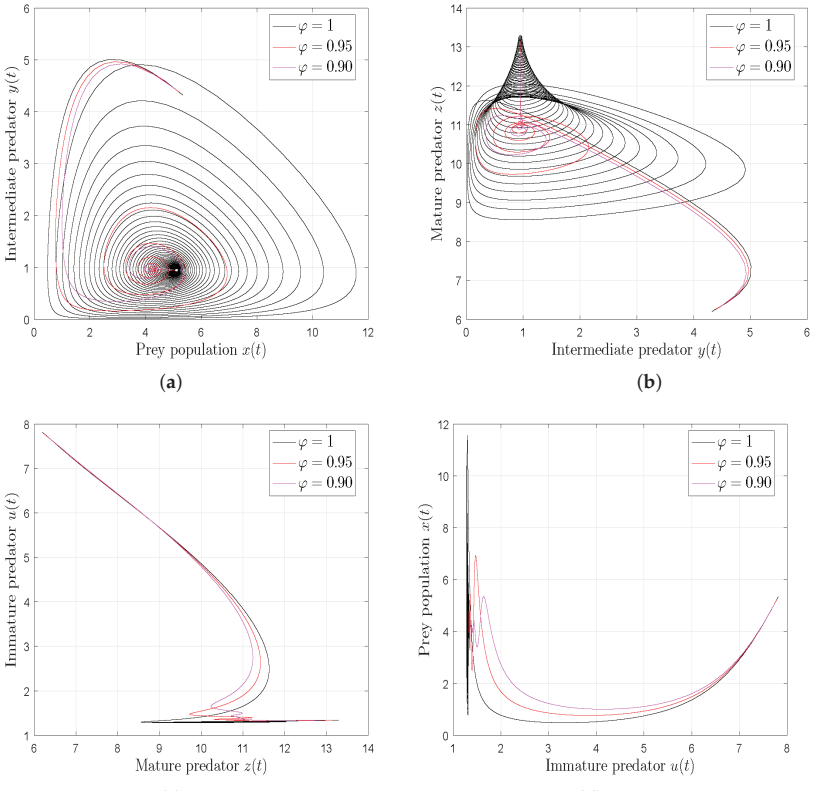

Figure 8. Two-dimensional chaotic phase plot for food web mathematical System (13) with generalized Caputo fractional operator when $\rho = 0.80$.

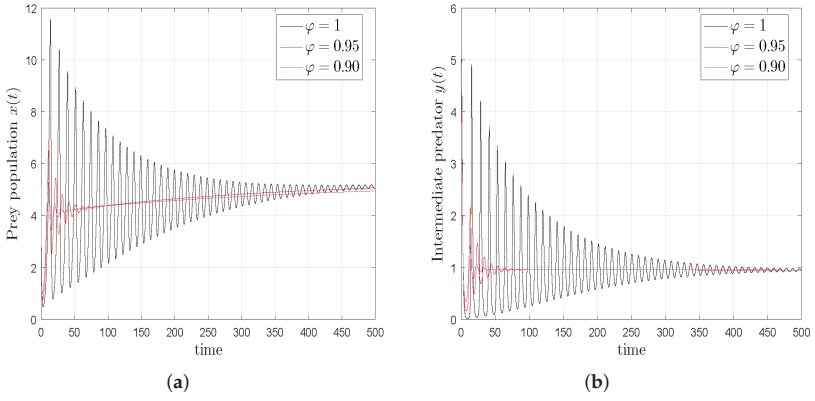

Figure 9. *Cont.*

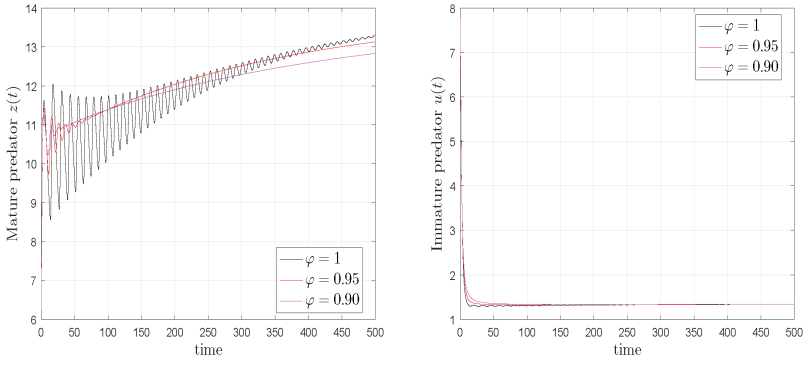

(c) **(d)**

Figure 9. Time series graphical representations for food web mathematical System (13) with generalized Caputo fractional operator when $\rho = 0.80$.

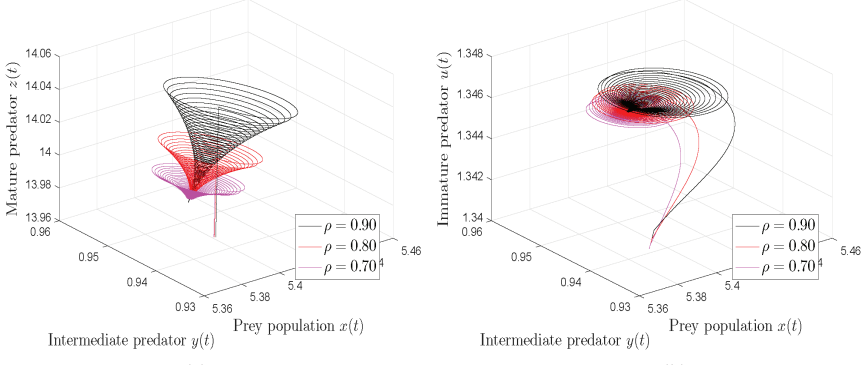

(a) **(b)**

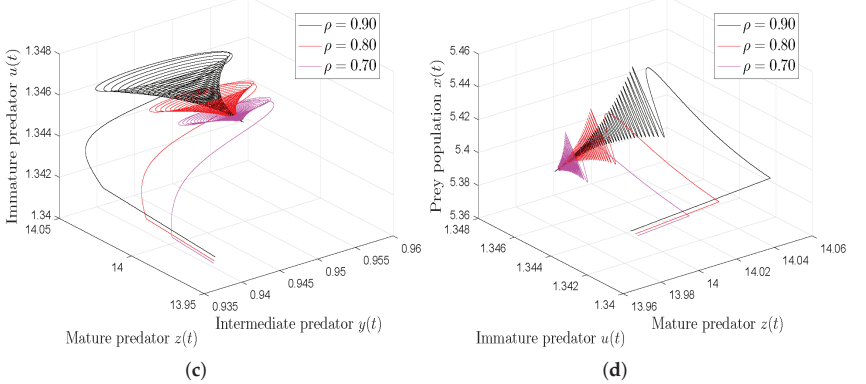

(c) **(d)**

Figure 10. Three-dimensional chaotic phase plot for food web mathematical System (13) with generalized Caputo fractional operator when $\varphi = 0.90$.

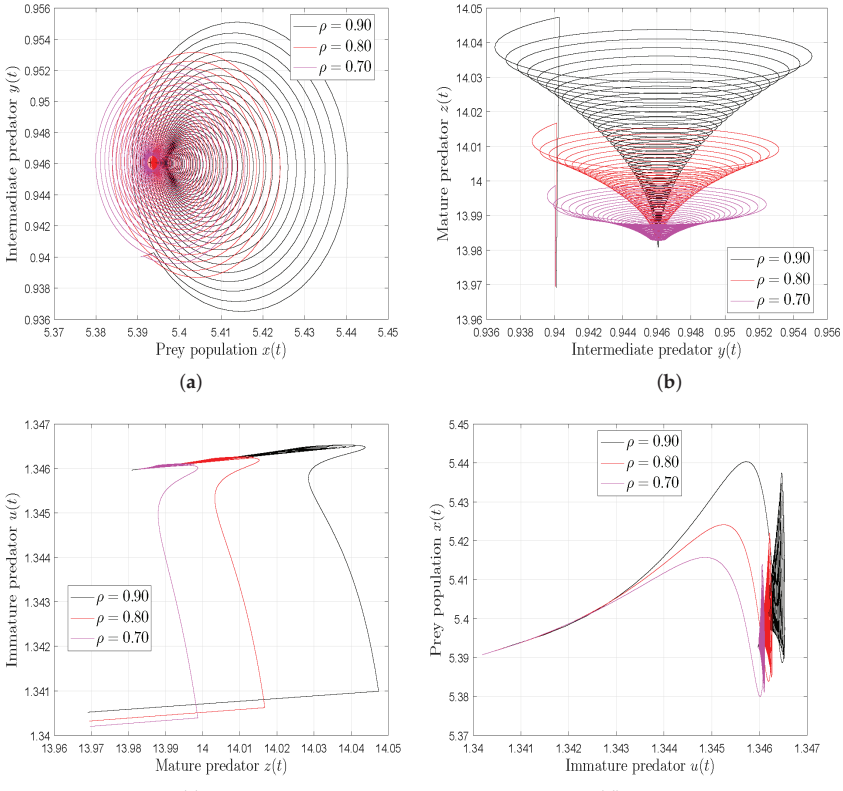

Figure 11. Two-dimensional chaotic phase plot for food web mathematical System (13) with generalized Caputo fractional operator when $\varphi = 0.90$.

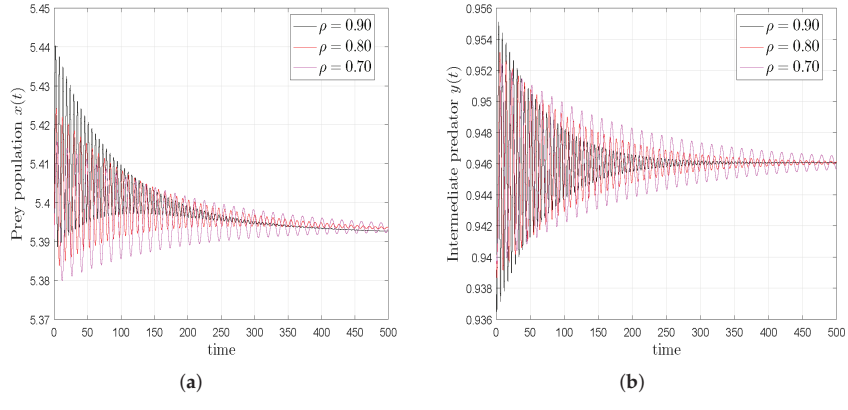

Figure 12. *Cont.*

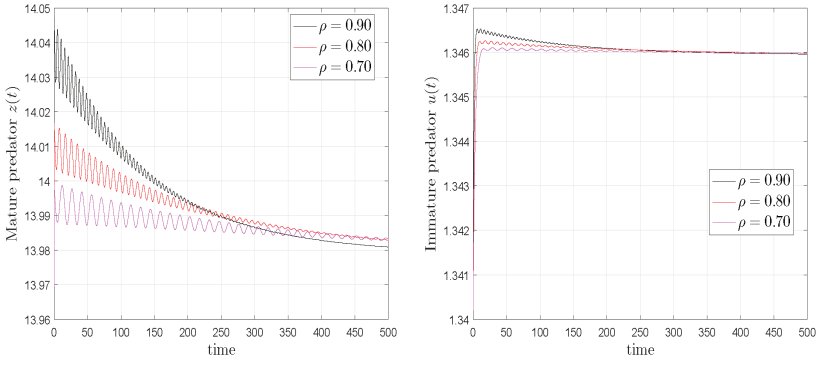

(**c**) (**d**)

Figure 12. Time series graphical representations for food web mathematical System (13) with generalized Caputo fractional operator when $\varphi = 0.90$.

8. Conclusions

Here, we examined a three-species food web model. According to this model, top predators are stage-structured, with a mature predator having a cannibalism trait. In the absence of the predator, the prey grows logistically at the first level. Food consumption at different levels of the food web is described by Lotka–Volterra functional responses. The proposed mathematical model of the food web was examined using the generalized Caputo fractional derivative. Using a fixed-point hypothesis, this study presented an investigation of the existence and uniqueness of the fractional food web system. The algorithm described in this study is based on a numerical technique called 'predictor–corrector', which allows the approximate solution of the fractional food web model to be found. We demonstrated the stability of this numerical method. The fractional food web model was geometrically presented under the generalized Caputo operator for different choices of φ and ρ. The new dynamical behaviour and phase portrait were demonstrated for various fractional orders (φ) and the value of ρ. This graphical illustration showed how the order of derivatives and the system parameters greatly affect the system. The new generalized fractional derivative will be used in future efforts to model other biological systems with memory or with hereditary properties, as well as to identify other important properties of this new generalized derivative.

Author Contributions: Conceptualization, S.K. and A.K.; methodology, A.K. and S.K.; software, A.K. and B.S.T.A.; validation, S.K., S.S.A. and B.S.T.A.; formal analysis, A.K. and S.K.; investigation, S.K. and S.S.A.; resources, S.K. and A.K.; data curation, S.K. and B.S.T.A.; writing—original draft preparation, S.K., A.K. and S.S.A.; writing—review and editing, A.K. and B.S.T.A.; visualization, A.K.; supervision, S.K. and B.S.T.A.; project administration, S.S.A. and S.K.; funding acquisition, S.K. and S.S.A. All authors have read and agreed to the published version of the manuscript.

Funding: This research received no external funding.

Institutional Review Board Statement: Not applicable.

Informed Consent Statement: Not applicable.

Data Availability Statement: All data available inside text.

Acknowledgments: All authors extended their appreciation ti Distinguished Scientist Fellowship Program (DSFP) at King Saud University, Saudi Arabia.

Conflicts of Interest: The authors declare no conflict of interest.

References

1. Naji, R.K. Global stability and persistence of three species food web involving omnivory. *Iraqi J. Sci.* **2012**, *53*, 866–876.
2. McCann, K.; Hastings, A. Re–evaluating the omnivory–stability relationship in food webs. *Proc. R. Soc. Lond. Ser. B Biol. Sci.* **1997**, *264*, 1249–1254. [CrossRef]
3. Nath, B.; Das, K.P. Density dependent mortality of intermediate predator controls chaos-conclusion drawn from a tri-trophic food chain. *J. Korean Soc. Ind. Appl. Math.* **2018**, *22*, 179–199.
4. Gakkhar, S.; Priyadarshi, A.; Banerjee, S. Complex behaviour in four species food-web model. *J. Biol. Dyn.* **2012**, *6*, 440–456. [CrossRef]
5. Kondoh, M.; Kato, S.; Sakato, Y. Food webs are built up with nested subwebs. *Ecology* **2010**, *91*, 3123–3130. [CrossRef]
6. Holt, R.D.; Grover, J.; Tilman, D. Simple rules for interspecific dominance in systems with exploitative and apparent competition. *Am. Nat.* **1994**, *144*, 741–771. [CrossRef]
7. Huang, C.; Qiao, Y.; Huang, L.; Agarwal, R.P. Dynamical behaviours of a food-chain model with stage structure and time delays. *Adv. Differ. Equ.* **2018**, 186. [CrossRef]
8. Naji, R.K.; Ridha, H.F. The dynamics of four species food web model with stage structure. *Int. J. Technol. Enhanc. Emerg. Eng. Res.* **2016**, *4*, 13–32.
9. Persson, L.; Roos, A.M.D.; Claessen, D.; Byström, P.; Lövgren, J.; Sjögren, S.; Svanbäck, R.; Wahlström, E.; Westman, E. Gigantic cannibals driving a whole-lake trophic cascade. *Proc. Natl. Acad. Sci. USA* **2003**, *100*, 4035–4039. [CrossRef]
10. Van den Bosch, F.; Gabriel, W. Cannibalism in an age-structured predator-prey system. *Bull. Math. Biol.* **1997**, *59*, 551–567. [CrossRef]
11. Jurado-Molina, J.; Gatica, C.; Cubillos, L.A. Incorporating cannibalism into an age-structured model for the chilean hake. *Fish. Res.* **2006**, *82*, 30–40. [CrossRef]
12. Kohlmeier, C.; Ebenhöh, W. The stabilizing role of cannibalism in a predator-prey system. *Bull. Math. Biol.* **1995**, *57*, 401–411. [CrossRef]
13. Diekmann, O.; Nisbet, R.; Gurney, W.; Van den Bosch, F. Simple mathematical models for cannibalism: A critique and a new approach. *Math. Biosci.* **1986**, *78*, 21–46. [CrossRef]
14. Bhattacharyya, J.; Pal, S. Coexistence of competing predators in a coral reef ecosystem. *Nonlinear Anal. Real World Appl.* **2011**, *12*, 965–978. [CrossRef]
15. Kumar, S.; Kumar, A.; Samet, B.; Dutta, H. A study on fractional host–parasitoid population dynamical model to describe insect species. *Numer. Methods Partial. Differ. Equ.* **2021**, *37*, 1673–1692. [CrossRef]
16. Kumar, S.; Kumar, A.; Jleli, M. A numerical analysis for fractional model of the spread of pests in tea plants. *Numer. Methods Partial. Differ. Equ.* **2022**, *38*, 540–565. [CrossRef]
17. Kumar, S.; Kumar, A.; Samet, B.; Gómez-Aguilar, J.; Osman, M. A chaos study of tumor and effector cells in fractional tumor-immune model for cancer treatment. *Chaos Solitons Fractals* **2020**, *141*, 110321. [CrossRef]
18. Kumar, A.; Kumar, S. A study on eco-epidemiological model with fractional operators. *Chaos Solitons Fractals* **2022**, *156*, 111697. [CrossRef]
19. Kumar, A.; Alshahrani, B.; Yakout, H.; Abdel-Aty, A.-H.; Kumar, S. Dynamical study on three-species population eco-epidemiological model with fractional order derivatives. *Results Phys.* **2021**, *24*, 104074. [CrossRef]
20. Kumar, S.; Kumar, A.; Abdel-Aty, A.-H.; Alharthi, M. A study on four-species fractional population competition dynamical model. *Results Phys.* **2021**, *24*, 104089. [CrossRef]
21. Kilbas, A.A.; Srivastava, H.M.; Trujillo, J.J. *Theory and Applications of Fractional Differential Equations*; Elsevier: Amsterdam, The Netherlands, 2006.
22. Atangana, A.; Baleanu, D. New fractional derivatives with nonlocal and non-singular kernel: Theory and application to heat transfer model. *arXiv* **2016**, arXiv:1602.03408.
23. Caputo, M.; Fabrizio, M. A new definition of fractional derivative without singular kernel. *Prog. Fract. Differ. Appl.* **2015**, *1*, 1–13.
24. Khan, A.; Abdeljawad, T.; Gomez-Aguilar, J.; Khan, H. Dynamical study of fractional order mutualism parasitism food web module. *Chaos Solitons Fractals* **2020**, *134*, 109685. [CrossRef]
25. Katugampola, U.N. New approach to a generalized fractional integral. *Appl. Math. Comput.* **2011**, *218*, 860–865. [CrossRef]
26. Katugampola, U.N. A new approach to generalized fractional derivatives. *arXiv* **2011**, arXiv:1106.0965.
27. Odibat, Z.; Baleanu, D. Numerical simulation of initial value problems with generalized Caputo-type fractional derivatives. *Appl. Numer. Math.* **2020**, *156*, 94–105. [CrossRef]
28. Alqahtani, R.T.; Ahmad, S.; Akgül, A. Dynamical analysis of bio-ethanol production model under generalized nonlocal operator in Caputo sense. *Mathematics* **2021**, *9*, 2370. [CrossRef]
29. Erturk, V.S.; Kumar, P. Solution of a COVID-19 model via new generalized Caputo-type fractional derivatives. *Chaos Solitons Fractals* **2020**, *139*, 110280. [CrossRef]
30. Liu, Y.; Roberts, J.; Yan, Y. A note on finite difference methods for nonlinear fractional differential equations with non-uniform meshes. *Int. J. Comput. Math.* **2018**, *95*, 1151–1169. [CrossRef]
31. Dimitrov, Y. Approximations of the Fractional Integral and Numerical Solutions of Fractional Integral Equations. *Commun. Appl. Math. Comput.* **2021**, *3*, 545–569. [CrossRef]

32. Diethelm, K.; Ford, N.J.; Freed, A.D. A predictor–corrector approach for the numerical solution of fractional differential equations. *Nonlinear Dyn.* **2002**, *29*, 3–22. [CrossRef]
33. Kumar, P.; Erturk, V.S.; Kumar, A. A new technique to solve generalized Caputo type fractional differential equations with the example of computer virus model. *J. Math. Ext.* **2021**, *15*, 1–23. [CrossRef]
34. Ibrahim, H.A.; Naji, R.K. The complex dynamic in three species food webmodel involving stage structure and cannibalism. *AIP Conf. Proc.* **2020**, *2292*, 020006.

fractal and fractional

MDPI

Article

Hermite–Hadamard-Type Inequalities for h-Convex Functions Involving New Fractional Integral Operators with Exponential Kernel

Yaoqun Wu

School of Information Engineering, Shaoyang University, Shaoyang 422000, China; 201731510071@smail.xtu.edu.cn

Abstract: In this paper, we use two new fractional integral operators with exponential kernel about the midpoint of the interval to construct some Hermite–Hadamard type fractional integral inequalities for h-convex functions. Taking two integral identities about the first and second derivatives of the function as auxiliary functions, the main results are obtained by using the properties of h-convexity and the module. In order to illustrate the application of the results, we propose four examples and plot function images to intuitively present the meaning of the inequalities in the main results, and we verify the correctness of the conclusion. This study further expands the generalization of Hermite–Hadamard-type inequalities and provides some research references for the study of Hermite–Hadamard-type inequalities.

Keywords: fractional integrals operators; exponential kernel; Hermite–Hadamard-type inequalities; h-convex function

MSC: 26D15; 26A51; 26A33

Citation: Wu, Y. Hermite–Hadamard-Type Inequalities for h-Convex Functions Involving New Fractional Integral Operators with Exponential Kernel. *Fractal Fract.* **2022**, *6*, 309. https://doi.org/10.3390/fractalfract6060309

Academic Editors: António M. Lopes, Norbert Herencsar, Alireza Alfi, Liping Chen and Sergio Adriani David

Received: 8 April 2022
Accepted: 26 May 2022
Published: 1 June 2022

1. Introduction

If $g : I \subseteq \mathbb{R} \to \mathbb{R}$, and $m, n \in I$ with $m < n$, then

$$g(\frac{m+n}{2}) \leq \frac{g(m)+g(n)}{2}, \tag{1}$$

which is called Jensen's inequality [1]. Afterward, Hermite and Hadamard insert the integral mean value of convex function g in inequality (1) to obtain the following classical Hermite–Hadamard's inequality [2,3] .

Let $g : I \subseteq \mathbb{R} \to \mathbb{R}$ be a convex function and $m, n \in I$ with $m < n$, then

$$g(\frac{m+n}{2}) \leq \frac{1}{n-m}\int_m^n g(x)dx \leq \frac{g(m)+g(n)}{2}. \tag{2}$$

If g is concave, the inequalities (2) hold in the reversed direction. We note that this inequality can make a bounded estimation of the integral mean on $[m, n]$, so it has wide applications in numerical integration. For the research on the popularization and application of the Hermite–Hadamard's inequality, the readers can refer to [4–10].

The research shows that the fractional-order phenomenon is widespread, and the fractional calculus modeling method is more accurate and reliable than the traditional integer order method. Therefore, the fractional calculus method has been one of the hot research topics in the academic community. Recently, the research results of fractional order on the Hermite–Hadamard's inequality are also numerous. For example, there are Riemann–Liouville fractional integral inequalities [11–14], conformable fractional integrals inequalities [15], k-Riemann–CLiouville fractional integrals inequalities [16], and local fractional integrals inequalities [17–19]. Because fractional integral operators have relatively

convenient applications in some special fields, the research on fractional operator type integral inequalities is becoming more and more abundant. Set et al. [20] used Raina's fractional integral operators to obtain new Hermite–Hadamard-Mercer-type inequalities. Srivastava et al. [21] introduced the generalized left-side and right-side fractional integral operators with a certain modified Mittag–CLeffler kernel and utilized this general family of fractional integral operators to investigate the interesting Chebyshev inequality. In refs. [18,22], Sun presented two local fractional integral operators with a Mittag–Leffler kernel to establish some Hermite–Hadamard-type inequalities for generalized h-convex functions and generalized preinvex functions, respectively; afterward, Xu et al. [23] studied Hermite–Hadamard–Mercer for generalized h-convex functions with the help of the two local fractional integral operators.

In [24], Ahmad et al. proposed two new fractional integral operators with exponential kernels and establish some inequalities related to the right side of the Hermite–Hadamard's inequality. Subsequently, Wu et al. [25] studied the bound for the left side of the Hermite–Hadamard's inequality involving these integral operators. Budak et al. [26] utilized these integral operators with exponential kernels to established some Hermite–CHadamard and Ostrowski type inequalities. On the application of the new integral operators having exponential kernels in Hermite–Hadamard-type inequalities, Du and Zhou et al. extended them to interval-valued and interval-valued co-ordinated, see [27,28]. The new fractional integral operators with exponential kernels are given as follows.

Definition 1 ([24]). *Let $g \in L(m,n)$. The fractional integrals $\mathcal{I}^{\beta}_{m^+}g(\xi)$ and $\mathcal{I}^{\beta}_{n^-}g(\xi)$ of order $\beta \in (0,1)$ are, respectively, defined by*

$$\mathcal{I}^{\beta}_{m^+}g(\xi) = \frac{1}{\beta}\int_m^{\xi} exp\Big(-\frac{1-\beta}{\beta}(\xi-u)\Big)g(u)du, \xi > m, \tag{3}$$

and

$$\mathcal{I}^{\beta}_{n^-}g(\xi) = \frac{1}{\beta}\int_{\xi}^{n} exp\Big(-\frac{1-\beta}{\beta}(u-\xi)\Big)g(u)du, \xi < n. \tag{4}$$

Some known results about (3) and (4) in refs [24,25] are stated as follows.

Theorem 1 ([24]). *Let $g:[m,n]\to\mathbb{R}$ be a positive function with $0 \le m < n$ and $g \in L(m,n)$. If g is a convex function on $[m,n]$, then the following inequalities about (3) and (4) hold.*

$$g(\frac{m+n}{2}) \le \frac{1-\beta}{2(1-exp(-\rho))}[\mathcal{I}^{\beta}_{m^+}g(n) + \mathcal{I}^{\beta}_{n^-}g(m)] \le \frac{g(m)+g(n)}{2}, \tag{5}$$

where $\rho = \frac{1-\beta}{\beta}(n-m)$.

Theorem 2 ([24]). *Let $g: I \subseteq \mathbb{R} \to \mathbb{R}$ be a differentiable function on I. If $|g'|$ is convex on $[m,n]$, $m,n \in I$, then the following inequality about (3) and (4) holds.*

$$\left|\frac{g(m)+g(n)}{2} - \frac{1-\beta}{2(1-exp(-\rho))}\Big[\mathcal{I}^{\beta}_{m^+}g(n) + \mathcal{I}^{\beta}_{n^-}g(m)\Big]\right| \le \frac{n-m}{2\rho}\tanh(\frac{\rho}{4})(|g'(m)| + |g'(n)|). \tag{6}$$

Theorem 3 ([25]). *Let $g: I \subseteq \mathbb{R} \to \mathbb{R}$ be a differentiable function on I. If $|g'|$ is convex on $[m,n]$, $m,n \in I$, then the following inequality about (3) and (4) holds:*

$$\left|\frac{1-\beta}{2(1-exp(-\rho))}\Big[\mathcal{I}^{\beta}_{m^+}g(n) + \mathcal{I}^{\beta}_{n^-}g(m)\Big] - g\Big(\frac{m+n}{2}\Big)\right| \le \frac{n-m}{2}\left[\frac{1}{2} - \frac{\tanh(\frac{\rho}{4})}{\rho}\right](|g'(m)| + |g'(n)|). \tag{7}$$

These Hermite–Hadamard-type integral inequalities involving the fractional integral operators (3) and (4) are structurally in the form of "$\mathcal{I}^{\beta}_{m^+}g(n)+\mathcal{I}^{\beta}_{n^-}g(m)$" for convex functions. In this paper, our main purpose is to apply the definition of h-convexity and the properties of modules to propose some new Hermite–Hadamard-type fractional integral inequalities about fractional integral operators (3) and (4) for generalized h-convex function, whose integral operators involving the midpoint of the interval $[m,n]$ is in the form of "$\mathcal{I}^{\beta}_{\frac{m+n}{2}^+}g(n)+\mathcal{I}^{\beta}_{\frac{m+n}{2}^-}g(m)$". Some numerical examples are given to illustrate the correctness of the results.

2. Results

In the subsequent text, we denote $\rho=\frac{1-\beta}{\beta}(n-m)$ for $\beta\in(0,1)$. In order to obtain our results, the following definition of h-convex function proposed by Varošanec in [29] will be used in the subsequent text.

Definition 2 ([29]). *Let $h:\Omega\to\mathbb{R}$ be a positive function. We say that $g:\Xi\to\mathbb{R}$ is an h-convex function, if g is nonnegative and for all $u,v\in\Xi$ and $\zeta\in(0,1)$, we have*

$$g(\zeta u+(1-\zeta)v)\le h(\zeta)g(u)+h(1-\zeta)g(v). \tag{8}$$

If inequality (8) is reversed, then g is said to be h-concave.

Remark 1. *Obviously, if $h(\zeta)=\zeta$, then h-convex function derives the classical convex function.*

Theorem 4. *Let $g:[m,n]\to\mathbb{R}$ be a positive function with $0\le m<n$, and $g(x)\in L[m,n]$. If g is an h-convex function on $[m,n]$, then the following inequalities for integral operators (3) and (4) hold.*

$$\begin{aligned}\frac{1-\exp(-\frac{\rho}{2})}{\rho h(\frac{1}{2})}g\Big(\frac{m+n}{2}\Big)&\le\frac{\beta}{n-m}\Big(\mathcal{I}^{\beta}_{\frac{m+n}{2}^+}g(n)+\mathcal{I}^{\beta}_{\frac{m+n}{2}^-}g(m)\Big)\\&\le[g(m)+g(n)]\int_0^{\frac{1}{2}}\exp(-\rho t)[h(t)+h(1-t)]dt.\end{aligned} \tag{9}$$

Proof. Since g is an h-convex function on $[m,n]$, we obtain

$$g\Big(\frac{x+y}{2}\Big)\le h(\frac{1}{2})g(x)+h(\frac{1}{2})g(y). \tag{10}$$

For $x=tm+(1-t)n$, $y=(1-t)m+tn$ in (10), $t\in[0,1]$, we have

$$g\Big(\frac{m+n}{2}\Big)\le h(\frac{1}{2})g\big(tm+(1-t)n\big)+h(\frac{1}{2})g\big((1-t)m+tn\big).$$

Multiplying both sides of the above inequality by $\exp(-\rho t)$, and integrating the resulting inequality with respect to t over $[0,\frac{1}{2}]$, we obtain

$$\begin{aligned}&\frac{g\big(\frac{m+n}{2}\big)(1-\exp(-\frac{\rho}{2}))}{\rho h(\frac{1}{2})}=\frac{g\big(\frac{m+n}{2}\big)}{h(\frac{1}{2})}\int_0^{\frac{1}{2}}\exp(-\rho t)dt\\&\le\int_0^{\frac{1}{2}}\exp(-\rho t)g\Big(tm+(1-t)n\Big)dt+\int_0^{\frac{1}{2}}\exp(-\rho t)g\Big((1-t)m+tn\Big)dt\\&=\frac{\beta}{n-m}\frac{1}{\beta}\int_{\frac{m+n}{2}}^{n}\exp\Big(-\frac{1-\beta}{\beta}(n-x)\Big)g(x)dx+\frac{\beta}{n-m}\frac{1}{\beta}\int_m^{\frac{m+n}{2}}\exp\Big(-\frac{1-\beta}{\beta}(y-m)\Big)g(y)dy\\&=\frac{\beta}{n-m}\Big(\mathcal{I}^{\beta}_{\frac{m+n}{2}^+}g(n)+\mathcal{I}^{\beta}_{\frac{m+n}{2}^-}g(m)\Big).\end{aligned} \tag{11}$$

Thus, the first inequality of (9) holds.

On the other hand, note that g is an h-convex function for $t \in [0,1]$, we get

$$g\big(tm+(1-t)n\big) \le h(t)g(m)+h(1-t)g(n)$$

and

$$g\big((1-t)m+tn\big) \le h(1-t)g(m)+h(t)g(n).$$

Adding the above two inequalities, we have

$$g\big(tm+(1-t)n\big)+g\big((1-t)m+tn\big) \le [h(t)+h(1-t)][g(m)+g(n)]. \tag{12}$$

Multiplying both sides of the inequality (12) by $\exp(-\rho t)$, and integrating the result with respect to t over $[0,\frac{1}{2}]$, we obtain

$$\begin{aligned}&\int_0^{\frac{1}{2}} \exp(-\rho t)g\Big(tm+(1-t)n\Big)dt+\int_0^{\frac{1}{2}} \exp(-\rho t)g\Big((1-t)m+tn\Big)dt\\ \le&[g(m)+g(n)]\int_0^{\frac{1}{2}} \exp(-\rho t)[h(t)+h(1-t)]dt.\end{aligned} \tag{13}$$

By (11), the inequality (13) becomes

$$\frac{\beta}{n-m}\Big(\mathcal{I}^{\beta}_{\frac{m+n}{2}+}g(n)+\mathcal{I}^{\beta}_{\frac{m+n}{2}-}g(m)\Big) \le [g(m)+g(n)]\int_0^{\frac{1}{2}} \exp(-\rho t)[h(t)+h(1-t)]dt. \tag{14}$$

Thus, the second inequality of (9) holds. This completes the proof. □

Corollary 1. *Under the conditions of Theorem 4, for $\beta \to 1$, we obtain*

$$g\big(\frac{m+n}{2}\big) \le \frac{2h(\frac{1}{2})}{n-m}\int_m^n g(x)dx \le [g(m)+g(n)]2h(\frac{1}{2})\int_0^{\frac{1}{2}}[h(t)+h(1-t)]dt. \tag{15}$$

Proof. By (9), that is

$$\begin{aligned}g\big(\frac{m+n}{2}\big) &\le \frac{h(\frac{1}{2})(1-\beta)}{1-\exp(-\frac{\rho}{2})}\Big(\mathcal{I}^{\beta}_{\frac{m+n}{2}+}g(n)+\mathcal{I}^{\beta}_{\frac{m+n}{2}-}g(m)\Big)\\ &\le [g(m)+g(n)]\frac{\rho h(\frac{1}{2})}{1-\exp(-\frac{\rho}{2})}\int_0^{\frac{1}{2}} \exp(-\rho t)[h(t)+h(1-t)]dt.\end{aligned} \tag{16}$$

By calculating, we have

$$\lim_{\beta\to 1}\frac{1-\beta}{1-\exp(-\frac{\rho}{2})}=\frac{2}{n-m},$$

and

$$\lim_{\beta\to 1}\frac{\rho\exp(-\rho t)}{1-\exp(-\frac{\rho}{2})}=2.$$

Thus, from the inequality (16) for $\beta \to 1$, we obtain the inequality (15). □

Remark 2. *Taking $h(t)=t$ in (15), we obtain the classical Hermite–Hadamard inequality for convex function (2).*

Corollary 2. *If we take $h(t) = t$ in Theorem 4, then the following fractional integral inequality for the convex function is obtained.*

$$g\Big(\frac{m+n}{2}\Big) \leq \frac{1-\beta}{2\big(1-\exp(-\frac{\rho}{2})\big)}\Big(\mathcal{I}^{\beta}_{\frac{m+n}{2}^{+}}g(n) + \mathcal{I}^{\beta}_{\frac{m+n}{2}^{-}}g(m)\Big) \leq \frac{g(m)+g(n)}{2}, \tag{17}$$

which is Theorem 2 proved by Budak in ref. [26].

In order to obtain our results, according to Lemma 1 in ref. [26], we can obtain the following identity.

Lemma 1 ([26])**.** *Let $g : [m,n] \to \mathbb{R}$ be a differentiable function with $m < n$. If $g' \in L[m,n]$, then the following identity involving fractional integral operators (3) and (4) holds.*

$$\begin{aligned} &g\Big(\frac{m+n}{2}\Big) - \frac{1-\beta}{2\Big(1-\exp\big(-\frac{\rho}{2}\big)\Big)}\Big(\mathcal{I}^{\beta}_{\frac{m+n}{2}^{+}}g(n) + \mathcal{I}^{\beta}_{\frac{m+n}{2}^{-}}g(m)\Big) \\ =&\frac{n-m}{2\Big(1-\exp(-\frac{\rho}{2})\Big)}\Bigg[\int_0^{\frac{1}{2}}\big(\exp(-\rho t)-1\big)g'\Big(tm+(1-t)n\Big)dt \\ &+\int_{\frac{1}{2}}^{1}\big(1-\exp(-\rho(1-t))\big)g'\Big(tm+(1-t)n\Big)dt\Bigg]. \end{aligned} \tag{18}$$

Theorem 5. *Let $g : [m,n] \to \mathbb{R}$ be a differentiable function with $m < n$. If $g'(u) \in L[m,n]$, and $|g'|$ is h-convex on $[m,n]$, then the following fractional integral inequality holds.*

$$\begin{aligned} &\left|g\Big(\frac{m+n}{2}\Big) - \frac{1-\beta}{2\Big(1-\exp\big(-\frac{\rho}{2}\big)\Big)}\Big(\mathcal{I}^{\beta}_{\frac{m+n}{2}^{+}}g(n) + \mathcal{I}^{\beta}_{\frac{m+n}{2}^{-}}g(m)\Big)\right| \\ \leq&\frac{n-m}{2\Big(1-\exp(-\frac{\rho}{2})\Big)}\int_0^{\frac{1}{2}}\big(1-\exp(-\rho t)\big)\Big(h(t)+h(1-t)\Big)\Big(|g'(m)|+|g'(n)|\Big)dt. \end{aligned} \tag{19}$$

Proof. Since $|g'|$ is h-convex on $[m,n]$ and h is a nonnegative function, by Lemma 1, we obtain

$$
\begin{aligned}
&\left|g\left(\frac{m+n}{2}\right)-\frac{1-\beta}{2\Big(1-\exp\left(-\frac{\rho}{2}\right)\Big)}\left(\mathcal{I}^{\beta}_{\frac{m+n}{2}^{+}}g(n)+\mathcal{I}^{\beta}_{\frac{m+n}{2}^{-}}g(m)\right)\right| \\
\leq&\frac{n-m}{2\Big(1-\exp(-\frac{\rho}{2})\Big)}\left[\int_0^{\frac{1}{2}}\left(1-\exp(-\rho t)\right)\left|g'\Big(tm+(1-t)n\Big)\right|dt\right. \\
&\left.+\int_{\frac{1}{2}}^{1}\left(1-\exp(-\rho(1-t))\right)\left|g'\Big(tm+(1-t)n\Big)\right|dt\right] \\
=&\frac{n-m}{2\Big(1-\exp(-\frac{\rho}{2})\Big)}\left[\int_0^{\frac{1}{2}}\left(1-\exp(-\rho t)\right)\left|g'\Big(tm+(1-t)n\Big)\right|dt\right. \\
&\left.+\int_0^{\frac{1}{2}}\left(1-\exp(-\rho t)\right)\left|g'\Big((1-t)m+tn\Big)\right|dt\right] \\
\leq&\frac{n-m}{2\Big(1-\exp(-\frac{\rho}{2})\Big)}\left[\int_0^{\frac{1}{2}}\left(1-\exp(-\rho t)\right)\Big(h(t)|g'(m)|+h(1-t)|g'(n)|\Big)dt\right. \\
&\left.+\int_0^{\frac{1}{2}}\left(1-\exp(-\rho t)\right)\Big(h(1-t)|g'(m)|+h(t)|g'(n)|\Big)dt\right] \\
=&\frac{n-m}{2\Big(1-\exp(-\frac{\rho}{2})\Big)}\int_0^{\frac{1}{2}}\left(1-\exp(-\rho t)\right)\Big(h(t)+h(1-t)\Big)\Big(|g'(m)|+|g'(n)|\Big)dt. \qquad (20)
\end{aligned}
$$

This completes the proof. □

Remark 3. *For $\beta \to 1$, by calculating, we obtain*

$$\lim_{\beta\to 1}\frac{1-\beta}{2[1-\exp(-\frac{\rho}{2})]}=\frac{1}{n-m},$$

and

$$\lim_{\beta\to 1}\frac{1-\exp(-\rho t)}{2\Big(1-\exp(-\frac{\rho}{2})\Big)}=t.$$

Thus, from the inequality (19) for $\beta \to 1$, we obtain the following inequality

$$\left|g\left(\frac{m+n}{2}\right)-\frac{1}{n-m}\int_m^n g(u)du\right|\leq(n-m)\Big(|g'(m)|+|g'(n)|\Big)\int_0^{\frac{1}{2}}t\Big(h(t)+h(1-t)\Big)dt. \qquad (21)$$

Remark 4. *Taking $h(t)=t$ in (21), we obtain the following inequality*

$$\left|g\left(\frac{m+n}{2}\right)-\frac{1}{n-m}\int_m^n g(u)du\right|\leq\frac{n-m}{8}\Big(|g'(m)|+|g'(n)|\Big),$$

which is Theorem 2.2 proved by U. Kirmaci in ref. [30].

Corollary 3. *If we take $h(t) = t$ in Theorem 5, then the following fractional integral inequality for convex function is obtained.*

$$\begin{aligned}&\left|g\big(\frac{m+n}{2}\big) - \frac{1-\beta}{2\Big(1-\exp\big(-\frac{\rho}{2}\big)\Big)}\Big(\mathcal{I}^{\beta}_{\frac{m+n}{2}^{+}}g(n) + \mathcal{I}^{\beta}_{\frac{m+n}{2}^{-}}g(m)\Big)\right| \\ \leq &\frac{n-m}{2\Big(1-\exp(-\frac{\rho}{2})\Big)}\Big(|g'(m)| + |g'(n)|\Big)\Big(\frac{1}{2} + \frac{\exp(-\frac{\rho}{2})-1}{\rho}\Big). \end{aligned} \tag{22}$$

Proof. If $h(t) = t$, by (19) we obtain

$$\begin{aligned}&\int_0^{\frac{1}{2}} \big(1-\exp(-\rho t)\big)\Big(h(t) + h(1-t)\Big)dt \\ =&\int_0^{\frac{1}{2}} \big(1-\exp(-\rho t)\big)dt \\ =&\frac{1}{2} + \frac{\exp(-\frac{\rho}{2})-1}{\rho}.\end{aligned}$$

This completes the proof. □

Lemma 2. *Let $g : [m,n] \to \mathbb{R}$ be a twice differentiable function on $[m,n]$ with $m < n$. If $g''(x) \in L[m,n]$, then the following identity involving fractional integral operators (3) and (4) holds.*

$$\begin{aligned}&g\big(\frac{m+n}{2}\big) - \frac{1-\beta}{2\Big(1-\exp\big(-\frac{\rho}{2}\big)\Big)}\Big(\mathcal{I}^{\beta}_{\frac{m+n}{2}^{+}}g(n) + \mathcal{I}^{\beta}_{\frac{m+n}{2}^{-}}g(m)\Big) \\ =&\frac{(n-m)^2}{2\Big(1-\exp(-\frac{\rho}{2})\Big)}\left[\int_0^{\frac{1}{2}}\Big(\frac{1-\exp(-\rho t)}{\rho} - t\Big)g''\Big(tm + (1-t)n\Big)dt \right. \\ &\left. + \int_{\frac{1}{2}}^{1}\Big(\frac{1-\exp(-\rho(1-t))}{\rho} - (1-t)\Big)g''\Big(tm + (1-t)n\Big)dt\right].\end{aligned} \tag{23}$$

Proof. Using integration by parts, we have

$$\begin{aligned}&\int_0^{\frac{1}{2}} \big(\exp(-\rho t) - 1\big)g'\Big(tm + (1-t)n\Big)dt \\ =&\int_0^{\frac{1}{2}} \exp(-\rho t)g'\Big(tm + (1-t)n\Big)dt - \int_0^{\frac{1}{2}} g'\Big(tm + (1-t)n\Big)dt \\ =&-\frac{1}{\rho}\left[\int_0^{\frac{1}{2}} g'\Big(tm + (1-t)n\Big)d\big(\exp(-\rho t)\big)\right] - \int_0^{\frac{1}{2}} g'\Big(tm + (1-t)n\Big)dt \\ =&-\frac{1}{\rho}\left[\exp(-\frac{\rho}{2})g'(\frac{m+n}{2}) - g'(n) - (m-n)\int_0^{\frac{1}{2}}\exp(-\rho t)g''\Big(tm + (1-t)n\Big)dt\right] \\ &-\frac{1}{2}g'(\frac{m+n}{2}) + (m-n)\int_0^{\frac{1}{2}} tg''\Big(tm + (1-t)n\Big)dt.\end{aligned} \tag{24}$$

Similarly, one has

$$
\begin{aligned}
&\int_{\frac{1}{2}}^{1}(1-\exp(-\rho(1-t)))g'\Big(tm+(1-t)n\Big)dt\\
=&\int_{\frac{1}{2}}^{1}g'\Big(tm+(1-t)n\Big)dt-\int_{\frac{1}{2}}^{1}\exp(-\rho(1-t))g'\Big(tm+(1-t)n\Big)dt\\
=&\int_{\frac{1}{2}}^{1}g'\Big(tm+(1-t)n\Big)dt-\frac{1}{\rho}\int_{\frac{1}{2}}^{1}g'\Big(tm+(1-t)n\Big)d\big(\exp(-\rho(1-t))\big)\\
=&g'(m)-\frac{1}{2}g'(\frac{m+n}{2})-(m-n)\int_{\frac{1}{2}}^{1}tg''\Big(tm+(1-t)n\Big)dt\\
&-\frac{1}{\rho}\Big[g'(m)-\exp(-\frac{\rho}{2})g'(\frac{m+n}{2})-(m-n)\int_{\frac{1}{2}}^{1}\exp(-\rho(1-t))g''\Big(tm+(1-t)n\Big)dt\Big].
\end{aligned}
\tag{25}
$$

Adding (24) and (25), we obtain

$$
\begin{aligned}
&\int_{0}^{\frac{1}{2}}\big(\exp(-\rho t)-1\big)g'\Big(tm+(1-t)n\Big)dt+\int_{\frac{1}{2}}^{1}(1-\exp(-\rho(1-t)))g'\Big(tm+(1-t)n\Big)dt\\
=&g'(m)-g'(\frac{m+n}{2})+(m-n)\int_{0}^{\frac{1}{2}}tg''\Big(tm+(1-t)n\Big)dt-(m-n)\int_{\frac{1}{2}}^{1}tg''\Big(tm+(1-t)n\Big)dt\\
&-\frac{1}{\rho}\Big[g'(m)-g'(n)-(m-n)\int_{0}^{\frac{1}{2}}\exp(-\rho t)g''\Big(tm+(1-t)n\Big)dt\\
&-(m-n)\int_{\frac{1}{2}}^{1}\exp(-\rho(1-t))g''\Big(tm+(1-t)n\Big)dt\Big]\\
=&(m-n)\int_{\frac{1}{2}}^{1}g''\Big(tm+(1-t)n\Big)dt+(m-n)\int_{0}^{\frac{1}{2}}\Big(t+\frac{\exp(-\rho t)}{\rho}\Big)g''\Big(tm+(1-t)n\Big)dt\\
&-\frac{m-n}{\rho}\int_{0}^{1}g''\Big(tm+(1-t)n\Big)dt-(m-n)\int_{\frac{1}{2}}^{1}\Big(t-\frac{\exp(-\rho(1-t))}{\rho}\Big)g''\Big(tm+(1-t)n\Big)dt\\
=&(m-n)\int_{0}^{\frac{1}{2}}\Big(t-\frac{1-\exp(-\rho t)}{\rho}\Big)g''\Big(tm+(1-t)n\Big)dt\\
&+(m-n)\int_{\frac{1}{2}}^{1}\Big(1-t-\frac{1-\exp(-\rho(1-t))}{\rho}\Big)g''\Big(tm+(1-t)n\Big)dt
\end{aligned}
\tag{26}
$$

$$
\begin{aligned}
=&(n-m)\int_{0}^{\frac{1}{2}}\Big(\frac{1-\exp(-\rho t)}{\rho}-t\Big)g''\Big(tm+(1-t)n\Big)dt\\
&+(n-m)\int_{\frac{1}{2}}^{1}\Big(\frac{1-\exp(-\rho(1-t))}{\rho}+t-1\Big)g''\Big(tm+(1-t)n\Big)dt.
\end{aligned}
$$

Substituting (26) into (18), we have

$$
\begin{aligned}
&g(\frac{m+n}{2})-\frac{1-\beta}{2\Big(1-\exp\big(-\frac{\rho}{2}\big)\Big)}\Big(\mathcal{I}^{\beta}_{\frac{m+n}{2}^{+}}g(n)+\mathcal{I}^{\beta}_{\frac{m+n}{2}^{-}}g(m)\Big)\\
=&\frac{(n-m)^2}{2\Big(1-\exp(-\frac{\rho}{2})\Big)}\Big[\int_{0}^{\frac{1}{2}}\Big(\frac{1-\exp(-\rho t)}{\rho}-t\Big)g''\Big(tm+(1-t)n\Big)dt\\
&+\int_{\frac{1}{2}}^{1}\Big(\frac{1-\exp(-\rho(1-t))}{\rho}+t-1\Big)g''\Big(tm+(1-t)n\Big)dt\Big].
\end{aligned}
$$

This completes the proof. □

Theorem 6. *Let $g:[m,n]\to\mathbb{R}$ be a twice differentiable function with $m<n$. If $g''(u)\in L[m,n]$, and $|g''|$ is h-convex on $[m,n]$, then the following fractional integral inequality holds.*

$$\left|g\Big(\frac{m+n}{2}\Big)-\frac{1-\beta}{2\Big(1-\exp\left(-\frac{\rho}{2}\right)\Big)}\Big(\mathcal{I}^{\beta}_{\frac{m+n}{2}+}g(n)+\mathcal{I}^{\beta}_{\frac{m+n}{2}-}g(m)\Big)\right|$$
$$\leq\frac{(n-m)^2\Big(|g''(m)|+|g''(n)|\Big)}{2\Big(1-\exp(-\frac{\rho}{2})\Big)}\int_0^{\frac{1}{2}}\Big(\frac{1-\exp(-\rho t)}{\rho}+t\Big)\Big(h(t)+h(1-t)\Big)dt. \tag{27}$$

Proof. Since $|g''|$ is h convex on $[m,n]$, by Lemma 2, we can obtain

$$\left|g\Big(\frac{m+n}{2}\Big)-\frac{1-\beta}{2\Big(1-\exp\left(-\frac{\rho}{2}\right)\Big)}\Big(\mathcal{I}^{\beta}_{\frac{m+n}{2}+}g(n)+\mathcal{I}^{\beta}_{\frac{m+n}{2}-}g(m)\Big)\right|$$
$$\leq\frac{(n-m)^2}{2\Big(1-\exp(-\frac{\rho}{2})\Big)}\left[\int_0^{\frac{1}{2}}\left|\frac{1-\exp(-\rho t)}{\rho}-t\right|\Big|g''\Big(tm+(1-t)n\Big)\Big|dt\right.$$
$$\left.+\int_{\frac{1}{2}}^{1}\left|\frac{1-\exp(-\rho(1-t))}{\rho}-(1-t)\right|\Big|g''\Big(tm+(1-t)n\Big)\Big|dt\right]$$
$$=\frac{(n-m)^2}{2\Big(1-\exp(-\frac{\rho}{2})\Big)}\left[\int_0^{\frac{1}{2}}\left|\frac{1-\exp(-\rho t)}{\rho}-t\right|\Big|g''\Big(tm+(1-t)n\Big)\Big|dt\right.$$
$$\left.+\int_0^{\frac{1}{2}}\left|\frac{1-\exp(-\rho t)}{\rho}-t\right|\Big|g''\Big((1-t)m+tn\Big)\Big|dt\right]$$

$$=\frac{(n-m)^2}{2\Big(1-\exp(-\frac{\rho}{2})\Big)}\int_0^{\frac{1}{2}}\left|\frac{1-\exp(-\rho t)}{\rho}-t\right|\Big(\Big|g''\Big(tm+(1-t)n\Big)\Big|+\Big|g''\Big((1-t)m+tn\Big)\Big|\Big)dt$$
$$\leq\frac{(n-m)^2}{2\Big(1-\exp(-\frac{\rho}{2})\Big)}\int_0^{\frac{1}{2}}\Big(\frac{1-\exp(-\rho t)}{\rho}+t\Big)\Big(h(t)+h(1-t)\Big)\Big(|g''(m)|+|g''(n)|\Big)dt. \tag{28}$$

This completes the proof. □

Corollary 4. *If we take $h(t)=t$ in Theorem 6, then the following fractional integral inequality for convex function is obtained.*

$$\left|g\Big(\frac{m+n}{2}\Big)-\frac{1-\beta}{2\Big(1-\exp\left(-\frac{\rho}{2}\right)\Big)}\Big(\mathcal{I}^{\beta}_{\frac{m+n}{2}+}g(n)+\mathcal{I}^{\beta}_{\frac{m+n}{2}-}g(m)\Big)\right|$$
$$\leq\frac{(n-m)^2\Big(|g''(m)|+|g''(n)|\Big)}{2\Big(1-\exp(-\frac{\rho}{2})\Big)}\Big(\frac{1}{2\rho}+\frac{\exp(-\frac{\rho}{2})-1}{\rho^2}+\frac{1}{8}\Big). \tag{29}$$

Proof. By $h(t)=t$ and the proof of Corollary 3, it is easy to obtain the desired result. □

3. Numerical Examples

To illustrate our main conclusions, we will present four examples to show these conclusions in this section.

Example 1. *From Corollary 2, we get the following inequalities*

$$\frac{2(1-\exp(-\frac{\rho}{2}))}{1-\beta}g(\frac{m+n}{2}) \leq \left(\mathcal{I}^{\beta}_{\frac{m+n}{2}+}g(n)+\mathcal{I}^{\beta}_{\frac{m+n}{2}-}g(m)\right) \leq \frac{1-\exp(-\frac{\rho}{2})}{1-\beta}[g(m)+g(n)].$$

Taking $g(\xi) = e^{2\xi}$, we know that g is an h-convex function for $h(t) = t$. It meets the conditions of Corollary 2 for $\beta \in [0,1]$. If we choose $m = 1, n = 3$, then the following formulas are drawn.

$$\begin{aligned}
\frac{2(1-\exp(-\frac{\rho}{2}))}{1-\beta}g(\frac{m+n}{2}) =& \frac{1-\exp(-\frac{\rho}{2})}{1-\beta}2e^4,\\
\left(\mathcal{I}^{\beta}_{\frac{m+n}{2}+}g(n)+\mathcal{I}^{\beta}_{\frac{m+n}{2}-}g(m)\right) =& \frac{1}{\beta}\Big[\int_2^3 \exp\Big(-\frac{1-\beta}{\beta}(3-u)\Big)e^{2u}du\\
&+\int_1^2 \exp\Big(-\frac{1-\beta}{\beta}(u-1)\Big)e^{2u}du\Big],\\
=& \frac{e^6-e^{5-\frac{1}{\beta}}}{\beta+1}-\frac{e^2-e^{5-\frac{1}{\beta}}}{3\beta-1},\\
\frac{1-\exp(-\frac{\rho}{2})}{1-\beta}[g(m)+g(n)] =& \frac{1-\exp(-\frac{\rho}{2})}{1-\beta}(e^2+e^6).
\end{aligned}$$

We plot the function image of the above three functions for $\beta \in [0,1]$, as shown in Figure 1. From the position relationship of the image, we can see that the middle term of the inequalities is just between the left and right images, and the left image is at the bottom, and the right image is at the top. These show that the inequalities relationship in Corollary 2 is tenable.

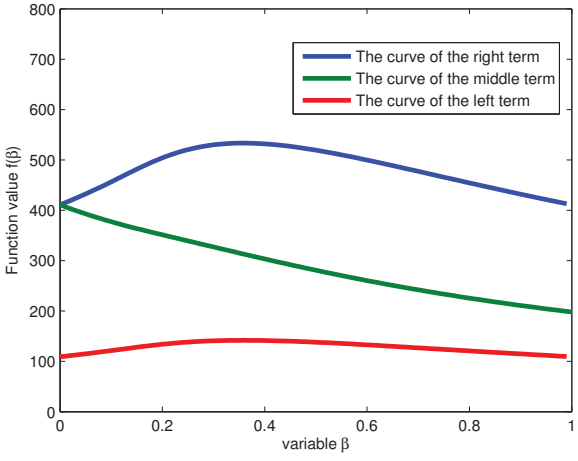

Figure 1. The image description of Corollary 2 for $h(t) = t$ and $g(\xi) = e^{2\xi}$.

Specidically, if we choose $\beta = \frac{1}{2}$, then we have

$$\begin{aligned}
\frac{2(1-\exp(-\frac{\rho}{2}))}{1-\beta}g(\frac{m+n}{2}) =& 138.0505,\\
\left(\mathcal{I}^{\beta}_{\frac{m+n}{2}+}g(n)+\mathcal{I}^{\beta}_{\frac{m+n}{2}-}g(m)\right) =& 280.9551,\\
\frac{1-\exp(-\frac{\rho}{2})}{1-\beta}[g(m)+g(n)] =& = 519.3728.
\end{aligned}$$

This further verifies that the conclusion of Corollary 2 is correct.

Example 2. *From Corollary 3, we get the following inequalities*

$$\left|\frac{2\left(1-\exp\left(-\frac{\rho}{2}\right)\right)}{1-\beta}g\left(\frac{m+n}{2}\right)-\left(\mathcal{I}^{\beta}_{\frac{m+n}{2}+}g(n)+\mathcal{I}^{\beta}_{\frac{m+n}{2}-}g(m)\right)\right|$$
$$\leq\frac{n-m}{1-\beta}\left(|g'(m)|+|g'(n)|\right)\left(\frac{1}{2}+\frac{\exp(-\frac{\rho}{2})-1}{\rho}\right).$$

Taking $g(\xi)=\xi^3$, we know that $|g'|$ is an h-convex function for $h(t)=t$. It meets the conditions of Corollary 3 for $\beta\in[0,1]$. If we choose $m=1,n=3$, then the following formulas are drawn.

$$\left|\frac{2\left(1-\exp\left(-\frac{\rho}{2}\right)\right)}{1-\beta}g\left(\frac{m+n}{2}\right)-\left(\mathcal{I}^{\beta}_{\frac{m+n}{2}+}g(n)+\mathcal{I}^{\beta}_{\frac{m+n}{2}-}g(m)\right)\right|$$
$$=\left|\frac{2\left(1-\exp(-\frac{\rho}{2})\right)}{1-\beta}g(2)-\frac{1}{\beta}\left[\int_2^3\exp\left(-\frac{1-\beta}{\beta}(3-u)\right)u^3du+\int_1^2\exp\left(-\frac{1-\beta}{\beta}(u-1)\right)u^3du\right]\right|$$
$$=\left|\frac{16\left(1-\exp(-\frac{\rho}{2})\right)}{1-\beta}-\frac{-76\beta^3+156\beta^2-108\beta+28}{(\beta-1)^4}-\frac{\exp(1-\frac{1}{\beta})(40\beta^3-72\beta^2+48\beta-16)}{(\beta-1)^4}\right|,$$

$$\frac{n-m}{1-\beta}\left(|g'(m)|+|g'(n)|\right)\left(\frac{1}{2}+\frac{\exp(-\frac{\rho}{2})-1}{\rho}\right)=\frac{60}{1-\beta}\left(\frac{1}{2}+\frac{\exp(-\frac{\rho}{2})-1}{\rho}\right).$$

We plot the function image of the above two functions for $\beta\in[0,1]$, as shown in Figure 2. From the position relationship of the image, we can see that the left image is at the bottom, and the right image is at the top. These show that the inequality relationship in Corollary 3 is tenable.

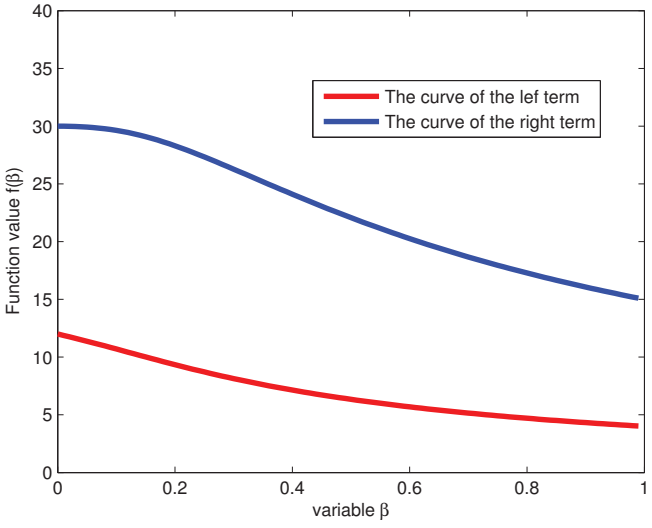

Figure 2. The image description of Corollary 3 for $h(t)=t$ and $g(\xi)=\xi^3$.

Specifically, if we choose $\beta = \frac{1}{3}$, then we have

$$\left|\frac{2\Big(1-\exp\left(-\frac{\rho}{2}\right)\Big)}{1-\beta}g\Big(\frac{m+n}{2}\Big) - \Big(\mathcal{I}^{\beta}_{\frac{m+n}{2}^{+}}g(n) + \mathcal{I}^{\beta}_{\frac{m+n}{2}^{-}}g(m)\Big)\right| = 7.7820,$$

$$\frac{n-m}{1-\beta}\Big(|g'(m)| + |g'(n)|\Big)\Big(\frac{1}{2} + \frac{\exp(-\frac{\rho}{2})-1}{\rho}\Big) = 25.5450.$$

This further verifies that the conclusion of Corollary 3 is correct.

Example 3. *From Corollary 4, we get the following inequalities*

$$\begin{aligned}&\left|\frac{2\Big(1-\exp\left(-\frac{\rho}{2}\right)\Big)}{1-\beta}g\Big(\frac{m+n}{2}\Big) - \Big(\mathcal{I}^{\beta}_{\frac{m+n}{2}^{+}}g(n) + \mathcal{I}^{\beta}_{\frac{m+n}{2}^{-}}g(m)\Big)\right|\\ \leq&\frac{(n-m)^2}{1-\beta}\Big(|g''(m)| + |g''(n)|\Big)\Big(\frac{1}{2\rho} + \frac{\exp(-\frac{\rho}{2})-1}{\rho^2} + \frac{1}{8}\Big).\end{aligned}$$

Taking $g(\xi) = e^{3\xi}$, we know that $|g''|$ is an h-convex function for $h(t) = t$. It meets the conditions of Corollary 4 for $\beta \in [0,1]$. If we choose $m = 1, n = 3$, then the following formulas are drawn.

$$\begin{aligned}&\left|\frac{2\Big(1-\exp\left(-\frac{\rho}{2}\right)\Big)}{1-\beta}g\Big(\frac{m+n}{2}\Big) - \Big(\mathcal{I}^{\beta}_{\frac{m+n}{2}^{+}}g(n) + \mathcal{I}^{\beta}_{\frac{m+n}{2}^{-}}g(m)\Big)\right|\\ =&\left|\frac{2\Big(1-\exp(-\frac{\rho}{2})\Big)}{1-\beta}g(2) - \frac{1}{\beta}\Big[\int_2^3 \exp\Big(-\frac{1-\beta}{\beta}(3-u)\Big)e^{3u}du + \int_1^2 \exp\Big(-\frac{1-\beta}{\beta}(u-1)\Big)e^{3u}du\Big]\right|\\ =&\left|\frac{(2e^6)\Big(1-\exp(-\frac{\rho}{2})\Big)}{1-\beta} - \frac{e^9 - e^{7-\frac{1}{\beta}}}{2\beta+1} + \frac{e^3 - e^{7-\frac{1}{\beta}}}{4\beta-1}\right|,\end{aligned}$$

$$\frac{(n-m)^2}{1-\beta}\Big(|g''(m)| + |g''(n)|\Big)\Big(\frac{1}{2\rho} + \frac{\exp(-\frac{\rho}{2})-1}{\rho^2} + \frac{1}{8}\Big) = \frac{4(9e^9+9e^3)}{1-\beta}\Big(\frac{1}{2\rho} + \frac{\exp(-\frac{\rho}{2})-1}{\rho^2} + \frac{1}{8}\Big).$$

We only plot the function image of the above two functions for $\beta \in [0, 0.5]$, as shown in Figure 3. From the position relationship of the image, we can see that the left image is at the bottom, and the right image is at the top. These show that the inequality relationship in Corollary 4 is tenable for $\beta \in [0,1]$, because the growth rate of the right term is much faster than that of the left term in interval $\beta \in [0.5, 1]$.

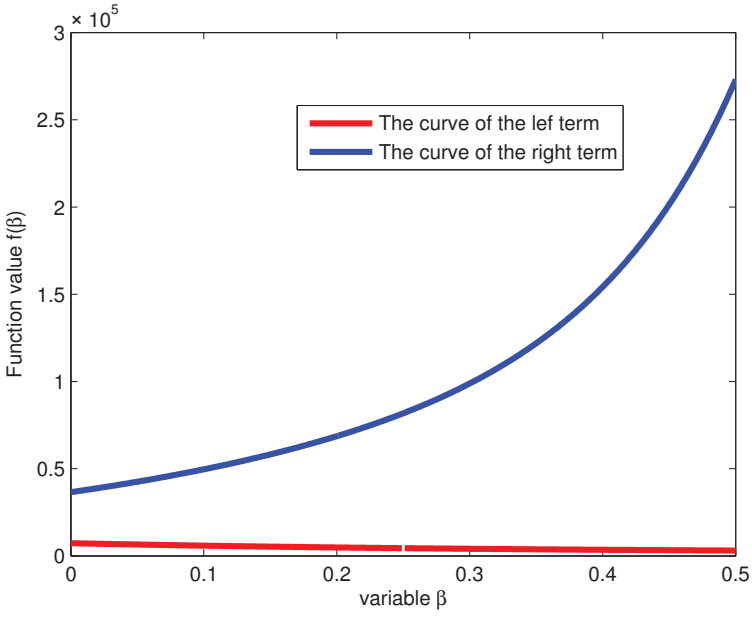

Figure 3. The image description of Corollary 4 for $h(t) = t$ and $g(\xi) = e^{3\xi}$.

Specifically, if we choose $\beta = 0.01$, then we have

$$\left|\frac{2\left(1-\exp\left(-\frac{\rho}{2}\right)\right)}{1-\beta}g\left(\frac{m+n}{2}\right) - \left(\mathcal{I}^{\beta}_{\frac{m+n}{2}+}g(n) + \mathcal{I}^{\beta}_{\frac{m+n}{2}-}g(m)\right)\right| = 7150.1,$$

$$\frac{(n-m)^2}{1-\beta}\left(|g''(m)| + |g''(n)|\right)\left(\frac{1}{2\rho} + \frac{\exp(-\frac{\rho}{2})-1}{\rho^2} + \frac{1}{8}\right) = 37669.$$

This further verifies that the conclusion of Corollary 4 is correct.

Example 4. *Taking $g(\xi) = e^{2\xi}$ and $h(t) = e^t$ for $t \in [0,1]$, we know that g is an h-convex function by Remark 5 in ref. [29]. It meets the conditions of Theorem 4 for $\beta \in [0,1]$. If we choose $m = 2, n = 4$, then the following formulas are drawn.*

$$\begin{aligned}
\frac{1-\exp(-\frac{\rho}{2})}{\rho h(\frac{1}{2})}g\left(\frac{m+n}{2}\right) &= \frac{1-\exp(-\frac{\rho}{2})}{\rho e^{\frac{1}{2}}}e^6 = \frac{\left[1-\exp(-\frac{1-\beta}{\beta})\right]\beta}{2(1-\beta)}e^{\frac{11}{2}},\\
\frac{\beta}{n-m}\left(\mathcal{I}^{\beta}_{\frac{m+n}{2}+}g(n) + \mathcal{I}^{\beta}_{\frac{m+n}{2}-}g(m)\right) &= \frac{1}{2}\Big[\int_3^4 \exp\Big(-\frac{1-\beta}{\beta}(4-u)\Big)e^{2u}du\\
&\quad + \int_2^3 \exp\Big(-\frac{1-\beta}{\beta}(u-2)\Big)e^{2u}du\Big],\\
&= \frac{\beta}{2}\Big[\frac{e^8 - e^{7-\frac{1}{\beta}}}{\beta+1} - \frac{e^4 - e^{7-\frac{1}{\beta}}}{3\beta-1}\Big],\\
[g(m)+g(n)]\int_0^{\frac{1}{2}}\exp(-\rho t)[h(t)+h(1-t)]dt &= [g(2)+g(4)]\int_0^{\frac{1}{2}}\exp(-\rho t)[e^t + e^{(1-t)}]dt\\
&= (e^4+e^8)\beta\Big[\frac{\exp(\frac{3}{2}-\frac{1}{\beta})-1}{3\beta-2} - \frac{e-\exp(\frac{3}{2}-\frac{1}{\beta})}{\beta-2}\Big].
\end{aligned}$$

We plot the function image of the above three functions for $\beta \in [0,1]$, as shown in Figure 4. From the position relationship of the image, we can see that the middle term of the inequalities is just between the left and right images, and the left image is at the bottom, and the right image is at the top. These show that the inequalities relationship in Theorem 4 for $h(t) = e^t$ is tenable.

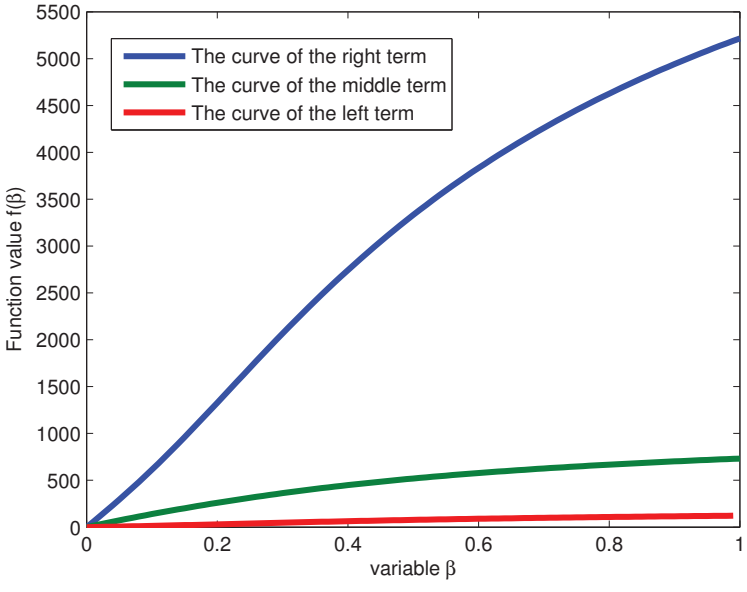

Figure 4. The image description of Theorem 2 for $h(t) = e^t$ and $g(\xi) = e^{2\xi}$.

Specifically, if we choose $\beta = 0.001$, then we have

$$\frac{1-\exp(-\frac{\rho}{2})}{\rho h(\frac{1}{2})} g\left(\frac{m+n}{2}\right) = 0.1225,$$

$$\frac{\beta}{n-m}\left(\mathcal{I}^{\beta}_{\frac{m+n}{2}+} g(n) + \mathcal{I}^{\beta}_{\frac{m+n}{2}-} g(m)\right) = 1.5164,$$

$$[g(m)+g(n)]\int_0^{\frac{1}{2}} \exp(-\rho t)[h(t)+h(1-t)]dt = [g(2)+g(4)]\int_0^{\frac{1}{2}} \exp(-\rho t)[e^t + e^{(1-t)}]dt = 5.6479.$$

This further verifies that the conclusion of Theorem 4 is correct.

4. Conclusions and Discussion

In this study, using two integral operators with exponential kernel proposed by Ahmad et al. in ref. [24], we establish the new Hermite–Hadamard's integral inequality for h-convex functions. Two midpoint type inequalities are also obtained in which the absolute values of the first derivative and the second derivative of the function are h-convex functions, respectively. The integral operators (3) and (4) involved in the results obtained in this paper are integral operators about the same midpoint of the interval, which is different from the integral operators about the two ends of the interval used in refs [24,25]. For different cases of $h(t) = t$ and $h(t) = e^t$, we construct four numerical examples that intuitively show the size relationship of the function values of the inequalities through the function image, and verify the correctness of the results.

Because fractional integral operators are widely used in the field of engineering technology, such as mathematical models, and different integral operators are suitable for different types of practical problems, our research on the fractional integral operator-

type integral inequalities will also expand the practical application scope of Hermite–Hadamard-type inequalities. We know that there are many fractional integral operators involved in other disciplines, which will also inspire us to use other types of integral operators to further study these kinds of inequalities, which also provide a direction for our future research.

Funding: This research received no external funding.

Institutional Review Board Statement: Not applicable.

Informed Consent Statement: Not applicable.

Data Availability Statement: Not applicable.

Conflicts of Interest: The author declares no conflict interest.

References

1. Jensen, J.L.W.V. Sur les functions convexes et les inegalites entre les valeurs moyennes. *Acta Math.* **1906**, *30*, 175–193. [CrossRef]
2. Hadamard, J. Etude sur les proprietes des fonctions entieres et en particulier d'une fonction considree par Riemann. *J. Math. Pures Appl.* **1893**, *58*, 171–215.
3. Hermite, C.H. Sur deux limites d'une integrale definie. *Mathesis* **1883**, *3*, 82.
4. Kashuri, A.; Iqbal, S.; Liko, R.; Gao, W.; Samraiz, M. Integral inequalities for s-convex functions via generalized conformable fractional integral operators. *Adv. Differ. Equ.* **2020**, *217*, 1–20. [CrossRef]
5. Han, J.; Mohammed, P.O.; Zeng, H. Generalized fractional integral inequalities of Hermite-CHadamard-type for a convex function. *Open Math.* **2020**, *18*, 794–806. [CrossRef]
6. Noor, M.A.; Noor, K.I.; Rashid, S. Some new class of preinvex functions and inequalities. *Mathematics* **2019**, *7*, 29. [CrossRef]
7. Sun, W.B.; Liu, Q. New Hermite-Hadamard type inequalities for (α, m)-convex functions and applications to special means. *J. Math. Inequal* **2017**, *11*, 383–394. [CrossRef]
8. Işcan, I. Hermite-CHadamard type inequalities for harmonically convex functions. *Hacet. J. Math. Stat.* **2014**, *43*, 935–942.
9. Liao, J.G.; Wu, S.H.; Du, T.S. The Sugeno integral with respect to α-preinvex functions. *Fuzzy Sets Syst.* **2020**, *379*, 102–114. [CrossRef]
10. Delavar, M.R.; De La Sen, M. A mapping associated to h-convex version of the Hermite-CHadamard inequality with applications. *J. Math. Inequal.* **2020**, *14*, 329–335. [CrossRef]
11. Sarikaya, M.Z.; Set, E.; Yaldiz, H.; Başak, N. Hermite-Hadamard's inequalities for fractional integrals and related fractional inequalities. *Math. Comput. Model.* **2013**, *57*, 2403–2407. [CrossRef]
12. Ozdemir, M.E.; Dragomir, S.S.; Yıldız, Ç. The Hadamard inequalities for convex function via fractional integrals. *Acta Math. Sci.* **2013**, *33*, 1293–1299. [CrossRef]
13. Srivastava, H.M.; Sahoo, S.K.; Mohammed, P.O.; Kodamasingh, B.; Hamed, Y.S. New Riemann-CLiouville fractional-order inclusions for convex functions via interval-valued settings associated with pseudo-order relations. *Fractal Fract.* **2022**, *6*, 212. [CrossRef]
14. Awan, M.U.; Kashuri, A.; Nisar, K.S.; Javed, M.Z.; Iftikhar, S.; Kumam, P.; Chaipunya, P. New fractional identities, associated novel fractional inequalities with applications to means and error estimations for quadrature formulas. *J. Inequalities Appl.* **2022**, *2022*, 3. [CrossRef]
15. Set, E.; Sarikaya, M.Z.; G$\ddot{}$ozpinar, A. Some Hermite-CHadamard type inequalities for convex functions via conformable fractional integrals and related inequalities. *Creat. Math. Inform.* **2017**, *26*, 221–229. [CrossRef]
16. Du, T.S.; Awan, M.U.; Kashuri, A.; Zhao, S.S. Some k-fractional extensions of the trapezium inequalities through generalized relative semi-(m, h)-preinvexity. *Appl. Anal.* **2021**, *100*, 642–662. [CrossRef]
17. Du, T.S.; Wang, H.; Khan, M.A.; Zhang, Y. Certain integral inequalities considering generalized m-convexity on fractal sets and their applications. *Fractals* **2019**, *27*, 1950117. [CrossRef]
18. Sun, W.B. Some new inequalities for generalized h-convex functions involving local fractional integral operators with Mittag-Leffler kernel. *Math. Meth. Appl. Sci.* **2021**, *44*, 4985–4998. [CrossRef]
19. Sun, W.B. Hermite-Hadamard type local fractional integral inequalities for generalized s-preinvex functions and their generalization. *Fractals* **2021**, *29*, 2150098. [CrossRef]
20. Set, E.; Çelik, B.; Ozdemir, M.E.; Aslan, M. Some new results on Hermite-CHadamard-CMercer-type inequalities using a general family of fractional integral operators. *Fractal Fract.* **2021**, *5*, 68. [CrossRef]
21. Srivastava, H.M.; Kashuri, A.; Mohammed, P.O.; Nonlaopon, K. Certain inequalities pertaining to some new generalized fractional integral operators. *Fractal Fract.* **2021**, *5*, 160. [CrossRef]
22. Sun, W.B. Hermite-Hadamard type local fractional integral inequalities with Mittag-Leffler kernel for generalized preinvex functions. *Fractals* **2021**, *29*, 2150253. [CrossRef]

23. Xu, P.; Butt, S.I.; Yousaf, S; Aslam, A; Zia, T.J. Generalized fractal Jensen-CMercer and Hermite-CMercer type inequalities via *h*-convex functions involving Mittag-CLeffler kernel. *Alex. Eng. J.* **2022**, *61*, 4837–4846. [CrossRef]
24. Ahmad, B.; Alsaedi, A.; Kirane, M.; Torebek, B.T. Hermite-Hadamard, Hermite-Hadamard-Fejér, Dragomir-Agarwal and Pachpatte type inequalities for convex functions via new fractional integrals. *J. Comput. Appl. Math.* **2019**, *353*, 120–129. [CrossRef]
25. Wu, X.; Wang, J.R.; Zhang, J. Hermite-CHadamard-type inequalities for convex functions via the fractional integrals with exponential kernel. *Mathematics* **2019**, *7*, 845. [CrossRef]
26. Budak, H.; Sarikaya, M.Z.; Usta, F.; Yildirim, H. Some Hermite-CHadamard and Ostrowski type inequalities for fractional integral operators with exponential kernel. *Acta Comment. Univ. Tartu. Math.* **2019**, *23*, 25–36.
27. Zhou, T.C.; Yuan, Z.R.; Du, T.S. On the fractional integral inclusions having exponential kernels for interval-valued convex functions. *Math. Sci.* **2021**. [CrossRef]
28. Du, T.S.; Zhou, T.C. On the fractional double integral inclusion relations having exponential kernels via interval-valued co-ordinated convex mappings. *Chaos Solitons Fractals* **2022**, *156*, 111846. [CrossRef]
29. Varošanec, S. On *h*-convexity. *J. Math. Anal. Appl.* **2007**, *326*, 303–311. [CrossRef]
30. Kirmaci, U.S. Inequalities for differentiable mappings and applications to special means of real numbers and to midpoint formula. *Appl. Math. Comput.* **2004**, *147*, 137–146. [CrossRef]

fractal and fractional

MDPI

Article

Regularization for a Sideways Problem of the Non-Homogeneous Fractional Diffusion Equation

Yonggang Chen [1,†], Yu Qiao [2,†] and Xiangtuan Xiong [2,*]

[1] School of Science, China University of Petroleum (East China), Qingdao 266580, China; chenyg@upc.edu.cn
[2] Department of Mathematics, Northwest Normal University, Lanzhou 730070, China; 15514358907@163.com
* Correspondence: xiangtuanxion@nwnu.edu.cn
† These authors contributed equally to this work.

Abstract: In this article, we investigate a sideways problem of the non-homogeneous time-fractional diffusion equation, which is highly ill-posed. Such a model is obtained from the classical non-homogeneous sideways heat equation by replacing the first-order time derivative by the Caputo fractional derivative. We achieve the result of conditional stability under an a priori assumption. Two regularization strategies, based on the truncation of high frequency components, are constructed for solving the inverse problem in the presence of noisy data, and the corresponding error estimates are proved.

Keywords: sideways problem; non-homogeneous fractional diffusion equation; ill-posedness; stability estimate; regularization method

Citation: Chen, Y.; Qiao, Y.; Xiong, X. Regularization for a Sideways Problem of the Non-Homogeneous Fractional Diffusion Equation. *Fractal Fract.* **2022**, *6*, 312. https://doi.org/10.3390/fractalfract6060312

Academic Editors: António M. Lopes, Alireza Alfi, Liping Chen and Sergio Adriani David

Received: 11 May 2022
Accepted: 31 May 2022
Published: 2 June 2022

Publisher's Note: MDPI stays neutral with regard to jurisdictional claims in published maps and institutional affiliations.

1. Introduction

Fractional partial differential equations arose from the studies of Lévy motion [1], continuous random walk [2] and high-frequency financial data [3], which has a wide range of applications in some scientific fields, such as chemistry, physics, mechanical engineering, fluid mechanics, signal processing and systems identification, control theory, electron transportation, viscoelasticity, image processing, and so on [4–13]. Moreover, fractional derivatives have been found to be more flexible in describing some practical phenomena than the traditional integer-order derivatives. In particular, fractional diffusion equations play an extremely important role in the study of some anomalous diffusion processes. These equations can describe the dynamics of various non-local and complex systems. Kinds of anomalous diffusion can be modeled by the following time-fractional diffusion equation: find the temperature $u(x,t)$ from known boundary temperature $u(1,t)=\psi(t)$ measurements satisfying the following system

$$\begin{cases} \frac{\partial^\nu u}{\partial t^\nu} - u_{xx} = 0, & x>0, t>0, \\ u(x,0)=0, & x>0, \\ u(1,t)=\psi(t), & t>0, \\ u(x,t)\mid_{x\to\infty} \text{bounded}, \end{cases} \tag{1}$$

where $\psi(t)$ is given function (usually in $L^2(\mathbb{R})$), $\frac{\partial^\nu u}{\partial t^\nu}$ is the Caputo fractional derivative of order ν $(0<\nu\le 1)$ defined by [14]

$$\frac{\partial^\nu u}{\partial t^\nu} = \frac{1}{\Gamma(1-\nu)}\int_0^t \frac{\partial u(x,s)}{\partial s}\frac{ds}{(t-s)^\nu}, \quad 0<\nu<1, \tag{2}$$

$$\frac{\partial^\nu u}{\partial t^\nu} = \frac{\partial u(x,t)}{\partial t}, \quad \nu=1. \tag{3}$$

The problem (1) in the case of $\nu = 1$, i.e., the following problem

$$\begin{cases} u_t - u_{xx} = 0, & x > 0, t > 0, \\ u(x,0) = 0, & x > 0, \\ u(1,t) = \varphi(t), & t > 0, \\ u(x,t) \mid_{x\to\infty} \textit{bounded}, \end{cases} \tag{4}$$

has been studied extensively in recent decades by many methods [15–28]. Tuan et al. [29] and Triet et al. [30] extended this work to the non-linear case.

When $0 < \nu < 1$, Xiong et al. [31,32] proposed an optimal filtering regularization method for calculating an approximate solution of the fractional sideways heat equation where the spatial domain is the interval [0, 1]. Li et al. [33] tackled the inverse problem of recovering the temperature and flux distribution in the domain $0 \le x < 1$ for (1) from the boundary data at $x = 1$, but the conditional stability result is not given. Zheng et al. [34–36] obtains a stable estimate of temperature distribution by utilizing the spectral regularization method, and numerical example shows that the computational effect of their methods are satisfactory. Zhang [37] applied a Tikhonov-type regularized method to construct an approximate solution and overcome the ill-posedness of (1). The a-posteriori convergence estimates of logarithmic and double logarithmic types for the regularized method are derived. Moreover, the authors verify the effectiveness of their method by doing the numerical experiments. Furthermore, there are also some articles that discuss the fractional sideways heat equation in 2-dimensional and higher-dimensions in space (see, e.g., [38–43] and the references therein).

To the best of our knowledge, few investigations has been performed with respect to a sideways problem of the non-homogeneous diffusion equation, and estimating the heat flux at the inaccessible surface is more difficult than estimating temperature. Liu and Chang in [44] addressed a three-dimensional non-homogeneous sideways heat equation in a cuboid by a Fourier sine series method, and the analysis of the regularization parameter and the stability of solution was worked out. According to them, this method is quite accurate. Luan in [45] discussed the two-dimensional non-homogeneous heat equation in the presence of a general source term, and proposed a kernel regularization method to recover the temperature and heat flux distribution from the given data. However, the above two articles only consider the case of integer order. Hence, in contrast to the previous work, we consider a sideways problem of the non-homogeneous time-fractional diffusion equation, which occurs in many applications related to reaction-diffusion

$$\begin{cases} \frac{\partial^\alpha u}{\partial t^\alpha} - u_{xx} = f(x,t), & x > 0, t > 0, \\ u(x,0) = 0, & x > 0, \\ u(1,t) = g(t), & t > 0, \\ u(x,t) \mid_{x\to\infty} \textit{bounded}, \end{cases} \tag{5}$$

where the function $f(x,t)$ is the heat source density. We first obtain an analytical solution to (5) via Fourier transform, and give the result of conditional stability under an a priori assumption. Due to the problem considered is severely ill-posed, it is impossible to solve it using classical numerical methods. Therefore, we propose dynamic spectral and Fourier regularization method, the goal here consists of recovering not only the temperature but also the heat flux distribution from the given data. Furthermore, for both regularization strategies, in the presence of noisy data, we establish and prove the stability and convergence estimates in the whole domain, i.e., including the case $0 < x < 1$ and the case $x = 1$.

The remainder of the paper is organized as follows: in Section 2, we give an analysis on the ill-posedness of the non-homogeneous fractional sideways heat equation. The conditional stability result is then given in Section 3. In Sections 4 and 5, error estimates for determination of temperature and flux distribute are derived. Finally, we draw a conclusion to our method.

2. Mathematical Analysis of the Problem

In order to simplify the discussion, our theoretical analysis will be performed in $L^2(\mathbb{R})$ and define all functions to be zero for $t < 0$. Let $\hat{g}$ denote the Fourier transform of $g(t)$ defined by

$$\hat{g}(\xi) =: \frac{1}{\sqrt{2\pi}} \int_{-\infty}^{\infty} g(t) e^{-i\xi t} dt,$$

and $\|\cdot\|_p$ denotes the norm in Sobolev space $H_p(\mathbb{R})$ defined by

$$\|u(0,\cdot)\|_p := \left(\int_{-\infty}^{\infty} (1+\xi^2)^p |\hat{u}(0,\xi)|^2 d\xi \right)^{\frac{1}{2}}.$$

When $p = 0$, $\|\cdot\|_p = \|\cdot\|$ denotes the $L^2(\mathbb{R})$ norm. Furthermore, we introduce the following norm

$$\|f(x,\cdot)\|_{L^2(0,1;H_p(\mathbb{R}))} = \left(\int_0^1 \|f(x,\cdot)\|_p^2 dx \right)^{\frac{1}{2}}.$$

Applying the Fourier transform with respect to t to both sides of (1), we obtain in the frequency space the following second order ordinary differential equation

$$\begin{cases} \hat{u}_{xx}(x,\xi) - (i\xi)^{\alpha} \hat{u}(x,\xi) = -\hat{f}(x,\xi), & \xi \in \mathbb{R}, \\ \hat{u}(1,\xi) = \hat{g}(\xi), & \xi \in \mathbb{R}, \\ \hat{u}(x,\xi) \mid_{x\to\infty} \textit{bounded}, & \xi \in \mathbb{R}. \end{cases} \tag{6}$$

The standard calculation procedure yields the solution of (6) as

$$\hat{u}(x,\xi) = e^{\tau(\xi)(1-x)} \hat{g}(\xi) + \int_x^1 \hat{f}(s,\xi) \frac{\sinh\big(\tau(\xi)(s-x)\big)}{\tau(\xi)} ds, \quad 0 \le x < 1, \tag{7}$$

and equivalently

$$u(x,t) = \frac{1}{\sqrt{2\pi}} \int_{-\infty}^{\infty} \left(e^{\tau(\xi)(1-x)} \hat{g}(\xi) + \int_x^1 \hat{f}(s,\xi) \frac{\sinh\big(\tau(\xi)(s-x)\big)}{\tau(\xi)} ds \right) e^{i\xi t} d\xi, \; 0 \le x < 1, \tag{8}$$

where

$$\tau(\xi) := (i\xi)^{\frac{\alpha}{2}} = |\xi|^{\frac{\alpha}{2}} \big(\cos(\frac{\alpha\pi}{4}) + isign(\xi) \sin(\frac{\alpha\pi}{4}) \big), \qquad \forall \xi \in \mathbb{R}. \tag{9}$$

Note that the real part of $\tau(\xi)$ is increasing positive function of ξ. Hence, the term $|e^{(1-x)\tau(\xi)}|$ and $|\sinh\big(\tau(\xi)(s-x)\big)|$ increase rather quickly when $|\xi| \to \infty$, small errors in the data can blow up and ultimately destroy the solution for $x \in [0,1)$. Comparing this with homogeneous fractional sideways heat equation [31], it is no doubt that the problem (5) is much more ill-posed, and some regularization methods are in order.

Remark 1. *We do not consider the case $f(x,t) = 0$ in this paper. In fact, if $f(x,t) = 0$, our problem is a homogeneous time-fractional sideways heat problem. We only note that, using our method, we obtain again the results of [33].*

Remark 2. *By using the Fourier transform, the solution of general problem (5) where the data g is fixed at an specific point $x_0 \in (0,1]$, can be expressed as*

$$\hat{u}(x,\xi) = e^{\tau(\xi)(x_0-x)} \hat{g}(\xi) + \int_x^{x_0} \hat{f}(s,\xi) \frac{\sinh\big(\tau(\xi)(s-x)\big)}{\tau(\xi)} ds, \quad 0 \le x < 1. \tag{10}$$

If we put $x_0 = 1$ in (10), we will obtain (7). In this context, the similar property can be acquired for this general problem and it is also an ill-posed problem. Furthermore, the similarity in (10) and (7) indicates that the methods using in the present paper are also applicable to solve the general problem.

Lemma 1 ([45]). *For arbitrary $z \in \mathbb{C}$, $x \in [0,1)$ and $\eta \in (x,1]$, we have*

$$\left|\frac{\sinh\big((\eta-x)z\big)}{z}\right| \le \frac{e^{(\eta-x)\Re(z)}}{|z|}, \tag{11}$$

$$\left|\frac{\sinh\big((\eta-x)z\big)}{z}\right| \le (\eta-x)e^{(\eta-x)|z|}, \tag{12}$$

$$|\cosh(xz)| \le e^{x\Re(z)} \le e^{x|z|}, \tag{13}$$

where $\Re(z)$ denotes the real parts of z.

Lemma 2 ([45]). *For arbitrary $c, d, p > 0$, the following inequality holds*

$$(c+d)^p \le \begin{cases} c^p + d^p, & 0 < p \le 1, \\ 2^{p-1}(c^p + d^p), & p > 1. \end{cases}$$

Lemma 3. *If $s \ne 0$, then the function $h(s) = \frac{e^{(1-x)s}}{s}$ gets its minimum $h_{\min} = (1-x)e$ at $s = \frac{1}{1-x}$.*

So as to acquire a more sharp convergence, we use the following a priori condition

$$\|u(0,\cdot)\| \le E. \tag{14}$$

Furthermore, since the $\sinh(\cdot)$ function is exponentially increasing, we must find a sharply decreasing function to suppress its growth. Therefore, we also give the following assumption

$$\int_0^1 |\hat{f}(s,\xi)|^2 ds < e^{-3|\xi|^{\frac{\alpha}{2}}}, \quad \forall \xi \in \mathbb{R}. \tag{15}$$

and the measured data (g_δ, f_δ) satisfy

$$\|g - g^\delta\| + \|f - f^\delta\|_{L^2(0,1;L^2(\mathbb{R}))} \le \delta. \tag{16}$$

Throughout this paper, we denote the real part and imaginary part of $\tau(\xi)$ as follows

$$a := \Re(\tau(\xi)), \quad b := \Im(\tau(\xi)). \tag{17}$$

3. A Conditional Stability Estimate

The object of stability estimates is to describe how much the development of solution from data magnifies errors, when noise contaminated the data. Next, we give the main results of this part.

Theorem 1. *Suppose that $\hat{u}(x,\xi)$ given by (7) be the exact solution of problem (5) in the frequency space, and (16) is satisfied, then the following estimate holds for $0 \le x < 1$*

$$\begin{aligned}\|u(x,t)\| \le & \sqrt{C_1\big(\big\|\hat{g}\big\|^2 + \big\|\hat{f}\big\|^2_{L^2(0,1;L^2(\mathbb{R}))}\big)} \\ & + \sqrt{2^{x+2}\big\|\hat{u}(0,\xi)\big\|^{2-2x}\big(\big\|\hat{g}\big\|^{2x} + \big\|\hat{f}\big\|^{2x}_{L^2(0,1;L^2(\mathbb{R}))}\big) + C_2\big\|\hat{f}\big\|^2_{L^2(0,1;L^2(\mathbb{R}))}}.\end{aligned}$$

where C_1 and C_2 are constants that only depends on x.

Proof. By the Parseval's identity, we have

$$\begin{aligned}\|u(x,t)\|^2 =&\|\hat{u}(x,\xi)\|^2\\ =&\underbrace{\int_{|\xi|\le 1}\left|e^{\tau(1-x)}\hat{g}+\int_x^1 \hat{f}\frac{\sinh\left(\tau(s-x)\right)}{\tau}ds\right|^2 d\xi}_{A_1}\\ &+\underbrace{\int_{|\xi|>1}\left|e^{\tau(1-x)}\hat{g}+\int_x^1 \hat{f}\frac{\sinh\left(\tau(s-x)\right)}{\tau}ds\right|^2 d\xi}_{A_2}.\end{aligned} \tag{18}$$

Next, we divide the argument into two steps.
Step 1. Estimate the term A_1 in (18). By Lemma 2, we have

$$A_1 \le \underbrace{2\int_{|\xi|\le 1}\left|e^{\tau(1-x)}\hat{g}\right|^2 d\xi}_{A_{11}} + \underbrace{2\int_{|\xi|\le 1}\left|\int_x^1 \hat{f}\frac{\sinh\left(\tau(s-x)\right)}{\tau}ds\right|^2 d\xi}_{A_{12}}. \tag{19}$$

Note that

$$|\tau| = |\xi|^{\frac{\alpha}{2}} \le 1, \tag{20}$$

we obtain

$$A_{11} \le 2\int_{|\xi|\le 1} e^{2|\tau|(1-x)}|\hat{g}|^2 d\xi \le 2e^{2(1-x)}\left\|\hat{g}\right\|^2. \tag{21}$$

Using Cauchy–Schwarz integral inequality, (12) yields

$$\begin{aligned}A_{12} \le& 2\int_{|\xi|\le 1}\left(\int_x^1 |\hat{f}|^2 ds\right)\left(\int_x^1 \left|\frac{\sinh(\tau(s-x))}{\tau}\right|^2 ds\right)d\xi\\ \le& 2\int_{|\xi|\le 1}\left(\int_x^1 |\hat{f}|^2 ds\right)\left(\int_x^1 e^{2|\tau|(s-x)}ds\right)d\xi\\ \le& e^{2(1-x)}\left\|\hat{f}\right\|^2_{L^2(0,1;L^2(\mathbb{R}))}.\end{aligned} \tag{22}$$

Substituting (21) and (22) into (19), we obtain

$$A_1 \le C_1\left(\left\|\hat{g}\right\|^2 + \left\|\hat{f}\right\|^2_{L^2(0,1;L^2(\mathbb{R}))}\right), \tag{23}$$

where

$$C_1 = 2e^{2(1-x)}. \tag{24}$$

Step 2. Estimate the term A_2 in (18). Again, in view of Lemma 2, we have

$$A_2 \le \underbrace{2\int_{|\xi|>1}\left|e^{\tau(1-x)}\hat{g}\right|^2 d\xi}_{A_{21}} + \underbrace{2\int_{|\xi|>1}\left|\int_x^1 \hat{f}\frac{\sinh\left(\tau(s-x)\right)}{\tau}ds\right|^2 d\xi}_{A_{22}}. \tag{25}$$

We first estimate A_{21}. Using (7) and Lemma 2, we have

$$\begin{aligned}A_{21} =&2\int_{|\xi|>1}\left|e^{-\tau x}\left[\hat{u}(0,\xi) - \int_0^1 \hat{f}\frac{\sinh(\tau s)}{\tau}\right]\right|^2 d\xi\\ \le&\underbrace{4\int_{|\xi|>1}|e^{-\tau x}|^2|\hat{u}(0,\xi)|^2 d\xi}_{\tilde{A_{21}}} + \underbrace{4\int_{|\xi|>1}|e^{-\tau x}|^2\left|\int_0^1 \hat{f}\frac{\sinh(\tau s)}{\tau}ds\right|^2 d\xi}_{\tilde{A_{22}}}.\end{aligned}$$

By (17), Lemma 2, Hölder inequality, we have

$$\begin{aligned}
\tilde{A_{21}} &= \int_{|\xi|>1} \left(|\hat{u}(0,\xi)|^2\right)^{1-x} \left[e^{-2a}\left|\hat{u}(0,\xi) - \int_0^1 \hat{f}\frac{\sinh(\tau s)}{\tau}ds + \int_0^1 \hat{f}\frac{\sinh(\tau s)}{\tau}ds\right|^2\right]^x d\xi \\
&\le \int_{|\xi|>1} \left(|\hat{u}(0,\xi)|^2\right)^{1-x} \left[\left(2e^{-2a}\left|\hat{u}(0,\xi) - \int_0^1 \hat{f}\frac{\sinh(\tau s)}{\tau}ds\right|^2\right)^x \right. \\
&\quad \left. + \left(2e^{-2a}\left|\int_0^1 \hat{f}\frac{\sinh(\tau s)}{\tau}ds\right|^2\right)^x\right] d\xi \\
&= \int_{|\xi|>1} \left(|\hat{u}(0,\xi)|^2\right)^{1-x} \left(2e^{-2a}\left|\hat{u}(0,\xi) - \int_0^1 \hat{f}\frac{\sinh(\tau s)}{\tau}ds\right|^2\right)^x d\xi \\
&\quad + \int_{|\xi|>1} \left(|\hat{u}(0,\xi)|^2\right)^{1-x} \left(2e^{-2a}\left|\int_0^1 \hat{f}\frac{\sinh(\tau s)}{\tau}ds\right|^2\right)^x d\xi \\
&\le \left(\int_{|\xi|>1} |\hat{u}(0,\xi)|^2 d\xi\right)^{1-x} \left(\int_{|\xi|>1} 2e^{-2a}\left|\hat{u}(0,\xi) - \int_0^1 \hat{f}\frac{\sinh(\tau s)}{\tau}ds\right|^2 d\xi\right)^x \\
&\quad + \left(\int_{|\xi|>1} |\hat{u}(0,\xi)|^2 d\xi\right)^{1-x} \left(\int_{|\xi|>1} 2e^{-2a}\left|\int_0^1 \hat{f}\frac{\sinh(\tau s)}{\tau}ds\right|^2 d\xi\right)^x.
\end{aligned}$$

By. Cauchy–Schwarz integral inequality and (11), we obtain

$$\begin{aligned}
2e^{-2a}\left|\int_0^1 \hat{f}\frac{\sinh(\tau s)}{\tau}ds\right|^2 &\le 2e^{-2a}\left(\int_0^1 |\hat{f}|^2 ds\right)\left(\int_0^1 |\frac{\sinh(\tau s)}{\tau}|^2 ds\right) \\
&\le 2e^{-2a}\left(\int_0^1 |\hat{f}|^2 ds\right)\left(\int_0^1 \frac{e^{2sa}}{|\tau|^2}ds\right) \\
&\le 2\left(\int_0^1 |\hat{f}|^2 ds\right)\frac{1}{2a|\tau|^2}.
\end{aligned} \tag{26}$$

Therefore,

$$\begin{aligned}
\tilde{A_{21}} &\le \left(\int_{|\xi|>1} |\hat{u}(0,\xi)|^2 d\xi\right)^{1-x} \left(\int_{|\xi|>1} |\sqrt{2}\hat{g}|^2 d\xi\right)^x \\
&\quad + \left(\int_{|\xi|>1} |\hat{u}(0,\xi)|^2 d\xi\right)^{1-x} \left(\int_{|\xi|>1} 2\left(\int_0^1 |\hat{f}|^2 ds\right)\frac{1}{2a|\tau|^2}d\xi\right)^x \\
&\le \|\hat{u}(0,\xi)\|^{2-2x} \|\sqrt{2}\hat{g}\|^{2x} + 2^x \|\hat{u}(0,\xi)\|^{2-2x} \|\hat{f}\|^{2x}_{L^2(0,1;L^2(\mathbb{R}))} \\
&= 2^x \|\hat{u}(0,\xi)\|^{2-2x} \left(\|\hat{g}\|^{2x} + \|\hat{f}\|^{2x}_{L^2(0,1;L^2(\mathbb{R}))}\right).
\end{aligned}$$

Likewise, we have

$$\begin{aligned}
\tilde{A_{22}} &\le \left(\int_{|\xi|>1} \left|\int_0^1 \hat{f}\frac{\sinh(\tau s)}{\tau}ds\right|^2 d\xi\right)^{1-x} \left(\int_{|\xi|>1} e^{-2a}\left|\int_0^1 \hat{f}\frac{\sinh(\tau s)}{\tau}ds\right|^2 d\xi\right)^x \\
&\le \left[\int_{|\xi|>1} \left(\int_0^1 |\hat{f}|^2 ds\right)\left(\int_0^1 e^{2|\tau|s}ds\right)\right]^{1-x} \left(\int_{|\xi|>1} \left(\int_0^1 |\hat{f}|^2 ds\right)\frac{1}{2a|\tau|^2}d\xi\right)^x \\
&\le \left[\int_{|\xi|>1} \left(\int_0^1 |\hat{f}|^2 ds\right)\frac{e^{2|\tau|}}{2|\tau|}\right]^{1-x} \|\hat{f}\|^{2x}_{L^2(0,1;L^2(\mathbb{R}))} \\
&\le e^{1-x} \|\hat{f}\|^2_{L^2(0,1;L^2(\mathbb{R}))}.
\end{aligned}$$

Combining the estimates of $\tilde{A_{21}}$ with $\tilde{A_{22}}$, we obtain

$$A_{21} \leq 2^{x+2}\|\hat{u}(0,\xi)\|^{2-2x}(\|\hat{g}\|^{2x} + \|\hat{f}\|^{2x}_{L^2(0,1;L^2(\mathbb{R}))}) + 4e^{1-x}\|\hat{f}\|^2_{L^2(0,1;L^2(\mathbb{R}))}. \tag{27}$$

Next, we estimate A_{22}. By Cauchy–Schwarz integral inequality, (12) and Lemma 3, we obtain

$$\begin{aligned} A_{22} \leq & 2\int_{|\xi|>1}\left(\int_x^1 |\hat{f}|^2 ds\right)\left(\int_x^1 \left|\frac{\sinh(\tau(s-x))}{\tau}\right|^2 ds\right)d\xi \\ \leq & 2\int_{|\xi|>1}\left(\int_x^1 |\hat{f}|^2 ds\right)\left(\int_x^1 e^{2|\tau|(s-x)} ds\right)d\xi \\ \leq & 2\int_{|\xi|>1}\left(\int_x^1 |\hat{f}|^2 ds\right)\frac{e^{2|\tau|(1-x)}}{2|\tau|}d\xi \\ \leq & 2(1-x)e\|\hat{f}\|^2_{L^2(0,1;L^2(\mathbb{R}))}. \end{aligned} \tag{28}$$

Inserting (27) and (28) into (25), we have

$$A_2 \leq 2^{x+2}\|\hat{u}(0,\xi)\|^{2-2x}(\|\hat{g}\|^{2x} + \|\hat{f}\|^{2x}_{L^2(0,1;L^2(\mathbb{R}))}) + C_2\|\hat{f}\|^2_{L^2(0,1;L^2(\mathbb{R}))}, \tag{29}$$

where

$$C_2 = 4e^{1-x} + 2(1-x)e. \tag{30}$$

Substituting (23) and (29) into (18), and using Lemma 2, we obtain

$$\begin{aligned} \|\hat{u}(x,\xi)\| \leq & \sqrt{A_1} + \sqrt{A_2} \\ \leq & \sqrt{C_1(\|\hat{g}\|^2 + \|\hat{f}\|^2_{L^2(0,1;L^2(\mathbb{R}))})} \\ & + \sqrt{2^{x+2}\|\hat{u}(0,\xi)\|^{2-2x}(\|\hat{g}\|^{2x} + \|\hat{f}\|^{2x}_{L^2(0,1;L^2(\mathbb{R}))}) + C_2\|\hat{f}\|^2_{L^2(0,1;L^2(\mathbb{R}))}}, \end{aligned}$$

where C_1 and C_2 is given by (24) and (30), respectively. □

4. Determination of the Temperature Distribution

In this part, we use the dynamic spectral method to recover the temperature distribution from the measured data. Since the matter of instability lies in the noise of data in the high frequency components, naturally a "corrector" is added to these in order to control their growth. As a result, one may obtain a stable approximation. Suppose β is the regularization parameter, motivated by [31], we contemplate the following regularized solutions in the frequency domain:

Method 1

$$\hat{u}^\delta_\beta(x,\xi) = \begin{cases} e^{\tau(\xi)(1-x)}\hat{g}^\delta(\xi) + \int_x^1 \hat{f}^\delta(s,\xi)\frac{\sinh(\tau(\xi)(s-x))}{\tau(\xi)}ds, & e^{-a(1-x)} \geq \sqrt{\beta}, \\ \frac{e^{-2a(1-x)}}{\beta}\left[e^{\tau(\xi)(1-x)}\hat{g}^\delta(\xi) + \int_x^1 \hat{f}^\delta(s,\xi)\frac{\sinh(\tau(\xi)(s-x))}{\tau(\xi)}ds\right], & e^{-a(1-x)} < \sqrt{\beta}. \end{cases} \tag{31}$$

Method 2

$$\hat{v}^\delta_\beta(x,\xi) = \begin{cases} e^{\tau(\xi)(1-x)}\hat{g}^\delta(\xi) + \int_x^1 \hat{f}^\delta(s,\xi)\frac{\sinh(\tau(\xi)(s-x))}{\tau(\xi)}ds, & e^{-a(1-x)} \geq \sqrt{\beta}, \\ \frac{e^{-a(1-x)}}{\sqrt{\beta}}\left[e^{\tau(\xi)(1-x)}\hat{g}^\delta(\xi) + \int_x^1 \hat{f}^\delta(s,\xi)\frac{\sinh(\tau(\xi)(s-x))}{\tau(\xi)}ds\right], & e^{-a(1-x)} < \sqrt{\beta}. \end{cases} \tag{32}$$

Method 3

$$\hat{w}_\beta^\delta(x,\xi)=\begin{cases} e^{\tau(\xi)(1-x)}\hat{g}^\delta(\xi)+\int_x^1 \hat{f}^\delta(s,\xi)\frac{\sinh(\tau(\xi)(s-x))}{\tau(\xi)}ds, & e^{-a(1-x)}\geq\sqrt{\beta},\\ \frac{e^{-\frac{a}{2}(1-x)}}{\beta^{\frac{1}{4}}}\left[e^{\tau(\xi)(1-x)}\hat{g}^\delta(\xi)+\int_x^1 \hat{f}^\delta(s,\xi)\frac{\sinh(\tau(\xi)(s-x))}{\tau(\xi)}ds\right], & e^{-a(1-x)}<\sqrt{\beta}. \end{cases} \tag{33}$$

Generally,

$$\hat{\mu}_\beta^\delta(x,\xi)=\begin{cases} e^{\tau(\xi)(1-x)}\hat{g}^\delta(\xi)+\int_x^1 \hat{f}^\delta(s,\xi)\frac{\sinh(\tau(\xi)(s-x))}{\tau(\xi)}ds, & e^{-a(1-x)}\geq\sqrt{\beta},\\ \frac{e^{-\gamma a(1-x)}}{\sqrt{\beta}^\gamma}\left[e^{\tau(\xi)(1-x)}\hat{g}^\delta(\xi)+\int_x^1 \hat{f}^\delta(s,\xi)\frac{\sinh(\tau(\xi)(s-x))}{\tau(\xi)}ds\right], & e^{-a(1-x)}<\sqrt{\beta}, \end{cases} \tag{34}$$

where $\gamma>0$ is a real number. Because the three spectral methods are very similar, then we only give the properties of the first two methods.

Remark 3. *It is apparently that the regularization solutions approach the exact solution if $\beta\to 0$ as $\delta\to 0$.*

Lemma 4. *If condition (14) and (15) hold, $B(\xi)=\hat{u}(0,\xi)-\int_0^1 \hat{f}\frac{\sinh(\tau s)}{\tau}ds$, then*

$$\left\|B(\xi)\right\|\leq E+N_1,$$

where N_1 is a constant.

Proof. Successively using the triangle inequality, (14), Cauchy–Schwarz integral inequality, (12) and (15), we obtain

$$\begin{aligned}\left\|B(\xi)\right\|\leq&\left\|\hat{u}(0,\xi)\right\|+\left\|\int_0^1 \hat{f}\frac{\sinh(\tau s)}{\tau}ds\right\|\\ \leq&E+\left[\int_{-\infty}^{\infty}\left(\int_0^1\left|\frac{\sinh(\tau s)}{\tau}\right|^2 ds\int_0^1|\hat{f}|^2 ds\right)d\xi\right]^{\frac{1}{2}}\\ \leq&E+\left[\int_{-\infty}^{\infty}\left(\int_0^1|se^{s|\tau|}|^2 ds\int_0^1|\hat{f}|^2 ds\right)d\xi\right]^{\frac{1}{2}}\\ \leq&E+\left(\int_{-\infty}^{\infty}\frac{1}{2|\xi|^{\frac{\alpha}{2}}}e^{-|\xi|^{\frac{\alpha}{2}}}d\xi\right)^{\frac{1}{2}}.\end{aligned}$$

It is easy to know that the generalized integral on the right-hand side of the last inequality converges, here we introduce the notation

$$N_1:=\left(\int_{-\infty}^{\infty}\frac{1}{2|\xi|^{\frac{\alpha}{2}}}e^{-|\xi|^{\frac{\alpha}{2}}}d\xi\right)^{\frac{1}{2}}. \tag{35}$$

Therefore,

$$\left\|B(\xi)\right\|\leq E+N_1,$$

where N_1 is a constant. □

Theorem 2. *Let $\hat{u}(x,\xi)$ given by (7) be the exact solution of problem (5) in the frequency space, $\hat{u}_\beta^\delta(x,\xi)$ given by (31) be the regularized solution, condition (14)–(16) hold. If the regularization parameter β is selected dynamically*

$$\beta(x)=2^{2x-2}\left(\frac{x}{2-x}\right)^{x-2}\left(\frac{\delta}{E+2N_1}\right)^{2(1-x)}. \tag{36}$$

Then, for a fixed $x \in (0,1)$, we have

$$\left\|u_\beta^\delta(x,\cdot)-u(x,\cdot)\right\| \le \frac{2^{1-x}}{2-x}\left(\frac{x}{2-x}\right)^{-\frac{x}{2}}\delta^x\left(E+2N_1\right)^{1-x}+\delta\sqrt{(1-x)e}. \tag{37}$$

Proof. By the triangle inequality, we have

$$\left\|u_\beta^\delta(x,\cdot)-u(x,\cdot)\right\| \le \underbrace{\left\|u_\beta^\delta(x,\cdot)-u_\beta(x,\cdot)\right\|}_{\mathcal{I}_1}+\underbrace{\left\|u_\beta(x,\cdot)-u(x,\cdot)\right\|}_{\mathcal{I}_2}. \tag{38}$$

Next , we divide the argument into two steps.

Step 1. Estimate the term $\mathcal{I}_1$ in (38). It follows immediately from Parseval's equality and the triangle inequality that

$$\begin{aligned}
\mathcal{I}_1 =& \left\|\hat{u}_\beta^\delta(x,\cdot)-\hat{u}_\beta(x,\cdot)\right\| \\
=& \left\| \min\left\{1,\frac{e^{-2a(1-x)}}{\beta}\right\}\left[e^{\tau(1-x)}\left(\hat{g}^\delta-\hat{g}\right)+\int_x^1\left(\hat{f}^\delta-\hat{f}\right)\frac{\sinh\left(\tau(s-x)\right)}{\tau}ds\right]\right\| \\
\le& \underbrace{\left\| \min\left\{1,\frac{e^{-2a(1-x)}}{\beta}\right\}e^{\tau(1-x)}\left(\hat{g}^\delta-\hat{g}\right)\right\|}_{\bar{\mathcal{I}}_1} \\
&+\underbrace{\left\| \min\left\{1,\frac{e^{-2a(1-x)}}{\beta}\right\}\int_x^1\left(\hat{f}^\delta-\hat{f}\right)\frac{\sinh\left(\tau(s-x)\right)}{\tau}ds\right\|}_{\bar{\mathcal{I}}_2}.
\end{aligned}$$

By (17) and (16), we obtain

$$\bar{\mathcal{I}}_1 \le \left\|\frac{e^{-2a(1-x)}}{\beta}e^{(a+bi)(1-x)}\left(\hat{g}^\delta-\hat{g}\right)\right\|_{e^{-a(1-x)}<\sqrt{\beta}} = \left\|\frac{e^{(-a+bi)(1-x)}}{\beta}\left(\hat{g}^\delta-\hat{g}\right)\right\| \le \delta\beta^{-\frac{1}{2}}.$$

Using Cauchy–Schwarz integral inequality, (12), Lemma 3 and (16) yields

$$\begin{aligned}
\bar{\mathcal{I}}_2 \le& \left\|\int_x^1\left(\hat{f}^\delta-\hat{f}\right)\frac{\sinh\left(\tau(x-s)\right)}{\tau}ds\right\| \\
\le& \left\|\left(\int_x^1\left|\hat{f}^\delta-\hat{f}\right|^2ds\right)\left(\int_x^1 e^{2(s-x)|\tau|}ds\right)\right\| \\
\le& \left\|\left(\int_x^1\left|\hat{f}^\delta-\hat{f}\right|^2ds\right)\frac{e^{2(1-x)|\tau|}}{2|\tau|}\right\| \\
\le& \delta\sqrt{(1-x)e}.
\end{aligned}$$

Hence,

$$\mathcal{I}_1 \le \delta\beta^{-\frac{1}{2}}+\delta\sqrt{(1-x)e}. \tag{39}$$

Step 2. Estimate the term $\mathcal{I}_2$ in (38). Again, by the Parseval's identity and the triangle inequality,

$$\begin{aligned}
\mathcal{I}_2 =& \left\|\hat{u}_\beta(x,\cdot) - \hat{u}(x,\cdot)\right\| \\
=& \left\| \min\left\{1, \frac{e^{-2a(1-x)}}{\beta}\right\} \right. \\
& \left. \cdot \left(e^{\tau(1-x)}\hat{g} + \int_x^1 \hat{f}\frac{\sinh\left(\tau(s-x)\right)}{\tau}ds\right) - \left(e^{\tau(1-x)}\hat{g} + \int_x^1 \hat{f}\frac{\sinh\left(\tau(s-x)\right)}{\tau}ds\right)\right\| \\
\leq& \underbrace{\left\|\left(1 - \min\left\{1, \frac{e^{-2a(1-x)}}{\beta}\right\}\right)e^{\tau(1-x)}\hat{g}\right\|}_{\tilde{\mathcal{I}}_1} \\
& + \underbrace{\left\|\left(1 - \min\left\{1, \frac{e^{-2a(1-x)}}{\beta}\right\}\right)\int_x^1 \hat{f}\frac{\sinh\left(\tau(s-x)\right)}{\tau}ds\right\|}_{\tilde{\mathcal{I}}_2}.
\end{aligned}$$

We start by estimating the first term above. Let

$$B_1(a) = \left(1 - \frac{e^{-2a(1-x)}}{\beta}\right)e^{-ax}.$$

Using (7) and (17), we obtain

$$\begin{aligned}
\tilde{\mathcal{I}}_1 =& \left\|\left(1 - \min\left\{1, \frac{e^{-2a(1-x)}}{\beta}\right\}\right)e^{-\tau x}\left[\hat{u}(0,\xi) - \int_0^1 \hat{f}\frac{\sinh(\tau s)}{\tau}ds\right]\right\| \\
\leq& \sup_{e^{-2a(1-x)}\leq\beta} B_1(a)\left\|\hat{u}(0,\xi) - \int_0^1 \hat{f}\frac{\sinh(\tau s)}{\tau}ds\right\|.
\end{aligned}$$

By elementary calculations, it is easy to find the zero point a^* of $B_1'(a)$ satisfies

$$e^{-2a^*(1-x)} = \frac{\beta x}{2-x},$$

and a^* maximize the function $B_1(a)$. Thus,

$$B_1(a) \leq B_1(a^*) = \left(1 - \frac{x}{2-x}\right)\left(\frac{\beta x}{2-x}\right)^{\frac{x}{2(1-x)}}. \tag{40}$$

Using Lemma 4, we have

$$\tilde{\mathcal{I}}_1 \leq \left(1 - \frac{x}{2-x}\right)\left(\frac{\beta x}{2-x}\right)^{\frac{x}{2(1-x)}}(E + N_1).$$

Now we estimate $\tilde{\mathcal{I}}_2$. Using Cauchy–Schwarz integral inequality, (12), (17), (15), (40), (9) and (10) yields

$$\begin{aligned}
\tilde{\mathcal{I}}_2 \leq & \left\| \left(1-\frac{e^{-2a(1-x)}}{\beta}\right) e^{-ax} \int_x^1 \hat{f} \frac{\sinh(\tau(s-x))}{\tau} ds e^{ax} \right\| \\
\leq & \sup_{e^{-2a(1-x)} \leq \beta} B_1(a) \left[\int_{-\infty}^{\infty} \left(\int_x^1 |\hat{f}|^2 ds \right) \left(\int_x^1 e^{2|\tau|(s-x)} ds \right) e^{2ax} d\xi \right]^{\frac{1}{2}} \\
\leq & \sup_{e^{-2a(1-x)} \leq \beta} B_1(a) \left[\int_{-\infty}^{\infty} \left(\int_x^1 |\hat{f}|^2 ds \right) \frac{e^{2|\tau|(1-x)}}{2|\tau|} e^{2|\tau|x} d\xi \right]^{\frac{1}{2}} \\
\leq & \left(1-\frac{x}{2-x}\right) \left(\frac{\beta x}{2-x}\right)^{\frac{x}{2(1-x)}} N_1.
\end{aligned}$$

Therefore,

$$\mathcal{I}_2 \leq \left(1-\frac{x}{2-x}\right) \left(\frac{\beta x}{2-x}\right)^{\frac{x}{2(1-x)}} \left(E+2N_1\right). \tag{41}$$

Substituting (39) and (40) into (38), we obtain

$$\|u_\beta^\delta(x,\cdot) - u(x,\cdot)\| \tag{42}$$

$$\leq \delta \beta^{-\frac{1}{2}} + \delta\sqrt{(1-x)e} + \left(1-\frac{x}{2-x}\right) \left(\frac{\beta x}{2-x}\right)^{\frac{x}{2(1-x)}} \left(E+2N_1\right) := h_1(\beta). \tag{43}$$

Minimizing the right-hand side of (42) with respect to β, we can obtain (36). Hence, (37) hold. □

Theorem 3. *Let $\hat{u}(x,\xi)$ given by (7) be the exact solution of problem (5) in the frequency space, $\hat{v}_\beta^\delta(x,\xi)$ given by (32) be the regularized solution, condition (14)–(16) hold. If the regularization parameter β is selected dynamically*

$$\beta(x) = x^{-2} \left(\frac{\delta}{E+2N_1}\right)^{2(1-x)}. \tag{44}$$

Then, for a fixed $x \in (0,1)$, we have

$$\left\|v_\beta^\delta(x,\cdot) - u(x,\cdot)\right\| \leq \delta^x \left(E+2N_1\right)^{1-x} + \delta\sqrt{(1-x)e}. \tag{45}$$

Proof. By the triangle inequality, we have

$$\left\|v_\beta^\delta(x,\cdot) - u(x,\cdot)\right\| \leq \underbrace{\left\|v_\beta^\delta(x,\cdot) - v_\beta(x,\cdot)\right\|}_{\mathcal{I}_3} + \underbrace{\left\|v_\beta(x,\cdot) - u(x,\cdot)\right\|}_{\mathcal{I}_4}. \tag{46}$$

Next, we divide the argument into two steps.

Step 1. Estimate the term $\mathcal{I}_3$ in (45). Taking a similar procedure of the estimate of $\mathcal{I}_1$, we have

$$\begin{aligned}\mathcal{I}_3 =&\left\|\hat{v}_\beta^\delta(x,\cdot)-\hat{v}_\beta(x,\cdot)\right\|\\ \le&\left\|\min\left\{1,\frac{e^{-a(1-x)}}{\sqrt{\beta}}\right\}e^{\tau(1-x)}\left(\hat{g}^\delta-\hat{g}\right)\right\|\\ &+\left\|\min\left\{1,\frac{e^{-a(1-x)}}{\sqrt{\beta}}\right\}\int_x^1\left(\hat{f}^\delta-\hat{f}\right)\frac{\sinh\left(\tau(s-x)\right)}{\tau}ds\right\| \qquad (47)\\ \le&\left\|\frac{e^{-a(1-x)}}{\sqrt{\beta}}e^{(a+bi)(1-x)}\left(\hat{g}^\delta-\hat{g}\right)\right\|_{e^{-a(1-x)}<\sqrt{\beta}}+\left\|\int_x^1\left(\hat{f}^\delta-\hat{f}\right)\frac{\sinh\left(\tau(s-x)\right)}{\tau}ds\right\|\\ \le&\delta\beta^{-\frac{1}{2}}+\delta\sqrt{(1-x)e}.\end{aligned}$$

Step 2. Estimate the term $\mathcal{I}_4$ in (45). By the Parseval's identity, we have

$$\begin{aligned}\mathcal{I}_4 =&\left\|\hat{v}_\beta(x,\cdot)-\hat{u}(x,\cdot)\right\|\\ \le&\underbrace{\left\|\left(1-\min\left\{1,\frac{e^{-a(1-x)}}{\sqrt{\beta}}\right\}\right)e^{\tau(1-x)}\hat{g}\right\|}_{\tilde{\mathcal{I}}_3}\\ &+\underbrace{\left\|\left(1-\min\left\{1,\frac{e^{-a(1-x)}}{\sqrt{\beta}}\right\}\right)\int_x^1\hat{f}\frac{\sinh\left(\tau(s-x)\right)}{\tau}ds\right\|}_{\tilde{\mathcal{I}}_4}.\end{aligned}$$

We start by estimating the first term above. Let

$$B_2(a)=\left(1-\frac{e^{-a(1-x)}}{\sqrt{\beta}}\right)e^{-ax}.$$

Using (7) and (17), we obtain

$$\begin{aligned}\tilde{\mathcal{I}}_3=&\left\|\left(1-\min\left\{1,\frac{e^{-a(1-x)}}{\sqrt{\beta}}\right\}\right)e^{-\tau x}\left[\hat{u}(0,\xi)-\int_0^1\hat{f}\frac{\sinh(\tau s)}{\tau}ds\right]\right\|\\ \le&\sup_{e^{-a(1-x)}\le\sqrt{\beta}}B_2(a)\left\|\hat{u}(0,\xi)-\int_0^1\hat{f}\frac{\sinh(\tau s)}{\tau}ds\right\|.\end{aligned}$$

By elementary calculations, it is easy to find the zero point a^* of $B_2'(a)$ satisfies

$$e^{-a^*(1-x)}=\sqrt{\beta}x,$$

and a^* maximize the function $B_2(a)$. Thus,

$$B_2(a)\le B_2(a^*)=(1-x)\left(\sqrt{\beta}x\right)^{\frac{x}{1-x}}. \qquad (48)$$

By Lemma 4, we have

$$\tilde{\mathcal{I}}_3\le(1-x)\left(\sqrt{\beta}x\right)^{\frac{x}{1-x}}\left(E+N_1\right).$$

Now we estimate $\tilde{\mathcal{I}}_4$. Using Cauchy–Schwarz integral inequality, (12), (17), (15), (9), (47) and (35) yields

$$\begin{aligned}\tilde{\mathcal{I}}_4 \leq & \left\| \left(1-\frac{e^{-a(1-x)}}{\sqrt{\beta}}\right) e^{-ax} \int_x^1 \hat{f} \frac{\sinh\left(\tau(x-s)\right)}{\tau} ds e^{ax} \right\| \\ \leq & \sup_{e^{-a(1-x)} \leq \sqrt{\beta}} B_2(a) \left[\int_{-\infty}^{\infty} \left(\int_x^1 |\hat{f}|^2 ds \right) \left(\int_x^1 e^{2|\tau|(s-x)} ds \right) e^{2ax} d\xi \right]^{\frac{1}{2}} \\ \leq & (1-x)\left(\sqrt{\beta}x\right)^{\frac{x}{1-x}} N_1.\end{aligned}$$

Therefore,

$$\mathcal{I}_4 \leq (1-x)\left(\sqrt{\beta}x\right)^{\frac{x}{1-x}} \left(E+2N_1\right). \tag{49}$$

Substituting (46) and (48) into (45), we obtain

$$\left\| v_\beta^\delta(x,\cdot) - u(x,\cdot) \right\| \leq \delta\beta^{-\frac{1}{2}} + \delta\sqrt{(1-x)e} + (1-x)\left(\sqrt{\beta}x\right)^{\frac{x}{1-x}} \left(E+2N_1\right) := h_2(\beta). \tag{50}$$

Minimizing the right-hand side of (49) with respect to β, we can obtain (43). Hence, (44) hold. □

Remark 4. *In Theorems 2 and 3, we choose the regularization parameter β to depend on the position of x , which will justify our use of the phrase "dynamic spectral". Moreover, we can find that the estimate of Theorem 3 is better than the estimate of Theorem 2.*

It is easy to see that two errors in Theorems 2 and 3 are not near to zero, if δ fixed and x tend to zero. Hence, the convergence of the approximate solution is very slow when x is in a neighborhood of zero. In addition, considering that the $\sinh(\cdot)$ function is exponentially increasing, to retain the continuous dependence of the solution at $x = 0$, we have to introduce some stronger a priori assumptions

$$\left\| u(0,\cdot) \right\|_p \leq E, \quad p > 0, \tag{51}$$

$$\left(1+\xi^2\right)^p \int_0^1 \left|\hat{f}(s,\xi)\right|^2 ds < e^{-3|\xi|^{\frac{\alpha}{2}}}, \quad \forall \xi \in \mathbb{R}. \tag{52}$$

Next , we only give error estimate at $x = 0$ for (32).

Lemma 5. *Let condition (50) and (51) hold, $\tilde{B}(\xi) = \left(1+\xi^2\right)^{\frac{p}{2}} \left[\hat{u}(0,\xi) - \int_0^1 \hat{f} \frac{\sinh(\tau s)}{\tau} ds\right]$, then*

$$\|\tilde{B}(\xi)\| \leq E + N_1,$$

where N_1 is a constant.

Theorem 4. *Let $\hat{u}(x,\xi)$ given by (7) be the exact solution of problem (5) in the frequency space, $\hat{v}_\beta^\delta(x,\xi)$ given by (32) be the regularized solution, condition (16), (50), (51) hold. The regularization parameter β is chosen as*

$$\beta = \frac{1}{\left(C(a^*)\delta^{-r}\right)^2}, \tag{53}$$

where $0 < r < 1$, $C(a^*) = \frac{2p}{a^*\alpha+2p} < 1$, a^* is a constant. Then, the following inequality hold

$$\left\| v_\beta^\delta(0,\cdot) - u(0,\cdot) \right\| \leq C(a^*)\delta^{1-r} + \delta\sqrt{e} + \left[1-C(a^*)\right] \left(r \ln \frac{1}{\delta} \right)^{-\frac{2p}{\alpha}} \left(E+2N_1\right), \quad p > 0. \tag{54}$$

Proof. By the triangle inequality, we have

$$\left\|v_\beta^\delta(0,\cdot)-u(0,\cdot)\right\| \le \underbrace{\left\|v_\beta^\delta(0,\cdot)-v_\beta(0,\cdot)\right\|}_{\mathcal{I}_5} + \underbrace{\left\|v_\beta(0,\cdot)-u(0,\cdot)\right\|}_{\mathcal{I}_6}. \tag{55}$$

Next, we divide the argument into two steps.

Step 1. Estimate the term $\mathcal{I}_5$ in (54). In view of the Parseval's equality, the triangle inequality, Cauchy–Schwarz integral inequality, (12), Lemma 3 and (16), we have

$$\begin{aligned}
\mathcal{I}_5 =& \left\|\hat{v}_\beta^\delta(0,\cdot)-\hat{v}_\beta(0,\cdot)\right\| \\
\le& \left\| \min\{1,\frac{e^{-a}}{\sqrt{\beta}}\}e^{\tau}\left(\hat{g}^\delta-\hat{g}\right)\right\| + \left\| \min\left\{1,\frac{e^{-a}}{\sqrt{\beta}}\right\}\int_0^1\left(\hat{f}^\delta-\hat{f}\right)\frac{\sinh(\tau s)}{\tau}ds\right\| \\
\le& \left\| \frac{e^{-a}}{\sqrt{\beta}}e^{(a+bi)}\left(\hat{g}^\delta-\hat{g}\right)\right\|_{e^{-a}<\sqrt{\beta}} + \left\| \int_0^1\left(\hat{f}^\delta-\hat{f}\right)\frac{\sinh(\tau s)}{\tau}ds\right\| \\
\le& \delta\beta^{-\frac{1}{2}} + \left[\int_{-\infty}^{\infty}\left(\int_0^1|\hat{f}^\delta-\hat{f}|^2ds\right)\left(\int_0^1 e^{2s|\tau|}ds\right)d\xi\right]^{\frac{1}{2}} \\
\le& \delta\beta^{-\frac{1}{2}} + \delta\sqrt{e}.
\end{aligned}$$

Step 2. Estimate the term $\mathcal{I}_6$ in (54). By the Parseval's equality and the triangle inequality, we obtain

$$\begin{aligned}
\mathcal{I}_6 =& \left\|\hat{v}_\beta(0,\cdot)-\hat{u}(0,\cdot)\right\| \\
\le& \underbrace{\left\|\left(1-\min\left\{1,\frac{e^{-a}}{\sqrt{\beta}}\right\}\right)e^{\tau}\hat{g}\right\|}_{\tilde{\mathcal{I}}_5} + \underbrace{\left\|\left(1-\min\left\{1,\frac{e^{-a}}{\sqrt{\beta}}\right\}\right)\int_0^1\hat{f}\frac{\sinh(\tau s)}{\tau}ds\right\|}_{\tilde{\mathcal{I}}_6}.
\end{aligned}$$

We start by estimating the first term above. Let

$$B_3(a) = \left(1-\frac{e^{-a}}{\sqrt{\beta}}\right)a^{-\frac{2p}{\alpha}}.$$

Using (7), and note that $a \le |\xi|^{\frac{\alpha}{2}}$, we obtain

$$\begin{aligned}
\tilde{\mathcal{I}}_5 =& \left\|\left(1-\min\left\{1,\frac{e^{-a}}{\sqrt{\beta}}\right\}\right)\left[\hat{u}(0,\xi)-\int_0^1\hat{f}\frac{\sinh(\tau s)}{\tau}ds\right]\right\| \\
\le& \sup_{e^{-a}\le\sqrt{\beta}}\left(1-\frac{e^{-a}}{\sqrt{\beta}}\right)\left(1+\xi^2\right)^{-\frac{p}{2}}\left\|\left[\hat{u}(0,\xi)-\int_0^1\hat{f}\frac{\sinh(\tau s)}{\tau}ds\right]\left(1+\xi^2\right)^{\frac{p}{2}}\right\| \\
\le& \sup_{e^{-a}\le\sqrt{\beta}}B_3(a)\left\|\left[\hat{u}(0,\xi)-\int_0^1\hat{f}\frac{\sinh(\tau s)}{\tau}ds\right]\left(1+\xi^2\right)^{\frac{p}{2}}\right\|.
\end{aligned}$$

By elementary calculations, it is easy to find the zero point a^* of $B_3'(a)$ satisfies

$$\frac{e^{-a^*}}{\sqrt{\beta}} = C(a^*),$$

where

$$C(a^*) = \frac{2p}{a^*\alpha+2p} < 1, \tag{56}$$

and a^* maximize the function $B_3(a)$. Thus,

$$B_3(a) \le B_3(a^*) = \big[1 - C(a^*)\big] \left(\ln \frac{1}{\sqrt{\beta} C(a^*)} \right)^{-\frac{2p}{\alpha}}. \tag{57}$$

By Lemma 5, we obtain

$$\tilde{\mathcal{I}}_5 \le \big[1 - C(a^*)\big] \left(\ln \frac{1}{\sqrt{\beta} C(a^*)} \right)^{-\frac{2p}{\alpha}} \big(E + N_1\big).$$

Now we estimate $\tilde{\mathcal{I}}_6$. Using (56) and Lemma 5 yields

$$\begin{aligned}
\tilde{\mathcal{I}}_6 \le & \left\| \left(1 - \frac{e^{-a}}{\sqrt{\beta}}\right) \big(1 + \xi^2\big)^{-\frac{p}{2}} \int_0^1 \hat{f} \frac{\sinh(\tau s)}{\tau} ds \big(1 + \xi^2\big)^{\frac{p}{2}} \right\| \\
\le & \sup_{e^{-a(1-x)} \le \sqrt{\beta}} B_3(a) \left\| \int_0^1 \hat{f} \frac{\sinh(\tau s)}{\tau} ds \big(1 + \xi^2\big)^{\frac{p}{2}} \right\| \\
\le & \big[1 - C(a^*)\big] \left(\ln \frac{1}{\sqrt{\beta} C(a^*)} \right)^{-\frac{2p}{\alpha}} N_1.
\end{aligned}$$

Therefore,

$$\mathcal{I}_6 \le \big[1 - C(a^*)\big] \left(\ln \frac{1}{\sqrt{\beta} C(a^*)} \right)^{-\frac{2p}{\alpha}} \big(E + 2N_1\big). \tag{58}$$

Then, by (54), we have

$$\begin{aligned}
\big\| v_\beta^\delta(x, \cdot) - u(x, \cdot) \big\| \le & \delta \beta^{-\frac{1}{2}} + \delta \sqrt{e} + \big[1 - C(a^*)\big] \left(\ln \frac{1}{\sqrt{\beta} C(a^*)} \right)^{-\frac{2p}{\alpha}} \big(E + 2N_1\big) \\
= & C(a^*) \delta^{1-r} + \delta \sqrt{e} + \big[1 - C(a^*)\big] \left(r \ln \frac{1}{\delta} \right)^{-\frac{2p}{\alpha}} \big(E + 2N_1\big).
\end{aligned}$$

where $C(a^*)$ is given by (55). □

Remark 5. *If we replace the assumption (14) and (15) by (50) and (51), then the convergence* $\|u_\beta^\delta(x, \cdot) - u(x, \cdot)\|_p$ *and* $\|v_\beta^\delta(x, \cdot) - u(x, \cdot)\|_p$ *is also hold.*

Remark 6. *From a theoretical point of view, Theorem 4 has obtained the stability estimate for the endpoint* $x = 0$, *since* $\lim_{\delta \to 0} \|v_\beta^\delta(0, \cdot) - u(0, \cdot)\| = 0$.

Remark 7. *In 1987, Eldén [19] proved that it is impossible to obtain the error asymptotically better than logarithmic rate at* $x = 0$. *So our estimates is reasonable, although the logarithmic term* $\ln \frac{1}{\delta}$ *implies the convergence rate is very slow.*

5. Determination of Flux Structure and Error Estimate

In this section, we use the Fourier regularization method to recover the flux distribution from the measure data. Differentiating the variable x on the right-hand side of (7), we obtain the following formula for the heat flux, denoted by

$$\hat{u}_x(x, \xi) = -\tau(\xi) e^{(1-x)\tau(\xi)} \hat{g}^\delta - \int_x^1 \hat{f}^\delta \cosh\big(\tau(\xi)(s - x)\big) ds, \quad 0 \le x < 1.$$

The method we adopt is to eliminate all high frequencies from the solution, and instead consider (5) for $|\xi| \leq \xi_{\max}$. Then, we obtain a regularized solution

$$\hat{u}_x^{\delta,\xi_{\max}}(x,\xi) = \Big[-\tau(\xi)e^{(1-x)\tau(\xi)}\hat{g}^\delta - \int_x^1 \hat{f}^\delta \cosh\big(\tau(\xi)(s-x)\big)ds\Big]\chi_{\max}. \tag{59}$$

where $\xi_{\max}$ is the regularization parameter, $\chi_{\max}$ is the characteristic function of the interval $[-\xi_{\max}, \xi_{\max}]$.

Theorem 5. *Let $\hat{u}(x,\xi)$ given by (7) be the exact solution of problem (5) in the frequency space, $\hat{u}_x^{\delta,\xi_{\max}}(x,\xi)$ given by (58) be the regularized solution, condition (14)–(16) hold. If the regularization parameter $\xi_{\max}$ is selected by*

$$\xi_{\max} = \left(\ln\frac{E}{\delta}\right)^{\frac{2}{\alpha}}. \tag{60}$$

Then for a fixed $x \in (0,1)$, we have

$$\begin{aligned}&\big\|u_x^{\delta,\xi_{\max}}(x,\cdot) - u_x(x,\cdot)\big\|\\ \leq&\left(2\ln\frac{E}{\delta} + \big(\ln\frac{E}{\delta}\big)^{-\frac{1}{2}}\right)E^{1-x}\delta^x + \epsilon_1\sqrt{2}E^{-x}\delta^x\big(E+N_1\big) + \left(\ln\frac{E}{\delta}\right)^{-\frac{1}{2}}N_2,\end{aligned}$$

where $\epsilon_1 = \max\{\frac{1}{x}, \ln\frac{E}{\delta}\}$, N_1 and N_2 are some constants.

Proof. By the triangle inequality, we have

$$\big\|u_x^{\delta,\xi_{\max}}(x,\cdot) - u_x(x,\cdot)\big\| \leq \underbrace{\big\|u_x^{\delta,\xi_{\max}}(x,\cdot) - u_x^{\xi_{\max}}(x,\cdot)\big\|}_{\mathcal{J}_1} + \underbrace{\big\|u_x^{\xi_{\max}}(x,\cdot) - u_x(x,\cdot)\big\|}_{\mathcal{J}_2}. \tag{61}$$

Next , we divide the argument into two steps.

Step 1. Estimate the term $\mathcal{J}_1$ in (60). It follows immediately from Parseval's equality and Lemma 2 that

$$\begin{aligned}\mathcal{J}_1 =&\big\|\hat{u}_x^{\delta,\xi_{\max}}(x,\cdot) - \hat{u}_x^{\xi_{\max}}(x,\cdot)\big\|\\ =&\left[\int_{|\xi|\leq\xi_{\max}}\big|\tau e^{\tau(1-x)}\big(\hat{g}-\hat{g}^\delta\big) + \int_x^1\big(\hat{f}-\hat{f}^\delta\big)\cosh\big(\tau(s-x)\big)ds\big|^2 d\xi\right]^{\frac{1}{2}}\\ \leq&\underbrace{\left[\int_{|\xi|\leq\xi_{\max}} 2\big|\tau e^{\tau(1-x)}\big(\hat{g}-\hat{g}^\delta\big)\big|^2 d\xi\right]^{\frac{1}{2}}}_{\bar{\mathcal{J}}_1}\\ &+\underbrace{\left[\int_{|\xi|\leq\xi_{\max}} 2\big|\int_x^1\big(\hat{f}-\hat{f}^\delta\big)\cosh\big(\tau(s-x)\big)ds\big|^2 d\xi\right]^{\frac{1}{2}}}_{\bar{\mathcal{J}}_2}.\end{aligned}$$

By (16) and (59), we obtain

$$\bar{\mathcal{J}}_1 \leq 2\delta\sup_{|\xi|\leq\xi_{\max}}\big|\tau e^{\tau(1-x)}\big| \leq 2\delta|\tau|e^{|\tau|(1-x)} \leq 2\delta\xi_{\max}^{\frac{\alpha}{2}}e^{\xi_{\max}^{\frac{\alpha}{2}}(1-x)} = 2E^{1-x}\delta^x\ln\frac{E}{\delta}. \tag{62}$$

Using Cauchy–Schwarz integral inequality, (13), (59) and (16) yields

$$\begin{aligned}\bar{\mathcal{J}}_2 \leq & \left[\int_{|\xi|\leq\xi_{\max}} 2\left(\int_x^1 e^{2|\tau|(s-x)}ds\right)\left(\int_x^1 |\hat{f}-\hat{f}^\delta|^2 ds\right)d\xi\right]^{\frac{1}{2}} \\ \leq & \xi_{\max}^{-\frac{\alpha}{4}} e^{(1-x)\xi_{\max}^{\frac{\alpha}{2}}} \left\|\hat{f}-\hat{f}^\delta\right\|_{L^2(0,1;L^2(\mathbb{R}))} \\ \leq & \left(\ln\frac{E}{\delta}\right)^{-\frac{1}{2}} E^{1-x}\delta^x.\end{aligned} \tag{63}$$

Thus , by (61) and (62)

$$\mathcal{J}_1 \leq \left(2\ln\frac{E}{\delta} + \left(\ln\frac{E}{\delta}\right)^{-\frac{1}{2}}\right)E^{1-x}\delta^x. \tag{64}$$

Step 2. Estimate the term $\mathcal{J}_2$ in (60). Again, using the Parseval's identity and Lemma 2, we have

$$\begin{aligned}\mathcal{J}_2 = & \left\|\hat{u}_x^{\xi_{\max}}(x,\cdot) - \hat{u}_x(x,\cdot)\right\| \\ = & \left[\int_{|\xi|>\xi_{\max}} \left|\tau e^{\tau(1-x)}\hat{g} + \int_x^1 \hat{f}\cosh\left(\tau(s-x)\right)ds\right|^2 d\xi\right]^{\frac{1}{2}} \\ \leq & \underbrace{\left[\int_{|\xi|>\xi_{\max}} 2\left|\tau e^{\tau(1-x)}\hat{g}\right|^2 d\xi\right]^{\frac{1}{2}}}_{\tilde{\mathcal{J}}_1} + \underbrace{\left[\int_{|\xi|>\xi_{\max}} 2\left|\int_x^1 \hat{f}\cosh\left(\tau(s-x)\right)ds\right|^2 d\xi\right]^{\frac{1}{2}}}_{\tilde{\mathcal{J}}_2}.\end{aligned}$$

We first estimate $\tilde{\mathcal{J}}_1$. Let

$$B_4(|\xi|) = \sqrt{2}|\xi|^{\frac{\alpha}{2}} e^{-x|\xi|^{\frac{\alpha}{2}}}.$$

By (7), we have

$$\begin{aligned}\tilde{\mathcal{J}}_1 = & \left[\int_{|\xi|>\xi_{\max}} 2\left|\tau e^{-\tau x}\left(\hat{u}(0,\xi) - \int_0^1 \hat{f}\frac{\sinh(\tau s)}{\tau}ds\right)\right|^2 d\xi\right]^{\frac{1}{2}} \\ \leq & \sup_{|\xi|>\xi_{\max}} B_4(|\xi|)\left|\hat{u}(0,\xi) - \int_0^1 \hat{f}\frac{\sinh(\tau s)}{\tau}ds\right|.\end{aligned}$$

By elementary calculations, it is easy to find the unique zero point $|\xi^*|$ of $B_4'(|\xi|)$ is

$$|\xi^*| = \left(\frac{1}{x}\right)^{\frac{2}{\alpha}},$$

and $|\xi^*|$ maximize the function $B_4(|\xi|)$. Thus,

$$\sup_{|\xi|>\xi_{\max}} B_4(|\xi|) = \begin{cases}\sqrt{2}|\xi^*|^{\frac{\alpha}{2}} e^{-x|\xi^*|^{\frac{\alpha}{2}}} \leq \sqrt{2}|\xi^*|^{\frac{\alpha}{2}} e^{-x\xi_{\max}^{\frac{\alpha}{2}}}, & \xi_{\max} < |\xi^*|, \\ \sqrt{2}\xi_{\max}^{\frac{\alpha}{2}} e^{-x\xi_{\max}^{\frac{\alpha}{2}}}, & \xi_{\max} \geq |\xi^*|.\end{cases}$$

By (59), we have

$$\sup_{|\xi|>\xi_{\max}} B_4(|\xi|) \leq \left\{\frac{1}{x}, \ln\frac{E}{\delta}\right\}\sqrt{2}e^{-x\ln\frac{E}{\delta}} := \epsilon_1\sqrt{2}E^{-x}\delta^x,$$

where

$$\epsilon_1 = \max\left\{\frac{1}{x}, \ln\frac{E}{\delta}\right\}. \tag{65}$$

Therefore , by Lemma 4, we obtain

$$\tilde{\mathcal{J}}_1 \le \epsilon_1\sqrt{2}E^{-x}\delta^x\big(E+N_1\big).$$

Now we estimate $\tilde{\mathcal{J}}_2$. Using Cauchy–Schwarz integral inequality, (13) and (15) yields

$$\begin{aligned}\tilde{\mathcal{J}}_2 \le& \left[\int_{|\xi|>\xi_{\max}} 2\bigg(\int_x^1 e^{2|\tau|(s-x)}ds\bigg)\bigg(\int_x^1 |\hat{f}|^2 ds\bigg)d\xi\right]^{\frac{1}{2}}\\ \le& \left[\int_{|\xi|>\xi_{\max}} \bigg(\frac{1}{|\xi|^{\frac{\alpha}{2}}}e^{2|\xi|^{\frac{\alpha}{2}}(1-x)}\bigg)\bigg(\int_x^1 |\hat{f}|^2 ds\bigg)d\xi\right]^{\frac{1}{2}}\\ \le& \xi_{\max}^{-\frac{\alpha}{4}}\left[\int_{|\xi|>\xi_{\max}} e^{2|\xi|^{\frac{\alpha}{2}}(1-x)}e^{-3|\xi|^{\frac{\alpha}{2}}}d\xi\right]^{\frac{1}{2}}.\end{aligned}$$

Since the generalized integral on the right side of the last inequality converges for $0 < x < 1$, we introduce the notation

$$N_2 = \left[\int_{|\xi|>\xi_{\max}} e^{-|\xi|^{\frac{\alpha}{2}}}d\xi\right]^{\frac{1}{2}}. \tag{66}$$

Using (59), we have

$$\tilde{\mathcal{J}}_2 \le \left(\ln\frac{E}{\delta}\right)^{-\frac{1}{2}}N_2.$$

Thus,

$$\mathcal{J}_2 \le \epsilon_1\sqrt{2}E^{-x}\delta^x\big(E+N_1\big) + \left(\ln\frac{E}{\delta}\right)^{-\frac{1}{2}}N_2. \tag{67}$$

where ϵ_1 is given by (64). By substituting (63) and (66) into (60), we arrive at the final conclusion. □

Remark 8. *If we replace assumptions (14) and (15) by (50) and (51), then the convergence* $\|u_x^{\delta,\xi_{\max}}(x,\cdot) - u_x(x,\cdot)\|_p$ *also holds.*

Similarly, the accuracy of the regularized solution becomes progressively lower as $x \to 0$, and then we use the condition (50) and (51) to give convergence estimate at $x = 0$.

Theorem 6. *Let* $\hat{u}(x,\xi)$ *given by (7) be the exact solution of problem (5) in the frequency space,* $\hat{u}_x^{\delta,\xi_{\max}}(x,\xi)$ *given by (58) be the regularized solution, condition (16), (50) and (51) hold. If the regularization parameter* $\xi_{\max}$ *is selected by*

$$\xi_{\max} = \left(\ln\Big(\frac{E}{\delta}\Big(\ln\frac{E}{\delta}\Big)^{-\frac{2p}{\alpha}}\Big)\right)^{\frac{2}{\alpha}}. \tag{68}$$

Then, for $p > \frac{\alpha}{2}$, *we have*

$$\big\|u_x^{\delta,\xi_{\max}}(0,\cdot) - u_x(0,\cdot)\big\| \le \big(2\epsilon_2^{-1} + \epsilon_2^{\frac{1}{2}}\big)E\left(\ln\frac{E}{\delta}\right)^{-\frac{2p}{\alpha}} + \sqrt{2}\epsilon_2^{\frac{2p}{\alpha}-1}\big(E+N_1\big) + \epsilon_2^{\frac{1}{2}+\frac{2p}{\alpha}}N_2, \tag{69}$$

where $\epsilon_2 = \left(\ln\Big(\frac{E}{\delta}\Big(\ln\frac{E}{\delta}\Big)^{-\frac{2p}{\alpha}}\Big)\right)^{-1}$, N_1 *and* N_2 *are some constants.*

Proof. By the triangle inequality, we have

$$\left\|u_x^{\delta,\xi_{\max}}(0,\cdot)-u_x(0,\cdot)\right\| \le \underbrace{\left\|u_x^{\delta,\xi_{\max}}(0,\cdot)-u_x^{\xi_{\max}}(0,\cdot)\right\|}_{\mathcal{J}_3} + \underbrace{\left\|u_x^{\xi_{\max}}(0,\cdot)-u_x(0,\cdot)\right\|}_{\mathcal{J}_4}. \tag{70}$$

Next , we divide the argument into two steps.

Step 1. Estimate the term $\mathcal{J}_3$ in (69). Taking a similar procedure of the estimate of $\mathcal{J}_1$, and by (67), we obtain

$$\begin{aligned}
\mathcal{J}_3 =& \left\|\hat{u}_x^{\delta,\xi_{\max}}(0,\cdot)-\hat{u}_x^{\xi_{\max}}(0,\cdot)\right\| \\
\le& \left[\int_{|\xi|\le\xi_{\max}} 2\left|\tau e^{\tau}(\hat{g}-\hat{g}^{\delta})\right|^2 d\xi\right]^{\frac{1}{2}} + \left[\int_{|\xi|\le\xi_{\max}} 2\left|\int_0^1 (\hat{f}-\hat{f}^{\delta})\cosh(\tau s)ds\right|^2 d\xi\right]^{\frac{1}{2}} \\
\le& 2\delta \sup_{|\xi|\le\xi_{\max}} \left|\tau e^{\tau}\right| + \left[\int_{|\xi|\le\xi_{\max}} 2\left(\int_0^1 e^{2|\tau|s}ds\right)\left(\int_0^1 |\hat{f}-\hat{f}^{\delta}|^2 ds\right)d\xi\right]^{\frac{1}{2}} \\
\le& 2\delta\xi_{\max}^{\frac{\alpha}{2}} e^{\xi_{\max}^{\frac{\alpha}{2}}} + \xi_{\max}^{-\frac{\alpha}{4}} e^{\xi_{\max}^{\frac{\alpha}{2}}} \left\|\hat{f}^{\delta}-\hat{f}\right\|_{L^2(0,1;H_p(\mathbb{R}))} \\
\le& (2\epsilon_2^{-1}+\epsilon_2^{\frac{1}{2}}) E\left(\ln\frac{E}{\delta}\right)^{-\frac{2p}{\alpha}},
\end{aligned} \tag{71}$$

where

$$\epsilon_2 = \left(\ln\left(\frac{E}{\delta}\left(\ln\frac{E}{\delta}\right)^{-\frac{2p}{\alpha}}\right)\right)^{-1}. \tag{72}$$

Step 2. Estimate the term $\mathcal{J}_4$ in (69). By Lemma 2, we have

$$\begin{aligned}
\mathcal{J}_4 =& \left\|\hat{u}_x^{\xi_{\max}}(0,\cdot)-\hat{u}_x(0,\cdot)\right\| \\
\le& \underbrace{\left[\int_{|\xi|>\xi_{\max}} 2\left|\tau e^{\tau}\hat{g}\right|^2 d\xi\right]^{\frac{1}{2}}}_{\tilde{\mathcal{J}}_3} + \underbrace{\left[\int_{|\xi|>\xi_{\max}} 2\left|\int_0^1 \hat{f}\cosh(\tau s)ds\right|^2 d\xi\right]^{\frac{1}{2}}}_{\tilde{\mathcal{J}}_4}.
\end{aligned}$$

We first estimate $\tilde{\mathcal{J}}_3$. By (7), (9), (67)and Lemma 5, we have

$$\begin{aligned}
\tilde{\mathcal{J}}_3 =& \left[\int_{|\xi|>\xi_{\max}} 2\left|(1+\xi^2)^{-\frac{p}{2}}\tau\left(\hat{u}(0,\xi)-\int_0^1 \hat{f}\frac{\sinh(\tau s)}{\tau}ds\right)(1+\xi^2)^{\frac{p}{2}}\right|^2 d\xi\right]^{\frac{1}{2}} \\
\le& \sqrt{2}\xi_{\max}^{\frac{\alpha}{2}-p}\left\|(1+\xi^2)^{\frac{p}{2}}\left(\hat{u}(0,\xi)-\int_0^1 \hat{f}\frac{\sinh(\tau s)}{\tau}ds\right)\right\| \\
\le& \sqrt{2}\epsilon_2^{\frac{2p}{\alpha}-1}(E+N_1).
\end{aligned}$$

Now we estimate $\tilde{\mathcal{J}}_4$. Using Cauchy–Schwarz integral inequality, (13), (9), (51), (67) and (65) yields

$$\begin{aligned}
\tilde{\mathcal{J}}_4 \le& \left[\int_{|\xi|>\xi_{\max}} 2(1+\xi^2)^{-p}\left(\int_0^1 e^{2|\tau|s}ds\right)\left(\int_0^1 |\hat{f}|^2 ds\right)(1+\xi^2)^p d\xi\right]^{\frac{1}{2}} \\
\le& \left[\int_{|\xi|>\xi_{\max}} |\xi|^{-2p}\left(\frac{1}{|\xi|^{\frac{\alpha}{2}}}e^{2|\xi|^{\frac{\alpha}{2}}}\right)\left(\int_0^1 |\hat{f}|^2 ds\right)(1+\xi^2)^p d\xi\right]^{\frac{1}{2}} \\
\le& \xi_{\max}^{-(\frac{\alpha}{4}+p)}\left[\int_{|\xi|>\xi_{\max}} e^{-|\xi|^{\frac{\alpha}{2}}}d\xi\right]^{\frac{1}{2}} \\
=& \epsilon_2^{\frac{1}{2}+\frac{2p}{\alpha}} N_2.
\end{aligned}$$

Then

$$\mathcal{J}_4 \le \sqrt{2}\epsilon_2^{\frac{2p}{\alpha}-1}\left(E+N_1\right)+\epsilon_2^{\frac{1}{2}+\frac{2p}{\alpha}}N_2, \tag{73}$$

where ϵ_2 is given by (71). The Theorem now follows from equations (69)–(72). □

Remark 9. *Since the regularization parameter $\xi_{\max} \to \infty$ as $\delta \to 0$, we can easily find that, for $p > \frac{\alpha}{2}$, $\epsilon_2 \to 0$ ($\delta \to 0$). In addition, note that for $p > \frac{\alpha}{2}$ there hold*

$$\ln\left(\frac{E}{\delta}\left(\ln\frac{E}{\delta}\right)^{-\frac{2p}{\alpha}}\right)\left(\ln\frac{E}{\delta}\right)^{-\frac{2p}{\alpha}} = \left(\ln\frac{E}{\delta}\right)^{1-\frac{2p}{\alpha}} - \frac{2p}{\alpha}\left[\ln\left(\ln\frac{E}{\delta}\right)\right]\left(\ln\frac{E}{\delta}\right)^{-\frac{2p}{\alpha}} \to 0, \quad \delta \to 0.$$

Therefore,

$$\lim_{\delta\to 0}\left\|u_x^{\delta,\xi_{\max}}(0,\cdot)-u_x(0,\cdot)\right\| = 0, \quad p > \frac{\alpha}{2}.$$

Remark 10. *In 2007, Qian [46] proved that it is impossible to obtain the error asymptotically better than logarithmic rate at $x = 0$. So our estimates is reasonable.*

6. Conclusions

In this paper, we have considered the problem of finding a function $u(x,t)$ satisfying (5). This is a sideways problem for non-homogeneous fractional heat equation, and the problem is ill-posed. To regularize the problem, we propose the dynamic spectral method and Fourier method, which are rather simple and convenient for dealing with some ill-posed problems. Error estimations between the approximate solution and the exact one, established from noise data g_δ and f_δ, are given. In fact, the paper extends the work in [33]. It is worth noting that the obtained estimates are sufficient to prove the results, but most of them are quite rough and can be improved.

As we all know, the most common regularization methods are the Tikhonov method, iterative method, quasi-reversibility method, truncation method, quasi-boundary value method and spectral method. The main difference between these methods is their convergence order. We can compare the convergence rate of errors by using different methods to discuss the problem. In addition, the dynamic spectral method and Fourier method can easily be extended to multi-dimensional case, which needs further study.

Author Contributions: Formal analysis, Y.C. and Y.Q.; Supervision, X.X. All authors have read and agreed to the published version of the manuscript.

Funding: This research received no external funding.

Institutional Review Board Statement: Not applicable.

Informed Consent Statement: Written informed consent has been obtained from the patients to publish this paper.

Data Availability Statement: Not applicable.

Conflicts of Interest: The authors declare no conflict of interest.

References

1. Meerschaert, M.M.; Scheffer, H.P. Semistable Lévy motion. *Fract. Calc. Appl. Anal.* **2002**, *5*, 27–54.
2. Barkai, E.; Metzler, R.; Klafter, J. From continuous time random walks to the fractional Fokker-Planck equation. *Phys. Rev. E Stat. Phys. Plasmas Fluids Relat. Interdiscip. Top.* **2000**, *61*, 132–138. [CrossRef] [PubMed]
3. Raberto, M.; Scalas, E.; Mainardi, F. Waiting-times and returns in high-frequency financial data: An empirical study. *Phys. A Stat. Mech. Its Appl.* **2002**, *314*, 749–755. [CrossRef]
4. Sabatier, J.; Lanusse, P.; Melchior, P.; Oustaloup, A. *Fractional Order Differentiation and Robust Control Design*; Springer: Dordrecht, The Netherlands, 2015.
5. Das, S.; Pan, I. *Fractional Order Signal Processing*; Springer: Berlin/Heidelberg, Germany, 2012.
6. Vilela Mendes, R. A fractional calculus interpretation of the fractional volatility model. *Nonlinear Dyn.* **2009**, *55*, 395–399. [CrossRef]

7. Roul, P. Analytical approach for nonlinear partial differential equations of fractional order. *Commun. Theor. Phys.* **2013**, *60*, 269–277. [CrossRef]
8. Roul, P. A high accuracy numerical method and its convergence for time-fractional Black-Scholes equation governing European options. *Appl. Numer. Math.* **2020**, *151*, 472–493. [CrossRef]
9. Li, C.P.; Wang, Z. The discontinuous Galerkin finite element method for Caputo-type nonlinear conservation law. *Math. Comput. Simul.* **2020**, *169*, 51–73. [CrossRef]
10. Sun, H.G.; Chen, Y.Q.; Chen, W. Random-order fractional differential equation models. *Signal Process.* **2011**, *91*, 525–530. [CrossRef]
11. Atangana, A.; Qureshi, S. Modeling attractors of chaotic dynamical systems with fractal-fractional operators. *Chaos Solitons Fractals* **2019**, *123*, 320–337. [CrossRef]
12. Liu, Q.; Liu, F.; Turner, I.; Anh, V.; Gu, Y. A RBF meshless approach for modeling a fractal mobile/immobile transport model. *Appl. Math. Comput.* **2014**, *226*, 336–347. [CrossRef]
13. Saqib, M.; Khan, I.; Shafie, S. Application of Atangana-Baleanu fractional derivative to MHD channel flow of CMC-based-CNT's nanofluid through a porous medium. *Chaos Solitons Fractals* **2018**, *116*, 79–85. [CrossRef]
14. Podlubny, I. *Fractional Differential Equations*; Academic Press: San Diego, CA, USA, 1999.
15. Zheng, Z.M.; Li, Z.P.; Xiong, X.T. An improved error bound on the boundary inversion for a sideways heat equation. *São Paulo J. Math. Sci.* **2020**, *14*, 287–300. [CrossRef]
16. Qian, Z. Regularization methods for the sideways heat equation and the idea of modifying the "kernel" in the frequency domain. *Commun. Appl. Math. Comput.* **2012**, *26*, 298–311. (In Chinese)
17. Carasso, A. Determining surface temperatures from interior observations. *SIAM J. Appl. Math.* **1982**, *42*, 558–574. [CrossRef]
18. Eldén, L. Modified equations for approximating the solution of a Cauchy problem for the heat equation. *Inverse Ill-Posed Probl.* **1987**, *4*, 345–350.
19. Eldén, L. Approximations for a Cauchy problem for the heat equation. *Inverse Probl.* **1987**, *3*, 263–273.
20. Nguyen, H.T.; Luu, V.C.H. Two new regularization methods for solving sideways heat equation. *J. Inequal. Appl.* **2015**, *2015*, 1–17. [CrossRef]
21. Wang, J.R. Uniform convergence of wavelet solution to the sideways heat equation. *Acta Math. Sin.* **2010**, *26*,1981–1992. [CrossRef]
22. Qiu, C.Y.; Fu, C.L.; Zhu, Y.B. Wavelets and regularization of the sideways heat equation. *Comput. Math. Appl.* **2003**, *46*, 821–829. [CrossRef]
23. Fu, C.L.; Qiu, C.Y. Wavelet and error estimation of surface heat flux. *J. Comput. Appl. Math.* **2003**, *150*, 143–155.
24. Seidman, T.I.; Eldén, L. An "optimal filtering" method for the sideways heat equation. *Inverse Probl.* **1990**, *6*, 681–696. [CrossRef]
25. Xiong, X.T.; Fu, C.L.; Li, H.F. Fourier regularization method of a sideways heat equation for determining surface heat flux. *J. Math. Anal. Appl.* **2006**, *317*, 331–348. [CrossRef]
26. Xiong, X.T.; Fu, C.L.; Li, H.F. Central difference method of a non-standard inverse heat conduction problem for determining surface heat flux from interior observations. *Appl. Math. Comput.* **2006**, *173*, 1265–1287. [CrossRef]
27. Eldén, L. Numerical solution of the sideways heat equation. In *Inverse Problems in Diffusion Processes*; SIAM: Philadelphia, PA, USA, 1995; pp.130–150.
28. Murio, D.A. The mollification method and the numerical solution of the inverse heat conduction problem by finite differences. *Comput. Math. Appl.* **1989**, *17*, 1385–1396. [CrossRef]
29. Huy Tuan, N.; Lesnic, D.; Quoc Viet, T.; Van Au, V. Regularization of semilinear sideways heat equation. *IMA J. Appl. Math.* **2019**, *84*, 258–291. [CrossRef]
30. Anh Triet, N.; O'Regan, D.; Baleanu, D.; Hoang Luc, N.; Can, N. A filter method for inverse nonlinear sideways heat equation. *Adv. Differ. Equ.* **2020**, *149*, 1–18. [CrossRef]
31. Xiong, X.T.; Guo, H.B.; Liu, X.H. An inverse problem for a fractional diffusion equation. *J. Comput. Appl. Math.* **2012**, *236*, 4474–4484. [CrossRef]
32. Xiong, X.T.; Bai, E.P. An optimal filtering method for the sideways fractional heat equation. *J. Northwest Norm. Univ.* **2020**, *56*, 14–16, 47. (In Chinese)
33. Li, M.; Xi, X.X.; Xiong, X.T. Regularization for a fractional sideways heat equation. *J. Comput. Appl. Math.* **2014**, *255*, 28–43. [CrossRef]
34. Zheng, G.H.; Wei, T. Spectral regularization method for solving a time-fractional inverse diffusion problem. *Appl. Math. Comput.* **2011**, *218*, 396–405. [CrossRef]
35. Zheng, G.H.; Wei, T. Spectral regularization method for a Cauchy problem of the time fractional advection-dispersion equation. *J. Comput. Appl. Math.* **2010**, *233*, 2631–2640. [CrossRef]
36. Zheng, G.H.; Wei, T. Spectral regularization method for the time fractional inverse advection-dispersion equation. *Math. Comput. Simul.* **2010**, *81*, 37–51. [CrossRef]
37. Zhang, H.W.; Zhang, X.J. Tikhonov-type regularization method for a sideways problem of the time-fractional diffusion equation. *AIMS Math.* **2021**, *6*, 90–101. [CrossRef]
38. Qian, Z.; Fu, C.L. Regularization strategies for a two-dimensional inverse heat conduction problem. *Inverse Probl.* **2007**, *23*, 1053–1068. [CrossRef]

39. Liu, S.S.; Feng, L.X. An Inverse Problem for a Two-Dimensional Time-Fractional Sideways Heat Equation. *Math. Probl. Eng.* **2020**, *2020*, 1–13. [CrossRef]
40. Liu, S.S.; Feng, L.X. A revised Tikhonov regularization method for a Cauchy problem of two-dimensional heat conduction equation. *Math. Probl. Eng.* **2018**, *2018*, 1–8. [CrossRef]
41. Xiong, X.T.; Xue, X.M. Fractional Tikhonov method for an inverse time-fractional diffusion problem in 2-dimensional space. *Bull. Malays. Math. Sci. Soc.* **2020**, *43*, 25–38. [CrossRef]
42. Xiong, X.T.; Zhou, Q.; Hon, Y.C. An inverse problem for fractional diffusion equation in 2-dimensional case: Stability analysis and regularization. *J. Math. Anal. Appl.* **2012**, *393*, 185–199. [CrossRef]
43. Guo, L.; Murio, D.A. A mollified space-marching finite-different algorithm for the two-dimensional inverse heat conduction problem with slab symmetry. *Inverse Probl.* **1991**, *7*, 247–259. [CrossRef]
44. Liu, C.S.; Chang, C.W. A spring-damping regularization of the Fourier sine series solution to the inverse Cauchy problem for a 3D sideways heat equation. *Inverse Probl. Sci. Eng.* **2020**, *29*, 196–219. [CrossRef]
45. Luan, T.N.; Khanh, T.Q. Determination of temperature distribution and thermal flux for two-dimensional inhomogeneous sideways heat equations. *Adv. Comput. Math.* **2020**, *46*, 1–28. [CrossRef]
46. Qian, Z.; Fu, C.L.; Xiong, X.T. A modified method for determining the surface heat flux of IHCP. *Inverse Probl. Sci. Eng.* **2007**, *15*, 249–265. [CrossRef]

symmetry

MDPI

Article

Noether and Lie Symmetry for Singular Systems Involving Mixed Derivatives

Chuan-Jing Song

School of Mathematical Sciences, Suzhou University of Science and Technology, Suzhou 215009, China; songchuanjingsun@126.com

Abstract: Singular systems play an important role in many fields, and some new fractional operators, which are general, have been proposed recently. Therefore, singular systems on the basis of the mixed derivatives including the integer order derivative and the generalized fractional operators are studied. Firstly, Lagrange equations within mixed derivatives are established, and the primary constraints are presented for the singular systems. Then the constrained Hamilton equations are constructed by introducing the Lagrange multipliers. Thirdly, Noether symmetry, Lie symmetry and the corresponding conserved quantities for the constrained Hamiltonian systems are investigated. And finally, an example is given to illustrate the methods and results.

Keywords: generalized operator; singular system; primary constraint; constrained Hamilton equation; Noether symmetry; Lie symmetry; conserved quantity

Citation: Song, C.-J. Noether and Lie Symmetry for Singular Systems Involving Mixed Derivatives. *Symmetry* **2022**, *14*, 1225. https://doi.org/10.3390/sym14061225

Academic Editor: António M. Lopes

Received: 21 April 2022
Accepted: 10 June 2022
Published: 13 June 2022

1. Introduction

Fractional calculus is a hot topic recently. Many results have been obtained in fractional calculus and its applications [1–7]. Since fractional derivatives were used to deal with dissipative forces for nonconservative systems by Riewe [8,9] in 1996, fractional variational problems became popular. For example, Klimek [10] studied Lagrangian and Hamiltonian fractional sequential mechanics; Muslih and Baleanu [11] established the Hamiltonian formulation of the systems with linear velocities within the Riemann–Liouville fractional derivative; Agrawal [12], investigated the fractional variational calculus in terms of the Riesz fractional derivative; Luo [13] studied the fractional Birkhoffian mechanics in terms of the combined Riemann-Liouville fractional derivative and the combined Caputo fractional derivative; Song and Agrawal [14] presented the Euler-Lagrange equations involving the Caputo fractional derivative for singular systems, and so on [15,16]. Especially, in 2010, Agrawal [17] introduced a new kernel $\kappa_\alpha(t,\tau)$ (or $\kappa_\alpha(\tau,t)$), on which the generalized fractional derivatives are defined. Only when the parameter set is specified, and the kernel $\kappa_\alpha(t,\tau)$ is equal to $(t-\tau)^{\alpha-1}/\Gamma(\alpha)$, can the Riemann-Liouville fractional derivative, the Caputo fractional derivative, the Riesz-Riemann-Liouville fractional derivative and the Riesz-Caputo fractional derivative be obtained. Besides, the kernel can also be replaced with other kernels, and the entire theories of classical and fractional variational calculus can be redeveloped. Therefore, the generalized fractional derivatives are more general.

Singular system is another keyword of this paper. Singular system plays an important role in field theory, because many important physical systems in field theory are singular ones, such as the Yang-Mills field, the gravitational field, the electromagnetic field, supersymmetry, superstring, supergravity, relativistic moving particles and so on [18]. Singular system has two forms, one is expressed by a Lagrangian, and the other is expressed by a Hamiltonian. When a singular system is expressed in the form of the Hamiltonian, there exist inherent constraints among the canonical variables, and the corresponding system is called a constrained Hamiltonian system [19,20]. The constrained Hamiltonian system also has many applications, such as in quantum field theories of anyons and theories of condensed matter [19,21,22].

In this paper, we intend to study the fractional calculus of variations for singular systems on the basis of generalized fractional derivatives. After the fractional differential equations of motion are established, the next step is to find solutions to them. The symmetry method in mechanics is one of the most effective methods. The symmetry method mainly contains three kinds of methods, namely, the Noether symmetry method, the Lie symmetry method and the Mei symmetry method [23]. This paper focuses on the Noether symmetry method and the Lie symmetry method. The Noether symmetry method was introduced by a German female mathematician Noether [24]. Noether symmetry is an invariance of the Hamilton action under the infinitesimal transformations of time and coordinates, and can lead to a conserved quantity. Lie symmetry is an invariance of the differential equations under the infinitesimal transformations of time and coordinates. Lie symmetry can also lead to a conserved quantity under certain conditions. Many results have been obtained with Noether symmetry and Lie symmetry, including both integer order calculus and fractional order calculus [25–46], we only refer to them briefly here.

2. Preliminaries on the Generalized Operators

Generalized operators were introduced by Agrawal [17] in 2010. He defined the operator K_M^α as

$$K_M^\alpha f(t) = m\int_{t_1}^{t} \kappa_\alpha(t,\tau)f(\tau)\mathrm{d}\tau + \omega\int_{t}^{t_2} \kappa_\alpha(\tau,t)f(\tau)\mathrm{d}\tau,\ \alpha > 0, \tag{1}$$

where $t_1 < t < t_2$, $M =< t_1, t, t_2, m, \omega >$ is a parameter set, m and ω are two real numbers, $\kappa_\alpha(t,\tau)$ is a kernel which may depend on a parameter α. It is easy to verify that the operator K_M^α is a linear operator and satisfies the following integration by parts formula,

$$\int_{t_1}^{t_2} g(t)K_M^\alpha f(t)\mathrm{d}t = \int_{t_1}^{t_2} f(t)K_{M^*}^\alpha g(t)\mathrm{d}t \tag{2}$$

where $M^* =< t_1, t, t_2, \omega, m >$.

The operators A_M^α and B_M^α were defined by Agrawal as

$$A_M^\alpha f(t) = D^n K_M^{n-\alpha} f(t),\ n-1 < \alpha < n, \tag{3}$$

$$B_M^\alpha f(t) = K_M^{n-\alpha} D^n f(t),\ n-1 < \alpha < n, \tag{4}$$

where D means the classical integer order derivative $\mathrm{d}/\mathrm{d}t$, n is an integer. Both operators are also linear and they satisfy the following integration by parts formulae,

$$\int_{t_1}^{t_2} g(t)A_M^\alpha f(t)\mathrm{d}t = (-1)^n\int_{t_1}^{t_2} f(t)B_{M^*}^\alpha g(t)\mathrm{d}t + \sum_{j=0}^{n-1}(-D)^{n-1-j}g(t)A_M^{\alpha+j-n}f(t)\Big|_{t=t_1}^{t=t_2} \tag{5}$$

$$\int_{t_1}^{t_2} g(t)B_M^\alpha f(t)\mathrm{d}t = (-1)^n\int_{t_1}^{t_2} f(t)A_{M^*}^\alpha g(t)\mathrm{d}t + \sum_{j=0}^{n-1}(-1)^j A_{M^*}^{\alpha+j-n}g(t)D^{n-1-j}f(t)\Big|_{t=t_1}^{t=t_2} \tag{6}$$

where $M^* =< t_1, t, t_2, \omega, m >$, n is an integer, $n-1 < \alpha < n$.

Specifically, if we let $\kappa_\alpha(t,\tau) = (t-\tau)^{\alpha-1}/\Gamma(\alpha)$ and let $M = M_1 =< t_1, t, t_2, 1, 0 >$, $M = M_2 =< t_1, t, t_2, 0, 1 >$ and $M = M_3 =< t_1, t, t_2, 1/2, 1/2 >$, then the operator A_M^α reduces to the left Riemann-Liouville, the right Riemann-Liouville and the Riesz-Riemann-Liouville fractional derivative operators, respectively. Similarly, the operator B_M^α reduces to the left Caputo, the right Caputo and the Riesz-Caputo fractional derivative operators, respectively.

In this text we set $0 < \alpha < 1$. We begin with variational problems and the primary constraints.

3. Variational Problems and the Primary Constraints

3.1. The Variational Problem and the Primary Constraint with the Operator A_M^α

Hamilton action with the operator A_M^α is defined as

$$I_A[\boldsymbol{q_A}(\cdot)] = \int_{t_1}^{t_2} L_A\big(t, \boldsymbol{q_A}, \dot{\boldsymbol{q}}_{\boldsymbol{A}}, \boldsymbol{A_M^\alpha q_A}\big)\mathrm{d}t \tag{7}$$

where $\boldsymbol{q_A} = (q_{A1}, q_{A2}, \cdots, q_{An})$, $q_{Ai} \in C^2([t_1, t_2]; \mathbb{R})$, $i = 1, 2, \cdots, n$, $\dot{\boldsymbol{q}}_{\boldsymbol{A}} = \big(\dot{q}_{A1}, \dot{q}_{A2}, \cdots, \dot{q}_{An}\big)$, $\boldsymbol{A_M^\alpha q_A} = \big(A_M^\alpha q_{A1}, A_M^\alpha q_{A2}, \cdots, A_M^\alpha q_{An}\big)$, $0 < \alpha < 1$ and $L_A(\cdot, \cdot, \cdot, \cdot) \in C^2([t_1, t_2] \times \mathbb{R}^n \times \mathbb{R}^n \times \mathbb{R}^n; \mathbb{R})$.

Then

$$\delta I_A = 0 \tag{8}$$

with

$$\boldsymbol{q_A}(t_1) = \boldsymbol{q_{A1}},\ \boldsymbol{q_A}(t_2) = \boldsymbol{q_{A2}},\ \delta\dot{q}_{Ai} = \frac{\mathrm{d}}{\mathrm{d}t}\delta q_{Ai},\ \delta A_M^\alpha q_{Ai} = A_M^\alpha \delta q_{Ai},\ i = 1, 2, \cdots, n \tag{9}$$

is called the Hamilton principle with the operator A_M^α, where $\boldsymbol{q_{A1}} = (q_{A11}, q_{A12}, \cdots, q_{A1n})$, $\boldsymbol{q_{A2}} = (q_{A21}, q_{A22}, \cdots, q_{A2n})$.

From Equations (5), (8) and (9), we obtain

$$\frac{\partial L_A}{\partial q_{Ai}} - \frac{\mathrm{d}}{\mathrm{d}t}\frac{\partial L_A}{\partial \dot{q}_{Ai}} - B_{M^*}^\alpha \frac{\partial L_A}{\partial A_M^\alpha q_{Ai}} + m\kappa_{1-\alpha}(t_2, t)\frac{\partial L_A(t_2)}{\partial A_M^\alpha q_{Ai}} - \omega\kappa_{1-\alpha}(t, t_1)\frac{\partial L_A(t_1)}{\partial A_M^\alpha q_{Ai}} = 0 \tag{10}$$

where $L_A(t_1) = L_A\big(t_1, \boldsymbol{q_A}(t_1), \dot{\boldsymbol{q}}_{\boldsymbol{A}}(t_1), \boldsymbol{A_M^\alpha q_A}(t_1)\big)$, $L_A(t_2) = L_A\big(t_2, \boldsymbol{q_A}(t_2), \dot{\boldsymbol{q}}_{\boldsymbol{A}}(t_2), \boldsymbol{A_M^\alpha q_A}(t_2)\big)$, $i = 1, 2, \cdots, n$. Equation (10) is called the Lagrange equation with the operator A_M^α.

Define the generalized momenta and the Hamiltonian as

$$p_{Ai} = \frac{\partial L_A\big(t, \boldsymbol{q_A}, \dot{\boldsymbol{q}}_{\boldsymbol{A}}, \boldsymbol{A_M^\alpha q_A}\big)}{\partial \dot{q}_{Ai}},\ p_{Ai}^\alpha = \frac{\partial L_A\big(t, \boldsymbol{q_A}, \dot{\boldsymbol{q}}_{\boldsymbol{A}}, \boldsymbol{A_M^\alpha q_A}\big)}{\partial A_M^\alpha q_{Ai}}, \tag{11}$$

$$H_A = p_{Ai}\dot{q}_{Ai} + p_{Ai}^\alpha \cdot A_M^\alpha q_{Ai} - L_A\big(t, \boldsymbol{q_A}, \dot{\boldsymbol{q}}_{\boldsymbol{A}}, \boldsymbol{A_M^\alpha q_A}\big),\ i = 1, 2, \cdots, n. \tag{12}$$

In this paper, we assume that $A_M^\alpha q_{Ai} = u_{Ai}\big(t, \boldsymbol{q_A}, \dot{\boldsymbol{q}}_{\boldsymbol{A}}, \boldsymbol{p_A^\alpha}\big)$ (or $\boldsymbol{A_M^\alpha q_A} = \boldsymbol{u_A}\big(t, \boldsymbol{q_A}, \dot{\boldsymbol{q}}_{\boldsymbol{A}}, \boldsymbol{p_A^\alpha}\big)$), where $\boldsymbol{p_A^\alpha} = \big(p_{A1}^\alpha, p_{A2}^\alpha, \cdots, p_{An}^\alpha\big)$, $\boldsymbol{u_A} = (u_{A1}, u_{A2}, \cdots, u_{An})$.

Define the elements H_{Aij}, $i, j = 1, 2, \cdots, n$, of the Hessian matrix $\big[H_{Aij}\big]$ as

$$H_{Aij} = \frac{\partial^2 L_A}{\partial \dot{q}_{Ai}\partial \dot{q}_{Aj}},\ i, j = 1, 2, \cdots, n, \tag{13}$$

then the Lagrangian is called regular if $\det\big[H_{Aij}\big] \neq 0$, and if $\det\big[H_{Aij}\big] = 0$, then the Lagrangian L_A is called singular. In this text, we assume that $\det\big[H_{Aij}\big] = 0$ and $\mathrm{rank}\big[H_{Aij}\big] = R$, $0 \leq R < n$. In the sequel, we will discuss two cases, i.e., $1 \leq R < n$ and $R = 0$.

Firstly, when $1 \leq R < n$, which means that only $\dot{q}_{A\sigma}$, $\sigma = 1, 2, \cdots, R$, can be determined from Equation (11) while $\dot{q}_{A\rho}$, $\rho = R+1, R+2, \cdots, n$, are random. From Equation (11), we express $\dot{q}_{A\sigma}$, $\sigma = 1, 2, \cdots, R$, as

$$\dot{q}_{A\sigma} = f_A^\sigma\big(t, \boldsymbol{q_A}, \boldsymbol{p_A^\alpha}, \boldsymbol{p_{AE}}, \dot{\boldsymbol{q}}_{\boldsymbol{AF}}\big),\ \Big(\text{or } \dot{\boldsymbol{q}}_{\boldsymbol{AE}} = \boldsymbol{f_A^E}\big(t, \boldsymbol{q_A}, \boldsymbol{p_A^\alpha}, \boldsymbol{p_{AE}}, \dot{\boldsymbol{q}}_{\boldsymbol{AF}}\big)\Big), \tag{14}$$

where $\boldsymbol{p_{AE}} = (p_{A1}, p_{A2}, \cdots, p_{AR})$, $\dot{\boldsymbol{q}}_{\boldsymbol{AE}} = \big(\dot{q}_{A1}, \dot{q}_{A2}, \cdots, \dot{q}_{AR}\big)$, $\dot{\boldsymbol{q}}_{\boldsymbol{AF}} = \big(\dot{q}_{AR+1}, \dot{q}_{AR+2}, \cdots, \dot{q}_{An}\big)$, $\boldsymbol{f_A^E} = \big(f_A^1, f_A^2, \cdots, f_A^R\big)$, $1 \leq R < n$.

From Equations (11) and (14), we have

$$p_{Ai} = g_{Ai}\Big(t, \boldsymbol{q_A}, \boldsymbol{f_A^E}\big(t, \boldsymbol{q_A}, \boldsymbol{p_A^\alpha}, \boldsymbol{p_{AE}}, \dot{\boldsymbol{q}}_{\boldsymbol{AF}}\big), \dot{\boldsymbol{q}}_{\boldsymbol{AF}}, \boldsymbol{p_A^\alpha}\Big) = g_{Ai}\big(t, \boldsymbol{q_A}, \boldsymbol{p_A^\alpha}, \boldsymbol{p_{AE}}, \dot{\boldsymbol{q}}_{\boldsymbol{AF}}\big),\ i = 1, 2, \cdots, n. \tag{15}$$

For Equation (15), if $i = 1, 2, \cdots, R$, $1 \leq R < n$, then Equation (15) always holds. If $i = R+1, R+2, \cdots, n$, $1 \leq R < n$, then from the assumption $\operatorname{rank}\left[H_{Aij}\right] = R$, $1 \leq R < n$, we have

$$p_{A\rho} = g_{A\rho}(t, \boldsymbol{q_A}, \boldsymbol{p_{AE}}, \boldsymbol{p_A^\alpha}), \ (\text{or } \boldsymbol{p_{AF}} = \boldsymbol{g_{AF}}(t, \boldsymbol{q_A}, \boldsymbol{p_{AE}}, \boldsymbol{p_A^\alpha})), \tag{16}$$

where $\rho = R+1, R+2, \cdots, n$, $\boldsymbol{p_{AF}} = (p_{AR+1}, p_{AR+2}, \cdots, p_{An})$, $\boldsymbol{g_{AF}} = (g_{AR+1}, g_{AR+2}, \cdots, g_{An})$, $1 \leq R < n$. Equation (16) has another form

$$\phi_A(t, \boldsymbol{q_A}, \boldsymbol{p_A}, \boldsymbol{p_A^\alpha}) = \boldsymbol{p_{AF}} - \boldsymbol{g_{AF}}(t, \boldsymbol{q_A}, \boldsymbol{p_{AE}}, \boldsymbol{p_A^\alpha}) = 0, \tag{17}$$

where $\phi_A = (\phi_{A1}, \phi_{A2}, \cdots, \phi_{An-R})$, $1 \leq R < n$.

Secondly, when $R = 0$, which means that no $\dot{q}_{Ai}$, $i = 1, 2, \cdots, n$, can be determined from Equation (11). Then from Equation (11) and the assumption $\operatorname{rank}\left[H_{Aij}\right] = R$, $R = 0$, we have

$$p_{Ai} = g_{Ai}(t, \boldsymbol{q_A}, \boldsymbol{p_A^\alpha}), \ (\text{or } \boldsymbol{p_A} = \boldsymbol{g_A}(t, \boldsymbol{q_A}, \boldsymbol{p_A^\alpha})), \tag{18}$$

where $i = 1, 2, \cdots, n$, $\boldsymbol{p_A} = (p_{A1}, p_{A2}, \cdots, p_{An})$, $\boldsymbol{g_A} = (g_{A1}, g_{A2}, \cdots, g_{An})$. Then Equation (18) gives

$$\phi_A(t, \boldsymbol{q_A}, \boldsymbol{p_A}, \boldsymbol{p_A^\alpha}) = \boldsymbol{p_A} - \boldsymbol{g_A}(t, \boldsymbol{q_A}, \boldsymbol{p_A^\alpha}) = 0, \tag{19}$$

where $\phi_A = (\phi_{A1}, \phi_{A2}, \cdots, \phi_{An})$.

Incorporating Equations (17) and (19), we get

$$\phi_A(t, \boldsymbol{q_A}, \boldsymbol{p_A}, \boldsymbol{p_A^\alpha}) = 0, \tag{20}$$

where $\phi_A = (\phi_{A1}, \phi_{A2}, \cdots, \phi_{An-R})$, $0 \leq R < n$. Equation (20) is called primary constraint with the operator A_M^α.

Remark 1. *Let $\kappa_\alpha(t, \tau) = (t-\tau)^{\alpha-1}/\Gamma(\alpha)$, when $M = M_1$, $M = M_2$ and $M = M_3$, Equations (10) and (20) give the Lagrange equations and the primary constraints in terms of the left Riemann-Liouville, the right Riemann-Liouville and the Riesz-Riemann-Liouville fractional derivatives, respectively.*

3.2. The Variational Problem and the Primary Constraint with the Operator B_M^α

Hamilton action with the operator B_M^α is

$$I_B[\boldsymbol{q_B}(\cdot)] = \int_{t_1}^{t_2} L_B(t, \boldsymbol{q_B}, \dot{\boldsymbol{q}}_{\boldsymbol{B}}, \boldsymbol{B_M^\alpha q_B}) \mathrm{d}t, \tag{21}$$

where $\boldsymbol{q_B} = (q_{B1}, q_{B2}, \cdots, q_{Bn})$, $q_{Bi} \in C^2([t_1, t_2]; \mathbb{R})$, $i = 1, 2, \cdots, n$, $\dot{\boldsymbol{q}}_{\boldsymbol{B}} = \left(\dot{q}_{B1}, \dot{q}_{B2}, \cdots, \dot{q}_{Bn}\right)$, $\boldsymbol{B_M^\alpha q_B} = \left(B_M^\alpha q_{B1}, B_M^\alpha q_{B2}, \cdots, B_M^\alpha q_{Bn}\right)$, $L_B(\cdot, \cdot, \cdot, \cdot) \in C^2([t_1, t_2] \times \mathbb{R}^n \times \mathbb{R}^n \times \mathbb{R}^n; \mathbb{R})$ and $0 < \alpha < 1$. Then

$$\delta I_B = 0 \tag{22}$$

with

$$\boldsymbol{q_B}(t_1) = \boldsymbol{q_{B1}}, \ \boldsymbol{q_B}(t_2) = \boldsymbol{q_{B2}}, \ \delta\dot{q}_{Bi} = \frac{\mathrm{d}}{\mathrm{d}t}\delta q_{Bi}, \ \delta B_M^\alpha q_{Bi} = B_M^\alpha \delta q_{Bi}, \ i = 1, 2, \cdots, n \tag{23}$$

is called the Hamilton principle with the operator B_M^α, where $\boldsymbol{q_{B1}} = (q_{B11}, q_{B12}, \cdots, q_{B1n})$, $\boldsymbol{q_{B2}} = (q_{B21}, q_{B22}, \cdots, q_{B2n})$.

From Equations (6), (22) and (23), we obtain

$$\frac{\partial L_B}{\partial q_{Bi}} - \frac{\mathrm{d}}{\mathrm{d}t}\frac{\partial L_B}{\partial \dot{q}_{Bi}} - A_{M^*}^\alpha \frac{\partial L_B}{\partial B_M^\alpha q_{Bi}} = 0, \ i = 1, 2, \cdots, n. \tag{24}$$

Equation (24) is called the Lagrange equation with the operator B_M^α.

Define the generalized momenta and the Hamiltonian as

$$p_{Bi} = \frac{\partial L_B(t, \boldsymbol{q_B}, \dot{\boldsymbol{q}}_{\boldsymbol{B}}, \boldsymbol{B}_{\boldsymbol{M}}^{\boldsymbol{\alpha}} \boldsymbol{q_B})}{\partial \dot{q}_{Bi}},\ p_{Bi}^{\alpha} = \frac{\partial L_B(t, \boldsymbol{q_B}, \dot{\boldsymbol{q}}_{\boldsymbol{B}}, \boldsymbol{B}_{\boldsymbol{M}}^{\boldsymbol{\alpha}} \boldsymbol{q_B})}{\partial B_M^{\alpha} q_{Bi}}, \tag{25}$$

$$H_B = p_{Bi}\dot{q}_{Bi} + p_{Bi}^{\alpha} \cdot B_M^{\alpha} q_{Bi} - L_B(t, \boldsymbol{q_B}, \dot{\boldsymbol{q}}_{\boldsymbol{B}}, \boldsymbol{B}_{\boldsymbol{M}}^{\boldsymbol{\alpha}} \boldsymbol{q_B}),\ i = 1, 2, \cdots, n. \tag{26}$$

In this paper, we assume that $B_M^{\alpha} q_{Bi} = u_{Bi}(t, \boldsymbol{q_B}, \dot{\boldsymbol{q}}_{\boldsymbol{B}}, \boldsymbol{p}_{\boldsymbol{B}}^{\boldsymbol{\alpha}})$ (or $\boldsymbol{B}_{\boldsymbol{M}}^{\boldsymbol{\alpha}} \boldsymbol{q_B} = \boldsymbol{u_B}(t, \boldsymbol{q_B}, \dot{\boldsymbol{q}}_{\boldsymbol{B}}, \boldsymbol{p}_{\boldsymbol{B}}^{\boldsymbol{\alpha}})$), where $\boldsymbol{p}_{\boldsymbol{B}}^{\boldsymbol{\alpha}} = (p_{B1}^{\alpha}, p_{B2}^{\alpha}, \cdots, p_{Bn}^{\alpha})$, $\boldsymbol{u_B} = (u_{B1}, u_{B2}, \cdots, u_{Bn})$.

Define the elements $H_{Bij}, i, j = 1, 2, \cdots, n$, of the Hessian matrix $[H_{Bij}]$ as

$$H_{Bij} = \frac{\partial^2 L_B}{\partial \dot{q}_{Bi} \partial \dot{q}_{Bj}},\ i, j = 1, 2, \cdots, n, \tag{27}$$

then the Lagrangian is called regular if $\det[H_{Bij}] \neq 0$, and if $\det[H_{Bij}] = 0$, then the Lagrangian L_B is called singular. In this text, we assume that $\det[H_{Bij}] = 0$ and $\operatorname{rank}[H_{Bij}] = R$, $0 \leq R < n$. In the sequel, we will discuss two cases, i.e., $1 \leq R < n$ and $R = 0$.

Firstly, when $1 \leq R < n$, which means that only $\dot{q}_{B\sigma}, \sigma = 1, 2, \cdots, R$, can be determined from Equation (25) while $\dot{q}_{B\rho}, \rho = R+1, R+2, \cdots, n$, are random. From Equation (25), we express $\dot{q}_{B\sigma}, \sigma = 1, 2, \cdots, R$, $1 \leq R < n$, as

$$\dot{q}_{B\sigma} = f_B^{\sigma}(t, \boldsymbol{q_B}, \boldsymbol{p}_{\boldsymbol{B}}^{\boldsymbol{\alpha}}, \boldsymbol{p_{BE}}, \dot{\boldsymbol{q}}_{\boldsymbol{BF}}),\ \left(\text{or } \dot{\boldsymbol{q}}_{\boldsymbol{BE}} = \boldsymbol{f}_{\boldsymbol{B}}^{\boldsymbol{E}}(t, \boldsymbol{q_B}, \boldsymbol{p}_{\boldsymbol{B}}^{\boldsymbol{\alpha}}, \boldsymbol{p_{BE}}, \dot{\boldsymbol{q}}_{\boldsymbol{BF}})\right), \tag{28}$$

where $\boldsymbol{p_{BE}} = (p_{B1}, p_{B2}, \cdots, p_{BR})$, $\dot{\boldsymbol{q}}_{\boldsymbol{BE}} = (\dot{q}_{B1}, \dot{q}_{B2}, \cdots, \dot{q}_{BR})$, $\dot{\boldsymbol{q}}_{\boldsymbol{BF}} = (\dot{q}_{BR+1}, \dot{q}_{BR+2}, \cdots, \dot{q}_{Bn})$, $\boldsymbol{f}_{\boldsymbol{B}}^{\boldsymbol{E}} = (f_B^1, f_B^2, \cdots, f_B^R)$.

From Equations (25) and (28), we have

$$p_{Bi} = g_{Bi}\left(t, \boldsymbol{q_B}, \boldsymbol{f}_{\boldsymbol{B}}^{\boldsymbol{E}}(t, \boldsymbol{q_B}, \boldsymbol{p}_{\boldsymbol{B}}^{\boldsymbol{\alpha}}, \boldsymbol{p_{BE}}, \dot{\boldsymbol{q}}_{\boldsymbol{BF}}), \dot{\boldsymbol{q}}_{\boldsymbol{BF}}, \boldsymbol{p}_{\boldsymbol{B}}^{\boldsymbol{\alpha}}\right) = g_{Bi}(t, \boldsymbol{q_B}, \boldsymbol{p}_{\boldsymbol{B}}^{\boldsymbol{\alpha}}, \boldsymbol{p_{BE}}, \dot{\boldsymbol{q}}_{\boldsymbol{BF}}),\ i = 1, 2, \cdots, n. \tag{29}$$

For Equation (29), if $i = 1, 2, \cdots, R$, then Equation (29) always holds. If $i = R+1, R+2, \cdots, n$, then from the assumption $\operatorname{rank}[H_{Bij}] = R$, $1 \leq R < n$, we have

$$p_{B\rho} = g_{B\rho}(t, \boldsymbol{q_B}, \boldsymbol{p_{BE}}, \boldsymbol{p}_{\boldsymbol{B}}^{\boldsymbol{\alpha}}),\ (\text{or } \boldsymbol{p_{BF}} = \boldsymbol{g_{BF}}(t, \boldsymbol{q_B}, \boldsymbol{p_{BE}}, \boldsymbol{p}_{\boldsymbol{B}}^{\boldsymbol{\alpha}})), \tag{30}$$

where $\rho = R+1, R+2, \cdots, n$, $\boldsymbol{p_{BF}} = (p_{BR+1}, p_{BR+2}, \cdots, p_{Bn})$, $\boldsymbol{g_{BF}} = (g_{BR+1}, g_{BR+2}, \cdots, g_{Bn})$, $1 \leq R < n$. Equation (30) has another form

$$\phi_B(t, \boldsymbol{q_B}, \boldsymbol{p_B}, \boldsymbol{p}_{\boldsymbol{B}}^{\boldsymbol{\alpha}}) = \boldsymbol{p_{BF}} - \boldsymbol{g_{BF}}(t, \boldsymbol{q_B}, \boldsymbol{p_{BE}}, \boldsymbol{p}_{\boldsymbol{B}}^{\boldsymbol{\alpha}}) = 0, \tag{31}$$

where $\phi_B = (\phi_{B1}, \phi_{B2}, \cdots, \phi_{Bn-R})$, $1 \leq R < n$.

Secondly, when $R = 0$, which means that no $\dot{q}_{Bi}, i = 1, 2, \cdots, n$, can be determined from Equation (25). Then from Equation (25) and the assumption $\operatorname{rank}[H_{Bij}] = R$, $R = 0$, we have

$$p_{Bi} = g_{Bi}(t, \boldsymbol{q_B}, \boldsymbol{p}_{\boldsymbol{B}}^{\boldsymbol{\alpha}}),\ (\text{or } \boldsymbol{p_B} = \boldsymbol{g_B}(t, \boldsymbol{q_B}, \boldsymbol{p}_{\boldsymbol{B}}^{\boldsymbol{\alpha}})), \tag{32}$$

where $i = 1, 2, \cdots, n$, $\boldsymbol{p_B} = (p_{B1}, p_{B2}, \cdots, p_{Bn})$, $\boldsymbol{g_B} = (g_{B1}, g_{B2}, \cdots, g_{Bn})$. Then Equation (32) gives

$$\phi_B(t, \boldsymbol{q_B}, \boldsymbol{p_B}, \boldsymbol{p}_{\boldsymbol{B}}^{\boldsymbol{\alpha}}) = \boldsymbol{p_B} - \boldsymbol{g_B}(t, \boldsymbol{q_B}, \boldsymbol{p}_{\boldsymbol{B}}^{\boldsymbol{\alpha}}) = 0, \tag{33}$$

where $\phi_B = (\phi_{B1}, \phi_{B2}, \cdots, \phi_{Bn})$.

Incorporating Equations (31) and (33), we get

$$\phi_B(t, \boldsymbol{q_B}, \boldsymbol{p_B}, \boldsymbol{p}_{\boldsymbol{B}}^{\boldsymbol{\alpha}}) = 0, \tag{34}$$

where $\phi_B = (\phi_{B1}, \phi_{B2}, \cdots, \phi_{Bn-R})$, $0 \leq R < n$. Equation (34) is called the primary constraint with the operator B_M^{α}.

Remark 2. *Let $\kappa_\alpha(t,\tau)=(t-\tau)^{\alpha-1}/\Gamma(\alpha)$, when $M=M_1$, $M=M_2$ and $M=M_3$, Equations (24) and (34) give the Lagrange equations and the primary constraints in terms of the left Caputo, the right Caputo and the Riesz-Caputo fractional derivatives, respectively.*

We intend to transform the singular Lagrangian systems with the mixed derivatives (Equations (10), (20), (24) and (34)) into the constrained Hamiltonian systems in the following section.

4. Constrained Hamiltonian System and Consistency Condition

4.1. Constrained Hamilton Equation with the Operator A_M^α

From Equations (11) and (12), we have

$$\delta H_A=\dot{q}_{Ai}\cdot\delta p_{Ai}+\delta p_{Ai}^{\alpha}\cdot A_M^{\alpha}q_{Ai}-\frac{\partial L_A}{\partial q_{Ai}}\delta q_{Ai},\ i=1,2,\cdots,n, \tag{35}$$

where

$$\frac{\partial L_A}{\partial q_{Ai}}=\dot{p}_{Ai}+B_{M^*}^{\alpha}p_{Ai}^{\alpha}-m\kappa_{1-\alpha}(t_2,t)p_{Ai}^{\alpha}(t_2)+\omega\kappa_{1-\alpha}(t,t_1)p_{Ai}^{\alpha}(t_1) \tag{36}$$

From the Hamiltonian $H_A=H_A\left(t,\boldsymbol{q_A},\boldsymbol{p_A},\boldsymbol{p_A^{\alpha}}\right)$ we have,

$$\delta H_A=\frac{\partial H_A}{\partial q_{Ai}}\cdot\delta q_{Ai}+\frac{\partial H_A}{\partial p_{Ai}}\cdot\delta p_{Ai}+\frac{\partial H_A}{\partial p_{Ai}^{\alpha}}\cdot\delta p_{Ai}^{\alpha},\ i=1,2,\cdots,n. \tag{37}$$

Besides, taking isochronous variation of Equation (20), we have

$$\delta\phi_{Aa}=\frac{\partial\phi_{Aa}}{\partial q_{Ai}}\cdot\delta q_{Ai}+\frac{\partial\phi_{Aa}}{\partial p_{Ai}}\cdot\delta p_{Ai}+\frac{\partial\phi_{Aa}}{\partial p_{Ai}^{\alpha}}\cdot\delta p_{Ai}^{\alpha}=0,\ i=1,2,\cdots,n,\ a=1,2,\cdots,n-R,\ 0\le R<n. \tag{38}$$

Introducing the Lagrange multipliers $\lambda_{Aa}(t)$, $a=1,2,\cdots,n-R$, $0\le R<n$, and from Equations (35)–(38), we have

$$\begin{aligned}\dot{p}_{Ai}&=-B_{M^*}^{\alpha}p_{Ai}^{\alpha}-\tfrac{\partial H_A}{\partial q_{Ai}}+m\kappa_{1-\alpha}(t_2,t)p_{Ai}^{\alpha}(t_2)-\omega\kappa_{1-\alpha}(t,t_1)p_{Ai}^{\alpha}(t_1)-\lambda_{Aa}\tfrac{\partial\phi_{Aa}}{\partial q_{Ai}},\\ \dot{q}_{Ai}&=\tfrac{\partial H_A}{\partial p_{Ai}}+\lambda_{Aa}\tfrac{\partial\phi_{Aa}}{\partial p_{Ai}},\ A_M^{\alpha}q_{Ai}=\tfrac{\partial H_A}{\partial p_{Ai}^{\alpha}}+\lambda_{Aa}\tfrac{\partial\phi_{Aa}}{\partial p_{Ai}^{\alpha}},\ i=1,2,\cdots,n,\ a=1,2,\cdots,n-R,\ 0\le R<n.\end{aligned} \tag{39}$$

Equation (39) is called the constrained Hamilton equation with the operator A_M^α.

For simplicity, we introduce $H_{AT}=H_A+\lambda_{Aa}\phi_{Aa}$, $a=1,2,\cdots,n-R$, $0\le R<n$, then Equation (39) can be written as

$$\begin{aligned}\dot{p}_{Ai}&=-B_{M^*}^{\alpha}p_{Ai}^{\alpha}-\tfrac{\partial H_{AT}}{\partial q_{Ai}}+m\kappa_{1-\alpha}(t_2,t)p_{Ai}^{\alpha}(t_2)-\omega\kappa_{1-\alpha}(t,t_1)p_{Ai}^{\alpha}(t_1),\\ \dot{q}_{Ai}&=\tfrac{\partial H_{AT}}{\partial p_{Ai}},\ A_M^{\alpha}q_{Ai}=\tfrac{\partial H_{AT}}{\partial p_{Ai}^{\alpha}},\ i=1,2,\cdots,n,\ a=1,2,\cdots,n-R,\ 0\le R<n.\end{aligned} \tag{40}$$

Remark 3. *Let $\kappa_\alpha(t,\tau)=(t-\tau)^{\alpha-1}/\Gamma(\alpha)$, when $M=M_1$, $M=M_2$ and $M=M_3$, Equation (39) (or Equation (40)) gives the constrained Hamilton equations in terms of the left Riemann-Liouville, the right Riemann-Liouville and the Riesz-Riemann-Liouville fractional derivatives, respectively.*

4.2. Constrained Hamilton Equation with the Operator B_M^α

From Equations (25) and (26), we have

$$\delta H_B=\dot{q}_{Bi}\cdot\delta p_{Bi}+\delta p_{Bi}^{\alpha}\cdot B_M^{\alpha}q_{Bi}-\frac{\partial L_B}{\partial q_{Bi}}\delta q_{Bi},\ i=1,2,\cdots,n, \tag{41}$$

where

$$\frac{\partial L_B}{\partial q_{Bi}} = \dot{p}_{Bi} + A^{\alpha}_{M^*} p^{\alpha}_{Bi}. \tag{42}$$

From the Hamiltonian $H_B = H_B\left(t, \boldsymbol{q_B}, \boldsymbol{p_B}, \boldsymbol{p^{\alpha}_B}\right)$ we have,

$$\delta H_B = \frac{\partial H_B}{\partial q_{Bi}} \cdot \delta q_{Bi} + \frac{\partial H_B}{\partial p_{Bi}} \cdot \delta p_{Bi} + \frac{\partial H_B}{\partial p^{\alpha}_{Bi}} \cdot \delta p^{\alpha}_{Bi},\ i = 1, 2, \cdots, n. \tag{43}$$

Besides, taking isochronous variation of Equation (34), we have

$$\delta \phi_{Ba} = \frac{\partial \phi_{Ba}}{\partial q_{Bi}} \cdot \delta q_{Bi} + \frac{\partial \phi_{Ba}}{\partial p_{Bi}} \cdot \delta p_{Bi} + \frac{\partial \phi_{Ba}}{\partial p^{\alpha}_{Bi}} \cdot \delta p^{\alpha}_{Bi} = 0,\ i = 1, 2, \cdots, n,\ a = 1, 2, \cdots, n - R,\ 0 \le R < n. \tag{44}$$

Introducing the Lagrange multipliers $\lambda_{Ba}(t)$, $a = 1, 2, \cdots, n - R, 0 \le R < n$, and from Equations (41)–(44), we have

$$\begin{gathered} \dot{p}_{Bi} = -A^{\alpha}_{M^*} p^{\alpha}_{Bi} - \frac{\partial H_B}{\partial q_{Bi}} - \lambda_{Ba} \frac{\partial \phi_{Ba}}{\partial q_{Bi}}, \dot{q}_{Bi} = \frac{\partial H_B}{\partial p_{Bi}} + \lambda_{Ba} \frac{\partial \phi_{Ba}}{\partial p_{Bi}}, \\ B^{\alpha}_M q_{Bi} = \frac{\partial H_B}{\partial p^{\alpha}_{Bi}} + \lambda_{Ba} \frac{\partial \phi_{Ba}}{\partial p^{\alpha}_{Bi}},\ i = 1, 2, \cdots, n,\ a = 1, 2, \cdots, n - R,\ 0 \le R < n. \end{gathered} \tag{45}$$

Equation (45) is called the constrained Hamilton equation with the operator B^{α}_M.

For simplicity, we introduce $H_{BT} = H_B + \lambda_{Ba}\phi_{Ba}$, $a = 1, 2, \cdots, n - R, 0 \le R < n$, then Equation (45) can be written as

$$\begin{gathered} \dot{p}_{Bi} = -A^{\alpha}_{M^*} p^{\alpha}_{Bi} - \frac{\partial H_{BT}}{\partial q_{Bi}},\ \dot{q}_{Bi} = \frac{\partial H_{BT}}{\partial p_{Bi}},\ B^{\alpha}_M q_{Bi} = \frac{\partial H_{BT}}{\partial p^{\alpha}_{Bi}}, \\ i = 1, 2, \cdots, n,\ a = 1, 2, \cdots, n - R,\ 0 \le R < n. \end{gathered} \tag{46}$$

Remark 4. *Let $\kappa_{\alpha}(t, \tau) = (t - \tau)^{\alpha - 1}/\Gamma(\alpha)$, when $M = M_1$, $M = M_2$ and $M = M_3$, Equation (45) (or Equation (46)) gives the constrained Hamilton equations in terms of the left Caputo, the right Caputo and the Riesz-Caputo fractional derivatives, respectively.*

4.3. Consistency Conditions with Generalized Operators

Let $F = F(t, \boldsymbol{q}, \boldsymbol{p}, \boldsymbol{p^{\alpha}})$, $G = G(t, \boldsymbol{q}, \boldsymbol{p}, \boldsymbol{p^{\alpha}})$, we define the Poisson bracket as

$$\{F, G\} = \frac{\partial F}{\partial q_i} \frac{\partial G}{\partial p_i} - \frac{\partial F}{\partial p_i} \frac{\partial G}{\partial q_i},\ i = 1, 2, \cdots, n, \tag{47}$$

where $\boldsymbol{q} = (q_1, q_2, \cdots, q_n)$, $\boldsymbol{p} = (p_1, p_2, \cdots, p_n)$, $\boldsymbol{p^{\alpha}} = \left(p^{\alpha}_1, p^{\alpha}_2, \cdots, p^{\alpha}_n\right)$.

Then using the Poisson bracket and Equation (40), we obtain

$$\begin{gathered} \{\phi_{Aa}, H_A\} + \lambda_{Ab}\{\phi_{Aa}, \phi_{Ab}\} + \frac{\partial \phi_{Aa}}{\partial t} + \frac{\partial \phi_{Aa}}{\partial p^{\alpha}_{Ai}} \dot{p}^{\alpha}_{Ai} - \frac{\partial \phi_{Aa}}{\partial p_{Ai}} \left[B^{\alpha}_{M^*} p^{\alpha}_{Ai} - m\kappa_{1-\alpha}(t_2, t) p^{\alpha}_{Ai}(t_2) \right. \\ \left. + \omega \kappa_{1-\alpha}(t, t_1) p^{\alpha}_{Ai}(t_1)\right] = 0,\ i = 1, 2, \cdots, n,\ a, b = 1, 2, \cdots, n - R,\ 0 \le R < n. \end{gathered} \tag{48}$$

Equation (48) is called the consistency condition with the operator A^{α}_M.

Similarly, the consistency condition with the operator B^{α}_M has the form

$$\begin{gathered} \{\phi_{Ba}, H_B\} + \lambda_{Bb}\{\phi_{Ba}, \phi_{Bb}\} + \frac{\partial \phi_{Ba}}{\partial t} + \frac{\partial \phi_{Ba}}{\partial p^{\alpha}_{Bi}} \dot{p}^{\alpha}_{Bi} - \frac{\partial \phi_{Ba}}{\partial p_{Bi}} \cdot A^{\alpha}_{M^*} p^{\alpha}_{Bi} = 0, \\ i = 1, 2, \cdots, n,\ a, b = 1, 2, \cdots, n - R,\ 0 \le R < n. \end{gathered} \tag{49}$$

If $\det[\{\phi_{Aa}, \phi_{Ab}\}] \neq 0$(resp. $\det[\{\phi_{Ba}, \phi_{Bb}\}] \neq 0$), $a, b = 1, 2, \cdots, n - R, 0 \le R < n$, then all the Lagrange multipliers λ_{Aa} (resp. λ_{Ba}), $a = 1, 2, \cdots, n - R, 0 \le R < n$, can be calculated from Equation (48) (resp. Equation (49)).

If $\det[\{\phi_{Aa}, \phi_{Ab}\}] = 0$ (resp. $\det[\{\phi_{Ba}, \phi_{Bb}\}] = 0$), then the Lagrange multipliers λ_{Aa} (resp. λ_{Ba}), $a = 1, 2, \cdots, n - R$, $0 \le R < n$, cannot be calculated completely, and then the new constraint, which is called the secondary constraint, will be deduced. Therefore,

the secondary constraint arises from the consistency condition of the primary constraint. Similarly, if the consistency condition of the secondary constraint still cannot give all the Lagrange multipliers, then some new secondary constraints will be established. Anyway, no new secondary constraint will be produced after a finite number of steps for a system with finite degrees of freedom.

Remark 5. *Let* $\kappa_\alpha(t,\tau) = (t-\tau)^{\alpha-1}/\Gamma(\alpha)$, *when* $M = M_1$, $M = M_2$ *and* $M = M_3$ *, Equations (48) and (49) give the consistency conditions in terms of the left Riemann-Liouville, the left Caputo, the right Riemann-Liouville, the right Caputo, the Riesz-Riemann-Liouville and the Riesz-Caputo fractional derivatives, respectively.*

5. Noether Symmetry and Conserved Quantity

Noether symmetry is the invariance of the Hamilton action under the infinitesimal transformations of time and coordinates. We begin with Noether symmetry with the operator A_M^α.

5.1. Noether Symmetry with the Operator A_M^α

The Hamilton action with the operator A_M^α is

$$I_A = \int_{t_1}^{t_2} \left[p_{Ai}\dot{q}_{Ai} + p_{Ai}^\alpha \cdot A_M^\alpha q_{Ai} - H_A(t, \boldsymbol{q_A}, \boldsymbol{p_A}, \boldsymbol{p_A^\alpha}) \right] \mathrm{d}t,\ i = 1, 2, \cdots, n. \tag{50}$$

The infinitesimal transformations are

$$\begin{aligned} &\bar{t} = t + \Delta t,\ \overline{q}_{Ai}(\bar{t}) = q_{Ai}(t) + \Delta q_{Ai},\ \overline{p}_{Ai}(\bar{t}) = p_{Ai}(t) + \Delta p_{Ai}, \overline{p}_{Ai}^\alpha(\bar{t}) = p_{Ai}^\alpha(t) + \Delta p_{Ai}^\alpha, \\ &\Big(\text{or } \bar{t} = t + \Delta t,\ \overline{\boldsymbol{q}}_{\boldsymbol{A}}(\bar{t}) = \boldsymbol{q_A}(t) + \Delta \boldsymbol{q_A},\ \overline{\boldsymbol{p}}_{\boldsymbol{A}}(\bar{t}) = \boldsymbol{p_A}(t) + \Delta \boldsymbol{p_A}, \overline{\boldsymbol{p}}_{\boldsymbol{A}}^{\boldsymbol{\alpha}}(\bar{t}) = \boldsymbol{p_A^\alpha}(t) + \Delta \boldsymbol{p_A^\alpha} \Big), \end{aligned} \tag{51}$$

and the expanded forms are

$$\begin{aligned} \bar{t} &= t + \theta_A \xi_{A0}(t, \boldsymbol{q_A}, \boldsymbol{p_A}, \boldsymbol{p_A^\alpha}) + o(\theta_A), \\ \overline{q}_{Ai}(\bar{t}) &= q_{Ai}(t) + \theta_A \xi_{Ai}(t, \boldsymbol{q_A}, \boldsymbol{p_A}, \boldsymbol{p_A^\alpha}) + o(\theta_A), \\ \overline{p}_{Ai}(\bar{t}) &= p_{Ai}(t) + \theta_A \eta_{Ai}(t, \boldsymbol{q_A}, \boldsymbol{p_A}, \boldsymbol{p_A^\alpha}) + o(\theta_A), \\ \overline{p}_{Ai}^\alpha(\bar{t}) &= p_{Ai}^\alpha(t) + \theta_A \eta_{Ai}^\alpha(t, \boldsymbol{q_A}, \boldsymbol{p_A}, \boldsymbol{p_A^\alpha}) + o(\theta_A), \end{aligned} \tag{52}$$

where θ_A is a small parameter, ξ_{A0}, ξ_{Ai}, η_{Ai} and η_{Ai}^α, $i = 1, 2, \cdots, n$, are the infinitesimal generators of the infinitesimal transformations, $o(\theta_A)$ is the higher order of θ_A.

Neglecting the higher order of θ_A, we have

$$\begin{aligned} \Delta I_A &= \overline{I}_A - I_A = \int_{\bar{t}_1}^{\bar{t}_2} \left[\overline{p}_{Ai}\dot{\overline{q}}_{Ai} + \overline{p}_{Ai}^\alpha \cdot A_M^\alpha \overline{q}_{Ai} - H_A\left(\bar{t}, \overline{\boldsymbol{q}}_{\boldsymbol{A}}, \overline{\boldsymbol{p}}_{\boldsymbol{A}}, \overline{\boldsymbol{p}}_{\boldsymbol{A}}^{\boldsymbol{\alpha}}\right) \right] \mathrm{d}\bar{t} - I_A \\ &= \theta_A \int_{t_1}^{t_2} \Big[\lambda_{Aa} \tfrac{\partial \phi_{Aa}}{\partial p_{Ai}} \eta_{Ai} + \lambda_{Aa} \tfrac{\partial \phi_{Aa}}{\partial p_{Ai}^\alpha} \eta_{Ai}^\alpha - \tfrac{\partial H_A}{\partial q_{Ai}} \xi_{Ai} + \left(p_{Ai}^\alpha \tfrac{\mathrm{d}}{\mathrm{d}t} A_M^\alpha q_{Ai} - \tfrac{\partial H_A}{\partial t} \right) \xi_{A0} \\ &+ p_{Ai}^\alpha A_M^\alpha \left(\xi_{Ai} - \dot{q}_{Ai} \xi_{A0} \right) + \left(p_{Ai}^\alpha A_M^\alpha q_{Ai} - H_A \right) \dot{\xi}_{A0} + \omega p_{Ai}^\alpha q_{Ai}(t_2) \xi_{A0}(t_2) \tfrac{\mathrm{d}}{\mathrm{d}t} \kappa_{1-\alpha}(t_2, t) \\ &- m p_{Ai}^\alpha q_{Ai}(t_1) \xi_{A0}(t_1) \tfrac{\mathrm{d}}{\mathrm{d}t} \kappa_{1-\alpha}(t, t_1) + p_{Ai} \dot{\xi}_{Ai} \Big] \mathrm{d}t, \end{aligned} \tag{53}$$

where $\xi_{A0}(t_1) = \xi_{A0}\left(t_1, \boldsymbol{q_A}(t_1), \boldsymbol{p_A}(t_1), \boldsymbol{p_A^\alpha}(t_1)\right)$, $\xi_{A0}(t_2) = \xi_{A0}\left(t_2, \boldsymbol{q_A}(t_2), \boldsymbol{p_A}(t_2), \boldsymbol{p_A^\alpha}(t_2)\right)$ and $\overline{M} = < \bar{t}_1, \bar{t}, \bar{t}_2, m, \omega >$.

Noether symmetry requires that $\Delta I_A = 0$, that is,

$$\begin{aligned} &\lambda_{Aa} \tfrac{\partial \phi_{Aa}}{\partial p_{Ai}} \eta_{Ai} + \lambda_{Aa} \tfrac{\partial \phi_{Aa}}{\partial p_{Ai}^\alpha} \eta_{Ai}^\alpha - \tfrac{\partial H_A}{\partial q_{Ai}} \xi_{Ai} + \left(p_{Ai}^\alpha \tfrac{\mathrm{d}}{\mathrm{d}t} A_M^\alpha q_{Ai} - \tfrac{\partial H_A}{\partial t} \right) \xi_{A0} + p_{Ai} \dot{\xi}_{Ai} \\ &+ p_{Ai}^\alpha A_M^\alpha \left(\xi_{Ai} - \dot{q}_{Ai} \xi_{A0} \right) + \left(p_{Ai}^\alpha A_M^\alpha q_{Ai} - H_A \right) \dot{\xi}_{A0} + \omega p_{Ai}^\alpha q_{Ai}(t_2) \xi_{A0}(t_2) \tfrac{\mathrm{d}}{\mathrm{d}t} \kappa_{1-\alpha}(t_2, t) \\ &- m p_{Ai}^\alpha q_{Ai}(t_1) \xi_{A0}(t_1) \tfrac{\mathrm{d}}{\mathrm{d}t} \kappa_{1-\alpha}(t, t_1) = 0. \end{aligned} \tag{54}$$

Equation (54) is called the Noether identity with the operator A_M^α.

If we let $\Delta I_A = -\int_{t_1}^{t_2} \frac{\mathrm{d}}{\mathrm{d}t}(\Delta G_A)\mathrm{d}t$, where $\Delta G_A = \theta_A G_A$, $G_A = G_A\left(t, \boldsymbol{q_A}, \boldsymbol{p_A}, \boldsymbol{p_A^\alpha}\right)$ is called a gauge function with the operator A_M^α, then we obtain

$$\begin{array}{c}\lambda_{Aa}\frac{\partial \phi_{Aa}}{\partial p_{Ai}}\eta_{Ai} + \lambda_{Aa}\frac{\partial \phi_{Aa}}{\partial p_{Ai}^\alpha}\eta_{Ai}^\alpha - \frac{\partial H_A}{\partial q_{Ai}}\xi_{Ai} + \left(p_{Ai}^\alpha \frac{\mathrm{d}}{\mathrm{d}t}A_M^\alpha q_{Ai} - \frac{\partial H_A}{\partial t}\right)\xi_{A0} + p_{Ai}\dot{\xi}_{Ai} \\ + p_{Ai}^\alpha A_M^\alpha\left(\xi_{Ai} - \dot{q}_{Ai}\xi_{A0}\right) + \left(p_{Ai}^\alpha A_M^\alpha q_{Ai} - H_A\right)\dot{\xi}_{A0} + \omega p_{Ai}^\alpha q_{Ai}(t_2)\xi_{A0}(t_2)\frac{\mathrm{d}}{\mathrm{d}t}\kappa_{1-\alpha}(t_2, t) \\ - m p_{Ai}^\alpha q_{Ai}(t_1)\xi_{A0}(t_1)\frac{\mathrm{d}}{\mathrm{d}t}\kappa_{1-\alpha}(t, t_1) + G_A = 0.\end{array} \tag{55}$$

Equation (55) is called the Noether quasi-identity with the operator A_M^α.

Noether symmetry leads to a conserved quantity. We first present the definition of the conserved quantity.

Definition 1. *A quantity C is called a conserved quantity if and only if* $\mathrm{d}C/\mathrm{d}t = 0$ *holds.*

Therefore, we have

Theorem 1. *For the constrained Hamiltonian system with the operator* A_M^α *(Equation (39)), if the infinitesimal generators* ξ_{A0}, ξ_{Ai}, η_{Ai} *and* η_{Ai}^α *satisfy Equation (54), then there exists a conserved quantity*

$$\begin{array}{c}C_A = p_{Ai}\xi_{Ai} + \left(p_{Ai}^\alpha A_M^\alpha q_{Ai} - H_A\right)\xi_{A0} + \int_{t_1}^{t}\left\{p_{Ai}^\alpha A_M^\alpha\left(\xi_{Ai} - \dot{q}_{Ai}\xi_{A0}\right) + \left(\xi_{Ai} - \dot{q}_{Ai}\xi_{A0}\right)\right. \\ \left.\left[B_{M^*}^\alpha p_{Ai}^\alpha - m\kappa_{1-\alpha}(t_2, \tau)p_{Ai}^\alpha(t_2) + \omega\kappa_{1-\alpha}(\tau, t_1)p_{Ai}^\alpha(t_1)\right]\right\}\mathrm{d}\tau + \omega q_{Ai}(t_2)\xi_{A0}(t_2) \\ \cdot\int_{t_1}^{t} p_{Ai}^\alpha(\tau)\frac{\mathrm{d}}{\mathrm{d}\tau}\kappa_{1-\alpha}(t_2, \tau)\mathrm{d}\tau - m q_{Ai}(t_1)\xi_{A0}(t_1)\int_{t_1}^{t} p_{Ai}^\alpha(\tau)\frac{\mathrm{d}}{\mathrm{d}\tau}\kappa_{1-\alpha}(\tau, t_1)\mathrm{d}\tau = \text{const.}\end{array} \tag{56}$$

Proof of Theorem 1. From Equations (20), (39) and (54), we have

$$\begin{array}{c}\mathrm{d}C_A/\mathrm{d}t = \dot{p}_{Ai}\xi_{Ai} + p_{Ai}\dot{\xi}_{Ai} + \left(p_{Ai}^\alpha A_M^\alpha q_{Ai} - H_A\right)\dot{\xi}_{A0} + p_{Ai}^\alpha A_M^\alpha\left(\xi_{Ai} - \dot{q}_{Ai}\xi_{A0}\right) \\ + \left(\dot{p}_{Ai}^\alpha A_M^\alpha q_{Ai} + p_{Ai}^\alpha \cdot \frac{\mathrm{d}}{\mathrm{d}t}A_M^\alpha q_{Ai} - \frac{\partial H_A}{\partial t} - \frac{\partial H_A}{\partial q_{Ai}}\dot{q}_{Ai} - \frac{\partial H_A}{\partial p_{Ai}}\dot{p}_{Ai} - \frac{\partial H_A}{\partial p_{Ai}^\alpha}\dot{p}_{Ai}^\alpha\right)\xi_{A0} \\ + \left(\xi_{Ai} - \dot{q}_{Ai}\xi_{A0}\right)\left[B_{M^*}^\alpha p_{Ai}^\alpha - m\kappa_{1-\alpha}(t_2, t)p_{Ai}^\alpha(t_2) + \omega\kappa_{1-\alpha}(t, t_1)p_{Ai}^\alpha(t_1)\right] \\ + \omega q_{Ai}(t_2)\xi_{A0}(t_2)p_{Ai}^\alpha(t)\frac{\mathrm{d}}{\mathrm{d}t}\kappa_{1-\alpha}(t_2, t) - m q_{Ai}(t_1)\xi_{A0}(t_1)p_{Ai}^\alpha(t)\frac{\mathrm{d}}{\mathrm{d}t}\kappa_{1-\alpha}(t, t_1) \\ = \frac{\partial H_A}{\partial q_{Ai}}\xi_{Ai} - \lambda_{Aa}\frac{\partial \phi_{Aa}}{\partial p_{Ai}}\eta_{Ai} + \dot{p}_{Ai}\xi_{Ai} + \xi_{A0}\left(\dot{p}_{Ai}^\alpha \cdot A_M^\alpha q_{Ai} - \frac{\partial H_A}{\partial q_{Ai}}\dot{q}_{Ai} - \frac{\partial H_A}{\partial p_{Ai}}\dot{p}_{Ai} - \frac{\partial H_A}{\partial p_{Ai}^\alpha}\dot{p}_{Ai}^\alpha\right) \\ + \left(\xi_{Ai} - \dot{q}_{Ai}\xi_{A0}\right)\left[B_{M^*}^\alpha p_{Ai}^\alpha - m\kappa_{1-\alpha}(t_2, t)p_{Ai}^\alpha(t_2) + \omega\kappa_{1-\alpha}(t, t_1)p_{Ai}^\alpha(t_1)\right] - \lambda_{Aa}\frac{\partial \phi_{Aa}}{\partial p_{Ai}^\alpha}\eta_{Ai}^\alpha \\ = \dot{p}_{Ai}\xi_{A0}\lambda_{Aa}\frac{\partial \phi_{Aa}}{\partial p_{Ai}} - \lambda_{Aa}\frac{\partial \phi_{Aa}}{\partial q_{Ai}}\left(\xi_{Ai} - \dot{q}_{Ai}\xi_{A0}\right) - \lambda_{Aa}\frac{\partial \phi_{Aa}}{\partial p_{Ai}}\eta_{Ai} - \lambda_{Aa}\frac{\partial \phi_{Aa}}{\partial p_{Ai}^\alpha}\eta_{Ai}^\alpha + \lambda_{Aa}\frac{\partial \phi_{Aa}}{\partial p_{Ai}^\alpha}\dot{p}_{Ai}^\alpha\xi_{A0} \\ = -\lambda_{Aa}\frac{\partial \phi_{Aa}}{\partial q_{Ai}} \cdot \delta q_{Ai} - \lambda_{Aa}\frac{\partial \phi_{Aa}}{\partial p_{Ai}} \cdot \delta p_{Ai} - \lambda_{Aa}\frac{\partial \phi_{Aa}}{\partial p_{Ai}^\alpha} \cdot \delta p_{Ai}^\alpha = -\lambda_{Aa} \cdot \delta\phi_{Aa} = 0.\end{array}$$

The proof is completed. □

Theorem 2. *For the constrained Hamiltonian system with the operator* A_M^α *(Equation (39)), if there exists a gauge function* G_A *such that the infinitesimal generators* ξ_{A0}, ξ_{Ai}, η_{Ai} *and* η_{Ai}^α *satisfy Equation (55), then there exists a conserved quantity*

$$\begin{array}{c}C_{AG} = p_{Ai}\xi_{Ai} + \left(p_{Ai}^\alpha A_M^\alpha q_{Ai} - H_A\right)\xi_{A0} + \int_{t_1}^{t}\left\{p_{Ai}^\alpha A_M^\alpha\left(\xi_{Ai} - \dot{q}_{Ai}\xi_{A0}\right) + \left(\xi_{Ai} - \dot{q}_{Ai}\xi_{A0}\right)\right. \\ \left.\left[B_{M^*}^\alpha p_{Ai}^\alpha - m\kappa_{1-\alpha}(t_2, \tau)p_{Ai}^\alpha(t_2) + \omega\kappa_{1-\alpha}(\tau, t_1)p_{Ai}^\alpha(t_1)\right]\right\}\mathrm{d}\tau + \omega q_{Ai}(t_2)\xi_{A0}(t_2) \\ \cdot\int_{t_1}^{t} p_{Ai}^\alpha(\tau)\frac{\mathrm{d}}{\mathrm{d}\tau}\kappa_{1-\alpha}(t_2, \tau)\mathrm{d}\tau - m q_{Ai}(t_1)\xi_{A0}(t_1)\int_{t_1}^{t} p_{Ai}^\alpha(\tau)\frac{\mathrm{d}}{\mathrm{d}\tau}\kappa_{1-\alpha}(\tau, t_1)\mathrm{d}\tau + G_A = \text{const.}\end{array} \tag{57}$$

Proof of Theorem 2. From Equations (20), (39) and (55), we have $\mathrm{d}C_{AG}/\mathrm{d}t = 0$. □

Remark 6. *Let* $\kappa_\alpha(t, \tau) = (t-\tau)^{\alpha-1}/\Gamma(\alpha)$, *when* $M = M_1$, $M = M_2$ *and* $M = M_3$, *Equation (54), Equation (55), Theorem 1 and Theorem 2 give the Noether identities, Noether quasi-identities and conserved quantities in terms of the left Riemann-Liouville, the right Riemann-Liouville and the Riesz-Riemann-Liouville fractional derivatives, respectively.*

5.2. Noether Symmetry with the Operator B_M^α

The Hamilton action with the operator B_M^α is

$$I_B = \int_{t_1}^{t_2} \left[p_{Bi}\dot{q}_{Bi} + p_{Bi}^{\alpha} \cdot B_M^{\alpha} q_{Bi} - H_B(t, \boldsymbol{q_B}, \boldsymbol{p_B}, \boldsymbol{p_B^{\alpha}}) \right] \mathrm{d}t,\ i = 1, 2, \cdots, n. \tag{58}$$

The infinitesimal transformations are

$$\begin{array}{c} \bar{t} = t + \Delta t,\ \overline{q}_{Bi}(\bar{t}) = q_{Bi}(t) + \Delta q_{Bi},\ \overline{p}_{Bi}(\bar{t}) = p_{Bi}(t) + \Delta p_{Bi}, \overline{p}_{Bi}^{\alpha}(\bar{t}) = p_{Bi}^{\alpha}(t) + \Delta p_{Bi}^{\alpha}, \\ \left(\text{or } \bar{t} = t + \Delta t,\ \overline{\boldsymbol{q}}_{\boldsymbol{B}}(\bar{t}) = \boldsymbol{q_B}(t) + \Delta \boldsymbol{q_B},\ \overline{\boldsymbol{p}}_{\boldsymbol{B}}(\bar{t}) = \boldsymbol{p_B}(t) + \Delta \boldsymbol{p_B},\ \overline{\boldsymbol{p}}_{\boldsymbol{B}}^{\boldsymbol{\alpha}}(\bar{t}) = \boldsymbol{p_B^{\alpha}}(t) + \Delta \boldsymbol{p_B^{\alpha}} \right), \end{array} \tag{59}$$

and the expanded forms are

$$\begin{array}{c} \bar{t} = t + \theta_B \xi_{B0}(t, \boldsymbol{q_B}, \boldsymbol{p_B}, \boldsymbol{p_B^{\alpha}}) + o(\theta_B),\ \overline{q}_{Bi}(\bar{t}) = q_{Bi}(t) + \theta_B \xi_{Bi}(t, \boldsymbol{q_B}, \boldsymbol{p_B}, \boldsymbol{p_B^{\alpha}}) + o(\theta_B), \\ \overline{p}_{Bi}(\bar{t}) = p_{Bi}(t) + \theta_B \eta_{Bi}(t, \boldsymbol{q_B}, \boldsymbol{p_B}, \boldsymbol{p_B^{\alpha}}) + o(\theta_B), \\ \overline{p}_{Bi}^{\alpha}(\bar{t}) = p_{Bi}^{\alpha}(t) + \theta_B \eta_{Bi}^{\alpha}(t, \boldsymbol{q_B}, \boldsymbol{p_B}, \boldsymbol{p_B^{\alpha}}) + o(\theta_B), \end{array} \tag{60}$$

where θ_B is a small parameter, ξ_{B0}, ξ_{Bi}, η_{Bi} and η_{Bi}^{α} are the infinitesimal generators of the infinitesimal transformations, $o(\theta_B)$ is the higher order of θ_B.

Neglecting the higher order of θ_B, we have

$$\begin{array}{l} \Delta I_B = \overline{I}_B - I_B = \int_{\bar{t}_1}^{\bar{t}_2} \left[\overline{p}_{Bi}\dot{\bar{q}}_{Bi} + \overline{p}_{Bi}^{\alpha} \cdot B_{\overline{M}}^{\alpha} \overline{q}_{Bi} - H_B\left(\bar{t}, \overline{\boldsymbol{q}}_{\boldsymbol{B}}, \overline{\boldsymbol{p}}_{\boldsymbol{B}}, \overline{\boldsymbol{p}}_{\boldsymbol{B}}^{\boldsymbol{\alpha}} \right) \right] \mathrm{d}\bar{t} - I_B \\ = \theta_B \int_{t_1}^{t_2} \Big[\lambda_{Ba} \frac{\partial \phi_{Ba}}{\partial p_{Bi}} \eta_{Bi} + \lambda_{Ba} \frac{\partial \phi_{Ba}}{\partial p_{Bi}^{\alpha}} \eta_{Bi}^{\alpha} - \frac{\partial H_B}{\partial q_{Bi}} \xi_{Bi} + \left(p_{Bi}^{\alpha} \frac{\mathrm{d}}{\mathrm{d}t} B_M^{\alpha} q_{Bi} - \frac{\partial H_B}{\partial t} \right) \xi_{B0} \\ + p_{Bi}^{\alpha} B_M^{\alpha} \left(\xi_{Bi} - \dot{q}_{Bi} \xi_{B0} \right) + \left(p_{Bi}^{\alpha} B_M^{\alpha} q_{Bi} - H_B \right) \dot{\xi}_{B0} + \omega p_{Bi}^{\alpha} \kappa_{1-\alpha}(t_2, t) \dot{q}_{Bi}(t_2) \xi_{B0}(t_2) \\ - m p_{Bi}^{\alpha} \kappa_{1-\alpha}(t, t_1) \dot{q}_{Bi}(t_1) \xi_{B0}(t_1) + p_{Bi} \dot{\xi}_{Bi} \Big] \mathrm{d}t, \end{array} \tag{61}$$

where $\xi_{B0}(t_1) = \xi_{B0}\left(t_1, \boldsymbol{q_B}(t_1), \boldsymbol{p_B}(t_1), \boldsymbol{p_B^{\alpha}}(t_1)\right)$, $\xi_{B0}(t_2) = \xi_{B0}\left(t_2, \boldsymbol{q_B}(t_2), \boldsymbol{p_B}(t_2), \boldsymbol{p_B^{\alpha}}(t_2)\right)$.

Noether symmetry requires that $\Delta I_B = 0$, that is,

$$\begin{array}{c} \lambda_{Ba} \frac{\partial \phi_{Ba}}{\partial p_{Bi}} \eta_{Bi} + \lambda_{Ba} \frac{\partial \phi_{Ba}}{\partial p_{Bi}^{\alpha}} \eta_{Bi}^{\alpha} - \frac{\partial H_B}{\partial q_{Bi}} \xi_{Bi} + \left(p_{Bi}^{\alpha} \frac{\mathrm{d}}{\mathrm{d}t} B_M^{\alpha} q_{Bi} - \frac{\partial H_B}{\partial t} \right) \xi_{B0} + p_{Bi} \dot{\xi}_{Bi} \\ + p_{Bi}^{\alpha} B_M^{\alpha} \left(\xi_{Bi} - \dot{q}_{Bi} \xi_{B0} \right) + \left(p_{Bi}^{\alpha} B_M^{\alpha} q_{Bi} - H_B \right) \dot{\xi}_{B0} + \omega p_{Bi}^{\alpha} \kappa_{1-\alpha}(t_2, t) \dot{q}_{Bi}(t_2) \xi_{B0}(t_2) \\ - m p_{Bi}^{\alpha} \kappa_{1-\alpha}(t, t_1) \dot{q}_{Bi}(t_1) \xi_{B0}(t_1) = 0. \end{array} \tag{62}$$

Equation (62) is called the Noether identity with the operator B_M^α.

If we let $\Delta I_B = -\int_{t_1}^{t_2} \frac{\mathrm{d}}{\mathrm{d}t}(\Delta G_B)\mathrm{d}t$, where $\Delta G_B = \theta_B G_B$, $G_B = G_B\left(t, \boldsymbol{q_B}, \boldsymbol{p_B}, \boldsymbol{p_B^{\alpha}}\right)$ is called a gauge function with the operator B_M^α, then we obtain

$$\begin{array}{c} \lambda_{Ba} \frac{\partial \phi_{Ba}}{\partial p_{Bi}} \eta_{Bi} + \lambda_{Ba} \frac{\partial \phi_{Ba}}{\partial p_{Bi}^{\alpha}} \eta_{Bi}^{\alpha} - \frac{\partial H_B}{\partial q_{Bi}} \xi_{Bi} + \left(p_{Bi}^{\alpha} \frac{\mathrm{d}}{\mathrm{d}t} B_M^{\alpha} q_{Bi} - \frac{\partial H_B}{\partial t} \right) \xi_{B0} + p_{Bi} \dot{\xi}_{Bi} \\ + p_{Bi}^{\alpha} B_M^{\alpha} \left(\xi_{Bi} - \dot{q}_{Bi} \xi_{B0} \right) + \left(p_{Bi}^{\alpha} B_M^{\alpha} q_{Bi} - H_B \right) \dot{\xi}_{B0} + \omega p_{Bi}^{\alpha} \kappa_{1-\alpha}(t_2, t) \dot{q}_{Bi}(t_2) \xi_{B0}(t_2) \\ - m p_{Bi}^{\alpha} \kappa_{1-\alpha}(t, t_1) \dot{q}_{Bi}(t_1) \xi_{B0}(t_1) + \dot{G}_B = 0. \end{array} \tag{63}$$

Equation (63) is called the Noether quasi-identity with the operator B_M^α. Therefore, we have

Theorem 3 . *For the constrained Hamiltonian system with the operator B_M^α (Equation (45)), if the infinitesimal generators ξ_{B0}, ξ_{Bi}, η_{Bi} and η_{Bi}^{α} satisfy Equation (62), then there exists a conserved quantity*

$$\begin{array}{l} C_B = p_{Bi}\xi_{Bi} + \left(p_{Bi}^{\alpha} B_M^{\alpha} q_{Bi} - H_B \right) \xi_{B0} + \int_{t_1}^{t} \left[p_{Bi}^{\alpha} B_M^{\alpha} \left(\xi_{Bi} - \dot{q}_{Bi} \xi_{B0} \right) + \left(\xi_{Bi} - \dot{q}_{Bi} \xi_{B0} \right) A_{M^*}^{\alpha} p_{Bi}^{\alpha} \right] \mathrm{d}\tau \\ + \omega \dot{q}_{Bi}(t_2) \xi_{B0}(t_2) \cdot \int_{t_1}^{t} p_{Bi}^{\alpha}(\tau) \kappa_{1-\alpha}(t_2, \tau) \mathrm{d}\tau - m \dot{q}_{Bi}(t_1) \xi_{B0}(t_1) \int_{t_1}^{t} p_{Bi}^{\alpha}(\tau) \kappa_{1-\alpha}(\tau, t_1) \mathrm{d}\tau = \text{const.} \end{array} \tag{64}$$

Proof of Theorem 3. From Equations (34), (45) and (62), we have $\mathrm{d}C_B/\mathrm{d}t = 0$. □

Theorem 4. *For the constrained Hamiltonian system with the operator B_M^α (Equation (45)), if there exists a gauge function G_B such that the infinitesimal generators ξ_{B0}, ξ_{Bi}, η_{Bi} and η_{Bi}^α satisfy Equation (63), then there exists a conserved quantity*

$$\begin{array}{c} C_{BG} = p_{Bi}\xi_{Bi} + \int_{t_1}^{t}\left[p_{Bi}^{\alpha}B_M^{\alpha}\left(\xi_{Bi} - \dot{q}_{Bi}\xi_{B0}\right) + \left(\xi_{Bi} - \dot{q}_{Bi}\xi_{B0}\right)A_{M^*}^{\alpha}p_{Bi}^{\alpha}\right]\mathrm{d}\tau \\ +\omega\dot{q}_{Bi}(t_2)\xi_{B0}(t_2)\cdot\int_{t_1}^{t}p_{Bi}^{\alpha}(\tau)\kappa_{1-\alpha}(t_2,\tau)\mathrm{d}\tau + \left(p_{Bi}^{\alpha}B_M^{\alpha}q_{Bi} - H_B\right)\xi_{B0} \\ -m\dot{q}_{Bi}(t_1)\xi_{B0}(t_1)\int_{t_1}^{t}p_{Bi}^{\alpha}(\tau)\kappa_{1-\alpha}(\tau,t_1)\mathrm{d}\tau + G_B = \mathrm{const.} \end{array} \tag{65}$$

Proof of Theorem 4. From Equations (34), (45) and (63), we have $\mathrm{d}C_{BG}/\mathrm{d}t = 0$. □

Remark 7. *Let $\kappa_\alpha(t,\tau) = (t-\tau)^{\alpha-1}/\Gamma(\alpha)$, when $M = M_1$, $M = M_2$ and $M = M_3$, Equation (62), Equation (63), Theorem 3 and Theorem 4 give the Noether identities, the Noether quasi-identities and the conserved quantities in terms of the left Caputo, the right Caputo and the Riesz-Caputo fractional derivatives, respectively.*

Remark 8. *When the gauge function $G_A = 0$ (resp. $G_B = 0$), Theorem 2 (resp. Theorem 4) reduces to Theorem 1 (resp. Theorem 3). Hence, the Noether-quasi symmetry is more general than the Noether symmetry.*

6. Lie Symmetry and Conserved Quantity

Lie symmetry means an invariance of the differential equations under the infinitesimal transformations of time and coordinates. Lie symmetry can also lead to a conserved quantity under certain conditions.

6.1. Lie Symmetry with the Operator A_M^α

We rewrite the constrained Hamilton equation with the operator A_M^α (Equation (39)) as

$$\begin{array}{c} \dot{p}_{Ai} = -B_{M^*}^{\alpha}p_{Ai}^{\alpha} + f_{Ai}\left(t,\boldsymbol{q_A},\boldsymbol{p_A},\boldsymbol{p_A^\alpha}\right), \\ \dot{q}_{Ai} = S_{Ai}\left(t,\boldsymbol{q_A},\boldsymbol{p_A},\boldsymbol{p_A^\alpha}\right), \\ A_M^{\alpha}q_{Ai} = h_{Ai}\left(t,\boldsymbol{q_A},\boldsymbol{p_A},\boldsymbol{p_A^\alpha}\right),\ i = 1,2,\cdots,n. \end{array} \tag{66}$$

Then under the condition $\kappa_{1-\alpha}(t,t) = 0$, we have

$$\begin{array}{l} \dot{\bar{q}}_{Ai} - S_{Ai}\left(\bar{t},\bar{\boldsymbol{q}}_{\boldsymbol{A}},\bar{\boldsymbol{p}}_{\boldsymbol{A}},\bar{\boldsymbol{p}}_{\boldsymbol{A}}^{\boldsymbol{\alpha}}\right) = \frac{\mathrm{d}\bar{q}_{Ai}}{\mathrm{d}\bar{t}} - S_{Ai}\left(t+\Delta t,\boldsymbol{q_A}+\Delta\boldsymbol{q_A},\boldsymbol{p_A}+\Delta\boldsymbol{p_A},\boldsymbol{p_A^\alpha}+\Delta\boldsymbol{p_A^\alpha}\right) \\ = \frac{\mathrm{d}q_{Ai}+\mathrm{d}\Delta q_{Ai}}{\mathrm{d}t+\mathrm{d}\Delta t} - S_{Ai}\left(t+\Delta t,\boldsymbol{q_A}+\Delta\boldsymbol{q_A},\boldsymbol{p_A}+\Delta\boldsymbol{p_A},\boldsymbol{p_A^\alpha}+\Delta\boldsymbol{p_A^\alpha}\right) \\ = \frac{\left(\frac{\mathrm{d}q_{Ai}}{\mathrm{d}t}+\frac{\mathrm{d}\Delta q_{Ai}}{\mathrm{d}t}\right)\left(1-\frac{\mathrm{d}\Delta t}{\mathrm{d}t}\right)}{\left(1+\frac{\mathrm{d}\Delta t}{\mathrm{d}t}\right)\left(1-\frac{\mathrm{d}\Delta t}{\mathrm{d}t}\right)} - S_{Ai}\left(t+\Delta t,\boldsymbol{q_A}+\Delta\boldsymbol{q_A},\boldsymbol{p_A}+\Delta\boldsymbol{p_A},\boldsymbol{p_A^\alpha}+\Delta\boldsymbol{p_A^\alpha}\right) \\ = \dot{q}_{Ai} + \frac{\mathrm{d}\Delta q_{Ai}}{\mathrm{d}t} - \dot{q}_{Ai}\frac{\mathrm{d}\Delta t}{\mathrm{d}t} - S_{Ai}\left(t,\boldsymbol{q_A},\boldsymbol{p_A},\boldsymbol{p_A^\alpha}\right) - \frac{\partial S_{Ai}}{\partial t}\cdot\Delta t - \frac{\partial S_{Ai}}{\partial q_{Ak}}\cdot\Delta q_{Ak} - \frac{\partial S_{Ai}}{\partial p_{Ak}}\cdot\Delta p_{Ak} - \frac{\partial S_{Ai}}{\partial p_{Ak}^{\alpha}}\cdot\Delta p_{Ak}^{\alpha} \\ = \dot{q}_{Ai} - S_{Ai}\left(t,\boldsymbol{q_A},\boldsymbol{p_A},\boldsymbol{p_A^\alpha}\right) + \theta_A\left[\dot{\xi}_{Ai} - \dot{q}_{Ai}\dot{\xi}_{A0} - X_A^{(0)}(S_{Ai})\right], \end{array} \tag{67}$$

$$\text{where } X_A^{(0)} = \xi_{A0}\frac{\partial}{\partial t} + \xi_{Ak}\frac{\partial}{\partial q_{Ak}} + \eta_{Ak}\frac{\partial}{\partial p_{Ak}} + \eta_{Ak}^{\alpha}\frac{\partial}{\partial p_{Ak}^{\alpha}},\ k = 1,2,\cdots,n.$$

$$\begin{array}{c} A_M^{\alpha}\bar{q}_{Ai}(\bar{t}) - h_{Ai}\left(\bar{t},\bar{\boldsymbol{q}}_{\boldsymbol{A}},\bar{\boldsymbol{p}}_{\boldsymbol{A}},\bar{\boldsymbol{p}}_{\boldsymbol{A}}^{\boldsymbol{\alpha}}\right) = A_M^{\alpha}\bar{q}_{Ai}(\bar{t}) - h_{Ai}\left(t+\Delta t,\boldsymbol{q_A}+\Delta\boldsymbol{q_A},\boldsymbol{p_A}+\Delta\boldsymbol{p_A},\boldsymbol{p_A^\alpha}+\Delta\boldsymbol{p_A^\alpha}\right) \\ = A_M^{\alpha}q_{Ai} + A_M^{\alpha}\delta q_{Ai} + \Delta t\cdot\frac{\mathrm{d}}{\mathrm{d}t}A_M^{\alpha}q_{Ai} + \frac{\mathrm{d}}{\mathrm{d}t}[-m\kappa_{1-\alpha}(t,t_1)\Delta t_1 q_{Ai}(t_1) + \omega\kappa_{1-\alpha}(t_2,t)\Delta t_2 q_{Ai}(t_2)] \\ -h_{Ai}\left(t,\boldsymbol{q_A},\boldsymbol{p_A},\boldsymbol{p_A^\alpha}\right) - \frac{\partial h_{Ai}}{\partial t}\Delta t - \frac{\partial h_{Ai}}{\partial q_{Ak}}\Delta q_{Ak} - \frac{\partial h_{Ai}}{\partial p_{Ak}}\Delta p_{Ak} - \frac{\partial h_{Ai}}{\partial p_{Ak}^{\alpha}}\Delta p_{Ak}^{\alpha} \\ = A_M^{\alpha}q_{Ai} - h_{Ai}\left(t,\boldsymbol{q_A},\boldsymbol{p_A},\boldsymbol{p_A^\alpha}\right) + \theta_A\Big\{A_M^{\alpha}\left(\xi_{Ai} - \dot{q}_{Ai}\xi_{A0}\right) + \xi_{A0}\cdot\frac{\mathrm{d}}{\mathrm{d}t}A_M^{\alpha}q_{Ai} \\ +\frac{\mathrm{d}}{\mathrm{d}t}[-m\kappa_{1-\alpha}(t,t_1)\xi_{A0}(t_1)q_{Ai}(t_1) + \omega\kappa_{1-\alpha}(t_2,t)\xi_{A0}(t_2)q_{Ai}(t_2)] - X_A^{(0)}(h_{Ai})\Big\}, \end{array} \tag{68}$$

where

$$\begin{array}{l}\xi_{A0}(t_1)=\xi_{A0}\left(t_1,\boldsymbol{q_A}(t_1),\boldsymbol{p_A}(t_1),\boldsymbol{p_A^\alpha}(t_1)\right),\ \xi_{A0}(t_2)=\xi_{A0}\left(t_2,\boldsymbol{q_A}(t_2),\boldsymbol{p_A}(t_2),\boldsymbol{p_A^\alpha}(t_2)\right),\\ A_M^\alpha\overline{q}_{Ai}(\overline{t})=A_M^\alpha q_{Ai}+\Delta t\cdot\frac{\mathrm{d}}{\mathrm{d}t}A_M^\alpha q_{Ai}+\frac{\mathrm{d}}{\mathrm{d}t}[-m\kappa_{1-\alpha}(t,t_1)\Delta t_1 q_{Ai}(t_1)+\omega\kappa_{1-\alpha}(t_2,t)\Delta t_2 q_{Ai}(t_2)]\\ +A_M^\alpha\delta q_{Ai}.\\ \dot{\overline{p}}_{Ai}+B_{M^*}^\alpha\overline{p}_{Ai}^\alpha(\overline{t})-f_{Ai}\left(\overline{t},\overline{\boldsymbol{q_A}},\overline{\boldsymbol{p_A}},\overline{\boldsymbol{p_A^\alpha}}\right)=\frac{\mathrm{d}p_{Ai}+\mathrm{d}\Delta p_{Ai}}{\mathrm{d}t+\mathrm{d}\Delta t}+B_{M^*}^\alpha\overline{p}_{Ai}^\alpha(\overline{t})-f_{Ai}\left(\overline{t},\overline{\boldsymbol{q_A}},\overline{\boldsymbol{p_A}},\overline{\boldsymbol{p_A^\alpha}}\right)\\ =\frac{\left(\frac{\mathrm{d}p_{Ai}}{\mathrm{d}t}+\frac{\mathrm{d}\Delta p_{Ai}}{\mathrm{d}t}\right)\left(1-\frac{\mathrm{d}\Delta t}{\mathrm{d}t}\right)}{\left(1+\frac{\mathrm{d}\Delta t}{\mathrm{d}t}\right)\left(1-\frac{\mathrm{d}\Delta t}{\mathrm{d}t}\right)}+B_{M^*}^\alpha\overline{p}_{Ai}^\alpha-f_{Ai}\left(t+\Delta t,\boldsymbol{q_A}+\Delta\boldsymbol{q_A},\boldsymbol{p_A}+\Delta\boldsymbol{p_A},\boldsymbol{p_A^\alpha}+\Delta\boldsymbol{p_A^\alpha}\right)\\ =\dot{p}_{Ai}+B_{M^*}^\alpha p_{Ai}^\alpha-f_{Ai}\left(t,\boldsymbol{q_A},\boldsymbol{p_A},\boldsymbol{p_A^\alpha}\right)+\theta_A\Big[\dot{\eta}_{Ai}-\dot{p}_{Ai}\dot{\xi}_{A0}+B_{M^*}^\alpha\left(\eta_{Ai}^\alpha-\dot{p}_{Ai}^\alpha\xi_{A0}\right)+\xi_{A0}\cdot\frac{\mathrm{d}}{\mathrm{d}t}B_{M^*}^\alpha p_{Ai}^\alpha\\ -\omega\kappa_{1-\alpha}(t,t_1)\dot{p}_{Ai}^\alpha(t_1)\cdot\xi_{A0}(t_1)+m\kappa_{1-\alpha}(t_2,t)\dot{p}_{Ai}^\alpha(t_2)\cdot\xi_{A0}(t_2)-X_A^{(0)}(f_{Ai})\Big],\end{array}\tag{69}$$

where

$$B_{M^*}^\alpha\overline{p}_{Ai}^\alpha=B_{M^*}^\alpha p_{Ai}^\alpha+B_{M^*}^\alpha\delta p_{Ai}^\alpha+\Delta t\cdot\frac{\mathrm{d}}{\mathrm{d}t}B_{M^*}^\alpha p_{Ai}^\alpha-\omega\kappa_{1-\alpha}(t,t_1)\dot{p}_{Ai}^\alpha(t_1)\cdot\Delta t_1+m\kappa_{1-\alpha}(t_2,t)\dot{p}_{Ai}^\alpha(t_2)\cdot\Delta t_2.$$

Lie symmetry requires that

$$\begin{array}{c}\dot{\xi}_{Ai}-\dot{q}_{Ai}\dot{\xi}_{A0}-X_A^{(0)}(S_{Ai})=0,\\ A_M^\alpha\left(\xi_{Ai}-\dot{q}_{Ai}\xi_{A0}\right)+\frac{\mathrm{d}}{\mathrm{d}t}[-m\kappa_{1-\alpha}(t,t_1)\xi_{A0}(t_1)q_{Ai}(t_1)+\omega\kappa_{1-\alpha}(t_2,t)\xi_{A0}(t_2)q_{Ai}(t_2)]\\ +\xi_{A0}\cdot\frac{\mathrm{d}}{\mathrm{d}t}A_M^\alpha q_{Ai}-X_A^{(0)}(h_{Ai})=0,\\ \dot{\eta}_{Ai}-\dot{p}_{Ai}\dot{\xi}_{A0}+B_{M^*}^\alpha\left(\eta_{Ai}^\alpha-\dot{p}_{Ai}^\alpha\xi_{A0}\right)+\xi_{A0}\cdot\frac{\mathrm{d}}{\mathrm{d}t}B_{M^*}^\alpha p_{Ai}^\alpha-\omega\kappa_{1-\alpha}(t,t_1)\dot{p}_{Ai}^\alpha(t_1)\\ \cdot\xi_{A0}(t_1)+m\kappa_{1-\alpha}(t_2,t)\dot{p}_{Ai}^\alpha(t_2)\cdot\xi_{A0}(t_2)-X_A^{(0)}(f_{Ai})=0\end{array}\tag{70}$$

Equation (70) is called the determined equation for the constrained Hamiltonian system with the operator A_M^α (Equation (39)). Lie symmetry also leads to a conserved quantity under certain conditions. Therefore, we have

Theorem 5. *For the constrained Hamiltonian system with the operator A_M^α (Equation (39)), if the infinitesimal generators ξ_{A0}, ξ_{Ai}, η_{Ai} and η_{Ai}^α satisfy Equation (54) and the determined equation (Equation (70)), then there exists a conserved quantity Equation (56).*

Proof of Theorem 5. From Equations (20), (39) and (54), we can get the intended result. □

6.2. Lie Symmetry with the Operator B_M^α

We rewrite the constrained Hamilton equation with the operator B_M^α (Equation (45)) as

$$\begin{array}{c}\dot{p}_{Bi}=-A_{M^*}^\alpha p_{Bi}^\alpha+f_{Bi}\left(t,\boldsymbol{q_B},\boldsymbol{p_B},\boldsymbol{p_B^\alpha}\right),\\ \dot{q}_{Bi}=S_{Bi}\left(t,\boldsymbol{q_B},\boldsymbol{p_B},\boldsymbol{p_B^\alpha}\right),\\ B_M^\alpha q_{Bi}=h_{Bi}\left(t,\boldsymbol{q_B},\boldsymbol{p_B},\boldsymbol{p_B^\alpha}\right),\ i=1,2,\cdots,n\end{array}\tag{71}$$

Then under the condition $\kappa_{1-\alpha}(t,t)=0$, we have

$$\begin{array}{l}\dot{\overline{q}}_{Bi}-S_{Bi}\left(\overline{t},\overline{\boldsymbol{q_B}},\overline{\boldsymbol{p_B}},\overline{\boldsymbol{p_B^\alpha}}\right)=\frac{\mathrm{d}\overline{q}_{Bi}}{\mathrm{d}t}-S_{Bi}\left(t+\Delta t,\boldsymbol{q_B}+\Delta\boldsymbol{q_B},\boldsymbol{p_B}+\Delta\boldsymbol{p_B},\boldsymbol{p_B^\alpha}+\Delta\boldsymbol{p_B^\alpha}\right)\\ =\frac{\mathrm{d}q_{Bi}+\mathrm{d}\Delta q_{Bi}}{\mathrm{d}t+\mathrm{d}\Delta t}-S_{Bi}\left(t+\Delta t,\boldsymbol{q_B}+\Delta\boldsymbol{q_B},\boldsymbol{p_B}+\Delta\boldsymbol{p_B},\boldsymbol{p_B^\alpha}+\Delta\boldsymbol{p_B^\alpha}\right)\\ =\dot{q}_{Bi}-S_{Bi}\left(t,\boldsymbol{q_B},\boldsymbol{p_B},\boldsymbol{p_B^\alpha}\right)+\theta_B\Big[\dot{\xi}_{Bi}-\dot{q}_{Bi}\dot{\xi}_{B0}-X_B^{(0)}(S_{Bi})\Big],\end{array}\tag{72}$$

where

$$\begin{aligned} &X_B^{(0)} = \xi_{B0}\tfrac{\partial}{\partial t} + \xi_{Bk}\tfrac{\partial}{\partial q_{Bk}} + \eta_{Bk}\tfrac{\partial}{\partial p_{Bk}} + \eta^{\alpha}_{Bk}\tfrac{\partial}{\partial p^{\alpha}_{Bk}},\ k = 1, 2, \cdots, n. \\ &B^{\alpha}_M \overline{q}_{Bi}(\bar{t}) - h_{Bi}\left(\bar{t}, \overline{\boldsymbol{q}}_{\boldsymbol{B}}, \overline{\boldsymbol{p}}_{\boldsymbol{B}}, \overline{\boldsymbol{p}}^{\boldsymbol{\alpha}}_{\boldsymbol{B}}\right) = B^{\alpha}_M \overline{q}_{Bi}(\bar{t}) - h_{Bi}(t + \Delta t, \boldsymbol{q}_{\boldsymbol{B}} + \Delta \boldsymbol{q}_{\boldsymbol{B}}, \boldsymbol{p}_{\boldsymbol{B}} + \Delta \boldsymbol{p}_{\boldsymbol{B}}, \boldsymbol{p}^{\boldsymbol{\alpha}}_{\boldsymbol{B}} + \Delta \boldsymbol{p}^{\boldsymbol{\alpha}}_{\boldsymbol{B}}) \\ &= B^{\alpha}_M q_{Bi} - h_{Bi}(t, \boldsymbol{q}_{\boldsymbol{B}}, \boldsymbol{p}_{\boldsymbol{B}}, \boldsymbol{p}^{\boldsymbol{\alpha}}_{\boldsymbol{B}}) + \theta_B\Big[B^{\alpha}_M(\xi_{Bi} - \dot{q}_{Bi}\xi_{B0}) + \xi_{B0}\cdot \tfrac{\mathrm{d}}{\mathrm{d}t} B^{\alpha}_M q_{Bi} \\ &-m\kappa_{1-\alpha}(t, t_1)\xi_{B0}(t_1)\dot{q}_{Bi}(t_1) + \omega\kappa_{1-\alpha}(t_2, t)\xi_{B0}(t_2)\dot{q}_{Bi}(t_2) - X_B^{(0)}(h_{Bi})\Big], \end{aligned} \tag{73}$$

where

$$\begin{aligned} &\xi_{B0}(t_1) = \xi_{B0}(t_1, \boldsymbol{q}_{\boldsymbol{B}}(t_1), \boldsymbol{p}_{\boldsymbol{B}}(t_1), \boldsymbol{p}^{\boldsymbol{\alpha}}_{\boldsymbol{B}}(t_1)), \\ &\xi_{B0}(t_2) = \xi_{B0}(t_2, \boldsymbol{q}_{\boldsymbol{B}}(t_2), \boldsymbol{p}_{\boldsymbol{B}}(t_2), \boldsymbol{p}^{\boldsymbol{\alpha}}_{\boldsymbol{B}}(t_2)). \\ &\dot{\overline{p}}_{Bi} + A^{\alpha}_{M^*}\overline{p}^{\alpha}_{Bi}(\bar{t}) - f_{Bi}\left(\bar{t}, \overline{\boldsymbol{q}}_{\boldsymbol{B}}, \overline{\boldsymbol{p}}_{\boldsymbol{B}}, \overline{\boldsymbol{p}}^{\boldsymbol{\alpha}}_{\boldsymbol{B}}\right) = \tfrac{\mathrm{d}p_{Bi} + \mathrm{d}\Delta p_{Bi}}{\mathrm{d}t + \mathrm{d}\Delta t} + A^{\alpha}_{M^*}\overline{p}^{\alpha}_{Bi}(\bar{t}) - f_{Bi}\left(\bar{t}, \overline{\boldsymbol{q}}_{\boldsymbol{B}}, \overline{\boldsymbol{p}}_{\boldsymbol{B}}, \overline{\boldsymbol{p}}^{\boldsymbol{\alpha}}_{\boldsymbol{B}}\right) \\ &= \dot{p}_{Bi} + A^{\alpha}_{M^*}p^{\alpha}_{Bi} - f_{Bi}(t, \boldsymbol{q}_{\boldsymbol{B}}, \boldsymbol{p}_{\boldsymbol{B}}, \boldsymbol{p}^{\boldsymbol{\alpha}}_{\boldsymbol{B}}) + \theta_B\Big\{\dot{\eta}_{Bi} - \dot{p}_{Bi}\dot{\xi}_{B0} + A^{\alpha}_{M^*}\left(\eta^{\alpha}_{Bi} - \dot{p}^{\alpha}_{Bi}\xi_{B0}\right) + \xi_{B0}\cdot \tfrac{\mathrm{d}}{\mathrm{d}t}A^{\alpha}_{M^*}p^{\alpha}_{Bi} \\ &+ \tfrac{\mathrm{d}}{\mathrm{d}t}\left[-\omega\kappa_{1-\alpha}(t, t_1)p^{\alpha}_{Bi}(t_1)\cdot\xi_{B0}(t_1) + m\kappa_{1-\alpha}(t_2, t)p^{\alpha}_{Bi}(t_2)\cdot\xi_{B0}(t_2)\right] - X^{(0)}(f_{Bi})\Big\}. \end{aligned} \tag{74}$$

Lie symmetry requires that

$$\begin{aligned} &\dot{\xi}_{Bi} - \dot{q}_{Bi}\dot{\xi}_{B0} - X_B^{(0)}(S_{Bi}) = 0, \\ &B^{\alpha}_M\left(\xi_{Bi} - \dot{q}_{Bi}\xi_{B0}\right) + \xi_{B0}\cdot\tfrac{\mathrm{d}}{\mathrm{d}t}B^{\alpha}_M q_{Bi} - m\kappa_{1-\alpha}(t, t_1)\xi_{B0}(t_1)\dot{q}_{Bi}(t_1) \\ &+\omega\kappa_{1-\alpha}(t_2, t)\xi_{B0}(t_2)\dot{q}_{Bi}(t_2) - X_B^{(0)}(h_{Bi}) = 0, \\ &\dot{\eta}_{Bi} - \dot{p}_{Bi}\dot{\xi}_{B0} + A^{\alpha}_{M^*}\left(\eta^{\alpha}_{Bi} - \dot{p}^{\alpha}_{Bi}\xi_{B0}\right) + \xi_{B0}\cdot\tfrac{\mathrm{d}}{\mathrm{d}t}A^{\alpha}_{M^*}p^{\alpha}_{Bi} - X^{(0)}(f_{Bi}) \\ &+\tfrac{\mathrm{d}}{\mathrm{d}t}\left[-\omega\kappa_{1-\alpha}(t, t_1)p^{\alpha}_{Bi}(t_1)\cdot\xi_{B0}(t_1) + m\kappa_{1-\alpha}(t_2, t)p^{\alpha}_{Bi}(t_2)\cdot\xi_{B0}(t_2)\right] = 0. \end{aligned} \tag{75}$$

Equation (75) is called the determined equation for the constrained Hamiltonian system with the operator B^{α}_M (Equation (45)). Lie symmetry also leads to a conserved quantity under certain conditions. Therefore, we have

Theorem 6. *For the constrained Hamiltonian system with the operator B^{α}_M (Equation (45)), if the infinitesimal generators ξ_{B0}, ξ_{Bi}, η_{Bi} and η^{α}_{Bi} satisfy Equation (62) and the determined equation (Equation (75), then there exists a conserved quantity Equation (64).*

Proof of Theorem 6. From Equations (34), (45) and (62), we can get the intended result. □

7. An Example

Try to find the conserved quantity for the following singular system with the operator A^{α}_M, whose Lagrangian is

$$L_A = \dot{q}_{A1}q_{A2} - q_{A1}\dot{q}_{A2} + (q_{A1})^2 + (q_{A2})^2 + \frac{1}{2}\left[\left(A^{\alpha}_M q_{A1}\right)^2 + \left(A^{\alpha}_M q_{A2}\right)^2\right]. \tag{76}$$

From Equations (11) and (12), we have

$$\begin{aligned} &p_{A1} = \tfrac{\partial L_A}{\partial \dot{q}_{A1}} = q_{A2},\ p_{A2} = \tfrac{\partial L_A}{\partial \dot{q}_{A2}} = -q_{A1},\ p^{\alpha}_{A1} = \tfrac{\partial L_A}{\partial A^{\alpha}_M q_{A1}} = A^{\alpha}_M q_{A1},\ p^{\alpha}_{A2} = \tfrac{\partial L_A}{\partial A^{\alpha}_M q_{A2}} = A^{\alpha}_M q_{A2}, \\ &H_A = p_{A1}\dot{q}_{A1} + p_{A2}\dot{q}_{A2} + p^{\alpha}_{A1}A^{\alpha}_M q_{A1} + p^{\alpha}_{A2}A^{\alpha}_M q_{A2} - L_A = \tfrac{1}{2}\left[\left(A^{\alpha}_M q_{A1}\right)^2 + \left(A^{\alpha}_M q_{A2}\right)^2\right] \\ &-(q_{A1})^2 - (q_{A2})^2 = \tfrac{1}{2}\left[\left(p^{\alpha}_{A1}\right)^2 + \left(p^{\alpha}_{A2}\right)^2\right] - (q_{A1})^2 - (q_{A2})^2. \end{aligned} \tag{77}$$

Therefore, the Hamiltonian and the two primary constraints have the form

$$H_A = \frac{1}{2}\left[\left(p^{\alpha}_{A1}\right)^2 + \left(p^{\alpha}_{A2}\right)^2\right] - q^2_{A1} - q^2_{A2}, \tag{78}$$

$$\phi_{A1} = p_{A1} - q_{A2} = 0,\ \phi_{A2} = p_{A2} + q_{A1} = 0. \tag{79}$$

Then from Equation (48), the two Lagrange multipliers λ_{A1} and λ_{A2} can be calculated as

$$\begin{array}{c}\lambda_{A1}=-q_{A2}+\frac{1}{2}\left[B_{M^*}^{\alpha}p_{A2}^{\alpha}-mp_{A2}^{\alpha}(t_2)\kappa_{1-\alpha}(t_2,t)+\omega p_{A2}^{\alpha}(t_1)\kappa_{1-\alpha}(t,t_1)\right],\\ \lambda_{A2}=q_{A1}-\frac{1}{2}\left[B_{M^*}^{\alpha}p_{A1}^{\alpha}-mp_{A1}^{\alpha}(t_2)\kappa_{1-\alpha}(t_2,t)+\omega p_{A1}^{\alpha}(t_1)\kappa_{1-\alpha}(t,t_1)\right].\end{array} \tag{80}$$

Therefore, the constrained Hamilton equation with the operator A_M^{α} can be obtained. And we can also verify that under the condition $\frac{\mathrm{d}}{\mathrm{d}t}\kappa_{\alpha}(t,\tau)=-\frac{\mathrm{d}}{\mathrm{d}\tau}\kappa_{\alpha}(t,\tau)$,

$$\begin{array}{c}\xi_{A0}=1,\ \xi_{A1}=\xi_{A2}=0,\ \eta_{A1}=\eta_{A2}=0,\ \eta_{A1}^{\alpha}=\eta_{A2}^{\alpha}=0,\\ G_A=0\end{array} \tag{81}$$

is a solution to the Noether quasi-identity (Equation (55)). Then Theorem 2 gives

$$\begin{array}{c}C_{AG}=\frac{1}{2}\left[\left(p_{A1}^{\alpha}\right)^2+\left(p_{A2}^{\alpha}\right)^2\right]+q_{A1}^2+q_{A2}^2-\int_{t_1}^{t}\left\{p_{A1}^{\alpha}\frac{\mathrm{d}}{\mathrm{d}t}A_M^{\alpha}q_{A1}+p_{A2}^{\alpha}\frac{\mathrm{d}}{\mathrm{d}t}A_M^{\alpha}q_{A2}\right.\\ +\dot{q}_{A1}\left[B_{M^*}^{\alpha}p_{A1}^{\alpha}-m\kappa_{1-\alpha}(t_2,\tau)p_{A1}^{\alpha}(t_2)+\omega\kappa_{1-\alpha}(\tau,t_1)p_{A1}^{\alpha}(t_1)\right]\\ \left.+\dot{q}_{A2}\left[B_{M^*}^{\alpha}p_{A2}^{\alpha}-m\kappa_{1-\alpha}(t_2,\tau)p_{A2}^{\alpha}(t_2)+\omega\kappa_{1-\alpha}(\tau,t_1)p_{A2}^{\alpha}(t_1)\right]\right\}\mathrm{d}\tau=\text{const.}\end{array} \tag{82}$$

Specially, let $\kappa_{\alpha}(t,\tau)=(t-\tau)^{\alpha-1}/\Gamma(\alpha)$, when $M=M_1$ (or $M=M_2$ or $M=M_3$) and $\alpha\to 1$, we have $C_{AG}=-H_A=\text{const.}$

8. Results and Discussion

Based on the mixed integer order derivative and generalized operators, the singular Lagrange equations, primary constraints, constrained Hamilton equations, consistency conditions and conserved quantities were investigated. All are new works. In fact, Lie symmetry can lead to the Noether type conserved quantity as well as the Hojman conserved quantity. Here, we only presented the Noether type conserved quantity simply. Next, Lie symmetry and the Hojman conserved quantity, Mei symmetry and the Mei type conserved quantity and the relationships among the three symmetry methods will be studied. Singular systems on time scales is also a hot topic that needs to be investigated further.

Funding: This research was funded by the National Natural Science Foundation of China, grant numbers 12172241, 11802193, 11972241, the Natural Science Foundation of Jiangsu Province, grant number BK20191454 and the "Qinglan Project" of Jiangsu Province.

Institutional Review Board Statement: Not applicable.

Informed Consent Statement: Not applicable.

Conflicts of Interest: The authors declare no conflict of interest.

References

1. Kusnezov, D.; Bulgac, A.; Dang, G.D. Quantum Lévy processes and fractional kinetics. *Phys. Rev. Lett.* **1999**, *82*, 1136–1139. [CrossRef]
2. Naber, M. Time fractional Schrdinger equation. *J. Math. Phys.* **2004**, *45*, 3339–3352. [CrossRef]
3. Muslih, S.I.; Agrawal, O.P.; Baleanu, D. A fractional Dirac equation and its solution. *J. Phys. A Math. Theor.* **2010**, *43*, 055203. [CrossRef]
4. Metzler, R.; Klafter, J. The random walk's guide to anomalous diffusion: A fractional dynamics approach. *Phys. Rep.* **2000**, *339*, 1–77. [CrossRef]
5. Herrmann, R. Gauge invariance in fractional field theories. *Phys. Lett. A* **2008**, *372*, 5515–5522. [CrossRef]
6. Lazo, M.J. Gauge invariant fractional electromagnetic fields. *Phys. Lett. A* **2011**, *375*, 3541–3546. [CrossRef]
7. Wu, Q.; Huang, J.H. *Fractional Calculus*; Tsinghua University Press: Beijing, China, 2016.
8. Riewe, F. Nonconservative Lagrangian and Hamiltonian mechanics. *Phys. Rev. E* **1996**, *53*, 1890–1899. [CrossRef] [PubMed]
9. Riewe, F. Mechanics with fractional derivatives. *Phys. Rev. E* **1997**, *55*, 3581–3592. [CrossRef]
10. Klimek, M. Lagrangian and Hamiltonian fractional sequential mechanics. *Czechoslov. J. Phys.* **2002**, *52*, 1247–1253. [CrossRef]
11. Muslih, S.I.; Baleanu, D. Hamiltonian formulation of systems with linear velocities within Riemann–Liouville fractional derivatives. *J. Math. Anal. Appl.* **2005**, *304*, 599–606. [CrossRef]

12. Agrawal, O.P. Fractional variational calculus in terms of Riesz fractional derivatives. *J. Phys. A Math. Theor.* **2007**, *40*, 6287–6303. [CrossRef]
13. Luo, S.K.; Xu, Y.L. Fractional Birkhoffian mechanics. *Acta Mech.* **2015**, *226*, 829–844. [CrossRef]
14. Song, C.J.; Agrawal, O.P. Hamiltonian formulation of systems described using fractional singular Lagrangian. *Acta Appl. Math.* **2021**, *172*, 9. [CrossRef]
15. Rabei, E.M.; Nawafleh, K.I.; Hijjawi, R.S.; Muslih, S.I.; Baleanu, D. The Hamilton formalism with fractional derivatives. *J. Math. Anal. Appl.* **2007**, *327*, 891–897. [CrossRef]
16. Malinowska, A.B.; Torres, D.F.M. *Introduction to the Fractional Calculus of Variations*; Imp. Coll. Press: London, UK, 2012.
17. Agrawal, O.P. Generalized variational problems and Euler-Lagrange equations. *Comput. Math. Appl.* **2010**, *59*, 1852–1864. [CrossRef]
18. Li, Z.P. Canonical symmetry and Dirac conjecture for constrained system. In *Thirty Years of Nonholonomic Mechanics in China*; Chen, B., Mei, F.X., Eds.; Henan University Press: Kaifeng, China, 1994.
19. Li, Z.P. *Classical and Quantal Dynamics of Contrained Systems and Their Symmetrical Properties*; Beijing Polytechnic University Press: Beijing, China, 1993.
20. Cao, S. Canonicalization and Symmetry Theories of the Constrained Hamiltonian System. Master's Thesis, Zhejiang Sci-Tech University, Hangzhou, China, 2017.
21. Li, Z.P. *Contrained Hamiltonian Systems and Their Symmetrical Properties*; Beijing Polytechnic University Press: Beijing, China, 1999.
22. Li, Z.P.; Jiang, J.H. *Symmetries in Constrained Canonical Systems*; Science Press: Beijing, China, 2002.
23. Mei, F.X.; Wu, H.B.; Zhang, Y.F. Symmetries and conserved quantities of constrained mechanical systems. *Int. J. Dynam. Control* **2014**, *2*, 285–303. [CrossRef]
24. Noether, A.E. Invariante Variationsprobleme. *Nachr. Akad. Wiss. Gött. Math-Phys.* **1918**, *KI*, 235–258.
25. Song, C.J.; Zhang, Y. Conserved quantities for Hamiltonian systems on time scales. *Appl. Math. Comput.* **2017**, *313*, 24–36. [CrossRef]
26. Song, C.J.; Zhang, Y. Noether symmetry and conserved quantity for fractional Birkhoffian mechanics and its applications. *Fract. Calc. Appl. Anal.* **2018**, *21*, 509–526. [CrossRef]
27. Zhang, Y.; Tian, X. Conservation laws of nonholonomic nonconservative system based on Herglotz variational problems. *Phys. Lett. A* **2019**, *383*, 691–696. [CrossRef]
28. Zhang, Y. Lie symmetry and invariants for a generalized Birkhoffian system on time scales. *Chaos Solitons Fractals* **2019**, *128*, 306–312. [CrossRef]
29. Ding, J.J.; Zhang, Y. Conserved quantities and adiabatic invariants of fractional Birkhoffian system of Herglotz type. *Chin. Phys. B* **2020**, *29*, 044501. [CrossRef]
30. Zhou, Y.; Zhang, Y. Noether symmetries for fractional generalized Birkhoffian systems in terms of classical and combined Caputo derivatives. *Acta Mech.* **2020**, *231*, 3017–3029. [CrossRef]
31. Mei, F.X. *Analytical Mechanics (II)*; Beijing Institute of Technology Press: Beijing, China, 2013.
32. Mei, F.X. *Symmetry and Conserved Quantity of Constrained Mechanical Systems*; Beijing Institute of Technology Press: Beijing, China, 2004.
33. Mei, F.X.; Wu, H.B. *Dynamics of Constrained Mechanical Systems*; Beijing Institute of Technology Press: Beijing, China, 2009.
34. Cai, P.P.; Fu, J.L.; Guo, Y.X. Lie symmetries and conserved quantities of the constraint mechanical systems on time scales. *Rep. Math. Phys.* **2017**, *79*, 279–298. [CrossRef]
35. Han, Y.L.; Wang, X.X.; Zhang, M.L.; Jia, L.Q. Lie symmetry and approximate Hojman conserved quantity of Appell equations for a weakly nonholonomic system. *Nonlinear Dyn.* **2013**, *71*, 401–408. [CrossRef]
36. Chen, X.W.; Li, Y.M.; Zhao, Y.H. Lie symmetries, perturbation to symmetries and adiabatic invariants of Lagrange system. *Phys. Lett. A* **2005**, *337*, 274–278. [CrossRef]
37. Ding, N.; Fang, J.H. Lie symmetry and conserved quantities for nonholonomic Vacco dynamical systems. *Commun. Theor. Phys.* **2006**, *46*, 265–268.
38. Zhang, Y.; Xun, Y. Lie symmetries of constrained Hamiltonian system with the second type of constraints. *Acta Phys. Sin.* **2001**, *50*, 816–819. [CrossRef]
39. Song, C.J.; Shen, S.L. Noether symmetry method for Birkhoffian systems in terms of generalized fractional operators. *Theor. Appl. Mech. Lett.* **2021**, *11*, 100298. [CrossRef]
40. Jia, Q.L.; Wu, H.B.; Mei, F.X. Noether symmetries and conserved quantities for fractional forced Birkhoffian systems. *J. Math. Anal. Appl.* **2016**, *442*, 782–795. [CrossRef]
41. Zhou, S.; Fu, H.; Fu, J.L. Symmetry theories of Hamiltonian systems with fractional derivatives. *Sci. China Phys. Mech. Astron.* **2011**, *54*, 1847–1853.
42. Song, C.J.; Cheng, Y. Noether symmetry method for Hamiltonian mechanics involving generalized operators. *Adv. Math. Phys.* **2021**, *2021*, 1959643. [CrossRef]
43. Song, C.J.; Cheng, Y. Noether's theorems for nonshifted dynamic systems on time scales. *Appl. Math. Comput.* **2020**, *374*, 125086. [CrossRef]
44. Zhang, Y.; Zhai, X.H. Perturbation to Lie symmetry and adiabatic invariants for Birkhoffian systems on time scales. *Commun. Nonlinear Sci. Numer. Simul.* **2019**, *75*, 251–261. [CrossRef]

45. Song, C.J.; Cheng, Y. Conserved quantity and adiabatic invariant for Hamiltonian system with variable order. *Symmetry* **2019**, *11*, 1270. [CrossRef]
46. Zhang, Y. Herglotz's variational problem for non-conservative system with delayed arguments under Lagrangian framework and its Noether's Theorem. *Symmetry* **2020**, *12*, 845. [CrossRef]

mathematics

MDPI

Article

On Hilfer Generalized Proportional Nabla Fractional Difference Operators

Qiushuang Wang and Run Xu *

School of Mathematical Sciences, Qufu Normal University, Qufu 273165, China; qswang2020@163.com
* Correspondence: xurun2005@163.com

Abstract: In this paper, the Hilfer type generalized proportional nabla fractional differences are defined. A few important properties in the left case are derived and the properties in the right case are proved by Q-operator. The discrete Laplace transform in the sense of the left Hilfer generalized proportional fractional difference is explored. Furthermore, An initial value problem with the new operator and its generalized solution are considered.

Keywords: hilfer operator; generalized proportional fractional difference; Q-operator, discrete laplace transform; the initial value problem

MSC: 26A33

Citation: Wang, Q.; Xu, R. On Hilfer Generalized Proportional Nabla Fractional Difference Operators. *Mathematics* **2022**, *10*, 2654. https://doi.org/10.3390/math10152654

Academic Editors: António Lopes, Alireza Alfi, Liping Chen and Sergio Adriani David

Received: 5 July 2022
Accepted: 26 July 2022
Published: 28 July 2022

Publisher's Note: MDPI stays neutral with regard to jurisdictional claims in published maps and institutional affiliations.

1. Introduction

Fractional Calculus (FC), which can be traced back to the 17th century, is derived from integral calculus. A wide variety of concepts for fractional operators in the continuous setting have been defined in the literature so far, such as Riemann–Liouville, Hadamard, Caputo, proportional, Hilfer fractional operators, and so on; the reader can refer to [1–4] and the references therein. Fractional models are of great theoretical significance and practical value, compared to integer models, in real world problems. Therefore, FC has been widely used in mathematics, physics, engineering, etc. For more recent developments on fractional calculus, see the monographs [5–12].

It is generally known that Discrete Fractional Calculus (DFC) is the extension of FC. The models for DFC play an important role in modeling complex problems of discontinuous systems, which are far superior to their counterparts in continuous settings. Unlike FC of the continuous system, whose history is more than hundreds of years old, the idea of DFC is very recent. The theory of DFC has been investigated extensively since the 20th century, when Chapman [13] presented the definitions of the fractional delta sequential differences, in 1911. Similarly to the case of FC, there are many forms of definitions, such as Riemann–Liouville, Caputo, Hilfer, proportional discrete fractional operators, and so on (see [14–17]).

In addition to the study of fractional operators in FC or DFC, there have also been many directions to develop, for instance, fractional inequalities, fractional equations, etc. In particular, initial value problems with fractional differential or difference operators have been extensively studied. In 2020, Jonnalagadda and Gopal [18] defined the nabla αth-order and βth-type Hilfer fractional difference of f

$$\nabla_a^{\alpha,\beta} f(t) = \nabla_{a+n}^{-\beta(n-\alpha)} \nabla^n \nabla_a^{-(1-\beta)(n-\alpha)} f(t),\ t \in \mathbb{N}_{a+n},$$

where $0 \leq \beta \leq 1$, $n-1 < \alpha \leq n$ with $n \in \mathbb{N}^+$, and $\nabla_a^{-\alpha} f(t) = \sum_{k=a}^{t} \frac{(t-k+1)^{\overline{\alpha}}}{\Gamma(\alpha)} f(k)$ is the nabla Riemann–Liouville fractional sum defined in [19]. Furthermore, they explored the solution of the following initial value problem

$$\begin{cases} \nabla_a^{\alpha,\beta} y(t) = f(t, y(t)), & t \in \mathbb{N}_{a+1}, \\ \nabla_a^{-(1-\gamma)} y(t)|_{t=a} = y(a), \end{cases}$$

where $0 < \alpha \leq 1$, $0 \leq \beta \leq 1$ and $\gamma = \alpha + \beta - \alpha\beta$. Recently, motivated by the generalized proportional and Hilfer fractional continuous operators, which are defined in [20,21], respectively, Ahmed et al. [22] introduced the Hilfer generalized proportional fractional derivative of order α and type β of a function f

$$\mathcal{D}_a^{\alpha,\beta,\rho} f(x) = \mathcal{I}_a^{\beta(n-\alpha),\rho} \left[\mathcal{D}^\rho \left(\mathcal{I}_a^{(1-\beta)(n-\alpha),\rho} f \right) \right](x),$$

where $n-1 < \alpha < n$, $\rho \in (0,1]$, $0 \leq \beta \leq 1$ with $n \in \mathbb{N}_1$, $\mathcal{D}^\rho f(x) = (1-\rho) f(x) + \rho f'(x)$, and $\mathcal{I}$ is the generalized proportional fractional integral operator defined in [21]. Furthermore, they discussed the existence and uniqueness of the solution for the following nonlinear differential equation with a nonlocal initial condition

$$\begin{cases} \mathcal{D}_{a^+}^{\alpha,\beta,\rho} y(t) = f(t, y(t)), & t \in [a, T],\ T > a \geq 0, \\ \mathcal{I}_{a+}^{1-\gamma,\rho} y(t)|_{t=a} = \sum_{i=1}^m c_i x(\tau_i), & \gamma = \alpha + \beta - \alpha\beta,\ \tau_i \in (a, T), \end{cases}$$

where $0 < \alpha < 1$, $c_i \in \mathbb{R}$, $f : [a, T] \times \mathbb{R} \to \mathbb{R}$ is a continuous function and $\tau_i \in (a, T)$ satisfying $a < \tau_i < \cdots < \tau_m < T$ for $i = 1, \ldots, m$. For more studies that investigate and extend the fractional differential or fractional difference equation, we refer the reader to [16,17,23,24].

The goal of this paper is to introduce the Hilfer-type generalized proportional fractional difference, which is a discrete counterpart of the fractional derivative defined in [22]. Moreover, we shall study the following initial value problem

$$\begin{cases} {}_a\nabla_h^{\alpha,\beta,\rho} y(t) = f(t, y(t)), & t \in \mathbb{N}_{a+h,h}, \\ {}_a\nabla_h^{-(1-\gamma),\rho} y(t)|_{t=a+h} = \frac{h^{1-\gamma}}{(\rho-(\rho-1)h)^{1-\gamma}} y(a+h), \end{cases} \tag{1}$$

where $0 < \alpha < 1$, $0 \leq \beta \leq 1$, $0 < \rho \leq 1, \gamma = \alpha + \beta - \alpha\beta$, ${}_a\nabla_h^{\alpha,\beta,\rho}(\cdot)$ is the new difference operator of order α and type β (see Definition 7), and ${}_a\nabla_h^{-(1-\gamma),\rho}(\cdot)$ is the proportional fractional sum operator of order $(1-\gamma)$ (see Definition 4). The new operator can reduce to some known operators. Additionally, our results can provide a powerful tool for studying the qualitative properties for the solution of (1), such as existence, uniqueness, oscillation, and so on.

The structure of this article is as follows: In Section 2, we review some basic definitions and results of discrete calculus. In Section 3, two new fractional difference operators are introduced, and some corresponding properties for the left case are proved based on the definitions. We also prove the properties of the right case by Q-operator. Moreover, the h-Laplace transform for the left Hilfer generalized proportional fractional difference operator is developed. Additionally, the general solution of an initial value problem (1) with the new operator is discussed. Finally, the conclusion of the paper is given in Section 4.

2. Preliminaries

In this section, some definitions and results are given for later use in the following sections. The sets considered in this paper are $\mathbb{N}_a = \{a, a+1, a+2, \ldots\}$, ${}_b\mathbb{N} = \{\ldots b-2, b-1, b\}$, $\mathbb{N}_{a,h} = \{a, a+h, a+2h, \ldots\}$ and ${}_{b,h}\mathbb{N} = \{\ldots b-2h, b-h, b\}$ with the step $h > 0$.

For convenience, we give some of the notations to be used here. The h-backward operator is given by $\rho_h(t) = t - h$ for $t \in \mathbb{N}_{a,h}$. The nabla and delta h-difference operators are given as

$$\nabla_h f(t) = \frac{f(t) - f(t-h)}{h}, \quad t \in \mathbb{N}_{a+h,h},$$

$$\Delta_h f(t) = \frac{f(t+h) - f(t)}{h}, \quad t \in {}_{b-h,h}\mathbb{N}.$$

For $h = 1$, we get the following nabla and delta difference operators

$$\nabla f(t) = f(t) - f(t-1), \quad \Delta f(t) = f(t+1) - f(t).$$

They are also called the backward and the forward difference operator, respectively. The nabla and delta h-sums are given as

$$\left(\nabla_h^{-1} f\right)(t) = \int_a^t f(s)\nabla_h s = \sum_{k=\frac{a}{h}+1}^{\frac{t}{h}} f(kh)h, \quad t \in \mathbb{N}_{a+h,h},$$

$$\left(\Delta_h^{-1} f\right)(t) = \int_t^b f(s)\Delta_h s = \sum_{k=\frac{t}{h}}^{\frac{b}{h}-1} f(kh)h, \quad t \in {}_{b-h,h}\mathbb{N},$$

where ∇_h and Δ_h are derivative operators on the time scales $\{a, a+h, \ldots, t\}$ and $\{t, \ldots, b-h, b\}$, respectively.

For arbitrary $t, \alpha \in \mathbb{R}$, the generalized rising and falling h-factorial functions are defined by

$$t_h^{\overline{\alpha}} = h^\alpha \frac{\Gamma\left(\frac{t}{h} + \alpha\right)}{\Gamma\left(\frac{t}{h}\right)}, \quad \frac{t}{h}, \frac{t}{h} + \alpha \notin \{\cdots, -2, -1, 0\},$$

$$t_h^{(\alpha)} = h^\alpha \frac{\Gamma\left(\frac{t}{h} + 1\right)}{\Gamma\left(\frac{t}{h} + 1 - \alpha\right)}, \quad \frac{t}{h} + 1, \frac{t}{h} + 1 - \alpha \notin \{\cdots, -2, -1, 0\},$$

where $\Gamma(\cdot)$ is the Gamma function given as $\Gamma(x) = \int_0^\infty \xi^{x-1} e^{-\xi} d\xi$. When $h = 1$, we obtain the rising and falling factorial function: $t^{\overline{\alpha}} = \frac{\Gamma(t+\alpha)}{\Gamma(t)}$, $t^{(\alpha)} = \frac{\Gamma(t+1)}{\Gamma(t-\alpha+1)}$. It is clear that

$$\nabla_h t_h^{\overline{\alpha}} = \alpha\, t_h^{\overline{\alpha-1}}.$$

For $\rho \in (0, 1] \setminus \frac{h}{1-h}$, we introduce the h-proportional differences of order ρ defined in [16]

$$(\nabla_h^\rho f)(t) = (1-\rho) f(t) + \rho(\nabla_h f)(t), \quad t \in \mathbb{N}_{a+h,h},$$

$$({}_\ominus\Delta_h^\rho f)(t) = (1-\rho) f(t) - \rho(\Delta_h f)(t), \quad t \in {}_{b-h,h}\mathbb{N},$$

and

$$(\nabla_h^{n,\rho} f)(t) = \underbrace{(\nabla_h^\rho\, \nabla_h^\rho \cdots\, \nabla_h^\rho f)}_{n \text{ times}}(t), \quad ({}_\ominus\Delta_h^{n,\rho} f)(t) = \underbrace{({}_\ominus\Delta_h^\rho\, {}_\ominus\Delta_h^\rho \cdots\, {}_\ominus\Delta_h^\rho f)}_{n \text{ times}}(t).$$

When $h = 1$, we denote $(\nabla_1^\rho f)(t) = f(t) - \rho f(t-1)$ and $({}_\ominus\Delta_1^\rho f)(t) = f(t) - \rho f(t+1)$. Next, we recall some definitions and properties of discrete fractional operators as follows.

Definition 1 ([25]). *For $\alpha > 0$, the nabla left and right h-Riemann–Liouville fractional sums of f are given by*

$$\left({}_a\nabla_h^{-\alpha} f\right)(t) = \frac{1}{\Gamma(\alpha)} \int_a^t (t - \rho_h(s))_h^{\overline{\alpha-1}} f(s)\nabla_h s, \quad t \in \mathbb{N}_{a+h,h}, \tag{2}$$

$$\left({}_h\nabla_b^{-\alpha} f\right)(t) = \frac{1}{\Gamma(\alpha)} \int_t^b (s - \rho_h(t))_h^{\overline{\alpha-1}} f(s)\Delta_h s, \quad t \in {}_{b-h,h}\mathbb{N}. \tag{3}$$

Definition 2 ([25]). *For $\alpha > 0$, the nabla left and right h-Riemann–Liouville fractional differences of f are given by*

$$({}_a\nabla_h^{\alpha} f)(t) = \nabla_h^n \left({}_a\nabla_h^{-(n-\alpha)} f \right)(t), \quad t \in \mathbb{N}_{a+h,h}, \tag{4}$$

$$({}_h\nabla_b^{\alpha} f)(t) = (-1)^n \Delta_h^n \left({}_h\nabla_b^{-(n-\alpha)} f \right)(t), \quad t \in {}_{b-h,h}\mathbb{N}, \tag{5}$$

where $n-1 < \alpha < n$, $n := [\alpha] + 1$, and $[\alpha]$ is the greatest integer that is less than or equal to α.

Definition 3 ([26]). *For $\alpha > 0$, the nabla left and right h-Caputo fractional differences are defined by*

$$({}_a^{C}\nabla_h^{\alpha} f)(t) = {}_{a_h(\alpha)}\nabla_h^{-(n-\alpha)} (\nabla_h^n f)(t), \quad t \in \mathbb{N}_{a+nh,h}, \tag{6}$$

$$({}_h^{C}\nabla_b^{\alpha} f)(t) = (-1)^n \, {}_h\nabla_{b_h(\alpha)}^{-(n-\alpha)} (\Delta_h^n f)(t), \quad t \in {}_{b-nh,h}\mathbb{N}, \tag{7}$$

where $n = [\alpha] + 1$, and $a_h(\alpha) = a + (n-1)h$, $b_h(\alpha) = b - (n-1)h$.

Definition 4 ([16]). *For $\alpha \in \mathbb{C}$, $Re(\alpha) > 0$, the left and right generalized proportional fractional sums are defined by*

$$\begin{aligned} ({}_a\nabla_h^{-\alpha,\rho} f)(t) =& \frac{1}{\rho^{\alpha}\Gamma(\alpha)} \int_a^t {}_h\hat{e}_p(t-\tau+\alpha h, 0)(t-\rho_h(\tau))_h^{\overline{\alpha-1}} f(\tau)\nabla_h\tau \\ =& \frac{h}{\rho^{\alpha}\Gamma(\alpha)} \sum_{k=\frac{a}{h}+1}^{\frac{t}{h}} {}_h\hat{e}_p(t-kh+\alpha h, 0)(t-\rho_h(kh))_h^{\overline{\alpha-1}} f(kh), \quad t \in \mathbb{N}_{a+h,h}, \end{aligned} \tag{8}$$

$$\begin{aligned} ({}_h\nabla_b^{-\alpha,\rho} f)(t) =& \frac{1}{\rho^{\alpha}\Gamma(\alpha)} \int_t^b {}_h\hat{e}_p(\tau-t+\alpha h, 0)(\tau-\rho_h(t))_h^{\overline{\alpha-1}} f(\tau)\Delta_h\tau \\ =& \frac{h}{\rho^{\alpha}\Gamma(\alpha)} \sum_{k=\frac{t}{h}}^{\frac{b}{h}-1} {}_h\hat{e}_p(kh-t+\alpha h, 0)(kh-\rho_h(t))_h^{\overline{\alpha-1}} f(kh), \quad t \in {}_{b-h,h}\mathbb{N}, \end{aligned} \tag{9}$$

where the proportionality index $\rho \in (0,1]$, and the exponential function is given as

$${}_h\hat{e}_p(t,a) = \left(\frac{1}{1-ph}\right)^{\frac{t-a}{h}} = \left(\frac{\rho}{\rho-(\rho-1)h}\right)^{\frac{t-a}{h}}, \quad \text{for } p = \frac{\rho-1}{\rho}.$$

Some properties of the exponential function that will be important in the development of this article are described in the following remark.

Remark 1 ([16]). *For $t \in \mathbb{N}_{a,h}$, $\alpha > 0$, $\beta > 0$ and $0 < \rho \leq 1$, the following identities hold,*

(i) ${}_h\hat{e}_p(t,a) = {}_h\hat{e}_p(t-a,0) = {}_h\hat{e}_p(0,a-t)$.

(ii) $\nabla_h^{\rho}\left(c \cdot {}_h\hat{e}_p(t,a)\right) = 0$, for c is a constant.

(iii) $\nabla_h^{\rho}(g(t) \cdot {}_h\hat{e}_p(t,0)) = \rho(\nabla_h g)(t) \cdot {}_h\hat{e}_p(t-h,0)$.

(iv) ${}_a\nabla_h^{-\alpha,\rho}\left({}_h\hat{e}_p(t,0)(t-a)_h^{\overline{\beta-1}}\right) = \frac{\Gamma(\beta)}{\Gamma(\beta+\alpha)\rho^{\alpha}} {}_h\hat{e}_p(t+\alpha h,0)(t-a)_h^{\overline{\alpha+\beta-1}}$.

Definition 5 ([16]). *For $\rho \in (0,1]$ and $\alpha \in \mathbb{C}$, $Re(\alpha) > 0$, the left and right generalized proportional fractional differences are defined by*

$$({}_a\nabla_h^{\alpha,\rho} f)(t) = \nabla_h^{n,\rho}\left({}_a\nabla_h^{-(n-\alpha),\rho} f\right)(t), \quad t \in \mathbb{N}_{a+h,h}, \tag{10}$$

$$({}_h\nabla_b^{\alpha,\rho} f)(t) = {}_{\ominus}\Delta_h^{n,\rho}\left({}_h\nabla_b^{-(n-\alpha),\rho} f\right)(t), \quad t \in {}_{b-h,h}\mathbb{N}, \tag{11}$$

where $n = [Re(\alpha)] + 1$.

Remark 2 ([16]). *Clearly,* $\lim_{\alpha\to 0}({}_a\nabla_h^{\alpha,\rho} f)(t) = f(t)$, $\lim_{\alpha\to 1}({}_a\nabla_h^{\alpha,\rho} f)(t) = (\nabla_h^{\rho} f)(t)$.

Definition 6 ([16]). *For* $\rho \in (0,1]$ *and* $\alpha \in \mathbb{C}$, $Re(\alpha) > 0$, *the left and right Caputo generalized proportional fractional differences are defined by*

$$\left({}_a^{C}\nabla_h^{\alpha,\rho} f\right)(t) = {}_{a_h(\alpha)}\nabla_h^{-(n-\alpha),\rho}(\nabla_h^{n,\rho} f)(t), \tag{12}$$

$$\left({}_h^{C}\nabla_b^{\alpha,\rho} f\right)(t) = {}_h\nabla_{b_h(\alpha)}^{-(n-\alpha),\rho}({}_{\ominus}\Delta_h^{n,\rho} f)(t). \tag{13}$$

where $n = [Re(\alpha)] + 1$.

Theorem 1 (Composition Rule [16]). *Assume* $\alpha > 0$, $n = [\alpha] + 1$ *and* $\beta > 0$. *Then for any* $0 < \rho \le 1$, *we have*

(i) ${}_a\nabla_h^{\alpha,\rho}\left({}_a\nabla_h^{-\alpha,\rho} f\right)(t) = f(t)$.

(ii) ${}_a\nabla_h^{-\alpha,\rho}\left(\nabla_h^{\rho} f\right)(t) = \nabla_h^{\rho}\left({}_a\nabla_h^{-\alpha,\rho} f\right)(t) - \frac{(t-a)_h^{\overline{\alpha-1}}\, {}_h\hat{e}_p(t,a)}{\rho^{\alpha-1}\Gamma(\alpha)}\left(\frac{\rho}{\rho-(\rho-1)h}\right)^{\alpha-1} f(a)$.

(iii) ${}_a\nabla_h^{-\alpha,\rho}({}_a\nabla_h^{-\beta,\rho} f)(t) = {}_a\nabla_h^{-\beta,\rho}({}_a\nabla_h^{-\alpha,\rho} f)(t) = ({}_a\nabla_h^{-(\alpha+\beta),\rho} f)(t)$.

(iv) $\left({}_{a_h(\alpha)}\nabla_h^{-\alpha,\rho}\, {}_{a_h(\alpha)}\nabla_h^{\alpha,\rho} f\right)(t) = f(t) - {}_h\hat{e}_p(t-(n-1)h, a)$
$\cdot \sum_{j=1}^{n}\left(\frac{\rho}{\rho-(\rho-1)h}\right)^{\alpha-1}\frac{(t-a_h(\alpha))_h^{\overline{\alpha-j}}}{\rho^{\alpha-j}\Gamma(\alpha+1-j)}\left({}_{a_h(\alpha)}\nabla_h^{-(j-\alpha),\rho} f\right)(a+(n-1)h)$.

3. Main Results

In this section, we define the left and right generalized proportional fractional difference operators in the Hilfer sense and discuss some of their properties. In addition, we demonstrate a general solution of problem (1).

3.1. The Hilfer Generalized Proportional Fractional Difference and Some Related Operators

(1) First, like the nabla Hilfer-type fractional difference that is defined by the composition of the nabla Riemann–Liouville fractional sum and nabla integral difference ([18]), the Hilfer generalized proportional fractional difference operators are introduced as follows, based on the generalized proportional fractional sum and h-proportional difference.

Definition 7. *Let* $n-1 < \alpha < n$ *with* $n \in \mathbb{N}_1$, $\rho \in (0,1]$ *and* $0 \le \beta \le 1$. *Then the left and right Hilfer generalized proportional fractional difference of order* α *and type* β *of a function* f *are defined by*

$$\left({}_a\nabla_h^{\alpha,\beta,\rho} f\right)(t) = {}_a\nabla_h^{-\beta(n-\alpha),\rho}\cdot\nabla_h^{\rho}\cdot\, {}_a\nabla_h^{-(n-\alpha)(1-\beta),\rho} f(t),\ t \in \mathbb{N}_{a+h,h}, \tag{14}$$

$$\left({}_h\nabla_b^{\alpha,\beta,\rho} f\right)(t) = {}_h\nabla_b^{-\beta(n-\alpha),\rho}\cdot\, {}_{\ominus}\Delta_h^{\rho}\cdot\, {}_h\nabla_b^{-(n-\alpha)(1-\beta),\rho} f(t),\ t \in\, {}_{b-h,h}\mathbb{N}, \tag{15}$$

where ${}_a\nabla_h^{-\beta(n-\alpha),\rho}(\cdot)$, ${}_h\nabla_b^{-\beta(n-\alpha),\rho}(\cdot)$ *are generalized proportional fractional sum operators defined in* (8) *and* (9), *respectively.*

In particular, when $n = 1$, *Definition 7 is equivalent with*

$$\left({}_a\nabla_h^{\alpha,\beta,\rho} f\right)(t) = {}_a\nabla_h^{-\beta(1-\alpha),\rho}\cdot\nabla_h^{\rho}\cdot\, {}_a\nabla_h^{-(1-\alpha)(1-\beta),\rho} f(t), \tag{16}$$

$$\left({}_h\nabla_b^{\alpha,\beta,\rho} f\right)(t) = {}_h\nabla_b^{-\beta(1-\alpha),\rho}\cdot\, {}_{\ominus}\Delta_h^{\rho}\cdot\, {}_h\nabla_b^{-(1-\alpha)(1-\beta),\rho} f(t). \tag{17}$$

When $n = 1$ and $h = 1$, Definition 7 is equivalent with

$$\left({}_a\nabla_1^{\alpha,\beta,\rho} f\right)(t) = {}_a\nabla_1^{-\beta(1-\alpha),\rho} \cdot \nabla_1^{\rho} \cdot {}_a\nabla_1^{-(1-\alpha)(1-\beta),\rho} f(t), \tag{18}$$

$$\left({}_1\nabla_b^{\alpha,\beta,\rho} f\right)(t) = {}_1\nabla_b^{-\beta(1-\alpha),\rho} \cdot \ominus\Delta_1^{\rho} \cdot {}_1\nabla_b^{-(1-\alpha)(1-\beta),\rho} f(t). \tag{19}$$

Remark 3. *It is worth noting that:*

(i) For the special value of β, (14) coincides with the generalized Riemann–Liouville and Caputo type proportional fractional difference, respectively (see Definitions 5 and 6 with $n = 1$)

$$\begin{cases} \left({}_a\nabla_h^{\alpha,\beta,\rho} f\right)(t) = \nabla_h^{\rho} \cdot {}_a\nabla_h^{-(1-\alpha),\rho} f(t) = \left({}_a\nabla_h^{\alpha,\rho} f\right)(t), & \beta = 0, \\ {}_a\nabla_h^{-(1-\alpha),\rho} \cdot \nabla_h^{\rho} f(t) = \left({}_a^{C}\nabla_h^{\alpha,\rho} f\right)(t), & \beta = 1. \end{cases}$$

In addition, when $\beta = 0$, $\rho = 1$, we recover the h-Riemann–Liouville fractional difference (see Definition 2), and when $\beta = 1$, $\rho = 1$, we get the h-Caputo fractional difference (see Definition 3)

$$\begin{cases} \left({}_a\nabla_h^{\alpha,\beta,\rho} f\right)(t) = \nabla_h^{\rho} \cdot {}_a\nabla_h^{-(1-\alpha),\rho} f(t) = \left({}_a\nabla_h^{\alpha} f\right)(t), & \beta = 0,\ \rho = 1, \\ {}_a\nabla_h^{-(1-\alpha),\rho} \cdot \nabla_h^{\rho} f(t) = \left({}_a^{C}\nabla_h^{\alpha} f\right)(t), & \beta = 1,\ \rho = 1. \end{cases}$$

The corresponding results for the right case ${}_h\nabla_b^{\alpha,\beta,\rho}$ are similar.

(ii) Clearly,

$$\lim_{\alpha\to 0}\left({}_a\nabla_h^{\alpha,\beta,\rho} f\right)(t) = f(t),\ \lim_{\alpha\to 1}\left({}_a\nabla_h^{\alpha,\beta,\rho} f\right)(t) = \left(\nabla_h^{\rho} f\right)(t),$$
$$\lim_{\alpha\to 0}\left({}_h\nabla_b^{\alpha,\beta,\rho} f\right)(t) = f(t),\ \lim_{\alpha\to 1}\left({}_h\nabla_b^{\alpha,\beta,\rho} f\right)(t) = \left(\ominus\Delta_h^{\rho} f\right)(t).$$

Here are some properties for the left Hilfer generalized proportional fractional difference operator.

Theorem 2 (Composition Rule)**.** *Assume $0 < \alpha < 1$, $0 \le \beta \le 1$, $\rho \in (0, 1]$ and f is defined on $\mathbb{N}_{a+h,h}$. Let $\gamma = \alpha + \beta - \alpha\beta$. Then we obtain*

(i) $\left({}_a\nabla_h^{\alpha,\beta,\rho} f\right)(t) = {}_a\nabla_h^{-\beta(1-\alpha),\rho}\left({}_a\nabla_h^{\gamma,\rho} f\right)(t)$.

(ii) ${}_a\nabla_h^{-\alpha,\rho}\left({}_a\nabla_h^{\alpha,\beta,\rho} f\right)(t) = {}_a\nabla_h^{-\gamma,\rho}\left({}_a\nabla_h^{\gamma,\rho} f\right)(t)$.

(iii) ${}_a\nabla_h^{\alpha,\beta,\rho}\left({}_a\nabla_h^{-\alpha,\rho} f\right)(t) = {}_a\nabla_h^{-\beta(1-\alpha),\rho}\left({}_a\nabla_h^{\beta(1-\alpha),\rho} f\right)(t)$.

(iv) ${}_a\nabla_h^{\alpha,\beta,\rho}\left({}_a\nabla_h^{-\alpha,\rho} f\right)(t) = f(t) - {}_h\hat{e}_p(t,a)\left(\frac{1}{\rho-(\rho-1)h}\right)^{\beta-\alpha\beta-1}\frac{(t-a)_h^{\overline{\beta-\alpha\beta-1}}}{\Gamma(\beta-\alpha\beta)}$ $\left({}_a\nabla_h^{-(1-\beta+\alpha\beta),\rho} f\right)(a)$.

Proof. According to (16), we have

$$\begin{aligned}\left({}_a\nabla_h^{\alpha,\beta,\rho} f\right)(t) &= {}_a\nabla_h^{-\beta(1-\alpha),\rho} \cdot \nabla_h^{\rho} \cdot {}_a\nabla_h^{-(1-\alpha)(1-\beta),\rho} f(t) \\ &= {}_a\nabla_h^{-\beta(1-\alpha),\rho}\left({}_a\nabla_h^{\gamma,\rho} f\right)(t).\end{aligned}$$

The proof of (i) is completed.

Using (iii) of Theorem 1 and Definition 5, we have

$$\begin{aligned}
{}_a\nabla_h^{-\alpha,\rho}\Big({}_a\nabla_h^{\alpha,\beta,\rho}f\Big)(t) &= {}_a\nabla_h^{-\alpha,\rho}\Big({}_a\nabla_h^{-\beta(1-\alpha),\rho}\cdot\nabla_h^{\rho}\cdot\ {}_a\nabla_h^{-(1-\alpha)(1-\beta),\rho}\Big)f(t)\\
&= {}_a\nabla_h^{-\alpha-\beta+\alpha\beta,\rho}\cdot\nabla_h^{\rho}\Big({}_a\nabla_h^{-(1-\alpha)(1-\beta),\rho}f\Big)(t)\\
&= {}_a\nabla_h^{-\gamma,\rho}\cdot\nabla_h^{\rho}\Big({}_a\nabla_h^{-1+\gamma,\rho}f\Big)(t)\\
&= {}_a\nabla_h^{-\gamma,\rho}\Big({}_a\nabla_h^{\gamma,\rho}f\Big)(t).
\end{aligned}$$

The proof of (ii) is completed.
We use Theorem 1 (iii) and Definition 5 to prove (iii). Consider

$$\begin{aligned}
{}_a\nabla_h^{\alpha,\beta,\rho}\Big({}_a\nabla_h^{-\alpha,\rho}f\Big)(t) &= {}_a\nabla_h^{-\beta(1-\alpha),\rho}\cdot\nabla_h^{\rho}\cdot\ {}_a\nabla_h^{-(1-\beta)(1-\alpha),\rho}\Big({}_a\nabla_h^{-\alpha,\rho}f\Big)(t)\\
&= {}_a\nabla_h^{-\beta(1-\alpha),\rho}\cdot\nabla_h^{\rho}\Big({}_a\nabla_h^{-[1-\beta(1-\alpha)],\rho}f\Big)(t)\\
&= {}_a\nabla_h^{-\beta(1-\alpha),\rho}\Big({}_a\nabla_h^{\beta(1-\alpha),\rho}f\Big)(t).
\end{aligned}$$

The proof of (iii) is completed.
Consider the left-hand side of (iv). Using (iii) and Theorem 1 (iv) with $n=1$, we have

$$\begin{aligned}
&{}_a\nabla_h^{\alpha,\beta,\rho}\Big({}_a\nabla_h^{-\alpha,\rho}f\Big)(t)\\
&= {}_a\nabla_h^{-\beta(1-\alpha),\rho}\Big({}_a\nabla_h^{\beta(1-\alpha),\rho}f\Big)(t)\\
&= f(t) - {}_h\hat{e}_p(t,a)\Big(\frac{\rho}{\rho-(\rho-1)h}\Big)^{\beta-\alpha\beta-1}\frac{(t-a)_h^{\overline{\beta-\alpha\beta-1}}}{\rho^{\beta-\alpha\beta-1}\Gamma(\beta-\alpha\beta)}\Big({}_a\nabla_h^{-(1-\beta+\alpha\beta),\rho}f\Big)(a)\\
&= f(t) - {}_h\hat{e}_p(t,a)\Big(\frac{1}{\rho-(\rho-1)h}\Big)^{\beta-\alpha\beta-1}\frac{(t-a)_h^{\overline{\beta-\alpha\beta-1}}}{\Gamma(\beta-\alpha\beta)}\Big({}_a\nabla_h^{-(1-\beta+\alpha\beta),\rho}f\Big)(a).
\end{aligned}$$

The proof of (iv) is completed. □

(2) Now, we will consider the Q-operator, which is used to demonstrate the results corresponding to Theorem 2 (i)–(iii) for the right case.

The Q-operator is defined as follows: Suppose $a \equiv b \bmod 1$ and $f(t)$ is defined on $\mathbb{N}_a \cap {}_b\mathbb{N}$, then

$$(Qf)(t) = f(a+b-t),$$

which is used to connect the left and right fractional discrete operators.

Lemma 1 ([16]). *Assume $n-1<\alpha<n$ with $n\in\mathbb{N}_1$, $a\equiv b \bmod h$ and function f is defined on $\mathbb{N}_{a+h,h}\cap {}_{b-h,h}\mathbb{N}$. Then we have*

(i) $Q(\nabla_h^{\rho}f)(t) = {}_{\ominus}\Delta_h^{\rho}(Qf)(t)$.
(ii) $Q({}_a\nabla_h^{-\alpha,\rho}f)(t) = {}_h\nabla_b^{-\alpha,\rho}(Qf)(t)$.
(iii) $Q({}_a\nabla_h^{\alpha,\rho}f)(t) = {}_h\nabla_b^{\alpha,\rho}(Qf)(t)$.

Theorem 3. *Let $n-1<\alpha<n$ with $n\in\mathbb{N}_1$, $0\le\beta\le 1$, $\rho\in(0,1]$ and $a\equiv b \bmod h$. Suppose f is defined on $\mathbb{N}_{a+h,h}\cap {}_{b-h,h}\mathbb{N}$. Then,*

$$Q({}_a\nabla_h^{\alpha,\beta,\rho}f)(t) = {}_h\nabla_b^{\alpha,\beta,\rho}(Qf)(t). \tag{20}$$

Proof. With the help of Lemma 1, we arrive at

$$\begin{aligned} Q({}_a\nabla_h^{\alpha,\beta,\rho} f)(t) &= Q({}_a\nabla_h^{-\beta(n-\alpha),\rho} \cdot \nabla_h^{\rho} \cdot {}_a\nabla_h^{-(n-\alpha)(1-\beta),\rho} f)(t) \\ &= {}_h\nabla_b^{-\beta(n-\alpha),\rho} Q(\nabla_h^{\rho} \cdot {}_a\nabla_h^{-(n-\alpha)(1-\beta),\rho} f)(t) \\ &= \left({}_h\nabla_b^{-\beta(n-\alpha),\rho} \cdot \ominus\Delta_h^{\rho}\right) Q({}_a\nabla_h^{-(n-\alpha)(1-\beta),\rho} f)(t) \\ &= \left({}_h\nabla_b^{-\beta(n-\alpha),\rho} \cdot \ominus\Delta_h^{\rho} \cdot {}_h\nabla_b^{-(n-\alpha)(1-\beta),\rho}\right)(Qf)(t) = {}_h\nabla_b^{\alpha,\beta,\rho}(Qf)(t). \end{aligned}$$

The proof is completed. □

Theorem 4. *Assume* $0 < \alpha < 1$, $0 \le \beta \le 1$, $\rho \in (0, 1]$ *and* $a \equiv b \bmod h$. *Let* f *be defined on* $\mathbb{N}_{a+h,h} \cap {}_{b-h,h}\mathbb{N}$ *and* $\gamma = \alpha + \beta - \alpha\beta$. *Then we obtain*

(i) $\left({}_h\nabla_b^{\alpha,\beta,\rho} f\right)(t) = {}_h\nabla_b^{-\beta(1-\alpha),\rho}\left({}_h\nabla_b^{\gamma,\rho} f\right)(t)$.

(ii) ${}_h\nabla_b^{\alpha,\beta,\rho}\left({}_h\nabla_b^{-\alpha,\rho} f\right)(t) = {}_h\nabla_b^{-\beta(1-\alpha),\rho}\left({}_h\nabla_b^{\beta(1-\alpha),\rho} f\right)(t)$.

(iii) ${}_h\nabla_b^{-\alpha,\rho}\left({}_h\nabla_b^{\alpha,\beta,\rho} f\right)(t) = {}_h\nabla_b^{-\gamma,\rho}\left({}_h\nabla_b^{\gamma,\rho} f\right)(t)$.

Proof. Let $t \in \mathbb{N}_{a+h,h} \cap {}_{b-h,h}$. Then $a + b - t \in \mathbb{N}_{a+h,h} \cap {}_{b-h,h}$. If we apply Q-operator to equations of Theorem 2 (i)–(iii), then we can get the following identities

$$\begin{aligned} &{}_h\nabla_b^{\alpha,\beta,\rho}(Qf)(t) = {}_h\nabla_b^{-\beta(1-\alpha),\rho} \cdot {}_h\nabla_b^{\gamma,\rho}(Qf)(t), \\ &{}_h\nabla_b^{\alpha,\beta,\rho} \cdot {}_h\nabla_b^{-\alpha,\rho}(Qf)(t) = {}_h\nabla_b^{-\beta(1-\alpha),\rho} \cdot {}_h\nabla_b^{\beta(1-\alpha),\rho}(Qf)(t), \\ &{}_h\nabla_b^{-\alpha,\rho} \cdot {}_h\nabla_b^{\alpha,\beta,\rho}(Qf)(t) = {}_h\nabla_b^{-\gamma,\rho} \cdot {}_h\nabla_b^{\gamma,\rho}(Qf)(t), \end{aligned}$$

which are equal to the desired equations. Thus we complete the proof. □

(3) We review two types of the discrete Laplace transform to obtain the h-Laplace transform for ${}_a\nabla_h^{\alpha,\beta,\rho}$.

Definition 8 ([19]). *Assume* $f : \mathbb{N}_a \to \mathbb{R}$ *and* $s \in \mathbb{C} \setminus \{1\}$, *then the Laplace transform of* f *is defined by*

$$F(s) = \mathcal{N}_a\{f(t)\}(s) = \sum_{t=1}^{\infty}(1-s)^{t-1} f(t+a) = \sum_{t=a+1}^{\infty}(1-s)^{t-a-1} f(t). \tag{21}$$

Definition 9 ([16]). *Assume* $f : \mathbb{N}_{a,h} \to \mathbb{R}$, *then the h-Laplace transform of* f *is defined by*

$$F(s) = \mathcal{N}_{a,h}\{f(t)\}(s) = h\sum_{t=\frac{a}{h}+1}^{\infty}(1-hs)^{t-\frac{a}{h}-1} f(ht). \tag{22}$$

Note that (22) *is consistent with* (21) *when* $h = 1$, *and when* $a = 0$, (22) *is reduced to*

$$\mathcal{N}_{0,h}\{f(t)\}(s) = h\sum_{t=1}^{\infty}(1-hs)^{t-1} f(ht).$$

Lemma 2 ([16]). *Let* $\rho \in (0, 1]$, $\alpha \in \mathbb{C}$, $Re(\alpha) > 0$, *and* $n = [Re(\alpha)] + 1$. *Then the h-discrete Laplace transforms for fractional proportional difference and sum are given by*

$$\mathcal{N}_{a,h}\left\{\left({}_a\nabla_h^{\alpha,\rho} f\right)(t)\right\}(s) = \left(\frac{\rho}{\rho-(\rho-1)h}\right)^{n-\alpha-1}\frac{\mathcal{N}_{a,h}\{f(t)\}(s)}{(\rho s+1-\rho)^{-\alpha}},$$

and

$$\mathcal{N}_{a,h}\Big\{\Big({}_a\nabla_h^{-\alpha,\rho}f\Big)(t)\Big\}(s)=\left(\frac{\rho}{\rho-(\rho-1)h}\right)^{\alpha-1}\frac{\mathcal{N}_{a,h}\{f(t)\}(s)}{(\rho s+1-\rho)^{\alpha}}.$$

After carefully checking, it is worth noting that there is a typing mistake in [16], Remark 3.2: $\left(\frac{\rho}{\rho-(\rho-1)h}\right)^{h(\alpha-1)}$*, which should be* $\left(\frac{\rho}{\rho-(\rho-1)h}\right)^{\alpha-1}$*. By calculating, we find that the same problem occurs in [16], Lemma 3.1, Theorems 4.1 and 4.3. We have revised it in Theorem 1 (ii) and Lemma 2.*

Theorem 5 (The h-Laplace transform for ${}_a\nabla_h^{\alpha,\beta,\rho}$)**.** *Assume* $0<\alpha<1$, $0\le\beta\le1$, $\rho\in(0,1]$, *and let* $f:\mathbb{N}_{a+h,h}\to\mathbb{R}$. *Then, we have the h-Laplace transform for the Hilfer generalized proportional fractional difference operator given as*

$$\mathcal{N}_{a,h}\Big\{\Big({}_a\nabla_h^{\alpha,\beta,\rho}f\Big)(t)\Big\}(s)=\left(\frac{\rho}{\rho-(\rho-1)h}\right)^{-\alpha-1}(\rho s+1-\rho)^{\alpha}\mathcal{N}_{a,h}\{f(t)\}(s).\tag{23}$$

Proof. Set $\gamma=\alpha+\beta-\alpha\beta$, then $0<\gamma<1$. Using Lemma 2, we obtain

$$\begin{aligned}\mathcal{N}_{a,h}\Big\{\Big({}_a\nabla_h^{\alpha,\beta,\rho}f\Big)(t)\Big\}(s)=&\mathcal{N}_{a,h}\Big\{{}_a\nabla_h^{-\beta(1-\alpha),\rho}\Big({}_a\nabla_h^{\gamma,\rho}f\Big)(t)\Big\}(s)\\=&\left(\frac{\rho}{\rho-(\rho-1)h}\right)^{\beta(1-\alpha)-1}\frac{\mathcal{N}_{a,h}\Big\{\Big({}_a\nabla_h^{\gamma,\rho}f\Big)(t)\Big\}(s)}{(\rho s+1-\rho)^{\beta(1-\alpha)}}\\=&\left(\frac{\rho}{\rho-(\rho-1)h}\right)^{\beta(1-\alpha)-1-\gamma}\cdot(\rho s+1-\rho)^{\gamma-\beta(1-\alpha)}\mathcal{N}_{a,h}\{f(t)\}(s)\\=&\left(\frac{\rho}{\rho-(\rho-1)h}\right)^{-\alpha-1}(\rho s+1-\rho)^{\alpha}\mathcal{N}_{a,h}\{f(t)\}(s).\end{aligned}$$

Thus, we complete the proof. □

3.2. The Initial Value Problem for the New Fractional Difference

Here, we give a general solution of an initial value problem for the new fractional difference.

According to the generalized proportional fractional sum given in Definition 4, we have the following identity

$${}_a\nabla_h^{-(1-\gamma),\rho}y(t)|_{t=a+h}=\frac{h^{1-\gamma}}{(\rho-(\rho-1)h)^{1-\gamma}}y(a+h).$$

Hence, consider the following initial value problem for a nonlinear fractional difference equation,

$$\begin{cases}{}_a\nabla_h^{\alpha,\beta,\rho}y(t)=f(t,y(t)), & t\in\mathbb{N}_{a+2h,h},\ (24)\\ {}_a\nabla_h^{-(1-\gamma),\rho}y(t)|_{t=a+h}=\dfrac{h^{1-\gamma}}{(\rho-(\rho-1)h)^{1-\gamma}}y(a+h)\triangleq m, & (25)\end{cases}$$

where $0<\alpha<1$, $0\le\beta\le1$, $0<\rho\le1$, $\gamma=\alpha+\beta-\alpha\beta$, and m is a constant.

Theorem 6. *Let* $f:\mathbb{N}_{a+h,h}\to\mathbb{R}$ *be given and* $\alpha\in(0,1)$, $\beta\in[0,1]$, $\rho\in(0,1]$, $\gamma=\alpha+\beta-\alpha\beta$. *Then the initial value problem* (24) *and* (25) *has a general solution*

$$\begin{aligned}y(t)=&\,{}_{a+h}\nabla_h^{-\gamma,\rho}\cdot{}_a\nabla_h^{\beta(1-\alpha),\rho}f(t,y(t))+\frac{(t-a-h)_h^{\overline{\gamma-1}}}{\rho^{\gamma-1}\Gamma(\gamma)}\,{}_h\hat{e}_p(t,a+h)\eta(h,\rho,\gamma)m\\&+\frac{h^{2-\gamma}(\gamma-1)(t-a)_h^{\overline{\gamma-2}}}{\Gamma(\gamma)}\,{}_h\hat{e}_p(t,a+h)y(a+h),\end{aligned}\tag{26}$$

where $\eta(h,\rho,\gamma)=\left(\frac{\rho}{\rho-(\rho-1)h}\right)^{\gamma-1}$.

Proof. Applying the operator ${}_a\nabla_h^{\beta(1-\alpha),\rho}$ to the both sides of (24), we have for $t\in\mathbb{N}_{a+2h,h}$,

$$ {}_a\nabla_h^{\beta(1-\alpha),\rho}\cdot\ {}_a\nabla_h^{\alpha,\beta,\rho}y(t)=\ {}_a\nabla_h^{\beta(1-\alpha),\rho}f(t,y(t)). \tag{27}$$

Let $F(t,y(t))=\ {}_a\nabla_h^{\beta(1-\alpha)\rho}f(t,y(t))$. Then using (16), we get

$$ {}_a\nabla_h^{\beta(1-\alpha),\rho}\cdot\ {}_a\nabla_h^{-\beta(1-\alpha),\rho}\cdot\nabla_h^{\rho}\cdot\ {}_a\nabla_h^{-(1-\alpha)(1-\beta),\rho}y(t)=F(t,y(t)). \tag{28}$$

Besides, with the help of Theorem 1 (i), we have

$$ \nabla_h^{\rho}\cdot\ {}_a\nabla_h^{-(1-\gamma),\rho}y(t)=F(t,y(t)). \tag{29}$$

where $0<1-\gamma<1$.

From the definition of the generalized proportional fraction sum given as (8), we get

$$\begin{aligned}\left({}_a\nabla_h^{-(1-\gamma),\rho}y\right)(t)&=\frac{h}{\rho^{1-\gamma}\Gamma(1-\gamma)}\sum_{k=\frac{a}{h}+1}^{\frac{t}{h}}{}_h\hat{e}_p(t-kh+(1-\gamma)h,0)\overline{(t-\rho_h(kh))_h^{-\gamma}}y(kh)\\&=\frac{h}{\rho^{1-\gamma}\Gamma(1-\gamma)}\sum_{k=\frac{a+h}{h}+1}^{\frac{t}{h}}{}_h\hat{e}_p(t-kh+(1-\gamma)h,0)\overline{(t-\rho_h(kh))_h^{-\gamma}}y(kh)\\&\quad+\frac{h\cdot\overline{(t-\rho_h(a+h))_h^{-\gamma}}}{\rho^{1-\gamma}\Gamma(1-\gamma)}\ {}_h\hat{e}_p(t-a-h+(1-\gamma)h,0)y(a+h)\\&=\left({}_{a+h}\nabla_h^{-(1-\gamma),\rho}y\right)(t)\\&\quad+\frac{h\cdot\overline{(t-a)_h^{-\gamma}}}{\rho^{1-\gamma}\Gamma(1-\gamma)}\ {}_h\hat{e}_p(t-a-h+(1-\gamma)h,0)y(a+h),\end{aligned} \tag{30}$$

where the properties for ${}_h\hat{e}_p(\cdot,\cdot)$ are in Remark 1. Then, applying both sides of (29) by the operator ${}_{a+h}\nabla_h^{-\gamma,\rho}$, we obtain

$$\begin{aligned}{}_{a+h}\nabla_h^{-\gamma,\rho}\cdot\nabla_h^{\rho}&\left\{{}_{a+h}\nabla_h^{-(1-\gamma),\rho}y(t)+\frac{h\cdot\overline{(t-a)_h^{-\gamma}}}{\rho^{1-\gamma}\Gamma(1-\gamma)}\ {}_h\hat{e}_p(t-a-h+(1-\gamma)h,0)y(a+h)\right\}\\&=G(t,y(t)),\end{aligned} \tag{31}$$

with $G(t,y(t))=\ {}_{a+h}\nabla_h^{-\gamma,\rho}F(t,y(t))$. That is

$$\begin{aligned}&{}_{a+h}\nabla_h^{-\gamma,\rho}\cdot\nabla_h^{\rho}\cdot\ {}_{a+h}\nabla_h^{-(1-\gamma),\rho}y(t)\\&+\ {}_{a+h}\nabla_h^{-\gamma,\rho}\cdot\nabla_h^{\rho}\left\{\frac{h\cdot\overline{(t-a)_h^{-\gamma}}}{\rho^{1-\gamma}\Gamma(1-\gamma)}\ {}_h\hat{e}_p(t-a-h+(1-\gamma)h,0)y(a+h)\right\}\\&=G(t,y(t)).\end{aligned} \tag{32}$$

For the convenience of calculations, we rewrite the above equation as

$$I+J=G(t,y(t)),$$

where

$$I = {}_{a+h}\nabla_h^{-\gamma,\rho} \cdot \nabla_h^{\rho} \cdot {}_{a+h}\nabla_h^{-(1-\gamma),\rho} y(t),$$
$$J = {}_{a+h}\nabla_h^{-\gamma,\rho} \cdot \nabla_h^{\rho} \left\{ \frac{h \cdot (t-a)_h^{\overline{-\gamma}}}{\rho^{1-\gamma}\Gamma(1-\gamma)} \, {}_h\hat{e}_p(t-a-h+(1-\gamma)h, 0) y(a+h) \right\}.$$

In the following, we come to deal with the above two terms one by one.
First, we consider I. It follows from (30) and the fact $(h)_h^{\overline{-\gamma}} = h^{-\gamma}\Gamma(1-\gamma)$ that

$$\begin{aligned} &\left({}_{a+h}\nabla_h^{-(1-\gamma),\rho} y\right)(t)|_{t=a+h} \\ &= \left({}_a\nabla_h^{-(1-\gamma),\rho} y(t) - \frac{h \cdot (t-a)_h^{\overline{-\gamma}}}{\rho^{1-\gamma}\Gamma(1-\gamma)} \, {}_h\hat{e}_p(t-a-h+(1-\gamma)h, 0) y(a+h) \right)_{t=a+h} \\ &= m - \frac{h^{1-\gamma}}{\rho^{1-\gamma}} \, {}_h\hat{e}_p((1-\gamma)h, 0) y(a+h). \end{aligned} \tag{33}$$

In addition, from $\lim_{\alpha \to 0} ({}_a\nabla_h^{\alpha,\rho} f)(t) = f(t)$ (see Remark 2) and Definition 5, we have

$$\nabla_h^{\rho} \, {}_{a+h}\nabla_h^{-1,\rho} y(t) = \lim_{\alpha \to 1^-} \nabla_h^{\rho} \, {}_{a+h}\nabla_h^{-\alpha,\rho} y(t) = \lim_{\alpha \to 1^-} {}_{a+h}\nabla_h^{1-\alpha,\rho} y(t) = y(t).$$

Therefore, with the help of Theorem 1 (ii)–(iii), we get

$$\begin{aligned} I = \; & {}_{a+h}\nabla_h^{-\gamma,\rho} \cdot \nabla_h^{\rho} \left({}_{a+h}\nabla_h^{-(1-\gamma),\rho} y \right)(t) \\ = \; & \nabla_h^{\rho} \cdot {}_{a+h}\nabla_h^{-\gamma,\rho} \left({}_{a+h}\nabla_h^{-(1-\gamma),\rho} y \right)(t) \\ & - \tfrac{(t-a-h)_h^{\overline{\gamma-1}}}{\rho^{\gamma-1}\Gamma(\gamma)} \, {}_h\hat{e}_p(t, a+h) \left(\tfrac{\rho}{\rho-(\rho-1)h} \right)^{\gamma-1} \left\{ \left({}_{a+h}\nabla_h^{-(1-\gamma),\rho} y \right)(t)|_{t=a+h} \right\} \\ = \; & \nabla_h^{\rho} \cdot {}_{a+h}\nabla_h^{-1,\rho} y(t) - \tfrac{(t-a-h)_h^{\overline{\gamma-1}}}{\rho^{\gamma-1}\Gamma(\gamma)} \, {}_h\hat{e}_p(t-a-h, 0) \eta(h, \rho, \gamma) \\ & \cdot \left(m - \tfrac{h^{1-\gamma}}{\rho^{1-\gamma}} \, {}_h\hat{e}_p((1-\gamma)h, 0) y(a+h) \right) \\ = \; & y(t) - \tfrac{(t-a-h)_h^{\overline{\gamma-1}}}{\rho^{\gamma-1}\Gamma(\gamma)} \, {}_h\hat{e}_p(t-a-h, 0) \eta(h, \rho, \gamma) \left(m - \tfrac{h^{1-\gamma}}{\rho^{1-\gamma}} \, {}_h\hat{e}_p((1-\gamma)h, 0) y(a+h) \right). \end{aligned} \tag{34}$$

Using the fact that

$${}_h\hat{e}_p(t-a-h, 0) \cdot {}_h\hat{e}_p((1-\gamma)h, 0) = {}_h\hat{e}_p(t-a-\gamma h, 0),$$

where we use the definition of the exponential function, then

$$\begin{aligned} I = y(t) & - \frac{(t-a-h)_h^{\overline{\gamma-1}}}{\rho^{\gamma-1}\Gamma(\gamma)} \, {}_h\hat{e}_p(t-a-h, 0) \eta(h, \rho, \gamma) m \\ & + \frac{h^{1-\gamma}(t-a-h)_h^{\overline{\gamma-1}}}{\Gamma(\gamma)} \, {}_h\hat{e}_p(t-a-\gamma h, 0) \eta(h, \rho, \gamma) y(a+h). \end{aligned} \tag{35}$$

Define the last term of the above equation as

$$\Psi(t, h, \rho, \gamma) = \frac{h^{1-\gamma}(t-a-h)_h^{\overline{\gamma-1}}}{\Gamma(\gamma)} \, {}_h\hat{e}_p(t-a-\gamma h, 0) \eta(h, \rho, \gamma) y(a+h),$$

hence, (35) becomes

$$I = y(t) - \frac{(t-a-h)_h^{\overline{\gamma-1}}}{\rho^{\gamma-1}\Gamma(\gamma)} \, {}_h\hat{e}_p(t-a-h, 0) \eta(h, \rho, \gamma) m + \Psi(t, h, \rho, \gamma). \tag{36}$$

Now, consider the second term J in (32). Define

$$\Phi(t,h,\rho,\gamma) = \nabla_h^{\rho} \cdot {}_{a+h}\nabla_h^{-\gamma,\rho}\left\{\frac{h\cdot(t-a)_h^{\overline{-\gamma}}}{\rho^{1-\gamma}\Gamma(1-\gamma)}\,{}_h\hat{e}_p(t-a-h+(1-\gamma)h,0)y(a+h)\right\}.$$

Then, using Theorem 1 (ii) and Remark 1, we get

$$\begin{aligned}
J &= {}_{a+h}\nabla_h^{-\gamma,\rho}\cdot\nabla_h^{\rho}\left\{\frac{h\cdot(t-a)_h^{\overline{-\gamma}}}{\rho^{1-\gamma}\Gamma(1-\gamma)}\,{}_h\hat{e}_p(t-a-h+(1-\gamma)h,0)y(a+h)\right\}\\
&= \nabla_h^{\rho}\cdot{}_{a+h}\nabla_h^{-\gamma,\rho}\left\{\frac{h\cdot(t-a)_h^{\overline{-\gamma}}}{\rho^{1-\gamma}\Gamma(1-\gamma)}\,{}_h\hat{e}_p(t-a-h+(1-\gamma)h,0)y(a+h)\right\}\\
&\quad-\frac{(t-a-h)_h^{\overline{\gamma-1}}}{\rho^{\gamma-1}\Gamma(\gamma)}\,{}_h\hat{e}_p(t-a-h,0)\eta(h,\rho,\gamma)\left(\frac{h\cdot(h)_h^{\overline{-\gamma}}}{\rho^{1-\gamma}\Gamma(1-\gamma)}\,{}_h\hat{e}_p((1-\gamma)h,0)y(a+h)\right) \qquad (37)\\
&= \Phi(t,h,\rho,\gamma)-\frac{h^{1-\gamma}(t-a-h)_h^{\overline{\gamma-1}}}{\Gamma(\gamma)}\,{}_h\hat{e}_p(t-a-\gamma h,0)\eta(h,\rho,\gamma)y(a+h)\\
&= \Phi(t,h,\rho,\gamma)-\Psi(t,h,\rho,\gamma).
\end{aligned}$$

Similar to (30), we have

$$\begin{aligned}
&{}_{a+h}\nabla_h^{-\gamma,\rho}\left\{\frac{h\cdot(t-a)_h^{\overline{-\gamma}}}{\rho^{1-\gamma}\Gamma(1-\gamma)}\,{}_h\hat{e}_p(t-a-h+(1-\gamma)h,0)y(a+h)\right\}\\
&= {}_a\nabla_h^{-\gamma,\rho}\left\{\frac{h\cdot(t-a)_h^{\overline{-\gamma}}}{\rho^{1-\gamma}\Gamma(1-\gamma)}\,{}_h\hat{e}_p(t-a-h+(1-\gamma)h,0)y(a+h)\right\}\\
&\quad-\frac{h\cdot(t-a)_h^{\overline{\gamma-1}}}{\rho^{\gamma}\Gamma(\gamma)}\,{}_h\hat{e}_p(t-a-h+\gamma h,0)\left(\frac{h\cdot(h)_h^{\overline{-\gamma}}}{\rho^{1-\gamma}\Gamma(1-\gamma)}\,{}_h\hat{e}_p((1-\gamma)h,0)y(a+h)\right) \qquad (38)\\
&= {}_a\nabla_h^{-\gamma,\rho}\left\{\frac{h\cdot(t-a)_h^{\overline{-\gamma}}}{\rho^{1-\gamma}\Gamma(1-\gamma)}\,{}_h\hat{e}_p(t-a-h+(1-\gamma)h,0)y(a+h)\right\}\\
&\quad-\frac{h^{2-\gamma}}{\rho\Gamma(\gamma)}(t-a)_h^{\overline{\gamma-1}}\,{}_h\hat{e}_p(t-a,0)y(a+h).
\end{aligned}$$

Using Remark 1 and $\nabla_h(t-a)_h^{\overline{\gamma-1}} = (\gamma-1)(t-a)_h^{\overline{\gamma-2}}N$, it follows that

$$\begin{aligned}
\Phi(t,h,\rho,\gamma) &= \nabla_h^{\rho}\cdot{}_a\nabla_h^{-\gamma,\rho}\left\{\frac{h\cdot(t-a)_h^{\overline{-\gamma}}}{\rho^{1-\gamma}\Gamma(1-\gamma)}\,{}_h\hat{e}_p(t-a-h+(1-\gamma)h,0)y(a+h)\right\}\\
&\quad-\nabla_h^{\rho}\left(\frac{h^{2-\gamma}}{\rho\Gamma(\gamma)}(t-a)_h^{\overline{\gamma-1}}\,{}_h\hat{e}_p(t-a,0)y(a+h)\right)\\
&= \frac{h}{\rho^{1-\gamma}\Gamma(1-\gamma)}\,{}_h\hat{e}_p(-a-h+(1-\gamma)h,0)y(a+h)\\
&\quad\cdot\nabla_h^{\rho}\cdot{}_a\nabla_h^{-\gamma,\rho}\left\{{}_h\hat{e}_p(t,0)(t-a)_h^{\overline{-\gamma}}\right\} \qquad (39)\\
&\quad-\frac{h^{2-\gamma}}{\rho\Gamma(\gamma)}\,{}_h\hat{e}_p(-a,0)y(a+h)\cdot\nabla_h^{\rho}\left\{{}_h\hat{e}_p(t,0)(t-a)_h^{\overline{\gamma-1}}\right\}\\
&= \frac{h}{\rho}y(a+h)\cdot\nabla_h^{\rho}\,{}_h\hat{e}_p(t-a,0)-\frac{h^{2-\gamma}}{\Gamma(\gamma)}\,{}_h\hat{e}_p(t-a-h,0)y(a+h)\cdot\nabla_h(t-a)_h^{\overline{\gamma-1}}\\
&= -\frac{h^{2-\gamma}(\gamma-1)(t-a)_h^{\overline{\gamma-2}}}{\Gamma(\gamma)}\,{}_h\hat{e}_p(t-a-h,0)y(a+h).
\end{aligned}$$

Thus,

$$J = -\frac{h^{2-\gamma}(\gamma-1)(t-a)_h^{\overline{\gamma-2}}}{\Gamma(\gamma)}\, {}_h\hat{e}_p(t-a-h,0)y(a+h) - \Psi(t,h,\rho,\gamma). \tag{40}$$

Finally, substituting (36) and (40) back in (32) and arranging, we can obtain the general solution representation

$$\begin{aligned} y(t) = G(t,y(t)) &+ \frac{(t-a-h)_h^{\overline{\gamma-1}}}{\rho^{\gamma-1}\Gamma(\gamma)}\, {}_h\hat{e}_p(t-a-h,0)\eta(h,\rho,\gamma)m - \Psi(t,h,\rho,\gamma) \\ &+ \frac{h^{2-\gamma}(\gamma-1)(t-a)_h^{\overline{\gamma-2}}}{\Gamma(\gamma)}\, {}_h\hat{e}_p(t-a-h,0)y(a+h) + \Psi(t,h,\rho,\gamma). \end{aligned} \tag{41}$$

That is,

$$\begin{aligned} y(t) = {}_{a+h}\nabla_h^{-\gamma,\rho} \cdot {}_a\nabla_h^{\beta(1-\alpha),\rho} f(t,y(t)) &+ \frac{(t-a-h)_h^{\overline{\gamma-1}}}{\rho^{\gamma-1}\Gamma(\gamma)}\, {}_h\hat{e}_p(t,a+h)\eta(h,\rho,\gamma)m \\ &+ \frac{h^{2-\gamma}(\gamma-1)(t-a)_h^{\overline{\gamma-2}}}{\Gamma(\gamma)}\, {}_h\hat{e}_p(t,a+h)y(a+h). \end{aligned} \tag{42}$$

The proof of Theorem 6 is complete. □

Example 1. *For a given function $g(t) : \mathbb{N}_{a+2h,h} \to \mathbb{R}$ and a constant $\lambda \neq 0$, we give two examples to illustrate Theorem 6.*

(i) Consider the initial value problem

$$\begin{cases} {}_a\nabla_h^{\alpha,\beta,\rho} y(t) = g(t), & t \in \mathbb{N}_{a+2h,h}, \\ {}_a\nabla_h^{-(1-\gamma),\rho} y(t)|_{t=a+h} \triangleq m. \end{cases} \tag{43}$$

Then we deduce from Theorem 6 that the general solution of the above initial value problem is given by

$$\begin{aligned} y(t) = {}_{a+h}\nabla_h^{-\gamma,\rho} \cdot {}_a\nabla_h^{\beta(1-\alpha),\rho} g(t) &+ \frac{(t-a-h)_h^{\overline{\gamma-1}}}{\rho^{\gamma-1}\Gamma(\gamma)}\, {}_h\hat{e}_p(t,a+h)\eta(h,\rho,\gamma)m \\ &+ \frac{h^{2-\gamma}(\gamma-1)(t-a)_h^{\overline{\gamma-2}}}{\Gamma(\gamma)}\, {}_h\hat{e}_p(t,a+h)y(a+h). \end{aligned} \tag{44}$$

(ii) Consider the initial value problem

$$\begin{cases} {}_a\nabla_h^{\alpha,\beta,\rho} y(t) = \lambda y(t), & t \in \mathbb{N}_{a+2h,h}, \\ {}_a\nabla_h^{-(1-\gamma),\rho} y(t)|_{t=a+h} \triangleq m. \end{cases} \tag{45}$$

From Theorem 6, the general solution is given by

$$\begin{aligned} y(t) = \lambda\, {}_{a+h}\nabla_h^{-\gamma,\rho} \cdot {}_a\nabla_h^{\beta(1-\alpha),\rho} y(t) &+ \frac{(t-a-h)_h^{\overline{\gamma-1}}}{\rho^{\gamma-1}\Gamma(\gamma)}\, {}_h\hat{e}_p(t,a+h)\eta(h,\rho,\gamma)m \\ &+ \frac{h^{2-\gamma}(\gamma-1)(t-a)_h^{\overline{\gamma-2}}}{\Gamma(\gamma)}\, {}_h\hat{e}_p(t,a+h)y(a+h). \end{aligned} \tag{46}$$

With a similar proof to Theorem 6, we obtain the following corollary.

Corollary 1. *Consider the initial value problem*

$$\begin{cases} {}_{a-h}\nabla_h^{\alpha,\beta,\rho} y(t) = f(t, y(t)), & t \in \mathbb{N}_{a+h,h}, \\ {}_{a-h}\nabla_h^{-(1-\gamma),\rho} y(t)|_{t=a} = \frac{h^{1-\gamma}}{(\rho-(\rho-1)h)^{1-\gamma}} y(a) \triangleq c, \end{cases} \tag{47}$$

where $0 < \alpha < 1,\ 0 \le \beta \le 1,\ 0 < \rho \le 1, \gamma = \alpha + \beta - \alpha\beta$ *and* c *is a constant. We can get the general solution representation*

$$\begin{aligned} y(t) = {}_a\nabla_h^{-\gamma,\rho} \cdot {}_{a-h}\nabla_h^{\beta(1-\alpha),\rho} f(t, y(t)) + \frac{(t-a)_h^{\overline{\gamma-1}}}{\rho^{\gamma-1}\Gamma(\gamma)} {}_h\hat{e}_p(t, a)\eta(h, \rho, \gamma)c \\ + \frac{h^{2-\gamma}(\gamma-1)(t-a+h)_h^{\overline{\gamma-2}}}{\Gamma(\gamma)} {}_h\hat{e}_p(t, a)y(a). \end{aligned} \tag{48}$$

where $\eta(h, \rho, \gamma) = \left(\frac{\rho}{\rho-(\rho-1)h}\right)^{\gamma-1}$.

Remark 4. *Corollary 1 is more general compared with corresponding results of the initial value problem with existing difference operators.*

(i) Let $\beta = 0$ *in the initial problem* (47)*. Then the initial value problem*

$$\begin{cases} {}_{a-h}\nabla_h^{\alpha,\rho} y(t) = f(t, y(t)), & t \in \mathbb{N}_{a+h,h}, \\ {}_{a-h}\nabla_h^{-(1-\alpha),\rho} y(t)|_{t=a} = \frac{h^{1-\alpha}}{(\rho-(\rho-1)h)^{1-\alpha}} y(a) \triangleq c, \end{cases} \tag{49}$$

has the following general solution representation

$$\begin{aligned} y(t) = {}_a\nabla_h^{-\alpha,\rho} f(t, y(t)) + \frac{(t-a)_h^{\overline{\alpha-1}}}{\rho^{\alpha-1}\Gamma(\alpha)} {}_h\hat{e}_p(t, a)\eta(h, \rho, \alpha)c \\ + \frac{h^{2-\alpha}(\alpha-1)(t-a+h)_h^{\overline{\alpha-2}}}{\Gamma(\alpha)} {}_h\hat{e}_p(t, a)y(a). \end{aligned} \tag{50}$$

where $0 < \alpha < 1$, $\eta(h, \rho, \alpha) = \left(\frac{\rho}{\rho-(\rho-1)h}\right)^{\alpha-1}$ *and* c *is a constant.*

(ii) Let $\beta = 0,\ \rho = 1$, *and* $h = 1$ *in* (48)*. Then we obtain*

$$y(t) = \frac{(t-a+1)^{\overline{\alpha-1}}}{\Gamma(\alpha)} y(a) + {}_a\nabla^{-\alpha} f(t, y(t)), \tag{51}$$

which is the general solution representation of the following initial value problem [24]

$$\begin{cases} {}_{a-1}\nabla^{\alpha} y(t) = f(t, y(t)), & t \in \mathbb{N}_{a+1}, \\ {}_{a-1}\nabla^{-(1-\alpha)} y(t)|_{t=a} = y(a), \end{cases} \tag{52}$$

where $0 < \alpha < 1$. ${}_{a-1}\nabla^{-(1-\alpha)}(\cdot)$ *and* ${}_{a-1}\nabla^{\alpha}(\cdot)$ *are defined by Definition 1 and 2 for* $h = 1$, *respectively.*

Remark 5. *Here we only discuss the case of the left Hilfer generalized proportional fractional operator. The corresponding results for the right one can be obtained similarly.*

4. Conclusions

In this paper, we proposed the generalized proportional fractional difference in the sense of Hilfer, which is considered to be the analogy of the Hilfer generalized proportional fractional derivative. Also, our definition can reduce to some known operators, such as h-Riemann–Liouville, h-Caputo and generalized proportional fractional differences that

are defined in [16,25,26] respectively. We derived some important properties of the left Hilfer proportional fractional difference. We also employed the Q-operator that enables us to prove properties for the right Hilfer proportional fractional difference based on the left one and considered the h-Laplace transform. Finally, following the newly left difference, we obtained a general solution of an initial value problem for $0 < \alpha < 1$. In the future, high-order case for $\alpha \geq 1$ can be considered. Furthermore, the general solution is one of most important ways to studying the qualitative properties of the solutions of difference equations, such as existence, uniqueness, oscillation, and so on.

Author Contributions: Conceptualization, Q.W. and R.X.; results and proofs, Q.W. and R.X.; formal analysis, Q.W. and R.X.; writing—original manuscript, Q.W. and R.X.; writing—review and editing, Q.W. and R.X. All authors have read and agreed to the published version of the manuscript.

Funding: This research was funded by National Science Foundation of China grant number (11971015).

Institutional Review Board Statement: Not applicable.

Informed Consent Statement: Not applicable.

Data Availability Statement: Not applicable.

Acknowledgments: The authors are very grateful to the anonymous referees for their valuable suggestions and comments, which helped to improve the quality of the paper.

Conflicts of Interest: The authors declare that there is no conflict of interest regarding the publication of this paper.

References

1. Kilbas, A.A.; Marichev, O.I.; Samko, S.G. *Fractional Integrals and Derivatives: Theory and Applications*; Gordon and Breach: Yverdon, Switzerland, 1993.
2. Podlubny, I. Fractional differential equations. *Math. Sci. Eng.* **1999**, *198*, 41–119.
3. De Oliveira, E.C.; Machado, J.A.T. A review of definitions for fractional derivatives and integral. *Math. Probl. Eng.* **2014**, *2014*, 238459. [CrossRef]
4. Teodoro, G.S.; Machado, J.A.T.; De Oliveira, E.C. A review of definitions of fractional derivatives and other operators. *J. Comput. Phys.* **2019**, *388*, 195–208. [CrossRef]
5. Yang, F.; Wang, X. Dynamic characteristic of a new fractional-order chaotic system based on the Hopfield Neural Network and its digital circuit implementation. *Phys. Scr.* **2021**, *96*, 3. [CrossRef]
6. Jajarmi, A.; Baleanu, D.; Sajjadi, S.S.; Nieto, J.J. Analysis and some applications of a regularized Ψ-Hilfer fractional derivative. *J. Comput. Appl. Math.* **2022**, *415*, 114476. [CrossRef]
7. Yusuf, A.; Qureshi, S.; Mustapha, U.T.; Musa, S.S.; Sulaiman, T.A. Fractional modeling for improving scholastic performance of students with optimal control. *Int. J. Appl. Comput. Math.* **2022**, *8*, 1–20. [CrossRef]
8. Jajarmi, A.; Baleanu, D.; Zarghami Vahid, K.; Mobayen, S. A general fractional formulation and tracking control for immunogenic tumor dynamics. *Math. Methods Appl. Sci.* **2022**, *45*, 667–680. [CrossRef]
9. Qiu, L.; Zhang, M.; Qin, Q.H. Homogenization function method for time-fractional inverse heat conduction problem in 3D functionally graded materials. *Appl. Math. Lett.* **2021**, *122*, 107478. [CrossRef]
10. Abro, K.A.; Gomez-Aguilar, J.F. Fractional modeling of fin on non-Fourier heat conduction via modern fractional differential operators. *Arab. J. Sci. Eng.* **2021**, *46*, 2901–2910. [CrossRef]
11. Mozafarifard, M.; Toghraie, D.; Sobhani, H. Numerical study of fast transient non-diffusive heat conduction in a porous medium composed of solid-glass spheres and air using fractional Cattaneo subdiffusion model. *Int. Commun. Heat Mass Transf.* **2021**, *122*, 105192. [CrossRef]
12. Yavtushenko, I.O.; Makhmud-Akhunov, M.Y; Sibatov, R.T.; Kitsyuk, E.P.; Svetukhin, V.V. Temperature-Dependent Fractional Dynamics in Pseudo-Capacitors with Carbon Nanotube Array/Polyaniline Electrodes. *Nanomaterials* **2022**, *12*, 739. [CrossRef] [PubMed]
13. Chapman, S. On non-integral orders of summability of series and integrals. *Proc. Lond. Math. Soc.* **1911**, *2*, 369–409. [CrossRef]
14. Miller, K.S.; Ross, B. Fractional difference calculus. In Proceedings of the International Symposium on Univalent Functions, Fractional Calculus and Their Applications, Koriyama, Japan, May 1988.
15. Bohner, M.; Peterson, A.C. *Advances in Dynamic Equations on Time Scales*; Springer Science and Business Media: Boston, MA, USA, 2002.
16. Abdeljawad, T.; Jarad, F.; Alzabut, J. Fractional proportional differences with memory. *Eur. Phys. J. Spec. Top.* **2017**, *226*, 3333–3354. [CrossRef]
17. Haider, S.S.; Abdeljawad, T. On Hilfer fractional difference operator. *Adv. Differ. Equ.* **2020**, *2020*, 1–20. [CrossRef]

18. Jonnalagadda, J.M.; Gopal, N.S. On Hilfer-type nabla fractional differences. *Int. J. Differ. Equ.* **2020**, *15*, 91–107.
19. Atıcı, F.M.; Eloe, P.W. Discrete fractional calculus with the nabla operator. *Electron. J. Qual. Theory Differ. Equ.* **2009**, *2009*, 1–12. [CrossRef]
20. Hilfer, R. *Applications of Fractional Calculus in Physics*; World Scientific: Singapore, 2000.
21. Jarad, F.; Abdeljawad, T.; Alzabut, J. Generalized fractional derivatives generated by a class of local proportional derivatives. *Eur. Phys. J. Spec. Top.* **2017**, *226*, 3457–3471. [CrossRef]
22. Ahmed, I.; Kumam, P.; Jarad, F.; Borisut, P.; Jirakitpuwapat, W. On Hilfer generalized proportional fractional derivative. *Adv. Differ. Equ.* **2020**, *2020*, 1–18. [CrossRef]
23. Atıcı, F.M.; Eloe, P.W. Gronwall's inequality on discrete fractional calculus. *Comput. Math. Appl.* **2012**, *64*, 3193–3200. [CrossRef]
24. Abdeljawad, T.; Atıcı, F.M. On the definitions of nabla fractional operators. *Abstr. Appl. Anal.* **2012**, *2012*, 1–13. [CrossRef]
25. Jia, B.G.; Du, F.F.; Erbe, L.; Peterson, A. Asymptotic behavior of nabla half order h-difference equations. *J. Appl. Anal. Comput.* **2018**, *8*, 1707–1726.
26. Abdeljawad, T. On delta and nabla Caputo fractional differences and dual identities. *Discret. Dyn. Nat. Soc.* **2013**, *2013*, 406910. [CrossRef]

fractal and fractional

MDPI

Article

Solutions of Initial Value Problems with Non-Singular, Caputo Type and Riemann-Liouville Type, Integro-Differential Operators

Christopher N. Angstmann [1,*], Stuart-James M. Burney [1], Bruce I. Henry [1] and Byron A. Jacobs [2]

[1] School of Mathematics and Statistics, University of New South Wales, Sydney, NSW 2052, Australia
[2] Department of Mathematics and Applied Mathematics, University of Johannesburg, Johannesburg 2092, South Africa
* Correspondence: c.angstmann@unsw.edu.au

Abstract: Motivated by the recent interest in generalized fractional order operators and their applications, we consider some classes of integro-differential initial value problems based on derivatives of the Riemann–Liouville and Caputo form, but with non-singular kernels. We show that, in general, the solutions to these initial value problems possess discontinuities at the origin. We also show how these initial value problems can be re-formulated to provide solutions that are continuous at the origin but this imposes further constraints on the system. Consideration of the intrinsic discontinuities, or constraints, in these initial value problems is important if they are to be employed in mathematical modelling applications.

Keywords: fractional calculus; Caputo derivative; Riemann-Liouville derivative; integro-differential equations

MSC: 26A33; 34A08; 34A12; 45J05

Citation: Angstmann, C.N.; Burney, S.-J.M.; Henry, B.I.; Jacobs, B.A. Solutions of Initial Value Problems with Non-Singular, Caputo Type and Riemann-Liouville Type, Integro-Differential Operators. *Fractal Fract.* **2022**, *6*, 436. https://doi.org/10.3390/fractalfract6080436

Academic Editors: António Lopes, Alireza Alfi, Liping Chen and Sergio Adriani David

Received: 23 July 2022
Accepted: 10 August 2022
Published: 11 August 2022

1. Introduction

In recent years there has been a great deal of interest in generalisations of derivatives defined through operators, involving convolutions, of the form

$$ {}_0\mathcal{D}_t f(t) = \frac{d}{dt}\int_0^t K(t-\tau) f(\tau)\, d\tau \tag{1} $$

and

$$ {}_0^*\mathcal{D}_t f(t) = \int_0^t K(t-\tau) f'(\tau)\, d\tau, \tag{2} $$

where $K(t)$ is a suitably defined kernel, see for example [1] and references therein. If the kernel is given by

$$ K(t) = \frac{t^{-\alpha}}{\Gamma(1-\alpha)}, \quad 0 < \alpha < 1 \tag{3} $$

then Equation (1) defines the Riemann–Liouville fractional derivative of order α and Equation (2) defines the Caputo fractional derivative of order α (see for example [2]). Here, $f'(t) = \frac{df(t)}{dt}$, although we may also consider this to be the distributional derivative of a generalized function below. The kernel in Equation (3) is singular at $t = 0$, viz $\tau = t$ in Equations (1) and (2), so that the integral in these definitions is an improper integral in this case, but it is bounded whenever $f(t)$ is bounded on $[0, t]$, since $K(t)$ is locally integrable on $(0, t)$. Some researchers define

$$ K(t) = \frac{t^{-\alpha}}{\Gamma(1-\alpha)} H(t), \tag{4} $$

where

$$H(t) = \begin{cases} 1 & \text{if} \quad t > 0, \\ 0 & \text{otherwise,} \end{cases} \tag{5}$$

and some also take the lower limit in the integral as 0^+ [3].

There has been a growing interest in defining new operators along the lines of Equations (1) and (2) with $K(t)$ non-singular in $[0, t]$. For example, if

$$K(t) = \frac{1}{1-\alpha} \exp\left(-\frac{\alpha t}{1-\alpha}\right), \quad 0 < \alpha < 1, \tag{6}$$

then Equation (2) defines a Caputo–Fabrizio (CF) operator of order α [4,5]. If

$$K(t) = \frac{1}{1-\alpha} E_\alpha\left(-\frac{\alpha t^\alpha}{1-\alpha}\right), \quad 0 < \alpha < 1, \tag{7}$$

where

$$E_\alpha(z) = \sum_{k=0}^{\infty} \frac{z^k}{\Gamma(\alpha k + 1)} \tag{8}$$

is the Mittag–Leffler function, then Equation (2) defines an Atangana–Baleanu–Caputo (ABC) operator of order α [6]; and Equation (1) defines an Atangana–Baleanu–Riemann (ABR) operator of order α [6]. These operators with non-singular kernels have found widespread use in modelling applications, typically with integer order derivatives replaced with the fractional order operators. The main argument for their introduction has been that it provides a memory affect without possible problems from a singularity at the origin. However, the memory aspect and the fractional calculus aspect of these operators, with these non-singular kernels, has been challenged [7–9].

In modelling applications, there is interest in initial value problems (IVPs) of the form

$${}_0\mathcal{D}_t f(t) = \frac{d}{dt} \int_0^t K(t-\tau) f(\tau)\, d\tau = G(t), \quad f(0) = f_0, \tag{9}$$

and

$${}_0^*\mathcal{D}_t f(t) = \int_0^t K(t-\tau) f'(\tau)\, d\tau = G(t), \quad f(0) = f_0, \tag{10}$$

where $K(t)$ and $G(t)$ are right-continuous for $t \geq 0$ and differentiable for $t > 0$. Here, $K(t)$ and $G(t)$ are expected to be known functions and we solve for $f(t)$, which is specified at $t = 0$. We refer to IVPs of the form Equation (10) as generalized Caputo type IVPs and those of the form Equation (9) as generalized Riemann–Liouville type IVPs.

In recent work, we considered IVPs of the form of Equation (10) with ${}_0^*\mathcal{D}_t$ given by the CF operator, or the ABC operator, and we showed that, in general, these problems have solutions that are discontinuous at $t = 0$ [10]. Here, we have extended this work to show that the problems formulated in Equations (9) and (10), with non-singular kernels, in general, have solutions that are discontinuous at the origin. This includes the case with ${}_0\mathcal{D}_t$ given by the ABR operator. As a corollary, we showed that it is possible to re-formulate these IVPs with non-singular kernels to provide solutions that are continuous for $t \geq 0$, but this introduces additional constraints on the system. Consideration of these results is important for modelling applications that would seek to employ these IVPs.

We note that the IVPs in Equations (9) and (10) can be formulated as Volterra integral equations of the first kind and there has been a series of papers written on the existence of generalized solutions for these problems in cases where continuous solutions cannot be obtained (see, for example, [11,12]). The results that we have provided are related to this work. Note especially that the Volterra integral equation

$$\int_0^t K(t-\tau) F(\tau)\, d\tau = G(t) \tag{11}$$

must have $G(0) = 0$ if $K(t)$ and $F(t)$ are classical functions. However, solutions for $F(t)$ are possible with $G(0) \neq 0$ if $F(t)$ is a generalized function and if the integral is also interpreted in a generalized sense. It is important to include such generalized function solutions in modelling applications with Equation (11) because, while $F(t)$ is defined by Equation (11), $G(t)$ is not, so that $G(0)$ may be non-zero. For a useful reference on generalized functions and distributional derivatives see, for example, [13], and references there-in.

The remainder of this paper is organized as follows. In Section 2, we consider generalized Caputo type IVPs with non-singular kernels, and $K(0) \neq 0$, and we prove that these problems have solutions that are discontinuous at the origin if $G(0) \neq 0$ but continuous at the origin if $G(0) = 0$. In Section 3, we consider generalized Riemann–Liouville type IVPs, with non-singular kernels, and $K(0) \neq 0$, and we prove that these problems have solutions that are discontinuous at the origin if $G(0) \neq f_0 K(0)$ but continuous at the origin if $G(0) = f_0 K(0)$. In this section, we also consider a different generalized Riemann–Liouville type IVP, with non-singular kernels, and $K(0), K'(0) \neq 0$, where the initial value $f(0)$ is replaced by the right-hand limit, $\lim_{t\to 0^+} f(t) = f_0$. The solutions to this problem are discontinuous at the origin if $G(0) \neq K(0) f_0$ but continuous at the origin if $G(0) = K(0) f_0$. However, the form of the solution is very different to that which would be obtained by simply replacing $f(0)$ with f_0 in the generalized Riemann–Liouville type IVP considered earlier. In Section 4, we provide examples that illustrate each of the theorems. We conclude with a Discussion and Summary in Section 5.

Many of our results are framed in terms of Laplace transforms with the following notation: $\hat{y}(s)$ or $\mathcal{L}[y(t)](s)$ is used to denote the Laplace transform of a function $y(t)$ with respect to t, with Laplace transform variable s; $\mathcal{L}^{-1}[\hat{y}(s)](t)$ is used to denote the inverse Laplace transform of a function $\hat{y}(s)$. The Laplace transform

$$\hat{y}(s) = \int_0^\infty e^{-st} y(t)\, dt \tag{12}$$

exists if $y(t)$ is bounded of exponential order, i.e., there exists real valued parameters $\alpha, M, T > 0$ such that

$$e^{-\alpha t}|y(t)| \leq M \quad \forall t > T,$$

and is piecewise continuous with, at most, a finite number of discontinuities. The inverse Laplace transform $F(t) = \mathcal{L}^{-1}\left[\hat{F}(s)\right](t)$ exists if $\lim_{s\to\infty} \hat{F}(s) = 0$, and $\lim_{s\to\infty} s\hat{F}(s)$ is finite.

2. Caputo Type IVPs with Non-Singular Kernels

We begin with a consideration of Caputo type IVPs.

Definition 1. *Suppose that; $K(t)$ and $G(t)$ are real-valued and bounded functions, continuous for $t \geq 0$ and differentiable for $t > 0$; and $f(t)$ is a real-valued differentiable function, or generalized function that is differentiable in a distributional sense. Then a Caputo type IVP (C-IVP) is defined by the integro-differential equation*

$$ {}_0^*\mathcal{D}_t f(t) = \int_0^t K(t-\tau) f'(\tau)\, d\tau = G(t) \tag{13}$$

and the initial value $f(0) = f_0$ with $f_0 \in \mathbb{R}$.

Before considering the construction of the solution to the general IVP, it is enlightening to show the special case where the solution is right-continuous. This lemma will be useful to the proof of the later theorem.

Lemma 1. *The solution of a C-IVP (Definition 1), with $K(0) \neq 0$ and $G(0) = 0$, is given by*

$$f(t) = \mathcal{L}^{-1}\left[\frac{\hat{G}(s)}{s\hat{K}(s)}\right](t) + f_0 \tag{14}$$

and is right-continuous at $t = 0$.

Proof. We first note that the Laplace transforms $\hat{K}(s)$ and $\hat{G}(s)$ both exist and

$$\lim_{s\to\infty} s\hat{K}(s) = \lim_{t\to 0} K(t) = K(0) \tag{15}$$

and

$$\lim_{s\to\infty} s\hat{G}(s) = \lim_{t\to 0} G(t) = G(0). \tag{16}$$

We now take the Laplace transform of Equation (13) to write

$$\hat{K}(s)(s\hat{f}(s) - f_0) = \hat{G}(s). \tag{17}$$

Thus,

$$\hat{f}(s) = \frac{\hat{G}(s)}{s\hat{K}(s)} + \frac{f_0}{s} \tag{18}$$

and

$$\lim_{s\to\infty} s\hat{f}(s) = \lim_{s\to\infty} \frac{s\hat{G}(s)}{s\hat{K}(s)} + f_0 \tag{19}$$

$$= \lim_{t\to 0} \frac{G(0)}{K(0)} + f_0 \tag{20}$$

$$= f_0. \tag{21}$$

It now also follows that

$$\lim_{s\to\infty} \hat{f}(s) = 0. \tag{22}$$

The results in Equations (21) and (22) ensure that $f(t) = \mathcal{L}^{-1}\left[\hat{f}(s)\right](t)$ exists and is right-continuous at $t = 0$. □

Considering the more general case where $G(0) \neq 0$ we can find solutions of the IVP that are not right-continuous at the origin.

Theorem 1. *The solution of a C-IVP (Definition 1), with $K(0) \neq 0$, is given by*

$$f(t) = \mathcal{L}^{-1}\left[\frac{\hat{G}(s)}{s\hat{K}(s)}\right](t) + f_0 + \frac{G(0)}{K(0)}(H(t) - 1), \tag{23}$$

where $H(t)$ is the Heaviside function defined in Equation (5).

Proof. The proof follows by assuming the solution exists in the form of an ansatz, which is shown to be consistent via direct substitution into the IVP. We begin by taking an ansatz solution of the form

$$f(t) = f_c(t) + aH(t), \tag{24}$$

where $f_c(t)$ is right-continuous at $t = 0$ and differentiable for $t > 0$ and a is a real-valued constant. We then note

$$f_c(0) = f_0 \tag{25}$$

and

$$f'(t) = f_c'(t) + a\delta(t), \tag{26}$$

where $\delta(t)$ is the Dirac delta generalized function. Substitution of the ansatz solution into Equation (13) now yields

$$\int_0^t K(t-\tau) f_c'(\tau)\, d\tau = G(t) - aK(t). \tag{27}$$

To find an explicit expression for the constant a we consider $t = 0$ where the integral over classical functions vanishes. Thus, we require

$$a = \frac{G(0)}{K(0)}. \tag{28}$$

Substituting this expression for a into Equation (27) gives

$$\int_0^t K(t-\tau) f_c'(\tau)\, d\tau = L(t), \tag{29}$$

where

$$L(t) = G(t) - \frac{G(0)}{K(0)} K(t). \tag{30}$$

It is noticed that Equation (29) is of the same form as Equation (13) with $G(t)$ replaced by $L(t)$ and $L(0) = 0$. Hence, we can utilize Lemma 1 to find

$$f_c(t) = \mathcal{L}^{-1}\left[\frac{\hat{G}(s)}{s\hat{K}(s)}\right](t) + f_0 - \frac{G(0)}{K(0)}. \tag{31}$$

Thus, the final result, given by Equation (23), is then obtained by substituting Equations (28) and (31) into Equation (24). □

As an interesting exercise, an alternate proof of this theorem is given in Appendix A. It is interesting to note that the solution to the IVP with two different initial conditions will only differ by a constant. Another interesting special case occurs when the right-hand side of the equation and the kernel are equal.

Corollary 1. *The solution of a C-IVP (Definition 1) for the special case in which $G(t) = K(t)$ is given by*

$$f(t) = f_0 + H(t), \tag{32}$$

where $H(t)$ is the Heaviside function defined in Equation (5).

We should note that it is always possible to obtain continuous solutions by the addition of a function on the right-hand side of the IVP that is equal to $-G(0)$ when $t = 0$. As an example, we could consider the case below.

Corollary 2. *Suppose that; $K(t)$ and $G(t)$ are real-valued and bounded functions, continuous for $t \geq 0$ and differentiable for $t > 0$; $K(0) \neq 0$; and $f(0) = f_0$. Then*

$${}_0^*\mathcal{D}_t f(t) = \int_0^t K(t-\tau) f'(\tau)\, d\tau = G(t) - \frac{G(0)}{K(0)} K(t) \tag{33}$$

has a continuous and bounded solution for $t \geq 0$ given by

$$f(t) = \mathcal{L}^{-1}\left[\frac{\hat{G}(s)}{s\hat{K}(s)}\right](t) + f_0 - \frac{G(0)}{K(0)}. \tag{34}$$

Examples of Caputo type IVPs and their solutions are given in Section 4. In general, we see that the non-singular kernel necessitates that the solution be discontinuous at $t = 0$.

This needs to be kept in mind for any application of these type of IVPs in modelling situations and otherwise.

3. Riemann–Liouville Type IVPs with Non-Singular Kernels

Next, we will consider the solutions to Riemann–Liouville type IVPs. We again begin with a definition.

Definition 2. *Suppose that; $K(t)$ and $G(t)$ are real-valued and bounded functions, continuous for $t \geq 0$ and differentiable for $t > 0$; and $f(t)$ is a real-valued differentiable function, or generalized function that is differentiable in a distributional sense. Then a Riemann–Liouville type IVP of the first kind (RLI-IVP) is defined by the integro-differential equation*

$$ {}_0\mathcal{D}_t f(t) = \frac{d}{dt}\int_0^t K(t-\tau)f(\tau)\,d\tau = G(t) \tag{35}$$

and the initial condition $f(0) = f_0$ with $f_0 \in \mathbb{R}$.

It is helpful to first consider the special case where the IVP gives right-continuous solutions at the origin. Note that the condition here differs from the required condition on the right-hand side used in Lemma 1.

Lemma 2. *The solution of a RLI-IVP (Definition 2), with $K(0) \neq 0$ and $G(0) = K(0)f_0$, is given by*

$$ f(t) = \mathcal{L}^{-1}\left[\frac{\hat{G}(s)}{s\hat{K}(s)}\right](t) \tag{36}$$

and is right-continuous at $t = 0$.

Proof. We first take the Laplace transform of Equation (35) to write

$$ s\hat{K}(s)\hat{f}(s) = \hat{G}(s). \tag{37}$$

Thus,

$$ \hat{f}(s) = \frac{\hat{G}(s)}{s\hat{K}(s)} \tag{38}$$

and

$$ \lim_{s\to\infty} s\hat{f}(s) = \lim_{s\to\infty} \frac{s\hat{G}(s)}{s\hat{K}(s)} \tag{39}$$

$$ = \lim_{t\to 0} \frac{G(0)}{K(0)} \tag{40}$$

$$ = \frac{K(0)f_0}{K(0)} \tag{41}$$

$$ = f_0. \tag{42}$$

It now also follows that

$$ \lim_{s\to\infty} \hat{f}(s) = 0. \tag{43}$$

The results in Equations (42) and (43) ensure that $f(t) = \mathcal{L}^{-1}\Big[\hat{f}(s)\Big](t)$ exists and is right-continuous at $t = 0$. □

The general case again will display a discontinuity at the origin. It is interesting to note that as f_0 is varied the solution only shifts at $t = 0$.

Theorem 2. *The solution of a RLI-IVP (Definition 2), with $K(0) \neq 0$, is given by*

$$f(t) = \mathcal{L}^{-1}\left[\frac{\hat{G}(s)}{s\hat{K}(s)}\right](t) + \left(\frac{G(0)}{K(0)} - f_0\right)(H(t) - 1), \tag{44}$$

where $H(t)$ is the Heaviside function defined in Equation (5).

Proof. The proof relies on establishing a relationship between Equations (13) and (35) and then utilizing Theorem 1. By interchanging the order of functions in the convolution and applying Leibniz rule for differentiation under the integral sign, we can write

$$\frac{d}{dt}\int_0^t K(t-\tau)f(\tau)\,d\tau = \frac{d}{dt}\int_0^t K(\tau)f(t-\tau)\,d\tau \tag{45}$$

$$= K(t)f_0 + \int_0^t K(\tau)f'(t-\tau)\,d\tau \tag{46}$$

$$= K(t)f_0 + \int_0^t K(t-\tau)f'(\tau)\,d\tau. \tag{47}$$

We now use the result of Equation (47) in Equation (35) and rearrange terms to re-write this as

$$\int_0^t K(t-\tau)f'(\tau)\,d\tau = M(t), \tag{48}$$

where $M(t) = G(t) - K(t)f_0$. It is noticed that this equation is of the same form as Equation (13) but with $G(t)$ replaced by $M(t)$. The final result, given by Equation (44), is then obtained by applying Theorem 1 to Equation (48). □

As an interesting exercise, an alternate proof of this theorem is given in Appendix A. The initial condition of the IVP only changes the solution at $t = 0$. For $t > 0$, with given functions K and G, the solutions are identical for all values of f_0. Similarly to the Caputo type case the special case where the kernel and right-hand side of the IVP are equal gives an interesting solution.

Corollary 3. *The solution of a RLI-IVP (Definition 2) for the special case in which $G(t) = K(t)$ is given by*

$$f(t) = f_0 + (1 - f_0)H(t), \tag{49}$$

where $H(t)$ is the Heaviside function defined in Equation (5).

It is always possible to obtain continuous solutions to the IVP by the addition of a function on the right-hand side of the IVP that is equal to $f_0K(0) - G(0)$ when $t = 0$. An example is given below.

Corollary 4. *Suppose that; $K(t)$ and $G(t)$ are real-valued and bounded functions, continuous at $t = 0$ and differentiable for $t > 0$; $K(0) \neq 0$; and $f(0) = f_0$. Then*

$${}_0\mathcal{D}_t f(t) = \frac{d}{dt}\int_0^t K(t-\tau)\,f(\tau)\,d\tau = G(t) - \left(\frac{G(0)}{K(0)} - f_0\right)K(t) \tag{50}$$

has a continuous and bounded solution for $t \geq 0$ given by

$$f(t) = \mathcal{L}^{-1}\left[\frac{\hat{G}(s)}{s\hat{K}(s)}\right](t) + f_0 - \frac{G(0)}{K(0)}. \tag{51}$$

In IVPs with continuous solutions, giving the initial condition as either $f(0)$ or $\lim_{t\to 0} f(t)$ will be equivalent. This is not the case for either the Caputo or Riemann–Liouville type IVPs in general. Most interestingly, we find that the solution to Riemann–

Liouville IVPs will propagate as a functional form of t. To find the solutions with this alternate form of initial condition, we will first define an alternate form to the IVP.

Definition 3. *Suppose that; $K(t)$ and $G(t)$ are real-valued and bounded functions, continuous for $t \geq 0$ and differentiable for $t > 0$; and $f(t)$ is a real-valued differentiable function, or generalized function that is differentiable in a distributional sense. Then a Riemann–Liouville type IVP of the second kind (RLII-IVP) is defined by the integro-differential equation*

$$ {}_0\mathcal{D}_t f(t) = \frac{d}{dt}\int_0^t K(t-\tau)f(\tau)\,d\tau = G(t) \tag{52}$$

and the limiting condition $\lim_{t\to 0^+} f(t) = f_0$ with $f_0 \in \mathbb{R}$.

Similar to the previous theorems, we see that the general case will display a discontinuity at the origin.

Theorem 3. *The solution of a RLII-IVP (Definition 3), with $K(0), K'(0) \neq 0$, is given by*

$$ f(t) = \mathcal{L}^{-1}\left[\frac{\hat{G}(s)}{s\hat{K}(s)} - \left(1 - \frac{K(0)}{s\hat{K}(s)}\right)\left(\frac{G(0) - f_0K(0)}{K'(0)}\right)\right](t) + \frac{G(0) - f_0K(0)}{K'(0)}\delta(t), \tag{53}$$

where $\delta(t)$ is the Dirac delta generalized function.

Proof. The proof follows in a similar manner to that for Theorem 1. We begin by taking an ansatz solution of the form

$$ f(t) = f_c(t) + b\delta(t), \tag{54}$$

where $f_c(t)$ is right-continuous at $t = 0$ and differentiable for $t > 0$ and b is a real-valued constant. We then note $\lim_{t\to 0^+} f(t) = f_c(0)$, or equivalently, $f_c(0) = f_0$. Substitution of the ansatz solution into Equation (52) gives

$$ \frac{d}{dt}\int_0^t K(t-\tau)f_c(\tau)\,d\tau = G(t) - bK'(t). \tag{55}$$

To find an explicit expression for the constant b we consider the limit $t \to 0$ and employ the initial value theorem to find that the integral over classical functions gives

$$ \lim_{t\to 0}\frac{d}{dt}\int_0^t K(t-\tau)f_c(\tau)\,d\tau = \lim_{s\to\infty}\left(s\hat{K}(s)\cdot s\hat{f_c}(s)\right) = K(0)f_0. \tag{56}$$

Thus, we require

$$ b = \frac{G(0) - f_0K(0)}{K'(0)}. \tag{57}$$

Substituting this expression for b into Equation (55) yields

$$ \frac{d}{dt}\int_0^t K(t-\tau)f_c(\tau)\,d\tau = N(t), \tag{58}$$

where

$$ N(t) = G(t) - \left(\frac{G(0) - f_0K(0)}{K'(0)}\right)K'(t). \tag{59}$$

It is noticed that Equation (58) is of the same form as Equation (35) with $G(t)$ replaced by $N(t)$ and $N(0) = f_0K(0)$. Since $f_c(t)$ is is right-continuous at $t = 0$, we know that the initial and limiting condition are equal. Hence, we can utilize Lemma 2 to find

$$ f_c(t) = \mathcal{L}^{-1}\left[\frac{\hat{G}(s)}{s\hat{K}(s)} - \left(1 - \frac{K(0)}{s\hat{K}(s)}\right)\left(\frac{G(0) - f_0K(0)}{K'(0)}\right)\right](t). \tag{60}$$

Thus, the final result, given by Equation (53), is then obtained by substituting Equations (57) and (60) into Equation (54). □

As an interesting exercise, an alternate proof of this theorem is given in Appendix A. Again we can modify the IVP to ensure that solutions are continuous by the addition of a function on the right-hand side that is equal to $f_0K(0) - G(0)$ when $t = 0$. An example of this is given below.

Corollary 5. *Suppose that; $K(t)$ and $G(t)$ are real-valued and bounded functions, continuous for $t \geq 0$ and differentiable for $t > 0$; $K(0), K'(0) \neq 0$; and $\lim_{t\to 0^+} f(t) = f_0$. Then*

$$ {}_0\mathcal{D}_t f(t) = \frac{d}{dt}\int_0^t K(t-\tau)\, f(\tau)\, d\tau = G(t) - \left(\frac{G(0) - f_0K(0)}{K'(0)}\right)K'(t). \tag{61}$$

has a continuous and bounded solution for $t \geq 0$ given by

$$ f(t) = \mathcal{L}^{-1}\left[\frac{\hat{G}(s)}{s\hat{K}(s)} - \left(1 - \frac{K(0)}{s\hat{K}(s)}\right)\left(\frac{G(0) - f_0K(0)}{K'(0)}\right)\right](t). \tag{62}$$

4. Examples

In this section we present some examples of solutions to generalized Caputo and Riemann–Liouville type IVPs with non-singular kernels. In general, the solutions to RLI-IVPs and RLII-IVPs are equivalent for the special case in which the solution is right-continuous at $t = 0$. This can be seen from the initial condition, since $\lim_{t\to 0^+} f(t) = f(0)$ by the right-continuity of f. The solution to each example can be easily verified via direct substitution into the respective IVP.

4.1. C-IVP with $K(t) = 1 - t^2$

Consider the C-IVP with

$$ \int_0^t \Big(1 - (t-\tau)^2\Big) f'(\tau)\, d\tau = \cos(t)\exp(-t) \quad \text{and} \quad f(0) = f_0 \tag{63}$$

with $f_0 \in \mathbb{R}$. The solution of this IVP is given by

$$ f(t) = f_0 - 1 + \frac{1}{2}\Big(\cosh\Big(\sqrt{2}t\Big) + \exp(t)(\cos(t) + \sin(t))\Big) + H(t). \tag{64}$$

Notice that the solution has a discontinuity at $t = 0$.

4.2. C-IVP with $K(t) = 1 + t\exp(-t)$

Consider the C-IVP

$$ \int_0^t (1 + (t-\tau)\exp(\tau - t)) f'(\tau)\, d\tau = \sin(t) \quad \text{and} \quad f(0) = f_0, \tag{65}$$

with $f_0 \in \mathbb{R}$. The solution of this IVP is given by

$$ f(t) = f_0 + \frac{2}{3}\sin(t) + \frac{2\sqrt{5}}{15}\exp\left(\frac{-3t}{2}\right)\sinh\left(\frac{\sqrt{5}t}{2}\right). \tag{66}$$

This solution is continuous for all $t \in \mathbb{R}$, which is expected as $G(t) = \sin(t)$ vanishes at $t = 0$.

4.3. RLI-IVP with $K(t) = \cos(t) + \sin(t)$

Consider the RLI-IVP with

$$\frac{d}{dt}\int_0^t (\cos(t-\tau) + \sin(t-\tau))f(\tau)\,d\tau = g \quad \text{and} \quad f(0) = f_0 \tag{67}$$

with $g, f_0 \in \mathbb{R}$. The solution of this IVP is given by

$$f(t) = f_0 + (t - 2 + 2\exp(-t))g + (g - f_0)H(t). \tag{68}$$

Notice that the solution has a discontinuity at $t = 0$ unless $g = f_0$.

4.4. RLI-IVP with $K(t) = 1 + t\exp(-t)$

Consider the RLI-IVP with

$$\frac{d}{dt}\int_0^t (1 + (t-\tau)\exp(\tau - t))f(\tau)\,d\tau = \sin(t) \quad \text{and} \quad f(0) = f_0 \tag{69}$$

with $f_0 \in \mathbb{R}$. The solution of this IVP is given by

$$f(t) = f_0 + \frac{2}{3}\sin(t) + \frac{2\sqrt{5}}{15}\exp\left(\frac{-3t}{2}\right)\sinh\left(\frac{\sqrt{5}t}{2}\right) - f_0 H(t). \tag{70}$$

This solution has a discontinuity at $t = 0$ unless $f_0 = 0$. When $t > 0$, we see that Equation (70) is independent of the initial value f_0 and the difference between Equations (66) and (70) is equal to the precise value of f_0. This is illustrated in Figure 1, where there is a vertical shift of $f_0 = 1$ for the curve representing Equation (66) from the curve representing Equation (70). For the special case in which $f_0 = 0$, then Equation (66) is equivalent to Equation (70). This is true in general, where Equation (23) is equivalent to Equation (44) when $f_0 = 0$.

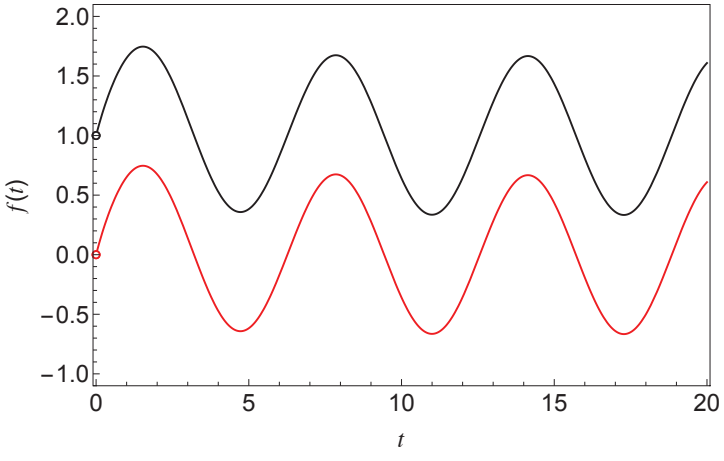

Figure 1. The black and red curves represent the IVP solutions given by Equations (66) and (70) respectively with $f_0 = 1$. The open circle on each curve indicates that both solutions are valid for $t > 0$.

4.5. RLII-IVP with $K(t) = \exp\left(\frac{\beta}{\beta-1}t\right)$

Consider the RLII-IVP

$$\frac{d}{dt}\int_0^t \exp\left(\frac{\beta}{\beta-1}(t-\tau)\right)f(\tau)\,d\tau = g \quad \text{and} \quad \lim_{t\to 0^+} f(t) = f_0 \tag{71}$$

with $g, f_0 \in \mathbb{R}$ and $\beta > 1$. The solution of this IVP is given by

$$f(t) = f_0 - \frac{\beta g t}{\beta - 1} + \frac{(g - f_0)(\beta - 1)}{\beta}\delta(t). \tag{72}$$

Notice that we have $\lim_{t\to 0^+} f(t) = f_0$ but due to the Dirac delta $f(0) \neq f_0$ unless $f_0 = g$.

4.6. RLII-IVP with $K(t) = \cos(t) + \sin(t)$

Consider the RLII-IVP with

$$\frac{d}{dt}\int_0^t (\cos(t-\tau) + \sin(t-\tau))f(\tau)\,d\tau = g \quad \text{and} \quad \lim_{t\to 0^+} f(t) = f_0 \tag{73}$$

with $g, f_0 \in \mathbb{R}$. The solution of this IVP is given by

$$f(t) = gt + (2\exp(-t) - 1)f_0 + (g - f_0)\delta(t). \tag{74}$$

In contrast to Equation (68), we see that Equation (74) is dependent on the initial value f_0. Consequently, varying f_0 will affect the form of Equation (74). This is illustrated in Figure 2, where the curves representing Equation (74) vary according to the specific value of f_0 and the curve representing Equation (68) remains unchanged. For the special case in which $g = f_0$, Equation (68) is equivalent to Equation (74).

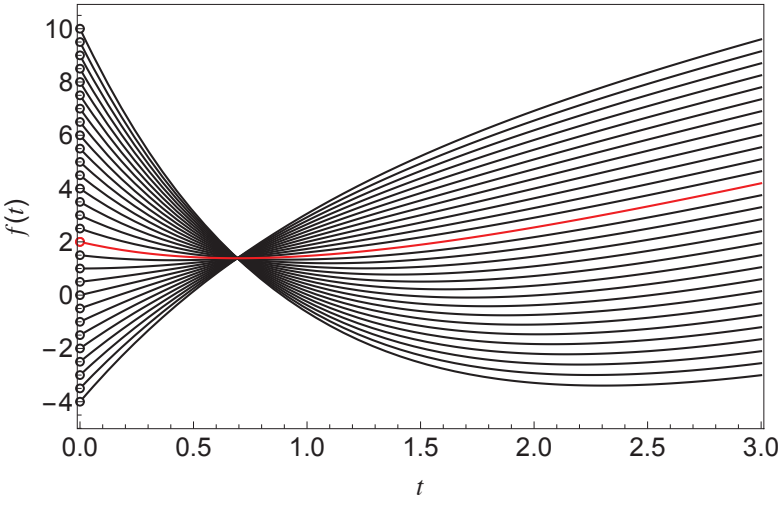

Figure 2. The black and red curves represent the IVP solutions given by Equations (68) and (74) respectively for varying values of f_0 with $g = 2$. The open circle on each curve indicates that both solutions are valid for $t > 0$.

5. Summary and Discussion

Here we have considered IVPs for integro-differential equations of the form $\mathcal{D}_t f(t) = G(t)$ where the operator $\mathcal{D}_t$ is either similar to the Riemann–Liouville derivative, or similar to the Caputo derivative, but with the singular kernel in those operators replaced by a non-singular kernel $K(t)$, and $K(0) \neq 0$. We have not attempted to motivate this replacement by modelling considerations; rather, we have sought to understand what the implications of such replacements would be in modelling applications. Our motivation in this pursuit has been guided by the plethora of integro-differential operators that have been introduced in recent years. In modelling applications, it would be expected that $G(t)$ and $K(t)$ are prescribed functions, and $f(t)$ is unknown except at the origin. We find that

the IVPs for these integro-differential equations with non-singular kernels, in general, have solutions that have intrinsic discontinuities at the origin. We also show that it is possible to re-formulate these IVPs so that solutions are guaranteed to be continuous at the origin but this comes at the cost of effectively constraining the right-hand side of the equations so that they are no longer just dependent on the prescribed function $G(t)$. These results are problematic for modelling applications which would seek to employ Riemann–Liouville type, or Caputo type, differential operators but with the singular kernel replaced by a non-singular kernel.

Author Contributions: Conceptualization, C.N.A., S.-J.M.B., B.I.H. and B.A.J.; formal analysis, C.N.A., S.-J.M.B., B.I.H. and B.A.J.; writing—original draft preparation, C.N.A., S.-J.M.B., B.I.H. and B.A.J.; writing—review and editing, C.N.A., S.-J.M.B., B.I.H. and B.A.J. All authors have read and agreed to the published version of the manuscript.

Funding: This research was funded by Australian Research Council grant number DP200100345.

Institutional Review Board Statement: Not applicable

Informed Consent Statement: Not applicable

Data Availability Statement: Not applicable

Conflicts of Interest: The authors declare no conflict of interest.

Appendix A

Here we present an alternative proof for Theorems 1–3. While each proof continues to rely on the assumption that the solutions take the form of an ansatz, the integrals are initially taken to be Riemann–Stieltjes integrals. These integrals can subsequently be reduced to standard Riemann integrals where traditional Laplace transform techniques can be employed. We begin with a proof of Theorem 1.

Appendix A.1. Theorem 1

Proof. We consider the problem

$$\int_0^t K(t-\tau)\, df(\tau) = G(t), \tag{A1}$$

where the integral is a Riemann–Stieltjes integral. Then Equation (13) can be recovered by identifying $f'(t) = \frac{df}{dt}$, as a classical derivative, or a distributional derivative. This can be evaluated as

$$\int_0^t K(t-\tau)\, df(\tau) = \sum_{k=0}^{m-1} K(t-c_k)(f(t_{k+1}) - f(t_k)) \tag{A2}$$

with $0 = t_0 < t_1 < \ldots < t_n = t$ and $c_k \in [t_k, t_{k+1}]$. We seek a solution of the form

$$f(t) = aH(t) + f_c(t), \tag{A3}$$

where $f_c(t)$ is right-continuous at $t = 0$ and differentiable for $t > 0$. Note that, by construction, $f(0) = f_c(0)$. Without loss of generality, for the partition in Equation (A2), we consider $t_1 = \epsilon$ then

$$\int_0^t K(t-\tau)\, df(\tau) = K(t-c_0)(f(\epsilon) - f(0)) + \int_\epsilon^t K(t-\tau)\, df(\tau) \tag{A4}$$

$$= K(t-c_0)(a + f_c(\epsilon) - f_c(0)) + \int_\epsilon^t K(t-\tau)\, df_c(\tau) \tag{A5}$$

where $c_0 \in [0, \epsilon]$. By taking the limit $\epsilon \to 0^+$ we can now write

$$\int_0^t K(t-\tau)\, df(\tau) = aK(t) + \int_{0^+}^t K(t-\tau)\, df_c(\tau). \tag{A6}$$

Given that $f_c(t)$ is a classical function that is right-continuous for $t \geq 0$ and differentiable for $t > 0$ we can now write

$$\int_0^t K(t-\tau)\, df(\tau) = aK(t) + \int_0^t K(t-\tau) f_c'(\tau), \tag{A7}$$

where the integral of the right-hand side is a standard Riemann integral. The original problem, with a solution of the form of Equation (A3), can thus be written as

$$\int_0^t K(t-\tau) f_c'(\tau)\, d\tau = G(t) - aK(t), \quad f_c(0) = f_0, \tag{A8}$$

but note that we now require, for consistency,

$$a = \frac{G(0)}{K(0)}, \tag{A9}$$

which defines an explicit a. Thus, Equation (A8), together with the consistency condition, Equation (A9), can be solved readily using Laplace transform methods to arrive at

$$f(t) = f_0 + \frac{G(0)}{K(0)}(H(t) - 1) + \mathcal{L}^{-1}\left[\frac{\hat{G}(s)}{s\hat{K}(s)}\right](t). \tag{A10}$$

□

Appendix A.2. Theorem 2

Proof. We consider the problem

$$\frac{d}{dt}\int_0^t K(t-\tau)\, dF(\tau) = G(t) \tag{A11}$$

where the integral is a Riemann–Stieltjes integral. Then Equation (35) can be recovered by identifying $\frac{dF}{dt} = f(t)$, as a classical derivative, or a distributional derivative, of $F(t)$. We now seek a solution of the form

$$F(t) = atH(t) + F_c(t) \tag{A12}$$

where $F_c(t)$ is right-continuous at $t = 0$ and differentiable for $t > 0$. Note that we identify

$$f(t) = aH(t) + at\delta(t) + F_c'(t) \tag{A13}$$
$$= aH(t) + F_c'(t) \tag{A14}$$
$$= aH(t) + f_c(t) \tag{A15}$$

and then $f(0) = f_c(0) = f_0$.

We begin by writing Equation (35) as

$$\lim_{\epsilon \to 0} \frac{1}{\epsilon}\left(\int_0^{t+\epsilon} K(t+\epsilon-\tau)\, dF(\tau) - \int_0^t K(t-\tau)\, dF(\tau)\right) = G(t), \tag{A16}$$

and then

$$\lim_{\epsilon\to 0}\frac{1}{\epsilon}\Bigg((K(t+\epsilon-c_0)-K(t-c_0))(F(\epsilon_0)-F(0)) + \int_{\epsilon_0}^{t+\epsilon} K(t+\epsilon-\tau)\,dF(\tau)-\int_{\epsilon_0}^{t} K(t-\tau)\,dF(\tau)\Bigg)=G(t) \tag{A17}$$

where $c_0\in(0,\epsilon_0)$. The remaining Riemann–Stieltjes integrals, with lower limit $\epsilon_0>0$, can now be written as Riemann integrals so that

$$\lim_{\epsilon\to 0}\frac{1}{\epsilon}\Bigg((K(t+\epsilon-c_0)-K(t-c_0))(F(\epsilon_0)-F(0)) + \int_{\epsilon_0}^{t+\epsilon} K(t+\epsilon-\tau)\,F'(\tau)\,d\tau-\int_{\epsilon_0}^{t} K(t-\tau)\,F'(\tau)\,d\tau\Bigg)=G(t) \tag{A18}$$

or equivalently, using Equation (A12),

$$\lim_{\epsilon\to 0}\frac{1}{\epsilon}\Bigg((K(t+\epsilon-c_0)-K(t-c_0))(a\epsilon_0+F_c(\epsilon_0)-F(0)) + \int_{\epsilon_0}^{t+\epsilon} K(t+\epsilon-\tau)\,(a+F_c'(\tau))\,d\tau-\int_{\epsilon_0}^{t} K(t-\tau)\,(a+F_c'(\tau))\,d\tau\Bigg)=G(t) \tag{A19}$$

After taking the limit $\epsilon_0\to 0$, and identifying $F_c'(\tau)=f_c(t)$, we now have

$$\frac{1}{\epsilon}\Bigg(\int_0^{t+\epsilon} K(t+\epsilon-\tau)\,(a+f_c(\tau))\,d\tau-\int_0^{t} K(t-\tau)\,(a+f_c(\tau))\,d\tau\Bigg)=G(t). \tag{A20}$$

After taking the limit $\epsilon\to 0$ this yields

$$\frac{d}{dt}\int_0^t K(t-\tau)\,(a+f_c(\tau))\,d\tau=G(t), \tag{A21}$$

or equivalently

$$\frac{d}{dt}\int_0^t K(t-\tau)\,f_c(\tau)\,d\tau=G(t)-aK(t). \tag{A22}$$

We now take Laplace transforms to write

$$s\hat{f}_c(s)=\frac{\hat{G}(s)}{\hat{K}(s)}-a. \tag{A23}$$

Considering the limit $s\to 0$ we have

$$f_c(0)=\frac{G(0)}{K(0)}-a, \tag{A24}$$

which defines

$$a=\frac{G(0)}{K(0)}-f_0. \tag{A25}$$

Using this in Equation (A23) and taking the inverse Laplace transform now yields

$$f_c(t)=f(0)-\frac{G(0)}{K(0)}+\mathcal{L}^{-1}\left[\frac{\hat{G}(s)}{s\hat{K}(s)}\right](t). \tag{A26}$$

Thus, the solution, given by Equation (44), is then obtained by substituting Equations (A25) and (A26) into Equation (A15). □

Appendix A.3. Theorem 3

Proof. We consider the problem

$$\frac{d}{dt}\int_0^t K(t-\tau)\,dF(\tau) = G(t) \tag{A27}$$

where the integral is a Riemann–Stieltjes integral. Then Equation (52) can be recovered by identifying $\frac{dF}{dt} = f(t)$, as a classical derivative, or a distributional derivative, of $F(t)$. Here we consider the possibility

$$F(t) = aH(t) + F_c(t) \tag{A28}$$

where $a > 0$, $H(t)$ is the Heaviside function and $F_c(t)$ is right-continuous at $t = 0$ and differentiable for $t \geq 0$. We then define

$$f(t) = F'(t) = a\delta(t) + F_c'(t) = a\delta(t) + f_c(t) \tag{A29}$$

where $f_c(t)$ is continuous for $t > 0$. Note that in this case we cannot consider the initial condition $f(0) = f_0$ but we can consider $\lim_{t\to 0^+} f(0) = f_0$ or equivalently $f_c(0) = f_0$. Hence, Equation (A27) can be written as

$$\lim_{\epsilon\to 0}\frac{1}{\epsilon}\left(\int_0^{t+\epsilon} K(t+\epsilon-\tau)\,dF(\tau) - \int_0^t K(t-\tau)\,dF(\tau)\right) = G(t), \tag{A30}$$

and then

$$\begin{aligned}\lim_{\epsilon\to 0}\frac{1}{\epsilon}\Bigg(&(K(t+\epsilon-c_0)-K(t-c_0))(F(\epsilon_0)-F(0))\\ &+\int_{\epsilon_0}^{t+\epsilon} K(t+\epsilon-\tau)\,dF(\tau) - \int_{\epsilon_0}^t K(t-\tau)\,dF(\tau)\Bigg) = G(t)\end{aligned} \tag{A31}$$

where $c_0 \in (0,\epsilon_0)$. The remaining Riemann–Stieltjes integrals can now be written as Riemann integrals with

$$\begin{aligned}\lim_{\epsilon\to 0}\frac{1}{\epsilon}\Bigg(&(K(t+\epsilon-c_0)-K(t-c_0))(a+F_c(\epsilon_0)-F(0))\\ &+\int_{\epsilon_0}^{t+\epsilon} K(t+\epsilon-\tau)\,f_c(\tau)\,d\tau - \int_{\epsilon_0}^t K(t-\tau)\,f_c(\tau)\,d\tau\Bigg) = G(t)\end{aligned} \tag{A32}$$

We can now consider the limit $\epsilon_0 \to 0$ to formally write

$$\begin{aligned}&\lim_{\epsilon_0\to 0}\lim_{\epsilon\to 0}\frac{1}{\epsilon}(K(t+\epsilon-c_0)-K(t-c_0))(a+F_c(\epsilon_0)-F_c(0))\\ &+\lim_{\epsilon_0\to 0}\lim_{\epsilon\to 0}\frac{1}{\epsilon}\left(\int_{\epsilon_0}^{t+\epsilon} K(t+\epsilon-\tau)\,f_c(\tau)\,d\tau - \int_{\epsilon_0}^t K(t-\tau)\,f_c(\tau)\,d\tau\right) = G(t)\end{aligned} \tag{A33}$$

and then taking the limit $\epsilon_0 \to 0$

$$\begin{aligned}&\lim_{\epsilon\to 0}\frac{1}{\epsilon}(K(t+\epsilon)-K(t))a\\ &+\lim_{\epsilon\to 0}\frac{1}{\epsilon}\left(\int_0^{t+\epsilon} K(t+\epsilon-\tau)\,f_c(\tau)\,d\tau - \int_0^t K(t-\tau)\,f_c(\tau)\,d\tau\right) = G(t)\end{aligned} \tag{A34}$$

Finally, taking the limit $\epsilon \to 0$ we have

$$\frac{d}{dt}\int_0^t K(t-\tau)\,f_c(\tau)\,d\tau = G(t) - aK'(t). \tag{A35}$$

We can now take the Laplace transform of this equation to write

$$s\hat{K}(s)\hat{f}_c(s) = \hat{G}(s) - a(s\hat{K}(s) - K(0)). \tag{A36}$$

We now solve for

$$\hat{f}_c(s) = \frac{\hat{G}(s)}{s\hat{K}(s)} - \frac{s\hat{K}(s) - K(0)}{s\hat{K}(s)}a. \tag{A37}$$

We can now find the initial condition $f_c(0)$ from

$$\lim_{s\to\infty} s\hat{f}_c(s) = \frac{\lim_{s\to\infty} s\hat{G}(s)}{\lim_{s\to\infty} s\hat{K}(s)} - \frac{\lim_{s\to\infty} s(s\hat{K}(s) - K(0))}{\lim_{s\to\infty} s\hat{K}(s)}a \tag{A38}$$

$$= \frac{G(0)}{K(0)} - \frac{K'(0)}{K(0)}a. \tag{A39}$$

We can solve for

$$a = \frac{G(0)}{K'(0)} - \frac{f_c(0)K(0)}{K'(0)}. \tag{A40}$$

We now take the Laplace transform of Equation (A37) to write

$$f_c(t) = \mathcal{L}^{-1}\left[\frac{\hat{G}(s)}{s\hat{K}(s)} - \frac{s\hat{K}(s) - K(0)}{s\hat{K}(s)}a\right](t) \tag{A41}$$

The solution, given by Equation (53), is now obtained by substituting the result for Equations (A40) and (A41) into Equation (A28). □

References

1. De Oliveira, E.C.; Tenreiro Machado, J.A. A Review of Definitions for Fractional Derivatives and Integral. *Math. Probl. Eng.* **2014**, *2014*, 238459. [CrossRef]
2. Li, C.; Qian, D.; Chen, Y. On Riemann-Liouville and Caputo Derivatives. *Discret. Dyn. Nat. Soc.* **2011**, *2011*, 562494. [CrossRef]
3. Ortigueira, M.D. A new look at the initial condition problem. *Mathematics* **2022**, *10*, 1771. [CrossRef]
4. Caputo, M.; Fabrizio, M. A new definition of fractional derivative without singular kernel. *Prog. Fract. Differ. Appl.* **2015**, *1*, 73–85.
5. Losada, J.; Nieto, J.J. Properties of a new fractional derivative without singular kernel. *Prog. Fract. Differ. Appl.* **2015**, *1*, 87–92.
6. Atangana, A.; Baleanu, D. New fractional derivatives with non-local and non-singular kernel. *Themal Sci.* **2016**, *20*, 763–769. [CrossRef]
7. Ortigueira, M.D.; Tenreiro Machado, J. A critical analysis of the Caputo-Fabrizio operator. *Commun. Nonlinear Sci. Numer. Simul.* **2018**, *59*, 608–611. [CrossRef]
8. Tarasov, V.E. Caputo–Fabrizio operator in terms of integer derivatives: Memory or distributed lag? *Comput. Appl. Math.* **2019**, *38*, 113. [CrossRef]
9. Hanyga, A. A comment on a controversial issue: A generalized fractional derivative cannot have a regular kernel. *Fract. Calc. Appl. Anal.* **2020**, *23*, 211–223. [CrossRef]
10. Angstmann, C.N.; Jacobs, B.A.; Henry, B.I.; Xu, Z. Intrinsic discontinuities in solutions of evolution equations involving fractional Caputo–Fabrizio and Atangana–Baleanu operators. *Mathematics* **2020**, *8*, 2023. [CrossRef]
11. Faleleev, M.V.; Sidorov, N.A.; Sidorov, D.N. Generalized solutions of Volterra integral equations of the first kind. *Lobachevskii J. Math.* **2005**, *20*, 47–57.
12. Sidorov, N.A.; Sidorov, D.N. Existence and construction of generalized solutions of nonlinear Volterra integral equations of the first kind. *Differ. Equ.* **2006**, *42*, 1312–1316. [CrossRef]
13. Ziemanian, A.H. An introduction to generalized functions and the generalized Laplace and Legendre transformations. *SIAM Rev.* **1968**, *10*, 1–24. [CrossRef]

fractal and fractional

MDPI

Article

Generalized Space-Time Fractional Stochastic Kinetic Equation

Junfeng Liu *, Zhigang Yao and Bin Zhang

School of Statistics and Data Science, Nanjing Audit University, Nanjing 211815, China
* Correspondence: junfengliu@nau.edu.cn

Abstract: In this paper, we study a class of nonlinear space-time fractional stochastic kinetic equations in $\mathbb{R}^d$ with Gaussian noise which is white in time and homogeneous in space. This type of equation constitutes an extension of the nonlinear stochastic heat equation involving fractional derivatives in time and fractional Laplacian in space. We firstly give a necessary condition on the spatial covariance for the existence and uniqueness of the solution. Furthermore, we also study various properties of the solution, such as Hölder regularity, the upper bound of second moment, and the stationarity with respect to the spatial variable in the case of linear additive noise.

Keywords: space-time fractional stochastic kinetic equations; caputo derivatives; gaussian index; hölder continuity

MSC: 60H05; 60H07; 60H15

Citation: Liu, J.; Yao, Z.; Zhang, B. Generalized Space-Time Fractional Stochastic Kinetic Equation. *Fractal Fract.* **2022**, *6*, 450. https://doi.org/10.3390/fractalfract6080450

Academic Editors: António Lopes, Alireza Alfi, Liping Chen and Sergio Adriani David

Received: 5 July 2022
Accepted: 16 August 2022
Published: 18 August 2022

Publisher's Note: MDPI stays neutral with regard to jurisdictional claims in published maps and institutional affiliations.

1. Introduction

Fractional stochastic partial differential equations (SPDEs for short) constitute a subclass of stochastic partial differential equations. The main characteristic of this class of stochastic equations is that they involve fractional derivatives and integrals, which replace the usual derivatives and integrals. The fractional stochastic partial differential equations received particular attention in the last several decades because they emerge in anomalous diffusion models in physics, among other areas of applications (see, for example, [1–8] and references therein).

The aim of the present article is to study the following space-time fractional stochastic kinetic equations, for any $(t,x) \in \mathbb{R}_+ \times \mathbb{R}^d$

$$\begin{cases} \left(\dfrac{\partial^\beta}{\partial t^\beta} + \nu(\mathrm{I}-\Delta)^{\gamma/2}(-\Delta)^{\alpha/2}\right)u(t,x) = I_t^{1-\beta}\big(\lambda\sigma(u(t,x))\dot{W}(t,x)\big), \\ u(0,x) = u_0(x), \quad x \in \mathbb{R}^d, \end{cases} \tag{1}$$

where $\beta \in (0,1]$, $\gamma \geq 0, \alpha > 0$ are some fractional parameters and ν and λ are two positive parameters, with λ being called the intensity of the noise. The coefficient $\sigma(\cdot)$ is a measurable function, and $\dot{W}$ is a Gaussian noise, white in time and correlated in space. Here, Δ is the d-dimensional Laplace operator and the operators $(I-\Delta)^{\gamma/2}, \gamma \geq 0$ and $(-\Delta)^{\alpha/2}, \alpha > 0$ are interpreted as the inverses of the Bessel and Riesz potentials, respectively. They are defined as follows. For a function f which is sufficiently smooth and small at infinity, the Riesz potential $(-\Delta)^{-\alpha/2}(f), 0 < \alpha < d$ is defined by

$$(-\Delta)^{-\alpha/2}(f)(x) := \frac{1}{\nu(\alpha)}\int_{\mathbb{R}^d} |x-y|^{-d+\alpha} f(y)dy,$$

with $\nu(\alpha) = \pi^{d/2}2^\alpha \frac{\Gamma(\alpha/2)}{\Gamma(\frac{d-\alpha}{2})}$. The Bessel potential $(I-\Delta)^{-\gamma/2}, \gamma \geq 0$ on $\mathbb{R}^d$ can be represented by

$$(I-\Delta)^{-\gamma/2}(f)(x) := \int_{\mathbb{R}^d} H_s(x-y)f(y)dy,$$

where $H_s(\cdot)$ is defined for $x \in \mathbb{R}^d/\{0\}$ by the formula $H_s(x) = \frac{1}{(4\pi)^{\gamma/2}\Gamma(\gamma/2)} \int_0^\infty \frac{1}{y^{1+\frac{d-\gamma}{2}}} e^{-\frac{\pi|x|^2}{y} - \frac{y}{4\pi}} dy$. For more details, one can consult Chapter V in [9] for the definitions about the Bessel and Riesz potentials. Furthermore, the composition of the Bessel and Riesz potentials plays an important role in describing the behaviour of the process at the spatial macro and microscales. These integral operators and their inverses can be defined as bounded operators on the fractional Sobolev spaces $\{H^\theta(\mathbb{R}^d); \theta \in \mathbb{R}\}$.

We will specify later the required conditions on the function $\sigma(\cdot)$ and the Gaussian noise $\dot{W}$. In Equarion (1), the time derivative operator $\frac{\partial^\beta}{\partial t^\beta}$ with order $\beta \in (0, 1]$ is defined in the *Caputo-Djrbashian* sense (for example, Caputo [3], Anh, and Leonenko [2]):

$$\frac{\partial^\beta}{\partial t^\beta} u(t,x) = \begin{cases} \frac{1}{\Gamma(1-\beta)} \left[\frac{\partial}{\partial t} \int_0^t \frac{u(s,x)}{(t-s)^\beta} ds - \frac{u(0,x)}{t^\beta} \right], & \text{if} \quad \beta \in (0,1), \\ \frac{\partial}{\partial t} u(t,x), & \text{if} \quad \beta = 1. \end{cases} \tag{2}$$

The deterministic counterparts of Equation (1) have received a lot of attention. This is because they appear to be very useful for modeling, being introduced to describe physical phenomena such as diffusion in porous media with fractal geometry, kinematics in viscoelastic media, relaxation processes in complex systems (including viscoelastic materials, glassy materials, synthetic polymers, biopolymers), propagation of seismic waves, anomalous diffusion and turbulence (see, for example, Anh and Leonenko [2], Caputo [3], Chen [10], Chen [11], Chen et al. [12], Meerschaert et al. [13], Nane [14], and references therein). Such equations are obtained from the classical diffusion equation by replacing the first or second-order derivative by a fractional derivative.

In this work, we mainly follow the studies in [1,2,15,16] and references therein, In particular, in [1], the authors showed a connection between the solution to the deterministic counterparts of Equation (1) and the theory of continuous-time random walks (CTRWs for short). In fact, they showed the existence of the stochastic processes which are the limits, in the weak sense, of sequences of CTRWs whose probability density function $p(t,x)$ are governed by general equations of the form

$$A_n \frac{\partial^{\beta_n}}{\partial t^{\beta_n}} p(t,x) + \cdots + A_0 \frac{\partial^{\beta_0}}{\partial t^{\beta_0}} p(t,x) = \mathcal{A} p(t,x),$$

where $\beta_n, \ldots, \beta_0 \in (0, 1]$ and $\mathcal{A}$ is the infinitesimal generator of a Lévy process. The Riesz–Bessel operator $(I-\Delta)^{\frac{\gamma}{2}}(-\Delta)^{\frac{\alpha}{2}}$ is a special case of $\mathcal{A}$. Hence, this motivates us considering equations of the form (1) containing the Caputo–Djrbashian derivative in this work. On the other hand, it might come natural to add just a additive Gaussian space-time white noise $\dot{W}(t,x)$ to the deterministic counterparts of Equation (1) and study the equation

$$\begin{cases} \left(\frac{\partial^\beta}{\partial t^\beta} + \nu(\mathrm{I}-\Delta)^{\gamma/2}(-\Delta)^{\alpha/2} \right) u(t,x) = \dot{W}(t,x), \\ u(0,x) = u_0(x), \quad x \in \mathbb{R}^d, \end{cases} \tag{3}$$

Hence, if we use time fractional Duhamel's principle (see, for example, [17]), we will get the mild (integral) solution of (1) to be of the form (informally):

$$u(t,x) = (\mathcal{G}u_0)_t(x) + \int_0^t \int_{\mathbb{R}^d} G_{t-s}(x-y) \frac{\partial^{1-\beta}}{\partial s^{1-\beta}} (\dot{W}(s,y)) dy dr, \tag{4}$$

where

$$(\mathcal{G}u_0)_t(x) = \int_{\mathbb{R}^d} G_t(x-y) u_0(y) dy.$$

It is not clear what the fractional derivative $\frac{\partial^{1-\beta}}{\partial s^{1-\beta}}\left(\dot{W}(s,y)\right)$ means. As explained in [18,19] and etc., one can remove the fractional derivative of the noise term in (4) in the following way. For $\beta \in (0,1)$, define the fractional integral operator $I_t^{1-\beta}$ as follows:

$$I_t^{1-\beta}u(t,x) := \frac{1}{\Gamma(1-\beta)}\int_0^t \frac{u(s,x)}{(t-r)^{\beta}}ds, \quad \beta \in (0,1).$$

Note that (see, for example, [18] and etc.), for every $\beta \in (0,1)$ and $g \in L^{\infty}(\mathbb{R}_+)$ or $g \in C(\mathbb{R}_+)$, $\partial_t^{\beta} I_t^{\beta} g(t) = g(t)$. Then, by using the fractional Duhamel's principle, mentioned above, the mild (integral) solution of Equation (3) will be (informally)

$$u(t,x) = (\mathcal{G}u_0)_t(x) + \int_0^t \int_{\mathbb{R}^d} G_{t-s}(x-y)W(ds,dy). \tag{5}$$

The time-fractional SPDEs (1) studied in this paper with $\gamma = 0$ may arise naturally by considering the heat equation in a material with thermal memory; see, for example, [12,18,19], etc.

The fractional SPDEs represent a combination of the deterministic fractional equations and the stochastic integration theory developped by Walsh (see [20], see also Dalang's seminal paper [21]). Several types of fractional SPDEs have been considered in Chen [10], Chen et al. [11], Chen et al. [22], Kim and Kim [12], Chen et al. [23], Foondun and Nane [24], Hu and Hu [25], Liu and Yan [26], Márquez-Carreras [15,16], Mijena and Nane [18,19], and references therein.

In this work, we are interested in space-time fractional SPDEs (1). It includes some widely studied particular cases. We refer, for example, to the classical stochastic heat equation with $\beta = 1$, $\gamma = 0$ and $\alpha = 2$ (see, e.g., Dalang [21], Khoshnevisan [27]), the fractional stochastic heat equation with $\beta = 1$, $\gamma = 0$ and $\alpha > 0$ (see examples Chen and Dalang [28,29], Foondun and Nane [24], Márquez-Carreras [16], Tudor [30]), the generalized fractional kinetic equation with $\beta = 0$, $\gamma \geq 0$ and $\alpha > 0$ (see [15]), the space-time fractional stochastic partial differential equation with $0 < \beta < 1$, $\gamma = 0$ and $0 < \alpha \leq 2$ (see [18,19]).

Our paper is motivated by the works of Anh and Leonenko [2], Márquez-Carreras [16], and Mijena and Nane [18,19]. We generalize the results of Márquez-Carreras [16] to the fractional-in-time diffusion equation and of Mijena and Nane [18] to fractional operator including Bessel operator $(I-\Delta)^{\gamma/2}$, which is essential for a study of (asymptotically) stationary solutions of Equation (1) (see Anh and Leonenko [2] for some details).

To be more precise, the novelty of this paper is that we extend the result in [15,18,31] by including in the model the Bessel operator $(I-\Delta)^{\frac{\gamma}{2}}$ with $\gamma \geq 0$ and by generalizing the stochastic noise, in the sense that we allow a more general structure for the spatial covariance of the Gaussian noise W in (1) (which is taken to be space-time white noise in [18] and colored by a Riesz kernel in space in [31]). The presence of this Bessel operator brings more flexibility to the model, by including for $\gamma = 0$ the situation treated in [15,18,31]. From the technical point of view, the appearance of the Bessel operator leads to a new expression of the fundamental solution associated with Equation (1). Indeed, we need new technical estimates for this kernel, which are obtained in Section 2.2. The Bessel operator is also essential in order to get an asymptotically stationary solution, as discussed in Section 4 of our work. Concretely, we study the existence and uniqueness of the solution to Equation (1) under global Lipschitz conditions on diffusion coefficient σ by using the random field approach of Walsh [20] and time fractional Duhamel's principle (see, e.g., [17,18]). Moreover, we study some new properties for the solution to time-space fractional SPDE (1), including an upper bound of the second moment, the Hölder regularity in time and space variables, and the (asymptotically) stationarity of the solution with respect to time and space variables in some particular case.

We organize this paper as follows: In Section 2, we introduce the Gaussian noise $\dot{W}(t,x)$, and we prove some properties of Green function $G_t(x)$ associated with the fractional heat type Equation (13). In Section 3, we give our main result about existence and

uniqueness of the solution and some properties of the solution, including the Hölder regularity and the behavior of the second moment. In Section 4, we study the linear additive case, with zero initial condition, i.e., $u_0(x) \equiv 0$ and $\sigma(x) \equiv 1$. We see that the solution of (1) is a Gaussian field with zero mean, with stationary increments, and a continuous covariance function in space, while it is not stationary in time but tends to a stationary process when the time goes to infinity.

2. Preliminaries

In this section, we recall some basic properties of the stochastic integral with respect to the Gaussian noise $\dot{W}$ appearing in Equation (1) and some basic facts on the solution to the fractional heat Equation (13).

2.1. Gaussian Noise

We denote by $C_0^\infty(\mathbb{R}_+ \times \mathbb{R}^d)$ the space of infinitely differentiable functions on $\mathbb{R}_+ \times \mathbb{R}^d$ with compact support and by $\mathcal{S}(\mathbb{R}^d)$ the Schwartz space of rapidly decreasing C^∞ functions in $\mathbb{R}^d$ and let $\mathcal{S}'(\mathbb{R}^d)$ denote its dual space of rapidly decreasing infinitely differentiable functions on $\mathbb{R}^d$. For $\varphi \in L^1(\mathbb{R}^d)$, we let $\mathcal{F}\varphi$ be the Fourier transform of φ defined by

$$\mathcal{F}\varphi(\xi) = \int_{\mathbb{R}^d} e^{-\mathrm{i}\xi\cdot x}\varphi(x)dx, \quad \xi \in \mathbb{R}^d. \tag{6}$$

We begin by introducing the framework in [21]. Let μ be a non-negative tempered measure on $\mathbb{R}^d$, i.e., a non-negative measure which satisfies:

$$\int_{\mathbb{R}^d} \left(\frac{1}{1+|\xi|^2}\right)^m \mu(d\xi) < \infty, \tag{7}$$

for some $m > 0$. Since the integrand is non-increasing in m, we may assume that $m \geq 1$ is an integer. Note that $1 + |\xi|^2$ behaves like a constant around 0, and like $|\xi|^2$ at ∞, and hence (7) is equivalent to

$$\int_{|\xi|\leq 1} \mu(d\xi) < \infty \quad \text{and} \quad \int_{|\xi|\geq 1} \frac{1}{|\xi|^{2m}}\mu(d\xi) < \infty,$$

for some integer $m \geq 1$.

Let $f : \mathbb{R}^d \to \mathbb{R}_+$ be the Fourier transform of a non-negative tempered measure μ in $\mathcal{S}'(\mathbb{R}^d)$, which is

$$\int_{\mathbb{R}^d} f(x)\varphi(x)dx = \int_{\mathbb{R}^d} \mathcal{F}\varphi(\xi)\mu(d\xi), \quad \forall \varphi \in \mathcal{S}(\mathbb{R}^d),$$

where $\mathcal{F}$ denotes the Fourier transform given by (6). Simple properties of the Fourier transform yield that, for any $\phi, \varphi \in \mathcal{S}(\mathbb{R}^d)$

$$\int_{\mathbb{R}^d}\int_{\mathbb{R}^d} \varphi(x)f(x-y)\phi(y)dxdy = \int_{\mathbb{R}^d} \mathcal{F}\varphi(\xi)\overline{\mathcal{F}\phi(\xi)}\mu(d\xi), \quad \forall \varphi, \phi \in \mathcal{S}(\mathbb{R}^d). \tag{8}$$

An approximation argument shows that the previous equality also holds for indicator functions $\varphi = 1_A$ and $\phi = 1_B$ with $A, B \in \mathcal{B}_b(\mathbb{R}^d)$, where $\mathcal{B}_b(\mathbb{R}^d)$ denotes the class of bounded Borel sets of $\mathbb{R}^d$, which is

$$\int_A\int_B f(x-y)dxdy = \int_{\mathbb{R}^d} \mathcal{F}1_A(\xi)\overline{\mathcal{F}1_B(\xi)}\mu(d\xi). \tag{9}$$

In this article, we consider a zero-mean Gaussian process $W = \{W(t, A); t \in [0, T], A \in \mathcal{B}_b(\mathbb{R}^d)\}$ with covariance

$$\mathbf{E}(W(t, A)W(s, B)) = (t \wedge s)\int_A\int_B f(x-y)dxdy,$$

on a complete probability space $(\Omega, \mathcal{F}, P)$.

Let $\mathcal{E}$ be the set of linear combinations of elementary functions $\{1_{[0,t]\times A}, t \geq 0, A \in \mathcal{B}_b(\mathbb{R}^d)\}$. With the Gaussian process W, we can associate a canoncial Hilbert space $\mathcal{H}$ which is defined as the closure of $\mathcal{E}$ with respect to the inner product $\langle \cdot, \cdot \rangle_{\mathcal{H}}$ defined by

$$\langle \varphi, \phi \rangle_{\mathcal{H}} = \int_{\mathbb{R}_+} \int_{\mathbb{R}^d} \int_{\mathbb{R}^d} \varphi(t,x) f(x-y) \phi(t,y) dx dy dt.$$

Alternatively, $\mathcal{H}$ can be defined as the completion of $C_0^\infty(\mathbb{R}_+ \times \mathbb{R}^d)$ with respect to the inner product $\langle \cdot, \cdot \rangle_{\mathcal{H}}$.

We denote by $W(\varphi)$ the random field indexed by functions $\varphi \in L^2(\mathbb{R}_+ \times \mathbb{R}^d)$ and for all $\varphi, \phi \in L^2(\mathbb{R}_+ \times \mathbb{R}^d)$, we have

$$\begin{aligned} \mathbf{E}(W(\varphi)W(\phi)) &= \int_{\mathbb{R}_+} \int_{\mathbb{R}^d} \int_{\mathbb{R}^d} \varphi(t,x) f(x-y) \phi(t,y) dx dy dt \\ &= \int_{\mathbb{R}_+} \int_{\mathbb{R}^d} \mathcal{F}\varphi(t,\cdot)(\xi) \overline{\mathcal{F}\phi(t,\cdot)(\xi)} \mu(d\xi) dt, \end{aligned} \tag{10}$$

where $\mathcal{F}\varphi(t,\cdot)(\xi)$ denotes the Fourier transform with respect to the space variable of $\varphi(t,x)$ only. Hence, $W(\varphi)$ can be represented as

$$W(\varphi) = \int_{\mathbb{R}_+} \int_{\mathbb{R}^d} \varphi(t,x) W(dx, dt).$$

Note that $W(\varphi)$ is $\mathcal{F}_t$-measurable whenever φ is supported on $[0,t] \times \mathbb{R}^d$.

Remark 1. *Since the spectral measure μ is non-trivial positive tempered measure, we can ensure that there exist positive constants c_1, c_2 and k such that*

$$c_1 < \int_{\{|\xi|<k\}} \mu(d\xi) < c_2. \tag{11}$$

As usual, the Gaussian process W can be extended to a *worthy martingale measure*, in the sense given by Walsh [20]. Dalang [21] presented an extension of Walsh's stochastic integral that requires the following integrability condition in terms of the Fourier transform of G

$$\int_0^T dt \int_{\mathbb{R}^d} \mu(d\xi) |\mathcal{F}G_t(\cdot)(\xi)|^2 < \infty, \tag{12}$$

where G is the fundamental solution of

$$\left(\frac{\partial^\beta}{\partial t^\beta} + \nu(I-\Delta)^{\gamma/2}(-\Delta)^{\alpha/2} \right) G_t(x) = 0. \tag{13}$$

Provided that (12) is satisfied and assuming conditions on $\sigma(\cdot)$ that will be described later, following Walsh [20], we will understand a solution of (1) to be a jointly measurable adapted process $\{u(t,x), (t,x) \in [0,T] \times \mathbb{R}^d\}$ satisfying the integral equation

$$u(t,x) = (\mathcal{G}u_0)_t(x) + \lambda \int_0^t \int_{\mathbb{R}^d} G_{t-s}(x-y) \sigma(u(s,y)) W(ds, dy), \tag{14}$$

where

$$(\mathcal{G}u_0)_t(x) = \int_{\mathbb{R}^d} G_t(x-y) u_0(y) dy,$$

and the stochastic integral in (14) is defined with respect to the $\mathscr{F}$-martingale measure $W(t,A)$. Next, we give the meaning of Walsh–Dalang integrals that is used in (14). (For the details, we refer the readers to Dalang [21]).

1. We say that $(t,x) \to \Phi_t(x)$ is an elementary random field when there exist $0 \leq a < b$, a $\mathcal{F}_a$-measurable random variable $X \in L^2(\Omega)$ and a deterministioc function $\phi \in L^2(\mathbb{R}^d)$ such that
$$\Phi_t(x) = X1_{[a,b)}(t)\phi(x), \quad t > 0, x \in \mathbb{R}^d.$$
2. If $h = h_t(x)$ is non-random and Φ is elementary as above, then we set
$$\int h\Phi dW := X \int_{[a,b)\times\mathbb{R}^d} h_t(x)\phi(x)W(dt,dx). \tag{15}$$
3. The stochastic integral in (15) is a Wiener integral, and it is well defined if and only if $h_t(x)\phi(x) \in L^2([a,b)\times\mathbb{R}^d)$.
4. Under the above notation, we have the Walsh isometry
$$\mathbf{E}\left(\left|\int h\Phi dW\right|^2\right) = \int_0^T ds \int_{\mathbb{R}^d} dy h_s(y)^2 \mathbf{E}(|\Phi_s(y)|^2).$$

2.2. Some Properties of the Fundamental Solution

We will give some estimates for the fundamental solution associated with Equation (1). The properties of this fundamental solution will play an important role in the sequel.

Let $G_t(x)$ be the fundamental solution of the fractional kinetic Equation (13) with $\beta \in (0,1], \nu > 0$, and $\gamma \geq 0, \alpha > 0$. Anh and Leonenko [2] showed that Equation (13) is equivalent to the Cauchy problem:
$$(\mathscr{D}_t^\beta \mathcal{F}G_t(\cdot))(\xi) + \nu|\xi|^\alpha(1+|\xi|^2)^{\gamma/2}\mathcal{F}G_t(\cdot)(\xi) = 0, \quad \mathcal{F}G_0(\cdot))(\xi) = 1 \tag{16}$$
and they also have proved that Equation (16) has a unique solution given by
$$\mathcal{F}G_t(\cdot)(\xi) = E_\beta(-\nu t^\beta|\xi|^\alpha(1+|\xi|^2)^{\gamma/2}), \quad \beta > 0, \tag{17}$$
where
$$E_\beta(x) = \sum_{j=0}^{\infty} \frac{x^j}{\Gamma(1+\beta j)}, \quad x > 0, \tag{18}$$
is the Mittag–Leffler function of order β. The inverse Fourier transform yields that
$$G_t(x) = (2\pi)^{-d} \int_{\mathbb{R}^d} e^{\mathrm{i}\langle\xi,x\rangle} E_\beta(-\nu t^\beta|\xi|^\alpha(1+|\xi|^2)^{\gamma/2}) d\xi. \tag{19}$$

We know that
$$E_\beta(-\nu t^\beta|\xi|^\alpha(1+|\xi|^2)^{\gamma/2}) \in L^1(\mathbb{R}^d), \tag{20}$$
for every $0 < \beta \leq 1$ if $\alpha + \gamma > d$. From this range, we see the role played by the parameter γ in Equation (17).

Moreover, one has the uniform estimates of the Mittag–Leffler function (e.g., Theorem 4 in Simon [32])
$$\frac{1}{1+\Gamma(1-\beta)x} \leq E_\beta(-x) \leq \frac{1}{1+\Gamma(1+\beta)^{-1}x}, \quad \text{for} \quad x > 0. \tag{21}$$

The following lemma gives a sharp estimate for the L^2-norm (in time) of the Green kernel. It extends Lemma 1 in [18] and Lemma 2.1 in [31].

Lemma 1. *For $0 < \beta < 1$ and $d < 2(\alpha+\gamma)$, we have the following*
$$\int_{\mathbb{R}^d} G_t(x)^2 dx \leq C_2 t^{-\frac{\beta d}{\alpha+\gamma}}. \tag{22}$$

where $B\Big(\frac{d}{\alpha+\gamma}, 2-\frac{d}{\alpha+\gamma}\Big)$ *is a Beta function. The (strictly) positive constant is given by* $C_2 = \frac{B\Big(\frac{d}{\alpha+\gamma}, 2-\frac{d}{\alpha+\gamma}\Big)}{\alpha+\gamma}\Big(\frac{\Gamma(1-\beta)}{\nu}\Big)^{\frac{d}{\alpha+\gamma}}\frac{2\pi^{d/2}}{\Gamma(d/2)}\frac{1}{(2\pi)^d}$.

Proof. Using the Plancherel's identity and the equality (17), we can write

$$\begin{aligned}\int_{\mathbb{R}^d} G_t(x)^2 dx &= \frac{1}{(2\pi)^d}\int_{\mathbb{R}^d} |\mathcal{F}G_t(\cdot)(\xi)|^2 d\xi \\ &= \frac{1}{(2\pi)^d}\int_{\mathbb{R}^d}\Big|E_\beta\Big(-\nu t^\beta |\xi|^\alpha (1+|\xi|^2)^{\gamma/2}\Big)\Big|^2 d\xi \\ &= \frac{2\pi^{d/2}}{\Gamma(d/2)}\frac{1}{(2\pi)^d}\int_0^{+\infty} r^{d-1}\Big(E_\beta\Big(-\nu t^\beta r^\alpha (1+r^2)^{\gamma/2}\Big)\Big)^2 dr,\end{aligned}$$

where we have used the integration in polar coordinates in the last equation above and the positive constant resulting from the integration over the angular spherical coordinates. Now using the upper bound in (21) and the fact $r^\alpha(1+r^2)^{\gamma/2} \geq r^{\alpha+\gamma}$ with $r>0$, we obtain, with the change of variable formula $z = \Gamma(1+\beta)^{-1}\nu t^\beta r^{\alpha+\gamma}$,

$$\begin{aligned}\int_0^{+\infty} r^{d-1}\Big(E_\beta\Big(-\nu t^\beta r^\alpha (1+r^2)^{\gamma/2}\Big)\Big)^2 dr &\leq \int_0^{+\infty} r^{d-1}\frac{1}{(1+\Gamma(1+\beta)^{-1}\nu t^\beta r^{\alpha+\gamma})^2}dr \\ &= \frac{1}{\alpha+\gamma}\Big(\frac{\Gamma(1+\beta)}{\nu}\Big)^{\frac{d}{\alpha+\gamma}} t^{-\frac{\beta d}{\alpha+\gamma}}\int_0^\infty z^{\frac{d}{\alpha+\gamma}-1}(1+z)^{-2}dz.\end{aligned}$$

Hence, $\int_0^\infty z^{\frac{d}{\alpha+\gamma}}(1+z)^{-2}dz < \infty$ if and only if $d < 2(\alpha+\gamma)$. In this case, we have

$$\int_0^\infty z^{\frac{d}{\alpha+\gamma}-1}(1+z)^{-2}dz = B\Big(\frac{d}{\alpha+\gamma}, 2-\frac{d}{\alpha+\gamma}\Big),$$

where $B\Big(\frac{d}{\alpha+\gamma}, 2-\frac{d}{\alpha+\gamma}\Big)$ is a Beta function. Then, we can conclude the proof of upper bound in (22). □

We now prove (12) under an integrability condition on the spectral measure μ given as follows, which is also known as the Dalang's condition (see, for example, [21]).

Hypothesis 1. *Assume that the spectral measure* μ *associated with the Gaussian noise* $\dot{W}$ *satisfies*

$$\int_{\mathbb{R}^d}\Big(\frac{1}{1+|\xi|^2}\Big)^\varrho \mu(d\xi) < \infty, \tag{23}$$

with the parameter ϱ *satisfying*

$$\varrho = \begin{cases}\alpha+\gamma, & \text{if} \quad 0<\beta<\frac{1}{2},\\ \frac{\alpha+\gamma}{2}, & \text{if} \quad \beta=\frac{1}{2},\\ \frac{\alpha+\gamma}{2\beta}, & \text{if} \quad \frac{1}{2}<\beta<1.\end{cases} \tag{24}$$

Remark 2. *If the parameter* $\beta = 1$, *Equation (1) reduces to the SPDE (1.1) studied in Márquez-Carreras [15], in which it is assumed (23) with* $\varrho = \frac{\alpha+\gamma}{2}$. *Thus, when* β *is close to one, the exponent* ϱ *in (24) coincides with the exponent studied in Lemma 2.1 in Márquez-Carreras [15]. On the other hand, our assumption (23) is weaker when* β *is close to zero.*

Let us now recall some of the main examples of spatial covariances for the noise which will be our guiding examples in the remainder of the present paper. Below, we denote by $|x|$ the Euclidean norm of $x \in \mathbb{R}^d$.

Example 1. *Let* $f(x) = \prod_{i=1}^{d} H_i(2H_i-1)|x_i|^{2H_i-2}$ *with* $1/2 < H_i < 1$ *for* $i = 1, \dots, d$. *Then,* $\mu(d\xi) = \prod_{i=1}^{d} H_i(2H_i-1)|\xi_i|^{-2H_i+1}d\xi$. *Thus, (23) is equivalent to* $\sum_{i=1}^{d}(2H_i-1) > d-2(\alpha+\gamma)$ *if* $0 < \beta < 1/2$, *it is equivalent to* $\sum_{i=1}^{d}(2H_i-1) > d-(\alpha+\gamma)$ *if* $\beta = 1/2$ *and when* $1/2 < \beta < 1$, *the condition (23) is equivalent to* $\sum_{i=1}^{d}(2H_i-1) > d-\frac{\alpha+\gamma}{\beta}$.

Example 2. *Let* $f(x) = \gamma_{\delta,d} = |x|^{-(d-\delta)}$ *be the Riesz kernel of order* $\delta \in (0,d)$, *then* $\mu(d\xi) = |\xi|^{-\delta}d\xi$ *and (23) is equivalent to* $2(\alpha+\gamma)+\delta > d$ *if* $0 < \beta < 1/2$, *(23) is equivalent to* $(\alpha+\gamma)+\delta > d$ *if* $\beta = 1/2$ *and (23) is equivalent to* $\frac{\alpha+\gamma}{\beta}+\delta > d$ *if* $1/2 < \beta < 1$. *This example is also considered in [31]. Their condition (used in Theorem 1.3 in this reference) reads* $\frac{\alpha}{\beta}+\delta > d$. *Our assumption (23) gives more flexibility when* β *is close to zero but as well as for* β *close to 1 (because of the new parameter* γ *in the expression of the Bessel operator* $(I-\Delta)^{\frac{\gamma}{2}}$.

Example 3. *For the Bessel kernel of order* $\tau > 0$ *given by* $f(x) = \gamma_\tau \int_0^\infty \omega^{\frac{\tau-d}{2}-1}e^{-\omega}e^{-\frac{|x|^2}{4\omega}}d\omega$. *Then,* $\mu(d\xi) = (1+|\xi|^2)^{-\frac{\tau}{2}}d\xi$. *Thus, (23) is equivalent to* $2(\alpha+\gamma)+\tau > d$ *if* $0 < \beta < 1/2$, *(23) is equivalent to* $(\alpha+\gamma)+\tau > d$ *if* $\beta = 1/2$ *and condition (23) is equivalent to* $\frac{\alpha+\gamma}{\beta}+\tau > d$ *if* $1/2 < \beta < 1$.

Example 4. *Let* $f(0) < \infty$ *(i.e.,* μ *is a finite measure). It corresponds to a spatially smooth noise* $\dot{W}$.

Example 5. *Suppose* $d = 1$ *and* $f = \delta_0$ *(i.e.,* μ *is the Lebesgue measure). This corresponds to a (rougher) noise* $\dot{W}$, *which is white in the spatial variable.*

For any $t \in \mathbb{R}_+$, denote by

$$N_t(\xi) = \int_0^t |\mathcal{F}G_u(\cdot)(\xi)|^2 du. \tag{25}$$

Then, we have the following

Proposition 1. *Assuming that* $t \in \mathbb{R}_+$ *and* $\xi \in \mathbb{R}^d$, *there exist (strictly) positive constants* $C_{2.i}(t), i = 1,2,3,4$ *(depending on t) such that*

$$N_t(\xi) \le C_{2.2}(t)\left(\frac{1}{1+|\xi|^2}\right)^{\alpha+\gamma}, \quad \text{if} \quad 0 < \beta < 1/2, \tag{26}$$

$$N_t(\xi) \le C_{2.3}(t)\left(\frac{1}{1+|\xi|^2}\right)^{\frac{\alpha+\gamma}{2}}, \quad \text{if} \quad \beta = 1/2, \tag{27}$$

and

$$N_t(\xi) \le C_{2.4}(t)\left(\frac{1}{1+|\xi|^2}\right)^{\frac{\alpha+\gamma}{2\beta}}, \quad \text{if} \quad 1/2 < \beta < 1. \tag{28}$$

The "constants" are defined as follows:

$$C_{2.2}(t) = t + \frac{2^{\alpha+\gamma}\Gamma(1+\beta)^2}{\nu^2(1-2\beta)}t^{1-2\beta},$$
$$C_{2.3}(t) = t + 2\nu^{-1}\Gamma(3/2)2^{\frac{\alpha+\gamma}{2}}t^{1/2},$$
$$C_{2.4}(t) = t + \frac{1}{2\beta-1}\Gamma(1+\beta)^{1/\beta}\nu^{-1/\beta}2^{\frac{\alpha+\gamma}{2\beta}}.$$

Proof. For any $t \in \mathbb{R}_+$, from Equations (17) and (25), we can rewrite $N_t(\xi)$ defined by (25) as

$$N_t(\xi) = \int_0^t \left| E_\beta(-\nu u^\beta |\xi|^\alpha (1+|\xi|^2)^{\gamma/2}) \right|^2 du.$$

We firstly prove the upper bound for $N_t(\xi)$. By using the upper bound in (21) and change of variable $x = \nu u^\beta |\xi|^\alpha (1+|\xi|^2)^{\gamma/2}$, one obtains

$$N_t(\xi) = \frac{1}{\beta}\left(\frac{1}{\nu|\xi|^\alpha(1+|\xi|^2)^{\gamma/2}}\right)^{\frac{1}{\beta}} \int_0^{\nu t^\beta |\xi|^\alpha (1+|\xi|^2)^{\gamma/2}} x^{\frac{1}{\beta}-1} E_\beta^2(-x)dx.$$

We will divide into two cases to estimate it according to the value of $|\xi|$. If $|\xi| \le 1$, and we claim that

$$\begin{aligned} N_t(\xi)1_{|\xi|\le 1} &\le \frac{1}{\beta}\left(\frac{1}{\nu|\xi|^\alpha(1+|\xi|^2)^{\gamma/2}}\right)^{\frac{1}{\beta}} \int_0^{\nu t^\beta |\xi|^\alpha (1+|\xi|^2)^{\gamma/2}} x^{\frac{1}{\beta}-1}\left(\frac{1}{1+\Gamma(1+\beta)^{-1}x}\right)^2 dx \\ &= t. \end{aligned}$$

If $|\xi| > 1$ and $1/2 < \beta < 1$, we have

$$\begin{aligned} N_t(\xi)1_{|\xi|>1} &\le \frac{1}{\beta}\left(\frac{1}{\nu|\xi|^\alpha(1+|\xi|^2)^{\gamma/2}}\right)^{\frac{1}{\beta}} \int_0^{\nu t^\beta |\xi|^\alpha (1+|\xi|^2)^{\gamma/2}} x^{\frac{1}{\beta}-1}\left(\frac{1}{1+\Gamma(1+\beta)^{-1}x}\right)^2 dx \\ &= \frac{1}{\beta}\left(\frac{\Gamma(1+\beta)}{\nu|\xi|^\alpha(1+|\xi|^2)^{\gamma/2}}\right)^{\frac{1}{\beta}} \int_0^{\nu\Gamma(1+\beta)^{-1}t^\beta |\xi|^\alpha (1+|\xi|^2)^{\gamma/2}} x^{\frac{1}{\beta}-1}(1+x)^{-2}dx \\ &\le \frac{1}{\beta}\left(\frac{\Gamma(1+\beta)}{\nu|\xi|^\alpha(1+|\xi|^2)^{\gamma/2}}\right)^{\frac{1}{\beta}} \int_0^{\nu\Gamma(1+\beta)^{-1}t^\beta |\xi|^\alpha (1+|\xi|^2)^{\gamma/2}} (1+x)^{\frac{1}{\beta}-3}dx \\ &\le \frac{1}{2\beta-1}\left(\frac{\Gamma(1+\beta)}{\nu}\right)^{\frac{1}{\beta}}\left(\frac{1}{|\xi|^\alpha(1+|\xi|^2)^{\gamma/2}}\right)^{\frac{1}{\beta}} \\ &\le \frac{1}{2\beta-1}\left(\frac{\Gamma(1+\beta)}{\nu}\right)^{\frac{1}{\beta}} 2^{\frac{\alpha+\gamma}{2\beta}}\left(\frac{1}{1+|\xi|^2}\right)^{\frac{\alpha+\gamma}{2\beta}}. \end{aligned}$$

On the other hand, with $|\xi| > 1$ and $0 < \beta < 1/2$, one obtains

$$\begin{aligned} N_t(\xi)1_{|\xi|>1} &\le \frac{1}{\beta}\left(\frac{\Gamma(1+\beta)}{\nu|\xi|^\alpha(1+|\xi|^2)^{\gamma/2}}\right)^{\frac{1}{\beta}} \int_0^{\nu\Gamma(1+\beta)^{-1}t^\beta |\xi|^\alpha (1+|\xi|^2)^{\gamma/2}} x^{\frac{1}{\beta}-3}dx \\ &= \frac{\Gamma(1+\beta)^2}{\nu^2(1-2\beta)}t^{1-2\beta}\left(\frac{1}{\nu|\xi|^\alpha(1+|\xi|^2)^{\gamma/2}}\right)^2 \\ &\le \frac{2^{\alpha+\gamma}\Gamma(1+\beta)^2}{\nu^2(1-2\beta)}t^{1-2\beta}\left(\frac{1}{1+|\xi|^2}\right)^{\alpha+\gamma}. \end{aligned}$$

For the critical case $\beta = 1/2$, one obtains that

$$\begin{aligned} N_t(\xi)1_{|\xi|>1} &\le 2\left(\frac{\Gamma(3/2)}{\nu|\xi|^\alpha(1+|\xi|^2)^{\gamma/2}}\right)^2 \int_0^{\nu\Gamma(3/2)^{-1}t^{1/2}|\xi|^\alpha(1+|\xi|^2)^{\gamma/2}} x(1+x)^{-2}dx \\ &\le 2\left(\frac{\Gamma(3/2)}{\nu|\xi|^\alpha(1+|\xi|^2)^{\gamma/2}}\right)^2 \int_0^{\nu\Gamma(3/2)^{-1}t^{1/2}|\xi|^\alpha(1+|\xi|^2)^{\gamma/2}} (1+x)^{-1}dx \\ &= 2\left(\frac{\Gamma(3/2)}{\nu|\xi|^\alpha(1+|\xi|^2)^{\gamma/2}}\right)^2 \ln\left(1+\nu\Gamma(3/2)^{-1}t^{1/2}|\xi|^\alpha(1+|\xi|^2)^{\gamma/2}\right) \\ &\le 2\nu^{-1}\Gamma(3/2)t^{1/2}2^{\frac{\alpha+\gamma}{2}}\left(\frac{1}{1+|\xi|^2}\right)^{\frac{\alpha+\gamma}{2}}. \end{aligned}$$

Then, combining the above estimates for $N_t(\xi)$ with $|\xi| \le 1$ and $|\xi| > 1$, respectively, we can conclude the proof of bounds (26)–(28). □

Remark 3. *From the above result, we see that Hypothesis 1 implies condition (12). In particular, the estimates (26)–(28) give the existence of the solution in the linear additive noise cas ($\sigma = 1$).*

3. Existence and Uniqueness

In this section, we will prove the existence and uniqueness of the mild solution to Equation (14). We first introduce a stronger integrability condition on the spectral measure μ than Hypothesis 1. While the existence and uniqueness of the solution can be obtained under Hypothesis 1, the new assumption presented below will be needed in order to prove certain properties of the solution.

Hypothesis 2. *Assume that the spectral measure μ associated with $\dot{W}$ satisfies*

$$\int_{\mathbb{R}^d}\left(\frac{1}{1+|\xi|^2}\right)^\eta \mu(d\xi) < \infty, \tag{29}$$

with some parameter η satisfying

$$\eta \in \begin{cases} (0, \alpha+\gamma), & \text{if} \quad 0 < \beta < \dfrac{1}{2}, \\ \left(0, \dfrac{\alpha+\gamma}{2}\right), & \text{if} \quad \beta = \dfrac{1}{2}, \\ \left(0, \dfrac{\alpha+\gamma}{2\beta}\right), & \text{if} \quad \dfrac{1}{2} < \beta < 1. \end{cases} \tag{30}$$

We will need the following estimates for the Green function given by (19) (their proof is given in Appendix A.

Proposition 2. *Supposing $\beta \in (0,1)$, then we have the following estimates for the temporal and spatial increments of the Green function $G_t(x)$ given by (19).*

1. *Under Hypothesis 1, for any $t, t' \in \mathbb{R}_+$ such that $t' < t$ and $x \in \mathbb{R}^d$, we have*

$$\int_0^{t'} ds \int_{\mathbb{R}^d} \mu(d\xi)|\mathcal{F}G_{t-s}(x-\cdot)(\xi) - \mathcal{F}G_{t'-s}(x-\cdot)(\xi)|^2 \le C_{3.1}|t-t'|^{2\beta}, \tag{31}$$

with $C_{3.1} = t^{1-2\beta}\int_{|\xi|\le 1}\mu(d\xi) + t^{-2\beta}\int_{|\xi|>1} N_{t'}(\xi)\mu(d\xi)$.

2. *Under Hypothesis 2, for any $t, t' \in \mathbb{R}_+$ such that $t' < t$ and $x \in \mathbb{R}^d$, we have*

$$\int_{t'}^{t} ds \int_{\mathbb{R}^d} \mu(d\xi) |\mathcal{F}G_{t-s}(x-\cdot)(\xi)|^2 \leq \begin{cases} C_{3.2}|t-t'|^{1-2\beta}, & \text{if } \ 0 < \beta < \frac{1}{2}, \\ C_{3.3}|t-t'|^{\frac{1}{2}}, & \text{if } \ \beta = \frac{1}{2}, \\ C_{3.4}|t-t'|, & \text{if } \ \frac{1}{2} < \beta < 1. \end{cases} \tag{32}$$

with

$$C_{3.2} = |t-t'|^{2\beta} \int_{|\xi|\leq 1} \mu(d\xi) + \frac{\Gamma(1+\beta)^2 2^{\alpha+\gamma}}{\nu^2(1-2\beta)} \int_{|\xi|>1} \left(\frac{1}{1+|\xi|^2}\right)^{\alpha+\gamma} \mu(d\xi),$$

$$C_{3.3} = \int_{|\xi|\leq 1} \mu(d\xi)|t-t'|^{\frac{1}{2}} + 2^{1+\frac{\alpha+\gamma}{2}} \frac{\Gamma(3/2)}{\nu} \int_{|\xi|>1} \left(\frac{1}{1+|\xi|^2}\right)^{\frac{\alpha+\gamma}{2}} \mu(d\xi),$$

$$C_{3.4} = \int_{|\xi|\leq 1} \mu(d\xi) + \frac{c}{2\beta-1} \left(\frac{\Gamma(1+\beta)}{\nu}\right)^{\frac{1}{\beta}} 2^{\frac{\alpha+\gamma}{2\beta}} \int_{|\xi|>1} \left(\frac{1}{1+|\xi|^2}\right)^{\frac{\alpha+\gamma}{2\beta}} \mu(d\xi).$$

3. *Under Hypothesis 2, for any $t \in \mathbb{R}_+$ and $x, x' \in \mathbb{R}^d$, $\rho_1 \in (0, \alpha+\gamma-\eta)$, $\rho_2 \in \left(0, \frac{\alpha+\gamma}{2} - \eta\right)$ and $\rho_3 \in \left(0, \frac{\alpha+\gamma}{2\beta} - \eta\right)$, we have*

$$\int_0^t ds \int_{\mathbb{R}^d} \mu(d\xi) \left|\mathcal{F}G_{t-s}(x-\cdot)(\xi) - \mathcal{F}G_{t-s}(x'-\cdot)(\xi)\right|^2 \leq \begin{cases} C_{3.5}|x'-x|^{2\rho_1}, & \text{if } \ 0 < \beta < \frac{1}{2}, \\ C_{3.6}|x'-x|^{2\rho_2}, & \text{if } \ \beta = \frac{1}{2}, \\ C_{3.7}|x'-x|^{2\rho_3}, & \text{if } \ \frac{1}{2} < \beta < 1. \end{cases} \tag{33}$$

with

$$C_{3.5} = Ct \int_{|\xi|\leq 1} \mu(d\xi) + C\frac{t^{1-2\beta}}{1-2\beta} \left(\frac{\Gamma(1+\beta)}{\nu}\right)^2 2^{\alpha+\gamma-\rho_1} \int_{|\xi|>1} \left(\frac{1}{1+|\xi|^2}\right)^{\alpha+\gamma-\rho_1} \mu(d\xi),$$

$$C_{3.6} = Ct \int_{|\xi|\leq 1} \mu(d\xi) + C2^{1+\frac{\alpha}{2}-\rho_2} t^{\frac{1}{2}} \frac{\Gamma(3/2)}{\nu} \int_{|\xi|>1} \left(\frac{1}{1+|\xi|^2}\right)^{\frac{\alpha+\gamma}{2}-\rho_2} \mu(d\xi),$$

$$C_{3.7} = Ct \int_{|\xi|\leq 1} \mu(d\xi) + C\frac{1}{2\beta-1} \left(\frac{\Gamma(1+\beta)}{\nu}\right)^{\frac{1}{\beta}} 2^{\frac{\alpha+\gamma}{2\beta}-\rho_3} \int_{|\xi|>1} \left(\frac{1}{1+|\xi|^2}\right)^{\frac{\alpha+\gamma}{2\beta}-\rho_3} \mu(d\xi).$$

Notice that all the constants depend on t although we omit it in the notation.

Remark 4.

1. *Our results of Proposition 2 extend the results in Mijena and Nane [18] to the space-time fractional SPDE with colored Gaussian noises and Khoshnevisan [27] to space-time fractional SPDE, respectively.*
2. *The above Proposition 2 also extends the results in Márquez-Carreras [15,16] to space-time fractional kinetic equation with spatially homogeneous Gaussian noise.*

Let us introduce some additional conditions that we need in order to prove our main results. The first condition is required for the existence-uniqueness result as well as for the upper bound on the second moment of the solution.

Assumption 1.

1. *We assume that the initial condition is a non-random bounded non-negative function* $u_0 : \mathbb{R}^d \to \mathbb{R}$.
2. *We assume that* $\sigma : \mathbb{R}^d \to \mathbb{R}^d$ *is Lipschitz continuous satisfying* $|\sigma(x)| \leq L_\sigma|x|$ *with* L_σ *being a positive constant. Moreover, for all* $x, y \in \mathbb{R}^d$,

$$|\sigma(x) - \sigma(y)| \leq L_\sigma|x - y|. \tag{34}$$

We may assume, with loss of generality, that L_σ *is also greater than* $\sigma(0)$. *Since* $|\sigma(x)| \leq |\sigma(0)| + L_\sigma|x|$, *it follows that* $|\sigma(x)| \leq L_\sigma(1 + |x|)$ *for all* $x \in \mathbb{R}^d$.

Now, we can prove the existence and uniqueness of mild solution of Equation (1) given by (14).

Theorem 1. *Under Assumption 1 and assuming that the spectral measure* μ *satisfies Hypothesis 1, then Equation (14) has a unique adapted solution and for any* $t \in \mathbb{R}_+$ *and* $p \geq 1$,

$$\sup_{(t,x)\in\mathbb{R}_+\times\mathbb{R}^d} \mathbf{E}(|u(t,x)|^p) < \infty.$$

Moreover, this unique solution is mean-square continuous.

Proof. The proof of existence and uniqueness is standard based on Picard's iterations. For more information, see, e.g., Walsh [20], Dalang [21]. We give a sketch of the proof. Define

$$\begin{aligned} u^{(0)}(t,x) &= (\mathcal{G}u_0)_t(x), \\ u^{(n+1)}(t,x) &= (\mathcal{G}u_0)_t(x) + \lambda \int_0^t \int_{\mathbb{R}^d} G_{t-s}(x-y)\sigma(u^{(n)}(s,y))W(ds,dy), \quad n \geq 0. \end{aligned} \tag{35}$$

We could easily prove that the sequence $\{u^{(n+1)}(t,x), n \geq 0\}$ is well-defined and then using Burkholder's inequality, we can show that, for any $n \geq 0$ and $t \in \mathbb{R}_+$,

$$\sup_{(t,x)\in\mathbb{R}_+\times\mathbb{R}^d} \mathbf{E}(|u^{(n+1)}(t,x)|^2) < \infty. \tag{36}$$

Moreover, by using an extension of Gronwall's lemma (for example, see Lemma 15 in Dalang [21]),

$$\sup_{n\geq 0} \sup_{(t,x)\in\mathbb{R}_+\times\mathbb{R}^d} \mathbf{E}(|u^{(n+1)}(t,x)|^2) < \infty. \tag{37}$$

The same kind of arguments allow us to check (36) and (37), changing the power 2 for $p > 2$. Moreover, we can also prove that $\{u^{(n+1)}(t,x), n \geq 0\}$ converges uniformly in L^p, denoting this limit by $u(t,x)$. We can check that $u(t,x)$ satisfies Equation (14). Then, it is adapted and satisfies

$$\sup_{(t,x)\in\mathbb{R}_+\times\mathbb{R}^d} \mathbf{E}(|u(t,x)|^p) < \infty.$$

The uniqueness can be accomplished by a similar argument.

The key to the continuity is to show that these Picard iterations are mean-square continuous. Then, it can be easily extended to $u(t,x)$. In order to show the ideas of the mean-square continuity, we give some steps of the proof for $\{u^{(n+1)}(t,x), n \geq 0\}$. As for the time increments, we have, for any $(t,x) \in \mathbb{R}_+ \times \mathbb{R}^d$ and $\delta > 0$ such that $t + \delta \in \mathbb{R}_+$,

$$\begin{aligned}
&\mathbf{E}\Big[|u^{(n+1)}(t+\delta,x)-u^{(n+1)}(t,x)|^2\Big]\\
&\le \lambda^2\mathbf{E}\left[\left|\int_0^t\int_{\mathbb{R}^d}[G_{t+\delta-u}(x-y)-G_{t-u}(x-y)]\sigma(u^{(n)}(u,y))W(ds,dy)\right|^2\right]\\
&+\lambda^2\mathbf{E}\left[\left|\int_t^{t+\delta}\int_{\mathbb{R}^d}G_{t+\delta-u}(x-y)\sigma(u^{(n)}(u,y))W(ds,dy)\right|^2\right].
\end{aligned}\tag{38}$$

Using the conditions imposed on σ and (36), we can bound the first term in (38) by

$$C\int_0^t du\int_{\mathbb{R}^d}\mu(d\xi)|\mathcal{F}G_{t+\delta-u}(\cdot)(\xi)-\mathcal{F}G_{t-u}(\cdot)(\xi)|^2,$$

which converges to zero as $\delta\downarrow 0$ according to (31). The second term in (38) can be proved by using the similar arguments by using (32). This proves the right continuity. The left continuity can be proved in the same way.

Concerning the spatial increment, we have, for any $(t,x),(t,z)\in\mathbb{R}_+\times\mathbb{R}^d$,

$$\begin{aligned}
&\mathbf{E}\Big[|u^{(n+1)}(t,x)-u^{(n+1)}(t,z)|^2\Big]\\
&\le C\lambda^2\int_0^t du\int_{\mathbb{R}^d}\mu(d\xi)|\mathcal{F}G_{t-u}(x-\cdot)(\xi)-\mathcal{F}G_{t-u}(z-\cdot)(\xi)|^2\\
&\le C\lambda^2\int_0^t du\int_{\mathbb{R}^d}\mu(d\xi)|e^{\mathrm{i}\langle x-z,\xi\rangle}-1|^2|\mathcal{F}G_{t-u}(z-\cdot)(\xi)|^2.
\end{aligned}\tag{39}$$

Then, thanks to (33), we can prove that the right hand of (39) converges to zero as $|x-z|\downarrow 0$. □

Remark 5. *Let us recall that Equation (1) with $\beta=1$ (fractional in space stochastic kinetic equation with factorization of the Laplacian) has been studied by Márquez-Carreras [15]. In this case, the Mittag–Leffler function reduces to $E_1(-x)=e^{-x}, x\ge 0$.*

When $\gamma=0$ and spatial kernel $f(\cdot)$ is the Riesz kernel, then the Equation (1) reduces to the SPDEs studied in Mijena and Nane [18,19]. In this reference, the authors studied the existence, uniqueness, and intermittence of the mild solution for the space-time fractional stochastic partial differential Equations (1).

For $\gamma=0$ and $\alpha=2$, the SPDE (1) reduces to the classical stochastic heat equation studied by many authors; see, for example, Dalang [21] and references therein.

Now, let us make the following assumption on the spectral measure μ in order to obtain a precise estimate for the upper bound of the second moment of the mild solution of (1).

Assumption 2. *We assume that the spectral measure μ satisfies*

$$\mu(d\xi)\asymp|\xi|^{-\delta}d\xi,\quad\text{with}\quad 0<\delta<d.\tag{40}$$

The symbol " $\asymp$ " means that, for every non-negative function h such that the integral in (41) are finite, there exist two positive and finite constants C and C' which may depend on h such that

$$C'\int_{\mathbb{R}^d}h(\xi)|\xi|^{-\delta}d\xi\le\int_{\mathbb{R}^d}h(\xi)\mu(d\xi)\le C\int_{\mathbb{R}^d}h(\xi)|\xi|^{-\delta}d\xi.\tag{41}$$

Remark 6. *The Riesz kernel of order $\delta\in(0,d)$ given in Example 2 obviously satisfies (40). The Bessel kernel given in Example 3 satisfies (40) and the constants in (41) are $C=1$ and $C'>0$ depending on δ and d (see [33]).*

We have the following results concerning the upper bound on the second moment of the mild solution to Equation (1).

Theorem 2. *Suppose $0 < d - \delta < (\alpha + \gamma)$ and $0 < \beta < 1$, if the spectral measure μ associated with the noise $\dot{W}$ satisfies Assumption 2, then, under the Assumption 1, there exist two positive and finite constants c and c' such that*

$$\sup_{x\in\mathbb{R}^d} \mathbf{E}\Big(|u(t,x)|^2\Big) \leq c \exp\Big\{c'\lambda^{\frac{2(\alpha+\gamma)}{(\alpha+\gamma)-\beta(d-\delta)}}t\Big\}, \tag{42}$$

for all $t > 0$.

Remark 7. *This theorem implies that, under some conditions, there exists some positive constant C such that*

$$\limsup_{t\to\infty} \frac{1}{t}\log \mathbf{E}|u(t,x)|^2 \leq C\lambda^{\frac{2(\alpha+\gamma)}{(\alpha+\gamma)-\beta(d-\delta)}},$$

for any fixed $x \in \mathbb{R}^d$.

Before giving the proof of Theorem 2, we state an important lemma needed in the proof of this theorem.

Lemma 2. *Supposing $0 < d - \delta < (\alpha + \gamma)$ and $0 < \beta < 1$, then there exists a positive constant C such that, for all $x, y \in \mathbb{R}^d$, we have*

$$\int_{\mathbb{R}^d}\int_{\mathbb{R}^d} G_t(x-z_1)G_t(y-z_2)f(z_1-z_2)dz_1dz_2 \leq Ct^{-\frac{\beta(d-\delta)}{\alpha+\gamma}}.$$

Proof. If we fix $t \in \mathbb{R}_+$, for any $x, y \in \mathbb{R}^d$, then, by using (8), we have

$$\int_{\mathbb{R}^d}\int_{\mathbb{R}^d} G_t(x-z_1)G_t(y-z_2)f(z_1-z_2)dz_1dz_2 = \int_{\mathbb{R}^d} \mathcal{F}G_t(x-\cdot)(\xi)\overline{\mathcal{F}G_t(y-\cdot)(\xi)}\mu(d\xi).$$

Recall that the spectral measure μ satisfies (40) (i.e., (41)) in Assumption 2. Thus, according to (17), we have

$$\int_{\mathbb{R}^d}\int_{\mathbb{R}^d} G_t(x-z_1)G_t(y-z_2)f(z_1-z_2)dz_1dz_2 \leq C_{\delta,d}\int_{\mathbb{R}^d} E_\beta^2(-\nu t^\beta|\xi|^\alpha(1+|\xi|^2)^{\gamma/2})|\xi|^{-\delta}d\xi. \tag{43}$$

Then, by the similar arguments in the proof of Lemma 1, based on the estimate on the Mittag–Leffler Function (21), we can conclude the proof. □

Now, we are ready to give the proof of Theorem 2. The idea used here is essentially due to [24].

Proof of Theorem 2. Recall the iterated sequences $\{u^{(n)}(t,x), n \geq 0, (t,x) \in [0,T]\times\mathbb{R}^d\}$ given by (35). Define

$$\begin{aligned} D_n(t,x) &:= \mathbf{E}\Big|u^{(n+1)}(t,x) - u^{(n)}(t,x)\Big|^2, \\ H_n(t) &= \sup_{x\in\mathbb{R}^d} D_n(t,x), \\ \Xi(t,y,n) &= \Big|\sigma(u^{(n)}(t,y)) - \sigma(u^{(n-1)}(t,y))\Big|. \end{aligned}$$

We will prove the result for $t \in [0,T]$, where $T > 0$ is some fixed number. We now use this notation together with the covariance formula (10) and the Assumption 1 on σ to write

$$D_n(t,x) = \lambda^2\int_0^t\int_{\mathbb{R}^d}\int_{\mathbb{R}^d} G_{t-s}(x-y)G_{t-s}(x-z)\mathbf{E}(\Xi(s,y,n)\Xi(s,z,n))f(y-z)dydzds.$$

Now, we estimate the expectation on the right hand side using Cauchy–Schwartz inequality:

$$\begin{aligned}\mathbf{E}(\Xi(s,y,n)\Xi(s,z,n)) &\le L_\sigma \mathbf{E}\Big(|u^{(n)}(s,y)-u^{(n-1)}(s,y)||u^{(n)}(s,z)-u^{(n-1)}(s,z)|\Big)\\ &\le L_\sigma^2\Big(\mathbf{E}|u^{(n)}(s,y)-u^{(n-1)}(s,y)|^2\Big)^{\frac{1}{2}}\Big(\mathbf{E}|u^{(n)}(s,z)-u^{(n-1)}(s,z)|^2\Big)^{\frac{1}{2}}\\ &\le L_\sigma^2(D_{n-1}(s,y)D_{n-1}(s,z))^{\frac{1}{2}}\\ &\le L_\sigma^2 H_{n-1}(s).\end{aligned}$$

Hence, we have for $0 < d-\delta < \alpha+\gamma$ by using Lemma 2

$$\begin{aligned}D_n(t,x) &\le \lambda^2 L_\sigma^2 \int_0^t H_{n-1}(s)\int_{\mathbb{R}^d}\int_{\mathbb{R}^d} G_{t-s}(x-y)G_{t-s}(x-z)f(y-z)dydzds\\ &\le C\lambda^2 L_\sigma^2\int_0^t H_{n-1}(s)(t-s)^{-\frac{\beta(d-\delta)}{\alpha+\gamma}}ds.\end{aligned}$$

We therefore have

$$H_n(t) \le C\lambda^2 L_\sigma^2\int_0^t H_{n-1}(s)(t-s)^{-\frac{\beta(d-\delta)}{\alpha+\gamma}}ds.$$

We now note that the integral appearing on the right-hand side of the above inequality is finite when $d-\delta < \frac{\alpha+\gamma}{\beta}$. Hence, by Lemma 3.3 in Walsh [20], the series $\sum_{n=0}^{\infty} H_n^{\frac{1}{2}}(t)$ converges uniformly on $[0,T]$. Therefore, the sequence $\{u^{(n)}(t,x), n\ge 0\}$ converges in L^2 and uniformly on $[0,T]\times\mathbb{R}^d$ and the limit satisfies (14). We can prove uniqueness in a similar way.

We now turn to the proof of the exponential bound. Set

$$A(t) := \sup_{x\in\mathbb{R}^d}\mathbf{E}|u(t,x)|^2.$$

We claim that there exist constants c and c' such that, for all $t>0$, we have

$$A(t) \le c + c'\lambda^2 L_\sigma^2\int_0^t A(s)(t-s)^{-\frac{\beta(d-\delta)}{\alpha+\gamma}}ds.$$

Recall the renewal inequality in Proposition 2.5 in Foondun, Liu, and Omaba [34] with $\rho = 1-\frac{\beta(d-\delta)}{\alpha+\gamma}$; then, one can prove the exponential upper bound. To prove this claim, we start with the mild formulation given by (14); then, take the second moment to obtain the following

$$\begin{aligned}\mathbf{E}|u(t,x)|^2 &= |(\mathcal{G}u_0)_t(x)|^2\\ &\quad+\lambda^2\int_0^t\int_{\mathbb{R}^d}\int_{\mathbb{R}^d} G_{t-s}(x-y)G_{t-s}(x-z)f(y-z)\mathbf{E}(\sigma(u(s,y))\sigma(u(s,z)))dydzds \qquad (44)\\ &:= I_1+I_2.\end{aligned}$$

Since u_0 is bounded, we have $I_1 \le c$ with some positive constant c. Next, we use the Assumption 1 on the coefficient σ together with Hölder's inequality to see that

$$\begin{aligned}\mathbf{E}(\sigma(u(s,y))\sigma(u(s,z))) &\le L_\sigma^2\mathbf{E}(u(s,y)u(s,z))\\ &\le L_\sigma^2[\mathbf{E}|u(s,y)|^2]^{\frac{1}{2}}[\mathbf{E}|u(s,z)|^2]^{\frac{1}{2}}\\ &\le L_\sigma^2\sup_{x\in\mathbb{R}^d}\mathbf{E}(|u(s,x)|^2).\end{aligned} \qquad (45)$$

Therefore, using Lemma 2, the second term I_2 is thus bounded as follows:

$$I_2 \leq c\lambda^2 L_\sigma^2 \int_0^t A(s)(t-s)^{-\frac{\beta(d-\delta)}{\alpha+\gamma}} ds.$$

Combining the above estimates, we obtain the desired result. □

Next, we analyze the Hölder regularity of the solution with respect to time and space variables. The next Theorem 3 extends and improves similar results known for (fractional) stochastic heat equation (e.g., Mijena and Nane [18] with $\gamma = 0$ in Equation (1), Chen and Dalang [28], corresponding to the case $0 < \alpha \leq 2, \gamma = 0$ and $\beta = 1$, Márquez-Carreras [15] with $\beta = 1$ in Equation (1)), and also extends some results for (1) with Gaussian white noise (e.g., Dalang [21]). We use a direct method to prove our regularity results in which the Fourier transform and the representation of the Green function (i.e., (17) and (19)) play a crucial role. We state the result as follows.

Theorem 3. *Under Assumption 1, assuming that the spectral measure μ satisfies Hypothesis 2, then, for every $t, s \in [0, T], T > 0$, $x, y \in \mathbb{R}^d$, $p \geq 2$, the solution $u(t, x)$ to Equation (1) satisfies*

$$\mathbf{E}(|u(t,x) - u(s,y)|^p) \leq C(|t-s|^{p\chi_1} + |x-y|^{p\chi_2}), \tag{46}$$

with $0 < \chi_1 < \min(\beta, \frac{1}{2} - \beta)$ and $0 < \chi_2 < \alpha + \gamma - \eta$ if $0 < \beta < \frac{1}{2}$, $0 < \chi_1 < \frac{1}{4}$ and $0 < \chi_2 < \frac{\alpha+\gamma}{2} - \eta$ if $\beta = \frac{1}{2}$, and $0 < \chi_1 < \beta - \frac{1}{2}$ and $0 < \chi_2 < \frac{\alpha+\gamma}{2\beta} - \eta$ if $\frac{1}{2} < \beta < 1$.

In particular, the random field u is (χ_1, χ_2)-Hölder continuous with respect to the time and space variables.

Proof. Since the function $(\mathcal{G}u_0)_t(x) = \int_{\mathbb{R}^d} G_t(x-y)u_0(y)dy$ is smooth for any $t > 0$, then, by Proposition 2, (38) and (39), we see that, for every $p \geq 2$ and any $0 < T < \infty$, there exists a finite constant $A_{p,T}$ such that

$$\mathbf{E}\Big(|u^{(n)}(t,x) - u^{(n)}(s,y)|^p\Big) \leq \begin{cases} A_{p,T}\Big(|t-s|^{\min(2\beta,1-2\beta)\frac{p}{2}} + |x-y|^{p\chi_2}\Big), & \text{if} \quad 0 < \beta < \dfrac{1}{2}, \\ A_{p,T}\Big(|t-s|^{\frac{p}{4}} + |x-y|^{p\chi_2}\Big), & \text{if} \quad \beta = \dfrac{1}{2} \\ A_{p,T}\Big(|t-s|^{(2\beta-1)\frac{p}{2}} + |x-y|^{p\chi_2}\Big), & \text{if} \quad \dfrac{1}{2} < \beta < 1. \end{cases} \tag{47}$$

with $\chi_2 \in (0, \alpha + \gamma - \eta)$ if $0 < \beta < \frac{1}{2}$, $\chi_2 \in (0, \frac{\alpha+\gamma}{2} - \eta)$ if $\beta = \frac{1}{2}$ and $\chi_2 \in (0, \frac{\alpha+\gamma}{2\beta} - \eta)$ if $\frac{1}{2} < \beta < 1$ simultaneously for all $t, s \in [0, T]$ and $x, y \in \mathbb{R}^d$. The right-hand side of this inequality does not depend on n. Hence, using Fatou's lemma, as n tends to infinity, we obtain the similar estimates for u, which also satisfies (47). Then, the conclusion of Theorem 3 is a consequence of the Kolmogorov continuity criterion for stochastic processes. □

Let us also make some discussion about the above regularity results.

Remark 8. *For β close to 1, the order of Hölder regularity of $u(t, x)$ in space is $(\alpha + \gamma)$-times the order of Hölder continuity to in time. This is coherent with the case in Márquez-Carreras [15]. When $\gamma = 0$ and $\alpha \in (0, 2]$, this happens always in the case of the solution of the (fractional) heat equation (with white noise), see Walsh [20].*

Remark 9. *If $d = 1$, $\alpha = 2$ and $\gamma = 0$ (so, somehow, the operator $(I - \Delta)^{\frac{\gamma}{2}}(-\Delta)^{\frac{\alpha}{2}}$ reduces to the Laplacian operator Δ and, moreover, we assume that η is close to one-half and β is close to 1, we obtain the well-known regularity of the solution to the heat equation with time-space white noise (which is Hölder continuous of order $\frac{1}{4}$ in time and of order $\frac{1}{2}$ in space).*

4. The Linear Additive Noise

In the last part of this work, we focus on the solution of (14) with $u_0(x) = 0$ and $\sigma = 1$. This is the additive noise case and in this situation the solution is Gaussian. We will study the stationarity of the solution, both in time and in space. The solution is stationary in space, but not in time.

In the following, we consider

$$U(t,x) = \int_0^t \int_{\mathbb{R}^d} G_{t-s}(x-y)W(ds,dy), \tag{48}$$

which is the mild solution of (1) when the initial condition $u_0(x) = 0, x \in \mathbb{R}^d$ and $\sigma(x) \equiv 1$, $x \in \mathbb{R}$.

Remark 10.

1. *As mentioned in the introduction, Anh and Leonenko [2] showed that the presence of the Bessel operator $-(I-\Delta)^{\gamma/2}$ with $\gamma \geq 0$ is essential to have an (asymptotically) stationary solution of SPDE (1). In fact, the linnear case requires the condition $0 < \alpha < d/2$ and $\alpha + \gamma > d/2$ that is to say the parameter $\gamma > 0$ is necessary.*
2. *On the other hand, the parameter $\gamma > 0$ of the Bessel operator is also useful in determining suitable conditions for the spectral density of the solutions of fractional kinetic equations belonging to $L^1(\mathbb{R}^d)$.*

Theorem 4. *Under Hypothesis 2 on the spectral measure μ associated with $\dot{W}$, then, for fixed $t \in \mathbb{R}_+$, the spatial covariance function of $U(t,x)$ given by (48) is*

$$R_t(x-z) = \int_{\mathbb{R}^d} \mu(d\xi) e^{\mathrm{i}\langle x-z,\xi\rangle} \int_0^t ds E_\beta^2(-\nu(t-s)^\beta |\xi|^\alpha (1+|\xi|^2)^{\gamma/2}).$$

In particular, for every $t \in \mathbb{R}_+$, the process $\left\{U(t,x), x \in \mathbb{R}^d\right\}$ is stationary.

Proof. We first calculate the spatial covariance for a fixed $t \in \mathbb{R}_+$. By means of the definition of Fourier transform, change of variable and Fubini's theorem, we obtain, for any $x, z \in \mathbb{R}^d$,

$$\begin{aligned}
\mathbf{E}(U(t,x)\overline{U(t,z)}) &= \int_0^t \int_{\mathbb{R}^d} \mathcal{F}G_{t-s}(x-\cdot)(\xi)\overline{\mathcal{F}G_{t-s}(z-\cdot)(\xi)}\mu(d\xi)ds \\
&= \int_0^t \int_{\mathbb{R}^d} e^{-\mathrm{i}\langle x-z,\xi\rangle} |\mathcal{F}G_{t-s}(\cdot)(\xi)|^2 \mu(d\xi)ds \\
&= \int_{\mathbb{R}^d} e^{-\mathrm{i}\langle x-z,\xi\rangle} \int_0^t E_\beta^2(-\nu(t-s)^\beta |\xi|^\alpha (1+|\xi|^2)^{\gamma/2})ds\mu(d\xi) \\
&= R_t(x-z),
\end{aligned}$$

where we have used the fact that

$$\begin{aligned}
&\int_0^t E_\beta^2(-\nu(t-s)^\beta |\xi|^\alpha (1+|\xi|^2)^{\gamma/2})ds \\
&\quad \leq \int_0^t \frac{1}{(1+\Gamma(1+\beta)^{-1}(t-s)^\beta |\xi|^\alpha (1+|\xi|^2)^{\gamma/2})^2} ds \\
&\quad \leq t.
\end{aligned}$$

Hence, for any fixed $t \in \mathbb{R}_+$, the process $\{U(t,x), x \in \mathbb{R}^d\}$ is a Gaussian field that has zero mean, stationary increments, and a continuous covariance function. □

Remark 11. *From the above result, one can obtain the spectral density of the process $x \to U(t,x)$. Indeeed, its spectral density $f_t(\xi)$ is given by*

$$f_t(\xi) = \int_0^t ds E_\beta^2(-\nu(t-s)^\beta |\xi|^\alpha (1+|\xi|^2)^{\gamma/2}) g(\xi).$$

where $g(\cdot)$ is the density of $\mu(\cdot)$ with respect to the Lebesgue measure.

The next result shows that the process (48) is not stationary in time, but, when t tends to infinity, it converges to a stationary process.

Theorem 5. *Under Hypothesis 2 on the spectral measure μ associated with $\dot{W}$, assuming $1/2 < \beta < 1$, then, for $t \in \mathbb{R}_+$, $\tau \in \mathbb{R}$ such that $t+\tau \in \mathbb{R}_+$, $x, z \in \mathbb{R}^d$, the asymptotic homogeneous spatial-temporal covariance function of $U(t+\tau, x)$ and $U(t,z)$ is*

$$R(\tau, x-z) = \int_{\mathbb{R}^d} \frac{e^{\mathrm{i}\langle x-z,\xi\rangle}}{\beta(\nu|\xi|^\alpha(1+|\xi|^2)^{\gamma/2})^{1/\beta}} \int_{\nu\tau^\beta|\xi|^\alpha(1+|\xi|^2)^{\gamma/2}}^\infty x^{1/\beta-1} E_\beta(-x) \cdot E_\beta\left(-\nu\left(\left(\frac{x}{\nu|\xi|^\alpha(1+|\xi|^2)^{\gamma/2}}\right)^{1/\beta} - \tau\right)^\beta |\xi|^\alpha (1+|\xi|^2)^{\gamma/2}\right) dx\mu(d\xi).$$

Moreover, $U(\cdot, x)$ is asymptotically in time an index-$\left(\beta - \frac{1}{2}\right)$ Gaussian field.

Proof. For $t, \tau \in \mathbb{R}_+$ (for $\tau \in \mathbb{R}_-$ such that $t+\tau \in \mathbb{R}_+$, we argue similarly), and $x, z \in \mathbb{R}^d$, we have

$$\begin{aligned}
&\mathbf{E}\left(U(t+\tau,x)\overline{U(t,z)}\right) \\
&= \int_0^t ds \int_{\mathbb{R}^d} \mu(d\xi) \mathcal{F}G_{t+\tau-s}(x-\cdot)(\xi) \overline{\mathcal{F}G_{t-s}(z-\cdot)(\xi)} \\
&= \int_0^t ds \int_{\mathbb{R}^d} \mu(d\xi) e^{\mathrm{i}\langle x-z,\xi\rangle} \mathcal{F}G_{t+\tau-s}(x-\cdot)(\xi) \mathcal{F}G_{t-s}(z-\cdot)(\xi) \\
&= \int_0^t ds \int_{\mathbb{R}^d} \mu(d\xi) e^{\mathrm{i}\langle x-z,\xi\rangle} E_\beta(-\nu(t+\tau-s)^\beta|\xi|^\alpha(1+|\xi|^2)^{\gamma/2}) E_\beta(-\nu(t-s)^\beta|\xi|^\alpha(1+|\xi|^2)^{\gamma/2}) \\
&= \int_{\mathbb{R}^d} e^{\mathrm{i}\langle x-z,\xi\rangle} \int_0^t E_\beta(-\nu(t+\tau-s)^\beta|\xi|^\alpha(1+|\xi|^2)^{\gamma/2}) E_\beta(-\nu(t-s)^\beta|\xi|^\alpha(1+|\xi|^2)^{\gamma/2}) ds\mu(d\xi).
\end{aligned}$$

Next, let us calculate the above integral with respect to s. In fact, with the change of variable $x = \nu(t+\tau-s)^\beta|\xi|^\alpha(1+|\xi|^2)^{\gamma/2}$, we have

$$\begin{aligned}
&\int_0^t E_\beta(-\nu(t+\tau-s)^\beta|\xi|^\alpha(1+|\xi|^2)^{\gamma/2}) E_\beta(-\nu(t-s)^\beta|\xi|^\alpha(1+|\xi|^2)^{\gamma/2}) ds \\
&\quad = \frac{1}{\beta(\nu|\xi|^\alpha(1+|\xi|^2)^{\gamma/2})^{1/\beta}} \int_{\nu\tau^\beta|\xi|^\alpha(1+|\xi|^2)^{\gamma/2}}^{\nu(t+\tau)^\beta|\xi|^\alpha(1+|\xi|^2)^{\gamma/2}} E_\beta(-x) x^{1/\beta-1} \\
&\qquad \cdot E_\beta\left(-\nu\left(\left(\frac{x}{\nu|\xi|^\alpha(1+|\xi|^2)^{\gamma/2}}\right)^{1/\beta} - \tau\right)^\beta |\xi|^\alpha(1+|\xi|^2)^{\gamma/2}\right) dx.
\end{aligned}$$

Moreover, as $t \to \infty$, we obtain

$$\begin{aligned}
&\lim_{t\to\infty} \int_0^t E_\beta(-\nu(t+\tau-s)^\beta|\xi|^\alpha(1+|\xi|^2)^{\gamma/2})E_\beta(-\nu(t-s)^\beta|\xi|^\alpha(1+|\xi|^2)^{\gamma/2})ds \\
&= \frac{1}{\beta(\nu|\xi|^\alpha(1+|\xi|^2)^{\gamma/2})^{1/\beta}} \int_{\nu\tau^\beta|\xi|^\alpha(1+|\xi|^2)^{\gamma/2}}^\infty x^{1/\beta-1}E_\beta(-x) \\
&\qquad \cdot E_\beta\left(-\nu\left(\left(\frac{x}{\nu|\xi|^\alpha(1+|\xi|^2)^{\gamma/2}}\right)^{1/\beta} - \tau\right)^\beta |\xi|^\alpha(1+|\xi|^2)^{\gamma/2}\right)dx,
\end{aligned}$$

which is finite because we have

$$\begin{aligned}
&\int_{\nu\tau^\beta|\xi|^\alpha(1+|\xi|^2)^{\gamma/2}}^\infty x^{1/\beta-1}E_\beta(-x)E_\beta\left(-\nu\left(\left(\frac{x}{\nu|\xi|^\alpha(1+|\xi|^2)^{\gamma/2}}\right)^{1/\beta} - \tau\right)^\beta |\xi|^\alpha(1+|\xi|^2)^{\gamma/2}\right)dx \\
&\le C_{\xi,\nu,\beta,\alpha,\gamma,\tau} \int_{\nu\tau^\beta|\xi|^\alpha(1+|\xi|^2)}^\infty x^{1/\beta-3}dx,
\end{aligned}$$

which is finite when $1/2 < \beta < 1$ (i.e., $\frac{1}{\beta} - 2 < 0$).

We now tackle the second part of this theorem. We assume that $x \in \mathbb{R}^d$, $t \in \mathbb{R}_+$ and $\tau \in \mathbb{R}_+$ are small (the negative case is similar). Then, from (31) and (32), when $1/2 < \beta < 1$, we have

$$\begin{aligned}
&\mathbf{E}\Big(|U(t+\tau,x) - U(t,x)|^2\Big) \\
&= \int_0^t ds \int_{\mathbb{R}^d} \mu(d\xi)|\mathcal{F}G_{t+\tau-s}(x-\cdot)(\xi) - \mathcal{F}G_{t-s}(x-\cdot)(\xi)|^2 \\
&\qquad + \int_t^{t+\tau} ds \int_{\mathbb{R}^d} \mu(d\xi)|\mathcal{F}G_{t+\tau-s}(x-\cdot)(\xi)|^2 \\
&\le C\Big(|\tau|^{2\beta} + |\tau|^{2\beta-1}\Big).
\end{aligned}$$

Then, we can complete the proof of the second part. □

5. Conclusions

In this article, we have studied the space-time fractional stochastic kinetic Equation (1) driven by spatially homogeneous Gaussian noise. The time fractional derivative $\frac{\partial^\beta}{\partial t^\beta}, 0 < \beta \le 1$ is defined in the Caputo–Djrbashian sense given by (2). The inverses of the Bessel and Riesz potentials are also included in Equation (1). First, the existence and uniqueness of solutions for the proposed fractional SPDEs (1) were obtained. In particular, when the covariance function of the Gaussian noise is given by the Riesz kernel, we have proved the upper bound for the second moment of the mild solution to Equation (1). Moreover, the main results have been proven based on the classical Picard's iterations and some estimates about the Fourier transform of the Green function given by (17). Next, we analyze the Hölder regularity of the mild solution to Equation (1) with respect to the time and space variables. Finally, in some special cases (i.e., $u_0(x) \equiv 0$ and $\sigma(u) \equiv 1$), we have studied the stationarity of the mild solution, both in time and space variables. We proved that the mild solution is stationary in space, but not in time.

Author Contributions: J.L.; Writing—original draft, J.L., Z.Y. and B.Z.; Writing, review and editing. All authors have read and agreed to the published version of the manuscript.

Funding: This research received no external funding.

Institutional Review Board Statement: Not applicable.

Informed Consent Statement: Not applicable.

Data Availability Statement: Not applicable.

Acknowledgments: The authors sincerely thank the reviewers for their constructive comments to improve the manuscript.

Conflicts of Interest: The authors declare no conflict of interest.

Appendix A

We will prove Proposition 2 in this appendix.

Proof of Proposition 2. For any $t, t' \in \mathbb{R}_+$ such that $t' < t$ and $x \in \mathbb{R}^d$, by using the fact

$$\mathcal{F}G_{t-s}(x-\cdot)(\xi) - \mathcal{F}G_{t'-s}(x-\cdot)(\xi) = e^{\mathrm{i}\langle \xi, x\rangle}(\mathcal{F}G_{t-s}(\cdot)(\xi) - \mathcal{F}G_{t'-s}(\cdot)(\xi)),$$

then from (17) and the absolute convergence of the series in (18), one obtains

$$\begin{aligned}\mathcal{F}G_{t-s}(\cdot)(\xi) - \mathcal{F}G_{t'-s}(\cdot)(\xi) &= \sum_{k=0}^{\infty} \frac{(-\nu|\xi|^\alpha(1+|\xi|^2)^{\gamma/2})^k}{\Gamma(1+k\beta)}\Big(|t-s|^{k\beta} - |t'-s|^{k\beta}\Big) \\ &\le \sum_{k=0}^{\infty} \frac{(-\nu|\xi|^\alpha(1+|\xi|^2)^{\gamma/2})^k}{\Gamma(1+k\beta)}\Big(|t-s|^{k} - |t'-s|^{k}\Big)^{\beta} \\ &\le |t-t'|^\beta \sum_{k=1}^{\infty} \frac{k^\beta(-\nu|\xi|^\alpha(1+|\xi|^2)^{\gamma/2})^k}{\Gamma(1+k\beta)} t^{(k-1)\beta},\end{aligned} \tag{A1}$$

for all $t, t' \in \mathbb{R}_+$, where the last inequality follows from the mean value theorem. Furthermore, since the series in (18) is absolutely convergent, then the series in the last inequality in (A1) can be bounded as follows with $0 < \beta < 1$:

$$\begin{aligned}\sum_{k=1}^{\infty} \frac{k^\beta(-\nu|\xi|^\alpha(1+|\xi|^2)^{\gamma/2})^k}{\Gamma(1+k\beta)} t^{(k-1)\beta} &= t^{-\beta}\sum_{k=1}^{\infty} \frac{k^\beta(-\nu|\xi|^\alpha(1+|\xi|^2)^{\gamma/2}t^\beta)^k}{\Gamma(1+k\beta)} \\ &\le -\nu t^{-\beta}|\xi|^\alpha(1+|\xi|^2)^{\gamma/2}\sum_{k=1}^{\infty} \frac{k(-\nu|\xi|^\alpha(1+|\xi|^2)^{\gamma/2}t^\beta)^{k-1}}{\Gamma(1+k\beta)} \\ &\le -\nu t^{-\beta}|\xi|^\alpha(1+|\xi|^2)^{\gamma/2}\sum_{k=1}^{\infty} \frac{(-\nu|\xi|^\alpha(1+|\xi|^2)^{\gamma/2}t^\beta)^{k-1}}{\Gamma(1+k\beta)} \\ &\le \frac{t^{-\beta}}{1+\Gamma(1+\beta)^{-1}\nu t^\beta|\xi|^\alpha(1+|\xi|^2)^{\gamma/2}}.\end{aligned} \tag{A2}$$

Then, we have

$$\begin{aligned}&\int_0^{t'} ds \int_{\mathbb{R}^d} \mu(d\xi)|\mathcal{F}G_{t-s}(x-\cdot)(\xi) - \mathcal{F}G_{t'-s}(x-\cdot)(\xi)|^2 \\ &\quad\le |t-t'|^{2\beta}\int_0^{t'} ds \int_{\mathbb{R}^d} \mu(d\xi)\frac{t^{-2\beta}}{(1+\Gamma(1+\beta)^{-1}\nu t^\beta|\xi|^\alpha(1+|\xi|^2)^{\gamma/2})^2} \\ &\quad:= A_1 + A_2,\end{aligned} \tag{A3}$$

with

$$A_1 = |t-t'|^{2\beta}\int_0^{t'} ds \int_{|\xi|\le 1} \mu(d\xi)\frac{t^{-2\beta}}{(1+\Gamma(1+\beta)^{-1}\nu t^\beta|\xi|^\alpha(1+|\xi|^2)^{\gamma/2})^2},$$

and

$$A_2 = |t-t'|^{2\beta}\int_0^{t'} ds \int_{|\xi|> 1} \mu(d\xi)\frac{t^{-2\beta}}{(1+\Gamma(1+\beta)^{-1}\nu t^\beta|\xi|^\alpha(1+|\xi|^2)^{\gamma/2})^2}.$$

Thus, with (11), we have

$$A_1 \le t^{1-2\beta} \int_{|\xi|\le 1} \mu(d\xi)|t-t'|^{2\beta},$$

and

$$A_2 \le t^{-2\beta} \int_{|\xi|>1} N_{t'}(\xi)\mu(d\xi)|t-t'|^{2\beta}.$$

Then, combining the above estimates for A_1, A_2 and Proposition 1, we can conclude the proof of (31).

Next, we can follow the similar arguments to prove (32) which will be divided into three cases. Firstly, with $0 < \beta < \frac{1}{2}$, we have

$$\begin{aligned}
&\int_{t'}^{t} ds \int_{\mathbb{R}^d} \mu(d\xi)|\mathcal{F}G_{t-s}(x-\cdot)(\xi)|^2 \\
&\quad = \int_{t'}^{t} ds \int_{\mathbb{R}^d} \mu(d\xi)|e^{\mathbf{i}\langle\xi,x\rangle}|^2 \Big| E_\beta(-\nu(t-s)^\beta|\xi|^\alpha(1+|\xi|^2)^{\gamma/2})\Big|^2 \\
&\quad \le \int_{\mathbb{R}^d} \mu(d\xi) \int_{t'}^{t} ds \Big(\frac{1}{1+\Gamma(1+\beta)^{-1}\nu(t-s)^\beta|\xi|^\alpha(1+|\xi|^2)^{\gamma/2}} \Big)^2 \\
&\quad \le \int_{|\xi|\le 1} \mu(d\xi)|t-t'| \\
&\qquad + \frac{\Gamma(1+\beta)^2 2^{\alpha+\gamma}}{\nu^2(1-2\beta)} \int_{|\xi|>1} \Big(\frac{1}{1+|\xi|^2} \Big)^{\alpha+\gamma} \mu(d\xi)|t-t'|^{1-2\beta} \\
&\quad = C_{3.2}|t-t'|^{1-2\beta}.
\end{aligned}$$

If $\frac{1}{2} < \beta < 1$, one obtains with Fubini's theorem

$$\begin{aligned}
&\int_{t'}^{t} ds \int_{\mathbb{R}^d} \mu(d\xi)|\mathcal{F}G_{t-s}(x-\cdot)(\xi)|^2 \\
&\quad = \int_{\mathbb{R}^d} \mu(d\xi) \int_{t'}^{t} \Big| E_\beta(-\nu(t-s)^\beta|\xi|^\alpha(1+|\xi|^2)^{\gamma/2})\Big|^2 ds \\
&\quad \le \int_{\mathbb{R}^d} \mu(d\xi) \int_{t'}^{t} \Big(\frac{1}{1+\Gamma(1+\beta)^{-1}\nu(t-s)^\beta|\xi|^\alpha(1+|\xi|^2)^{\gamma/2}} \Big)^2 ds.
\end{aligned}$$

Denote by

$$\begin{aligned}
M_{t,t'}(\xi) &:= \int_{t'}^{t} \Big(\frac{1}{1+\Gamma(1+\beta)^{-1}\nu(t-s)^\beta|\xi|^\alpha(1+|\xi|^2)^{\gamma/2}} \Big)^2 ds \\
&= \int_{0}^{t-t'} \Big(\frac{1}{1+\Gamma(1+\beta)^{-1}\nu u^\beta|\xi|^\alpha(1+|\xi|^2)^{\gamma/2}} \Big)^2 du.
\end{aligned}$$

Then, with the change of variable $x = \Gamma(1+\beta)^{-1}\nu u^\beta|\xi|^\alpha(1+|\xi|^2)^{\gamma/2}$, we have

$$M_{t,t'}(\xi) = \frac{1}{\beta}\Big(\frac{\Gamma(1+\beta)}{\nu|\xi|^\alpha(1+|\xi|^2)^{\gamma/2}} \Big)^{\frac{1}{\beta}} \int_0^{\Gamma(1+\beta)^{-1}\nu(t-t')^\beta|\xi|^\alpha(1+|\xi|^2)^{\gamma/2}} x^{\frac{1}{\beta}-1}(1+x)^{-2}dx.$$

For $|\xi| \le 1$, we have the following:

$$\begin{aligned}
M_{t,t'}(\xi)1_{\{|\xi|\le 1\}} &\le \frac{1}{\beta}\Big(\frac{\Gamma(1+\beta)}{\nu|\xi|^\alpha(1+|\xi|^2)^{\gamma/2}} \Big)^{\frac{1}{\beta}} \int_0^{\frac{\nu|\xi|^\alpha(1+|\xi|^2)^{\gamma/2}}{\Gamma(1+\beta)}(t-t')^\beta} x^{\frac{1}{\beta}-1}dx \\
&= |t-t'|.
\end{aligned} \tag{A4}$$

Now we will estimate $M_{t,t'}(\xi)$ when $|\xi| > 1$. In fact, with $0 < \eta < \frac{\alpha+\gamma}{2\beta}$, we have

$$\begin{aligned} M_{t,t'}(\xi)1_{\{|\xi|>1\}} &\le \frac{1}{\beta}\left(\frac{\Gamma(1+\beta)}{\nu|\xi|^\alpha(1+|\xi|^2)^{\gamma/2}}\right)^{\frac{1}{\beta}} \int_0^{\frac{\nu|\xi|^\alpha(1+|\xi|^2)^{\gamma/2}}{\Gamma(1+\beta)}(t-t')^\beta} (1+x)^{\frac{1}{\beta}-3}dx \\ &\le \frac{1}{2\beta-1}\left(\frac{\Gamma(1+\beta)}{\nu|\xi|^\alpha(1+|\xi|^2)^{\gamma/2}}\right)^{\frac{1}{\beta}} \\ &\le \frac{1}{2\beta-1}\left(\frac{\Gamma(1+\beta)}{\nu}\right)^{\frac{1}{\beta}} 2^{\frac{\alpha+\gamma}{2\beta}} \left(\frac{1}{1+|\xi|^2}\right)^{\frac{\alpha+\gamma}{2\beta}}. \end{aligned} \tag{A5}$$

Then, combining the estimates (A4) and (A5), we can obtain (32).
If $\beta = \frac{1}{2}$, by using the similar argument above, we have

$$\begin{aligned} &\int_{t'}^t ds \int_{\mathbb{R}^d} \mu(d\xi)|\mathcal{F}G_{t-s}(x-\cdot)(\xi)|^2 \\ &\quad= \int_{\mathbb{R}^d} \mu(d\xi) \int_{t'}^t \left|E_\beta(-\nu(t-s)^\beta|\xi|^\alpha(1+|\xi|^2)^{\gamma/2})\right|^2 ds \\ &\quad\le \int_{|\xi|\le 1} \mu(d\xi)|t-t'| \\ &\quad+ 2\left(\frac{\Gamma(3/2)}{\nu|\xi|^\alpha(1+|\xi|^2)^{\gamma/2}}\right)^2 \int_{|\xi|>1} \mu(d\xi) \int_0^{\Gamma(3/2)^{-1}\nu|t-t'|^{\frac{1}{2}}|\xi|^\alpha(1+|\xi|^2)^{\gamma/2}} x(1+x)^{-2}dx. \end{aligned}$$

and we have

$$\begin{aligned} &2\left(\frac{\Gamma(3/2)}{\nu|\xi|^\alpha(1+|\xi|^2)^{\gamma/2}}\right)^2 \int_0^{\Gamma(3/2)^{-1}\nu|t-t'|^{\frac{1}{2}}|\xi|^\alpha(1+|\xi|^2)^{\gamma/2}} x(1+x)^{-2}dx \\ &\le 2\left(\frac{\Gamma(3/2)}{\nu|\xi|^\alpha(1+|\xi|^2)^{\gamma/2}}\right)^2 \int_0^{\Gamma(3/2)^{-1}\nu|t-t'|^{\frac{1}{2}}|\xi|^\alpha(1+|\xi|^2)^{\gamma/2}} (1+x)^{-1}dx \\ &= 2\left(\frac{\Gamma(3/2)}{\nu|\xi|^\alpha(1+|\xi|^2)^{\gamma/2}}\right)^2 \ln\left(1+\Gamma(3/2)^{-1}\nu|t-t'|^{\frac{1}{2}}|\xi|^\alpha(1+|\xi|^2)^{\gamma/2}\right) \\ &\le 2^{1+\frac{\alpha+\gamma}{2}}\frac{\Gamma(3/2)}{\nu}\left(\frac{1}{1+|\xi|^2}\right)^{\frac{\alpha+\gamma}{2}}|t-t'|^{\frac{1}{2}}. \end{aligned}$$

Then, we have that

$$\begin{aligned} &\int_{t'}^t ds \int_{\mathbb{R}^d} \mu(d\xi)|\mathcal{F}G_{t-s}(x-\cdot)(\xi)|^2 \\ &\quad\le \left(\int_{|\xi|\le 1} \mu(d\xi)|t-t'|^{\frac{1}{2}} + 2^{1+\frac{\alpha+\gamma}{2}}\frac{\Gamma(3/2)}{\nu}\int_{|\xi|>1}\left(\frac{1}{1+|\xi|^2}\right)^{\frac{\alpha+\gamma}{2}}\mu(d\xi)\right)|t-t'|^{\frac{1}{2}}. \end{aligned}$$

Since

$$\mathcal{F}G_{t-s}(x-\cdot)(\xi) - \mathcal{F}G_{t-s}(x'-\cdot)(\xi) = (e^{i\langle\xi,x\rangle} - e^{i\langle\xi,x'\rangle})\mathcal{F}G_{t-s}(\cdot)(\xi),$$

then we have that

$$\begin{aligned} &\int_0^t ds \int_{\mathbb{R}^d} \mu(d\xi)\left|\mathcal{F}G_{t-s}(x-\cdot)(\xi) - \mathcal{F}G_{t-s}(x'-\cdot)(\xi)\right|^2 \\ &\quad= \int_0^t ds \int_{\mathbb{R}^d} \mu(d\xi)\left|e^{i\langle\xi,x\rangle} - e^{i\langle\xi,x'\rangle}\right|^2|\mathcal{F}G_{t-s}(\cdot)(\xi)|^2 \\ &\quad:= B_1 + B_2, \end{aligned}$$

with

$$B_1 = \int_0^t ds \int_{|\xi|\le 1} \mu(d\xi) \left| e^{\mathrm{i}\langle \xi, x\rangle} - e^{\mathrm{i}\langle \xi, x'\rangle} \right|^2 |\mathcal{F}G_{t-s}(\cdot)(\xi)|^2,$$
$$B_2 = \int_0^t ds \int_{|\xi|>1} \mu(d\xi) \left| e^{\mathrm{i}\langle \xi, x\rangle} - e^{\mathrm{i}\langle \xi, x'\rangle} \right|^2 |\mathcal{F}G_{t-s}(\cdot)(\xi)|^2.$$

The first term B_1 is easy and can be studied in the same way for any $0 < \beta < 1$. Indeed, the fact that the Fourier transform of Green function G given by (17) is bounded by 1, the mean value theorem, and property (11) imply that

$$\begin{aligned} B_1 &\le C \int_0^t ds \int_{|\xi|\le 1} \mu(d\xi) |\langle x - x', \xi\rangle|^2 \\ &\le Ct \int_{|\xi|\le 1} \mu(d\xi) |x - x'|^2. \end{aligned} \tag{A6}$$

The other term B_2 is a little involved. We distinguish three cases depending on the values of β. We first study the case $0 < \beta < \frac{1}{2}$. Let $0 < \rho_1 < \alpha + \gamma - \eta$. Applying the mean theorem, Fubini's theorem, the fact $1 - e^{-x} \le 1$ for all $x > 0$ and Hypothesis 2, then we have

$$\begin{aligned} B_2 &= \int_0^t ds \int_{|\xi|>1} \mu(d\xi) \left| e^{\mathrm{i}\langle \xi, x\rangle} - e^{\mathrm{i}\langle \xi, x'\rangle} \right|^2 |\mathcal{F}G_{t-s}(\cdot)(\xi)|^2 \\ &\le 4 \int_0^t ds \int_{|\xi|>1} \mu(d\xi) \left| \frac{1}{2} (e^{\mathrm{i}\langle \xi, x\rangle} - e^{\mathrm{i}\langle \xi, x'\rangle}) \right|^{2\rho_3} |\mathcal{F}G_{t-s}(\cdot)(\xi)|^2 \\ &\le C \int_0^t ds \int_{|\xi|>1} \mu(d\xi) |\xi|^{2\rho_1} |x - x'|^{2\rho_1} |E_\beta(-\nu(t-s)^\beta |\xi|^\alpha (1 + |\xi|^2)^{\gamma/2})|^2 \\ &\le Ct^{1-2\beta} \frac{\Gamma(1+\beta)^2}{(1-2\beta)\nu^2} 2^{\alpha+\gamma-\rho_1} \int_{|\xi|>1} \left(\frac{1}{1+|\xi|^2} \right)^{\alpha+\gamma-\rho_1} \mu(d\xi) |x - x'|^{2\rho_1}. \end{aligned} \tag{A7}$$

For the critical case $\beta = \frac{1}{2}$, by choosing $0 < \rho_2 < \frac{\alpha+\gamma}{2} - \eta$, then we have that

$$\begin{aligned} B_2 &\le C|x - x'|^{2\rho_2} \int_{|\xi|>1} \mu(d\xi) |\xi|^{2\rho_2} \int_0^t |E_\beta(-\nu(t-s)^\beta |\xi|^\alpha (1 + |\xi|^2)^{\gamma/2})|^2 ds \\ &\le 2Ct^{\frac{1}{2}} |x - x'|^{2\rho_2} \Gamma(3/2) \nu^{-1} \int_{|\xi|>1} \mu(d\xi) \frac{|\xi|^{2\rho_2}}{|\xi|^\alpha (1 + |\xi|^2)^{\gamma/2}} \\ &\le C 2^{1+\frac{\alpha+\gamma}{2}-\rho_2} t^{\frac{1}{2}} |x - x'|^{2\rho_2} \Gamma(3/2) \nu^{-1} \int_{|\xi|>1} \left(\frac{1}{1+|\xi|^2} \right)^{\frac{\alpha+\gamma}{2}-\rho_2} \mu(d\xi). \end{aligned} \tag{A8}$$

On the other hand, when $\frac{1}{2} < \beta < 1$, let $0 < \rho_3 < \frac{\alpha+\gamma}{2\beta} - \eta$, then the similar arguments yield that

$$\begin{aligned} B_2 &\le C \int_0^t ds \int_{|\xi|>1} \mu(d\xi) |\xi|^{2\rho_3} |x - x'|^{2\rho_3} |E_\beta(-\nu(t-s)^\beta |\xi|^\alpha (1 + |\xi|^2)^{\gamma/2})|^2 \\ &\le \frac{C}{(2\beta - 1)} \left(\frac{\Gamma(1+\beta)}{\nu} \right)^{\frac{1}{\beta}} 2^{\frac{\alpha+\gamma}{2\beta}-\rho_3} \int_{|\xi|>1} \left(\frac{1}{1+|\xi|^2} \right)^{\frac{\alpha+\gamma}{2\beta}-\rho_3} \mu(d\xi) \cdot |x - x'|^{2\rho_3}. \end{aligned} \tag{A9}$$

Then, we can conclude the proof of (33) by combining (A6)–(A9). □

References

1. Angulo, J.M.; Anh, V.V.; McVinish, R.; Ruiz-Medina, M.D. Fractional kinetic equations driven by Gaussian or infinitely divisible noise. *Adv. Appl. Prob.* **2005**, *37*, 366–392. [CrossRef]
2. Anh, V.V.; Leonenko, N.N. Spectral analysis of fractional kinetic equations with random data. *J. Stat. Phys.* **2001**, *104*, 1349–1387. [CrossRef]

3. Caputo, M. Linear models of dissipation whose *Q* is almost frequency independent, Part III. *Geophys. J. R. Astron. Soc.* **1967**, *13*, 529–539. [CrossRef]
4. Kilbas, A.A.; Srivastava, H.M.; Trujillo, J.J. *Theory and Applications of Fractional Differential Equations*; Elsevier: Amsterdam, The Netherlands, 2006.
5. Povstenko, Y. *Linear Fractional Diffusion-Wave Equation for Scientists and Engineers*; Birkhäuser: New York, NY, USA, 2015.
6. Povstenko, Y. *Fractional Thermoelasticity*; Springer: New York, NY, USA, 2015.
7. Compte, A.; Metzler, R. The generalized Cattaneo equation for the description of anomalous transport processes. *J. Phys. A.* **1997**, *30*, 7277–7289. [CrossRef]
8. Kotelenez, P. *Stochastic Ordinary and Stochastic Partial Differential Equations*; Springer: Berlin/Heidelberg, Germany, 2008.
9. Stein, E.M. *Singular Integrals and Differential Properties of Functions*; Princeton University Press: Princeton, NJ, USA, 1970.
10. Chen, L. Nonlinear stochastic time-fractional diffusion equations on: Moments, Hölder regularity and intermittency. *Trans. Am. Math. Soc.* **2017**, *369*, 8497–8535. [CrossRef]
11. Chen, L.; Hu, Y.; Nualart , D. Nonlinear stochastic time-fractional slow and fast diffusion equations on $\mathbb{R}^d$. *Stoch. Proc. Appl.* **2019**, *129*, 5073–5112. [CrossRef]
12. Chen, Z.-Q.; Kim, K.-H.; Kim, P. Fractional time stochastic partial differential equations. *Stoch. Process. Appl.* **2015**, *125*, 1470–1499. [CrossRef]
13. Meerschaert, M.M.; Nane, E.; Vellaisamy, P. Fractional Cauchy problems on bounded domains. *Ann. Probab.* **2009**, *37*, 979–1007. [CrossRef]
14. Nane, E. Fractional Cauchy problems on bounded domains: survey of recent results. In *Fractional Dynamics and Control*; Baleanu, D., Machado, J.A.T., Luo, A.C.J., Eds.; Springer: New York, NY, USA, 2012; pp. 185–198.
15. Márquez-Carreras, D. Generalized fractional kinetic equations: Another point of view. *Adv. Appl. Prob.* **2009**, *41*, 893–910. [CrossRef]
16. Márquez-Carreras, D. Generalized stochastic heat equation. In *Malliavin Calculus and Stochastic Analysis: A Festschrift in Honor of David Nualart*; Springer: Boston, MA, USA, 2012; Volume 34, pp. 281–297.
17. Umarov, S. On fractional Duhamel's principle and its applications. *J. Differ. Equ.* **2012**, *252*, 5217–5234. [CrossRef]
18. Mijena, J.B.; Nane, E. Space-time fractional stochastic partial differential equations. *Stoch. Process. Appl.* **2015**, *125*, 3301–3326. [CrossRef]
19. Mijena, J.B.; Nane, E. Intermittency and time fractional stochastic partial differential equation. *Potential Anal.* **2016**, *44*, 295–312. [CrossRef]
20. Walsh, J.B. An introduction to stochastic partial differential equations. In *Ecole d'été de Probabilités de St. Flour XIV*; Lecture Notes in Mathematics; Springer: Berlin/Heidelberg, Germany, 1986; Volume 1180, pp. 266–439.
21. Dalang, R. Extending the martingale measure stochastic integral with applications to spatially homogeneous SPDE's. *Electron. J. Probab.* **1999**, *4*, 1–29. [CrossRef]
22. Chen, L.; Hu, G. Hölder regularity for the nonlinear stochastic time-fractional slow and fastdiffusion equations on $\mathbb{R}^d$. *Fract. Calc. Appl. Anal.* **2022**, *25*, 608–629. [CrossRef]
23. Chen, L.; Hu, G.; Hu, Y.; Huang, J. Space-time fractional diffusions in Gaussian noisy enviroment. *Stochastics* **2017**, *89*, 171–206. [CrossRef]
24. Foondun, M.; Nane, E. Asymptotic properties of some space-time fractional stochastic equation. *Math. Z.* **2017**, *287*, 493–519. [CrossRef]
25. Hu, G.; Hu, Y. Fractional diffusion in Gaussian noisy environment. *Mathematics* **2015**, *3*, 131–152. [CrossRef]
26. Liu, J.; Yan, L. Solving a nonlinear fractional stochastic partial differential equation with fractional noise. *J. Theor. Probab.* **2016**, *29*, 307–347. [CrossRef]
27. Khoshnevisan, D. *Analysis of Stochastic Partial Differential Equations*; CBMS Regional Conference Series in Mathematics; The American Mathematical Society, Providence, RI, USA, 2014; Volume 119.
28. Chen, L.; Dalang, R.C. Moments, intermittency and growth indices for the nonlinear fractional stochastic heat equation. *Stoch. Partial. Differ. Equ. Anal. Comput.* **2015**, *3*, 360–397. [CrossRef]
29. Chen, L.; Kim, K. On comparision principle and strict positivity of the solutions to the nonlinear stochastic fractonal heat equation. *Ann. Inst. Henri Poincaré* **2017**, *53*, 358–388. [CrossRef]
30. Tudor, C.A. *Analysis of Variations for Self-Similar Processes*; Springer: Berlin/Heidelberg, Germany, 2013.
31. Foondun, M.; Mijena, J.; Nane, E. Nonlinear excitation for some space-time fractional stochastic equations in bounded domains. *Fract. Calc. Appl. Anal.* **2016**, *19*, 1527–1553. [CrossRef]
32. Simon, T. Comparing Fréchet and positive stable laws. *Electron. J. Probab.* **2014**, *19*, 1–25. [CrossRef]
33. Tudor, C.A.; Xiao, Y. Sample paths of the solution to the fractional-colored stochastic heat equation. *Stoch. Dyn.* **2017**, *17*, 1750004. [CrossRef]
34. Foondun, M.; Liu, W.; Omaba, M. Moment bounds for a class of fractional stochastic heat equations. *Ann. Probab.* **2017**, *45*, 2131–2153. [CrossRef]

symmetry

MDPI

Article

Hermite–Hadamard-Type Inequalities Involving Harmonically Convex Function via the Atangana–Baleanu Fractional Integral Operator

Muhammad Amer Latif [1], Humaira Kalsoom [2,*] and Muhammad Zainul Abidin [2,*]

[1] Department of Basic Sciences, King Faisal University, Hofuf 31982, Saudi Arabia
[2] Department of Mathematics, Zhejiang Normal University, Jinhua 321004, China
* Correspondence: humaira87@zju.edu.cn (H.K.); mzainulabidin@zjnu.edu.cn (M.Z.A.)

Abstract: Fractional integrals and inequalities have recently become quite popular and have been the prime consideration for many studies. The results of many different types of inequalities have been studied by launching innovative analytical techniques and applications. These Hermite–Hadamard inequalities are discovered in this study using Atangana–Baleanu integral operators, which provide both practical and powerful results. In this paper, a symmetric study of integral inequalities of Hermite–Hadamard type is provided based on an identity proved for Atangana–Baleanu integral operators and using functions whose absolute value of the second derivative is harmonic convex. The proven Hermite–Hadamard-type inequalities have been observed to be valid for a choice of any harmonic convex function with the help of examples. Moreover, fractional inequalities and their solutions are applied in many symmetrical domains.

Keywords: harmonic convex functions; Hermite–Hadamard-type inequalities; Atangana–Baleanu fractional integral operator; power-mean inequality; Hölder inequality

Citation: Amer Latif, M.; Kalsoom, H.; Zainul Abidin, M. Hermite–Hadamard-Type Inequalities Involving Harmonically Convex Function via the Atangana–Baleanu Fractional Integral Operator. *Symmetry* **2022**, *14*, 1774. https://doi.org/10.3390/sym14091774

Academic Editor: António M. Lopes

Received: 31 May 2022
Accepted: 2 July 2022
Published: 25 August 2022

1. Introduction

Integral inequalities are fundamental to our comprehension of the cosmos, and there are a great deal of straightforward methods available for determining the uniqueness and existence of linear and nonlinear differential equations in which symmetry is a significant factor. Convex functions are of great interest to researchers in many applied fields, such as convex programming, because they are extremely important for the theory of inequality in a wide range of applications. Convex functions are also of great interest to researchers in many theoretical fields, such as probability theory. It is good to start by recognizing this class of function.

Definition 1. *A function $f : I \subseteq \mathbb{R} \to \mathbb{R}$ is convex if for all $\varpi_1, \varpi_2 \in I$, the inequality*

$$f(t\varpi_1 + (1-t)\varpi_2) \leq tf(\varpi_1) + (1-t)f(\varpi_2) \tag{1}$$

holds. A function $f : I \to \mathbb{R}$ is concave in which the inequality (1) holds in the opposite direction.

In this case, convex functions play an important role in many areas of mathematics. They are especially important in the study of optimization problems where they are distinguished by a number of convenient properties. Moreover, convex functions are used to create a historical inequality, which is a kind of beautiful inequality in which one has the ability to express the lower and higher limits as arithmetic means. It is critical in numerical integration to understand the inequality described here because it is used in error estimation formulas such as the trapezoidal and midpoint formulas (for more details, see [1–7]):

$$f\left(\frac{\omega_1+\omega_2}{2}\right) \leq \frac{1}{\omega_2-\omega_1}\int_{\omega_1}^{\omega_2} f(x)dx \leq \frac{f(\omega_1)+f(\omega_2)}{2}, \tag{2}$$

where the function $f : I \to \mathbb{R}$ is convex on I and $f \in L^1([\omega_1, \omega_2])$.

One of the generalizations of the convex functions is the harmonic convex functions, which are defined as follows:

Definition 2 ([7]). *A function $f : I \subset \mathbb{R}\backslash\{0\} \to \mathbb{R}$ is harmonic convex if for all $\omega_1, \omega_2 \in I$, the inequality*

$$f\left(\frac{\omega_1\omega_2}{t\omega_2+(1-t)\omega_1}\right) \leq tf(\omega_1)+(1-t)f(\omega_2) \tag{3}$$

holds. A function $f : I \subset \mathbb{R}\backslash\{0\} \to \mathbb{R}$ is harmonic concave in which the inequality (3) holds in the opposite direction. For more details about harmonic convex functions, please see [8–11].

A variant of the Hermite–Hadamard inequality (2) for harmonic convex functions was proved by İşcan [7].

Theorem 1 ([7]). *Let $f : I \subset \mathbb{R}\backslash\{0\} \to \mathbb{R}$ be a harmonically convex function and $\omega_1, \omega_2 \in I$ with $\omega_1 < \omega_2$. If $f \in L[\omega_1, \omega_2]$; then, the following inequalities hold:*

$$f\left(\frac{2\omega_1\omega_2}{\omega_1+\omega_2}\right) \leq \frac{\omega_1\omega_2}{\omega_2-\omega_1}\int_{\omega_1}^{\omega_2}\frac{f(x)}{x^2}dx \leq \frac{f(\omega_1)+f(\omega_2)}{2}.$$

Convexity and integral inequality are topics that are explored in several works. This type of research is oriented on examining the properties of Hadamard, Bullen, Ostrowski, and Simpson-type inequalities, which can be discovered in the results of Static Neural Networks, as well as the properties of other types of inequalities. Every study introduced a new strategy and opened new application opportunities for the literature. The articles [12–18] offer additional information on convexity and integral inequalities in various directions:

Fractional integral inequalities benefit from the properties and definition of convexity, and it has recently become an immensely important topic of research. A newly emerged field in applied mathematics, called fractional analysis, is concerned with finding answers to open problems involving fractional-order derivatives. After discovering this solution, mathematicians have found themselves embarking on brand-new lines of inquiry due to how much research interest there has been in the field for decades. In addition to the Riemann–Liouville fractional integrals, fractional integral operators and fractional derivatives have become major parts of applied mathematics and applied sciences. Solutions to real-world problems are proposed by fractional integral and derivative operators, which also improve the relationship between mathematics and other disciplines when it comes to applications. Those interested in learning more about fractional integral and derivative operators should begin with the articles [19–46]. An important concept, not long ago, that has emerged is the Caputo–Fabrizio integral operator, which was established in the last few years. This is how it is defined:

Definition 3 ([47]). *Let $f \in H^1(0, \omega_2)$, $\omega_1 < \omega_2$, $\alpha \in [0, 1]$; then, the definition of the new Caputo fractional derivative is:*

$${}^{CF}D^{\alpha}f(x) = \frac{M(\alpha)}{1-\alpha}\int_{\omega_1}^{x} f'(t)\exp\left[-\frac{\alpha(x-t)}{1-\alpha}\right]dt, \tag{4}$$

such that $M(\alpha)$ is a normalization function.

The Caputo–Fabrizio fractional integral formula is:

Definition 4 ([21]). *Let $f \in H^1(0, \omega_2)$, $\omega_1 < \omega_2$, $\alpha \in [0,1]$ So, the left and right sides of the Caputo–Fabrizio fractional integral are:*

$$\left({}^{CF}_{\omega_1}I^{\alpha}\right)f(x) = \frac{1-\alpha}{B(\alpha)}f(x) + \frac{\alpha}{B(\alpha)}\int_{\omega_1}^{x} f(t)dt \tag{5}$$

and

$$\left({}^{CF}I^{\alpha}_{\omega_2}\right)f(x) = \frac{1-\alpha}{B(\alpha)}f(x) + \frac{\alpha}{B(\alpha)}\int_{x}^{\omega_2} f(t)dt, \tag{6}$$

where $B(\alpha)$ is normalization function.

Atangana–Baleanu [5] has found a solution to the problem of the Caputo–Fabrizio operator not being reduced to the original function in a special case, despite the fact that the operator is an effective tool in the solution of many systems of differential equations. The features of the Caputo–Fabrizio operator are present in the normalization function.

The power law is included in the kernel of some fractional order derivative and integral operators as well as some integral operators. Nature does not usually exhibit power law behavior. This novel derivative and integral operator incorporates the Mittag–Leffler function [48]. The Mittag–Leffler function is required to model nature. This improved the Atangana–Baleanu operator and piqued researchers' interest. That the work uses the Atangana–Baleanu operator for Hermite–Hadamard inequalities is unusual. When the parameter is set to zero, the Atangana–Baleanu original function can be derived and compared to the Caputo–Fabrizio results.

Definition 5 ([5]). *Let $f \in H^1(0, \omega_2)$, $\omega_1 < \omega_2$, $\alpha \in [0,1]$; then, the definition of the new fractional derivative is given below*

$${}^{ABC}_{\omega_1}D^{\alpha}_{x}[f(x)] = \frac{B(\alpha)}{1-\alpha}\int_{\omega_1}^{x} f'(t)E_{\alpha}\left[-\frac{\alpha(x-t)^{\alpha}}{1-\alpha}\right]dt. \tag{7}$$

Definition 6 ([5]). *Let $f \in H^1(0, \omega_2)$, $\omega_1 < \omega_2$, $\alpha \in [0,1]$; then, the definition of the new fractional derivative is given below:*

$${}^{ABC}_{\omega_1}D^{\alpha}_{x}[f(x)] = \frac{B(\alpha)}{1-\alpha}\frac{d}{dx}\int_{\omega_1}^{x} f(t)E_{\alpha}\left[-\frac{\alpha(x-t)^{\alpha}}{1-\alpha}\right]dt. \tag{8}$$

Equations (7) and (8) have a non-local kernel. In addition, in (8), as a result, the constant function returns to zero. The following is the definition of the associated integral operator for the Atangana–Baleanu fractional derivative:

Definition 7 ([5]). *The new fractional derivative with a non-local kernel of a function is associated with the fractional integral $f \in H^1(0, \omega_2)$ as defined:*

$$\left({}^{AB}_{\omega_1}I^{\alpha}\right)\{f(x)\} = \frac{1-\alpha}{B(\alpha)}f(x) + \frac{\alpha}{B(\alpha)\Gamma(\alpha)}\int_{\omega_1}^{x} f(t)(x-t)^{\alpha-1}dt, \tag{9}$$

where $\omega_1 < \omega_2$, $\alpha \in [0,1]$.

The authors of [22] described the integral operator's right-hand side as follows:

$${}^{AB}I^{\alpha}_{\omega_2}\{f(x)\} = \frac{1-\alpha}{B(\alpha)}f(x) + \frac{\alpha}{B(\alpha)\Gamma(\alpha)}\int_{x}^{\omega_2} f(t)(t-x)^{\alpha-1}dt, \tag{10}$$

where $\omega_1 < \omega_2$, $\alpha \in [0,1]$.

Mathematical concepts can be thought of as having practical and theoretical significance. Furthermore, among the qualities that make the concepts strong are that they solve

a deficiency, provide a new workplace orientation and are more functional than existing concepts. The significance and power of fractional analysis investigations can be better understood when seen from this perspective. The literature acknowledges an operator whose definition and properties are expressed because it is popular in the domain of usage and invention. The Atangana–Baleanu derivative and related integral operator have proven particularly useful. Although many investigations on this unusual operator have been completed in a short time, the results demonstrate that the operator is efficient and valuable. We advise academics to undertake their own independent research to learn more about new directions and trends in fractional calculus.

In [37], Set et al. proved new Hermite–Hadamard-type inequalities, which are for functions whose absolute value of the second derivatives are convex, using Atangana–Baleanu integral operators. Set et al. [37] used Atangana–Baleanu operators to generate new and general Hermite–Hadamard-type inequalities and to make discoveries that better explain physical phenomena in terms of the kernel structure and characteristics of the operator. Selecting α equal to 1 will give a different classical Hermite–Hadamard inequality. In the first place, an identity using Atangana–Baleanu was obtained by various integration techniques, and on the other hand, a modification is made in this identity, and hence, a new set of integral inequalities was proved.

During the course of the last three decades, the study of mathematical inequalities that make use of convex functions has been recognized as a prominent field of research. The researchers are looking for new generalizations of convex functions, and as a consequence, new findings are being added to the theory of inequality as a result of their efforts. Within the scope of the present investigation, we have made use of harmonic convex functions in order to generalize a number of findings that are valid for convex functions. The study initiated by Set et al. [37] provided a sound motivation for us to conduct similar research toward harmonic convex functions. We first set up an identity using an Atangana–Baleanu integral operator as well as the properties of harmonic convexity and the use of several integration techniques to obtain new results of Hermite–Hadamard type. We also try to make amendments in the main identity and applications of a number of known famous integral inequalities to prove a new variety of integral inequalities of Hermite–Hadamard type in the next section, with the property that the derivative of the function in absolute value having certain powers is harmonic convex. The proven Hermite–Hadamard-type inequalities have been observed to be valid for a choice of any harmonic convex function with the help of examples. Moreover, the Figure 1 shows the validity of Theorem 7 and Figure 2 shows the validity of Theorem 3.

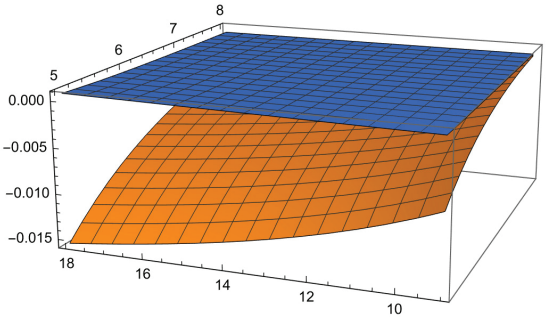

Figure 1. The graph shows the validity of Theorem 2.

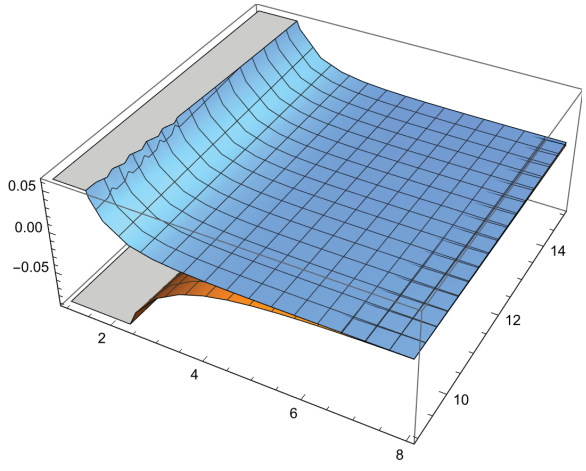

Figure 2. The graph shows the validity of Theorem 3.

2. Main Results

The following lemma will be used to show the Hermite–Hadamard-type integral inequalities for the first time in the literature of inequalities theory. The following result is actually a consequence of the sum of two symmetric integrals and is useful to obtain our results.

Lemma 1. *Let $f : I \subseteq (0,\infty) \to \mathbb{R}$ be differentiable mapping on I° (the interior of I) and $\varpi_1, \varpi_2 \in I^\circ$ with $\varpi_1 < \varpi_2$. Then, the Atangana–Baleanu identity holds for fractional integral operators*

$$\begin{aligned}\Phi_{f\circ h}\left({}^{AB}_{\frac{1}{\varpi_1}}I^{\alpha}_{\frac{1}{x}}, {}^{AB}_{\frac{1}{\varpi_2}}I^{\alpha}_{\frac{1}{x}}\right) :=& -\frac{\left(\frac{x-\varpi_1}{x\varpi_1}\right)^{\alpha+1}}{B(\alpha)\Gamma(\alpha)}\left[\frac{(\alpha-1)xf(\varpi_1)+\varpi_1(x-\varpi_1)\left(2f(\varpi_1)-f'(\varpi_1)\right)}{\varpi_1 x^2(x-\varpi_1)}\right]\\ &-\frac{\left(\frac{\varpi_2-x}{\varpi_2 x}\right)^{\alpha+1}}{B(\alpha)\Gamma(\alpha)}\left[\frac{(\alpha-1)xf(\varpi_2)+\varpi_2(\varpi_2-x)\left(2f(\varpi_2)-f'(\varpi_2)\right)}{\varpi_2 x^2(\varpi_2-x)}\right]\\ &+\frac{(\alpha-1)}{\varpi_1^2x^2}\left[{}^{AB}_{\frac{1}{\varpi_1}}I^{\alpha}_{\frac{1}{x}}\{(f\circ h)(x)\}-\frac{1-\alpha}{B(\alpha)}(f\circ h)(x)\right]-\frac{2\alpha B(\alpha+1)}{\varpi_1^2x^3(\alpha+1)B(\alpha)}\\ &\times\left[{}^{AB}_{\frac{1}{\varpi_1}}I^{\alpha+1}_{\frac{1}{x}}\left\{(h(x))^2(f\circ h)(x)\right\}+\frac{\alpha}{B(\alpha+1)}(h(x))^2(f\circ h)(x)\right]\\ &+\frac{(\alpha-1)}{\varpi_2^2x^2}\left[{}^{AB}_{\frac{1}{\varpi_2}}I^{\alpha}_{\frac{1}{x}}\{(f\circ h)(x)\}-\frac{1-\alpha}{B(\alpha)}(f\circ h)(x)\right]+\frac{2\alpha B(\alpha+1)}{\varpi_2^2x^3(\alpha+1)B(\alpha)}\end{aligned} \tag{11}$$

$$\times\left[{}^{AB}_{\frac{1}{\omega_2}}I^{\alpha+1}_{\frac{1}{x}}\left\{(h(x))^2(f\circ h)(x)\right\}+\frac{\alpha}{B(\alpha+1)}(h(x))^2(f\circ h)(x)\right]$$
$$-\frac{2}{\omega_1^2x^3}\left[{}^{AB}_{\frac{1}{\omega_1}}I^{\alpha}_{\frac{1}{x}}\{h(x)(f\circ h)(x)\}-\frac{1-\alpha}{B(\alpha)}h(x)(f\circ h)(x)\right]$$
$$+\frac{2}{\omega_2^2x^3}\left[{}^{AB}_{\frac{1}{\omega_2}}I^{\alpha}_{\frac{1}{x}}\{h(x)(f\circ h)(x)\}-\frac{1-\alpha}{B(\alpha)}h(x)(f\circ h)(x)\right]$$
$$=\frac{\omega_2x(\omega_2-x)}{B(\alpha)\Gamma(\alpha)}\left(\frac{\omega_2-x}{\omega_2x}\right)^{\alpha+1}\int_0^1\frac{t^{\alpha+1}}{(tx+(1-t)\omega_2)^4}f''\left(\frac{\omega_2x}{tx+(1-t)\omega_2}\right)dt$$
$$+\frac{\omega_1x(x-\omega_1)}{B(\alpha)\Gamma(\alpha)}\left(\frac{x-\omega_1}{x\omega_1}\right)^{\alpha+1}\int_0^1\frac{(1-t)^{\alpha+1}}{(t\omega_1+(1-t)x)^4}f''\left(\frac{\omega_1x}{t\omega_1+(1-t)x}\right)dt.$$

where $h(w)=\frac{1}{w}$, $w\in\left[\frac{1}{\omega_2},\frac{1}{\omega_1}\right]$, $x\in[\omega_1,\omega_2]$ *and* $\alpha\in[0,1]$.

Proof. We observe by integration by parts that

$$\frac{1}{B(\alpha)\Gamma(\alpha)}\int_0^1\frac{(1-t)^{\alpha}}{(t\omega_1+(1-t)x)^2}f'\left(\frac{\omega_1x}{t\omega_1+(1-t)x}\right)dt=\frac{1}{B(\alpha)\Gamma(\alpha)}$$
$$\times\left[\frac{1}{\alpha+1}\frac{f'(\omega_1)}{x^2}+\int_0^1\frac{(1-t)^{\alpha+1}}{\alpha+1}\frac{\omega_1x(x-\omega_1)}{(t\omega_1+(1-t)x)^4}f''\left(\frac{\omega_1x}{t\omega_1+(1-t)x}\right)dt\right.\tag{12}$$
$$\left.+\int_0^1\frac{(1-t)^{\alpha+1}}{\alpha+1}\frac{2(x-\omega_1)}{(t\omega_1+(1-t)x)^3}f'\left(\frac{\omega_1x}{t\omega_1+(1-t)x}\right)dt\right].$$

From (12), we obtain

$$\frac{\alpha-1}{B(\alpha)\Gamma(\alpha)}\int_0^1\frac{(1-t)^{\alpha}}{(t\omega_1+(1-t)x)^2}f'\left(\frac{\omega_1x}{t\omega_1+(1-t)x}\right)dt$$
$$+\frac{2\omega_1}{B(\alpha)\Gamma(\alpha)}\int_0^1\frac{(1-t)^{\alpha}}{(t\omega_1+(1-t)x)^3}f'\left(\frac{\omega_1x}{tx+(1-t)\omega_1}\right)dt=\frac{1}{B(\alpha)\Gamma(\alpha)}\tag{13}$$
$$\times\left[\frac{f'(\omega_1)}{x^2}+\omega_1x(x-\omega_1)\int_0^1\frac{(1-t)^{\alpha+1}}{(t\omega_1+(1-t)x)^4}f''\left(\frac{\omega_1x}{t\omega_1+(1-t)x}\right)dt\right].$$

By using the definition of Atangana–Baleanu fractional derivative, we observe that the following equalities hold

$$\begin{aligned}&\tfrac{\alpha-1}{B(\alpha)\Gamma(\alpha)}\int_0^1\tfrac{(1-t)^{\alpha}}{(t\omega_1+(1-t)x)^2}f'\left(\tfrac{\omega_1x}{t\omega_1+(1-t)x}\right)dt\\&=\tfrac{\alpha-1}{B(\alpha)\Gamma(\alpha)\omega_1x(x-\omega_1)}\int_0^1(1-t)^{\alpha}d\left[f\left(\tfrac{\omega_1x}{t\omega_1+(1-t)x}\right)\right]\\&=-\tfrac{(\alpha-1)f(\omega_1)}{B(\alpha)\Gamma(\alpha)\omega_1x(x-\omega_1)}+\tfrac{(\alpha-1)}{\omega_1x(x-\omega_1)}\left(\tfrac{\omega_1x}{x-\omega_1}\right)^{\alpha}\tfrac{\alpha}{B(\alpha)\Gamma(\alpha)}\int_{\frac{1}{x}}^{\frac{1}{\omega_1}}\left(w-\tfrac{1}{x}\right)^{\alpha-1}f\left(\tfrac{1}{w}\right)dw\\&=-\tfrac{(\alpha-1)f(\omega_1)}{B(\alpha)\Gamma(\alpha)\omega_1x(x-\omega_1)}+\tfrac{(\alpha-1)}{\omega_1x(x-\omega_1)}\left(\tfrac{\omega_1x}{x-\omega_1}\right)^{\alpha}\\&\times\left[{}^{AB}_{\frac{1}{\omega_1}}I^{\alpha}_{\frac{1}{x}}\{(f\circ h)(x)\}-\tfrac{1-\alpha}{B(\alpha)}(f\circ h)(x)\right]\end{aligned}\tag{14}$$

and

$$\begin{aligned}
&\frac{2\omega_1}{B(\alpha)\Gamma(\alpha)}\int_0^1 \frac{(1-t)^{\alpha}}{(t\omega_1+(1-t)x)^3} f'\left(\frac{\omega_1 x}{t\omega_1+(1-t)x}\right)dt\\
&=\frac{2}{x(x-\omega_1)B(\alpha)\Gamma(\alpha)}\int_0^1 \frac{(1-t)^{\alpha}}{t\omega_1+(1-t)x} d\left[f\left(\frac{\omega_1 x}{t\omega_1+(1-t)x}\right)\right]\\
&=-\frac{2f(\omega_1)}{x^2(x-\omega_1)B(\alpha)\Gamma(\alpha)}-\frac{2\alpha}{\alpha x B(\alpha)\Gamma(\alpha)}\int_0^1 \frac{(1-t)^{\alpha}}{(t\omega_1+(1-t)x)^2} f\left(\frac{\omega_1 x}{t\omega_1+(1-t)x}\right)dt\\
&\quad+\frac{2\alpha}{x^2(x-\omega_1)B(\alpha)\Gamma(\alpha)}\int_0^1 \frac{(1-t)^{\alpha-1}}{t\omega_1+(1-t)x} f\left(\frac{\omega_1 x}{t\omega_1+(1-t)x}\right)dt \qquad (15)\\
&=-\frac{2f(\omega_1)}{x^2(x-\omega_1)B(\alpha)\Gamma(\alpha)}-\frac{2\left(\frac{\omega_1 x}{x-\omega_1}\right)^{\alpha+1}B(\alpha+1)}{\omega_1^2 x^3(\alpha+1)B(\alpha)}\\
&\quad\times\left[{}^{AB}_{\frac{1}{\omega_1}}I^{\alpha+1}_{\frac{1}{x}}\left\{(h(x))^2(f\circ h)(x)\right\}+\frac{\alpha}{B(\alpha+1)}(h(x))^2(f\circ h)(x)\right]\\
&\quad+\frac{2\left(\frac{\omega_1 x}{x-\omega_1}\right)^{\alpha}}{\omega_1 x^2(x-\omega_1)}\left[{}^{AB}_{\frac{1}{\omega_1}}I^{\alpha}_{\frac{1}{x}}\{h(x)(f\circ h)(x)\}-\frac{1-\alpha}{B(\alpha)}h(x)(f\circ h)(x)\right].
\end{aligned}$$

By applying (14) and (15) in (13), we obtain

$$\begin{aligned}
&-\frac{\left(\frac{x-\omega_1}{x\omega_1}\right)^{\alpha+1}}{B(\alpha)\Gamma(\alpha)}\left[\frac{(\alpha-1)xf(\omega_1)+2\omega_1(x-\omega_1)f(\omega_1)-\omega_1(x-\omega_1)f'(\omega_1)}{\omega_1 x^2(x-\omega_1)}\right]\\
&\quad+\frac{(\alpha-1)}{\omega_1^2x^2}\left[{}^{AB}_{\frac{1}{\omega_1}}I^{\alpha}_{\frac{1}{x}}\{(f\circ h)(x)\}-\frac{1-\alpha}{B(\alpha)}(f\circ h)(x)\right]-\frac{2B(\alpha+1)}{\omega_1^2x^3(\alpha+1)B(\alpha)}\\
&\quad\times\left[{}^{AB}_{\frac{1}{\omega_1}}I^{\alpha+1}_{\frac{1}{x}}\left\{(h(x))^2(f\circ h)(x)\right\}+\frac{\alpha}{B(\alpha+1)}(h(x))^2(f\circ h)(x)\right] \qquad (16)\\
&\quad+\frac{2}{\omega_1^2x^3}\left[{}^{AB}_{\frac{1}{\omega_1}}I^{\alpha}_{\frac{1}{x}}\{h(x)(f\circ h)(x)\}-\frac{1-\alpha}{B(\alpha)}h(x)(f\circ h)(x)\right]\\
&=\frac{\omega_1x(x-\omega_1)}{B(\alpha)\Gamma(\alpha)}\left(\frac{x-\omega_1}{x\omega_1}\right)^{\alpha+1}\int_0^1\frac{(1-t)^{\alpha+1}}{(t\omega_1+(1-t)x)^4}f''\left(\frac{\omega_1x}{t\omega_1+(1-t)x}\right)dt.
\end{aligned}$$

Now, we consider the integral

$$\begin{aligned}
&\tfrac{1}{B(\alpha)\Gamma(\alpha)}\int_0^1\tfrac{t^{\alpha}}{(tx+(1-t)\omega_2)^2}f'\left(\tfrac{\omega_2x}{tx+(1-t)\omega_2}\right)dt\\
&=\tfrac{f'(\omega_2)}{x^2(\alpha+1)B(\alpha)\Gamma(\alpha)}-\tfrac{1}{B(\alpha)\Gamma(\alpha)}\int_0^1\tfrac{t^{\alpha+1}}{\alpha+1}\tfrac{\omega_2x(\omega_2-x)}{(tx+(1-t)\omega_2)^4}f''\left(\tfrac{\omega_2x}{tx+(1-t)\omega_2}\right)dt \qquad (17)\\
&-\tfrac{1}{B(\alpha)\Gamma(\alpha)}\int_0^1\tfrac{t^{\alpha+1}}{\alpha+1}\tfrac{2(\omega_2-x)}{(tx+(1-t)\omega_2)^3}f'\left(\tfrac{\omega_2x}{tx+(1-t)\omega_2}\right)dt.
\end{aligned}$$

which gives

$$\begin{aligned}
&\frac{\alpha-1}{B(\alpha)\Gamma(\alpha)}\int_0^1\frac{t^{\alpha}}{(tx+(1-t)\omega_2)^2}f'\left(\frac{\omega_2x}{tx+(1-t)\omega_2}\right)dt\\
&\quad+\frac{2\omega_2}{B(\alpha)\Gamma(\alpha)}\int_0^1\frac{t^{\alpha}}{(tx+(1-t)\omega_2)^3}f'\left(\frac{\omega_2x}{tx+(1-t)\omega_2}\right)dt \qquad (18)\\
&=\frac{f'(\omega_2)}{x^2B(\alpha)\Gamma(\alpha)}-\frac{\omega_2x(\omega_2-x)}{B(\alpha)\Gamma(\alpha)}\int_0^1\frac{t^{\alpha+1}}{(tx+(1-t)\omega_2)^4}f''\left(\frac{\omega_2x}{tx+(1-t)\omega_2}\right)dt.
\end{aligned}$$

It is easy to see that

$$\begin{aligned}\frac{\alpha-1}{B(\alpha)\Gamma(\alpha)}\int_0^1\frac{t^\alpha}{(tx+(1-t)\omega_2)^2}f'\left(\frac{\omega_2 x}{tx+(1-t)\omega_2}\right)dt\\ =\frac{(\alpha-1)f(\omega_2)}{\omega_2 x(\omega_2-x)B(\alpha)\Gamma(\alpha)}-\frac{(\alpha-1)\left(\frac{\omega_2 x}{\omega_2-x}\right)^\alpha}{\omega_2 x(\omega_2-x)}\\ \times\left[{}^{AB}_{\frac{1}{\omega_2}}I^\alpha_{\frac{1}{x}}\{(f\circ h)(x)\}-\frac{1-\alpha}{B(\alpha)}(f\circ h)(x)\right]\end{aligned}\tag{19}$$

and

$$\begin{aligned}\frac{2\omega_2}{B(\alpha)\Gamma(\alpha)}\int_0^1\frac{t^\alpha}{(tx+(1-t)\omega_2)^3}f'\left(\frac{\omega_2 x}{tx+(1-t)\omega_2}\right)dt\\ =\frac{2f(\omega_2)}{x^2B(\alpha)\Gamma(\alpha)}-\frac{2\left(\frac{\omega_2 x}{\omega_2-x}\right)^\alpha}{\omega_2x^2(\omega_2-x)}\left[{}^{AB}_{\frac{1}{\omega_2}}I^\alpha_{\frac{1}{x}}\{h(x)(f\circ h)(x)\}-\frac{1-\alpha}{B(\alpha)}h(x)(f\circ h)(x)\right]\\ -\frac{2\left(\frac{\omega_2 x}{\omega_2-x}\right)^{\alpha+1}\alpha B(\alpha+1)}{\omega_2^2x^3(\alpha+1)B(\alpha)}\times\left[{}^{AB}_{\frac{1}{\omega_2}}I^\alpha_{\frac{1}{x}}\left\{(h(x))^2(f\circ h)(x)\right\}+\frac{\alpha}{B(\alpha+1)}(h(x))^2(f\circ h)(x)\right].\end{aligned}\tag{20}$$

A combination of (18)–(20) gives us

$$\begin{aligned}-\frac{\left(\frac{\omega_2-x}{\omega_2x}\right)^{\alpha+1}}{B(\alpha)\Gamma(\alpha)}\left[\frac{(\alpha-1)xf(\omega_2)+2\omega_2(\omega_2-x)f(\omega_2)-\omega_2(\omega_2-x)f'(\omega_2)}{\omega_2x^2(\omega_2-x)}\right]\\ +\frac{(\alpha-1)}{\omega_2^2x^2}\left[{}^{AB}_{\frac{1}{\omega_2}}I^\alpha_{\frac{1}{x}}\{(f\circ h)(x)\}-\frac{1-\alpha}{B(\alpha)}(f\circ h)(x)\right]+\frac{2\alpha B(\alpha+1)}{\omega_2^2x^3(\alpha+1)B(\alpha)}\\ \times\left[{}^{AB}_{\frac{1}{\omega_2}}I^\alpha_{\frac{1}{x}}\left\{(h(x))^2(f\circ h)(x)\right\}+\frac{\alpha}{B(\alpha+1)}(h(x))^2(f\circ h)(x)\right]\\ +\frac{2}{\omega_2^2x^3}\left[{}^{AB}_{\frac{1}{\omega_2}}I^\alpha_{\frac{1}{x}}\{h(x)(f\circ h)(x)\}-\frac{1-\alpha}{B(\alpha)}h(x)(f\circ h)(x)\right]\\ =\frac{\omega_2x(\omega_2-x)}{B(\alpha)\Gamma(\alpha)}\left(\frac{\omega_2-x}{\omega_2x}\right)^{\alpha+1}\int_0^1\frac{t^{\alpha+1}}{(tx+(1-t)\omega_2)^4}f''\left(\frac{\omega_2x}{tx+(1-t)\omega_2}\right)dt.\end{aligned}\tag{21}$$

The addition of (16) and (21) gives the required result. □

We also recall some special functions which we use to give our estimates.

The Beta or the Euler integral of the first kind and hypergeometric functions are defined as

$$\mathbb{B}(\alpha,\beta)=\int_0^1 t^{\alpha-1}(1-t)^{\beta-1}dt,\quad \alpha,\beta>0.$$

$${}_2F_1(\alpha,\beta;\gamma,z)=\frac{1}{\mathbb{B}(\beta,\gamma-\beta)}\int_0^1 t^{\beta-1}(1-t)^{\gamma-\beta-1}(1-zt)^{-\alpha}dt,\quad \gamma>\beta>0,\quad |z|<1,$$

respectively, (see [35]). The regularized hypergeometric function is defined as

$${}_2\bar{F}_1(\alpha,\beta;\gamma,z)=\frac{{}_2F_1(\alpha,\beta;\gamma,z)}{\Gamma(\gamma)},$$

where $\Gamma(\gamma)$ is the gamma function.

We will now be able to generalize the Hermite–Hadamard-type inequalities using the harmonic convexity. One can easily observe that there is symmetry even in the estimates of $\left|\Phi_{f\circ h}\left({}^{AB}_{\frac{1}{\omega_1}}I^{\alpha}_{\frac{1}{x}}, {}^{AB}_{\frac{1}{\omega_2}}I^{\alpha}_{\frac{1}{x}}\right)\right|$.

Theorem 2. *Let $f : I \subseteq (0,\infty) \to \mathbb{R}$ be differentiable mapping on I° (the interior of I) and $\omega_1, \omega_2 \in I^\circ$ with $\omega_1 < \omega_2$. If $f'' \in L_1[\omega_1, \omega_2]$ and $\left|f''\right|$ is a harmonic convex mapping on $[\omega_1, \omega_2]$, then the following inequality for Atangana–Baleanu fractional integral operators holds*

$$\begin{aligned}&\left|\Phi_{f\circ h}\left({}^{AB}_{\frac{1}{\omega_1}}I^{\alpha}_{\frac{1}{x}}, {}^{AB}_{\frac{1}{\omega_2}}I^{\alpha}_{\frac{1}{x}}\right)\right| \\ &\leq \tfrac{\omega_2 x(\omega_2-x)}{B(\alpha)\Gamma(\alpha)}\left(\tfrac{\omega_2-x}{\omega_2 x}\right)^{\alpha+1}\left[\phi_1(\omega_1,\omega_2,\alpha;x)\left|f''(x)\right| + \phi_2(\omega_1,\omega_2,\alpha;x)\left|f''(\omega_2)\right|\right] \\ &+ \tfrac{\omega_1 x(x-\omega_1)}{B(\alpha)\Gamma(\alpha)}\left(\tfrac{x-\omega_1}{x\omega_1}\right)^{\alpha+1}\left[\phi_3(\omega_1,\omega_2,\alpha;x)\left|f''(\omega_1)\right| + \phi_4(\omega_1,\omega_2,\alpha;x)\left|f''(x)\right|\right],\end{aligned} \tag{22}$$

where

$$\begin{aligned}\phi_1(\omega_1,\omega_2,\alpha;x) &= \frac{\omega_2(\omega_2-2\alpha x)}{6\omega_2^4 x^2} + \frac{\alpha\left(\alpha^2+3\alpha+2\right){}_2F_1\left(1,\alpha+3;\alpha+4;1-\frac{x}{\omega_2}\right)}{6\omega_2^4(\alpha+3)} \\ &\quad - \frac{\alpha\left(\alpha^2-1\right){}_2F_1\left(1,\alpha+2;\alpha+3;1-\frac{x}{\omega_2}\right)}{6\omega_2^4(\alpha+2)},\end{aligned}$$

$$\begin{aligned}\phi_2(\omega_1,\omega_2,\alpha;x) &= \frac{\omega_2\left(2\omega_2^2-\alpha\omega_2 x+\alpha(\alpha+1)x^2\right)}{6\omega_2^4 x^3} \\ &\quad - \frac{\alpha(\alpha+1)(\alpha+2)\Gamma(\alpha+3)\,{}_2\tilde{F}_1\left(1,\alpha+3;\alpha+4;1-\frac{x}{\omega_2}\right)}{6\omega_2^4},\end{aligned}$$

$$\begin{aligned}\phi_3(\omega_1,\omega_2,\alpha;x) &= \frac{2\omega_1^2+\alpha(\alpha+1)x^2-\alpha\omega_1 x}{6\omega_1^3 x^3} \\ &\quad - \frac{\alpha(\alpha+1)(\alpha+2)\Gamma(\alpha+3)\,{}_2\tilde{F}_1\left(1,1;\alpha+4;1-\frac{\omega_1}{x}\right)}{6\omega_1^3 x},\end{aligned}$$

$$\begin{aligned}\phi_4(\omega_1,\omega_2,\alpha;x) &= \frac{\left(\omega_1^2-2\alpha\omega_1 x\right)(\alpha+2)-\alpha\left(\alpha^2-1\right)x^2}{6(\alpha+2)\omega_1^4 x^2} \\ &\quad + \frac{\alpha(\alpha+1)\Gamma(\alpha+3)(3\omega_1+(\alpha-1)x)\,{}_2\tilde{F}_1\left(1,1;\alpha+4;1-\frac{\omega_1}{x}\right)}{6\omega_1^4 x},\end{aligned}$$

$x \in [\omega_1,\omega_2]$, $\alpha \in [0,1]$, $q > 1$, $B(\alpha)$ and $\Gamma(\alpha)$ are the normalization and gamma function, respectively.

Proof. According to (11) of Lemma 1, we obtain

$$\begin{aligned}&\left|\Phi_{f\circ h}\left({}^{AB}_{\frac{1}{\omega_1}}I^{\alpha}_{\frac{1}{x}}, {}^{AB}_{\frac{1}{\omega_2}}I^{\alpha}_{\frac{1}{x}}\right)\right| \\ &\leq \tfrac{\omega_2 x(\omega_2-x)}{B(\alpha)\Gamma(\alpha)}\left(\tfrac{\omega_2-x}{\omega_2 x}\right)^{\alpha+1}\int_0^1 \tfrac{t^{\alpha+1}}{(tx+(1-t)\omega_2)^4}\left|f''\left(\tfrac{\omega_2 x}{tx+(1-t)\omega_2}\right)\right|dt \\ &+ \tfrac{\omega_1 x(x-\omega_1)}{B(\alpha)\Gamma(\alpha)}\left(\tfrac{x-\omega_1}{x\omega_1}\right)^{\alpha+1}\int_0^1 \tfrac{(1-t)^{\alpha+1}}{(t\omega_1+(1-t)x)^4}\left|f''\left(\tfrac{\omega_1 x}{t\omega_1+(1-t)x}\right)\right|dt.\end{aligned} \tag{23}$$

Since $\left|f''\right|$ is a harmonic convex mapping on $[\omega_1, \omega_2]$, we obtain

$$\begin{aligned}
&\int_0^1 \frac{t^{\alpha+1}}{(tx+(1-t)\omega_2)^4}\left|f''\left(\frac{\omega_2 x}{tx+(1-t)\omega_2}\right)\right|dt \\
&\leq \left|f''(x)\right|\int_0^1 \frac{t^{\alpha+1}(1-t)}{(tx+(1-t)\omega_2)^4}dt + \left|f''(\omega_2)\right|\int_0^1 \frac{t^{\alpha+2}}{(tx+(1-t)\omega_2)^4}dt \\
&= \left[\frac{\omega_2(\omega_2-2\alpha x)}{6\omega_2^4 x^2} + \frac{\alpha\left(\alpha^2+3\alpha+2\right){}_2F_1\left(1,\alpha+3;\alpha+4;1-\frac{x}{\omega_2}\right)}{6\omega_2^4(\alpha+3)}\right. \\
&\left. - \frac{\alpha\left(\alpha^2-1\right){}_2F_1\left(1,\alpha+2;\alpha+3;1-\frac{x}{\omega_2}\right)}{6\omega_2^4(\alpha+2)}\right]\left|f''(x)\right| + \left[\frac{\omega_2\left(2\omega_2^2-\alpha\omega_2 x+\alpha(\alpha+1)x^2\right)}{6\omega_2^4 x^3}\right. \\
&\left. - \frac{\alpha(\alpha+1)(\alpha+2)\Gamma(\alpha+3){}_2\tilde{F}_1\left(1,\alpha+3;\alpha+4;1-\frac{x}{\omega_2}\right)}{6\omega_2^4}\right]\left|f''(\omega_2)\right|
\end{aligned} \tag{24}$$

and

$$\begin{aligned}
&\int_0^1 \frac{(1-t)^{\alpha+1}}{(t\omega_1+(1-t)x)^4}\left|f''\left(\frac{\omega_1 x}{t\omega_1+(1-t)x}\right)\right|dt \\
&\leq \left|f''(\omega_1)\right|\left[\frac{2\omega_1^2+\alpha(\alpha+1)x^2-\alpha\omega_1 x}{6\omega_1^3 x^3}\right. \\
&\left. - \frac{\alpha(\alpha+1)(\alpha+2)x^2\Gamma(\alpha+3){}_2\tilde{F}_1\left(1,1;\alpha+4;1-\frac{\omega_1}{x}\right)}{6\omega_1^3 x^3}\right] \\
&+\left|f''(x)\right|\left[\frac{\left(\omega_1^2-2\alpha\omega_1 x\right)(\alpha+2)-\alpha\left(\alpha^2-1\right)x^2}{6(\alpha+2)\omega_1^4 x^2}\right. \\
&\left. + \frac{\alpha(\alpha+1)x\Gamma(\alpha+3)(3\omega_1+(\alpha-1)x){}_2\tilde{F}_1\left(1,1;\alpha+4;1-\frac{\omega_1}{x}\right)}{6\omega_1^4 x^2}\right].
\end{aligned} \tag{25}$$

Applying (24) and (25) together in (23), we obtain the desired result. □

Corollary 1. *The substitution of* $x = \frac{2\omega_1\omega_2}{\omega_1+\omega_2}$ *in Theorem 2 produces the following result*

$$\begin{aligned}
&\left|\Phi_{f\circ h}\left({}^{AB}_{\frac{1}{\omega_1}}I^{\alpha}_{\frac{\omega_1+\omega_2}{2\omega_1\omega_2}}, {}^{AB}_{\frac{1}{\omega_2}}I^{\alpha}_{\frac{\omega_1+\omega_2}{2\omega_1\omega_2}}\right)\right| \leq \frac{2\omega_1\omega_2(\omega_2-\omega_1)}{(\omega_1+\omega_2)^2 B(\alpha)\Gamma(\alpha)}\left(\frac{\omega_2-\omega_1}{2\omega_1\omega_2}\right)^{\alpha+1} \\
&\times\left\{\omega_2^2\left[\phi_1\left(\omega_1,\omega_2,\alpha;\frac{2\omega_1\omega_2}{\omega_1+\omega_2}\right)\left|f''\left(\frac{2\omega_1\omega_2}{\omega_1+\omega_2}\right)\right| + \phi_1\left(\omega_1,\omega_2,\alpha;\frac{2\omega_1\omega_2}{\omega_1+\omega_2}\right)\left|f''(\omega_2)\right|\right]\right. \\
&\left.+\omega_1^2\left[\phi_3\left(\omega_1,\omega_2,\alpha;\frac{2\omega_1\omega_2}{\omega_1+\omega_2}\right)\left|f''(\omega_1)\right| + \phi_4\left(\omega_1,\omega_2,\alpha;\frac{2\omega_1\omega_2}{\omega_1+\omega_2}\right)\left|f''\left(\frac{2\omega_1\omega_2}{\omega_1+\omega_2}\right)\right|\right]\right\},
\end{aligned} \tag{26}$$

where

$$\begin{aligned}
\phi_1\left(\omega_1,\omega_2,\alpha;\frac{2\omega_1\omega_2}{\omega_1+\omega_2}\right) &= \frac{\alpha\left(\alpha^2+3\alpha+2\right){}_2F_1\left(1,\alpha+3;\alpha+4;\frac{\omega_2-\omega_1}{\omega_1+\omega_2}\right)}{6\omega_2^4(\alpha+3)} \\
&- \frac{\alpha\left(\alpha^2-1\right){}_2F_1\left(1,\alpha+2;\alpha+3;\frac{\omega_2-\omega_1}{\omega_1+\omega_2}\right)}{6\omega_2^4(\alpha+2)} - \frac{(\omega_1+\omega_2)(\omega_1(4\alpha-1)-\omega_2)}{24\omega_1^2\omega_2^4},
\end{aligned}$$

$$\phi_2\left(\omega_1,\omega_2,\alpha;\frac{2\omega_1\omega_2}{\omega_1+\omega_2}\right)=\frac{(\omega_1+\omega_2)(\omega_1\alpha(\omega_1-\omega_2+2\omega_1\alpha)+(\omega_1+\omega_2))}{24\omega_1^3\omega_2^4}-\frac{\alpha(\alpha+1)(\alpha+2)\Gamma(\alpha+3)\,{}_2\tilde{F}_1\left(1,\alpha+3;\alpha+4;\frac{\omega_2-\omega_1}{\omega_1+\omega_2}\right)}{6\omega_2^4},$$

$$\phi_3\left(\omega_1,\omega_2,\alpha;\frac{2\omega_1\omega_2}{\omega_1+\omega_2}\right)=\frac{(\omega_1+\omega_2)\left(\alpha\omega_2(\omega_2-\omega_1)+(\omega_1+\omega_2)^2+2\alpha^2\omega_2^2\right)}{24\omega_1^4\omega_2^3}-\frac{\alpha(\alpha+1)(\alpha+2)(\omega_1+\omega_2)\Gamma(\alpha+3)\,{}_2\tilde{F}_1\left(1,1;\alpha+4;\frac{\omega_2-\omega_1}{2\omega_2}\right)}{12\omega_1^4\omega_2},$$

$$\phi_4\left(\omega_1,\omega_2,\alpha;\frac{2\omega_1\omega_2}{\omega_1+\omega_2}\right)=\frac{\left(\omega_1^2+2(1-2\alpha)\omega_1\omega_2\right)(\alpha+2)-(\alpha(4\alpha(\alpha+1)+3)-2)\omega_2^2}{24\omega_1^4\omega_2^2(\alpha+2)}+\frac{\alpha(\alpha+1)\Gamma(\alpha+3)(3\omega_1+2\alpha\omega_2+\omega_2)\,{}_2\tilde{F}_1\left(1,1;\alpha+4;\frac{\omega_2-\omega_1}{2\omega_2}\right)}{12\omega_1^4\omega_2},$$

$\alpha\in[0,1]$, $B(\alpha)$ and $\Gamma(\alpha)$ are the normalization and gamma function, respectively.

Theorem 3. *Let $f:I\subseteq(0,\infty)\to\mathbb{R}$ be differentiable mapping on I° (the interior of I) and $\omega_1,\omega_2\in I^\circ$ with $\omega_1<\omega_2$. If $f''\in L_1[\omega_1,\omega_2]$ and $\left|f''\right|^q$ is a harmonic convex mapping on $[\omega_1,\omega_2]$; then, the following inequality for Atangana–Baleanu fractional integral operators holds*

$$\begin{aligned}\left|\Phi_{f\circ h}\left({}^{AB}_{\frac{1}{\omega_1}}I^{\alpha}_{\frac{1}{x}},{}^{AB}_{\frac{1}{\omega_2}}I^{\alpha}_{\frac{1}{x}}\right)\right|&\leq\left(\frac{1}{\alpha p+p+1}\right)^{\frac{1}{p}}\left\{\frac{\omega_2x(\omega_2-x)}{B(\alpha)\Gamma(\alpha)}\left(\frac{\omega_2-x}{\omega_2x}\right)^{\alpha+1}\right.\\&\times\left[\varphi_1(\omega_1,\omega_2,q;x)\left|f''(x)\right|^q+\varphi_2(\omega_1,\omega_2,q;x)\left|f''(\omega_2)\right|^q\right]^{\frac{1}{q}}+\frac{\omega_1x(x-\omega_1)}{B(\alpha)\Gamma(\alpha)}\\&\left.\times\left(\frac{x-\omega_1}{x\omega_1}\right)^{\alpha+1}\left[\varphi_3(\omega_1,\omega_2,q;x)\left|f''(\omega_1)\right|^q+\varphi_4(\omega_1,\omega_2,q;x)\left|f''(x)\right|^q\right]^{\frac{1}{q}}\right\},\end{aligned}\tag{27}$$

where

$$\varphi_1(\omega_1,\omega_2,q;x)=\frac{\omega_2^{2-4q}-2\omega_2^{1-4q}x-4\omega_2^{2-4q}q+x^{2-4q}+4\omega_2^{1-4q}qx}{2(\omega_2-x)^2(8q^2-6q+1)},$$

$$\varphi_2(\omega_1,\omega_2,q;x)=\frac{\omega_2^{-4q}x^{-4q}\left(x\omega_2^{4q}(\omega_2(4q-2)-4qx+x)+\omega_2^2x^{4q}\right)}{2(8q^2-6q+1)(\omega_2-x)^2},$$

$$\varphi_3(\omega_1,\omega_2,q;x)=\frac{\omega_1^{-4q}x^{-4q}\left(x\omega_1^{4q}(\omega_1(4q-2)-4qx+x)+\omega_1^2x^{4q}\right)}{2(8q^2-6q+1)(\omega_1-x)^2},$$

$$\varphi_4(\omega_1,\omega_2,q;x)=\frac{\omega_1^{-4q}x^{-4q}\left(x^2\omega_1^{4q}-\omega_1x^{4q}(\omega_1(4q-1)+(2-4q)x)\right)}{2(8q^2-6q+1)(\omega_1-x)^2},$$

$p^{-1}+q^{-1}=1$, $x\in[\omega_1,\omega_2]$, $\alpha\in[0,1]$, $q>1$, $B(\alpha)$ and $\Gamma(\alpha)$ are the normalization and gamma function, respectively.

Proof. Taking the absolute value on both sides of Lemma 1, applying Hölder's inequality and using the fact that $\left|f''\right|^q$ is a harmonic convex mapping on $[\omega_1, \omega_2]$, we obtain

$$\begin{aligned}\left|\Phi_{f\circ h}\left({}^{AB}_{\frac{1}{\omega_1}}I^{\alpha}_{\frac{1}{x}}\,{}^{AB}_{\frac{1}{\omega_2}}I^{\alpha}_{\frac{1}{x}}\right)\right| &\leq \frac{\omega_2 x(\omega_2-x)}{B(\alpha)\Gamma(\alpha)}\left(\frac{\omega_2-x}{\omega_2 x}\right)^{\alpha+1}\left(\int_0^1 t^{p(\alpha+1)}dt\right)^{\frac{1}{p}}\\ &\times\left(\int_0^1 \frac{1}{(tx+(1-t)\omega_2)^{4q}}\left|f''\left(\frac{\omega_2 x}{tx+(1-t)\omega_2}\right)\right|^q dt\right)^{\frac{1}{q}}\\ &+\frac{\omega_1 x(x-\omega_1)}{B(\alpha)\Gamma(\alpha)}\left(\frac{x-\omega_1}{x\omega_1}\right)^{\alpha+1}\left(\int_0^1 (1-t)^{p(\alpha+1)}dt\right)^{\frac{1}{p}}\\ &\times\left(\int_0^1 \frac{1}{(t\omega_1+(1-t)x)^{4q}}\left|f''\left(\frac{\omega_1 x}{t\omega_1+(1-t)x}\right)\right|^q dt\right)^{\frac{1}{q}}.\end{aligned} \tag{28}$$

It is easy to observe that

$$\int_0^1 t^{p(\alpha+1)}dt = \int_0^1 (1-t)^{p(\alpha+1)}dt = \frac{1}{\alpha p+p+1}. \tag{29}$$

Since $\left|f''\right|^q$ is harmonic convex on $[\omega_1, \omega_2]$, we obtain

$$\begin{aligned}&\int_0^1 \frac{1}{(tx+(1-t)\omega_2)^{4q}}\left|f''\left(\frac{\omega_2 x}{tx+(1-t)\omega_2}\right)\right|^q dt\\ &\leq \int_0^1 \frac{\left[(1-t)\left|f''(x)\right|^q + t\left|f''(\omega_2)\right|^q\right]}{(tx+(1-t)\omega_2)^{4q}}dt\\ &= \left[\frac{\omega_2^{2-4q} - 2\omega_2^{1-4q}x - 4\omega_2^{2-4q}q + x^{2-4q} + 4\omega_2^{1-4q}qx}{2(\omega_2-x)^2(8q^2-6q+1)}\right]\left|f''(x)\right|^q\\ &+\left[\frac{\omega_2^{-4q}x^{-4q}\left(x\omega_2^{4q}(\omega_2(4q-2)-4qx+x)+\omega_2^2x^{4q}\right)}{2(8q^2-6q+1)(\omega_2-x)^2}\right]\left|f''(\omega_2)\right|^q\end{aligned} \tag{30}$$

and similarly, we obtain

$$\begin{aligned}&\int_0^1 \frac{1}{(t\omega_1+(1-t)x)^{4q}}\left|f''\left(\frac{\omega_1 x}{t\omega_1+(1-t)x}\right)\right|^q dt\\ &\leq \left[\frac{\omega_1^{-4q}x^{-4q}\left(x\omega_1^{4q}(\omega_1(4q-2)-4qx+x)+\omega_1^2x^{4q}\right)}{2(8q^2-6q+1)(\omega_1-x)^2}\right]\left|f''(\omega_1)\right|^q\\ &+\left[\frac{\omega_1^{-4q}x^{-4q}\left(x^2\omega_1^{4q}-\omega_1x^{4q}(\omega_1(4q-1)+(2-4q)x)\right)}{2(8q^2-6q+1)(\omega_1-x)^2}\right]\left|f''(x)\right|^q.\end{aligned} \tag{31}$$

Applying (29)–(31) in (28), we obtain (27). □

Corollary 2. *In Theorem 3, especially when we take* $x = \frac{2\omega_1\omega_2}{\omega_1+\omega_2}$, *we obtain*

$$\begin{aligned}&\left|\Phi_{f\circ h}\left({}^{AB}_{\frac{1}{\omega_1}}I^{\alpha}_{\frac{\omega_1+\omega_2}{2\omega_1\omega_2}}\,{}^{AB}_{\frac{1}{\omega_2}}I^{\alpha}_{\frac{\omega_1+\omega_2}{2\omega_1\omega_2}}\right)\right| \leq \frac{2\omega_1\omega_2(\omega_2-\omega_1)}{(\omega_1+\omega_2)^2B(\alpha)\Gamma(\alpha)}\left(\frac{1}{\alpha p+p+1}\right)^{\frac{1}{p}}\left(\frac{\omega_2-\omega_1}{2\omega_1\omega_2}\right)^{\alpha+1}\\ &\times\left\{\omega_2^2\left[\varphi_1\left(\omega_1,\omega_2,q;\frac{2\omega_1\omega_2}{\omega_1+\omega_2}\right)\left|f''\left(\frac{2\omega_1\omega_2}{\omega_1+\omega_2}\right)\right|^q + \varphi_2\left(\omega_1,\omega_2,q;\frac{2\omega_1\omega_2}{\omega_1+\omega_2}\right)\left|f''(\omega_2)\right|^q\right]^{\frac{1}{q}}\right.\\ &\left.+\omega_1^2\left[\varphi_3\left(\omega_1,\omega_2,q;\frac{2\omega_1\omega_2}{\omega_1+\omega_2}\right)\left|f''(\omega_1)\right|^q + \varphi_4\left(\omega_1,\omega_2,q;\frac{2\omega_1\omega_2}{\omega_1+\omega_2}\right)\left|f''\left(\frac{2\omega_1\omega_2}{\omega_1+\omega_2}\right)\right|^q\right]^{\frac{1}{q}}\right\},\end{aligned} \tag{32}$$

where

$$\varphi_1\left(\omega_1,\omega_2,q;\frac{2\omega_1\omega_2}{\omega_1+\omega_2}\right)=\frac{4\omega_1^2\left(\frac{2\omega_1\omega_2}{\omega_1+\omega_2}\right)^{-4q}+(\omega_1+\omega_2)\omega_2^{-4q}(\omega_1(4q-3)-4\omega_2q+\omega_2)}{2(8q^2-6q+1)(\omega_1-\omega_2)^2},$$

$$\varphi_2\left(\omega_1,\omega_2,q;\frac{2\omega_1\omega_2}{\omega_1+\omega_2}\right)=\frac{(\omega_1+\omega_2)^2\omega_2^{-4q}}{2(8q^2-6q+1)(\omega_1-\omega_2)^2}-\frac{2\omega_1\left(\frac{2\omega_1\omega_2}{\omega_1+\omega_2}\right)^{-4q}(2\omega_1q-2\omega_2q+\omega_2)}{(8q^2-6q+1)(\omega_1-\omega_2)^2},$$

$$\varphi_3\left(\omega_1,\omega_2,q;\frac{2\omega_1\omega_2}{\omega_1+\omega_2}\right)=\frac{(\omega_1+\omega_2)^2\omega_1^{-4q}}{2(8q^2-6q+1)(\omega_1-\omega_2)^2}-\frac{\omega_2\left(\frac{2\omega_1\omega_2}{\omega_1+\omega_2}\right)^{-4q}(\omega_1(2-4q)+4\omega_2q)}{(8q^2-6q+1)(\omega_1-\omega_2)^2},$$

$$\varphi_4\left(\omega_1,\omega_2,q;\frac{2\omega_1\omega_2}{\omega_1+\omega_2}\right)=\frac{2\omega_2^2\left(\frac{2\omega_1\omega_2}{\omega_1+\omega_2}\right)^{-4q}}{(8q^2-6q+1)(\omega_1-\omega_2)^2}-\frac{(\omega_1+\omega_2)\omega_1^{-4q}((4q-1)(\omega_1-\omega_2)+2\omega_2)}{2(8q^2-6q+1)(\omega_1-\omega_2)^2},$$

$p^{-1}+q^{-1}=1$, $x\in[\omega_1,\omega_2]$, $\alpha\in[0,1]$, $q>1$, $B(\alpha)$ and $\Gamma(\alpha)$ are the normalization and gamma function, respectively.

Theorem 4. *Let $f:I\subseteq(0,\infty)\to\mathbb{R}$ be differentiable mapping on I° (the interior of I) and $\omega_1,\omega_2\in I^\circ$ with $\omega_1<\omega_2$. If $f''\in L_1[\omega_1,\omega_2]$ and $\left|f''\right|^q$ is a harmonic convex mapping on $[\omega_1,\omega_2]$, then the following inequality for Atangana–Baleanu fractional integral operators holds*

$$\begin{aligned}\left|\Phi_{f\circ h}\left({}^{AB}_{\frac{1}{\omega_1}}I^{\alpha}_{\frac{1}{x}},{}^{AB}_{\frac{1}{\omega_2}}I^{\alpha}_{\frac{1}{x}}\right)\right|&\leq\frac{\omega_2x(\omega_2-x)}{B(\alpha)\Gamma(\alpha)}\left(\frac{\omega_2-x}{\omega_2x}\right)^{\alpha+1}\left[L^{-4p}_{-4p}(\omega_2,x)\right]^{\frac{1}{p}}\\&\times\left[\frac{\left|f''(x)\right|^q+(\alpha q+q+1)\left|f''(\omega_2)\right|^q}{(\alpha q+q+1)(\alpha q+q+2)}\right]^{\frac{1}{q}}+\frac{\omega_1x(x-\omega_1)}{B(\alpha)\Gamma(\alpha)}\left(\frac{x-\omega_1}{x\omega_1}\right)^{\alpha+1}\\&\times\left[L^{-4p}_{-4p}(x,\omega_1)\right]^{\frac{1}{p}}\left[\frac{(\alpha q+q+1)\left|f''(\omega_1)\right|^q+\left|f''(x)\right|^q}{(\alpha q+q+1)(\alpha q+q+2)}\right]^{\frac{1}{q}},\end{aligned}\tag{33}$$

where $p^{-1}+q^{-1}=1$, $x\in[\omega_1,\omega_2]$, $\alpha\in[0,1]$, $q>1$, $B(\alpha)$ and $\Gamma(\alpha)$ are the normalization and gamma function, respectively.

Proof. Taking the absolute value on both sides of Lemma 1, applying Hölder's inequality and using the fact that $\left|f''\right|^q$ is a harmonic convex mapping on $[\omega_1,\omega_2]$, we obtain

$$\begin{aligned}\left|\Phi_{f\circ h}\left({}^{AB}_{\frac{1}{\omega_1}}I^{\alpha}_{\frac{1}{x}},{}^{AB}_{\frac{1}{\omega_2}}I^{\alpha}_{\frac{1}{x}}\right)\right|&\leq\frac{\omega_2x(\omega_2-x)}{B(\alpha)\Gamma(\alpha)}\left(\frac{\omega_2-x}{\omega_2x}\right)^{\alpha+1}\left(\int_0^1\frac{1}{(tx+(1-t)\omega_2)^{4p}}dt\right)^{\frac{1}{p}}\\&\times\left(\int_0^1t^{q(\alpha+1)}\left[(1-t)\left|f''(x)\right|^q+t\left|f''(\omega_2)\right|^q\right]dt\right)^{\frac{1}{q}}\\&+\frac{\omega_1x(x-\omega_1)}{B(\alpha)\Gamma(\alpha)}\left(\frac{x-\omega_1}{x\omega_1}\right)^{\alpha+1}\left(\int_0^1\frac{1}{(t\omega_1+(1-t)x)^{4p}}dt\right)^{\frac{1}{p}}\\&\times\left(\int_0^1(1-t)^{q(\alpha+1)}\left[(1-t)\left|f''(\omega_1)\right|^q+t\left|f''(x)\right|^q\right]dt\right)^{\frac{1}{q}}.\end{aligned}\tag{34}$$

It is easy to observe that

$$\int_0^1\frac{1}{(tx+(1-t)\omega_2)^{4p}}dt=\frac{x^{1-4p}-\omega_2^{1-4p}}{(4p-1)(\omega_2-x)}$$

and

$$\int_0^1 \frac{1}{(t\omega_1+(1-t)x)^{4p}}dt = \frac{\omega_1^{1-4p}-x^{1-4p}}{(4p-1)(x-\omega_1)}.$$

It is not difficult to notice that

$$\int_0^1 t^{q(\alpha+1)}(1-t)dt = \int_0^1 t(1-t)^{q(\alpha+1)}dt = \frac{1}{(\alpha q+q+1)(\alpha q+q+2)}$$

and

$$\int_0^1 t^{q(\alpha+1)+1}dt = \int_0^1 (1-t)^{q(\alpha+1)+1}dt = \frac{1}{\alpha q+q+2}$$

Hence, (34) leads to the proof of the inequality (33). □

Corollary 3. *In Theorem 4, especially when we take* $x = \frac{2\omega_1\omega_2}{\omega_1+\omega_2}$*, we obtain*

$$\begin{aligned}
&\left|\Phi_{f\circ h}\left({}^{AB}_{\frac{1}{\omega_1}}I^{\alpha}_{\omega_1+\omega_2}, {}^{AB}_{\frac{1}{\omega_2}}I^{\alpha}_{\omega_1+\omega_2}\right)\right| \\
&\leq \frac{2\omega_1\omega_2(\omega_2-\omega_1)}{(\omega_1+\omega_2)^2B(\alpha)\Gamma(\alpha)}\left(\frac{\omega_2-\omega_1}{2\omega_1\omega_2}\right)^{\alpha+1}\left\{\omega_2^2\left[L_{-4p}^{-4p}\left(\omega_2,\frac{2\omega_1\omega_2}{\omega_1+\omega_2}\right)\right]^{\frac{1}{p}}\right. \\
&\times\left[\frac{\left|f''\left(\frac{2\omega_1\omega_2}{\omega_1+\omega_2}\right)\right|^q+(\alpha q+q+1)\left|f''(\omega_2)\right|^q}{(\alpha q+q+1)(\alpha q+q+2)}\right]^{\frac{1}{q}}+\omega_1^2\left[L_{-4p}^{-4p}\left(\frac{2\omega_1\omega_2}{\omega_1+\omega_2},\omega_1\right)\right]^{\frac{1}{p}} \\
&\left.\times\left[\frac{(\alpha q+q+1)\left|f''(\omega_1)\right|^q+\left|f''\left(\frac{2\omega_1\omega_2}{\omega_1+\omega_2}\right)\right|^q}{(\alpha q+q+1)(\alpha q+q+2)}\right]^{\frac{1}{q}}\right\},
\end{aligned} \tag{35}$$

where $p^{-1}+q^{-1}=1$, $x\in[\omega_1,\omega_2]$, $\alpha\in[0,1]$, $q>1$, $B(\alpha)$ *and* $\Gamma(\alpha)$ *are the normalization and gamma function, respectively.*

Theorem 5. *Let* $f: I\subseteq(0,\infty)\to\mathbb{R}$ *be differentiable mapping on* I° *(the interior of I) and* $\omega_1,\omega_2\in I^\circ$ *with* $\omega_1<\omega_2$*. If* $f''\in L_1[\omega_1,\omega_2]$ *and* $\left|f''\right|^q$ *is a harmonic convex mapping on* $[\omega_1,\omega_2]$*; then, the following inequality for Atangana–Baleanu fractional integral operators holds*

$$\begin{aligned}
&\left|\Phi_{f\circ h}\left({}^{AB}_{\frac{1}{\omega_1}}I^{\alpha}_{\frac{1}{x}}, {}^{AB}_{\frac{1}{\omega_2}}I^{\alpha}_{\frac{1}{x}}\right)\right| \leq \left\{\frac{\omega_2 x(\omega_2-x)}{B(\alpha)\Gamma(\alpha)}\left(\frac{\omega_2-x}{\omega_2 x}\right)^{\alpha+1}\right. \\
&\times\left[\frac{1}{p(\alpha p+p+1)}+\frac{\varphi_1(\omega_1,\omega_2,q;x)\left|f''(x)\right|^q+\varphi_2(\omega_1,\omega_2,q;x)\left|f''(\omega_2)\right|^q}{q}\right] \\
&+\frac{\omega_1 x(x-\omega_1)}{B(\alpha)\Gamma(\alpha)}\left(\frac{x-\omega_1}{x\omega_1}\right)^{\alpha+1}\left[\frac{1}{p(\alpha p+p+1)}\right. \\
&\left.\left.+\frac{\varphi_3(\omega_1,\omega_2,q;x)\left|f''(\omega_1)\right|^q+\varphi_4(\omega_1,\omega_2,q;x)\left|f''(x)\right|^q}{q}\right]\right\},
\end{aligned} \tag{36}$$

where $\varphi_1(\omega_1,\omega_2,q;x)$, $\varphi_1(\omega_1,\omega_2,q;x)$, $\varphi_1(\omega_1,\omega_2,q;x)$, *and* $\varphi_1(\omega_1,\omega_2,q;x)$ *are defined in Theorem 3,* $p^{-1}+q^{-1}=1$, $x\in[\omega_1,\omega_2]$, $\alpha\in[0,1]$, $q>1$, $B(\alpha)$ *and* $\Gamma(\alpha)$ *are normalization and gamma function, respectively.*

Proof. Taking the absolute value on both sides of Lemma 1, applying Young inequality $xy\leq\frac{x^p}{p}+\frac{y^q}{q}$ and using the harmonic convexity of $\left|f''\right|^q$ on $[\omega_1,\omega_2]$, we obtain

$$\left|\Phi_{f\circ h}\left({}^{AB}_{\frac{1}{\omega_1}}I^{\alpha}_{\frac{1}{x}},{}^{AB}_{\frac{1}{\omega_2}}I^{\alpha}_{\frac{1}{x}}\right)\right| \leq \frac{\omega_2 x(\omega_2-x)}{B(\alpha)\Gamma(\alpha)}\left(\frac{\omega_2-x}{\omega_2 x}\right)^{\alpha+1}\int_0^1 \frac{t^{\alpha+1}}{(tx+(1-t)\omega_2)^4}\left|f''\left(\frac{\omega_2 x}{tx+(1-t)\omega_2}\right)\right|dt$$
$$+\frac{\omega_1 x(x-\omega_1)}{B(\alpha)\Gamma(\alpha)}\left(\frac{x-\omega_1}{x\omega_1}\right)^{\alpha+1}\int_0^1 \frac{(1-t)^{\alpha+1}}{(t\omega_1+(1-t)x)^4}\left|f''\left(\frac{\omega_1 x}{t\omega_1+(1-t)x}\right)\right|dt$$
$$\leq \frac{\omega_2 x(\omega_2-x)}{B(\alpha)\Gamma(\alpha)}\left(\frac{\omega_2-x}{\omega_2 x}\right)^{\alpha+1}\left[\frac{1}{p}\int_0^1 t^{p(\alpha+1)}dt\right. \tag{37}$$
$$\left.+\frac{1}{q}\int_0^1 \frac{1}{(tx+(1-t)\omega_2)^{4q}}\left|f''\left(\frac{\omega_2 x}{tx+(1-t)\omega_2}\right)\right|^q dt\right]+\frac{\omega_1 x(x-\omega_1)}{B(\alpha)\Gamma(\alpha)}\left(\frac{x-\omega_1}{x\omega_1}\right)^{\alpha+1}$$
$$\times\left[\frac{1}{p}\int_0^1 (1-t)^{p(\alpha+1)}dt+\frac{1}{q}\int_0^1 \frac{1}{(t\omega_1+(1-t)x)^{4q}}\left|f''\left(\frac{\omega_1 x}{t\omega_1+(1-t)x}\right)\right|^q dt\right].$$

The integrals involved in (37) have already been evaluated in the proof of Theorem 3. This proves the proof of the result. □

Corollary 4. *In Theorem 3, especially when we take* $x=\frac{2\omega_1\omega_2}{\omega_1+\omega_2}$*, we obtain*

$$\left|\Phi_{f\circ h}\left({}^{AB}_{\frac{1}{\omega_1}}I^{\alpha}_{\frac{\omega_1+\omega_2}{2\omega_1\omega_2}},{}^{AB}_{\frac{1}{\omega_2}}I^{\alpha}_{\frac{\omega_1+\omega_2}{2\omega_1\omega_2}}\right)\right| \leq \frac{2\omega_1\omega_2}{(\omega_1+\omega_2)^2 B(\alpha)\Gamma(\alpha)}\left(\frac{\omega_2-\omega_1}{2\omega_1\omega_2}\right)^{\alpha+1}\left\{\omega_2^2\left[\frac{1}{p(\alpha p+p+1)}\right.\right.$$
$$\left.+\frac{\varphi_1\left(\omega_1,\omega_2,q;\frac{2\omega_1\omega_2}{\omega_1+\omega_2}\right)\left|f''\left(\frac{2\omega_1\omega_2}{\omega_1+\omega_2}\right)\right|^q+\varphi_2\left(\omega_1,\omega_2,q;\frac{2\omega_1\omega_2}{\omega_1+\omega_2}\right)\left|f''(\omega_2)\right|^q}{q}\right]+\omega_1^2\left[\frac{1}{p(\alpha p+p+1)}\right. \tag{38}$$
$$\left.\left.+\frac{\varphi_3\left(\omega_1,\omega_2,q;\frac{2\omega_1\omega_2}{\omega_1+\omega_2}\right)\left|f''(\omega_1)\right|^q+\varphi_4\left(\omega_1,\omega_2,q;\frac{2\omega_1\omega_2}{\omega_1+\omega_2}\right)\left|f''\left(\frac{2\omega_1\omega_2}{\omega_1+\omega_2}\right)\right|^q}{q}\right]\right\},$$

where $\varphi_1\left(\omega_1,\omega_2,q;\frac{2\omega_1\omega_2}{\omega_1+\omega_2}\right)$, $\varphi_1\left(\omega_1,\omega_2,q;\frac{2\omega_1\omega_2}{\omega_1+\omega_2}\right)$, $\varphi_1\left(\omega_1,\omega_2,q;\frac{2\omega_1\omega_2}{\omega_1+\omega_2}\right)$, *and* $\varphi_1\left(\omega_1,\omega_2,q;\frac{2\omega_1\omega_2}{\omega_1+\omega_2}\right)$ *are defined in Theorem 3,* $p^{-1}+q^{-1}=1$, $x\in[\omega_1,\omega_2]$, $\alpha\in[0,1]$, $q>1$, $B(\alpha)$ *is the normalization function and* $\Gamma(\alpha)$ *is the gamma function.*

Theorem 6. *Let* $f: I\subseteq(0,\infty)\to\mathbb{R}$ *be differentiable mapping on* I° *(the interior of I) and* $\omega_1,\omega_2\in I^\circ$ *with* $\omega_1<\omega_2$*. If* $f''\in L_1[\omega_1,\omega_2]$ *and* $\left|f''\right|^q$ *is a harmonic convex mapping on* $[\omega_1,\omega_2]$*, then the following inequality for Atangana–Baleanu fractional integral operators holds*

$$\left|\Phi_{f\circ h}\left({}^{AB}_{\frac{1}{\omega_1}}I^{\alpha}_{\frac{1}{x}},{}^{AB}_{\frac{1}{\omega_2}}I^{\alpha}_{\frac{1}{x}}\right)\right| \leq \left(\frac{1}{\alpha p+p+1}\right)^{\frac{1}{p}}\left\{\frac{\omega_2 x(\omega_2-x)}{B(\alpha)\Gamma(\alpha)}\left(\frac{\omega_2-x}{\omega_2 x}\right)^{\alpha+1}\right.$$
$$\times\left[\frac{x^{1-4p}-\omega_2^{1-4p}}{p(4p-1)(\omega_2-x)}+\frac{\left|f''(x)\right|^q+(\alpha q+q+1)\left|f''(\omega_2)\right|^q}{q(\alpha q+q+1)(\alpha q+q+2)}\right]+\frac{\omega_1 x(x-\omega_1)}{B(\alpha)\Gamma(\alpha)} \tag{39}$$
$$\left.\times\left(\frac{x-\omega_1}{x\omega_1}\right)^{\alpha+1}\left[\frac{\omega_1^{1-4p}-x^{1-4p}}{p(4p-1)(x-\omega_1)}\frac{(\alpha q+q+1)\left|f''(\omega_1)\right|^q+\left|f''(x)\right|^q}{q(\alpha q+q+1)(\alpha q+q+2)}\right]\right\},$$

where $p^{-1}+q^{-1}=1$, $x\in[\omega_1,\omega_2]$, $\alpha\in[0,1]$, $q>1$, $B(\alpha)$ *and* $\Gamma(\alpha)$ *are the normalization and gamma function, respectively.*

Proof. Taking the absolute value on both sides of Lemma 1, applying Young inequality $xy \leq \frac{x^p}{p} + \frac{y^q}{q}$ and using the harmonic convexity of $\left|f''\right|^q$ on $[\omega_1, \omega_2]$, we obtain

$$\begin{aligned}
&\left|\Phi_{f\circ h}\left({}^{AB}_{\frac{1}{\omega_1}}I^{\alpha}_{\frac{1}{x}}, {}^{AB}_{\frac{1}{\omega_2}}I^{\alpha}_{\frac{1}{x}}\right)\right| \\
&\leq \frac{\omega_2 x(\omega_2 - x)}{B(\alpha)\Gamma(\alpha)}\left(\frac{\omega_2 - x}{\omega_2 x}\right)^{\alpha+1}\int_0^1 \frac{t^{\alpha+1}}{(tx + (1-t)\omega_2)^4}\left|f''\left(\frac{\omega_2 x}{tx + (1-t)\omega_2}\right)\right|dt \\
&+\frac{\omega_1 x(x - \omega_1)}{B(\alpha)\Gamma(\alpha)}\left(\frac{x - \omega_1}{x\omega_1}\right)^{\alpha+1}\int_0^1 \frac{(1-t)^{\alpha+1}}{(t\omega_1 + (1-t)x)^4}\left|f''\left(\frac{\omega_1 x}{t\omega_1 + (1-t)x}\right)\right|dt
\end{aligned}$$

$$\begin{aligned}
&\leq \frac{\omega_2 x(\omega_2 - x)}{B(\alpha)\Gamma(\alpha)}\left(\frac{\omega_2 - x}{\omega_2 x}\right)^{\alpha+1}\left[\frac{1}{p}\int_0^1 \frac{1}{(tx + (1-t)\omega_2)^{4p}}dt\right. \\
&\left.+\frac{1}{q}\int_0^1 t^{q(\alpha+1)}\left|f''\left(\frac{\omega_2 x}{tx + (1-t)\omega_2}\right)\right|^q dt\right] \\
&+\frac{\omega_1 x(x - \omega_1)}{B(\alpha)\Gamma(\alpha)}\left(\frac{x - \omega_1}{x\omega_1}\right)^{\alpha+1}\left[\frac{1}{p}\int_0^1 \frac{1}{(t\omega_1 + (1-t)x)^{4p}}dt\right. \\
&\left.+\frac{1}{q}\int_0^1 (1-t)^{q(\alpha+1)}\left|f''\left(\frac{\omega_1 x}{t\omega_1 + (1-t)x}\right)\right|^q dt\right].
\end{aligned} \tag{40}$$

After solving the integrals involved in (40), we obtain (39). □

Corollary 5. *In Theorem 3, especially when we take* $x = \frac{2\omega_1\omega_2}{\omega_1+\omega_2}$, *we obtain*

$$\begin{aligned}
&\left|\Phi_{f\circ h}\left({}^{AB}_{\frac{1}{\omega_1}}I^{\alpha}_{\frac{1}{x}}, {}^{AB}_{\frac{1}{\omega_2}}I^{\alpha}_{\frac{1}{x}}\right)\right| \leq \left(\frac{1}{\alpha p + p + 1}\right)^{\frac{1}{p}}\left\{\frac{\omega_2 x(\omega_2 - x)}{B(\alpha)\Gamma(\alpha)}\left(\frac{\omega_2 - x}{\omega_2 x}\right)^{\alpha+1}\right. \\
&\times\left[\frac{x^{1-4p} - \omega_2^{1-4p}}{p(4p-1)(\omega_2 - x)} + \frac{\left|f''(x)\right|^q + (\alpha q + q + 1)\left|f''(\omega_2)\right|^q}{q(\alpha q + q + 1)(\alpha q + q + 2)}\right] + \frac{\omega_1 x(x - \omega_1)}{B(\alpha)\Gamma(\alpha)} \\
&\left.\times\left(\frac{x - \omega_1}{x\omega_1}\right)^{\alpha+1}\left[\frac{\omega_1^{1-4p} - x^{1-4p}}{p(4p-1)(x - \omega_1)}\frac{(\alpha q + q + 1)\left|f''(\omega_1)\right|^q + \left|f''(x)\right|^q}{q(\alpha q + q + 1)(\alpha q + q + 2)}\right]\right\},
\end{aligned} \tag{41}$$

where $p^{-1} + q^{-1} = 1$, $x \in [\omega_1, \omega_2]$, $\alpha \in [0, 1]$, $q > 1$, $B(\alpha)$ *and* $\Gamma(\alpha)$ *are the normalization and gamma function, respectively.*

Theorem 7. *Let* $f : I \subseteq (0, \infty) \to \mathbb{R}$ *be differentiable mapping on* I° *(the interior of I) and* $\omega_1, \omega_2 \in I^\circ$ *with* $\omega_1 < \omega_2$. *If* $f'' \in L_1[\omega_1, \omega_2]$ *and* $\left|f''\right|^q$ *is a harmonic convex mapping on* $[\omega_1, \omega_2]$, *then the following inequality for Atangana–Baleanu fractional integral operators holds*

$$\begin{aligned}
&\left|\Phi_{f\circ h}\left({}^{AB}_{\frac{1}{\omega_1}}I^{\alpha}_{\frac{1}{x}}, {}^{AB}_{\frac{1}{\omega_2}}I^{\alpha}_{\frac{1}{x}}\right)\right| \leq \frac{\omega_2 x(\omega_2 - x)}{B(\alpha)\Gamma(\alpha)}\left(\frac{\omega_2 - x}{\omega_2 x}\right)^{\alpha+1}[\psi_1(\omega_1, \omega_2, q; x)]^{1-\frac{1}{q}} \\
&\times\left[\psi_2(\omega_1, \omega_2, q; x)\left|f''(x)\right|^q + \psi_3(\omega_1, \omega_2, q; x)\left|f''(\omega_2)\right|^q\right]^{\frac{1}{q}} + \frac{\omega_1 x(x - \omega_1)}{B(\alpha)\Gamma(\alpha)}\left(\frac{x - \omega_1}{x\omega_1}\right)^{\alpha+1} \\
&\times[\psi_4(\omega_1, \omega_2, q; x)]^{1-\frac{1}{q}}\left[\psi_5(\omega_1, \omega_2, q; x)\left|f''(\omega_1)\right|^q + \psi_6(\omega_1, \omega_2, q; x)\left|f''(x)\right|^q\right]^{\frac{1}{q}}\Bigg\},
\end{aligned} \tag{42}$$

where

$$\psi_1(\varpi_1,\varpi_2,q;x)=\frac{\varpi_2\left(-\alpha x(\varpi_2+x)+\varpi_2(2\varpi_2+x)+\alpha^2x^2\right)}{6\varpi_2^4x^3}-\frac{\alpha\left(\alpha^2-1\right)\Gamma(\alpha+2)\,{}_2\tilde{F}_1\left(1,\alpha+2;\alpha+3;1-\frac{x}{\varpi_2}\right)}{6\varpi_2^4},$$

$$\psi_2(\varpi_1,\varpi_2,q;x)=\frac{\alpha\left(\alpha^2+3\alpha+2\right){}_2F_1\left(1,\alpha+3;\alpha+4;1-\frac{x}{\varpi_2}\right)}{6(\alpha+3)\varpi_2^4}-\frac{\alpha\left(\alpha^2-1\right){}_2F_1\left(1,\alpha+2;\alpha+3;1-\frac{x}{\varpi_2}\right)}{6(\alpha+2)\varpi_2^4}+\frac{\varpi_2(\varpi_2-2\alpha x)}{6\varpi_2^4x^2},$$

$$\psi_3(\varpi_1,\varpi_2,q;x)=\frac{\varpi_2\left(2\varpi_2^2-\alpha\varpi_2x+\alpha(\alpha+1)x^2\right)}{6\varpi_2^4x^3}-\frac{\alpha(\alpha+1)(\alpha+2)\Gamma(\alpha+3)\,{}_2\tilde{F}_1\left(1,\alpha+3;\alpha+4;1-\frac{x}{\varpi_2}\right)}{6\varpi_2^4},$$

$$\psi_4(\varpi_1,\varpi_2,q;x)=\frac{\varpi_1(2\varpi_1+x)+\alpha^2x^2-\alpha x(\varpi_1+x)}{6\varpi_1^3x^3}-\frac{\alpha\left(\alpha^2-1\right)x^2\Gamma(\alpha+2)\,{}_2\tilde{F}_1\left(1,1;\alpha+3;1-\frac{\varpi_1}{x}\right)}{6\varpi_1^3x^3},$$

$$\psi_5(\varpi_1,\varpi_2,q;x)=\frac{2\varpi_1^2-\alpha\varpi_1x+\alpha(\alpha+1)x^2}{6\varpi_1^3x^3}-\frac{\alpha(\alpha+1)(\alpha+2)x^2\Gamma(\alpha+3)\,{}_2\tilde{F}_1\left(1,1;\alpha+4;1-\frac{\varpi_1}{x}\right)}{6\varpi_1^3x^3},$$

$$\psi_5(\varpi_1,\varpi_2,q;x)=\frac{\left(\varpi_1^2-2\alpha\varpi_1x\right)(\alpha+2)-\alpha\left(\alpha^2-1\right)x^2}{\alpha+2}+\frac{\alpha(\alpha+1)x\Gamma(\alpha+3)(3\varpi_1+(\alpha-1)x)\,{}_2\tilde{F}_1\left(1,1;\alpha+4;1-\frac{\varpi_1}{x}\right)}{6\varpi_1^4x^2},$$

$q\geq 1$, $x\in[\varpi_1,\varpi_2]$, $\alpha\in[0,1]$, $B(\alpha)$ *and* $\Gamma(\alpha)$ *are the normalization and gamma function, respectively.*

Proof. Taking the absolute value on both sides of Lemma 1, applying power-mean inequality and using the fact that $\left|f''\right|^q$ is a harmonic convex mapping on $[\varpi_1,\varpi_2]$, we obtain

$$\begin{aligned}\left|\Phi_{f\circ h}\left({}^{AB}_{\frac{1}{\varpi_1}}I^{\alpha}_{\frac{1}{x}},{}^{AB}_{\frac{1}{\varpi_2}}I^{\alpha}_{\frac{1}{x}}\right)\right|&\leq\frac{\varpi_2x(\varpi_2-x)}{B(\alpha)\Gamma(\alpha)}\left(\frac{\varpi_2-x}{\varpi_2x}\right)^{\alpha+1}\left(\int_0^1\frac{t^{\alpha+1}}{(tx+(1-t)\varpi_2)^4}dt\right)^{1-\frac{1}{q}}\\&\times\left(\int_0^1\frac{t^{\alpha+1}\left[(1-t)\left|f''(x)\right|^q+t\left|f''(\varpi_2)\right|^q\right]}{(tx+(1-t)\varpi_2)^4}dt\right)^{\frac{1}{q}}\\&+\frac{\varpi_1x(x-\varpi_1)}{B(\alpha)\Gamma(\alpha)}\left(\frac{x-\varpi_1}{x\varpi_1}\right)^{\alpha+1}\left(\int_0^1\frac{(1-t)^{\alpha+1}}{(t\varpi_1+(1-t)x)^4}dt\right)^{1-\frac{1}{q}}\\&\times\left(\int_0^1\frac{(1-t)^{\alpha+1}\left[(1-t)\left|f''(\varpi_1)\right|^q+t\left|f''(x)\right|^q\right]}{(t\varpi_1+(1-t)x)^4}dt\right)^{\frac{1}{q}}.\end{aligned}\tag{43}$$

Evaluating the integrals involved in (43), we obtain (42). □

Corollary 6. *In Theorem 7, especially when we take* $x = \frac{2\omega_1\omega_2}{\omega_1+\omega_2}$, *we obtain*

$$\begin{aligned}
&\left|\Phi_{f\circ h}\left(\tfrac{1}{\omega_1}{}^{AB}I^{\alpha}_{\frac{\omega_1+\omega_2}{2\omega_1\omega_2}}, \tfrac{1}{\omega_2}{}^{AB}I^{\alpha}_{\frac{\omega_1+\omega_2}{2\omega_1\omega_2}}\right)\right| \leq \tfrac{2\omega_1\omega_2(\omega_2-\omega_1)}{(\omega_1+\omega_2)^2B(\alpha)\Gamma(\alpha)}\left(\tfrac{\omega_2-\omega_1}{2\omega_1\omega_2}\right)^{\alpha+1}\\
&\times\left\{\omega_2^2\left[\psi_1\left(\omega_1,\omega_2,q;\tfrac{2\omega_1\omega_2}{\omega_1+\omega_2}\right)\right]^{1-\frac{1}{q}}\left[\psi_2\left(\omega_1,\omega_2,q;\tfrac{2\omega_1\omega_2}{\omega_1+\omega_2}\right)\left|f''\left(\tfrac{2\omega_1\omega_2}{\omega_1+\omega_2}\right)\right|^q\right.\right.\\
&\left.+\psi_3\left(\omega_1,\omega_2,q;\tfrac{2\omega_1\omega_2}{\omega_1+\omega_2}\right)\left|f''(\omega_2)\right|^q\right]^{\frac{1}{q}}+\omega_1^2\left[\psi_4\left(\omega_1,\omega_2,q;\tfrac{2\omega_1\omega_2}{\omega_1+\omega_2}\right)\right]^{1-\frac{1}{q}}\\
&\left.+\left[\psi_5\left(\omega_1,\omega_2,q;\tfrac{2\omega_1\omega_2}{\omega_1+\omega_2}\right)\left|f''(\omega_1)\right|^q+\psi_6\left(\omega_1,\omega_2,q;\tfrac{2\omega_1\omega_2}{\omega_1+\omega_2}\right)\left|f''\left(\tfrac{2\omega_1\omega_2}{\omega_1+\omega_2}\right)\right|^q\right]^{\frac{1}{q}}\right\},
\end{aligned} \tag{44}$$

where

$$\begin{aligned}
\psi_1\left(\omega_1,\omega_2,q;\frac{2\omega_1\omega_2}{\omega_1+\omega_2}\right) &= \frac{(\omega_1+\omega_2)\left((\alpha(2\alpha-3)+2)\omega_1^2-(\alpha-3)\omega_1\omega_2+\omega_2^2\right)}{24\omega_1^3\omega_2^4}\\
&\quad-\frac{4\alpha\left(\alpha^2-1\right)\Gamma(\alpha+2)\,{}_2\tilde{F}_1\left(1,\alpha+2;\alpha+3;1-\frac{2\omega_1}{\omega_1+\omega_2}\right)}{24\omega_2^4},\\
\psi_2\left(\omega_1,\omega_2,q;\frac{2\omega_1\omega_2}{\omega_1+\omega_2}\right) &= \frac{(\omega_1+\omega_2)(\omega_1(4\alpha-1)-\omega_2)}{24\omega_1^2\omega_2^4}\\
&\quad+\frac{\alpha\left(\alpha^2-1\right){}_2F_1\left(1,\alpha+2;\alpha+3;\frac{\omega_2-\omega_1}{\omega_1+\omega_2}\right)}{6(\alpha+2)\omega_2^4}\\
&\quad-\frac{\alpha\left(\alpha^2+3\alpha+2\right){}_2F_1\left(1,\alpha+3;\alpha+4;\frac{\omega_2-\omega_1}{\omega_1+\omega_2}\right)}{6(\alpha+3)\omega_2^4},\\
\psi_3\left(\omega_1,\omega_2,q;\frac{2\omega_1\omega_2}{\omega_1+\omega_2}\right) &= \frac{(\omega_1+\omega_2)\left(2\omega_1^2\alpha^2+\omega_1\alpha(\omega_1-\omega_2)+(\omega_1+\omega_2)^2\right)}{24\omega_1^3\omega_2^4}\\
&\quad-\frac{4\alpha(\alpha+1)(\alpha+2)\Gamma(\alpha+3)\,{}_2\tilde{F}_1\left(1,\alpha+3;\alpha+4;1-\frac{2\omega_1}{\omega_1+\omega_2}\right)}{24\omega_2^4},\\
\psi_4\left(\omega_1,\omega_2,q;\frac{2\omega_1\omega_2}{\omega_1+\omega_2}\right) &= \frac{(\omega_1+\omega_2)\left(\omega_1^2+(\alpha(2\alpha-3)+2)\omega_2^2-(\alpha-3)\omega_1\omega_2\right)}{24\omega_1^4\omega_2^3}\\
&\quad-\frac{2\alpha\left(\alpha^2-1\right)(\omega_1+\omega_2)\omega_2^2\Gamma(\alpha+2)\,{}_2\tilde{F}_1\left(1,1;\alpha+3;\frac{\omega_2-\omega_1}{2\omega_2}\right)}{24\omega_1^4\omega_2^3},\\
\psi_5\left(\omega_1,\omega_2,q;\frac{2\omega_1\omega_2}{\omega_1+\omega_2}\right) &= \frac{\alpha\omega_2(\omega_2-\omega_1)+(\omega_1+\omega_2)^2+2\alpha^2\omega_2^2}{24\omega_1^4\omega_2^3}\\
&\quad-\frac{2\alpha(\alpha+1)(\alpha+2)(\omega_1+\omega_2)\omega_2^2\Gamma(\alpha+3)\,{}_2\tilde{F}_1\left(1,1;\alpha+4;\frac{\omega_2-\omega_1}{2\omega_2}\right)}{24\omega_1^4\omega_2^3},\\
\psi_6\left(\omega_1,\omega_2,q;\frac{2\omega_1\omega_2}{\omega_1+\omega_2}\right) &= \frac{(\alpha+2)\left(\omega_1^2+2(1-2\alpha)\omega_1\omega_2\right)-(\alpha(4\alpha(\alpha+1)+3)-2)\omega_2^2}{\alpha+2}\\
&\quad+\frac{2\alpha(\alpha+1)\omega_2\Gamma(\alpha+3)(3\omega_1+2\alpha\omega_2+\omega_2)\,{}_2\tilde{F}_1\left(1,1;\alpha+4;\frac{\omega_2-\omega_1}{2\omega_2}\right)}{24\omega_1^4\omega_2^2},
\end{aligned}$$

$q \geq 1$, $x \in [\omega_1,\omega_2]$, $\alpha \in [0,1]$, $q > 1$, $B(\alpha)$ and $\Gamma(\alpha)$ are the normalization and gamma function, respectively.

We mention here an important result to prove our next results for concave functions.

Theorem 8. *Let $h : I \subset (0,\infty) \to \mathbb{R}$ be an HA convex function and $[\omega_1,\omega_2] \subset I^\circ$ (the interior of I). Assume also that $w(t) \geq 0$ a.e. on $[\omega_1,\omega_2]$ with $\int_{\omega_1}^{\omega_2} w(t)dt > 0$, then*

$$h\left(\frac{\int_{\omega_1}^{\omega_2} w(t)dt}{\int_{\omega_1}^{\omega_2} \frac{w(t)}{t}dt}\right) \leq \frac{\int_{\omega_1}^{\omega_2} h(t)w(t)dt}{\int_{\omega_1}^{\omega_2} w(t)dt}.$$

Theorem 9. *Let $f : I \subseteq (0,\infty) \to \mathbb{R}$ be differentiable mapping on I° (the interior of I) and $\omega_1,\omega_2 \in I^\circ$ with $\omega_1 < \omega_2$. If $f'' \in L_1[\omega_1,\omega_2]$ and $\left|f''\right|^q$ is a harmonic-concave mapping on $[\omega_1,\omega_2]$; then, the following inequality for Atangana–Baleanu fractional integral operators holds*

$$\begin{aligned}
&\left|\Phi_{f\circ h}\left({}^{AB}_{\frac{1}{\omega_1}}I^{\alpha}_{\frac{1}{x}}, {}^{AB}_{\frac{1}{\omega_2}}I^{\alpha}_{\frac{1}{x}}\right)\right| \\
&\leq \frac{\omega_2 x(\omega_2-x)}{B(\alpha)\Gamma(\alpha)}\left(\frac{\omega_2-x}{\omega_2 x}\right)^{\alpha+1}\left|f''(\kappa_1(\omega_1,\omega_2,q;x))\right| \\
&+\frac{\omega_1 x(x-\omega_1)}{B(\alpha)\Gamma(\alpha)}\left(\frac{x-\omega_1}{x\omega_1}\right)^{\alpha+1}\left|f''(\kappa_2(\omega_1,\omega_2,q;x))\right|,
\end{aligned} \tag{45}$$

where

$$\kappa_1(\omega_1,\omega_2,q;x) = \frac{\alpha(\alpha+1)x^2\Gamma(\alpha+2)\,{}_2\tilde{F}_1\left(1,\alpha+2;\alpha+3;1-\frac{x}{\omega_2}\right)+\omega_2(\omega_2-\alpha x)}{2\omega_2^2x^2},$$

$$\kappa_2(\omega_1,\omega_2,q;x) = \frac{\alpha(\alpha+1)x\Gamma(\alpha+2)\,{}_2\tilde{F}_1\left(1,1;\alpha+3;1-\frac{\omega_1}{x}\right)+\omega_1-\alpha x}{2\omega_1 x},$$

$x \in [\omega_1,\omega_2]$, $\alpha \in [0,1]$, $B(\alpha)$ and $\Gamma(\alpha)$ are the normalization and gamma function, respectively.

Proof. Taking the absolute value on both sides of Lemma 1, applying Jensen's inequality for harmonic convex mappings and using the fact that if $\left|f''\right|^q$ is a harmonic-concave mapping on $[\omega_1,\omega_2]$ then $\left|f''\right|$ is a also a harmonic-concave mapping on $[\omega_1,\omega_2]$, we obtain

$$\begin{aligned}
&\left|\Phi_{f\circ h}\left({}^{AB}_{\frac{1}{\omega_1}}I^{\alpha}_{\frac{1}{x}}, {}^{AB}_{\frac{1}{\omega_2}}I^{\alpha}_{\frac{1}{x}}\right)\right| \\
&\leq \frac{\omega_2 x(\omega_2-x)}{B(\alpha)\Gamma(\alpha)}\left(\frac{\omega_2-x}{\omega_2 x}\right)^{\alpha+1}\int_0^1 \frac{t^{\alpha+1}}{(tx+(1-t)\omega_2)^4}\left|f''\left(\frac{\omega_2 x}{tx+(1-t)\omega_2}\right)\right|dt \\
&+\frac{\omega_1 x(x-\omega_1)}{B(\alpha)\Gamma(\alpha)}\left(\frac{x-\omega_1}{x\omega_1}\right)^{\alpha+1}\int_0^1 \frac{(1-t)^{\alpha+1}}{(t\omega_1+(1-t)x)^4}\left|f''\left(\frac{\omega_1 x}{t\omega_1+(1-t)x}\right)\right|dt \\
&\leq \frac{\omega_2 x(\omega_2-x)}{B(\alpha)\Gamma(\alpha)}\left(\frac{\omega_2-x}{\omega_2 x}\right)^{\alpha+1}\left|f''\left(\frac{\omega_2 x}{\int_0^1 \frac{t^{\alpha+1}}{(tx+(1-t)\omega_2)^3}}\right)\right|dt \\
&+\frac{\omega_1 x(x-\omega_1)}{B(\alpha)\Gamma(\alpha)}\left(\frac{x-\omega_1}{x\omega_1}\right)^{\alpha+1}\left|f''\left(\frac{\omega_1 x}{\int_0^1 \frac{t^{\alpha+1}}{(t\omega_1+(1-t)x)^3}}\right)\right|dt.
\end{aligned} \tag{46}$$

Evaluating the integrals involved in (46), we obtain (45). □

Corollary 7. *In Theorem 7, especially when we take* $x = \frac{2\omega_1\omega_2}{\omega_1+\omega_2}$, *we obtain*

$$\begin{aligned}\left|\Phi_{f\circ h}\left({}^{AB}_{\frac{1}{\omega_1}}I^{\alpha}_{\frac{\omega_1+\omega_2}{2\omega_1\omega_2}}, {}^{AB}_{\frac{1}{\omega_2}}I^{\alpha}_{\frac{\omega_1+\omega_2}{2\omega_1\omega_2}}\right)\right| &\leq \frac{2\omega_1\omega_2(\omega_2-\omega_1)}{(\omega_1+\omega_2)^2B(\alpha)\Gamma(\alpha)}\left(\frac{\omega_2-\omega_1}{2\omega_1\omega_2}\right)^{\alpha+1}\\ \times\left\{\omega_2^2\left|f''\left(\kappa_1\left(\omega_1,\omega_2,q;\frac{2\omega_1\omega_2}{\omega_1+\omega_2}\right)\right)\right|+\omega_1^2\left|f''\left(\kappa_2\left(\omega_1,\omega_2,q;\frac{2\omega_1\omega_2}{\omega_1+\omega_2}\right)\right)\right|\right\},\end{aligned} \tag{47}$$

where

$$\begin{aligned}&\kappa_1\left(\omega_1,\omega_2,q;\frac{2\omega_1\omega_2}{\omega_1+\omega_2}\right)\\ &=\frac{(\omega_1+\omega_2)(\omega_1+\omega_2-2\alpha\omega_1)+4\omega_1\alpha(\alpha+1)\Gamma(\alpha+2)\,{}_2\tilde{F}_1\left(1,\alpha+2;\alpha+3;1-\frac{2\omega_1}{\omega_1+\omega_2}\right)}{4\omega_1\omega_2(\omega_1+\omega_2)},\end{aligned}$$

$$\kappa_2\left(\omega_1,\omega_2,q;\frac{2\omega_1\omega_2}{\omega_1+\omega_2}\right)=\frac{2\alpha(\alpha+1)\omega_2\Gamma(\alpha+2)\,{}_2\tilde{F}_1\left(1,1;\alpha+3;\frac{\omega_2-\omega_1}{2\omega_2}\right)+\omega_1-2\alpha\omega_2+\omega_2}{4\omega_1\omega_2},$$

$x \in [\omega_1,\omega_2]$, $\alpha \in [0,1]$, $q > 1$, $B(\alpha)$ and $\Gamma(\alpha)$ are the normalization and gamma function, respectively.

Theorem 10. *Let $f : I \subseteq (0,\infty) \to \mathbb{R}$ be differentiable mapping on I° (the interior of I) and $\omega_1,\omega_2 \in I^\circ$ with $\omega_1 < \omega_2$. If $f'' \in L_1[\omega_1,\omega_2]$ and $\left|f''\right|^q$ is a harmonic-concave mapping on $[\omega_1,\omega_2]$, then the following inequality for Atangana–Baleanu fractional integral operators holds*

$$\begin{aligned}&\left|\Phi_{f\circ h}\left({}^{AB}_{\frac{1}{\omega_1}}I^{\alpha}_{\frac{1}{x}}, {}^{AB}_{\frac{1}{\omega_2}}I^{\alpha}_{\frac{1}{x}}\right)\right|\\ &\leq\frac{\omega_2x(\omega_2-x)}{B(\alpha)\Gamma(\alpha)}\left(\frac{\omega_2-x}{\omega_2x}\right)^{\alpha+1}[v_1(\omega_1,\omega_2,q;x)]^{\frac{1}{p}}\left|f''\left(\frac{2\omega_2^2x^2}{\omega_2+x}\right)\right|\\ &+\frac{\omega_1x(x-\omega_1)}{B(\alpha)\Gamma(\alpha)}\left(\frac{x-\omega_1}{x\omega_1}\right)^{\alpha+1}[v_2(\omega_1,\omega_2,q;x)]^{\frac{1}{p}}\left|f''\left(\frac{2\omega_1^2x^2}{x+\omega_1}\right)\right|,\end{aligned} \tag{48}$$

where

$$v_1(\omega_1,\omega_2,q;x)=\frac{\omega_2^{-4p}\,{}_2F_1\left(4p,\alpha p+p+1;\alpha p+p+2;1-\frac{x}{\omega_2}\right)}{\alpha p+p+1},$$

$$v_2(\omega_1,\omega_2,q;x)=\frac{x^{-4p}\,{}_2F_1\left(1,4p;\alpha p+p+2;1-\frac{\omega_1}{x}\right)}{\alpha p+p+1},$$

$x \in [\omega_1,\omega_2]$, $\alpha \in [0,1]$, $B(\alpha)$ and $\Gamma(\alpha)$ are the normalization and gamma function, respectively.

Proof. Taking the absolute value on both sides of Lemma 1, applying Hölder's inequality, using Jensen's inequality for harmonic convex mappings and using the fact that if $\left|f''\right|^q$ is a harmonic-concave mapping on $[\omega_1,\omega_2]$, we obtain

$$\begin{aligned}&\left|\Phi_{f\circ h}\left({}^{AB}_{\frac{1}{\omega_1}}I^{\alpha}_{\frac{1}{x}}, {}^{AB}_{\frac{1}{\omega_2}}I^{\alpha}_{\frac{1}{x}}\right)\right|\leq\frac{\omega_2x(\omega_2-x)}{B(\alpha)\Gamma(\alpha)}\left(\frac{\omega_2-x}{\omega_2x}\right)^{\alpha+1}\\ &\times\left(\int_0^1\frac{t^{p(\alpha+1)}}{(tx+(1-t)\omega_2)^{4p}}dt\right)^{\frac{1}{p}}\left(\int_0^1\left|f''\left(\frac{\omega_2x}{tx+(1-t)\omega_2}\right)\right|^q dt\right)^{\frac{1}{q}}\\ &+\frac{\omega_1x(x-\omega_1)}{B(\alpha)\Gamma(\alpha)}\left(\frac{x-\omega_1}{x\omega_1}\right)^{\alpha+1}\left(\int_0^1\frac{(1-t)^{p(\alpha+1)}}{(t\omega_1+(1-t)x)^{4p}}dt\right)^{\frac{1}{p}}\end{aligned} \tag{49}$$

$$\times\left(\int_0^1\left|f''\left(\frac{\omega_2 x}{t\omega_1+(1-t)x}\right)\right|^q dt\right)^{\frac{1}{q}} \leq \frac{\omega_2 x(\omega_2-x)}{B(\alpha)\Gamma(\alpha)}\left(\frac{\omega_2-x}{\omega_2 x}\right)^{\alpha+1}$$
$$\times\left(\int_0^1 \frac{t^{p(\alpha+1)}}{(tx+(1-t)\omega_2)^{4p}}dt\right)^{\frac{1}{p}}\left|f''\left(\frac{\omega_2 x}{\int_0^1 tx+(1-t)\omega_2 dt}\right)\right|^q + \frac{\omega_1 x(x-\omega_1)}{B(\alpha)\Gamma(\alpha)}$$
$$\times\left(\frac{x-\omega_1}{x\omega_1}\right)^{\alpha+1}\left(\int_0^1 \frac{(1-t)^{p(\alpha+1)}}{(t\omega_1+(1-t)x)^{4p}}dt\right)^{\frac{1}{p}}\left|f''\left(\frac{\omega_1 x}{\int_0^1 t\omega_1+(1-t)xdt}\right)\right|^q.$$

Evaluating the integrals involved in (49), we obtain (48). □

Corollary 8. *In Theorem 7, especially when we take* $x = \frac{2\omega_1\omega_2}{\omega_1+\omega_2}$, *we obtain*

$$\left|\Phi_{f\circ h}\left({}^{AB}_{\frac{1}{\omega_1}}I^{\alpha}_{\frac{\omega_1+\omega_2}{2\omega_1\omega_2}}, {}^{AB}_{\frac{1}{\omega_2}}I^{\alpha}_{\frac{\omega_1+\omega_2}{2\omega_1\omega_2}}\right)\right| \leq \frac{2\omega_1\omega_2(\omega_2-\omega_1)}{(\omega_1+\omega_2)^2 B(\alpha)\Gamma(\alpha)}\left(\frac{\omega_2-\omega_1}{2\omega_1\omega_2}\right)^{\alpha+1}$$
$$\times\left\{\omega_2^2\left[v_1\left(\omega_1,\omega_2,q;\frac{2\omega_1\omega_2}{\omega_1+\omega_2}\right)\right]^{\frac{1}{p}}\left|f''\left(\frac{8\omega_1^2\omega_2^3}{(3\omega_1+\omega_2)(\omega_1+\omega_2)}\right)\right|\right. \tag{50}$$
$$\left.+\omega_1^2\left[v_1\left(\omega_1,\omega_2,q;\frac{2\omega_1\omega_2}{\omega_1+\omega_2}\right)\right]^{\frac{1}{p}}\left|f''\left(\frac{8\omega_1^3\omega_2^2}{(\omega_1+\omega_2)(\omega_1+3\omega_2)}\right)\right|\right\},$$

where

$$v_1\left(\omega_1,\omega_2,q;\frac{2\omega_1\omega_2}{\omega_1+\omega_2}\right) = \frac{\omega_2^{-4p}\,{}_2F_1\left(4p,\alpha p+p+1;\alpha p+p+2;\frac{\omega_2-\omega_1}{\omega_1+\omega_2}\right)}{\alpha p+p+1},$$

$$v_2\left(\omega_1,\omega_2,q;\frac{2\omega_1\omega_2}{\omega_1+\omega_2}\right) = \frac{2^{-4p}\left(\frac{\omega_1\omega_2}{\omega_1+\omega_2}\right)^{-4p}\,{}_2F_1\left(1,4p;\alpha p+p+2;\frac{\omega_2-\omega_1}{2\omega_2}\right)}{\alpha p+p+1},$$

$x \in [\omega_1,\omega_2]$, $\alpha \in [0,1]$, $q > 1$, $B(\alpha)$ *and* $\Gamma(\alpha)$ *are the normalization and gamma function, respectively.*

Theorem 11. *Let* $f : I \subseteq (0,\infty) \to \mathbb{R}$ *be differentiable mapping on* I° *(the interior of I) and* $\omega_1,\omega_2 \in I^\circ$ *with* $\omega_1 < \omega_2$. *If* $f'' \in L_1[\omega_1,\omega_2]$ *and* $\left|f''\right|^q$ *is a harmonic-concave mapping on* $[\omega_1,\omega_2]$, *then the following inequality for Atangana–Baleanu fractional integral operators holds*

$$\left|\Phi_{f\circ h}\left({}^{AB}_{\frac{1}{\omega_1}}I^{\alpha}_{\frac{1}{x}}, {}^{AB}_{\frac{1}{\omega_2}}I^{\alpha}_{\frac{1}{x}}\right)\right| \leq \left(\frac{1}{\alpha p+p+1}\right)^{\frac{1}{p}}$$
$$\times\left\{\frac{\omega_2 x(\omega_2-x)}{B(\alpha)\Gamma(\alpha)}\left(\frac{\omega_2-x}{\omega_2 x}\right)^{\alpha+1}\left|f''\left(\frac{2\omega_2 x(1-2q)(\omega_2-x)}{\omega_2^{2-4q}-x^{2-4q}}\right)\right|^q\right. \tag{51}$$
$$\left.+\frac{\omega_1 x(x-\omega_1)}{B(\alpha)\Gamma(\alpha)}\left(\frac{x-\omega_1}{x\omega_1}\right)^{\alpha+1}\left|f''\left(\frac{2\omega_1 x(1-2q)(\omega_1-x)}{\omega_1^{2-4q}-x^{2-4q}}\right)\right|^q\right\},$$

where $x \in [\omega_1,\omega_2]$, $\alpha \in [0,1]$, $B(\alpha)$ *and* $\Gamma(\alpha)$ *are the normalization and gamma function, respectively.*

Proof. Taking the absolute value on both sides of Lemma 1, applying Hölder's inequality, using Jensen's inequality for harmonic convex mappings and using the fact that if $\left|f''\right|^q$ is a harmonic-concave mapping on $[\omega_1,\omega_2]$, we obtain

$$\left|\Phi_{f\circ h}\left({}^{AB}_{\frac{1}{\omega_1}}I^{\alpha}_{\frac{1}{x}},{}^{AB}_{\frac{1}{\omega_2}}I^{\alpha}_{\frac{1}{x}}\right)\right| \leq \frac{\omega_2 x(\omega_2-x)}{B(\alpha)\Gamma(\alpha)}\left(\frac{\omega_2-x}{\omega_2 x}\right)^{\alpha+1}$$
$$\times\left(\int_0^1 t^{p(\alpha+1)}dt\right)^{\frac{1}{p}}\left(\int_0^1 \frac{1}{(tx+(1-t)\omega_2)^{4q}}\left|f''\left(\frac{\omega_2 x}{tx+(1-t)\omega_2}\right)\right|^q dt\right)^{\frac{1}{q}}$$
$$+\frac{\omega_1 x(x-\omega_1)}{B(\alpha)\Gamma(\alpha)}\left(\frac{x-\omega_1}{x\omega_1}\right)^{\alpha+1}\left(\int_0^1 (1-t)^{p(\alpha+1)}dt\right)^{\frac{1}{p}}$$
$$\times\left(\int_0^1 \frac{1}{(t\omega_1+(1-t)x)^{4q}}\left|f''\left(\frac{\omega_1 x}{t\omega_1+(1-t)x}\right)\right|^q dt\right)^{\frac{1}{q}} \leq \frac{\omega_2 x(\omega_2-x)}{B(\alpha)\Gamma(\alpha)}\left(\frac{\omega_2-x}{\omega_2 x}\right)^{\alpha+1} \tag{52}$$
$$\times\left(\int_0^1 t^{p(\alpha+1)}dt\right)^{\frac{1}{p}}\left|f''\left(\frac{\omega_2 x}{\int_0^1 (tx+(1-t)\omega_2)^{1-4q}dt}\right)\right|^q + \frac{\omega_1 x(x-\omega_1)}{B(\alpha)\Gamma(\alpha)}$$
$$\times\left(\frac{x-\omega_1}{x\omega_1}\right)^{\alpha+1}\left(\int_0^1 (1-t)^{p(\alpha+1)}dt\right)^{\frac{1}{p}}\left|f''\left(\frac{\omega_1 x}{\int_0^1 (t\omega_1+(1-t)x)^{1-4q}dt}\right)\right|^q.$$

Evaluating the integrals involved in (52), we obtain (51). □

Corollary 9. *In Theorem 7, especially when we take* $x = \frac{2\omega_1\omega_2}{\omega_1+\omega_2}$, *we obtain*

$$\left|\Phi_{f\circ h}\left({}^{AB}_{\frac{1}{\omega_1}}I^{\alpha}_{\frac{\omega_1+\omega_2}{2\omega_1\omega_2}},{}^{AB}_{\frac{1}{\omega_2}}I^{\alpha}_{\frac{\omega_1+\omega_2}{2\omega_1\omega_2}}\right)\right| \leq \frac{2\omega_1\omega_2(\omega_2-\omega_1)}{B(\alpha)\Gamma(\alpha)(\omega_1+\omega_2)^2}\left(\frac{\omega_2-\omega_1}{\omega_1\omega_2}\right)^{\alpha+1}$$
$$\times\left(\frac{1}{\alpha p+p+1}\right)^{\frac{1}{p}}\left\{\omega_2^2\left|f''\left(\frac{4(1-2q)\omega_1\omega_2^3(\omega_1+\omega_2)^{4q}(\omega_2-\omega_1)}{\omega_2^{2-4q}(\omega_1+\omega_2)^{2-4q}-(2\omega_1\omega_2)^{2-4q}}\right)\right|\right. \tag{53}$$
$$\left.+\omega_1^2\left|f''\left(\frac{4(1-2q)\omega_1^3\omega_2(\omega_1+\omega_2)^{4q}(\omega_2-\omega_1)}{(2\omega_1\omega_2)^{2-4q}-\omega_1^{2-4q}(\omega_1+\omega_2)^{2-4q}}\right)\right|\right\},$$

where $x \in [\omega_1,\omega_2]$, $\alpha \in [0,1]$, $q > 1$, $B(\alpha)$ *and* $\Gamma(\alpha)$ *are the normalization and gamma function, respectively.*

Theorem 12. *Let* $f : I \subseteq (0,\infty) \to \mathbb{R}$ *be differentiable mapping on* I° *(the interior of I) and* $\omega_1,\omega_2 \in I^\circ$ *with* $\omega_1 < \omega_2$. *If* $f'' \in L_1[\omega_1,\omega_2]$ *and* $\left|f''\right|^q$ *is a harmonic-concave mapping on* $[\omega_1,\omega_2]$, *then the following inequality for Atangana–Baleanu fractional integral operators holds*

$$\left|\Phi_{f\circ h}\left({}^{AB}_{\frac{1}{\omega_1}}I^{\alpha}_{\frac{1}{x}},{}^{AB}_{\frac{1}{\omega_2}}I^{\alpha}_{\frac{1}{x}}\right)\right| \leq \left(\frac{1}{\alpha p+p+1}\right)^{\frac{1}{p}}$$
$$\times\left\{\frac{\omega_2 x(\omega_2-x)}{B(\alpha)\Gamma(\alpha)}\left(\frac{\omega_2-x}{\omega_2 x}\right)^{\alpha+1}\left|f''\left(\frac{2\omega_2 x(1-2q)(\omega_2-x)}{\omega_2^{2-4q}-x^{2-4q}}\right)\right|^q\right. \tag{54}$$
$$\left.+\frac{\omega_1 x(x-\omega_1)}{B(\alpha)\Gamma(\alpha)}\left(\frac{x-\omega_1}{x\omega_1}\right)^{\alpha+1}\left|f''\left(\frac{2\omega_1 x(1-2q)(\omega_1-x)}{\omega_1^{2-4q}-x^{2-4q}}\right)\right|^q\right\},$$

where $x \in [\omega_1,\omega_2]$, $\alpha \in [0,1]$, $B(\alpha)$ *and* $\Gamma(\alpha)$ *are the normalization and gamma function, respectively.*

Proof. Taking the absolute value on both sides of Lemma 1, applying Hölder's inequality, using Jensen's inequality for harmonic concave mappings and using the fact that if $\left|f''\right|^q$ is a harmonic-concave mapping on $[\omega_1,\omega_2]$, we obtain

$$\left|\Phi_{f\circ h}\left({}^{AB}_{\frac{1}{\omega_1}}I^{\alpha}_{\frac{1}{x}},{}^{AB}_{\frac{1}{\omega_2}}I^{\alpha}_{\frac{1}{x}}\right)\right| \leq \frac{\omega_2 x(\omega_2-x)}{B(\alpha)\Gamma(\alpha)}\left(\frac{\omega_2-x}{\omega_2 x}\right)^{\alpha+1}$$
$$\times\left(\int_0^1 t^{p(\alpha+1)}dt\right)^{\frac{1}{p}}\left(\int_0^1 \frac{1}{(tx+(1-t)\omega_2)^{4q}}\left|f''\left(\frac{\omega_2 x}{tx+(1-t)\omega_2}\right)\right|^q dt\right)^{\frac{1}{q}}$$
$$+\frac{\omega_1 x(x-\omega_1)}{B(\alpha)\Gamma(\alpha)}\left(\frac{x-\omega_1}{x\omega_1}\right)^{\alpha+1}\left(\int_0^1 (1-t)^{p(\alpha+1)}dt\right)^{\frac{1}{p}}$$
$$\times\left(\int_0^1 \frac{1}{(t\omega_1+(1-t)x)^{4q}}\left|f''\left(\frac{\omega_1 x}{t\omega_1+(1-t)x}\right)\right|^q dt\right)^{\frac{1}{q}} \leq \frac{\omega_2 x(\omega_2-x)}{B(\alpha)\Gamma(\alpha)}\left(\frac{\omega_2-x}{\omega_2 x}\right)^{\alpha+1} \tag{55}$$
$$\times\left(\int_0^1 t^{p(\alpha+1)}dt\right)^{\frac{1}{p}}\left|f''\left(\frac{\omega_2 x}{\int_0^1 (tx+(1-t)\omega_2)^{1-4q}dt}\right)\right|^q + \frac{\omega_1 x(x-\omega_1)}{B(\alpha)\Gamma(\alpha)}$$
$$\times\left(\frac{x-\omega_1}{x\omega_1}\right)^{\alpha+1}\left(\int_0^1 (1-t)^{p(\alpha+1)}dt\right)^{\frac{1}{p}}\left|f''\left(\frac{\omega_1 x}{\int_0^1 (t\omega_1+(1-t)x)^{1-4q}dt}\right)\right|^q.$$

Evaluating the integrals involved in (52), we obtain (51). □

Corollary 10. *In Theorem 12, especially when we take* $x = \frac{2\omega_1\omega_2}{\omega_1+\omega_2}$*, we obtain*

$$\left|\Phi_{f\circ h}\left({}^{AB}_{\frac{1}{\omega_1}}I^{\alpha}_{\frac{\omega_1+\omega_2}{2\omega_1\omega_2}},{}^{AB}_{\frac{1}{\omega_2}}I^{\alpha}_{\frac{\omega_1+\omega_2}{2\omega_1\omega_2}}\right)\right| \leq \frac{2\omega_1\omega_2(\omega_2-\omega_1)}{B(\alpha)\Gamma(\alpha)(\omega_1+\omega_2)^2}\left(\frac{\omega_2-\omega_1}{\omega_1\omega_2}\right)^{\alpha+1}$$
$$\times\left(\frac{1}{\alpha p+p+1}\right)^{\frac{1}{p}}\left\{\omega_2^2\left|f''\left(\frac{4(1-2q)\omega_1\omega_2^3(\omega_1+\omega_2)^{4q}(\omega_2-\omega_1)}{\omega_2^{2-4q}(\omega_1+\omega_2)^{2-4q}-(2\omega_1\omega_2)^{2-4q}}\right)\right|\right. \tag{56}$$
$$\left.+\omega_1^2\left|f''\left(\frac{4(1-2q)\omega_1^3\omega_2(\omega_1+\omega_2)^{4q}(\omega_2-\omega_1)}{(2\omega_1\omega_2)^{2-4q}-\omega_1^{2-4q}(\omega_1+\omega_2)^{2-4q}}\right)\right|\right\},$$

where $x \in [\omega_1,\omega_2]$ *,* $\alpha \in [0,1]$*,* $q > 1$*,* $B(\alpha)$ *and* $\Gamma(\alpha)$ *are the normalization and gamma function, respectively.*

Theorem 13. *Let* $f : I \subseteq (0,\infty) \to \mathbb{R}$ *be differentiable mapping on* I° *(the interior of I) and* $\omega_1,\omega_2 \in I^\circ$ *with* $\omega_1 < \omega_2$*. If* $f'' \in L_1[\omega_1,\omega_2]$ *and* $\left|f''\right|^q$ *is a harmonic-concave mapping on* $[\omega_1,\omega_2]$*, then the following inequality for Atangana–Baleanu fractional integral operators holds*

$$\left|\Phi_{f\circ h}\left({}^{AB}_{\frac{1}{\omega_1}}I^{\alpha}_{\frac{1}{x}},{}^{AB}_{\frac{1}{\omega_2}}I^{\alpha}_{\frac{1}{x}}\right)\right| \leq \left(\frac{\omega_2^{1-4p}-x^{1-4p}}{(1-4p)(\omega_2-x)}\right)^{\frac{1}{p}}\frac{\omega_2 x(\omega_2-x)}{B(\alpha)\Gamma(\alpha)}\left(\frac{\omega_2-x}{\omega_2 x}\right)^{\alpha+1}$$
$$\times\left|f''\left(\frac{\omega_2 x(q+q\alpha+1)(q+q\alpha+2)}{\omega_2+x+qx+qx\alpha}\right)\right|^q + \left(\frac{\omega_1^{1-4p}-x^{1-4p}}{(1-4p-1)(\omega_1-x)}\right)^{\frac{1}{p}} \tag{57}$$
$$\times\frac{\omega_1 x(x-\omega_1)}{B(\alpha)\Gamma(\alpha)}\left(\frac{x-\omega_1}{x\omega_1}\right)^{\alpha+1}\left|f''\left(\frac{\omega_1 x(q+q\alpha+1)(q+q\alpha+2)}{\omega_1+x+qx+qx\alpha}\right)\right|^q\Bigg\},$$

where $x \in [\omega_1,\omega_2]$ *,* $\alpha \in [0,1]$*,* $B(\alpha)$ *and* $\Gamma(\alpha)$ *are the normalization and gamma function, respectively.*

Proof. Taking the absolute value on both sides of Lemma 1, applying Hölder's inequality, using Jensen's inequality for harmonic concave mappings and using the fact that if $\left|f''\right|^q$ is a harmonic-concave mapping on $[\omega_1,\omega_2]$, we obtain

$$\begin{aligned}
\left|\Phi_{f\circ h}\left({}^{AB}_{\frac{1}{\omega_1}}I^{\alpha}_{\frac{1}{x}},{}^{AB}_{\frac{1}{\omega_2}}I^{\alpha}_{\frac{1}{x}}\right)\right| &\leq \frac{\omega_2 x(\omega_2-x)}{B(\alpha)\Gamma(\alpha)}\left(\frac{\omega_2-x}{\omega_2 x}\right)^{\alpha+1}\\
\times\left(\int_0^1\frac{1}{(tx+(1-t)\omega_2)^{4p}}dt\right)^{\frac{1}{p}}&\left(\int_0^1 t^{q(\alpha+1)}\left|f''\left(\frac{\omega_2 x}{tx+(1-t)\omega_2}\right)\right|^q dt\right)^{\frac{1}{q}}\\
+\frac{\omega_1 x(x-\omega_1)}{B(\alpha)\Gamma(\alpha)}&\left(\frac{x-\omega_1}{x\omega_1}\right)^{\alpha+1}\left(\int_0^1\frac{1}{(t\omega_1+(1-t)x)^{4p}}dt\right)^{\frac{1}{p}}\\
\times\left(\int_0^1(1-t)^{q(\alpha+1)}\right.&\left.\left|f''\left(\frac{\omega_1 x}{t\omega_1+(1-t)x}\right)\right|^q dt\right)^{\frac{1}{q}}\\
\leq\frac{\omega_2 x(\omega_2-x)}{B(\alpha)\Gamma(\alpha)}&\left(\frac{\omega_2-x}{\omega_2 x}\right)^{\alpha+1}\left(\int_0^1\frac{1}{(tx+(1-t)\omega_2)^{4p}}dt\right)^{\frac{1}{p}}\\
\times\left|f''\left(\frac{\omega_2 x}{\int_0^1 t^{q(\alpha+1)}(tx+(1-t)\omega_2)dt}\right)\right|^q&+\frac{\omega_1 x(x-\omega_1)}{B(\alpha)\Gamma(\alpha)}\left(\frac{x-\omega_1}{x\omega_1}\right)^{\alpha+1}\\
\left(\int_0^1(1-t)^{p(\alpha+1)}dt\right)^{\frac{1}{p}}&\left|f''\left(\frac{\omega_1 x}{\int_0^1(1-t)^{q(\alpha+1)}(t\omega_1+(1-t)x)dt}\right)\right|^q.
\end{aligned}\tag{58}$$

Evaluating the integrals involved in (52), we obtain (51). □

Corollary 11. *In Theorem 7, especially when we take* $x=\frac{2\omega_1\omega_2}{\omega_1+\omega_2}$*, we obtain*

$$\begin{aligned}
\left|\Phi_{f\circ h}\left({}^{AB}_{\frac{1}{\omega_1}}I^{\alpha}_{\frac{\omega_1+\omega_2}{2\omega_1\omega_2}},{}^{AB}_{\frac{1}{\omega_2}}I^{\alpha}_{\frac{\omega_1+\omega_2}{2\omega_1\omega_2}}\right)\right| &\leq \frac{2\omega_1\omega_2(\omega_2-\omega_1)}{B(\alpha)\Gamma(\alpha)(\omega_1+\omega_2)^2}\left(\frac{\omega_2-\omega_1}{\omega_1\omega_2}\right)^{\alpha+1}\\
\times\left(\frac{1}{\alpha p+p+1}\right)^{\frac{1}{p}}&\left\{\omega_2^2\left|f''\left(\frac{4(1-2q)\omega_1\omega_2^3(\omega_1+\omega_2)^{4q}(\omega_2-\omega_1)}{\omega_2^{2-4q}(\omega_1+\omega_2)^{2-4q}-(2\omega_1\omega_2)^{2-4q}}\right)\right|\right.\\
&\left.+\omega_1^2\left|f''\left(\frac{4(1-2q)\omega_1^3\omega_2(\omega_1+\omega_2)^{4q}(\omega_2-\omega_1)}{(2\omega_1\omega_2)^{2-4q}-\omega_1^{2-4q}(\omega_1+\omega_2)^{2-4q}}\right)\right|\right\},
\end{aligned}\tag{59}$$

where $x\in[\omega_1,\omega_2]$*,* $\alpha\in[0,1]$*,* $q>1$*,* $B(\alpha)$ *and* $\Gamma(\alpha)$ *are the normalization and gamma function, respectively.*

Now, we provide some examples to show the validity of the results that have been proved so far.

Example 1. *By using the all conditions of Theorem 2 and* $f:[\omega_1,\omega_2]\subset(0,\infty)\to\mathbb{R}$ *be defined as* $f(t)=t^2$*. Then,* f *is a harmonically convex on* $[\omega_1,\omega_2]$*. Suppose that* $\alpha=1$*,* $B(\alpha)=B(1)=1$ *and* $x=\frac{2\omega_1\omega_2}{\omega_1+\omega_2}$*; then*

$$\left|\Phi_{f\circ h}\left({}^{AB}_{\frac{1}{\omega_1}}I^{\alpha}_{\frac{1}{x}},{}^{AB}_{\frac{1}{\omega_2}}I^{\alpha}_{\frac{1}{x}}\right)\right|=-\frac{(u-v)^2\left(u^2(24v+1)+uv(24v+29)+18v^2\right)}{48u^3v^4}.\tag{60}$$

And

$$\begin{aligned}
&\frac{\omega_2 x(\omega_2-x)}{B(\alpha)\Gamma(\alpha)}\left(\frac{\omega_2-x}{\omega_2 x}\right)^{\alpha+1}\left[\phi_1(\omega_1,\omega_2,\alpha;x)\left|f''(x)\right|+\phi_2(\omega_1,\omega_2,\alpha;x)\left|f''(\omega_2)\right|\right]\\
&+\frac{\omega_1 x(x-\omega_1)}{B(\alpha)\Gamma(\alpha)}\left(\frac{x-\omega_1}{x\omega_1}\right)^{\alpha+1}\left[\phi_3(\omega_1,\omega_2,\alpha;x)\left|f''(\omega_1)\right|+\phi_4(\omega_1,\omega_2,\alpha;x)\left|f''(x)\right|\right]\\
&=\frac{4\omega_1\omega_2(\omega_2-\omega_1)}{(\omega_1+\omega_2)^2}\left(\frac{\omega_2-\omega_1}{2\omega_1\omega_2}\right)^2\\
&\times\left[\omega_2^2\left\{\phi_1\left(\omega_1,\omega_2,1;\frac{2\omega_1\omega_2}{\omega_1+\omega_2}\right)+\phi_2\left(\omega_1,\omega_2,1;\frac{2\omega_1\omega_2}{\omega_1+\omega_2}\right)\right\}\right.\\
&\left.+\omega_1^2\left\{\phi_3\left(\omega_1,\omega_2,1;\frac{2\omega_1\omega_2}{\omega_1+\omega_2}\right)+\phi_4\left(\omega_1,\omega_2,1;\frac{2\omega_1\omega_2}{\omega_1+\omega_2}\right)\right\}\right],
\end{aligned}\tag{61}$$

where

$$\phi_1\left(\omega_1,\omega_2,1;\frac{2\omega_1\omega_2}{\omega_1+\omega_2}\right)=\frac{(\omega_2-3\omega_1)}{24\omega_2^4\omega_1^2}+\frac{6\,{}_2F_1\left(1,4;5;\frac{\omega_2-\omega_1}{\omega_1+\omega_2}\right)}{24\omega_2^4},$$

$$\phi_2\left(\omega_1,\omega_2,1;\frac{2\omega_1\omega_2}{\omega_1+\omega_2}\right)=\frac{2\left(4\omega_1^2+\omega_1\omega_2+\omega_2^2\right)}{48\omega_2^4\omega_1^3}-\frac{6\,{}_2\tilde{F}_1\left(1,4;5;\frac{\omega_2-\omega_1}{\omega_1+\omega_2}\right)}{\omega_2^4},$$

$$\phi_3\left(\omega_1,\omega_2,1;\frac{2\omega_1\omega_2}{\omega_1+\omega_2}\right)=\frac{2\omega_1^2\left(\omega_1^2+\omega_1\omega_2+4\omega_2^2\right)}{6\omega_1^6\omega_2^3}-\frac{6\,{}_2\tilde{F}_1\left(1,1;5;\frac{\omega_2-\omega_1}{2\omega_2}\right)}{\omega_1^3},$$

$$\begin{aligned}
\phi_4\left(\omega_1,\omega_2,1;\frac{2\omega_1\omega_2}{\omega_1+\omega_2}\right)&=\frac{(\omega_1-3\omega_2)(\omega_1+\omega_2)}{72\omega_1^4\omega_2^2}\\
&+\frac{3(\omega_1+\omega_2)\,{}_2\tilde{F}_1\left(1,1;5;\frac{\omega_2-\omega_1}{2\omega_2}\right)}{2\omega_1^4\omega_2}.
\end{aligned}$$

Thus

$$=\frac{4\omega_1\omega_2^3(\omega_2-\omega_1)}{(\omega_1+\omega_2)^2}\left(\frac{\omega_2-\omega_1}{2\omega_1\omega_2}\right)^2\left[\phi_1\left(\omega_1,\omega_2,1;\frac{2\omega_1\omega_2}{\omega_1+\omega_2}\right)+\phi_2\left(\omega_1,\omega_2,1;\frac{2\omega_1\omega_2}{\omega_1+\omega_2}\right)\right]$$

$$\begin{aligned}
&+\frac{4\omega_2\omega_1^3(\omega_2-\omega_1)}{(\omega_1+\omega_2)^2}\left[\phi_3\left(\omega_1,\omega_2,1;\frac{2\omega_1\omega_2}{\omega_1+\omega_2}\right)+\phi_4\left(\omega_1,\omega_2,1;\frac{2\omega_1\omega_2}{\omega_1+\omega_2}\right)\right]\\
&=\frac{1}{72\omega_1^6\omega_2^3(\omega_1-\omega_2)(\omega_1+\omega_2)^2}\left[-\omega_1^9+\omega_1^8(6\omega_2-3)+\omega_1^7\omega_2\left(-264\omega_2^2+55\omega_2+6\right)\right.\\
&+\omega_1^6\omega_2^2\left(72\omega_2^2+52\omega_2-21\right)+3\omega_1^5\omega_2^3\left(24\omega_2^2-9\omega_2+20\right)\\
&+\omega_1^4\omega_2^4\left(120\omega_2^2-58\omega_2-141\right)-507\omega_1^2\omega_2^6+360\omega_1\omega_2^7-96\omega_2^8\\
&\left.-9\omega_1^3\omega_2^5(3\omega_2-38)+36\omega_1^3\omega_2^2(\omega_1+\omega_2)^3(\omega_1(4\omega_2-1)-\omega_2)\ln\left(\frac{\omega_1+\omega_2}{2\omega_2}\right)\right].
\end{aligned}\tag{62}$$

If we choose $1\le\omega_1\le 8$ *and* $9\le\omega_2\le 18$*, then the graph below validates the result of Theorem 2.*

Example 2. *By using all the conditions of Theorem 3 and $f:[\omega_1,\omega_2]\subset(0,\infty)\to\mathbb{R}$ be defined as $f(t)=t^2$. Then, f is a harmonically convex on $[\omega_1,\omega_2]$. Suppose that $\alpha=1$, $B(\alpha)=B(1)=1$, $x=\frac{2\omega_1\omega_2}{\omega_1+\omega_2}$ and $q=\frac{4}{3}$, then*

$$\left|\Phi_{foh}\left({}^{AB}_{\frac{1}{\omega_1}}I^{\alpha}_{\frac{1}{x}},{}^{AB}_{\frac{1}{\omega_2}}I^{\alpha}_{\frac{1}{x}}\right)\right|=-\frac{(u-v)^2\left(u^2(24v+1)+uv(24v+29)+18v^2\right)}{48u^3v^4}. \tag{63}$$

And

$$\begin{aligned}
&\left(\frac{1}{\alpha p+p+1}\right)^{\frac{1}{p}}\left\{\frac{\omega_2x(\omega_2-x)}{B(\alpha)\Gamma(\alpha)}\left(\frac{\omega_2-x}{\omega_2x}\right)^{\alpha+1}\right.\\
&\times\left[\varphi_1(\omega_1,\omega_2,q;x)\left|f''(x)\right|^q+\varphi_2(\omega_1,\omega_2,q;x)\left|f''(\omega_2)\right|^q\right]^{\frac{1}{q}}+\frac{\omega_1x(x-\omega_1)}{B(\alpha)\Gamma(\alpha)}\\
&\left.\times\left(\frac{x-\omega_1}{x\omega_1}\right)^{\alpha+1}\left[\varphi_3(\omega_1,\omega_2,q;x)\left|f''(\omega_1)\right|^q+\varphi_4(\omega_1,\omega_2,q;x)\left|f''(x)\right|^q\right]^{\frac{1}{q}}\right\},\\
&=2\left(\frac{1}{\alpha p+p+1}\right)^{\frac{1}{p}}\left\{\frac{2\omega_1\omega_2^3}{\omega_1+\omega_2}\left(\frac{\omega_2-\omega_1}{\omega_1+\omega_2}\right)\left(\frac{\omega_2-\omega_1}{2\omega_1\omega_2}\right)^2\right.\\
&\times\left[\varphi_1\left(\omega_1,\omega_2,q;\frac{2\omega_1\omega_2}{\omega_1+\omega_2}\right)+\varphi_2\left(\omega_1,\omega_2,q;\frac{2\omega_1\omega_2}{\omega_1+\omega_2}\right)\right]^{\frac{1}{q}}+\frac{2\omega_1^3\omega_2}{\omega_1+\omega_2}\left(\frac{\omega_2-\omega_1}{\omega_1+\omega_2}\right)\\
&\left.\times\left(\frac{\omega_2-\omega_1}{2\omega_1\omega_2}\right)^2\left[\varphi_3\left(\omega_1,\omega_2,q;\frac{2\omega_1\omega_2}{\omega_1+\omega_2}\right)+\varphi_4\left(\omega_1,\omega_2,q;\frac{2\omega_1\omega_2}{\omega_1+\omega_2}\right)\right]^{\frac{1}{q}}\right\}.
\end{aligned}$$

$$\begin{aligned}
&=\frac{v^2\left(\frac{q-1}{3q-1}\right)^{\frac{q-1}{q}}(v-u)^3}{uv(u+v)^2}\left(\frac{2^{-8q}v^{-4q}\left(\frac{uv}{u+v}\right)^{-8q}\left(\begin{array}{c}u^2\left(\begin{array}{c}v^{4q}\left(2^{4q+2}q\left(\frac{uv}{u+v}\right)^{4q}+2\right)\\+256^q(2q-1)\left(\frac{uv}{u+v}\right)^{8q}\end{array}\right)\\+2^{4q+1}(2q-1)uv^{4q+1}\left(\frac{uv}{u+v}\right)^{4q}\\-256^q(2q-1)v^2\left(\frac{uv}{u+v}\right)^{8q}\end{array}\right)}{(8q^2-6q+1)(u-v)^2}\right)^{1/q}\\
&\quad+\frac{u^2\left(\frac{q-1}{3q-1}\right)^{\frac{q-1}{q}}(v-u)^3}{uv(u+v)^2}\left(\frac{vu^{-4q}+u^{1-4q}-2^{1-4q}v\left(\frac{uv}{u+v}\right)^{-4q}}{-4qu+4qv+u-v}\right)^{1/q},
\end{aligned} \tag{64}$$

where

$$\begin{aligned}
\varphi_1(\omega_1,\omega_2,q;x)&=\frac{(\omega_1+\omega_2)^2}{2\omega_2^2(\omega_2-\omega_1)^2(8q^2-6q+1)}\\
&\times\left((1-4q)\omega_2^{2-4q}-\frac{4\omega_1\omega_2^{2-4q}}{\omega_1+\omega_2}+\left(\frac{2\omega_1\omega_2}{\omega_1+\omega_2}\right)^{2-4q}+\frac{8q\omega_1\omega_2^{2-4q}}{\omega_1+\omega_2}\right),
\end{aligned}$$

$$\begin{aligned}
\varphi_2\left(\omega_1,\omega_2,q;\frac{2\omega_1\omega_2}{\omega_1+\omega_2}\right)&=\frac{\omega_2^{-4q}\left(\frac{2\omega_1\omega_2}{\omega_1+\omega_2}\right)^{-4q+1}}{2(8q^2-6q+1)(\frac{\omega_2(\omega_2-\omega_1)}{\omega_1+\omega_2})^2}\\
&\times\left(\omega_2^{4q}\left(\omega_2(4q-2)+\frac{2\omega_1\omega_2}{\omega_1+\omega_2}(1-4q)\right)+\omega_2^2\left(\frac{2\omega_1\omega_2}{\omega_1+\omega_2}\right)^{4q-1}\right),
\end{aligned}$$

$$\varphi_3\left(\omega_1,\omega_2,q;\frac{2\omega_1\omega_2}{\omega_1+\omega_2}\right)=\frac{\omega_1^{-4q}\left(\frac{2\omega_1\omega_2}{\omega_1+\omega_2}\right)^{-4q}}{2(8q^2-6q+1)(\frac{\omega_1(\omega_2-\omega_1)}{\omega_1+\omega_2})^2}$$
$$\times\left(\frac{2\omega_1\omega_2}{\omega_1+\omega_2}\omega_1^{4q}(\omega_1(4q-2)+\frac{2(1-4q)\omega_1\omega_2}{\omega_1+\omega_2})+\omega_1^2\left(\frac{2\omega_1\omega_2}{\omega_1+\omega_2}\right)^{4q}\right),$$

$$\varphi_4\left(\omega_1,\omega_2,q;\frac{2\omega_1\omega_2}{\omega_1+\omega_2}\right)=\frac{\omega_1^{-4q}\left(\frac{2\omega_1\omega_2}{\omega_1+\omega_2}\right)^{-4q}}{2(8q^2-6q+1)(\frac{\omega_1(\omega_2-\omega_1)}{\omega_1+\omega_2})^2}$$
$$\times\left(\left(\frac{2\omega_1\omega_2}{\omega_1+\omega_2}\right)^2\omega_1^{4q}-\omega_1\left(\frac{2\omega_1\omega_2}{\omega_1+\omega_2}\right)^{4q}\left(\omega_1(4q-1)+\frac{4(1-2q)\omega_1\omega_2}{\omega_1+\omega_2}\right)\right).$$

If we choose $1\le\omega_1\le 8$ *and* $9\le\omega_2\le 18$, *then the graph below validates the result of Theorem 3.*

Author Contributions: Writing—original, software, M.A.L.; Writing—review and editing, Methodology, H.K.; Validation, Visualization, M.Z.A. All authors have read and agreed to the published version of the manuscript.

Funding: This research received no external funding.

Institutional Review Board Statement: Not applicable.

Informed Consent Statement: Not applicable.

Data Availability Statement: Not applicable.

Acknowledgments: The Chinese Government is to be acknowledged for providing postdoctoral studies to Humaira Kalsoom and Muhammad Zainul Abidin.

Conflicts of Interest: The authors declare that they have no competing interest.

References

1. Akdemir, A.O.; Set, E.; Özdemir, M.E.; Yalcin, A. New generalizations for functions whose second derivatives are GG-convex, *Uzbek Math. J.* **2018**, *4*, 22–34.
2. Bakula, M.K.; Özdemir, M.E.; Pecaric, J.P. Hadamard type inequalities for m-convex and (α,m)-convex functions. *J. Inequal. Pure Appl. Math.* **2008**, *9*, 12.
3. Chen, F.; Wu, S. Fejér and Hermite-Hadamard type inqequalities for harmonically convex functions. *J. Appl. Math.* **2014**, *2014*, 386806. [CrossRef]
4. Dragomir, S.S.; Pearce, C.E.M. *Selected Topics on Hermite-Hadamard Inequalities and Applications*; RGMIA Monographs, Victoria University: Footscray, Australia, 2000.
5. Dragomir, S.S.; Agarwal, R.P. Two inequalities for differentiable mappings and applications to special means of real numbers and to trapezoidal formula. *Appl. Math. Lett.* **1998**, *11*, 91–95. [CrossRef]
6. Hadamard, J. Étude sur les propriétés des fonctions entières en particulier d'une fonction considérée par Riemann. *J. Math. Pures Appl.* **1893**, *58*, 171–215.
7. İşcan, İ. Hermite-Hadamard type inequalities for harmonically convex functions. *Hacet. J. Math. Stat.***2014**, *43*, 935–942. [CrossRef]
8. Awan, M.U.; Akhtar, N.; Iftikhar, S.; Noor, M.A.; Chu, Y.M. New Hermite–Hadamard type inequalities for n-polynomial harmonically convex functions. *J. Inequal. Appl.* **2020**, *2020*, 1–12. [CrossRef]
9. Latif, M.A.; Hussain, S.; Chu, Y. Generalized Hermite–Hadamard type inequalities for differentiable harmonically-convex and harmonically quasi-convex functions. *J. Math. Inequal.* **2021**, *15*, 755–766. [CrossRef]
10. You, X.X.; Ali, M.A.; Budak, H.; Agarwal, P.; Chu, Y.M. Extensions of Hermite–Hadamard inequalities for harmonically convex functions via generalized fractional integrals. *J. Inequal. Appl.* **2021**, *2021*, 1–22. [CrossRef]
11. Chu, Y.M.; Rashid, S.; Abdeljawad, T.; Khalid, A.; Kalsoom, H. On new generalized unified bounds via generalized exponentially harmonically s-convex functions on fractal sets. *Adv. Differ. Equ. 2021*, *2021*, 1–33. [CrossRef]
12. Kirmaci, U.K.; Bakula, M.K.; Ozdemir, M.E.; Pečarić, J. Hadamard-type inequalities of s-convex functions. *Appl. Math. Comput.* **2007**, *193*, 26–35. [CrossRef]
13. Kavurmaci, H.; Avci, M.; Özdemir, M.E. New inequalities of Hermite-Hadamard type for convex functions with applications. *J. Inequal. Appl.* **2011**, *2011*, 86. [CrossRef]
14. Mohammed, P.O.; Abdeljawad, T.; Zeng, S.; Kashuri, A. Fractional Hermite-Hadamard integral inequalities for a new class of convex functions. *Symmetry* **2020**, *12*, 1485. [CrossRef]

15. Shi, D.-P.; Xi, B.-Y.; Qi, F. Hermite-Hadamard type inequalities for Riemann-Liouville fractional integrals of (α, m)-convex functions. *Fract. Differ. Calc.* **2014**, *4*, 31–43. [CrossRef]
16. Vivas-Cortez, M.; Abdeljawad, T.; Mohammed, P.O.; Rangel-Oliveros, Y. Simpson's integral inequalities for twice differentiable convex functions. *Math. Probl. Eng.* **2020**, *2020*, 1936461. [CrossRef]
17. Zhang, T.-Y.; Ji, A.-P.; Qi, F. On integral inequalities of Hermite-Hadamard type for s-geometrically convex functions. *Abstr. Appl. Anal.* **2012**, *2012*, 560–586. [CrossRef]
18. Zhang, T.-Y.; Ji, A.-P.; Qi, F. Some inequalities of Hermite-Hadamard type for GA-convex functions with applications to means. *Le Mat.* **2013**, *68*, 229–239.
19. Almeida, R. A Caputo fractional derivative of a function with respect to another function. *Commun. Nonlinear Sci. Numer. Simul.* **2017**, *44*, 460–481. [CrossRef]
20. Abdeljawad, T.; Mohammed, P.O.; Kashuri, A. New modified conformable fractional integral inequalities of Hermite-Hadamard type with applications. *J. Funct. Space* **2020**, *2020*, 4352357. [CrossRef]
21. Abdeljawad, T.; Baleanu, D. On fractional derivatives with exponential kernel and their discrete versions. *Rep. Math. Phys.* **2017**, *80*, 11–27. [CrossRef]
22. Abdeljawad, T.; Baleanu, D. Integration by parts and its applications of a new nonlocal fractional derivative with Mittag-Leffler nonsingular kernel. *J. Nonlinear Sci. Appl.* **2017**, *10*, 1098–1107. [CrossRef]
23. Baleanu, D.; Mohammed, P.O.; Vivas-Cortez, M.; Rangel-Oliveros, Y. Some modifications in conformable fractional integral inequalities. *Adv. Differ. Equ.* **2020**, *2020*, 374. [CrossRef]
24. Bardaro, C.; Butzer, P.L.; Mantellini, I. The foundations of fractional calculus in the Mellin transform setting with applications. *J. Fourier Anal. Appl.* **2015**, *21*, 961–1017. [CrossRef]
25. Baleanu, D.; Mohammed, P.O.; Zeng, S. Inequalities of trapezoidal type involving generalized fractional integrals. *Alex. Eng. J.* **2020**, *59*, 2975–2984. [CrossRef]
26. Fernandez, A.; Mohammed, P.O. Hermite-Hadamard inequalities in fractional calculus defined using Mittag-Leffler kernels. *Math. Methods Appl. Sci.* **2020**, *44*, 8414–8431. [CrossRef]
27. Gunawan, H.; Eridani. Fractional integrals and generalized Olsen inequalities. *Kyungpook Math. J.* **2009**, *49*, 31–39. [CrossRef]
28. Han, J.; Mohammed, P.O.; Zeng, H. Generalized fractional integral inequalities of Hermite-Hadamard-type for a convex function. *Open Math.* **2020**, *18*, 794–806. [CrossRef]
29. İşcan, İ. Hermite-Hadamard-Fejér type inequalities for convex functions via fractional integrals. *Stud. Univ. Babes Bolyai Math.* **2015**, *60*, 355–366.
30. İşcan, İ.; Wu, S. Hermite-Hadamard type inequalities for harmonically convex functions via fractional integrals. *Appl. Math. Comput.* **2014**, *238*, 237–244. [CrossRef]
31. İşcan, İ.; Kunt, M.; Yazici, N. Hermite-Hadamard-Fejér type inequalities for harmonically convex functions via fractional integrals. *New Trends Math. Sci.* **2016**, *4*, 239–253. [CrossRef]
32. Kilbas, A.A.; Srivastava, H.M.; Trujillo, J.J. *Theory and Applications of Fractional Differential Equations*; North-Holland Mathematics Studies; Elsevier Sci. B.V.: Amsterdam, The Netherlands, 2006; Volume 204.
33. Kunt, M.; İşcan, İ. On new Hermite-Hadamard-Fejér type inequalities for p-convex functions via fractional integrals. *Commun. Math. Model. Appl.* **2017**, *2*, 1–15. [CrossRef] [PubMed]
34. Mohammed, P.O.; Sarikaya, M.Z.; Baleanu, D. On the generalized Hermite-Hadamard inequalities via the tempered fractional integrals. *Symmetry* **2020**, *12*, 595. [CrossRef]
35. Mehmood, S.; Zafar, F.; Asmin, N. New Hermite-Hadamard-Fejér type inequalities for (h_1,h_2)-convex functions via fractional calculus. *ScienceAsia* **2020**, *46*, 102–108. [CrossRef]
36. Qi, F.; Mohammed, O.P.; Yao, J.C.; Yao, Y.H. Generalized fractional integral inequalities of Hermite-Hadamard type for (α ,m)-convex functions. *J. Inequal. Appl.* **2019**, *2019*, 135. [CrossRef]
37. Set, E.; Butt, S.I.; Akdemir, A.O.; Karaoğlan, A.; Abdeljawad, T. New integral inequalities for differentiable convex functions via Atangana-Baleanu fractional integral operators. *Chaos Solitons Fractals* **2021**, *143*, 110554. [CrossRef]
38. Sarikaya, M.Z.; Yaldiz, H. On generalization integral inequalities for fractional integrals. *Nihonkai Math. J.* **2014**, *25*, 93–104.
39. Sarikaya, M.Z.; Set, E.; Yaldiz, H.; Basak, N. Hermite-Hadamard's inequalities for fractional integrals and related fractional inequalities. *Math. Comput. Model.* **2013**, *57*, 2403–2407. [CrossRef]
40. Mohammed, P.O.; Brevik, I. A new version of the Hermite-Hadamard inequality for Riemann-Liouville fractional integrals. *Symmetry* **2020**, *12*, 610. [CrossRef]
41. Mohammed, P.O.; Sarikaya, M.Z. Hermite-Hadamard type inequalities for F-convex function involving fractional integrals. *J. Inequal. Appl.* **2018**, *2018*, 359. [CrossRef]
42. Mohammed, P.O.; Abdeljawad, T. Modification of certain fractional integral inequalities for convex functions. *Adv. Differ. Equ.* **2020**, *2020*, 69. [CrossRef]
43. Mohammed, P.O.; Sarikaya, M.Z. On generalized fractional integral inequalities for twice differentiable convex functions. *J. Comput. Appl. Math.* **2020**, *372*, 112740. [CrossRef]
44. Mohammed, P.O.; Abdeljawad, T. Integral inequalities for a fractional operator of a function with respect to another function with nonsingular kernel. *Adv. Differ. Equ.* **2020**, *2020*, 363. [CrossRef]

45. Mohammed, P.O. Hermite-Hadamard inequalities for Riemann-Liouville fractional integrals of a convex function with respect to a monotone function. *Math. Methods Appl. Sci.* **2019**, *44*, 2314–2324. [CrossRef]
46. Macdonald, I.G. *Symmetric Functions and Orthogonal Polynomials*; American Mathematical Soc.: Providence, RI, USA, 1997.
47. Caputo, M.; Fabrizio, M.A. A new definition of fractional derivative without singular kernel. *Prog. Fract. Differ. Appl.* **2015**, *1*, 73–85.
48. Atangana, A.; Baleanu, D. New fractional derivatives with non-local and non-singular kernel, theory and application to heat transfer model. *Therm. Sci.* **2016**, *20*, 763–769. [CrossRef]

mathematics

MDPI

Article

Analytical Investigations into Anomalous Diffusion Driven by Stress Redistribution Events: Consequences of Lévy Flights

Josiah D. Cleland [1,2,*] and Martin A. K. Williams [1,2,3]

[1] School of Natural Sciences, Massey University, Palmerston North 4442, New Zealand
[2] Riddet Institute, Palmerston North 4474, New Zealand
[3] The MacDiarmid Institute for Advanced Materials and Nanotechnology, Wellington 6140, New Zealand
* Correspondence: j.cleland2@massey.ac.nz

Abstract: This research is concerned with developing a generalised diffusion equation capable of describing diffusion processes driven by underlying stress-redistributing type events. The work utilises the development of an appropriate continuous time random walk framework as a foundation to consider a new generalised diffusion equation. While previous work has explored the resulting generalised diffusion equation for jump-timings motivated by stick-slip physics, here non-Gaussian probability distributions of the jump displacements are also considered, specifically Lévy flights. This work illuminates several features of the analytic solution to such a generalised diffusion equation using several known properties of the Fox H function. Specifically demonstrated are the temporal behaviour of the resulting position probability density function, and its normalisation. The reduction of the proposed form to expected known solutions upon the insertion of simplifying parameter values, as well as a demonstration of asymptotic behaviours, is undertaken to add confidence to the validity of this equation. This work describes the analytical solution of such a generalised diffusion equation for the first time, and additionally demonstrates the capacity of the Fox H function and its properties in solving and studying generalised Fokker–Planck equations.

Keywords: generalized; fractional; diffusion; Fokker–Planck

MSC: 60G65

Citation: Cleland, J.; Williams, M.A.K. Analytical Investigations into Anomalous Diffusion Driven by Stress Redistribution Events: Consequences of Lévy Flights. *Mathematics* **2022**, *10*, 3235. https://doi.org/10.3390/math10183235

Academic Editors: António M. Lopes, Alireza Alfi, Liping Chen and Sergio A. David

Received: 15 August 2022
Accepted: 3 September 2022
Published: 6 September 2022

1. Introduction

Diffusion is a widespread phenomena, occurring across a vast array of physical systems. The study of diffusive systems in a physical and mathematical sense may be divided into those exhibiting Gaussian or non-Gaussian behaviours. These two classes of diffusive process are also often referred to as normal (Gaussian) and anomalous (non-Gaussian) diffusion, although there have been more recent works to suggest some overlap between these classes [1,2]. Classification of a process into one of the two categories is based on the value of the characteristic exponent of the time dependence of the second moment of the probability density function (PDF). In the instance where the process occurs in a spatially symmetric manner, the second moment and mean squared displacement are equivalent and thus,

$$\mu_2(t) = \langle x^2 \rangle(t) = t^{\gamma}. \tag{1}$$

In Equation (1), γ plays the role of the characteristic exponent. Normal diffusion is said to occur for $\gamma = 1$ and when $\gamma \neq 1$ the process is described as anomalous. Anomalous diffusion is abundant amongst the natural world, and as a consequence of this prevalence it has been the subject of widespread study, of which there is a rich history. As specific examples, it has been observed in charge carrier transport in amorphous semiconductors [3,4], in flow in porous systems [5], in quantum optics [6,7], as well as many other systems [8,9]. In a mathematical context, two predominant branches of study exist, one

extends from the works of Langevin, aiming to produce a stochastic description of a single trajectory. The second branch is concerned with the time evolution of the entire ensemble of a process, with early works in this vain formulated by the likes of Fokker, Planck, and Smoluchowski [10].

In prior work by the authors, a generalized diffusion equation was derived from an underlying continuous time random walk (CTRW) [11] that possessed a timing distribution associated with stress redistributing systems. The intention of that work was to explore the ability of fractional or non-Markovian models to describe dynamics within physical systems with stress redistributing features (such as those found in earthquake dynamics, physical gels, and many stick-slip models). It could be said that the mentioned work focused on the *temporal* implications of stress redistribution for resulting diffusive processes. The present research explores the spatial implications which follow from *stress re-distributing* processes driving anomalous diffusion. In order to capture these spatial features, we employ non-Gaussian distributions of the displacements in the underlying CTRW framework. Specifically the class of probability density functions known as *stable Lévy distributions* are inserted for the displacement probability densities in the underlying CTRW.

This article will be structured as follows, Section 2 will give a brief overview of the underlying CTRW framework, Section 3 outlines the consequences of incorporating Lévy stable probability densities in the CTRW in terms of the resulting generalised diffusion equation, the probability density current, and the displacement PDF. Section 3 finishes with the demonstration of the normalisation and reduction properties of the obtained solution to the generalised diffusion equation. Finally, Section 4 covers the key findings and provides some concluding remarks.

2. CTRW

The CTRW framework was first described by Weiss and Montroll, and has been employed in the studies of a number of stochastic processes [12]. The CTRW is built up from the stochastic exploration of a walker through space, where the displacements x are interrupted by waiting times t. These variables are drawn from a continuous probability density function (PDF) $\Psi(x,t)$. In the instance that there exists no correlations between the size of the displacement and the waiting time (decoupled CTRW), the following expressions hold

$$\lambda(x) = \int_0^\infty \Psi(x,t)dt \tag{2}$$

$$\omega(t) = \int_{-\infty}^\infty \Psi(x,t)dx, \tag{3}$$

where $\lambda(x)$ and $\omega(t)$ are the step-length and waiting time PDFs, respectively. The decoupled framework allows $\Psi(x,t)$ to be factored into the independent distributions $\lambda(x)$ and $\omega(t)$. From these distributions, an arrival PDF, $\eta(x,t)$ describing the probability density of a walker arriving at various positions x in time t, may be constructed. The PDF $\eta(x,t)$ is defined as,

$$\eta(x,t) = \int_{-\infty}^\infty \int_0^t \eta(x',t')\lambda(x-x')\omega(t-t')dt'dx' + \delta(x)\delta(t). \tag{4}$$

The first term of Equation (4) describes the probability associated with a walker at x' at time, t' having made a jump of length $x-x'$ in the remaining time $t-t'$, summed over all x and all causally relevant t. Whilst the second term represents the initial conditions, here at time $t=0$ the walker is localized at a position defined by $\delta(x)$. The position PDF, $P(x,t)$ is then defined as the probability density of arriving and remaining at a position x at time t, defined as

$$P(x,t) = \int_0^t \eta(x,t')\Phi(t-t')dt', \tag{5}$$

where $\Phi(t)$ is referred to as the survival PDF which provides the probability density for a waiting time longer than t, defined as

$$\Phi(t) = 1 - \int_0^t \omega(t')dt'. \tag{6}$$

The typical progress from this point is to pass into the Fourier–Laplace space. This simplifies the expressions through the known transform properties of convolutions [13]. Transforming Equations (4) and (6), then substituting them into the Fourier–Laplace equivalent of Equation (5), provides the following form for $P(k,u)$ [14],

$$P(k,u) = \frac{1-\hat{\omega}(u)}{u}\frac{1}{1-\hat{\lambda}(k)\hat{\omega}(u)}. \tag{7}$$

3. Lévy Flight

If the CTRW contains a Lévy stable distribution for the displacements, then such behaviour corresponds to the following Fourier space, small k approximation,

$$\hat{\lambda}(k) \sim 1 - \sigma^{\mu}|k|^{\mu}, \tag{8}$$

with $\mu \in [1,2]$ [15]. The waiting time PDF, $\omega(t)$ utilised in this work is the gamma distribution, which takes the following functional form,

$$\omega(t) = \frac{t^{\gamma-1}}{\tau^{\gamma}\Gamma(\gamma)}\exp\left(\frac{-t}{\tau}\right). \tag{9}$$

Equation (9) has been connected with the timing of stress-redistribution events, motivating its use in the present study [11,16,17]. The PDF $\omega(t)$ appears in the Laplace space as,

$$\hat{\omega}(u) = \frac{1}{\tau^{\gamma}\left(\frac{1}{\tau}+u\right)^{\gamma}} \tag{10}$$

Inserting Equations (10) and (8) into Equation (7) yields the following expression for the PDF in the Fourier–Laplace space

$$P(k,u) = \frac{1}{u}\cdot\frac{1}{1+\frac{D_{\gamma,\mu}|k|^{\mu}}{((\frac{1}{\tau}+u)^{\gamma}-\frac{1}{\tau^{\gamma}})}}, \tag{11}$$

where $D_{\alpha,\mu} = \frac{\sigma^{\mu}}{\tau^{\alpha}}$ is the generalised space-time diffusion coefficient.

3.1. Generalised Diffusion Equation

From Equation (11) we can outline a generalised diffusion equation [18]. The generalised diffusion equation appears as,

$$\frac{\partial}{\partial t}P(x,t) = D_{\alpha,\mu}\frac{\partial}{\partial t}\int_0^t \exp\left(-\frac{(t-t')}{\tau}\right)(t-t')^{\gamma-1}E_{\gamma,\gamma}\left(\frac{(t-t')^{\gamma}}{\tau^{\gamma}}\right)\frac{\partial^{\mu}}{\partial|x|^{\mu}}P(x,t')dt', \tag{12}$$

where, $\frac{\partial^{\mu}}{\partial|x|^{\mu}}$ is the Riesz space-fractional derivative [19,20]. The Riesz space-fractional derivative is defined as

$$\frac{\partial^{\mu}}{\partial|x|^{\mu}}f(x) = F^{-1}\Big[|k|^{\mu}f(k)\Big](x), \tag{13}$$

which in the x space is (for $1 < \mu \leq 2$),

$$\frac{\partial^{\mu}}{\partial|x|^{\mu}}f(x) = \frac{-1}{2\cos(\pi\mu/2)}\frac{1}{\Gamma(2-\mu)}\frac{\partial^2}{\partial x^2}\left(\int_{-\infty}^{x}\frac{f(x')}{(x-x')^{\mu-1}}dx' + \int_x^{\infty}\frac{f(x')}{(x'-x)^{\mu-1}}dx'\right). \tag{14}$$

Equation (12) therefore represents the extension of non-locality to include both temporal and spatial domains.

3.1.1. Probability Density Current

There exists a well known connection between the diffusion equation and the continuity equation. The continuity equation states that the total change in concentration at a particular location (the change in probability density in this case) and the divergence of the concentration current at the same location (probability density current in this case) must be zero, in the instance of a conserved quantity. Another way of expressing this is simply to state that in the instance of a conserved quantity the change in this quantity in a defined region must balance the flow of this quantity into and out of the region, or, more succinctly

$$P_t(x,t) = -\frac{\partial}{\partial x} J(x,t). \tag{15}$$

where in Equation (15) $J(x,t)$ is the probability density current (PDC). This provides a useful starting point for investigations into how a given generalised diffusion equation varies from the standard or *normal* case. Writing the PDC in a generalised form consistent with fractional calculus

$$J(x,t) = -{}_0G_t^{1-\gamma} \frac{\partial^{\mu-1}}{\partial |x|^{\mu-1}} P(x,t). \tag{16}$$

where in Equation (16) the operator ${}_0G_t^{1-\gamma}$ is defined as,

$${}_0G_t^{1-\gamma} f(t) = \frac{\partial}{\partial t} \int_0^t \exp\left(-\frac{(t-t')}{\tau}\right)(t-t')^{\gamma-1} E_{\gamma,\gamma}\left(\frac{(t-t')^{\gamma}}{\tau^{\gamma}}\right) f(t')dt'. \tag{17}$$

It is no longer accurate to describe the PDC, $J(x,t)$, as moving down the gradient of the PDF. In order to establish precisely to what this generalised PDC is sensitive to, we outline its mathematical relationship connection with the position PDF:

$$J(x,t) = -{}_0G_t^{1-\gamma}\left[\frac{-1}{\cos\left(\frac{\pi(\mu-1)}{2}\right)}\left({}_{-\infty}D_x^{\mu-1}P(x,t) + {}_xD_{\infty}^{\mu-1}P(x,t)\right)\right]. \tag{18}$$

where the operators ${}_{-\infty}D_x^{\mu-1}$ and ${}_xD_{\infty}^{\mu-1}$ in Equation (18) are the left and right Riemann–Liouville fractional derivatives (with $0 < \mu - 1 \leq 1$) [21], respectively,

$$J(x,t) =_0 G_t^{1-\gamma}\left[\frac{1}{\cos\left(\frac{\pi(\mu-1)}{2}\right)}\frac{1}{\Gamma(2-\mu)}\frac{\partial}{\partial x}\left(\int_{-\infty}^{x}\frac{P(x',t)}{(x-x')^{\mu-1}}dx' - \int_x^{\infty}\frac{P(x',t)}{(x'-x)^{\mu-1}}dx'\right)\right]. \tag{19}$$

Thus, there is still a gradient that the PDC will be directed down, which is intuitive in the case of normal diffusion. However, the gradient is the now, rather than simply being the slope of the PDF, the gradient in question is the derivative of the factor

$$\left(\int_{-\infty}^{x}\frac{P(x',t)}{(x-x')^{\mu-1}}dx' - \int_x^{\infty}\frac{P(x',t)}{(x'-x)^{\mu-1}}dx'\right). \tag{20}$$

This object is positive or negative depending on the position x being considered, which follows from the symmetry of $P(x,t)$. Equally, Equation (19) outlines a measure of the non-local allocation of probability density. It constructs a difference from the weighted sum of probability above and below the point of interest x. It is the gradient of this non-local description that guides the flow of probability density. The presence of the generalised time derivative captures the non-local behaviour in time, which persists over a regime whose extent is governed by τ. The origins of the occurrence of non-local behaviour in

time has been discussed in previous work [11], while the appearance of spatially non-local behaviour, can result from the inclusion of a power law distribution of the displacements such as those originating in systems exhibiting stress driven phenomena [22].

3.2. Displacement PDF

Beginning with Equation (11), the first modification made here is to express it as a Fox H function [23] (for further details, and a summary of useful properties see Appendix A),

$$P(k,u) = \frac{1}{u} H_{1,1}^{1,1}\left[\frac{D_{\gamma,\mu}|k|^{\mu}}{((\frac{1}{\tau}+u)^{\gamma} - \frac{1}{\tau^{\gamma}})}\middle|_{(0,1)}^{(0,1)}\right]. \tag{21}$$

Taking the inverse Fourier (cosine) transform, and following up with the inverse Laplace transform yields,

$$P(x,t) = \frac{1}{2\sqrt{\pi}}\int_0^t \exp\left(-\frac{t}{\tau}\right)\mathcal{L}^{-1}\left\{\frac{1}{|x|}H_{1,3}^{2,1}\left[\frac{(u^{\gamma}-\frac{1}{\tau^{\gamma}})|x|^{\mu}}{2^{\mu}D_{\gamma,\mu}}\middle|_{(\frac{1}{2},\frac{\mu}{2})(1,1)(1,\frac{\mu}{2})}^{(1,1)}\right]\right\}(t')dt'. \tag{22}$$

As a brief aside, here it is pointed out that if only the Fourier inversion is evaluated, it is possible to construct an integral decomposition precisely as described by Chechin et al. and Sokolov [24,25], however, rather than the decomposition involving the Gaussian propagator, it would would now involve the Lévy propagator (using the same Laplace-type transform structure). To our knowledge this has *not* been described in the literature.

3.2.1. Subordinator Form

It will now be illustrated briefly how a connection of the kind outlined by Sokolov [25], may be defined in this case in relation to the standard Lévy position PDF. Beginning with Equation (21) the first step is to make the following substitution,

$$\frac{u}{K(u)} = \left(\left(\frac{1}{\tau}+u\right)^{\gamma} - \frac{1}{\tau^{\gamma}}\right). \tag{23}$$

In this instance $K(u)$ is the Laplace transform of the memory kernel as defined in Sokolov's work, which is the time derivative of the memory kernels as defined by Tateishi [26]. After the evaluation of the inverse Fourier transform, Equation (21) becomes,

$$P(x,\frac{u}{K(u)}) = \frac{1}{\sqrt{\pi}u|x|}H_{1,3}^{2,1}\left[\frac{|x|^{\mu}\frac{u}{K(u)}}{D_{\gamma,\mu}2^{\mu}}\middle|_{(\frac{1}{2},\frac{\mu}{2}),(1,1)(1,\frac{\mu}{2})}^{(1,1)}\right]. \tag{24}$$

Using the Laplace transform properties of the H function allows the following representation,

$$P\left(x,\frac{u}{K(u)}\right) = \int_0^{\infty}\frac{1}{\sqrt{\pi}|x|\mu}H_{2,3}^{2,1}\left[\frac{|x|}{D_{\gamma,\mu}2\tau^{\frac{1}{\mu}}}\middle|_{(\frac{1}{2},\frac{1}{2})(1,\frac{1}{\mu}),(1,\frac{1}{2})}^{(1,\frac{1}{\mu}),(1,\frac{1}{\mu})}\right]\frac{1}{K(u)}\exp\left(-\tau\frac{u}{K(u)}\right)d\tau. \tag{25}$$

Cancelling out the coefficients of the H function, then introducing a new pair $(1,\frac{1}{2})$ symmetrically and using the Legendre duplication formula yields,

$$P\left(x,\frac{u}{K(u)}\right) = \int_0^{\infty}\frac{1}{|x|\mu}H_{2,2}^{1,1}\left[\frac{|x|}{D_{\gamma,\mu}\tau^{\frac{1}{\mu}}}\middle|_{(1,1),(1,\frac{1}{2})}^{(1,\frac{1}{\mu})(1,\frac{1}{2})}\right]\frac{1}{K(u)}\exp\left(-\tau\frac{u}{K(u)}\right)d\tau. \tag{26}$$

This form describes the connection between the standard Lévy solution and the generalised form studied within this work. The form of the connection is the subordinator type structure, as described by Sokolov.

Returning now to Equation (22) we continue to work on revealing $P(x,t)$. Prior to the full inversion of the Laplace transform in Equation (22), we first prepare the H function. This is achieved by first expressing the H - function in its series form as described in the text by Mathai and Saxena [27]. This gives the following result,

$$\mathcal{L}^{-1}\Big\{\frac{1}{|x|}H^{2,1}_{1,3}\Big[\frac{(u^\gamma-\frac{1}{\tau^\gamma})|x|^\mu}{2^\mu D_{\gamma,\mu}}\Big|^{(1,1)}_{(\frac{1}{2},\frac{\mu}{2})(1,1)(1,\frac{\mu}{2})}\Big]\Big\}(t)=\frac{1}{|x|}\mathcal{L}^{-1}\Big\{\sum_{n=0}^{\infty}\Big(\frac{\Gamma\Big(1-\frac{2}{\mu}(\frac{1}{2}+n)\Big)\Gamma\Big(\frac{2}{\mu}(\frac{1}{2}+n)\Big)}{\Gamma\Big(\frac{1}{2}+n\Big)\Gamma(n+1)}$$
$$\frac{(-1)^n}{\frac{\mu}{2}}\Big(\frac{\tau^\gamma|x|^\mu(u^\gamma-\frac{1}{\tau}^\gamma)2}{2^\mu\sigma^\mu\mu}\Big)^{\frac{2}{\mu}(\frac{1}{2}+n)}\Big)+\sum_{n=0}^{\infty}\Big(\frac{\Gamma\Big(\frac{1}{2}-\frac{\mu}{2}(1+n)\Big)\Gamma(1+n)}{\Gamma\big(\frac{\mu}{2}(1+n)\big)\Gamma(1+n)}$$
$$\times(-1)^n\Big(\frac{\tau^\gamma|x|^\mu(u^\gamma-\frac{1}{\tau}^\gamma)}{2^\mu\sigma^\mu}\Big)^{1+n}\Big)\Big\}(t). \tag{27}$$

Now the binomial theorem is used to expand the $(u^\gamma-\frac{1}{\tau}^\gamma)$ terms,

$$(u^\gamma-\frac{1}{\tau}^\gamma)^A=u^{\gamma A}(1-\frac{1}{u^\gamma\tau^\gamma})^A=u^{\gamma A}\sum_{m=0}^{\infty}\binom{A}{m}\Big(-\frac{1}{u^\gamma\tau^\gamma}\Big)^m, \tag{28}$$

where $\binom{A}{m}$ are the binomial coefficients. Thus,

$$\mathcal{L}^{-1}\Big\{\frac{1}{u|x|}H^{2,1}_{1,3}\Big[\frac{(u^\gamma-\frac{1}{\tau^\gamma})|x|^\mu}{2^\mu D_{\gamma,\mu}}\Big|^{(1,1)}_{(\frac{1}{2},\frac{\mu}{2})(1,1)(1,\frac{\mu}{2})}\Big]\Big\}(t)=\mathcal{L}^{-1}\Big\{\sum_{n=0}^{\infty}\sum_{m=0}^{\infty}\Big(\frac{\Gamma\Big(1-\frac{2}{\mu}(\frac{1}{2}+n)\Big)}{\Gamma\Big(\frac{1}{2}+n\Big)}$$
$$\frac{\Gamma\Big(\frac{2}{\mu}(\frac{1}{2}+n)\Big)\Gamma\Big(\frac{2}{\mu}(\frac{1}{2}+n)+1\Big)}{\Gamma(n+1)\Gamma(m+1)\Gamma\Big(\frac{\mu}{2}(\frac{1}{2}+n)+1-m\Big)}\frac{(-1)^n}{\frac{\mu}{2}}\Big(\frac{\tau^\gamma|x|^\mu u^\gamma 2}{2^\mu\sigma^\mu\mu}\Big)^{\frac{2}{\mu}(\frac{1}{2}+n)}\Big)\Big(-\frac{1}{u^\gamma\tau^\gamma}\Big)^m$$
$$+\sum_{n=0}^{\infty}\sum_{m=0}^{\infty}\Big(\frac{\Gamma\Big(\frac{1}{2}-\frac{\mu}{2}(1+n)\Big)\Gamma(1+n)\Gamma(2+n)}{\Gamma(\frac{\mu}{2}(1+n))\Gamma(1+n)\Gamma(m+1)\Gamma(2+n-m)}(-1)^n\Big(\frac{\tau^\gamma|x|^\mu u^\gamma}{2^\mu\sigma^\mu}\Big)^{1+n}\Big)\Big(-\frac{1}{u^\gamma\tau^\gamma}\Big)^m\Big\}(t).$$

Which, when put back into a Fox H-function form, and Laplace inverted appears as

$$P(x,t)=\frac{1}{\sqrt{\pi}}\int_0^t\exp\Big(-\frac{t'}{\tau}\Big)\sum_{m=0}^{\infty}\frac{1}{\Gamma(m+1)}\Big(-\frac{t'^\gamma}{\tau^\gamma}\Big)^m\frac{1}{t'|x|}H^{2,2}_{3,4}\Big[\frac{\tau^\gamma|x|^\mu}{2^\mu\sigma^\mu t'^\gamma}\Big|^{(1,1)(0,1)(\gamma m,\gamma)}_{(\frac{1}{2},\frac{\mu}{2})(1,1)(1,\frac{\mu}{2})(m,1)}\Big]dt'. \tag{29}$$

An equivalent form may be found by first using the shift theorem for the Laplace inversion, rather than removing the $1/u$ factor as an integral from $0\to t$. Keeping it in the u-space, it becomes $\frac{1}{u-\frac{1}{\tau}}$ and inverting the Laplace transform in its entirety

$$P(x,t)=\frac{1}{\sqrt{\pi}}\exp\Big(-\frac{t}{\tau}\Big)\sum_{m=0}^{\infty}\sum_{j=0}^{\infty}\frac{1}{\Gamma(m+1)}\Big(-\frac{t^\gamma}{\tau^\gamma}\Big)^m\Big(\frac{t}{\tau}\Big)^j\frac{1}{t|x|}H^{2,2}_{3,4}\Big[\frac{\tau^\gamma|x|^\mu}{\sigma^\mu t^\gamma}\Big|^{(1,1)(0,1)(1+j+\gamma m,\gamma)}_{(\frac{1}{2},\frac{\mu}{2})(1,1)(1,\frac{\mu}{2})(m,1)}\Big]. \tag{30}$$

The solution $P(x,t)$ is contained within Figure 1 for a range of values of μ and γ. It is of note that, through the methods of solution adopted in this article, the spatial parameter μ may have its range of values extended to $\mu\in(0,2]$, however the additional constraint that $\mu\neq\gamma$ is present if $\mu\in(0,1]$.

3.2.2. Normalisation

The normalisation of Equation (29) can be demonstrated using the Mellin transform, as shown before in the work of Sandev et al. [28]. After the evaluation of the Mellin transform, Equation (29) becomes,

$$\int_0^t\exp\Big(-\frac{t'}{\tau}\Big)\sum_{m=0}^{\infty}\frac{1}{\Gamma(m+1)}\Big(\frac{t'^\gamma}{\tau^\gamma}\Big)^m\frac{1}{t'}\frac{1}{\Gamma(\gamma m)\Gamma(1-m)}dt'. \tag{31}$$

Equation (31) has an equivalent form in terms of the Fox H function, after expressing it in this manner and taking the Laplace transform reveals

$$\frac{1}{u}H_{2,2}^{1,1}\left[-\frac{1}{(u+\tau)^{\gamma}\tau^{\gamma}}\middle|\begin{matrix}(1,\gamma)(1,1)\\(0,1),(1,\gamma)\end{matrix}\right]=\frac{1}{u}\left(1+\frac{1}{(u+\tau)^{\gamma}\tau^{\gamma}}\right)^{0}=\frac{1}{u} \tag{32}$$

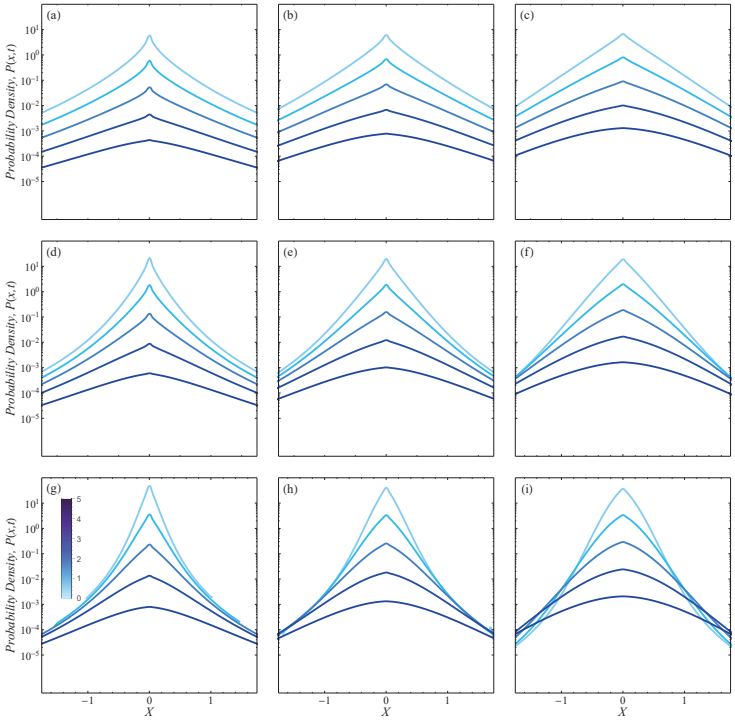

Figure 1. Position probability density functions corresponding to increasing values of γ and μ in Equation (29), where X is dimensionless, $X = x/\sigma$. The value of γ ranges from $\gamma = 1/4$ (first row), to $\gamma = 3/4$ (third row), in increments of $1/4$ and μ ranges from $3/2$ (first column) to $5/2$ (third column) in increments of $1/2$. The colours correspond to units of time, t/τ, within the open range $(0, 5)$ (light blue to dark blue). These figures have used the values of τ and σ to be $\tau = \sigma = 1$.

3.2.3. Reduction $\gamma \to 1$

If $\gamma \to 1$, Equation (29) should reduce to the standard Lévy solution. The first step is to remove the factor $(-1)^m$ from the Fox H function followed by taking the factor (-1) into the Fox H function, both via the relations discussed in Skibinski et al. [29]

$$P(x,t)=\frac{1}{\sqrt{\pi}}\int_0^t\frac{(-1)}{t'|x|}H_{1,2}^{1,1}\left[\frac{\tau^{\gamma}|x|^{\mu}}{2^{\mu}\sigma^{\mu}t'}\middle|\begin{matrix}(0,1)\\(\frac{1}{2},\frac{\mu}{2})(1,\frac{\mu}{2})\end{matrix}\right]. \tag{33}$$

Laplace transforming this to resolve the integral, provides the following expression for $P(x,u)$

$$P(x,u)=\frac{1}{\sqrt{\pi}}\frac{(-1)}{u|x|}H_{1,3}^{2,1}\left[\frac{\tau^{\gamma}|x|^{\mu}u}{2^{\mu}\sigma^{\mu}}\middle|\begin{matrix}(0,1)\\(0,1)(\frac{1}{2},\frac{\mu}{2})(1,\frac{\mu}{2})\end{matrix}\right]. \tag{34}$$

The inversion of this followed by bringing the factor (-1) back into the H function, enables the cancellation of the coefficient pair $(0,1)$.

$$P(x,t) = \frac{1}{\sqrt{\pi}} \frac{1}{|x|} H_{1,2}^{1,1}\left[\frac{\tau^{\gamma}|x|^{\mu}}{2^{\mu}\sigma^{\mu}t} \middle|_{(\frac{1}{2},\frac{\mu}{2})(1,\frac{\mu}{2})}^{(1,1)} \right]. \tag{35}$$

From this expression you may simply remove μ from the Fox H function (see known properties [30]), insert a symmetric coefficient pair $(1,\frac{1}{2})$ followed by the employment of the Legendre duplication formula on the coefficient pairs $(1,\frac{1}{2})$ and $(\frac{1}{2},\frac{1}{2})$ to complete the extraction of the standard Lévy form, as required [11].

$$P(x,t) = \frac{1}{|x|\mu} H_{2,2}^{1,1}\left[\frac{\tau|x|}{\sigma t^{\frac{1}{\mu}}} \middle|_{(1,1)(1,\frac{1}{2})}^{(1,\frac{1}{\mu})(1,\frac{1}{2})} \right]. \tag{36}$$

3.2.4. Reduction $\mu \to 2$

If $\mu \to 2$ the Gaussian propagator should be recovered and that is now demonstrated. Starting from Equation (29) we set $\mu \to 2$, which gives,

$$P(x,t) = \frac{1}{\sqrt{\pi}} \int_0^t \exp\left(-\frac{t'}{\tau}\right) \sum_{m=0}^{\infty} \frac{1}{\Gamma(m+1)} \left(-\frac{t'^{\gamma}}{\tau^{\gamma}}\right)^m \frac{1}{t'|x|} H_{3,4}^{2,2}\left[\frac{\tau^{\gamma}x^2}{4\sigma^2 t'^{\gamma}} \middle|_{(\frac{1}{2},1)(1,1)(1,1)(m,1)}^{(1,1)(0,1)(\gamma m,\gamma)} \right] dt'. \tag{37}$$

We then combine coefficients by way of the Legendre duplication relation, and then reduce the H function to give,

$$P(x,t) = \frac{1}{2} \int_0^t \exp\left(-\frac{t'}{\tau}\right) \sum_{m=0}^{\infty} \frac{1}{\Gamma(m+1)} \left(\frac{t'^{\gamma}}{\tau^{\gamma}}\right)^m \frac{1}{t'|x|} H_{2,2}^{1,1}\left[\frac{\tau^{\frac{\gamma}{2}}|x|}{\sigma t'^{\frac{\gamma}{2}}} \middle|_{(1,1)(m,\frac{1}{2})}^{(0,\frac{1}{2})(\gamma m,\frac{\gamma}{2})} \right] dt'. \tag{38}$$

This is the integral form identified for the Gaussian CTRW case, as required.

3.2.5. Short Timescale Asymptotics

In the very small t regime, such that $\exp\left(-\frac{t}{\tau}\right) \approx 1$, and the dominant term of the series over m is $m = 0$, in which case the solution to Equation (29) reduces to the following integral form,

$$\begin{aligned} P(x,t) &= \frac{1}{\sqrt{\pi}} \int_0^t \frac{1}{t'|x|} H_{2,3}^{2,1}\left[\frac{\tau^{\gamma}|x|^{\mu}}{2^{\mu}\sigma^{\mu}t'^{\gamma}} \middle|_{(\frac{1}{2},\frac{\mu}{2})(1,1)(1,\frac{\mu}{2})}^{(1,1)(0,\gamma)} \right] dt' \\ &= \frac{1}{\sqrt{\pi}} \frac{1}{|x|} H_{2,3}^{2,1}\left[\frac{\tau^{\gamma}|x|^{\mu}}{2^{\mu}\sigma^{\mu}t^{\gamma}} \middle|_{(\frac{1}{2},\frac{\mu}{2})(1,1)(1,\frac{\mu}{2})}^{(1,1)(1,\gamma)} \right]. \end{aligned} \tag{39}$$

Which is the solution to the Riemann–Liouville space-time fractional diffusion equation.

3.2.6. Long Timescale Asymptotics

In order to explore the long timescale asymptotic behaviour, the first step is to remove the factor $(-1)^m$ by way of property 3.5 of the work of Skibinski [29]. Following this, the Fox H function may be expressed in the series form as described in brief in the article of Metzler et al. [31] and in detail in the landmark text by Saxena and Mathai [27]. The series form contains a nested pair of summations, one between 0 and ∞ and the other from 1 to 3. The latter has only one non-zero component (corresponding to the coefficient pair $(\frac{1}{2},\frac{\mu}{2})$) which we now outline,

$$\frac{1}{t|x|}H_{3,4}^{2,2}\left[\frac{\tau^{\gamma}|x|^{\mu}}{2^{\mu}\sigma^{\mu}t^{\gamma}}\middle|_{(\frac{1}{2},\frac{\mu}{2})(1,1)(1,\frac{\mu}{2})(m,1)}^{(1,1)(0,1)(\gamma m,\gamma)}\right]=\frac{1}{t|x|}\sum_{n=0}^{\infty}\left(\frac{\tau^{\gamma}|x|^{\mu}}{2^{\mu}\sigma^{\mu}t^{\gamma}}\right)^{\left(\frac{1}{2}+n\right)\frac{2}{\mu}}\frac{2}{\mu}$$
$$\frac{\Gamma\left(m-\frac{2}{\mu}\left(\frac{1}{2}+n\right)\right)\Gamma\left(1-\frac{2}{\mu}\left(\frac{1}{2}+n\right)\right)\Gamma\left(\frac{2}{\mu}\left(\frac{1}{2}+n\right)\right)}{\Gamma\left(-\frac{2\gamma}{\mu}\left(\frac{1}{2}+n\right)\right)\Gamma\left(\gamma m-\frac{2\gamma}{\mu}\left(\frac{1}{2}+n\right)\right)\Gamma\left(\frac{1}{2}+n\right)\Gamma(n+1)}. \tag{40}$$

Reinserting Equation (40) into Equation (29), then collecting the series over m and expressing this as an H function, yields

$$P(x,t)=\frac{1}{\sqrt{\pi}}\int_0^t\exp\left(-\frac{t'}{\tau}\right)\frac{1}{t|x|}\sum_{n=0}^{\infty}\left(\frac{\tau^{\gamma}|x|^{\mu}}{2^{\mu}\sigma^{\mu}t^{\gamma}}\right)^{\left(\frac{1}{2}+n\right)\frac{2}{\mu}}\frac{2}{\mu}$$
$$\frac{\Gamma\left(\frac{2}{\mu}\left(\frac{1}{2}+n\right)\right)\Gamma\left(1-\frac{2}{\mu}\left(\frac{1}{2}+n\right)\right)}{\Gamma\left(-\frac{2\gamma}{\mu}\left(\frac{1}{2}+n\right)\right)\Gamma\left(\frac{1}{2}+n\right)\Gamma(n+1)}H_{1,2}^{1,1}\left[-\frac{t^{\gamma}}{\tau^{\gamma}}\middle|_{(0,1)(1+\frac{2\gamma}{\mu}\left(\frac{1}{2}+n\right),\gamma)}^{(1+\frac{2}{\mu}\left(\frac{1}{2}+n\right),1)}\right]dt'. \tag{41}$$

The Fox H function contained in Equation (41) is able to be connected with the Wright function and this allows asymptotic behaviour to be readily extracted via the work of Wright [32]. Using the relationships identified by Wright, the following form can be extracted (using theorem 1 within, and the integer $M=1$)

$$P(x,t)=\frac{1}{\sqrt{\pi}}\int_0^t\exp\left(-\frac{t'}{\tau}\right)\frac{1}{t|x|}\sum_{n=0}^{\infty}\left(\frac{\tau^{\gamma}|x|^{\mu}}{2^{\mu}\sigma^{\mu}t^{\gamma}}\right)^{\left(\frac{1}{2}+n\right)\frac{2}{\mu}}\frac{2}{\mu}$$
$$\frac{\Gamma\left(\frac{2}{\mu}\left(\frac{1}{2}+n\right)\right)\Gamma\left(1-\frac{2}{\mu}\left(\frac{1}{2}+n\right)\right)}{\Gamma\left(-\frac{2\gamma}{\mu}\left(\frac{1}{2}+n\right)\right)\Gamma\left(\frac{1}{2}+n\right)\Gamma(n+1)}\left(\frac{t}{\tau}\right)^{(\gamma-1)\frac{2}{\mu}\left(\frac{1}{2}+n\right)}\gamma^{\frac{2}{\mu}\left(\frac{1}{2}+n\right)}\exp\left(\frac{t}{\tau}\right)dt'. \tag{42}$$

After simplifying Equation (42) it may be recombined into the following H function expression

$$\begin{aligned}P(x,t)&=\frac{1}{\sqrt{\pi}}\int_0^t\frac{1}{t'|x|}H_{2,3}^{2,1}\left[\frac{\tau|x|^{\mu}}{2^{\mu}\sigma^{\mu}t'}\middle|_{(\frac{1}{2},\frac{\mu}{2})(1,1)(1,\frac{\mu}{2})}^{(1,1)(0,1)}\right]dt'\\&=\frac{1}{\sqrt{\pi}}\frac{1}{|x|}H_{1,2}^{2,0}\left[\frac{\gamma\tau|x|^{\mu}}{2^{\mu}\sigma^{\mu}t}\middle|_{(\frac{1}{2},\frac{\mu}{2})(1,\frac{\mu}{2})}^{(1,1)}\right]\\&=\frac{1}{\sqrt{\pi}}\frac{1}{|x|}H_{2,3}^{2,1}\left[\frac{\gamma\tau|x|^{\mu}}{2^{\mu}\sigma^{\mu}t}\middle|_{(1,\frac{\mu}{2})(\frac{1}{2},\frac{\mu}{2})(1,\frac{\mu}{2})}^{(1,1)(1,\frac{\mu}{2})}\right]\\&=\frac{1}{\sqrt{\pi}}\frac{1}{|x|}H_{2,2}^{1,1}\left[\frac{\gamma\tau|x|^{\mu}}{\sigma^{\mu}t}\middle|_{(1,\mu)(1,\frac{\mu}{2})}^{(1,1)(1,\frac{\mu}{2})}\right].\end{aligned} \tag{43}$$

To summarise the steps involved in Equation (43), the integral is first evaluated after a reduction is afforded due to the symmetry of the coefficients. The symmetric coefficients $(1,\frac{\mu}{2})$ are then inserted to allow the Legendre duplication formula to be used to combine the coefficient pair $(1,\frac{\mu}{2})(\frac{1}{2},\frac{\mu}{2})$. Thus it can be seen that for sufficiently large timescales the standard Lévy form is recovered. It is of note, however, that the anomalous exponent γ remains present. It represents a lingering signature of the subdiffusive behaviour that was present on shorter timescales, which is analogous to the observations made in the work of Cleland and Williams [11] for long timescales.

4. Discussion and Conclusions

This research is concerned with developing a generalised diffusion equation capable of describing diffusion processes driven by underlying stress-redistributing (SR) type events. Previous work [11] has explored the resulting diffusion equation in the instance that only the timing of these SR jump-inducing events is considered. However, the present research incorporates spatial implications as well, encoded within the chosen displacement PDF in the underlying CTRW. The encoding was introduced via a Lévy stable PDF exhibiting the inverse power law tails also observed in SR models [22]. The resulting generalised diffusion equation was found in the so called *hydrodynamic limit*, which corresponds to the small k regime in the Fourier space, and its memory kernel was extracted. Its structure is different from that which was studied in Ref. [11] with regard to the spatial derivative, which is now fractional. The implications of a fractional derivative were explored in Section 3.1.1, within the context of the flow of probability current. The non-local nature of these derivatives was also demonstrated in Section 3.1.1, as the flow of PDC was determined to be directed down a non-local gradient. Section 3.2 then delved into the solution to the generalised diffusion equation discussed within this article. In obtaining the solution to Equation (12) via its Fourier and Laplace form, a small detour was taken to highlight a new subordinator connection to the standard Lévy PDF. This subordinator form mirrored extremely closely the form highlighted by Checkin et al. and Sokolov [24,25], however, differing slightly in the inclusion of the standard Lévy PDF. After this brief detour, the derivation of the solution to Equation (12) continued. Several relations closely connected with the Fox H function were exploited in the determination of the final PDF form, which is given in Equation (29) and shown in Figure 1. The employment of these Fox H function properties is something that has become an important tool in the study of fractional derivative equations in recent years [11,28,33,34]. Sections 3.2.2–3.2.4 deal with important behaviours that any solution of Equation (12) would be expected to have, confirming its validity. Specifically, in Section 3.2.2 the normalisation condition was confirmed, ensuring that $P(x,t)$ is a PDF. Section 3.2.3 demonstrated that in the instance $\gamma \to 1$ $P(x,t)$ relaxed back to the standard Lévy PDF. Finally, Section 3.2.4 outlined the nature of the reduction back to the PDF described in the work of Cleland and Williams [11], upon the occurrence of $\mu \to 2$. This work represents the first time both spatial and temporal features of stress-redistribution driven diffusion have been encoded within a generalised diffusion equation. It is hoped that the analytic features outlined within this work will be of great use in the modelling of systems demonstrating diffusion driven by these stick-slip dynamics.

Author Contributions: Conceptualization, J.D.C.; methodology, J.D.C.; formal analysis, J.D.C.; investigation, J.D.C.; writing—original draft preparation, J.D.C.; writing—review and editing, J.D.C. and M.A.K.W.; supervision, M.A.K.W.; project administration, M.A.K.W.; funding acquisition, M.A.K.W. All authors have read and agreed to the published version of the manuscript.

Funding: This research was funded by the Riddet Institute.

Conflicts of Interest: The authors declare no conflict of interest.

Appendix A. Fox *H*-Function

The definition of the Fox H-function appears in terms of the Mellin–Barnes type integral as follows [27,30],

$$H_{p,q}^{m,n}(z) = H_{p,q}^{m,n}\left[z\middle|\begin{matrix}(a_1,A_1),\ldots,(a_p,A_p)\\(b_1,B_1),\ldots,(b_p,B_p)\end{matrix}\right] = \frac{1}{2\pi i}\int_{\Omega}\theta(s)z^s\,ds, \tag{A1}$$

where $\theta(s)$ is the ratio of products of gamma functions, hence the mention of Barnes in the integral name. Specifically we have

$$\theta(s) = \frac{\prod_{j=1}^{m} \Gamma(b_j - B_j s) \prod_{j=1}^{n} \Gamma(1 - a_j + A_j s)}{\prod_{j=m+1}^{q} \Gamma(1 - b_j + B_j s) \prod_{j=n+1}^{p} \Gamma(a_j - A_j s)}. \tag{A2}$$

With the parameters defined such that, $0 \leq n \leq p, 1 \leq m \leq q, a_i, b_j \in \mathbb{C}, A_i, B_j \in \mathbb{R}^+, i = 1, \ldots, p, j = 1, \ldots, q$. The integration contour, Ω is chosen to run from $c - i\infty \to c + i\infty$ such that it avoids the poles of $\theta(s)$. There is a very useful expansion for the Fox H-function given in Ref. [28], it appears as

$$H_{p,q}^{m,n}(z) = H_{p,q}^{m,n}\left[z \middle| \begin{matrix} (a_1, A_1), \ldots, (a_p, A_p) \\ (b_1, B_1), \ldots, (b_p, B_p) \end{matrix} \right]$$

$$= \sum_{h=1}^{m} \sum_{k=0}^{\infty} \frac{\prod_{j=1, j\neq h}^{m} \Gamma(b_j - B_j \frac{b_h + k}{B_h}) \prod_{j=1}^{n} \Gamma(1 - a_j + A_j \frac{b_h + k}{B_h})}{\prod_{j=m+1}^{q} \Gamma(1 - b_j + B_j \frac{b_h + k}{B_h}) \prod_{j=n+1}^{p} \Gamma(a_j - A_j \frac{b_h + k}{B_h})} \frac{(-1)^k z^{\frac{b_h + k}{B_h}}}{k! B_h}. \tag{A3}$$

These functions are of great importance to anomalous diffusion as they provide a closed form in which to represent the non-Gaussian distributions that occur [35].

Appendix A.1. Expansion Formulae

Let m, n, p, and q be non-negative integers such that $1 \leq m \leq q, 0 \leq n \leq p$. Further, let $A_j, j = 1, \ldots, p$ and $B_j, j = 1, \ldots, q$ be positive numbers and $a_j, j = 1, \ldots, p$ and $b_j, j = 1, \ldots, q$ be complex numbers and $\mu > 0$ where

$$\mu = \sum_{j=1}^{p} B_j - \sum_{j=1}^{p} A_j. \tag{A4}$$

Then, if ω and η are complex numbers such that $\omega \neq 0$ and $\eta \neq 0$, then the following results hold:

Formula I

$$H_{p,q}^{m,n}\left[\eta\omega \middle| \begin{matrix} (a_1, A_1), \ldots, (a_p, A_p) \\ (b_1, B_1), \ldots, (b_q, B_q) \end{matrix} \right] = \eta^{\frac{b_1}{B_1}} \sum_{r=0}^{\infty} \frac{\left(1 - \eta^{\frac{1}{B_q}}\right)^r}{r!} H_{p,q}^{m,n}\left[\omega \middle| \begin{matrix} (a_1, A_1), \ldots, (a_p, A_p) \\ (b_1 + r, B_1), \ldots, (b_q, B_q) \end{matrix} \right] \tag{A5}$$

where η is arbitrary for $m = 1$, and for $m > 1$ $|\eta^{\frac{1}{B_1}} - 1| < 1$, $\arg(\eta\omega) = B_1, \arg(\eta^{\frac{1}{B_1}}) + \arg(\omega)$, and $|\arg(\eta^{\frac{1}{B_1}})| < \frac{\pi}{2}$.

Formula II

$$H_{p,q}^{m,n}\left[\eta\omega \middle| \begin{matrix} (a_1, A_1), \ldots, (a_p, A_p) \\ (b_1, B_1), \ldots, (b_q, B_q) \end{matrix} \right] = \eta^{\frac{b_q}{B_q}} \sum_{r=0}^{\infty} \frac{\left(\eta^{\frac{1}{B_q}} - 1\right)^r}{r!} H_{p,q}^{m,n}\left[\omega \middle| \begin{matrix} (a_1, A_1), \ldots, (a_p, A_p) \\ (b_1, B_1), \ldots, (b_q + r, B_q) \end{matrix} \right] \tag{A6}$$

where $q > m, |\eta^{\frac{1}{B_q}} - 1| < 1 \arg(\eta\omega) = B_q \arg(\eta^{\frac{1}{B_q}}) + \arg(\omega)$, and $|\arg(\eta^{\frac{1}{B_q}})| < \frac{\pi}{2}$.

Formula III

$$H_{p,q}^{m,n}\left[\eta\omega \middle| \begin{matrix} (a_1, A_1), \ldots, (a_p, A_p) \\ (b_1, B_1), \ldots, (b_q, B_q) \end{matrix} \right] = \eta^{\frac{a_1 - 1}{A_1}} \sum_{r=0}^{\infty} \frac{\left(1 - \eta^{-\frac{1}{A_1}}\right)^r}{r!} H_{p,q}^{m,n}\left[\omega \middle| \begin{matrix} (a_1 - r, A_1), \ldots, (a_p, A_p) \\ (b_1, B_1), \ldots, (b_q, B_q) \end{matrix} \right] \tag{A7}$$

where $n > 0, \Re\left(\eta^{\frac{1}{A_1}}\right) > \frac{1}{2}, \arg(\eta\omega) = A_1 \arg(\eta^{\frac{1}{A_1}}) + \arg(\omega)$, and $|\arg(\eta^{\frac{1}{A_1}})| < \frac{\pi}{2}$.

Formula IV

$$H_{p,q}^{m,n}\left[\eta\omega\middle|\begin{matrix}(a_1,A_1),\ldots,(a_p,A_p)\\(b_1,B_1),\ldots,(b_q,B_q)\end{matrix}\right]=\eta^{\frac{a_q-1}{A_q}}\sum_{r=0}^{\infty}\frac{\left(\eta^{-\frac{1}{A_p}}-1\right)^r}{r!}H_{p,q}^{m,n}\left[\omega\middle|\begin{matrix}(a_1,A_1),\ldots,(a_p-r,A_p)\\(b_1,B_1),\ldots,(b_q,B_q)\end{matrix}\right] \tag{A8}$$

where $p>n, \Re\left(\eta^{\frac{1}{A_p}}\right)>\frac{1}{2}$, $\arg(\eta\omega)=A_p\arg(\eta^{\frac{1}{A_p}})+\arg(\omega)$, and $|\arg(\eta^{\frac{1}{A_q}})|<\frac{\pi}{2}$.

Appendix A.2. Transformation Properties

Laplace Transform

Let either $\alpha>0, |\arg a|<\frac{1}{2}\pi\alpha$ or $\alpha=0$ and $\Re(\delta)<-1$. Further assume that $\alpha>0;\rho,\alpha,u\in C,\sigma>0$, satisfy the condition: $\Re(\rho)+\sigma\min_{1\le j\le m}\left[\frac{\Re(b_j)}{B_j}\right]>0$ for $\alpha>0$ or $\alpha=0,\mu\ge 0$; and $\Re(\rho)+\sigma\min_{1\le j\le m}\left[\frac{b_j}{B_j}+\frac{\Re(\delta)+\frac{1}{2}}{\mu}\right]>0$ for $\alpha=0$ and $\mu<0$. Then for $\Re(u)>0$, there holds the formula,

$$\mathcal{L}\left[t^{\rho-1}H_{p,q+1}^{m,n}\left[at^{\sigma}\middle|\begin{matrix}(a_p,A_p)\\(b_q,B_q)\end{matrix}\right]\right](u)=u^{-\rho}H_{p,q}^{m,n}\left[au^{-\sigma}\middle|\begin{matrix}(a_p,A_p)\\(b_q,B_q),(1-\rho,\sigma)\end{matrix}\right] \tag{A9}$$

for $\Re(u)>0, u\in C$.

With the inverse given by

$$\mathcal{L}^{-1}\left[u^{-\rho}H_{p,q}^{m,n}\left[au^{-\sigma}\middle|\begin{matrix}(a_p,A_p)\\(b_q,B_q)\end{matrix}\right]\right](t)=t^{\rho-1}H_{p+1,q}^{m,n}\left[at^{\sigma}\middle|\begin{matrix}(a_p,A_p)\\(b_q,B_q),(1-\rho,\sigma)\end{matrix}\right] \tag{A10}$$

where $\rho,a,u\in C, \Re(u)>0,\sigma>0, \Re(\rho)+\sigma\max_{1\le i\le n}\left[\frac{1}{A_i}-\frac{\Re(a_i)}{A_i}\right]>0, |\arg(a)|<\frac{1}{2}\pi\theta, \theta=-\sigma$.

Fourier Cosine Transform

$$\int_0^{\infty}x^{\rho-1}\cos(ax)H_{p,q+1}^{m,n}\left[bx^{\sigma}\middle|\begin{matrix}(a_p,A_p)\\(b_q,B_q),(1-\rho,\sigma)\end{matrix}\right]dx=\frac{2^{\rho-1}\sqrt{\pi}}{a^{\rho}}H_{p+2,q}^{m,n+1}\left[ba^{-\sigma}2^{\sigma}\middle|\begin{matrix}(\frac{(2-\rho)}{2},\frac{\sigma}{2})(a_p,A_p)(\frac{(1-\rho)}{2},\frac{\sigma}{2})\\(b_q,B_q),(1-\rho,\sigma)\end{matrix}\right] \tag{A11}$$

where $a,\alpha,\sigma>0,\rho,b\in C; |\arg b|<\frac{1}{2}\pi\alpha$;

$$\Re(\rho)+\sigma\min_{1\le j\le m}\Re\left(\frac{b_j}{B_j}\right)>0;\Re(\rho)+\sigma\max_{1\le j\le n}\left[\frac{(a_j-1)}{A_j}\right]<1$$

References

1. Yin, Q.Q.; Li, Y.Y.; Marchesoni, F.; Nayak, S.; Ghosh, P.K. Non-Gaussian normal diffusion in low dimensional systems. *Front. Phys.* **2021**, *16*, 1–14. [CrossRef]
2. Abe, S. Fokker-Planck approach to non-Gaussian normal diffusion: Hierarchical dynamics for diffusing diffusivity. *Phys. Rev. E* **2020**, *102*, 042136. [CrossRef] [PubMed]
3. Gu, Q.; Schiff, E.A.; Grebner, S.; Wang, F.; Schwarz, R. Non-Gaussian transport measurements and the Einstein relation in amorphous silicon. *Phys. Rev. Lett.* **1996**, *76*, 3196–3199. [CrossRef] [PubMed]
4. Scher, H.; Shlesinger, M.F.; Bendler, J.T. Time-scale invariance in transport and relaxation. *Phys. Today* **1991**, *44*, 26–34. [CrossRef]
5. Klammler, F.; Kimmich, R. Geometrical restrictions of incoherent transport of water by diffusion in protein of silica fineparticle systems and by flow in a sponge—A study of anomalous properties using an nmr field-gradient technique. *Croat. Chem. Acta* **1992**, *65*, 455–470.
6. Schaufler, S.; Schleich, W.P.; Yakovlev, V.P. Keyhole look at Lévy flights in subrecoil laser cooling. *Phys. Rev. Lett.* **1999**, *83*, 3162–3165. [CrossRef]
7. Schaufler, S.; Schleich, W.P.; Yakovlev, V.P. Scaling and asymptotic laws in subrecoil laser cooling. *Europhys. Lett.* **1997**, *39*, 383–388. [CrossRef]

8. Balescu, R. Anomalous transport in turbulent plasmas and continuous-time random-walks. *Phys. Rev. E* **1995**, *51*, 4807–4822. [CrossRef]
9. Barkai, E.; Silbey, R. Diffusion of tagged particle in an exclusion process. *Phys. Rev. E* **2010**, *81*, 041129. [CrossRef]
10. Fokker, A.D. The median energy of rotating electrical dipoles in radiation fields. *Ann. der Phys.* **1914**, *43*, 810–820. [CrossRef]
11. Cleland, J.; Williams, M.A.K. Anomalous diffusion driven by the redistribution of internal stresses. *Phys. Rev. E* **2021**, *104*, 014123. [CrossRef]
12. Montroll, E.W.; Weiss, G.H. Random walks on lattices. II. *J. Math. Phys.* **1965**, *6*, 167–181. [CrossRef]
13. Klafter, J.; Sokolov, I. *First Steps in Random Walks. From Tools to Applications*; OUP Oxford: Oxford, UK, 2011.
14. Shlesinger, M.F. Origins and applications of the Montroll-Weiss continuous time random walk. *Eur. Phys. J. B* **2017**, *90*, 1–5. [CrossRef]
15. Metzler, R.; Klafter, J. The random walk's guide to anomalous diffusion: A fractional dynamics approach. *Phys. Rep.-Rev. Sect. Phys. Lett.* **2000**, *339*, 1–77. [CrossRef]
16. Vivirschi, B.N.; Boboc, P.C.; Baran, V.; Nicolin, A.I. Scale-free distributions of waiting times for earthquakes. *Phys. Scr.* **2020**, *95*, 044011. [CrossRef]
17. Bialecki, M. On mechanistic explanation of the shape of the universal curve of earthquake recurrence time distributions. *Acta Geophys.* **2015**, *63*, 1205–1215. [CrossRef]
18. Povstenko, Y. *Linear Fractional Diffusion-Wave Equation for Scientists and Engineers*; Springer: Cham, Switzerland, 2015. [CrossRef]
19. Samko, S.G.; Kilbas, A.A.; Marichev, O.I. Fractional integrals and derivatives: Theory and applications. *Teor. Mater. Fiz* **1993**, *3*, 397–414.
20. Kilbas, A.; Srivastava, H.; Trujillo, J. *Theory and Applications Of Fractinal Differential Equations*; Elsevier: Amsterdam, The Netherlands, 2006; Volume 204, [CrossRef]
21. Podlubny, I. (Ed.) Chapter 2—Fractional derivatives and integrals. In *Fractional Differential Equations*; Mathematics in Science and Engineering; Elsevier: Amsterdam, The Netherlands, 1999; Volume 198, pp. 41–119. [CrossRef]
22. Pica Ciamarra, M.; Lippiello, E.; De Arcangelis, L.; Godano, C. Statistics of slipping event sizes in granular seismic fault models. *EPL (Europhys. Lett.)* **2011**, *95*, 54002. [CrossRef]
23. Fox, C. The g and h functions as symmetrical fourier kernels. *Trans. Am. Math. Soc.* **1961**, *98*, 395–429.
24. Chechkin, A.V.; Sokolov, I.M. Relation between generalized diffusion equations and subordination schemes. *Phys. Rev. E* **2021**, *103*, 032133. [CrossRef]
25. Sokolov, I.M. Solutions of a class of non-Markovian fokker-Planck equations. *Phys. Rev. E* **2002**, *66 Pt 1*, 041101. [CrossRef] [PubMed]
26. Tateishi, A.A.; Ribeiro, H.V.; Lenzi, E.K. The role of fractional time-derivative operators on anomalous diffusion. *Front. Phys.* **2017**, *5*, 52. [CrossRef]
27. Mathai, A.M.; Saxena, R.K. *The H-Function with Applications in Statistics and Other Disciplines*; John Wiley & Sons: Hoboken, NJ, USA, 1978.
28. Sandev, T.; Chechkin, A.V.; Korabel, N.; Kantz, H.; Sokolov, I.M.; Metzler, R. Distributed-order diffusion equations and multifractality: Models and solutions. *Phys. Rev. E* **2015**, *92*, 042117. [CrossRef]
29. Skibiński, P. Some expansion theorems for the H-function. *Ann. Pol. Math.* **1970**, *23*, 125–138. [CrossRef]
30. Mathai, A.; Saxena, R.; Haubold, H. *The H-Function: Theory and Applications*; Springer: Berlin/Heidelberg, Germany, 2009. [CrossRef]
31. Sandev, T.; Metzler, R.; Tomovski, Z. Fractional diffusion equation with a generalized Riemann-Liouville time fractional derivative. *J. Phys. A Math. Theor.* **2011**, *44*, 255203. [CrossRef]
32. Wright, E.M. The asymptotic expansion of the generalized hypergeometric function. *Proc. Lond. Math. Soc.* **1940**, *s2-46*, 389–408. [CrossRef]
33. Langlands, T. Solution of a modified fractional diffusion equation. *Appl. Anal. Acta. Phys. Pol. B* **2003**, *630*, 259–279. [CrossRef]
34. Awad, E.; Metzler, R. Crossover dynamics from superdiffusion to subdiffusion: Models and solutions. *Fract. Calc. Appl. Anal.* **2020**, *23*, 55–102. [CrossRef]
35. Soury, H.; Alouini, M.S. On the symmetric alpha-stable distribution with application to symbol error rate calculations. In Proceedings of the 2016 IEEE 27th Annual International Symposium on Personal, Indoor, and Mobile Radio Communications (Pimrc), Valencia, Spain, 4–8 September 2016; pp. 990–995.

fractal and fractional

MDPI

Article

Some Results on a New Refinable Class Suitable for Fractional Differential Problems

Laura Pezza [1,*] and Luca Tallini [2]

[1] Department of Basic and Applied Sciences for Engineering (SBAI), University La Sapienza of Rome, 00161 Rome, Italy
[2] Facoltá di Scienze della Comunicazione, University of Teramo, 64100 Teramo, Italy
* Correspondence: laura.pezza@uniroma1.it

Abstract: In recent years, we found that some multiscale methods applied to fractional differential problems, are easy and efficient to implement, when we use some fractional refinable functions introduced in the literature. In fact, these functions not only generate a multiresolution on $\mathbb{R}$, but also have fractional (non-integer) derivative satisfying a very convenient recursive relation. For this reason, in this paper, we describe this class of refinable functions and focus our attention on their approximating properties.

Keywords: fractional refinable functions; fractional differential problems; collocation method

Citation: Pezza, L.; Tallini, L. Some Results on a New Refinable Class Suitable for Fractional Differential Problems. *Fractal Fract.* **2022**, *6*, 521. https://doi.org/10.3390/fractalfract6090521

Academic Editors: António Lopes, Alireza Alfi, Liping Chen and Sergio Adriani David

Received: 22 June 2022
Accepted: 2 August 2022
Published: 15 September 2022

Publisher's Note: MDPI stays neutral with regard to jurisdictional claims in published maps and institutional affiliations.

1. Introduction

In the last decades, fractional calculus has increased in popularity, owing to the awareness that many physical problems, such as viscoelasticity, Brownian motion, medical issues and so forth, require fractional derivatives to be modeled appropriately. For a better understanding, please see [1,2].

Analytical solutions for certain problems have been found. They are expressed through the Mittag–Leffler function [3], which is a series expansion, and thus require numerical tools to be computed. For this issue and for the other unsolved problems, the literature provides many ways to numerically solve fractional differential problems. Most of the methods employ the quadrature rule to compute the fractional derivatives [4]; others use spectral or Galerkin methods [5].

In recent papers [5–7], the authors proved that the multiscale collocation methods are easy and efficient to implement, when using certain fractional refinable functions introduced in [6,8]. In fact, these functions not only generate a multiresolution on $\mathbb{R}$, but also satisfy a fractional derivative convenient formula. Moreover, the collocation technique allows one to obtain an algebraic system from a differential problem.

The coefficient matrix is given by the collocation of basis functions into the collocation nodes. In this way, the result is given by the solution (often in a least-squares sense) of a linear algebraic system. The goal of this paper is to prove further approximating properties of this class of fractional refinable functions with respect to [6,8], suitable to the solution of fractional differential problems.

More precisely, in [6,8], we proved the basis properties of the class $\varphi_{\alpha,h}$, for $\alpha > 2$. The novelty of this paper, is that here we prove that these properties are also valid for $\alpha > 1$ and that other important approximating and smoothing properties can be proved, e.g., the order of polynomial reproducibility. In this way, we enlarge the class of fractional refinable functions from $\alpha > 2$ to $\alpha > 1$ and thus, also its applicability to *a wider class of fractional differential problems* . Furthermore, we prove that all the properties derive from a suitable convolution formula. Note that when we apply these functions to a differential problem with fractional derivative γ, we have to choose refinable functions of approximation order α such that $\alpha - \gamma > 1$.

The paper is organized as folllows. Section 3 introduces some fractional derivative definitions, that can be computed by numerical quadrature rules. We choose the Caputo derivative for several reasons: computational efficiency, minor regularity required, stability [2]. Section 4 explains Multiresolution Analysis (MRA) properties on $\mathbb{R}$ and on the interval. Section 5 describes the collocation and the Galerkin methods constructed with MRA. Section 6 lists the main properties of the fractional B-splines, introduced in [9,10], emphasizing the fractional derivative properties. Section 7 describes the new class of fractional refinable functions constructed introduced by [6,8], through a convolution formula involving the functions in [11] and with a continuos dependence from a parameter h. We prove that these functions satisfy new properties that are similar to those of the fractional B-splines, such as, for example, the polynomial reproducibility. Furthermore, we prove a differentiation formula that makes them particularly interesting in the fractional derivative context. In the conclusions, we explain all the advantages of this new class of fractional refinable functions, including an example on polynomial reproducibility.

2. Fractional Derivatives

The fractional derivative can be defined in many ways: for example, in the Caputo sense or in the Riemann Liouville way.

The Caputo definition of the *fractional derivative* is:

$$ {}_cD_t^\gamma\, y(t) := \left(\mathcal{J}^{(k-\gamma)} y^{(k)}\right)(t)\,, \qquad k-1<\gamma<k\,, \quad k\in\mathbb{N}\,, \qquad t>0\,, \tag{1}$$

where $\mathcal{J}^{(\beta)}$ is the *Riemann–Liouville integral operator*

$$ \left(\mathcal{J}^{(\beta)} y\right)(t) := \frac{1}{\Gamma(\beta)} \int_0^t y(\tau)\,(t-\tau)^{\beta-1}\,d\tau \quad \beta\in\mathbb{R}, \tag{2}$$

and Γ denotes Euler's gamma function

$$ \Gamma(\beta) := \int_0^\infty \tau^{\beta-1}\,\mathrm{e}^{-\tau}\,d\tau\,. \tag{3}$$

Hence,

$$ {}_cD_t^\gamma\, y(t) := \frac{1}{\Gamma(k-\gamma)} \int_0^t y^{(k)}(\tau)\,(t-\tau)^{k-\gamma-1}\,d\tau, \quad k=\lceil\gamma\rceil. \tag{4}$$

For example, if $\gamma=0.5$ then $k=1$ and:

$$ {}_cD_t^{0.5} y(t) := \frac{1}{\Gamma(0.5)} \int_0^t \frac{y'(\tau)}{\sqrt{(t-\tau)}}\,d\tau\,. \tag{5}$$

If, for example, $y(t)=t^n$ then

$$ {}_cD_t^\gamma y(t) := \frac{\Gamma(n+1-\gamma)}{\Gamma(n+1)} t^{n-\gamma}. \tag{6}$$

Riemann–Liouville definition is instead

$$ {}_{RL}D\gamma\, y(t) := \frac{d^k}{dt^k}\left(\mathcal{J}^{(\gamma)} y\right)(t)\,, \qquad t>0\,. \tag{7}$$

They both reduce to the usual differential operator when $\gamma\in\mathbb{N}$. In the general case, we have the following relation between the Caputo and the Riemann derivatives

$$ {}_cD^\gamma\, y(t) =_{RL} D^\gamma\left(y(t) - \sum_{l=0}^{k} \frac{t^l}{l!} y^{(l)}(0^+)\right). \tag{8}$$

The definitions coincide for homogenous boundary initial conditions.

In the Fourier domain one has

$$\mathcal{F}\left(D^{\gamma}, y(t)\right) = (i\omega)^{\gamma}\mathcal{F}(y(t)), \qquad \gamma \in \mathbb{R}^{+}, \omega \in \mathbb{C} \tag{9}$$

where $\mathcal{F}(y)$ is the Fourier transform of the function y.

3. MRA and Refinable Spaces

A sequence of functional spaces $\{V_j, j \in \mathbb{Z}\} \subset L^2(\mathbb{R})$, forms a multiresolution analysis (MRA) of $L^2(\mathbb{R})$ if

1. $V_j \subset V_{j+1}$, $j \in \mathbb{Z}$,
2. $\overline{\cup_{j\in\mathbb{Z}} V_j} = L^2(\mathbb{R})$;
3. $\bigcap_{j\in\mathbb{Z}} V_j = \{0\}$;
4. $f(t) \in V_j \leftrightarrow f(2t) \in V_{j+1}$, $j \in \mathbb{Z}$;
5. there exists a $L^2(\mathbb{R})$-stable basis in V_0.

MRA Based on Refinable Functions

An MRA can be generated by a *refinable function* ϕ, i.e., a function that satisfies a *refinement functional equation*

$$\phi(t) = \sum_{k\in\mathbb{Z}} a_k\, \phi(2\,t - k), \qquad t \in \mathbb{R}. \tag{10}$$

It is known that if the mask coefficients $\{a_k, k \in \mathbb{Z}\}$ form a finite sequence and have some particular properties, then the existence of a unique solution to (10) in $L^2(\mathbb{R})$, can be proved [12]. Moreover, the shifted refinable functions $\{\phi(t-k), k \in \mathbb{Z}\}$ give rise to a stable basis in V_0, i.e., the space they span.

It is important to associate (10) with its symbol

$$b^n(z) = \sum_k a_k\, z^k$$

When the mask is an infinity sequence, under suitable conditions the solution exists as proved in [8].

Now, we can define the spaces V_j of the multiresolution:

$$V_j := \overline{\text{span}\left\{\phi_{jk}(t) := \phi(2^j\, t - k), k \in \mathbb{Z}\right\}}, \qquad j \in \mathbb{Z}, \qquad t \in \mathbb{R}. \tag{11}$$

Since we are taking into account differential problems of order n with initial conditions, it is also important to define an MRA on an interval $[0, T]$, belonging to $Ł^2([0, T])$.

Let us suppose that the support of ϕ is compact, i.e., $supp\,\phi = [0, \sigma]$. Then, we can define an MRA on the interval.

$$V_j^0[0, T] = \overline{\text{span}\left\{\phi_{jk}^0(t), k \in \mathcal{N}_j\right\}, \quad j \geq j_0, \quad t \in [0, T]}, \tag{12}$$

where

$\phi_{jk}^0(t) := \{\phi_{jk}|_{[0,T]} : \phi_{jk}(0) = \phi_{jk}'(0) = \cdots = \phi_{jk}^{(n-1)}(0) = 0\}$;

$\mathcal{N}_j \subset \mathbb{Z}$, with $\#\mathcal{N}_j = N_j = 2^j + \sigma - 1$, is the set of admissible index k and j_0 is the initial multiresolution scale, i.e., the minimal index such that supp $\phi_{j_0 0}^0 \subset [0, \sigma]$.

4. The Collocation Method and the Galerkin Method

We use the MRA to approximate each fractional differential problem by the collocation method and Galerkin method. For both methods, we pose the solution in the following form:

$$y_j(t) = \sum_{k \in \mathcal{N}_j} c_{jk}\, \zeta_{jk}(t) \tag{13}$$

where ζ_{jk} is a refinable function generating an MRA.

- In the collocation method, we substitute (13) in the differential problem and we collocate it in the dyadic nodes $\{t_p = p/2^s,\, p = 0, \ldots, N_s, s \geq j\}$. So, we obtain a linear algebraic system in N_s equations and N_j unknowns $\{c_{jk}\}_{k=1}^{N_j}$. Usually, we solve the system by least-squares method.
- In the Galerkin method, we rewrite the differential problem in a weak form, and we substitute (13), using ζ_{jk} as trial and test functions. In this way, the resulting linear algebraic system, will contain as the coefficient matrix, the integrals between u and the test (trial) functions ζ_{jk} (Stiffness matrix).

In this way, the differential problem is converted into a system of algebraic equations that is suitable for computer programming.

Note.

If u also depends on x, i.e., $u(t, x)$, then the coefficients are $c_{jk} = c_{jk}(x)$ [5,6].

5. Fractional B-Splines

A particular class of refinable functions is provided by the cardinal B-Splines of degree n, i.e., functions that are positive and compactly supported in $[0, n+1]$, in each interval of the partition are polynomials of degree at most n and in $\mathbb{R}$ have regularity $C^{n-1}(\mathbb{R})$. The Fourier transform of the classical B-Splines is:

$$\hat{B}_n(\omega) = \left(\frac{1 - e^{-i\omega}}{i\omega}\right)^{n+1}, \qquad n = 0, 1, \cdots \tag{14}$$

We can define a *fractional B-Spline* starting with its Fourier transform obtained introducing a fractional (non-integer) exponent in (14):

$$\hat{B}_\alpha(\omega) = \left(\frac{1 - e^{-i\omega}}{i\omega}\right)^{\alpha+1}, \quad \alpha > -1 \tag{15}$$

It is proven that for $\alpha > -1$, the antitransform B_α is in $L^1(\mathbb{R})$, while B_α is in $L^2(\mathbb{R})$ for $\alpha > -1/2$ [9].

In the time domain, the cardinal B-Splines B_n, are defined in the following way. Let $t_+ := \max(0, t)$ be the usual truncated power function and the finite difference operator

$$\Delta^n v(t) := \sum_{k \in \mathbb{N}_0} (-1)^k \binom{n}{k} v(t - k), \qquad n \in \mathbb{N} \tag{16}$$

Then, $B_n(t)$ can be defined as:

$$B_n(t) := \frac{\Delta^{n+1} t_+^n}{(n+1)!}, \tag{17}$$

whose *symbol* is

$$b^n(z) = \frac{1}{2^n}(1 + z)^{n+1}$$

In the *non-integer case*, we define the *generalized finite difference operator*

$$\Delta^{\gamma} v(t) := \sum_{k \in \mathbb{N}_0} (-1)^k \binom{\gamma}{k} v(t-k), \qquad \gamma \in \mathbb{R}^+. \tag{18}$$

When $\gamma \in \mathbb{N}$, $\{\binom{\gamma}{k}\}_k$ is a compactly supported sequence and we get the usual finite difference operator.

On the other hand, when $\gamma \in \mathbb{R}^+ \backslash \mathbb{N}$, then

$$\binom{\gamma}{k} := \frac{\Gamma(\gamma+1)}{k!\,\Gamma(\gamma-k+1)} = O(k^{-\gamma-1}), \qquad k \in \mathbb{N}_0, \quad \gamma \in \mathbb{R}^+$$

and thus the sequence $\{\binom{\gamma}{k}\}_k$ is absolutely summable and the limit of the series (18) exists under suitable hypothesis on v. [9]

The *fractional B-spline*, i.e., the B-spline of non-integer order, in the time domain is defined as:

$$B_{\alpha}(t) := \frac{\Delta^{\alpha+1} t_+^{\alpha}}{\Gamma(\alpha+1)}, \qquad \alpha > -\frac{1}{2}, \tag{19}$$

The following theorem writes, with a different proof with respect to [9].

Theorem 1. *The fractional derivative of a B-Spline is a fractional B-Spline. More precisely,*

$$D^{\gamma} B_n(x) = \frac{\Delta^{n+1} t_+^{n-\gamma}(x)}{\Gamma(n+1-\gamma)} = \Delta^{\gamma} B_{n-\gamma}(x) \tag{20}$$

In fact, one has

$$D^{\gamma} B_n(x) = D^{\gamma} \frac{\Delta^{n+1} t_+^{n}(x)}{(n+1)!} = \Delta^{n+1} \frac{D^{\gamma} t_+^{n}(x)}{(n+1)!} =$$

$$\frac{\Gamma(n+1)}{\Gamma(n+1-\gamma)} \frac{\Delta^{n+1} t_+^{n-\gamma}(x)}{(n+1)!} = \frac{\Delta^{n+1} t_+^{n-\gamma}(x)}{\Gamma(n+1-\gamma)}$$

Proof. Now, for the rule of the difference finite operator composition

$$\Delta^{\gamma} \Delta^{n-\gamma+1} = \Delta^{n+1},$$

it is easy to verify that

$$\frac{\Delta^{n+1} t_+^{n-\gamma}(x)}{\Gamma(n+1-\gamma)} = \frac{\Delta^{\gamma} \Delta^{n-\gamma+1} t_+^{n-\gamma}(x)}{\Gamma(n+1-\gamma)} = \Delta^{\gamma} B_{n-\gamma}(x).$$

The theorem is proved. □

It is also worthwhile to define the symbol b^{α} of B_{α}, i.e.,

$$b^{\alpha}(z) = \frac{1}{2^{\alpha}} (1+z)^{\alpha+1}$$

5.1. Main Properties of Fractional B-Splines

In the study by [9], fractional B-splines are introduced for the first time and their main properties are proved. We summarize these properties in the following propositions avoiding the proof.

Proposition 1. *The fractional B-Splines B_α belong to $L^1(\mathbb{R})$, for $\alpha > -1$ and to the Sobolev space $W_2^r(\mathbb{R})$, $0 \leq r < \alpha + \frac{1}{2}$,for $\alpha > -\frac{1}{2}$; where $W_2^r(\mathbb{R})$, represents the Banach subspace of $L^2(\mathbb{R})$, equipped with the norm*

$$||f||_r = ||f||_2 + ||D^r f||_2$$

Proposition 2. *When $\alpha > -1/2$, the fractional B-Splines are α-order continuous, i.e., they can be derived up to the order α but ∂^α is in general only bounded.*

Moreover, they generate an MRA of $L^2(\mathbb{R})$

Proposition 3. *The fractional B-splines reproduce polynomials up to degree $\lceil \alpha \rceil$, but they do not satisfy Strang and Fix theory. In fact, they have fractional approximation order $\alpha + 1$, instead of $\lceil \alpha \rceil + 1$.*

For the CAGD and isogeometric context, it is important to know that they form a partition of unity for $\alpha > -1$.

Proposition 4. *It is also important to consider the following fractional derivation rule that is a generalization of the Formula (20)*

$$D^\gamma \left(B_\alpha \right) = \Delta^\gamma B_{\alpha - \gamma} \tag{21}$$

where D^γ is the usual derivative of order γ.

There is also a formula that allows us to assume that a fractional B-spline preserves the order of approximation of any refinable function of order α.

Proposition 5. *Let ϕ_α be a refinable function generating an MRA in $L^2(\mathbb{R})$, of order of approximation α. Then, ϕ_α can be factorized as*

$$\phi_\alpha = B_\alpha * \phi_0, \tag{22}$$

$\alpha \geq 0$ and ϕ_0 is a distribution such that $\int \phi_0 = 1$ [10].

Let us observe that all the previous propositions can be proved by starting from Proposition 5.

5.2. Fractional Derivative of Refinable Functions

If we consider a generic function ϕ_α of order α, it is possible to generalize the differentiation rule (21).

In fact, let it be that $\phi_0 \in \mathcal{C}^0(\mathbb{R})$, then $\phi_\alpha \in \mathcal{C}^{\lceil \alpha \rceil}(\mathbb{R})$ and

$$D^\gamma \phi_\alpha = D^\gamma \left(B_\alpha * \phi_0 \right) = \Delta^\gamma \left(B_{\alpha - \gamma} * \phi_0 \right) = \Delta^\gamma \phi_{\alpha - \gamma}\,, \qquad 0 < \gamma \leq \alpha\,. \tag{23}$$

The claim follows from some results in [10].

For shifted functions $\phi_{\alpha,k}(t)$, we obtain a similar result.

Proposition 6. *Let $\phi_{\alpha,k}(t) := \phi_\alpha(t - k)$. Then,*

$$D_t^\gamma \, \phi_{\alpha,k} = \Delta^\gamma \, \phi_{\alpha - \gamma, k}\,, \qquad 0 < \gamma \leq \alpha\,. \tag{24}$$

Let us note that since $\phi \in L^2(\mathbb{R})$ and the generalized binomial coefficients decay similar to $k^{-\gamma - 1}$ as $k \to +\infty$, thus the series in (24) converges. Thus, in practical computation, $\Delta^\gamma \phi_{\alpha - \gamma, k}$ is a finite sum.

6. Fractional GP Refinable Functions

We present here the main results regarding a new class of refinable functions of fractional order α, obtained starting by a suitable refinable function (of support $[0,2]$) introduced in [11]. We consider

$$\phi_{\alpha,h} = \frac{1}{2} B_{\alpha-2} * \phi_{1,\hat{h}}\,, \qquad 0 \le \alpha \le h\,, \tag{25}$$

where $\phi_{\hat{h}} \in L^2(\mathbb{R})$ is the *elementary refinable function*, solution of the refinement equation

$$\phi_{1,\hat{h}}(t) = \sum_{k=0}^{2} a_{\hat{h},k}\, \phi_h(2t-k)\,, \qquad t \in \mathbb{R}\,, \tag{26}$$

with mask coefficients in [11] and $\hat{h} = h - \alpha + 1$. h is a real *shape parameter* that controls the shape of $\phi_{\alpha,h}$. The symbol of $\phi_{n,h}$ in general is

$$b_h^n(z) = \frac{1}{2^h}[(1+z)^{n+1} + 4(2^{h-n}-1)z(1+z)^{n-1}].$$

that, for $n = 1$ reduces to

$$b_h^1(z) = \frac{1}{2^h}[(1+z)^2 + 4(2^{h-1}-1)z].$$

In the Fourier domain, the definition of $\phi_{\alpha,h}$ becomes:

$$\mathcal{F}(\phi_{\alpha,h})(\omega) = \left(\frac{1-e^{-i\omega}}{i\omega}\right)^{\alpha-1} \hat{\phi}_{\hat{h}}(\omega)$$

We observe that when $\alpha \in \mathbb{N}$, $\alpha \ge 0$, then $\phi_{\alpha,h}$ is compactly supported, belongs to $\in C^{\alpha-1}(\mathbb{R})$ and is a GP function as in [11]; in particular for $h = \alpha$ it reduces to a cardinal B-Spline. Instead, when α is not an integer but $h = \alpha$, then $\phi_{\alpha,\alpha}$ is a fractional B-spline in [9].

It is easy to show that $\phi_{\alpha,h}$ can be also obtained by placing a fractional index in the mask of $\phi_{n,h}$, i.e., $a_{\alpha,h,k} = \frac{1}{h}\left[\binom{\alpha+1}{k} + 4(2^{h-\alpha}-1)\binom{\alpha-1}{k-1}\right]$ and, in this case $\phi_{\alpha,h}$ becomes:

$$b_h^\alpha(z) = \frac{1}{2^h}[(1+z)^{\alpha+1} + 4(2^{h-\alpha}-1)z(1+z)^{\alpha-1}]$$

Therefore, it is not difficult to prove that:

$$b_h^\alpha(z) = \frac{1}{2} b^{\alpha-2}(z)\, b_{\hat{h}}^1(z) \tag{27}$$

where

$$b^{\alpha-2}(z) = \frac{1}{2^{\alpha-2}}(1+z)^{\alpha-1} \quad \text{and } \hat{h} = h - \alpha + 1$$

In fact,

$$b_h^\alpha(z) = \frac{1}{2^h}(1+z)^{\alpha-1}[(1+z)^2 + (2^{h-\alpha+2}) - 2^2)z] =$$

$$= \frac{1}{2^{\alpha-2}}\frac{1}{2^{h-\alpha+2}}(1+z)^{\alpha-1}[(z^2 + (2^{h-\alpha+2}) - 2)z + 1].$$

Observe that from (29), we deduce that $B_{\alpha-2}$ carries all the approximation properties of $\varphi_{\alpha,h}$. In fact, since $\phi_{\hat{h}}$ is summable, the convolution preserves all the properties of $B_{\alpha-2}$. So, we have the following theorem,

Theorem 2. *For any admissible α and h, $\phi_{\alpha,h}$ belongs to $C^{\lfloor \alpha \rfloor - 2}(\mathbb{R})$ (and decays to the infinity rather rapidly so that in practice it can be assumed compactly supported).*

Moreover, it has derivative $\partial^{\alpha-1}$, but it is only bounded, not necessary continuous; one says that it is α- continous. As for the order of approximation, $\phi_{\alpha,h}$ has order of approximation *$\alpha - 1$ and order of polynomial reproducibility $\lceil \alpha \rceil - 1$; so it does not verify the Strang and Fix theory.*

Finally, the differentiation rule is specified in

$$D_t^{\gamma} \phi_{\alpha,h}(t) = \Delta^{\gamma} \phi_{\alpha-\gamma,h-\alpha+2}(t) =$$

$$\sum_{k \in \mathbb{N}_0} (-1)^k \binom{\alpha}{k} \phi_{\alpha-\gamma,h-\alpha+2}(t-k), \quad 0 < \gamma \leq \alpha\,.$$

Proof. The properties of $\phi_{\alpha,h}$ are the same properties of $B_{\alpha-2}$ [9] that are preserved through the convolution Formula (27) since $\phi_{1,\hat{h}}$ is summable. □

7. Conclusions

Since, as in the classical B-spline case, the fractional derivative of a GP refinable function is a GP fractional refinable function, we deal in this paper with fractional GP functions stemming from the fractional derivative of GP refinable functions. In this way, we obtain a class of refinable functions, closed with respect to the fractional derivative.

Another advantage of these fractional GP refinable functions ϕ_h^{α} with respect to the GP refinable function, is that, in practice, due to the rapid decay of ϕ_h^{α}, their supports appear strictly contained in the supports $[0, n+1]$ of $\phi_{n,h}$, but the order of exactness is the same, i.e., $n-1$. This property, in addition to derivative Formulas (23) and (24), renders them highly suitable for solving fractional differential problems, as shown in [5,6].

More precisely, if, for example, we consider ϕ_h^{α}, with $\alpha = 1.5$, then the order of polynomial reproducibility is $\lceil \alpha \rceil - 1 = 1$, that is the straight line can be reproduced, in the same manner as classical GP refinable, when $n = 1$, and support $[0, 2]$.

Author Contributions: Conceptualization, L.P. and L.T.; methodology, L.P.; software, L.T.; validation, L.P. and L.T.; formal analysis, L.P.; investigation, L.P.; resources, L.P.; data curation, L.P. and Luca Tallini; writing—original draft preparation, L.P. and L.T.; writing—review and editing, L.P. and L.T.; visualization, L.P. and L.T.; supervision, L.P. and L.T.; project administration, L.P. and Luca Tallini; funding acquisition, L.P. All authors have read and agreed to the published version of the manuscrip.

Funding: This research received no external funding.

Acknowledgments: We would like to thank Francesca Pitolli and our daughter Irene Tallini for all the precious suggestions they gave us.

Conflicts of Interest: The authors declare no conflict of interest.

References

1. Kimeu, J.M. Fractional Calculus: Definitions and Applications. Ph.D. Thesis, Western Kentucky University, Bowling Green, KY, USA, 2009
2. Lino, P.; Maione, G.; Garrappa, R.; Holm, S. An approach to optimal integer and fractional-order modeling of electro-injectors in compression-ignition engines. *Control. Eng. Pract.* **2021**, *115*, 104890. [CrossRef]
3. Garrappa, R.; Popolizio, M. Evaluation of generalized Mittag–Leffler functions on the real line. *Adv. Comput. Math.* **2013**, *39*, 205–225. [CrossRef]
4. Pedas, A.; Tamme, E. On the convergence of spline collocation methods for solving fractional differential equations. *J. Comput. Appl. Math.* **2011**, *235*, 3502–3514. [CrossRef]
5. Pezza, L.; Pitolli, F. A fractional spline collocation-Galerkin method, for the fractional diffusion equation. *CAIM* **2018**, *9*, 104–120. [CrossRef]
6. Pezza, L.; Pitolli, F. A multiscale collocation method for fractional differential problems. *Math. Comput. Simul.* **2018**, *147*, 210–219. [CrossRef]
7. Pezza, L.; Pitolli, F. A Fractional Spline Collocation Method for the Fractional Order Logistic Equation. In *Approximation Theory XV: San Antonio 2016, Proceedings in Mathematics and Statistics;* Fasshauer, G., Schumaker, L., Eds.; Springer: Berlin/Heidelberg, Germany, 2017; Volume 201; pp. 307–318.
8. Pezza, L. Fractional GP Refinable Functions. *Rend. Mat. Ser. VII* **2007**, *27*, 73–87.

9. Unser, M.; Blu, T. Fractional splines and wavelets. *SIAM Rev.* **2000**, *42*, 43–67. [CrossRef]
10. Unser, M.; Blu, T. Wavelet theory demystified. *IEEE Trans. Sig. Proc.* **2003**, *51*, 470–483. [CrossRef]
11. Gori, L.; Pitolli, F. A class of totally positive refinable functions. *Rend. Mat. Ser. VII* **2000**, *20*, 305–322.
12. Dahmen, W.; Micchelli, C.A. Using the refinement equation for evaluating integrals of wavelets. *SIAMJ Numer. Anal.* **1993**, *30*, 507–537. [CrossRef]

mathematics

MDPI

Article

The Power Fractional Calculus: First Definitions and Properties with Applications to Power Fractional Differential Equations

El Mehdi Lotfi [1], Houssine Zine [2], Delfim F. M. Torres [2,*] and Noura Yousfi [1]

[1] Laboratory of Analysis, Modeling and Simulation (LAMS), Faculty of Sciences Ben M'sik, Hassan II University of Casablanca, Sidi Othman, Casablanca P.O. Box 7955, Morocco
[2] Center for Research and Development in Mathematics and Applications (CIDMA), Department of Mathematics, University of Aveiro, 3810-193 Aveiro, Portugal
* Correspondence: delfim@ua.pt

Abstract: Using the Laplace transform method and the convolution theorem, we introduce new and more general definitions for fractional operators with non-singular kernels, extending well-known concepts existing in the literature. The new operators are based on a generalization of the Mittag–Leffler function, characterized by the presence of a key parameter p. This power parameter p is important to enable researchers to choose an adequate notion of the derivative that properly represents the reality under study, to provide good mathematical models, and to predict future dynamic behaviors. The fundamental properties of the new operators are investigated and rigorously proved. As an application, we solve a Caputo and a Riemann–Liouville fractional differential equation.

Keywords: generalized Mittag–Leffler function; fractional calculus; non-singular kernels; integro-differential equations

MSC: 26A33; 33E12; 34A08; 44A10

Citation: Lotfi, E.M.; Zine, H.; Torres, D.F.M.; Yousfi, N. The Power Fractional Calculus: First Definitions and Properties with Applications to Power Fractional Differential Equations. *Mathematics* **2022**, *10*, 3594. https://doi.org/10.3390/math10193594

Academic Editors: António Lopes, Alireza Alfi, Liping Chen and Sergio Adriani David

Received: 24 August 2022
Accepted: 28 September 2022
Published: 1 October 2022

1. Introduction

Fractional calculus theory plays a crucial role in bridging the gap on the modeling of many neglected phenomena with memory effects. Unlike Markov-chain processes, where the current value of the function under consideration depends only on that of the recent past, long-range memory is naturally included under fractional modeling [1,2].

An in-depth examination of the literature of fractional calculus confirms that the modeling of memory effects has undergone several transformations in recent years, namely by considering the exponential effect under the Caputo–Fabrizio derivative [3], the Mittag–Leffler effect with Atangana–Baleanu and Al-Refai operators [4,5], and the new generalized fractional operator of Hattaf [6]. Here, we propose new, and more general, fractional operators based on a generalized Mittag–Leffler function, which we call the "power Mittag–Leffler function". Our new mathematical concept allows us to unify and extend the fractional literature by developing a family of power fractional operators (PFOs) that expand the existing generalized fractional operators and their many consequences [3–6]. Broadly speaking, the exponential function is converted to the expanded power function, and the generalized Mittag–Leffler function is transformed into the power Mittag–Leffler counterpart that we propose here.

Advanced mathematical results have recently been proved in the framework of fractional calculus: see, e.g., [7–11] and the references therein. However, to effectively describe realistic phenomena, all available definitions suffer from some limitations, depending on the application at hand, which has motivated us to propose here new, more general, notions, containing the key power parameter p. The currently introduced power fractional calculus enables the generalization and unification of many of the cited results, allowing engineers, researchers, and scientists to select the appropriate fractional derivative with respect to

the phenomenon under study in a natural way via the presence of the parameter p in our new definitions.

The action of the parameter p on a system is illustrated in the numerical simulation phase, where it is essential to find the appropriate value of p to describe real data with the adopted model, to describe the current trajectories to correctly predict the asymptotic behavior in the future: see our section devoted to the resolution of some power fractional differential equations (PFDEs). Furthermore, the defined power fractional derivative derives its legitimacy from the construction of its inverse power fractional integral operator (PFIO), using the Laplace transform and the convolution theorem. Finally, we claim that our PFOs have considerable potential, both for the development of mathematical modeling, in various fields, and in the mathematics discipline itself. All these reasons support the originality, importance, relevance and robustness of our definitions and results.

The paper is organized as follows. Section 2 is devoted to the introduction of the new power Mittag–Leffler function (Definition 1) accompanied with its convergence (Theorem 1). Section 3 contains novel definitions of the PFOs in both Caputo (Definition 2) and Riemann–Liouville senses (Definition 3), as well as establishing the connection between them (Theorem 3). Section 4 is dedicated to the discovery of the corresponding PFIO (Definition 4). To show the significance and usefulness of our PFOs, the resolution of two PFDEs is performed in Section 5. Section 6 concludes the paper and highlights some directions for future research.

2. The Power Mittag–Leffler Function

In this section, we introduce a new generalization of the Mittag–Leffler function, which we call the *power Mittag–Leffler* function.

Definition 1 (The Power Mittag–Leffler function)**.** *The Power Mittag-Leffler function is defined as*

$$ {}^{p}E_{\alpha,\beta}(z) := \sum_{n=0}^{\infty} \frac{(z \ln p)^n}{\Gamma(\alpha n + \beta)}, \quad z \in \mathbb{C}, \tag{1}$$

where $p \in \mathbb{R}_{+}^{*}$, *and* $\min(\alpha, \beta) > 0$.

Remark 1. *Note that our power Mittag–Leffler function* (1) *generalizes many important Mittag–Leffler functions that exist in the literature:*

1. *if* $\alpha = \beta = 1$ *and* $p = e$, *then we immediately obtain the classical exponential function,*

$$ {}^{e}E_{1,1}(z) = \sum_{n=0}^{\infty} \frac{z^n}{\Gamma(n+1)} = \sum_{n=0}^{\infty} \frac{z^n}{n!} = \exp(z); $$

2. *if* $\beta = 1$ *and* $p = e$, *then we obtain the celebrated Mittag–Leffler function, as defined in 1902 [12]:*

$$ {}^{e}E_{\alpha,1}(z) = \sum_{n=0}^{\infty} \frac{z^n}{\Gamma(\alpha n + 1)}; $$

3. *if* $p = 1$, *then we obtain the generalization defined in 1905 by Wiman [13],*

$$ {}^{e}E_{\alpha,\beta}(z) = \sum_{n=0}^{\infty} \frac{z^n}{\Gamma(\alpha n + \beta)}. $$

Similarly, further generalizations introduced by various authors, e.g., Prabhakar [14], Shukla and Prajapati [15], Salim [16], Salim and Faraj [17], and Khan and Ahmed [18], can also be obtained as particular cases of our power Mittag–Leffler function. *Readers interested in such generalizations are referred to [19].*

Theorem 1. *The power Mittag–Leffler function* ${}^{p}E_{\alpha,\beta}(z)$ *is absolutely convergent for all values of* $z \in \mathbb{C}$.

Proof. We rewrite ${}^{p}E_{\alpha,\beta}(z)$ in the power series form:

$$ {}^{p}E_{\alpha,\beta}(z) := \sum_{n=0}^{\infty} a_n z^n, \quad z \in \mathbb{C}, \tag{2}$$

where $a_n = \dfrac{(\ln p)^{\,n}}{\Gamma(\alpha n + \beta)}$. Using Stirling's formula, we get

$$\Gamma(\alpha n + \beta) = \left(\frac{\alpha n + \beta - 1}{e}\right)^{\alpha n + \beta - 1} \sqrt{2\pi(\alpha n + \beta - 1)}(1 + o(1)).$$

Then,

$$a_n = (\ln p)^{\,n} \cdot \left[\left(\frac{e}{\alpha n + \beta - 1}\right)^{\alpha n + \beta - 1} (2\pi(\alpha n + \beta - 1))^{-1/2}\right](1 + o(1)).$$

It follows, from Cauchy's criterion, that

$$a_n^{1/n} = (\ln p).\left[\left(\frac{e}{\alpha n + \beta - 1}\right)^{\alpha + \frac{\beta}{n} - \frac{1}{n}} \big(2\pi(\alpha n + \beta - 1)\big)^{-1/2n}\right]\big(1 + o(1)\big) \longrightarrow 0$$

as $n \longrightarrow \infty$ when $\alpha > 0$, which leads to the absolute convergence for all values of $z \in \mathbb{C}$ with the radius of convergence of the power series being infinite. □

3. The Power Fractional Derivatives

In this section, we present a new fractional derivative. Along the text, $f \in H^1(a,b)$ is a sufficiently smooth function on $[a,b]$ with $a, b \in \mathbb{R}$, where $H^1(a,b)$ is the Sobolev space $W^{1,2}(a,b)$, which is a Hilbert space. In addition, we adopt the following notations:

$$\phi(\alpha) := \frac{1-\alpha}{N(\alpha)}, \quad \psi(\alpha) := \frac{\alpha}{N(\alpha)},$$

where $0 \le \alpha < 1$ and $N(\alpha)$ is a normalization function obeying $N(0) = N(1^-) = 1$, with $N(1^-) = \lim_{\alpha \to 1^-} N(\alpha)$. In applications, the choice of a suitable and concrete normalization function N may depend on the phenomenon under study. Along the paper, we denote

$$\mu_\alpha := \frac{\alpha}{1-\alpha}.$$

Definition 2 (The power fractional derivative of order α in the Caputo sense)**.** *Let* $0 \le \alpha < 1$ *and* $\min(\beta, p) > 0$. *The power fractional derivative of order* α *in the Caputo sense, of a function* $f \in H^1(a,b)$ *with respect to the weight function* $w(t)$, *is defined as*

$${}^{pC}D_{a,t,w}^{\alpha,\beta,p} f(t) = \frac{1}{\phi(\alpha)} \frac{1}{w(t)} \int_a^t {}^{p}E_{\beta,1}\Big[-\mu_\alpha (t-s)^{\beta}\Big](wf)'(s)ds, \tag{3}$$

where $w \in C^1([a,b])$ *with* $w > 0$ *on* $[a,b]$.

We note that "pC" in the operator ${}^{pC}D_{a,t,w}^{\alpha,\beta,p}$ stands for "power Caputo".

Remark 2. *Our power fractional derivative in the Caputo sense given by Definition 2 generalizes many existing notions found in the literature:*

1. *if $w(t) \equiv 1$, $p = e$, and $\beta = 1$, then we obtain the Caputo–Fabrizio fractional derivative [3] given by*
$$ {}^{pC}D^{\alpha,1,e}_{a,t,1} f(t) = \frac{1}{\phi(\alpha)} \int_a^t \exp[-\mu_\alpha(t-s)] f'(s) ds;$$
2. *if $w(t) \equiv 1$, $p = e$, and $\beta = \alpha$, then we get the Atangana–Baleanu fractional derivative [4] given by*
$$ {}^{pC}D^{\alpha,\alpha,e}_{a,t,1} f(t) = \frac{1}{\phi(\alpha)} \int_a^t {}^{e}E_{\alpha,1}[-\mu_\alpha(t-s)^\alpha] f'(s) ds;$$
3. *if $p = e$ and $\beta = \alpha$, then we obtain the weighted Atangana–Baleanu fractional derivative defined by Al-Refai in [5], given by*
$$ {}^{pC}D^{\alpha,\alpha,e}_{a,t,w} f(t) = \frac{1}{\phi(\alpha)} \frac{1}{w(t)} \int_a^t {}^{e}E_{\alpha,1}[-\mu_\alpha(t-s)^\alpha] (wf)'(s) ds;$$
4. *if $p = e$, then we obtain the weighted generalized fractional derivative introduced by Hattaf [6], which is given by*
$$ {}^{pC}D^{\alpha,\beta,e}_{a,t,w} f(t) = \frac{1}{\phi(\alpha)} \frac{1}{w(t)} \int_a^t {}^{e}E_{\beta,1}[-\mu_\alpha(t-s)^\beta] (wf)'(s) ds.$$

Remark 3. *It is worth observing that the power fractional derivative in the Caputo sense satisfies the following two properties:*

$$ {}^{pC}D^{0,\beta,p}_{a,t,w} f(t) = f(t) - \frac{w(a)}{w(t)} f(a) \tag{4}$$

and

$$ {}^{pC}D^{\alpha,\beta,p}_{a,t,1} f(t) = 0 \text{ for any constant function } f(t). \tag{5}$$

Definition 3 (The power fractional derivative of order α in the Riemann–Liouville sense)**.** *Let $0 \le \alpha < 1$ and $\min(p, \beta) > 0$. The power fractional derivative of order α in the Riemann–Liouville sense, of a function $f \in H^1(a,b)$ with respect to the weight function $w(t)$, is defined as*

$$ {}^{pRL}D^{\alpha,\beta,p}_{a,t,w} f(t) = \frac{1}{\phi(\alpha)} \frac{1}{w(t)} \frac{d}{dt} \int_a^t (wf)(s) \, {}^{p}E_{\beta,1}\left[-\mu_\alpha (t-s)^\beta\right] ds, \tag{6}$$

where $w \in C^1([a,b])$ with $w > 0$ on $[a,b]$.

Remark 4. *The statements of Remark 2 are also verified in the Riemann–Liouville sense.*

Remark 5. *The following property of the power fractional derivative in the Riemann–Liouville sense is satisfied:*

$$ {}^{pRL}D^{0,\beta,p}_{a,t,w} f(t) = f(t). \tag{7}$$

Theorem 2. *The power fractional derivatives in the Caputo and Riemann–Liouville senses are linear operators.*

Proof. We easily see that

$$ {}^{pC}D^{\alpha,\beta,p}_{a,t,w} (c_1 f(t) + c_2 g(t)) = c_1 \, {}^{pC}D^{\alpha,\beta,p}_{a,t,w} f(t) + c_2 \, {}^{pC}D^{\alpha,\beta,p}_{a,t,w} g(t), \tag{8}$$

and

$$ {}^{pRL}D^{\alpha,\beta,p}_{a,t,w} (c_1 f(t) + c_2 g(t)) = c_1 \, {}^{pRL}D^{\alpha,\beta,p}_{a,t,w} f(t) + c_2 \, {}^{pRL}D^{\alpha,\beta,p}_{a,t,w} g(t), \tag{9}$$

for all scalars c_1 and c_2 and all functions $f, g \in H^1(a,b)$. □

Theorem 3. *Let wf be an analytic function. Then,*

$$ {}^{p_{RL}}D^{\alpha,\beta,p}_{a,t,w} f(t) = {}^{p_C}D^{\alpha,\beta,p}_{a,t,w} f(t) + \frac{1}{\phi(\alpha)} \frac{1}{w(t)} {}^{p}E_{\beta,1}\Big[-\mu_\alpha (t-a)^\beta\Big](wf)(a). \tag{10} $$

Proof. Because of the analyticity of the function wf, we get

$$ (wf)(x) = \sum_{n=0}^{+\infty} \frac{(wf)^{(n)}(t)}{n!}(x-t)^n $$

and

$$ \begin{aligned} {}^{p_{RL}}D^{\alpha,\beta,p}_{a,t,w} f(t) &= \frac{1}{\phi(\alpha)} \frac{1}{w(t)} \frac{d}{dt} \int_a^t \sum_{k=0}^{\infty} \frac{(-\mu_\alpha (t-s)^\beta \ln p)^k}{\Gamma(\beta k+1)} \sum_{n=0}^{+\infty} \frac{(wf)^{(n)}(t)}{n!}(s-t)^n ds \\ &= \frac{1}{\phi(\alpha)} \frac{1}{w(t)} \frac{d}{dt} \sum_{n=0}^{+\infty}\sum_{k=0}^{+\infty} \frac{(-1)^n(-\mu_\alpha \ln p)^k (wf)^{(n)}(t)}{n!\Gamma(\beta k+1)} \int_a^t (t-s)^{\beta k+n} ds \\ &= \frac{1}{\phi(\alpha)} \frac{1}{w(t)} \frac{d}{dt} \sum_{n=0}^{+\infty}\sum_{k=0}^{+\infty} \frac{(-1)^n(-\mu_\alpha \ln p)^k (wf)^{(n)}(t)(t-a)^{\beta k+n+1}}{n!\Gamma(\beta k+1)(\beta k+n+1)} \\ &= \frac{1}{\phi(\alpha) w(t)} \Bigg[\sum_{n=0}^{+\infty}\sum_{k=0}^{+\infty} \frac{(-1)^n(-\mu_\alpha \ln p)^k}{n!\Gamma(\beta k+1)(\beta k+n+1)} (wf)^{(n+1)}(t)(t-a)^{\beta k+n+1} \\ &\quad + \sum_{n=0}^{+\infty}\sum_{k=0}^{+\infty} \frac{(-1)^n(-\mu_\alpha \ln p)^k}{n!\Gamma(\beta k+1)} (wf)^{(n)}(t)(t-a)^{\beta k+n} \Bigg] \\ &= \frac{1}{\phi(\alpha) w(t)} \Bigg[\sum_{n=0}^{+\infty}\sum_{k=0}^{+\infty} \frac{(-1)^n(-\mu_\alpha \ln p)^k}{n!\Gamma(\beta k+1)} (wf)^{(n+1)}(t) \int_a^t (t-x)^{\beta k+n} dx \\ &\quad + \sum_{n=0}^{+\infty} \frac{(-1)^n}{n!} (wf)^{(n)}(t)(t-a)^n \sum_{k=0}^{+\infty} \frac{(-\mu_\alpha \ln p)^k}{\Gamma(\beta k+1)} (t-a)^{\beta k} \Bigg] \\ &= {}^{p_C}D^{\alpha,\beta,p}_{a,t,w} f(t) + \frac{1}{\phi(\alpha)} \frac{1}{w(t)} {}^{p}E_{\beta,1}[-\mu_\alpha (t-a)^\beta](wf)(a). \end{aligned} $$

The proof is complete. □

4. The Power Fractional Integral

With the intention of establishing the associated power fractional integral, we begin this section by computing the Laplace transform of the power fractional derivatives in Caputo and Riemann–Liouville senses multiplied by $w(t)$.

Lemma 1. *Let $f \in H^1(a,b)$ and $w \in C^1([a,b])$ with $w > 0$ on $[a,b]$. The following equalities hold:*

$$ \mathcal{L}\Big\{ w(t)\, {}^{p_C}D^{\alpha,\beta,p}_{0,t,w} f(t) \Big\}(s) = \frac{1}{\phi(\alpha)} \frac{s^\beta \mathcal{L}\{w(t)f(t)\}(s) - s^{\beta-1} w(0) f(0)}{s^\beta + \mu_\alpha \ln p}; \tag{11} $$

and

$$ \mathcal{L}\Big\{ w(t)\, {}^{p_{RL}}D^{\alpha,\beta,p}_{0,t,w} f(t) \Big\}(s) = \frac{1}{\phi(\alpha)} \frac{s^\beta \mathcal{L}\{w(t)f(t)\}(s)}{s^\beta + \mu_\alpha \ln p}. \tag{12} $$

Proof. We begin by proving the first statement of Lemma 1:

$$\begin{aligned}
\mathcal{L}\{w(t)\,{}^{pC}D^{\alpha,\beta,p}_{0,t,w}f(t)\}(s) &= \frac{1}{\phi(\alpha)}\mathcal{L}\Big\{{}^{p}E_{\beta,1}\Big[-\mu_\alpha t^\beta\Big]*(wf)'(t)\Big\}(s)\\
&= \frac{1}{\phi(\alpha)}\mathcal{L}\Big\{{}^{p}E_{\beta,1}\Big[-\mu_\alpha t^\beta\Big]\Big\}(s)\cdot\mathcal{L}\{(wf)'(t)\}(s).\\
&= \frac{1}{\phi(\alpha)}\sum_{n=0}^{+\infty}\frac{(\ln p)^n}{\Gamma(\beta n+1)}\mathcal{L}\Big\{(-\mu_\alpha t^\beta)^n\Big\}(s)\cdot\mathcal{L}\{(wf)'(t)\}(s)\\
&= \frac{1}{\phi(\alpha)}\frac{s^{\beta-1}}{s^\beta+\mu_\alpha\ln p}\mathcal{L}\{(wf)'(t)\}(s),\ \left|\frac{\mu_\alpha\ln p}{s^\beta}\right|<1\\
&= \frac{1}{\phi(\alpha)}\frac{s^\beta\mathcal{L}\{(wf)(t)\}(s)-s^{\beta-1}(wf)(0)}{s^\beta+\mu_\alpha\ln p}.
\end{aligned}$$

To prove the second statement, we get:

$$\begin{aligned}
\mathcal{L}\{w(t)\,{}^{p_{RL}}D^{\alpha,\beta,p}_{0,t,w}f(t)\}(s) &= \frac{1}{\phi(\alpha)}\mathcal{L}\Big\{\frac{d}{dt}\big({}^{p}E_{\beta,1}[-\mu_\alpha t^\beta]*(wf)(t)\big)\Big\}(s)\\
&= \frac{s}{\phi(\alpha)}\mathcal{L}\Big\{\big({}^{p}E_{\beta,1}[-\mu_\alpha t^\beta]*(wf)(t)\big)\Big\}(s)\\
&= \frac{s}{\phi(\alpha)}\mathcal{L}\Big\{\big({}^{p}E_{\beta,1}[-\mu_\alpha t^\beta]\Big\}(s).\mathcal{L}\Big\{(wf)(t)\Big\}(s)\\
&= \frac{1}{\phi(\alpha)}\frac{s^\beta\mathcal{L}\{w(t)f(t)\}(s)}{s^\beta+\mu_\alpha\ln p}.
\end{aligned}$$

The result is proved. □

Theorem 4. *The fractional differential equation*

$$^{p_{RL}}D^{\alpha,\beta,p}_{0,t,w}y(t)=f(t) \tag{13}$$

has a unique solution given by

$$y(t)=\phi(\alpha)f(t)+\ln p\cdot\psi(\alpha)\,{}^{RL}I^{\beta}_{0,w}f(t), \tag{14}$$

where ${}^{RL}I^{\beta}_{0,w}$ *is the standard weighted Riemann–Liouville fractional integral of order* β *given by*

$${}^{RL}I^{\beta}_{0,w}f(t)=\frac{1}{\Gamma(\beta)}\frac{1}{w(t)}\int_0^t(t-x)^{\beta-1}w(x)f(x)dx. \tag{15}$$

Proof. The equality (13) is equivalent to

$$\mathcal{L}\Big\{w(t)\,{}^{p_{RL}}D^{\alpha,\beta,p}_{0,t,w}y(t)\Big\}(s)=\mathcal{L}\Big\{w(t)f(t)\Big\}(s).$$

Using Lemma 1, we conclude that

$$\begin{aligned}
\mathcal{L}\{w(t)\,{}^{p_{RL}}D^{\alpha,\beta,p}_{0,t,w}f(t)\}(s) &= \phi(\alpha)\mathcal{L}\Big\{w(t)f(t)\Big\}(s)+\psi(\alpha)\frac{\ln p}{s^\beta}\mathcal{L}\Big\{w(t)f(t)\Big\}(s)\\
&= \phi(\alpha)\mathcal{L}\Big\{w(t)f(t)\Big\}(s)+\psi(\alpha)\frac{\ln p}{\Gamma(\beta)}\mathcal{L}\Big\{t^{\beta-1}*w(t)f(t)\Big\}(s)\\
&= \mathcal{L}\Big\{\phi(\alpha)w(t)f(t)+\psi(\alpha)\frac{\ln p}{\Gamma(\beta)}t^{\beta-1}*w(t)f(t)\Big\}(s).
\end{aligned}$$

Moreover, the action of the inverse Laplace transform yields

$$y(t) = \phi(\alpha) f(t) + \ln p . \psi(\alpha)^{RL} I^{\beta}_{0,w} f(t), \tag{16}$$

which completes the proof. □

Our Theorem 4 allows us to define an appropriate inverse operator for power fractional differentiation.

Definition 4 (The power fractional integral of order α). *Let $0 \leq \alpha < 1$ and $\min(p, \beta) > 0$. The power fractional integral of order α, of a function $f \in H^1(a, b)$ with respect to the weight function $w(t)$, is defined by*

$${}^{p} I^{\alpha,\beta,p}_{a,t,w} f(t) = \phi(\alpha) f(t) + \ln p \cdot \psi(\alpha)^{RL} I^{\beta}_{a,w} f(t), \tag{17}$$

where $w \in C^1([a, b])$ with $w > 0$ on $[a, b]$.

5. Examples of Power Fractional Differential Equations

In this section, we treat two examples of power fractional differential equations (PFDEs). Our first example considers a non-autonomous PFDE in the Riemann–Liouville sense.

Example 1. *Consider the following non-autonomous PFDE on $[0, 100]$:*

$${}^{p}{}_{RL} D^{\alpha,\beta,p}_{0,t,\frac{1}{t^2}} x(t) = t^2, \quad x(0) = 0. \tag{18}$$

Using Theorem 4, we obtain that

$$\begin{aligned} x(t) &= \phi(\alpha) t^2 + \ln p \cdot \psi(\alpha) \cdot {}^{p} I^{\alpha,\beta,p}_{0,t,\frac{1}{t^2}} t^2 \\ &= \phi(\alpha) t^2 + \ln p \cdot \psi(\alpha) \frac{t^{\beta+2}}{\Gamma(\beta+1)}. \end{aligned} \tag{19}$$

The action of the parameter p on the obtained solution is shown in Figure 1.

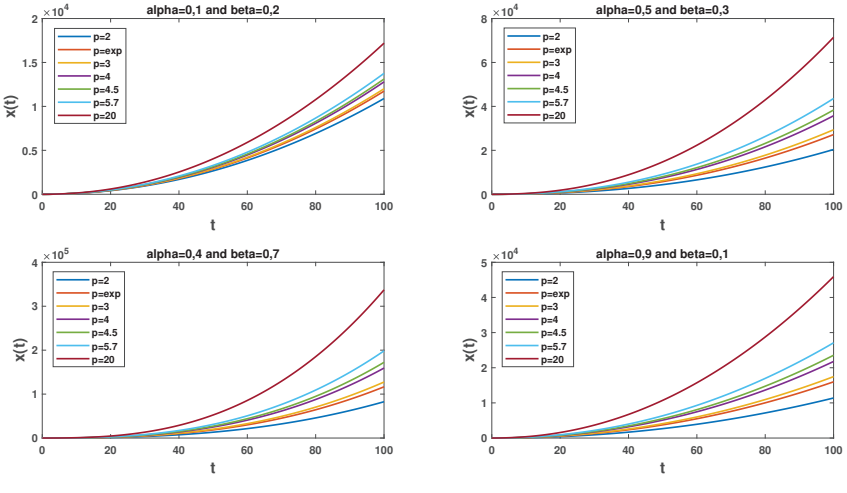

Figure 1. Impact of the power parameter p on the solution $x(t)$ (19) of problem (18) of Example 1 with different values of orders α and β.

We now consider an autonomous PFDE in the Caputo sense.

Example 2. *Consider the following autonomous PFDE:*

$$ {}^{pC}D^{\alpha,\beta,p}_{0,t,w}x(t) = Ax(t) + B, \quad x(0) = x_0. \tag{20}$$

The action of the Laplace transform on both sides of Equation (20) yields:

$$\mathcal{L}\Big\{w(t)\,{}^{pC}D^{\alpha,\beta,p}_{0,t,w}x(t)\Big\}(s) = A\mathcal{L}\{w(t)x(t)\}(s) + B\mathcal{L}\{w(t)\}(s).$$

Using Lemma 1, we obtain that

$$\begin{aligned}
\mathcal{L}\{w(t)x(t)\}(s) &= \frac{B(1-\alpha)s^\beta + \alpha A\ln p}{[N(\alpha)-(1-\alpha)A]s^\beta - \alpha A\ln p}\mathcal{L}\{w(t)\}(s) \\
&\quad + \frac{N(\alpha)w(0)x(0)s^{\beta-1}}{[N(\alpha)-(1-\alpha)A]s^\beta - \alpha A\ln p} \\
&= \frac{N(\alpha)w(0)x(0)}{[N(\alpha)-(1-\alpha)A]}\frac{s^{\beta-1}}{s^\beta - \frac{\alpha A\ln p}{[N(\alpha)-(1-\alpha)A]}} \\
&\quad + \frac{B(1-\alpha)}{[N(\alpha)-(1-\alpha)A]}\frac{s^{\beta-1}}{s^\beta - \frac{\alpha A\ln p}{[N(\alpha)-(1-\alpha)A]}}s\mathcal{L}\{w(t)\}(s) \\
&\quad + \frac{\alpha B\ln p}{[N(\alpha)-(1-\alpha)A]}\frac{1}{s^\beta - \frac{\alpha A\ln p}{[N(\alpha)-(1-\alpha)A]}}\mathcal{L}\{w(t)\}(s) \\
&= \frac{N(\alpha)w(0)x_0}{[N(\alpha)-(1-\alpha)A]}\mathcal{L}\left\{{}^pE_{\beta,1}\left(\frac{\alpha A}{[N(\alpha)-(1-\alpha)A]}t^\beta\right)\right\}(s) \\
&\quad + \frac{(1-\alpha)B}{[N(\alpha)-(1-\alpha)A]}\mathcal{L}\left\{{}^pE_{\beta,1}\left(\frac{\alpha A}{[N(\alpha)-(1-\alpha)A]}t^\beta\right)\right\}(s) \\
&\quad \times\big(\mathcal{L}\{w'(t)\}(s) + w(0)\big) \\
&\quad + \frac{B}{A}\mathcal{L}\left\{\frac{d}{dt}\,{}^pE_{\beta,1}\left(\frac{\alpha A}{[N(\alpha)-(1-\alpha)A]}t^\beta\right)\right\}(s)\mathcal{L}\{w(t)\}(s).
\end{aligned}$$

The effect of the inverse Laplace transform operator yields

$$\begin{aligned}
w(t)x(t) &= \frac{N(\alpha)w(0)x_0}{[N(\alpha)-(1-\alpha)A]}\,{}^pE_{\beta,1}\left(\frac{\alpha A}{[N(\alpha)-(1-\alpha)A]}t^\beta\right) \\
&\quad + \frac{(1-\alpha)B}{[N(\alpha)-(1-\alpha)A]}\,{}^pE_{\beta,1}\left(\frac{\alpha A}{[N(\alpha)-(1-\alpha)A]}t^\beta\right) * w'(t) \\
&\quad + \frac{(1-\alpha)Bw(0)}{[N(\alpha)-(1-\alpha)A]}\,{}^pE_{\beta,1}\left(\frac{\alpha A}{[N(\alpha)-(1-\alpha)A]}t^\beta\right) \\
&\quad + \frac{B}{A}\left(\frac{d}{dt}\,{}^pE_{\beta,1}\left(\frac{\alpha A}{[N(\alpha)-(1-\alpha)A]}t^\beta\right)\right) * w(t).
\end{aligned}$$

Applying the integration by parts formula on $\left(\frac{d}{dt}\,{}^pE_{\beta,1}\left(\frac{\alpha A}{[N(\alpha)-(1-\alpha)A]}t^\beta\right)\right) * w(t)$*, we can state that the solution to problem* (20) *is given by*

$$\begin{aligned}
x(t) &= \frac{-B}{A} + \frac{N(\alpha)w(0)}{[N(\alpha)-(1-\alpha)A]w(t)}\left(x_0 + \frac{B}{A}\right)\,{}^pE_{\beta,1}\left(\frac{\alpha A}{[N(\alpha)-(1-\alpha)A]}t^\beta\right) \\
&\quad - \frac{AN(\alpha)}{A[N(\alpha)-(1-\alpha)A]w(t)}\,{}^pE_{\beta,1}\left(\frac{\alpha A}{[N(\alpha)-(1-\alpha)A]}t^\beta\right) * w'(t).
\end{aligned}$$

6. Conclusions

In this paper, some new mathematical concepts, enabling the introduction of a new extended fractional calculus, are provided. The new approach allows choice of the most

appropriate notion of differentiation to suitably describe real dynamic phenomena under study, describing the observed trajectories and correctly predicting future behaviors. More precisely, we introduce the "power Mittag–Leffler function" ${}^{p}E_{\alpha,\beta}(\cdot)$ that extends several important functions: the Mittag–Leffler function ${}^{e}E_{\alpha,1}(\cdot)$, first introduced by Mittag–Leffler in [12]; the function ${}^{e}E_{\alpha,\beta}(\cdot)$ of Wiman [13]; and those introduced by Prabhakar [14] and Salim [16]. With the help of the new power Mittag–Leffler function, we then introduce the new power fractional derivatives ${}^{p_C}D^{\alpha,\beta,p}_{a,t,w}(\cdot)$ and ${}^{p_{RL}}D^{\alpha,\beta,p}_{a,t,w}(\cdot)$, which generalize those available in the literature, namely the Caputo–Fabrizio [3], Atangana–Baleanu [4], weighted Atangana–Baleanu [5], and weighted generalized fractional derivatives [6]. Moreover, an appropriate power fractional integral operator (PFIO) ${}^{p}I^{\alpha,\beta,p}_{a,t,w}(\cdot)$ is introduced, which is an important tool for the solution of power fractional differential equations (PFDEs). As examples, we investigated two PFDEs. The first is a non-autonomous PFDE: using our PFIO, we compute its solution and illustrate, numerically, the impact of the parameter p on the solution. The second example considered is an autonomous PFDE and its solution is obtained using the Laplace transform operator.

Here, we have only introduced the power fractional calculus and provided the most fundamental results with some applications to power fractional differential equations. In future work, several investigations may be designed to develop the new fractional calculus, which will enable the setting up of numerous applications on many parallel domains, e.g., in the fractional neural networks framework, analogously to what is done in [20–22].

Author Contributions: Conceptualization, E.M.L., H.Z., D.F.M.T. and N.Y.; validation, E.M.L., H.Z., D.F.M.T. and N.Y.; formal analysis, E.M.L., H.Z., D.F.M.T. and N.Y.; investigation, E.M.L., H.Z., D.F.M.T. and N.Y.; writing—original draft preparation, E.M.L., H.Z., D.F.M.T. and N.Y.; writing—review and editing, E.M.L., H.Z., D.F.M.T. and N.Y. All authors have read and agreed to the published version of the manuscript.

Funding: This research was funded by Fundação para a Ciência e a Tecnologia (FCT), grant number UIDB/04106/2020 (CIDMA).

Data Availability Statement: Not applicable.

Acknowledgments: The authors would like to express their gratitude to two anonymous reviewers for their constructive comments and suggestions, which helped them to enrich the paper.

Conflicts of Interest: The authors declare no conflict of interest. The funders had no role in the design of the study; in the collection, analyses, or interpretation of data; in the writing of the manuscript, or in the decision to publish the results.

References

1. Ding, L.; Luo, Y.; Lin, Y.; Huang, Y. Revisiting the relations between Hurst exponent and fractional differencing parameter for long memory. *Physica A* **2021**, *566*, 125603. [CrossRef]
2. Kee, C.Y.; Chua, C.; Zubair, M.; Ang, L.K. Fractional modeling of urban growth with memory effects. *Chaos* **2022**, *32*, 083127. [CrossRef] [PubMed]
3. Caputo, M.; Fabrizio, M. A new definition of fractional derivative without singular kernel. *Progr. Fract. Differ. Appl.* **2015**, *1*, 73–85. [CrossRef]
4. Atangana, A.; Baleanu, D. New fractional derivatives with non-local and non-singular kernel: Theory and application to heat transfer model. *Therm. Sci.* **2016**, *20*, 763–769. [CrossRef]
5. Al-Refai, M. On weighted Atangana-Baleanu fractional operators. *Adv. Differ. Equ.* **2020**, *2020*, 3. [CrossRef]
6. Hattaf, K. A new generalized definition of fractional derivative with non-singular kernel. *Computation* **2020**, **8**, 49. [CrossRef]
7. Zine, H.; Torres, D.F.M. A stochastic fractional calculus with applications to variational principles. *Fractal Fract.* **2020**, *4*, 38. [CrossRef]
8. Boukhouima, A.; Hattaf, K.; Lotfi, E.M.; Mahrouf, M.; Torres, D.F.M.; Yousfi, N. Lyapunov functions for fractional-order systems in biology: Methods and applications. *Chaos Solitons Fractals* **2020**, *140*, 110224. [CrossRef]
9. Zine, H.; Lotfi, E.M.; Torres, D.F.M.; Yousfi, N. Weighted generalized fractional integration by parts and the Euler-Lagrange equation. *Axioms* **2022**, *11*, 178. [CrossRef]
10. Zine, H.; Lotfi, E.M.; Torres, D.F.M.; Yousfi, N. Taylor's formula for generalized weighted fractional derivatives with nonsingular kernels. *Axioms* **2022**, *11*, 231. [CrossRef]

11. Boukhouima, A.; Zine, H.; Lotfi, E.M.; Mahrouf, M.; Torres, D.F.M.; Yousfi, N. Lyapunov functions and stability analysis of fractional-order systems. In *Mathematical Analysis of Infectious Diseases*; Elsevier: London, UK, 2022; Chapter 8, pp. 125–136. [CrossRef]
12. Mittag-Leffler, G.M. Sur la nouvelle fonction $E^{\alpha}(x)$. *C. R. L'Acad. Sci. Paris* **1903**, *137*, 554–558.
13. Wiman, A. Über den Fundamentalsatz in der Teorie der Funktionen $E^{a}(x)$. *Acta Math.* **1905**, *29*, 191–201. [CrossRef]
14. Prabhakar, T.R. A singular integral equation with a generalized Mittag Leffler function in the kernel. *Yokohama Math. J.* **1971**, *19*, 7–15.
15. Shukla, A.K.; Prajapati, J.C. On a generalization of Mittag-Leffler function and its properties. *J. Math. Anal. Appl.* **2007**, **336**, 797–811. [CrossRef]
16. Salim, T.O. Some properties relating to the generalized Mittag-Leffler function. *Adv. Appl. Math. Anal.* **2009**, *4*, 21–30.
17. Salim, T.O.; Faraj, A.W. A generalization of Mittag-Leffler function and integral operator associated with fractional calculus. *J. Fract. Calc. Appl.* **2012**, *3*, 1–13.
18. Khan, M.A.; Ahmed, S. On some properties of the generalized Mittag-Leffler function. *SpringerPlus* **2013**, *2*, 337. [CrossRef]
19. Khan, N.; Ghayasuddin, M.; Shadab, M. Some generating relations of extended Mittag-Leffler functions. *Kyungpook Math. J.* **2019**, *59*, 325–333. [CrossRef]
20. Xiao, J.; Guo, X.; Li, Y.; Wen, S.; Shi, K.; Tang, Y. Extended analysis on the global Mittag-Leffler synchronization problem for fractional-order octonion-valued BAM neural networks. *Neural Netw.* **2022**, *154*, 491–507. [CrossRef]
21. Xiao, J.; Zhong, S.; Wen, S. Unified analysis on the global dissipativity and stability of fractional-order multidimension-valued memristive neural networks with time delay. *IEEE Trans. Neural Netw. Learn. Syst.* **2021**. [CrossRef]
22. Xiao, J.; Li, Y. Novel synchronization conditions for the unified system of multi-dimension-valued neural networks. *Mathematics* **2022**, *10*, 3031. [CrossRef]

mathematics

MDPI

Article

Thermoelastic Analysis of Functionally Graded Nanobeams via Fractional Heat Transfer Model with Nonlocal Kernels

Doaa Atta [1,3], Ahmed E. Abouelregal [2,3,*] and Fahad Alsharari [2]

[1] Department of Mathematics, College of Science, Qassim University, P.O. Box 6644, Buraydah 51482, Saudi Arabia
[2] Department of Mathematics, College of Science and Arts, Jouf University, Al-Qurayyat 77455, Saudi Arabia
[3] Department of Mathematics, Faculty of Science, Mansoura University, Mansoura 35516, Egypt
* Correspondence: ahabogal@ju.edu.sa

Abstract: The small size and clever design of nanoparticles can result in large surface areas. This gives nanoparticles enhanced properties such as greater sensitivity, strength, surface area, responsiveness, and stability. This research delves into the phenomenon of a nanobeam vibrating under the influence of a time-varying heat flow. The nanobeam is hypothesized to have material properties that vary throughout its thickness according to a unique exponential distribution law based on the volume fractions of metal and ceramic components. The top of the FG nanobeam is made entirely of ceramic, while the bottom is made of metal. To address this issue, we employ a nonlocal modified thermoelasticity theory based on a Moore–Gibson–Thompson (MGT) thermoelastic framework. By combining the Euler–Bernoulli beam idea with nonlocal Eringen's theory, the fundamental equations that govern the proposed model have been constructed based on the extended variation principle. The fractional integral form, utilizing Atangana–Baleanu fractional operators, is also used to formulate the heat transfer equation in the suggested model. The strength of a thermoelastic nanobeam is improved by performing detailed parametric studies to determine the effect of many physical factors, such as the fractional order, the small-scale parameter, the volume fraction indicator, and the periodic frequency of the heat flow.

Keywords: non-homogeneous beams; nonlocal kernels; fractional thermoelasticity; MGT model; heat flow

MSC: 35B40; 35Q79; 35J55; 45F15; 73B30

Citation: Atta, D.; Abouelregal, A.E.; Alsharari, F. Thermoelastic Analysis of Functionally Graded Nanobeams via Fractional Heat Transfer Model with Nonlocal Kernels. *Mathematics* **2022**, *10*, 4718. https://doi.org/10.3390/math10244718

Academic Editors: António Lopes, Alireza Alfi, Liping Chen and Sergio Adriani David

Received: 10 November 2022
Accepted: 8 December 2022
Published: 12 December 2022

1. Introduction

Many areas of cutting-edge engineering focus on understanding and manipulating the processes that lead to pore development in nanostructures. Technological advancements in lithography and solid-state synthesis have opened up a wide range of options for building nanoscale mechanical devices with a tunable distribution of material characteristics along several axes. These mechanical nano-devices may exhibit the properties of functionally graded materials (FGMs), materials with a varied porosity variation, or both, depending on the production method. The characteristics of FGMs and the many ways porosity is dispersed in FGM structures significantly impact the mechanical response of nanostructured materials and should be investigated in detail [1]. Based on adaptable design concepts of component characteristics and mechanical qualities, FGM structures are created to suit the functional requirements of various engineering issues.

FGMs are innovative composite materials pioneered by Japanese researchers. Because FGMs' mechanical characteristics vary consistently and smoothly in the directions they are applied, they are not susceptible to the delamination problem that plagues laminated composites [2]. Both the metal and ceramic components are extremely durable and resistant to heat and corrosion. They are used in several industries, such as aerospace, nuclear,

automotive, civil engineering, etc., because of their superior features and benefits [3]. In addition, they are used in solar cells, MEMS and NEMS, micro- and nano-witches, transistors, actuators, sensor systems, AFM, and conversion devices [4].

Amiri Delouei et al. [5] obtained an exact general analytical solution to the heat conduction issue in an axisymmetric cylinder using a functionally graded material with bidirectionally varying thermal conductivity. It is presumed that the radial and longitudinal thermal conductivity factors are power functions of the radius. They also, in [6], found an analytical solution to the problem of steady-state heat transmission in a hollow sphere of functionally graded material. They treated the temperature distribution as a two-dimensional problem with a radial and tangential component because the conductivity factors in both directions are functions of radius. The shear deformation model (ST) was utilized by Avey et al. [7] to create a mathematical and computational model of the thermoelastic stability problem of composite cylinders reinforced with carbon nanotubes (CNTs) during uniform temperature loading. The basic partial differential equations (PDEs) for CNT-patterned cylindrical shells are developed inside a modified version of the Donnell-type shell concept, which accounts for the impact of transverse shear elastic deformation. Kaur et al. [8] proposed new applications for one-dimensional Euler–Bernoulli magneto-electro-piezo-thermoelastic (MEPT) nanoscale beams. The two-temperature heat transfer equation has also been taken into account. Pinola et al. [9] investigated the bending problems of micro- and nanobeams by proposing a nonlocal stress–strain relationship that changes over time. They did this by using a stress-driven integral framework and fractional-order operators.

Due to their increased performance and wide range of applications in fields such as nano/microelectromechanical systems (NEMS/MEMS) and flexible electronics, nanostructured materials and nanoparticles have recently garnered the interest of the global scientific community. Nano-switches, nanosensors, nanoactuators, and nanogenerators are only a few examples of the many potential uses of these technologies [10]. The nanoscale significantly affects the mechanical properties of micro and soft structures due to the small size influence. On the other hand, classical continuum mechanics' constitutive equation does not consider size effects. This makes it hard to accurately describe nanomaterials' thermal and mechanical engineering properties [11,12].

When studying the mechanical properties of nanostructures, it is crucial to account for their size and the magnitude of the impact they have. Continuum mechanics has been used to address this issue as an alternative to small-scale investigations and molecular dynamics (MD) simulations. It is evident that conventional elasticity theories cannot account for the size effect, and numerous nonclassical models have been developed to do so. The most widely used of these approaches is Eringen's nonlocal elasticity theory [13–15], which has been effectively implemented in the dynamic and static studies of nanostructured materials. To explain mechanical phenomena that depend on size, nonlocal continuum notions have been proposed, along with the appropriate scale parameters. High-order strain gradient concepts [16–18], rotation gradient models [19], and couple-stress theories [20,21] are all examples of this type of framework. This paper examines the nonlocal Eringen elasticity concept, a common tool for analyzing nanostructures' static and dynamic properties [13,14]. In place of a straight linear relationship between stress state and strains, the constitutive equation in nonlocal systems uses a convolutional integral.

Fractional calculus analyzes differential and integral operators of either real or complex order. A correspondence between Leibniz and de l'Hôpital in 1695 provides the earliest known explanation of fractional-order differentials, focusing on the interpretation of $\frac{d^{\alpha}}{dt^{\alpha}}(f(t))$ when t is not an integer. Liouville, Riemann, Laurent, Abel, Riesz, Weyl, Hardy and Littlewood, and Caputo are a few brilliant mathematicians who built upon and advanced fractional calculus. There are benefits and drawbacks to using several definitions of fractional derivatives [22].

The fractional-order analogy to integral calculus began practically concurrently, but the mathematics and, notably, the applications are much further along. This finding has

arisen due to several variables, one of which is the absence of techniques to connect a system's geometric and physical aspects with the fractional operator's associated order. Fractional calculus has recently played a significant role in several disciplines, including mechanics, Brownian motion, electrical, chemistry, biology, fluid dynamics, economics, and viscoelasticity, most notably in control theory, non-Fourier heat conduction, and signal and image processing. The inherent multiscale character of these operators is fascinating. Memory effects, in which a system's response depends on what it has done in the past, are made possible by time-fractional operators. In contrast, space-fractional operators make it possible for effects that are not local and do not depend on the scale [23].

To address the demand for real-world modeling problems in various domains, such as computational fluid dynamics, viscoelasticity, biology, physics, and engineering, several academics have discovered that developing new fractional derivatives with various singular or non-singular kernels is important. Two fractional derivatives based on the extended Mittag–Leffler function were presented, one in the Liouville–Caputo sense and the other in the Riemann–Liouville concept. Caputo and Fabrizio [24] offered an exponential-function-based solution to the single-kernel issue inherent in the standard definitions of fractional derivatives, including the Liouville–Caputo and Riemann–Liouville fractional derivatives. Unfortunately, this player has certain problems, such as the fact that it is not local. Not only that, but the matching integral in the fractional derivative is not a fractional integral. Atangana and Baleanu [25,26] successfully overcame these challenges.

Zhang and Li [27] devised the fundamental architecture of the Caputo–Fabrizio fractional-order differential equations (CF-FODEs) with multiple delays and an exponential Euler difference form. A fractional PECE approach is then suggested to resolve this implicit difference after research demonstrates that the acquired difference form (i.e., time-discrete CF-FODEs) falls within the range of implicit Euler differences. One category of fast ONNs (FONNs), which has Caputo derivatives (IPFONNs) piecewise, was described by Zhang et al. [28]. The differential inclusion concept is used to probe the existence of Filippov solutions for discontinuous IPFONNs. Several decision theorems have also been developed for IPFONNs, including those concerning the existence and uniqueness of the periodic solution, global exponential stability, and impulsively controlling global stabilization. Several systems have been defined using these terms [29–39].

A more extended dynamical theory of thermoelasticity was developed by Lord and Shulman [38], utilizing a variant of the thermal transfer equation that accounts for the time required for acceleration of the heat flow. The theory accounts for the impact of the coupling between temperature and strain rate; however, the coupled equations that follow are both hyperbolic. This resolves the seeming conundrum of unlimited propagation speed in the current coupled theory of thermoelasticity. By employing the extended theory, we can achieve a competitive solution with a solution found using the standard coupled theory. Green and Naghdi [39] used Fourier's law and the displacement-temperature-flux rate to propose a replacement model without considering energy dissipation. The most noticeable feature of this theory is that the thermal stream disregards energy waste compared to the classical theory linked to heat transfer and Fourier's equation. Three distinct types of constitutive response functions were used in the Green–Naghdi (GN) theory, which relied on Fourier's law for the displacement-temperature-flux rate. The most noticeable feature of this model is that the thermal stream disregards energy waste compared to the classical model linked to heat transfer and Fourier's equation. The Green–Naghdi (GN) theory makes use of three distinct forms (types I, II, and III) of constitutive response functions [39–41].

Recently, Quintanilla [42] introduced the MGT model of associated thermoelasticity based on the Moore–Gibson–Thompson (MGT) heat transmission equation. It is possible to see the energy balance equation (heat conduction equation) as a unified formulation incorporating LS theory, the GN model, and energy dissipation. Some investigators have recently focused on expanding MGT thermoelasticity investigation in various areas; some of these developments are discussed below. Based on the MGT heat transfer

equation for two temperatures, Quintanilla [43] created the MGT thermoelasticity study. Abouelregal et al. [44–49] have analyzed several papers using the MGT thermoelastic model to learn more about the spread of thermal and mechanical waves.

It is important to remember that most of the sources mentioned above and studies on micro- and nanobeam modeling assume the material is homogeneous and does not account for temperature variation's impact. According to the literature, most relevant research has ignored the effect of temperature change, and a few studies have considered the fractional differential thermal conductivity equation, including non-singular kernels. There is little literature on functionally gradient materials and extended thermoelastic theory in micro- and nanostructures. According to the authors, fractional calculus with nonlocal and non-singular kernels of conventional and nonlocal elasticity theory is explored for the first time. Using a generalized heat equation with fractional differential operators, we can analyze the nonlinear response of functionally graded nonlocal nanobeams.

This paper proposes a thermomechanical model that contributes to theoretical and practical guidance for the field of thermoelasticity, which may include some problems of energy, physics, engineering, and biotechnology. The governing equations are derived from generalized Hamilton's principle and nonlocal theory, Euler–Bernoulli theory, and the MGT-heat transfer equation, including the fractional-order differential operator. Although the classical fractional derivative has many desirable qualities, the singularity of its kernel is a major drawback of this operator. Different definitions of fractional derivatives, such as the Caputo–Fabrizio [2] and the Atangana–Baleanu [3], have been suggested to address this issue. Because the proposed model is based on the nonlocal Eringen theory, it can be used to study and create nanosensors and nanoactuators by taking into account the effects of the nanoscale.

The vibration sensitivity of the functionally graded nanobeams was investigated using the model that has been proposed. This means metal-like materials' characteristics may be continuously modified across their thickness. As a result, the FGM microbeam undergoes a continual transformation in its elastic-plastic, thermo-mechanical behavior from one surface to the next. In addition to being exposed to non-uniform heat flow, the nanobeam is made of isotropic material. The governing differential equations were transformed into dimensionless form, and then the Laplace transform method was applied as a solution strategy. A well-proven approximation algorithm was used to find the reflection of the Laplace transforms. Graphical representations are presented to investigate the effect of nonlocal factors, fractional derivatives, heat flux pulses, and relaxation time on the nanobeam resonator. In addition, comparisons were made with previous studies, which are considered special cases of the current work. These results could be used in many areas, such as biology, electronics, accelerometers, sensors, resonators, etc. This research has practical implications for the development of NEMS/MEMS-based sensors, actuators, and devices used in fields as diverse as marine, aeronautical, navigation, and other applications.

2. Formulation and Mathematical Model

2.1. Linear Theory of Nonlocal Elasticity

In the case of isotropic materials, the local stress, τ_{ij}, local strain, e_{ij}, and temperature change, θ, at a point, x, in the local elasticity theory are governed by classical linear constitutive relations [40]:

$$\tau_{ij} = 2\mu e_{ij} + \lambda e_{kk} - \gamma\theta\delta_{ij} \tag{1}$$

where local strain, e_{ij}, is given by

$$e_{kl} = 0.5(u_{k,l} + u_{l,k}) \tag{2}$$

In Equations (1) and (2), λ and μ are Lamé's, $\gamma = \alpha_t(3\lambda + 2\mu) = E\alpha_t/(1 - 2\nu)$ is the coupling parameter, α_t is the coefficient of thermal expansion, E denotes Young modulus, ν is Poisson's ratio, u_k are the displacement vector components, $\theta = T - T_0$ is the variation of

temperature, T is the temperature distribution, T_0 is the environmental temperature, and δ_{ij} denotes Kronecker's delta function.

The reaction of structures can be predicted using classical continuum models, but only up to a certain size threshold, below which they fail to produce accurate predictions. The small-scale effect has been taken into account by nonlocal continuum models. Continuum modeling is complicated by including a size parameter in nonlocal concepts. Using a nonlocal stress model, the dynamic behavior of the nanostructure is investigated. Using spatial integrals that are weighted averages of the contributions of corresponding strain tensors at the relevant place, Eringen's nonlocal elasticity model [13–15] derives its fundamental equations. Therefore, the theory uses a spatially integral constitutive relationship to account for the impact at small scales. The constitutive relationship that is predicated by the nonlocal theory of elasticity is given by the following [50,51]:

$$\sigma_{kl}(x) = \int \tau_{kl}(x') \mathcal{K}_{\xi}(|x - x'|, \xi) dV(x'), \forall\, x \in V \tag{3}$$

where the nonlocal stress tensor at every position x is denoted by the symbol σ_{kl}.

Moreover, $\mathcal{K}_{\xi}(|x - x'|, \xi)$ signifies the nonlocal kernel function and $|x - x'|$ indicates the Euclidean distance. In addition, $\xi = e_0 l_i / l_e$ is a material constant in which l_i and l_e are the internal and exterior characteristic lengths of the nanobeam, respectively, and e_0 is a dimensionless quantity that may be measured experimentally. Classical theories can be applied in the region where $l_i / l_e \gg 1$. If $l_i / l_e \sim 1$, classical theories cannot accurately predict the results; instead, atomistic or nonlocal theories should be used.

The literature typically employs the differential form of constitutive equations rather than the integral form because of the difficulty in addressing the integral constitutive equations. Using the proper kernel function, $\mathcal{K}_{\xi}$, in the aforementioned integral form of the equation, a differential version of the constitutive equations was supplied by Eringen [17–19] and can be constructed as

$$\sigma_{kl} - \xi^2 \frac{\partial^2 \sigma_{kl}}{\partial x^2} = \tau_{kl} = 2\mu e_{kl} + \lambda e_{mm} - \gamma \theta \delta_{kl} \tag{4}$$

2.2. Fractional Heat Conduction with Non-Singular Kernels

The process of transferring thermal energy between two bodies occurs when they are at different temperatures. To illustrate the basic idea behind heat transfer, Fourier's law is applied. Fourier's law shows the relationship between heat flow and temperature gradient, as in the following relationship:

$$q_i = -K_{ij} \theta_{,j} \tag{5}$$

The equation that describes energy can be written as follows [45,46]:

$$\rho C_E \frac{\partial \theta}{\partial t} + \gamma T_0 \frac{\partial u_{k,k}}{\partial t} = -q_{i,i} + Q \tag{6}$$

In Equations (5) and (6), q_i denotes the heat flux components, $K_{ij} = K_i \delta_{ij}$ indicates the thermal conductivity tensor, C_E symbolizes the specific heat, ρ is the density of the material; and Q signifies the internal energy supply.

Applying Fourier's law (1) in conjunction with the energy Equation (3) produces a parabola for heat transfer. This allows heat waves and turbulence to travel unlimitedly within the medium. This indicates that any thermal disturbance at the boundary is instantly sensed anywhere within the material, regardless of the location's distance from the heat source. This phenomenon is not recognized in the physical world because it is in direct conflict with the principle of causation.

Green and Naghdi suggested three alternative models of thermoelasticity, each with its own set of modifications to the constitutive requirements that make it possible to deal with

a broader category of heat problems. It is shown that the Green–Naghdi heat conduction equation (GN-III) can be changed in the following way [40]:

$$q_i = -K_{ij}\theta_{,j} + K^*_{ij}\vartheta_{,j} \tag{7}$$

where $K^*_{ij} = K^*_i\delta_{ij}$ are material constants, and the function ϑ denotes the gradient of thermal displacement and satisfies $\dot{\vartheta} = \theta$.

By introducing the concept of phase lag, τ_0 (relaxation time), of the heat flux, Equation (7) was modified based on the Moore–Gibson–Thompson equation concept as [42,43]

$$\left(1 + \tau_0\frac{\partial}{\partial t}\right)\dot{q}_i = -K_{ij}\dot{\theta}_{,j} - K^*_{ij}\theta_{,j} \tag{8}$$

Fractional derivatives are a part of fractional calculus that play a crucial role in real-world modeling phenomena within different branches of engineering and science. With the help of fractional calculus, many mathematical models of real problems were produced in various fields of engineering and science. Models in physics, engineering, and other disciplines frequently use the following Riemann–Liouville fractional derivative formula [52]

$$D^\alpha_t f(t) = \frac{1}{\Gamma(1-\alpha)}\frac{d}{dt}\int_0^t (t-\xi)^{-\alpha} f(\xi)d\xi,\ 0 < \alpha \leq 1 \tag{9}$$

The single kernel problem in the current fractional-order derivatives models, such as the Liouville–Caputo and Riemann–Liouville fractional derivatives, was overcome by Caputo and Fabrizio [24] by introducing an exponential function. The basic definitions in the Riemann–Liouville and Caputo concepts deal with singular kernels. Several criticisms of Caputo and Fabrizio's fractional derivatives operator have been discussed, as the integral kernel was shown to be non-singular but still non-local. The derivative operators of Caputo and Fabrizio also lack the concept of a fractional integral. That is why Atangana and Baleanu (AB) [25,26] used the extended Mittag–Leffler function to create two fractional derivatives based on the Caputo and Riemann–Liouville concepts to address the problem of non-singularity and non-localization of the kernels.

The Atangana–Baleanu derivative of fractional order α, $(0 < \alpha \leq 1)$ of function $f(t)$ and m involving the Mittag–Leffler function is defined as [25,26]:

$$D^\alpha_t f(t) = \frac{1}{1-\alpha}\int_0^t \frac{\partial f(\xi)}{\partial \xi} E_\alpha\left[-\frac{\alpha(t-\xi)^\alpha}{1-\alpha}\right]d\xi,\ 0 < \alpha \leq 1 \tag{10}$$

The Laplace transform to Atangana–Baleanu fractional derivative is given by [53]:

$$\mathcal{L}\left[D^{(\alpha)}_t f(t)\right] = \frac{1}{1-\alpha}\frac{s^\alpha \mathcal{L}[f(t)] - s^{\alpha-1}f(0)}{s^\alpha + \frac{\alpha}{1-\alpha}}, s > 0 \tag{11}$$

To better understand the development and behavior of the dynamical system, the AB factor has seen extensive application over the past six years. The two fields in which AB operators were most used were physical sciences and engineering. In this context, we may derive a modified model of fractional heat transfer with a one-phase lag and MGT equation by inserting the fractional Atangana–Baleanu derivative operator into Equation (5), which can be expressed as follows [36,47]:

$$(\mathbf{1} + \boldsymbol{\tau_0 D^\alpha_t})\dot{\boldsymbol{q}}_{\boldsymbol{i}} = -\boldsymbol{K_{ij}}\dot{\boldsymbol{\theta}}_{\boldsymbol{,j}} - \boldsymbol{K^*_{ij}}\boldsymbol{\theta}_{\boldsymbol{,j}} \tag{12}$$

When Equations (3) and (10) are put together, we obtain the fractional-order MGT heat transfer equation with a phase delay, which looks like this:

$$\left(K_{ij}\dot{\theta}_{,j}\right)_{,i} + \left(K^{*}_{ij}\theta_{,j}\right)_{,i} = (1+\tau_0 D^{\alpha}_{t})\left(\rho C_E \frac{\partial^2\theta}{\partial t^2} + \beta_{ij}\, T_0 \frac{\partial^2 u_{k,k}}{\partial t^2}\right) \tag{13}$$

2.3. Material Properties

There has been a rise in interest in functionally graded materials (FGMs) for various uses. The qualities of the two raw materials that go into making FGMs are preserved, and the components are distributed on a continuous grade scale. One of the FGMs made by combining ceramic and metal, for instance, has the strength of metal but the heat resistance and corrosion resistance of ceramic. It is also an excellent material for withstanding high temperatures. Unlike traditional composites, which often have discrete phases, FGMs exhibit continually variable material characteristics, meaning that many analytical methods may not be immediately relevant to FGMs [54]. Properties such as thermal conductivity, corrosion resistance, specific heat, hardness, and stiffness ratio are continuously graded due to slow variations in the volume fraction of constituents and nonidentical structure in the preferred direction [55]. With these benefits, FGMs are superior to homogeneous composites in various contexts. As a result of their unique qualities, FGMs have been the subject of several attempts at improvement. Different sizes and structures have led to the introduction of many classes of FGMs thus far. In addition, several other fabrication procedures, including a gas-based approach, a liquid process method, and a solid process method, can be used to create FGMs.

Heterogeneous composite nanobeams consist of different materials at different scales, starting with ceramic and ending with metal via an uninterrupted structural transition through the thickness of the beam. Along with the beam thickness trend, the modulus of elasticity, material density, thermal conductivity modulus, and coupling parameters are expected to vary due to the nature of FGMs. Except for the Poisson ratio, the current model displays the effective material gradient property $P(z)$ along the thickness axis, as in the following relationship [56,57]:

$$P(z) = P_m e^{-n_p(h-2z)/h} \tag{14}$$

where the intermediate value of the graded parameter n_p is determined by the left and right bounds of the physical characteristic, i.e.,

$$n_p = ln\sqrt{\frac{P_m}{P_c}} \tag{15}$$

where c and m represent the two primary components, ceramic and metal, respectively.

According to its material properties (full metal), the studied beam has a metal-rich bottom plane ($z = h/2$) and a ceramic-rich (full-ceramic) top plane ($z = -h/2$). By setting the power index constants to zero ($n_p = 0$ or $P_m = P_c$), we may simplify the solution method and the results to that of a thick beam of isotropic materials (pure metal-like nanobeams).

3. Problem Formulation

As shown in Figure 1, a functionally graded nanobeam will be considered with dimensions of length (L), width (b), and height (h), and its cross-section is regular rectangular with area $A = bh$. The coordinate system (x, y, z) will be used, with the xy plane positioned at the neutral surface of the microbial beam and the origin x axis located at the centroid of the left end. The x-axis, y-axis for width, and z-axis for depth are all shown here. It will be assumed that the variables u, v, and w represent the offsets of the x, y, and z axis,

respectively. The nanobeam under consideration is described with the Euler–Bernoulli beam hypothesis.

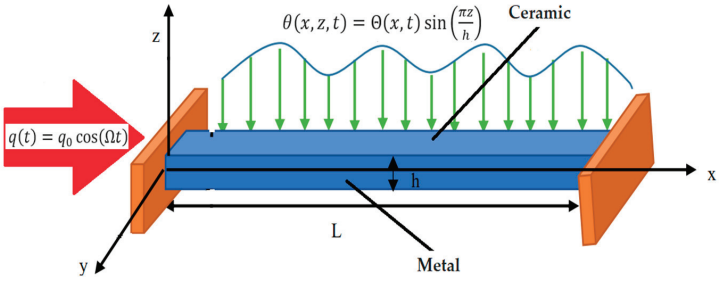

Figure 1. Configuration of FG thermoelastic nanobeam.

The cross sections continue to be planar and normal to the longitudinal axis in the Euler–Bernoulli beam theory. In this case, the displacements may be provided by

$$u = -z\frac{\partial w}{\partial x},\ v = 0, w(x, y, z, t) = w(x, t) \tag{16}$$

By combining Equations (14) and (16), the following forms of the nonlocal differential constitutive Equation (4) can be found:

$$\sigma_x - \xi^2\frac{\partial^2\sigma_x}{\partial x^2} = -E_m\left[ze^{\frac{n_{E\alpha}(2z-h)}{h}}\frac{\partial^2 w}{\partial x^2} + \alpha_{Tm}\theta e^{\frac{n_{E\alpha}(2z-h)}{h}}\right] \tag{17}$$

where $\alpha_{Tm} = \frac{\alpha_m}{1-2\nu_m}$, σ_x is the axial nonlocal thermal stress, and the quantity $n_{E\alpha} = \ln\sqrt{E_m\alpha_m/E_c\alpha_c}$, α_c and E_c, respectively, are the thermal expansion factor of ceramics and Young's modulus.

The bending moment, $M(x, t)$, of the thermoelastic FG nanobeams can be calculated as follows [58]:

$$M = b\int_{-h/2}^{h/2} z\sigma_x dz \tag{18}$$

The bending moment can be calculated when the nonlocal constitutive Equation (17) is included in Equation (18). Multiplying Equation (17) by $\frac{12}{h^3}$ and integrating with respect to the variable z from $-h/2$ to $h/2$, the bending moment may be expressed as

$$M - \xi^2\frac{\partial^2 M}{\partial x^2} = -bh^2E_m\left[h\mu_E\frac{\partial^2 w}{\partial x^2} + \alpha_{Tm}\mu_K M_T\right] \tag{19}$$

where M_T is the thermal moment, which is defined by the formula:

$$M_T = \frac{12}{h^3}\int_{-h/2}^{h/2}\theta z dz \tag{20}$$

with

$$\mu_E = \frac{\left(-2n_{E\alpha}\cosh(n_{E\alpha}) + \left(2+n_{E\alpha}^2\right)\mathrm{shin}(n_{E\alpha})\right)}{4n_{E\alpha}^3}\sqrt{\frac{E_c\alpha_c}{E_m\alpha_m}},$$
$$\mu_K = \frac{(n_{E\alpha}\cosh(n_{E\alpha}) - \mathrm{shin}(n_{E\alpha}))}{2n_{E\alpha}^2}\sqrt{\frac{E_c\alpha_c}{E_m\alpha_m}}.$$

The Hamiltonian notion was used to develop the equation of motion that describes motion. The equation below, which is based on Newton's second law of motion, may be used to describe the beam's oscillation in a transverse direction [59]:

$$\frac{\partial^2 M}{\partial x^2} = \mu_\rho A\frac{\partial^2 w}{\partial t^2} \tag{21}$$

where $\mu_\rho = \frac{\left(1-e^{-2n_\rho}\right)\rho_m}{2n_\rho}$.

When Equation (19) is plugged into Equation (21), the differential motion Equation (21) can be expressed as:

$$\frac{\partial^4 w}{\partial x^4} + \frac{\mu_\rho}{E_m h A \mu_E}\left(\frac{\partial^2 w}{\partial t^2} - \xi^2 \frac{\partial^4 w}{\partial t^2 \partial x^2}\right) + \frac{\alpha_{m\mu_K}}{E_m A^2 \mu_E}\frac{\partial^2 M_T}{\partial x^2} = 0 \tag{22}$$

In addition, Equations (19) and (21) can be used to figure out the flexure moment, M, in the following way:

$$M(x,t) = \xi^2 A \mu_\rho \frac{\partial^2 w}{\partial t^2} - bh^2 E_m \left[h\mu_E \frac{\partial^2 w}{\partial x^2} + \alpha_{Tm}\mu_K M_T\right] \tag{23}$$

The fractional MGT heat transfer equation without singular kernels may be represented using Equations (13) and (14) as

$$\begin{aligned}(1+\tau_0 D_t^\alpha)\left[\rho_m C_{Em} e^{n_{\rho C_E}(2z-h)/h}\frac{\partial^2\theta}{\partial t^2} - z\gamma_m e^{n_\gamma(2z-h)/h} T_0 \frac{\partial^2}{\partial t^2}\left(\frac{\partial^2 w}{\partial x^2}\right)\right] \\ = e^{n_K(2z-h)/h}\left(K_m\frac{\partial}{\partial t} + K_m^*\right)\left[\frac{\partial^2\theta}{\partial x^2} + \frac{\partial^2\theta}{\partial z^2} + \frac{2n_K}{h}\frac{\partial\theta}{\partial z}\right]\end{aligned} \tag{24}$$

Equation (14) is used to compute the parameters n_K, n_γ, and $n_{\rho C_E}$ for the ceramic and metal content properties. Furthermore, the definitions for the parameters γ_m and $\rho_m C_{Em}$ are

$$\gamma_m = \frac{E_m \alpha_m}{1-2\nu_m}, \chi_m = \frac{K_m}{\rho_m C_{Em}}$$

The investigated nanobeam is assumed to have no heat conduction along its surfaces at the planes $z = \pm h/2$. In addition, if the nanobeam is tiny enough, the temperature gradient across the plate's thickness should follow a sinusoidal pattern as

$$\theta(x,z,t) = \Theta(x,t)\sin\left(\frac{\pi z}{h}\right) \tag{25}$$

By substituting Equation (25) into the heat Equation (24) and then integrating it throughout the width of the beam, we can derive the following equation:

$$\left(\frac{\partial}{\partial t} + \frac{K_m^*}{K_m}\right)\left[\frac{\partial^2}{\partial x^2} - \left(\frac{\pi}{h}\right)^2\right]\Theta = (1+\tau_0 D_t^\alpha)\left[\frac{\overline{\mu}_{\rho C_E}}{\chi_m}\frac{\partial^2\Theta}{\partial t^2} - \frac{\overline{\mu}_\gamma \gamma_m h T_0}{K_m}\frac{\partial^2}{\partial t^2}\left(\frac{\partial^2 w}{\partial x^2}\right)\right] \tag{26}$$

where

$$\begin{aligned}\overline{\mu}_{\rho C_E} = \frac{\mu_{\rho C_E}}{\mu_K}, \overline{\mu}_\gamma = \frac{\mu_\gamma}{\mu_K}, \mu_{\rho C_E} = \frac{2n_{\rho C_E}\left(1+e^{-2n_{\rho C_E}}\right)}{\pi^2 + 4\left(n_{\rho C_E}\right)^2}, \\ \mu_K = \frac{2n_K\left(1+e^{-2n_K}\right)}{\pi^2+4(n_K)^2}, \mu_\gamma = \frac{n_\gamma\left(1+e^{-2n_\gamma}\right)+e^{-2n_\gamma}-1}{4(n_\gamma)^2}.\end{aligned}$$

To obtain a more relevant result, the nondimensional variables described below can be regarded:

$$\begin{aligned}\{x', z', u', w', L', h', \xi'\} = c_0\eta_0\{x,z,u,w,L,h,\xi\}, \Theta' = \frac{\Theta}{T_0}, \\ \sigma'_x = \frac{\sigma_x}{E_m}, \{t', \tau'_0\} = c_0^2\eta_0\{t,\tau_0\}, \quad M' = \frac{M}{bh^3 E_m \mu_E \eta\varepsilon}.\end{aligned} \tag{27}$$

With the help of Equation (27) and the elimination of primes, the fundamental governing equations may be written in a form that is free of dimensions, as follows:

$$\frac{\partial^4 w}{\partial x^4} + A_1\left(\frac{\partial^2 w}{\partial t^2} - \xi^2\frac{\partial^4 w}{\partial t^2\partial x^2}\right) = -A_2\frac{\partial^2\Theta}{\partial x^2} \tag{28}$$

$$\left(\frac{\partial}{\partial t} + \frac{K_m^*}{c_0^2\eta_0 K_m}\right)\left[\frac{\partial^2}{\partial x^2} - \left(\frac{\pi}{h}\right)^2\right]\Theta = (1+\tau_0 D_t^\alpha)\left[A_3\frac{\partial^2\Theta}{\partial t^2} - A_4\frac{\partial^2}{\partial t^2}\left(\frac{\partial^2 w}{\partial x^2}\right)\right] \tag{29}$$

$$M(x,t) = A_1\left(\xi\frac{\partial^2 w}{\partial t^2} - \frac{\partial^2 w}{\partial x^2}\right) - A_2\Theta \tag{30}$$

where

$$A_1 = \frac{\mu_\rho}{h^2\mu_E}, A_2 = \frac{T_0\alpha_{m\overline{\mu}_{E\alpha}}}{h},\ A_3 = \overline{\mu}_{\rho C_E}, A_4 = \frac{\overline{\mu}_\gamma\gamma_m h}{\eta_0 K_m}$$

4. Solution of the Transformed Domain

To solve this problem, we will use the Laplace transform technique in the system of partial differential Equations (31)–(33). It is assumed here that the starting circumstances of the problem are

$$\Theta(x,0) = 0 = \frac{\partial\Theta(x,0)}{\partial t}, w(x,0) = 0 = \frac{\partial w(x,0)}{\partial t} \tag{31}$$

The following versions of governing Equations (28)–(30) result from applying the Laplace transformation method:

$$\left(\frac{d^4}{dx^4} - \xi^2 A_1 s^2\frac{d^2}{dx^2} + A_1 s^2\right)\overline{w} = -A_2\frac{d^2\overline{\Theta}}{dx^2} \tag{32}$$

$$\left(\frac{d^2}{dx^2} - \phi_2\right)\overline{\Theta} = -\phi A_4\frac{d^2\overline{w}}{dx^2} \tag{33}$$

$$\overline{M}(x,t) = A_1\left(\xi^2 s^2\overline{w} - \frac{d^2\overline{w}}{dx^2}\right) - A_2\overline{\Theta} \tag{34}$$

where

$$\phi_1 = 1 + \frac{\tau_0 s^\alpha}{s^\alpha(1-\alpha)+\alpha},\ \phi = \frac{\phi_1}{\left(s + \frac{K_m^*}{c_0^2\eta_0 K_m}\right)}, \phi_2 = \left(\frac{\pi}{h}\right)^2 + \phi A_3$$

By first deleting either $\overline{w}$ or $\overline{\Theta}$ from Equations (32) and (33), we can derive the following differential equation:

$$\left(D^6 - AD^4 + BD^2 - C\right)\left\{\overline{\Theta}, \overline{w}\right\}(x) = 0 \tag{35}$$

where

$$A = \xi^2 A_1 s^2 + \phi_2 + \phi A_2 A_4,\ B = A_1 s^2 + \phi\xi^2 A_1 A_3 s^2,\ C = \phi_2 A_1 s^2, D = \frac{d}{dx}.$$

When the following equation is satisfied by the parameters m_n^2, $n = 1,2,3$,

$$m^6 - Am^4 + Bm^2 - C = 0 \tag{36}$$

The following is a factorization that may be performed on Equation (35):

$$\left(D^2 - m_1^2\right)\left(D^2 - m_2^2\right)\left(D^2 - m_3^2\right)\left\{\overline{\Theta}, \overline{w}\right\}(x) = 0 \tag{37}$$

Equation (37) has a general solution that can be expressed as

$$\left\{\overline{w}, \overline{\Theta}\right\}(x) = \sum_{n=1}^{3}\{1, \beta_n\}\left(H_n e^{-m_n x} + R_n e^{m_n x}\right) \tag{38}$$

where the parameters H_n and R_n stand in for the integration constants, and $\beta_n = -\frac{\phi A_4 m_n^2}{m_n^2 - \phi_2}$.

The displacement $\overline{u}$ can be determined by incorporating Equation (38) into Equation (16) as follows:

$$\overline{u}(x) = -z\frac{d\overline{w}}{dx} = z\sum_{n=1}^{3} m_n\left(H_n e^{-m_n x} - R_n e^{m_n x}\right) \tag{39}$$

Equations (34) and (38) can be used to calculate the solution of the bending moment, $\overline{M}$, as

$$\overline{M}(x) = \sum_{n=1}^{3}\left(\xi^2 s^2 A_1 - m_n^2 A_1 - A_2\beta_n\right)\left(H_n e^{-m_n x} + R_n e^{m_n x}\right) \tag{40}$$

In addition, the strain, $\overline{e}$, can be calculated as follows:

$$\overline{e}(x) = \frac{d\overline{u}}{dx} = -z\sum_{n=1}^{3} m_n^2\left(H_n e^{-m_n x} + R_n e^{m_n x}\right) \tag{41}$$

5. Application

The boundary conditions will be responsible for determining the integration constants H_n and R_n, where $n = 1$, 2, and 3. In the present work, the nanobeam is assumed to be simply supported at both ends. Therefore, the mechanical boundary conditions can be represented as follows:

$$w(0,t) = 0 = w(L,t), \frac{\partial^2 w(0,t)}{\partial x^2} = 0 = \frac{\partial^2 w(L,t)}{\partial x^2} \tag{42}$$

In addition to this, we will assume that the beginning of the nanobeam ($x = 0$) is subjected to a dimensionless and time-dependent heat transfer rate denoted by $q(t)$. In this particular scenario, we take into account the heat flow, $q(t)$, which varies periodically, and e is represented mathematically as

$$q(t) = q_0\cos(\Omega t)\ ,\ \Omega > 0 \text{ on } x = 0 \tag{43}$$

where Ω is the thermal oscillation frequency and q_0 is the heat flow intensity.

Using the modified model of fractional MGT heat transfer (12), then we have

$$(1 + \tau_0 D_t^{\alpha})\frac{\partial q(t)}{\partial t} = -e^{n_K(2z-h)/h}\left(K_m\frac{\partial}{\partial t} + K_m^*\right)\frac{\partial\theta}{\partial x} \tag{44}$$

With the help of the nondimensional quantitates given in Equation (25) and using (44), we get

$$(1 + \tau_0 D_t^{\alpha})Q_0\sin(\Omega t) = -e^{n_K(2z-h)/h}\left(\frac{\partial}{\partial t} + \frac{K_m^*}{c_0^2\eta_0 K_m}\right)\frac{\partial\theta}{\partial x} \tag{45}$$

where Q_0 is a constant parameter.

It is possible to obtain the following equation by inserting (27) into the heat Equation (45) and integrating along the beam's thickness with respect to z:

$$(1 + \tau_0 D_t^{\alpha})\sin(\Omega t) = \psi\left(\frac{\partial}{\partial t} + \frac{K_m^*}{c_0^2\eta_0 K_m}\right)\frac{\partial\Theta}{\partial x} \tag{46}$$

where $\psi = \frac{2n_K\left(1+e^{-2n_K}\right)}{Q_0(4{n_K}^2+\pi^2)}$.

In addition, it is assumed that the opposite end of the nanobeam is thermally isolated. We can express this boundary condition mathematically as

$$\frac{\partial\Theta}{\partial x} = 0 \text{ on } x = L \tag{47}$$

When the Laplace transform is applied to the boundary conditions (42), (46), and (47), we get

$$\begin{array}{c} \overline{w}(0,s) = 0 = \overline{w}(L,s) \\ \frac{d^2\overline{w}(0,s)}{dx^2} = 0 = \frac{d^2\overline{w}(L,s)}{dx^2} = 0 \\ \frac{d\overline{\Theta}(0,s)}{dx} = \frac{\phi_1 \Omega \phi}{\psi\left(s^2+\Omega^2\right)} = G(s) \\ \frac{d\overline{\Theta}(L,s)}{dx} = 0 \end{array} \tag{48}$$

Six linear equations may be obtained by substituting Equation (38) into the boundary conditions mentioned above:

$$\sum_{n=1}^{3}(C_n + C_{n+1}) = 0 \tag{49}$$

$$\sum_{n=1}^{3}\left(C_n e^{-m_n L} + C_{n+1} e^{m_n L}\right) = 0 \tag{50}$$

$$\sum_{n=1}^{3} m_n^2 (C_n + C_{n+1}) = 0 \tag{51}$$

$$\sum_{n=1}^{3} m_n^2 \left(C_n e^{-m_n L} + C_{n+1} e^{m_n L}\right) = 0 \tag{52}$$

$$\sum_{n=1}^{3} m_n (\beta_n C_n - \beta_{n+1} C_{n+1}) = G(s) \tag{53}$$

$$\sum_{n=1}^{3} m_n \left(\beta_n C_n e^{-m_n L} - \beta_{n+1} C_{n+1} e^{m_n L}\right) = 0 \tag{54}$$

The unknowns in this system of linear equations are H_n and R_n, where $n = 1, 2, 3$.

6. Inversion of the Laplace Transforms

Numerical calculations using Mathematica have been used to determine the research formulas for fields obtained in the physical field of silicon nanobeams. The Riemann sum approximation method is used to generate numerical results for evaluating the areas of the physical domain under study. Honig and Hirdes [60] give some thought to cataloging these methods. By using residue calculus, the original solution might be inverted.

7. Validation of the Numerical Scheme

The finite element method (FEM) is widely accepted as the method of choice for modeling linear and nonlinear systems across many application areas. To obtain the numerical solution to a difficult issue, this method is often employed. The finite element approach was utilized by Abbas et al. [61–63] in order to study a variety of extended thermoelastic diffusion problems. In this section, the finite element method is briefly introduced to validate the Honig and Hirdes approach [60]. Equations (28) and (29) may be converted to a finite element formulation by using the conventional process suggested by Abbas et al. [61–63], and the time derivatives of the unknown studied field variables can be computed using implicit methods. To validate the method and the numerical results, a comparison of the numerical results was performed using the Honig and Hirdes technique [60] and the finite element method [61–63] (see Table 1).

The finite element method is better than the integrative transformation method in the case of applications with irregular shapes and complex boundary conditions. It is mentioned that in the case of the finite element method, the price of the calculations is expensive and requires a large memory and also that its standards are strict and guarantee stability and non-volatility. In contrast, the general method of Laplace transforms is easier to use in the case of regular geometric shapes and simple boundary conditions, as in the case of the present problem.

Table 1. Comparison between Honig and Hirdes technique and finite element method.

x	Temperature θ		Deflection w	
	Honig and Hirdes	**Finite Element**	**Honig and Hirdes**	**Finite Element**
0	0.0350153	0.0346686	0	0
0.1	0.0060144	0.00595485	0.0603709	0.0597732
0.2	0.00376662	0.00372933	0.0315896	0.0312768
0.3	0.00185514	0.00183677	−0.00144551	−0.0014312
0.4	0.000452097	0.000447621	−0.00675736	−0.00669046
0.5	0.000568924	0.000563291	−0.00139024	−0.00137648
0.6	0.0000632165	0.0000625906	0.00116959	0.00115801
0.7	0.000109421	0.000108337	0.000647093	0.000640686
0.8	0.0000444636	0.0000440233	−0.0000806691	−0.0000798704
0.9	0.0000122177	0.0000120968	−0.000167537	−0.000165878
1	0.0000133683	0.000013236	0	0

8. Numerical Outcomes and Analysis

The resulting equations are used in this part to characterize the thermo-mechanical resonance responses of FGM nanoscale beams as a function of size through the use of several numerical case studies. In the case studies, aluminum and alumina (aluminum oxide) are used to represent the metal and ceramic phases of the nanoscale beam. Here are some details of each of them [64,65]:

Ceramic (alumina):

$$E_c = 393\ \text{GPa}, \quad \nu_c = 0.33, \quad \rho_c = 3960\ \text{Kg/m}^3,\ T_0 = 293\text{K},$$
$$\alpha_c = 8.7 \times 10^{-6}\text{K}^{-1}, \quad \chi_c = 1.06 \times 10^{-6}\text{m}^2/\text{s}, \quad K_c = 1.78\ \text{W/(m K)}.$$

Metal (aluminum):

$$E_m = 70\ \text{GPa}, \quad \nu_m = 0.35, \quad \rho_m = 2700\ \text{Kg/m}^3, T_0 = 293\text{K},$$
$$\alpha_m = 23.1 \times 10^{-6}\text{K}^{-1}, \quad \chi_m = 84.18 \times 10^{-6}\text{m}^2/\text{s}, \quad K_m = 237\ \text{W/(m K)}.$$

The beam size ratios used in the equations are as follows: $L/h = 20$ and $b/h = 0.5$. If h is different, then so must be b. We will choose a beam length range of $L(1 \ : \ 100) \times 10^{-9}$, stipulating that this is suitable for nanoscale beams. The instantaneous time, t, will be expressed in picoseconds $(1 : 100) \times 10^{-12}$ s, while the phase-delay value, τ_0, will also be interpreted as having a precision of 1 picosecond $(1 : 100) \times 10^{-12}$ s. When $L = 1$, $z = h/6$, and $t = 0.12$, the numerical calculations and figures were created for the nondimensional physical variables (θ, w, u, and M) with various nanobeam lengths $(0 \le x \le 1)$.

In the discussion and analysis, the influence of the nonlocal parameter ξ, the periodic frequency Ω of the applied heat flow, and the fractional differentiation parameter α will be considered. In addition, to verify the proposed thermoelasticity model, a comparison will be made between it and the previous corresponding models.

8.1. Validation of the Proposed Thermal Model

The analytical solutions for deflection, $\boldsymbol{w}$, and temperature, $\boldsymbol{\theta}$, were verified in the case of the present developed thermal model by comparing the results obtained with the corresponding results available in some of the literature. For validation, we compared the present numerical results in the presence of fractional differentiation with those reported in the literature [56,66] in the absence of fractional differentiation. The findings of this study provide insight into the instability of nano-beam-based microdevices and can direct

researchers toward optimizing their overall performance. Furthermore, the results of this study provide an explanation for the differences found in the literature when comparing the nanosystem's responses without considering modified models, such as nonclassical concepts, small-scale influences, and external force modifications to the results obtained.

Despite the difference in quantities, Table 2 displays data showing good agreement between those obtained and those published in [56,66]. As a result, the excellent accuracy of our model is demonstrated by the strong correlation between our results and those from investigations. As for the fractional case, it is noted that the different distributions in the case of using the fractional derivatives of AB are affected by the past more than the traditional derivative. The findings of the completed study are in good accord with data found in the open literature, as shown by the theoretical results, which are supplied in Table 2.

Table 2. Comparison of the temperature, θ, and deflection, w and with Refs. [56,66].

x	Temperature θ			Deflection w		
	Present	**Ref. [56]**	**Ref. [66]**	**Present**	**Ref. [56]**	**Ref. [66]**
0	0.033902	0.052003	0.0624035	0	0	0
0.1	0.006218	0.00893227	0.0107187	0.057221	0.0717278	0.0896598
0.2	0.003576	0.0055940	0.00671279	0.031654	0.0375322	0.0469152
0.3	0.001987	0.00275515	0.00330618	−0.00028	−0.00171744	−0.0021468
0.4	0.000346	0.000671431	0.000805718	−0.00665	−0.00802855	−0.0100357
0.5	0.000593	0.000844937	0.00101392	−0.00180	−0.00165178	−0.00206472
0.6	0.000109	0.000093886	0.000112663	0.001030	0.00138961	0.00173702
0.7	0.000103	0.000162506	0.000195007	0.000742	0.00076882	0.00096103
0.8	0.00005645	0.00006604	0.000079242	−0.000009	−0.00009584	−0.0001198
0.9	0.00000662	0.000018145	0.00002177	−0.00017	−0.0001991	−0.0002488
1	0.00000151	0.000019854	0.00002382	0	0	0

8.2. Impact of Fractional Derivative Parameter

In this work, we suggest an approximation to the solution of the fractional heat transfer equation defined by a non-singular fractional derivative. Our research employs the fractional derivative introduced by Atangana–Baleanu (AB) and Caputo. Fractional versions have a tremendous advantage over their conventional counterparts by having unlimited degrees of freedom for orders of derivatives and fully explaining the memory effect. To accomplish this, graphical illustrations have been developed to physically assess the consequences and compare the outcomes of the fractional derivatives for FGM nanoscale beams as compared to those of the classical approaches.

Due to the influence of fractional order, α, in this subsection we will examine how the FG material reacts when subjected to a varying heat flux at regular intervals and how the reactions are distributed. The numerical solutions are computed for the situation when $\Omega = 3$, $\tau_0 = 0.02$, and $\xi = 0.002$. The AB fractional derivative operator was used to graphically illustrate the temperature increment, θ, the bending moment, M, the transverse vibration deviation, w, and the longitudinal displacement, u, in fractional thermoelastic for different fractional order values (see Figures 2–5). When $\alpha = 0.9$, 0.8, and 0.7, the Atangana–Baleanu fractional derivative operator is utilized, and when $\alpha = 1$, the classical nonfractional derivative is employed.

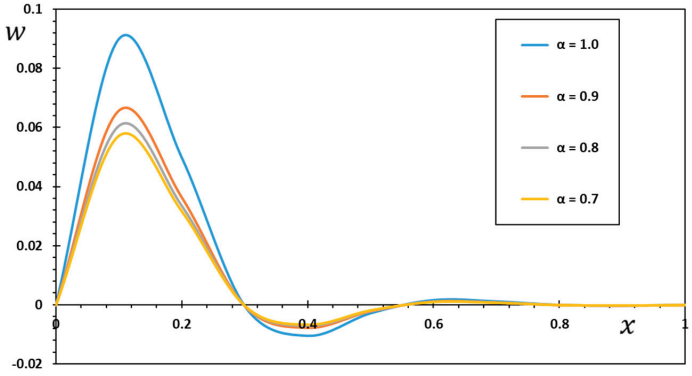

Figure 2. Effect of fractional order, α, on the deflection, w.

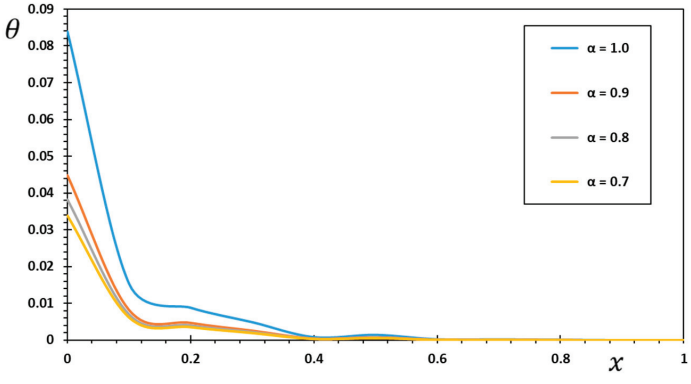

Figure 3. Effect of fractional order, α, on the temperature, θ.

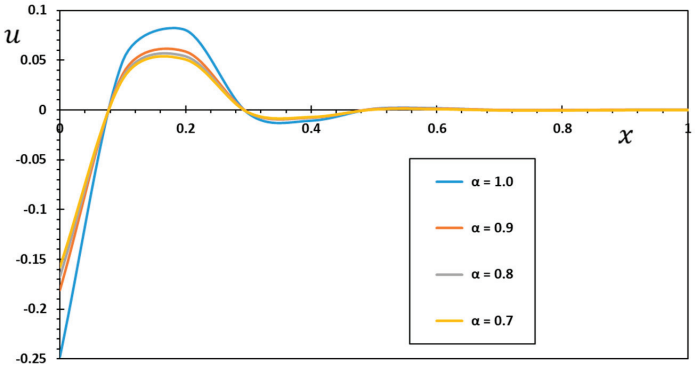

Figure 4. Effect of fractional order, α, on the displacement, u.

For various values of the fractional order parameter, α, the relationship between the thermal deflection, w, and the distance, x, is shown in Figure 2. Figure 2 shows that the boundary requirements of the problem (48) are always satisfied by the zero values of the dispersed deflection, w, at the endpoints of the nanobeam. The nanobeam's highest deflection occurs towards the first edge of the nanobeam due to the heat flow to which it is exposed, as opposed to other areas on the axial axis.

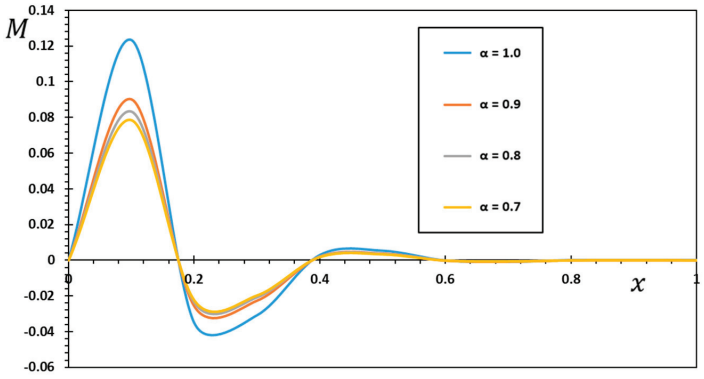

Figure 5. Effect of fractional order, α, on the bending moment, M.

In Figure 3, we see how the fractional-order, α, choices affect the temperature fluctuation, θ, with distance, x, when subjected to an irregular thermal flow. Figure 3 demonstrates that as x increases, the temperature, θ, drops. Additionally, it is apparent from the nanobeam's heat diffusion distribution curves that the most significant values of thermal diffusion are acquired near the beginning of the beam. The heat wave then weakens in its ability to reach the other side as x is increased, and eventually, after a certain threshold has been passed, it vanishes altogether. In contrast to predictions based on traditional heat transfer models, the speed with which heat waves travel through the material is limited.

In comparison with the work of previous authors [67,68], these results are found to be compatible, and the conclusions are valid. In addition, this paper claims that theoretical models utilizing the Atangana–Baleanu fractional operator are superior at elucidating the true features of observed occurrences. To better explain complex situations in the real world, Atangana and Baleanu introduced the derivative using the Mittag–Leffler function. Thus, this new model of thermal conduction will definitely lead to understanding the new behavior of heat flow in nanobeams.

Figure 4 depicts the effect of the fractional-order parameter, α, on a heterogeneous nanobeam to produce a range of displacement values, u, as a function of distance, x. We can see from the figure that the distortion, u, anisotropy increases as we move right on the beam axis. The magnitude of the displacement, u, gradually changes from positive to negative x values. As the value of the fractional order parameter increases, the figure displays a more significant displacement away from the plane $x = 0$. This is because the heat source experiences periodic and transient fluctuations. The axial displacement, u, of the nanobeam is reduced as the fractional parameters increase. Hence, it can be considered that the fractional derivative's order affects the dynamics of thermal deformation in nanobeams at least in this present problem. By applying fractional-order derivatives in modeling techniques, a dynamic system aids in describing memory's characteristics and efficacy (effectiveness, utility) as crucial elements in many nanostructured systems.

In Figure 5, we see how the fractional parameter affects the relationship between the thermal bending moment, M, and the distance, x. This image shows how the modulus can affect the bending moment of the nanobeam, M. It has also been shown that the peak bending moment grows under all conditions as the fractional parameter grows. The bending moments, M, calculated using the fractional derivative are offered as more minor in Figure 5 compared to those computed using the thermoelastic model with integer derivatives. The outcome of this investigation has shown that as the fractional order falls, the bending moment reduces. The fractional operator with the bending property developed by Atangana and Băleanu is responsible for this significant result.

The figures demonstrate how the rate at which waves travel can be affected by varying the value of the fractional-order parameter, α. Therefore, it could be crucial to think about

it while creating new materials for practical applications. In other words, when the values of the fractional order rise, it is possible to see the reduction of all curves in the different physical fields. This figure illustrates that when the current results are compared to those of [32], there is good agreement between the two data sets. As for the fractional case, it is noted that the different distributions in the case of using the fractional derivatives of AB are affected by the past more than the traditional derivative.

More practical recommendations are included in the current publication. It generally provides robust answers that converge rapidly on issues with an actual physical world component. The results can be helpful in cases where a perfect solution is not required and unnecessary complications must be avoided. However, it must be admitted that additional research on the topic may reveal hitherto unexplored possibilities, allowing for the development of more nuanced conclusions and extremely fruitful outcomes. As well as providing closed-form solutions to the specified issues, the detailed analysis has demonstrated the convergence of approximation results to precise answers. The convergence phenomena have proven that the suggested method is reliable. As a result, the fractional derivative of the Atangana–Baleanu in the Caputo concept can be used to describe fractional heat transfer equations.

8.3. The Effect of Nonlocal Parameter

Nonlocal elasticity concepts have received much interest from researchers interested in designing or analyzing micro- or nanostructures. The models serve as models with bridging scales in the investigation of issues involving several scales because they extend the fundamental ideas in the classical theory of elasticity to approximate the behavior of particles as tiny as molecules or atoms. It is clear from the governing equations that these theories portray that they include one or more parameters in addition to the conventional constants. Because of these characteristics, also known as small-scale parameters, it is possible to investigate the size impact.

In contrast to earlier studies, the current study focuses on the extent to which nonlocal parameters affect the dynamic response of a functionally graded nanostructure in the context of physical and geometrical characteristics coupled with thermoelasticity theory involving differential operators of fractional orders. The nanostructure's length is also considered because nonlocal events significantly affect how the nanostructure responds to vibrations. This study shows the variations in outcomes depending on conventional and non-conventional assumptions, in line with its intended purpose.

In this category, through Figures 6–9, we have investigated how small-scale ξ characteristics affect the fluctuations of several field variables (w, θ, u, and M). The remaining effective parameters ($\Omega = 3$, $\tau_0 = 0.02$, and $\alpha = 0.8$) are assumed to remain unchanged in this case. When the value $\xi = 0$ was present, the prior scenario (conventional beam theory) was suggested, but when $\xi = 0.001$, $\xi = 0.003$, and $\xi = 0.005$ were present, the nonlocal elasticity theory (Eringen's theory) was indicated. We show that the thermal deflection, temperature increment, bending moment, and axial displacement are very sensitive to the nonlocal parameter. The nonlocal parameter enhances the mechanical waves in all the fields examined. It can be explored that the influence of the nonlocal parameter on the axial changes of the nanobeam in different modes is prominent and, therefore, more significant. As shown in Figures 6–9, as the value of the nonlocal parameter ξ at given x increases, the temperature curves decrease, and the amount of other physical fields increases. A softening impact was seen as the nonlocal parameter was increased. After the non-locality impact was introduced, the values of the major field variables under study decreased for both the mechanical and thermal systems.

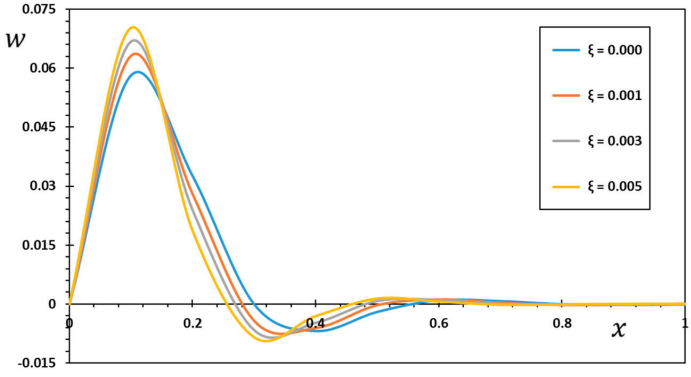

Figure 6. The thermal deflection, w, under various nonlocal parameter ξ values.

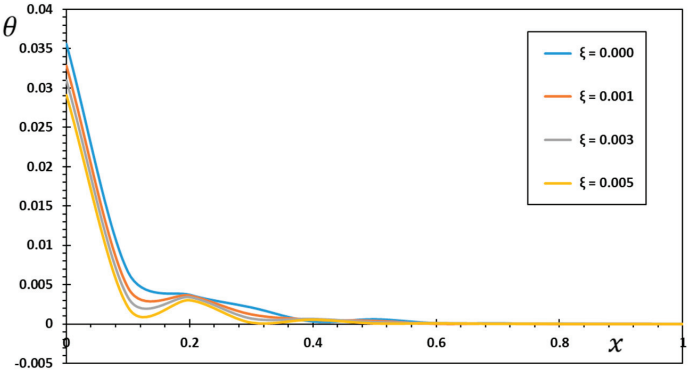

Figure 7. The dimensionless temperature, θ, under various nonlocal parameter ξ values.

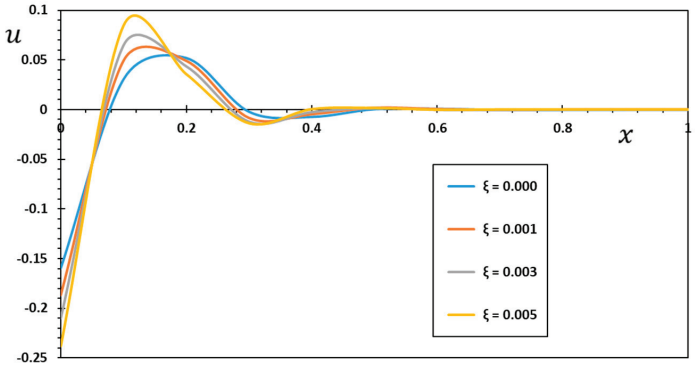

Figure 8. The axial displacement, u, under various nonlocal parameter ξ values.

In addition, it is clear from Figure 8 that throughout the axial direction of the beam, the axial displacement, u, increases with the nonlocal parameter at specific periods and decreases with it at others. Figure 6 shows that at $\xi = 0.005$, the size of the deflection, w, is at its maximum. In Figure 9, it can be seen that the bending moment, M, profile grows in size when the nonlocal parameter values are raised. In addition, the displacement amount in the case of the local heat transfer model is less than the equivalent displacement curve for the nonlocal version (see Figure 8). As a result, to obtain trustworthy results, the nonlocal

component of the motion equation must be taken into account, as it can change the results significantly. For this reason, future studies examining the mechanical behavior of micro- and nanostructures composed of FG materials may use the results of the proposed nonlocal theory as a valuable size-dependent framework. When the length-scale characteristics are considered, the curves demonstrate that we have a Stiffer nanosystem. So, considering nonclassical models will increase the system deflection and dynamic deformation. In addition, there are larger discrepancies between the nonlocal thermoelastic concept and traditional elasticity theory.

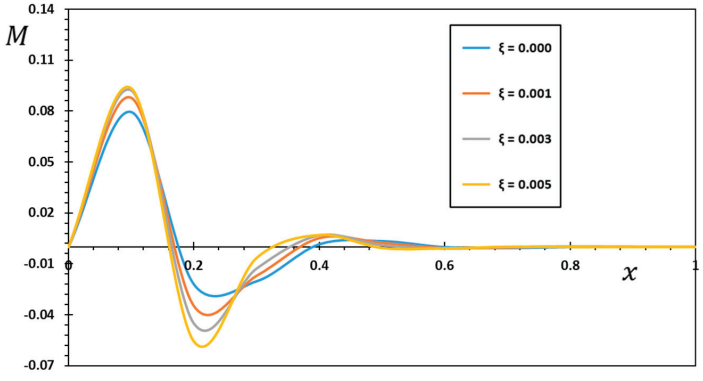

Figure 9. The bending moment, M, under various nonlocal parameter ξ values.

Researchers can use the results of this study to learn more about the instability of nanobeam-based tiny devices and make adjustments to their designs to boost their overall performance. As an added extra, this study's results provide a rationale for why nonclassical frameworks, small-scale influences, and external dynamic and thermal force improvements to theoretical and experimental data provide different results when analyzing the reactions of the nano-system. Small-scale parameters are shown to be sensitive to the structure's geometry, the qualities of the material it is made of, and the loads placed on it by means of the nonlocal interaction range factor. For this reason, ultra-small electronics based on nanostructures can only be modeled using nonlocal models.

8.4. The Effect of the Gradient Index

This subsection investigates the thermoelastic interaction of a functionally graded (FG) nanobeam using the nonlocal Euler–Bernoulli beam theory and the MGT heat transfer model. It is assumed that the FG nanobeam has material properties that change throughout its thickness. The length scale parameter (nonlocal parameter) is incorporated into this nonclassical (nonlocal) nanobeam framework to account for the small-scale effect.

It is investigated in Figures 10–13 how the variability of the physically analyzed fields of the FG nanobeam is affected by the impact of the graded parameter n_p. Here, it is assumed that other parameters that often play a role remain unchanged ($\alpha = 0.8$, $\tau_0 = 0.02$ and $\xi = 0.003$).

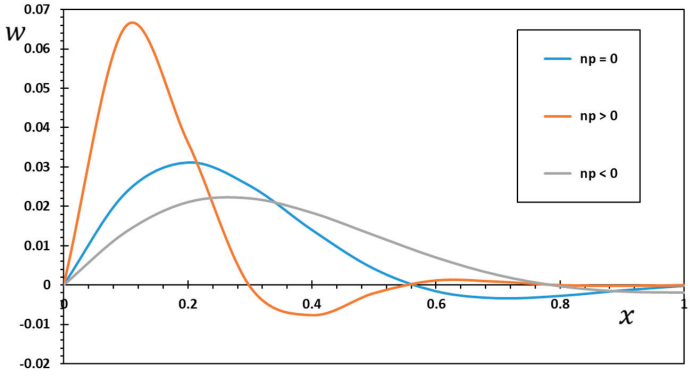

Figure 10. Effect of the gradient indicator on the dimensionless deflection, w.

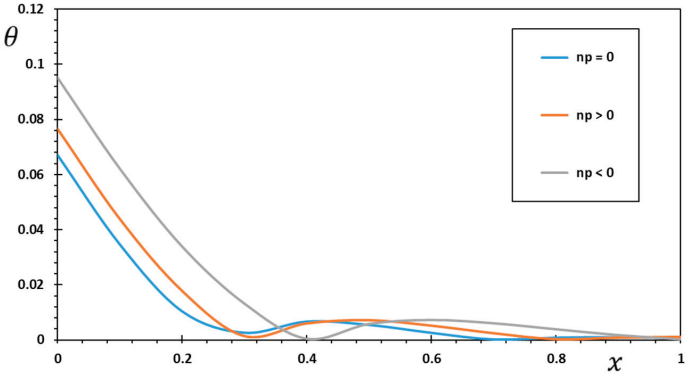

Figure 11. Effect of the gradient indicator on the dimensionless temperature, θ.

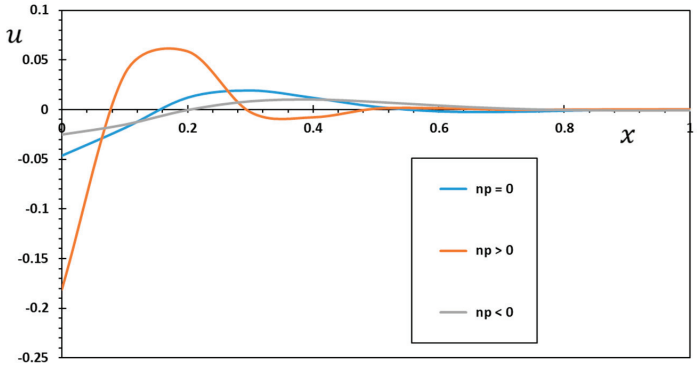

Figure 12. Effect of the gradient indicator on the dimensionless displacement, u.

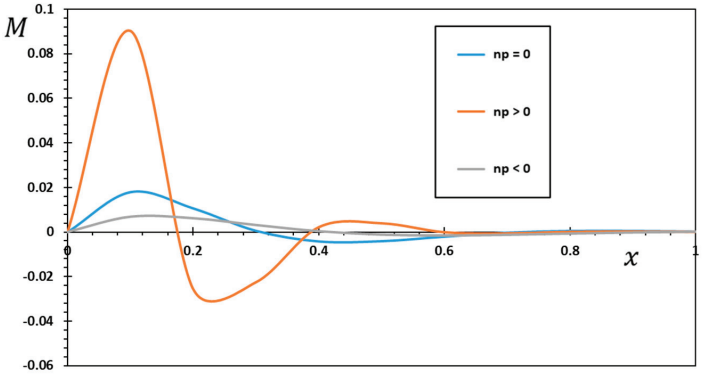

Figure 13. Effect of the gradient indicator on the dimensionless bending moment, M.

For three separate values of the graded parameter n_p, two values for the effective varying material properties ($n_p > 0$ and $n_p < 0$), and zero value $n_p = 0$ for isotropic materials, the studied physical variables were calculated and investigated. The amplitudes of the nondimensional field variables examined are also shown to grow when the graded index $n_p > 0$ (see Figures 10–13). Once n_p is specified, the nondimensional variables have their minimum values at $n_p = 0$.

Increasing the gradient coefficient leads to an increase in the nondimensional deflections and a decrease in the dimensionless temperature. This is because the stiffness of the FG nanobeam increases as the gradient coefficient increases. When the gradient indicator is changed, there is a sudden shift in the responses, but once $n_p = 0$ is reached, all the curves flatten out. In fact, FGMs are favored over conventional laminates because they offer uniformly smooth property variations throughout the whole surface, something that was not possible before when taking the interface between laminate plies into account [69]. In addition, while the individual plies of a composite laminate often behave in an anisotropic way, FGMs behave the same everywhere, even though they are made of different materials. The authors feel that the analyzed results will serve as a reference for other investigators to compare their findings because they are unaware of any previous work on the thermoelastic interactions in FG nanobeams.

9. Conclusions

This paper thoroughly studies a mathematical fractional thermoelastic framework for a functionally graded Euler–Bernoulli nanobeam subjected to a periodic heat flow. Variations in through-thickness features range from purely ceramic to purely metallic. The model employs both nonlocal elasticity theory and generalized MGT thermoelasticity with fractional derivative operators. The Atangana–Baleanu (AB) fractional derivative operator without singular kernels is a novel definition introduced by the revised heat conduction equation. Both analytical and numerical studies show that the nonhomogeneity parameter (gradient indicator), the nonlocal parameter, and the fractional differential operators significantly impact field variables. According to the results of the previous research:

- Thermomechanical responses of the FG nanobeam are shown to be significantly impacted by nonlocal effects, as demonstrated by numerical data.
- Magnitudes are bigger in the novel nonlocal beam model compared to the traditional (local) beam model. Therefore, the small-scale effects (also called nonlocal effects) must be considered when figuring out how nanostructures behave mechanically.
- The success of nonlocal beam models depends heavily on carefully selecting the nonlocal parameter's value.
- The FG nanobeam's responses can be adjusted by selecting appropriate values for the gradient indicator, which significantly impacts the responses.

- There were significant discrepancies between the variances of the thermoelastic models and the fractional thermoelastic models. Changes in the rate of change of the temperature variation depend strongly on the value of the fractional parameter of the Atangana–Baleanu fractional derivative operator. Therefore, the fractional parameter is becoming more effective as a measure of heat conduction.
- With fractional derivatives, the values of the fields under study are less than those predicted by standard thermoelastic models. Therefore, the fractional parameter should be chosen to reduce the medium's effect on the elastic wave.
- Composite materials with FGM characteristics are superior to traditional homogenous materials in various contexts. The biomedical and defense industries also extensively use FGMs, most notably as medical implants and bulletproof vests. The automotive sector, the steel sector, the energy sector, etc., are just a few more areas where FGM has been found useful.
- With this new perspective on investigating thermal deformations in solid mechanics, we can understand the Atangana–Baleanu fractional derivative operator in heat and mass transfer systems. Application of the method and concepts given herein to other thermoelasticity and thermodynamic problems is possible.

Author Contributions: Conceptualization, D.A.; Methodology, D.A.; Software, A.E.A. and F.A.; Validation, F.A.; Formal analysis, F.A.; Investigation, A.E.A.; Resources, D.A. and F.A.; Data curation, A.E.A.; Writing—original draft, A.E.A. and F.A.; Writing—review & editing, A.E.A.; Visualization, F.A.; Funding acquisition, F.A. All authors have read and agreed to the published version of the manuscript.

Funding: This research was funded by Qassim University grant number [QU-IF-4-5-1-29618].

Data Availability Statement: The numerical data used to support the findings of this study are included in the article.

Acknowledgments: The authors extend their appreciation to the Deputyship for Research and Innovation, Ministry of Education, Saudi Arabia, for funding this research work through project number (QU-IF-4-5-1-29618). The authors also thank Qassim University for technical support.

Conflicts of Interest: The authors declared no potential conflict of interest concerning the research, authorship, and publication of this article.

References

1. Faghidian, S.A.; Żur, K.K.; Reddy, J.N.; Ferreira, A.J.M. On the wave dispersion in functionally graded porous Timoshenko-Ehrenfest nanobeams based on the higher-order nonlocal gradient elasticity. *Compos. Struct.* **2022**, *279*, 114819. [CrossRef]
2. Pham, Q.-H.; Tran, V.K.; Tran, T.T.; Nguyen, P.-C.; Malekzadeh, P. Dynamic instability of magnetically embedded functionally graded porous nanobeams using the strain gradient theory. *Alex. Engin. J.* **2022**, *61*, 10025–10044. [CrossRef]
3. Akgöz, B.; Civalek, Ö. Thermo-mechanical buckling behavior of functionally graded microbeams embedded in elastic medium. *Int. J. Eng. Sci.* **2014**, *85*, 90–104. [CrossRef]
4. Ghayesh, M.H.; Farokhi, H.; Amabili, M. Nonlinear behaviour of electrically actuated MEMS resonators. *Int. J. Eng. Sci.* **2013**, *71*, 137–155. [CrossRef]
5. Amiri Delouei, A.; Emamian, A.; Karimnejad, S.; Sajjadi, H. A closed-form solution for axisymmetric conduction in a finite functionally graded cylinder. *Int. Communic. Heat Mass Trans.* **2019**, *108*, 104280. [CrossRef]
6. Amiri Delouei, A.; Emamian, A.; Karimnejad, S.; Sajjadi, H.; Jing, D. Two-dimensional analytical solution for temperature distribution in FG hollow spheres: General thermal boundary conditions. *Int. Communic. Heat Mass Trans.* **2020**, *113*, 104531. [CrossRef]
7. Avey, M.; Fantuzzi, N.; Sofiyev, A. Mathematical modeling and analytical solution of thermoelastic stability problem of functionally graded nanocomposite cylinders within different theories. *Mathematics* **2022**, *10*, 1081. [CrossRef]
8. Kaur, I.; Singh, K.; Ghita, G.M.D.; Craciun, E.-M. Modeling of a magneto-electro-piezo-thermoelastic nanobeam with two temperature subjected to ramp type heating. *Proc. Rom. Acad. Ser. A* **2022**, *23*, 141–149.
9. Pinnola, F.P.; Barretta, R.; Marotti de Sciarra, F.; Pirrotta, A. Analytical solutions of viscoelastic nonlocal Timoshenko beams. *Mathematics* **2022**, *10*, 477. [CrossRef]
10. Wang, S.; Kang, W.; Yang, W.; Zhang, Z.; Li, Q.; Liu, M.; Wang, X. Hygrothermal effects on buckling behaviors of porous bi-directional functionally graded micro-/nanobeams using two-phase local/nonlocal strain gradient theory. *Eur. J. Mech.-A/Solids* **2022**, *94*, 104554. [CrossRef]

11. Civalek, Ö.; Uzun, B.; Yayl, M.Ö.; Akgöz, B. Size-dependent transverse and longitudinal vibrations of embedded carbon and silica carbide nanotubes by nonlocal finite element method. *Eur. Phys. J. Plus* **2020**, *135*, 381. [CrossRef]
12. Dangi, C.; Lal, R.; Sukavanam, N. Effect of surface stresses on the dynamic behavior of bi-directional functionally graded nonlocal strain gradient nanobeams via generalized differential quadrature rule. *Eur. J. Mech.-A/Solids* **2021**, *90*, 104376. [CrossRef]
13. Eringen, A.C. On differential equations of nonlocal elasticity and solutions of screw dislocation and surface waves. *J. Appl. Phys.* **1983**, *54*, 4703–4710. [CrossRef]
14. Eringen, A.C.; Edelen, D.G.B. On nonlocal elasticity. *Int. J. Eng. Sci.* **1972**, *10*, 233–248. [CrossRef]
15. Eringen, A.C. Linear theory of nonlocal elasticity and dispersion of plane waves. *Int. J. Eng. Sci.* **1972**, *10*, 425–435. [CrossRef]
16. Mindlin, R.D.; Eshel, N.N. On first strain-gradient theories in linear elasticity. *Int. J. Solids Struct.* **1968**, *4*, 109–124. [CrossRef]
17. Askes, H.; Aifantis, E.C. Gradient elasticity in statics and dynamics: An overview of formulations, length scale identification procedures, finite element implementations and new results. *Int. J. Solids Struct.* **2011**, *48*, 1962–1990. [CrossRef]
18. Lam, D.C.C.; Yang, F.; Chong, A.C.M.; Wang, J.; Tonga, P. Experiments and theory in strain gradient elasticity. *J. Mech. Phys. Solids* **2003**, *51*, 1477–1508. [CrossRef]
19. Grekova, E.F.; Porubov, A.V.; dell'Isola, F. Reduced linear constrained elastic and viscoelastic homogeneous Cosserat media as acoustic metamaterials. *Symmetry* **2020**, *12*, 521. [CrossRef]
20. Toupin, R.A. Elastic materials with couple-stresses. *Arch. Ration Mech. Anal.* **1962**, *11*, 385–414. [CrossRef]
21. Toupin, R.A. Theories of elasticity with couple-stress. *Arch. Ration Mech. Anal.* **1964**, *17*, 85–112. [CrossRef]
22. Atangana, A.; Secer, A. A note on fractional order derivatives and table of fractional derivatives of some special functions. *Abst. Appl. Analy.* **2013**, *2013*, 279681. [CrossRef]
23. Patnaik, S.; Hollkamp, J.P.; Semperlotti, F. Applications of variable-order fractional operators: A review. *Proc. R. Soc. A Math. Phys. Eng. Sci.* **2020**, *476*, 20190498. [CrossRef] [PubMed]
24. Caputo, M.; Fabrizio, M. A new definition of fractional derivative without singular kernel. *Prog. Fract. Differ. Appl.* **2015**, *1*, 73–85.
25. Atangana, A.; Baleanu, D. New fractional derivative with nonlocal and nonsingular kernel. *Therm. Sci.* **2016**, *20*, 757. [CrossRef]
26. Atangana, A.; Baleanu, D. New fractional derivatives with nonlocal and non-singular kernel: Theory and application to heat transfer model. *Therm. Sci.* **2016**, *20*, 763–769. [CrossRef]
27. Saad, K.M. New fractional derivative with non-singular kernel for deriving Legendre spectral collocation method, Alex. *Eng. J.* **2020**, *59*, 1909–1917.
28. Dokuyucu, M.A.; Dutta, H.; Yildirim, C. Application of nonlocal and non-singular kernel to an epidemiological model with fractional order. *Math. Methods Appl. Sci.* **2021**, *44*, 3468–3484. [CrossRef]
29. Sabatier, J. Non-Singular kernels for modelling power law type long memory behaviours and beyond. *Cybern. Sys.* **2020**, *51*, 383–401. [CrossRef]
30. Aljahdaly, N.H.; Agarwal, R.P.; Shah, R.; Botmart, T. Analysis of the time fractional-order coupled burgers equations with non-singular kernel operators. *Mathematics* **2021**, *9*, 2326. [CrossRef]
31. Anastassiou, G.A. Multiparameter fractional differentiation with non singular kernel. *Probl. Anal.-Iss. Analy.* **2021**, *10*, 15–30. [CrossRef]
32. Heydari, M.H.; Hosseininia, M. A new variable-order fractional derivative with non-singular Mittag–Leffler kernel: Application to variable-order fractional version of the 2D Richard equation. *Engin. Comput.* **2022**, *38*, 1759. [CrossRef]
33. Jena, R.M.; Chakraverty, S. Singular and Nonsingular Kernels Aspect of Time-Fractional Coupled Spring-Mass System. *ASME J. Comput. Nonlinear Dynam.* **2022**, *17*, 021001. [CrossRef]
34. Atangana, A.; Akgül, A.; Owolabi, K.M. Analysis of fractal fractional differential equations. *Alex. Eng. J.* **2020**, *59*, 1117–1134. [CrossRef]
35. Atangana, A.; Qureshi, S. Modeling attractors of chaotic dynamical systems with fractal-fractional operators. *Chaos Solitons Fractals* **2019**, *123*, 320–337. [CrossRef]
36. Saad, K.M.; Gómez-Aguilar, J.F. Analysis of reaction–diffusion system via a new fractional derivative with non-singular kernel. *Phys. A Stat. Mech. Its Appl.* **2018**, *509*, 703–716. [CrossRef]
37. Fernandez, A.; Baleanu, D. Classes of operators in fractional calculus: A case study. *Math. Methods Appl. Sci.* **2021**, *44*, 9143–9162. [CrossRef]
38. Lord, H.W.; Shulman, Y. A generalized dynamical theory of thermoelasticity. *J. Mech. Phys. Solids* **1967**, *15*, 299–309. [CrossRef]
39. Green, A.E.; Naghdi, P.M. Thermoelasticity without energy dissipation. *J. Elast.* **1993**, *31*, 189–208. [CrossRef]
40. Green, A.E.; Naghdi, P.M. On undamped heat waves in an elastic solid. *J. Therm. Stress.* **1992**, *15*, 253–264. [CrossRef]
41. Green, A.E.; Naghdi, P.M. A re-examination of the basic postulates of thermomechanics. *Proc. R. Soc. Lond. A.* **1991**, *432*, 171–194.
42. Quintanilla, R. Moore–Gibson–Thompson thermoelasticity. *Math. Mech. Solids* **2019**, *24*, 4020–4031. [CrossRef]
43. Quintanilla, R. Moore-Gibson-Thompson thermoelasticity with two temperatures. *Appl. Eng. Sci.* **2020**, *1*, 100006. [CrossRef]
44. Moaaz, O.; Abouelregal, A.E.; Alsharari, F. Analysis of a transversely isotropic annular circular cylinder immersed in a magnetic field using the Moore–Gibson–Thompson thermoelastic model and generalized Ohm's law. *Mathematics* **2022**, *10*, 3816. [CrossRef]
45. Abouelregal, A.E.; Dassios, I.; Moaaz, O. Moore–Gibson–Thompson Thermoelastic Model Effect of Laser-Induced Microstructures of a Microbeam Sitting on Visco-Pasternak Foundations. *Appl. Sci.* **2022**, *12*, 9206. [CrossRef]

46. Abouelregal, A.E.; Mohammed, F.A.; Benhamed, M.; Zakria, A.; Ahmed, I.-E. Vibrations of axially excited rotating micro-beams heated by a high-intensity laser in light of a thermo-elastic model including the memory-dependent derivative. *Math. Comp. Simul.* **2022**, *199*, 81–99. [CrossRef]
47. Moaaz, O.; Abouelregal, A.E.; Alesemi, M. Moore–Gibson–Thompson Photothermal Model with a Proportional Caputo Fractional Derivative for a Rotating Magneto-Thermoelastic Semiconducting Material. *Mathematics* **2022**, *10*, 3087. [CrossRef]
48. Abouelregal, A.E. Generalized thermoelastic MGT model for a functionally graded heterogeneous unbounded medium containing a spherical hole. *Eur. Phys. J. Plus* **2022**, *137*, 953. [CrossRef]
49. Abouelregal, A.E.; Mohammad-Sedighi, H.; Shirazi, A.H.; Malikan, M.; Eremeyev, V.A. Computational analysis of an infinite magneto-thermoelastic solid periodically dispersed with varying heat flow based on nonlocal Moore–Gibson–Thompson approach. *Contin. Mech. Thermodyn.* **2022**, *34*, 1067–1085. [CrossRef]
50. Abouelregal, A.E.; Moustapha, M.V.; Nofal, T.A.; Rashid, S.; Ahmad, H. Generalized thermoelasticity based on higher-order memory-dependent derivative with time delay. *Results Phys.* **2021**, *20*, 103705. [CrossRef]
51. Eringen, A.C.; Wegner, J. Nonlocal Continuum Field Theories. *ASME Appl. Mech. Rev. March.* **2003**, *56*, B20–B22. [CrossRef]
52. Miller, K.S.; Ross, B. *An introduction to the Fractional Integrals and Derivatives, Theory and Applications*; John Wiley and Sons Inc.: New York, NY, USA, 1993.
53. Atangana, A.; Baleanu, D. Caputo-Fabrizio derivative applied to groundwater flow within confined aquifer. *J. Eng. Mech.* **2017**, *143*, D4016005. [CrossRef]
54. Zhang, N.; Khan, T.; Guo, H.; Shi, S.; Zhong, W.; Zhang, W. Functionally graded materials: An overview of stability, buckling, and free vibration analysis. *Advan. Mater. Sci. Eng.* **2019**, *2019*, 1354150. [CrossRef]
55. Gupta, A.; Talha, M. Recent development in modeling and analysis of functionally graded materials and structures. *Prog. Aero. Sci.* **2015**, *79*, 1–14. [CrossRef]
56. Abouelregal, A.E.; Mohammed, W.W.; Mohammad-Sedighi, H. Vibration analysis of functionally graded microbeam under initial stress via a generalized thermoelastic model with dual-phase lags. *Arch. Appl. Mech.* **2021**, *91*, 2127–2142. [CrossRef]
57. Abouelregal, A.E.; Ahmad, H.; Yao, S.-W. Functionally graded piezoelectric medium exposed to a movable heat flow based on a heat equation with a memory-dependent derivative. *Materials* **2020**, *13*, 3953. [CrossRef] [PubMed]
58. Oden, J.T.; Ripperger, E.A. *Mechanics of Elastic Structures*; Hemisphere/McGraw-Hill: New York, NY, USA, 1981.
59. Peng, W.; Chen, L.; He, T. Nonlocal thermoelastic analysis of a functionally graded material microbeam. *Appl. Math. Mech.-Engl. Ed.* **2021**, *42*, 855. [CrossRef]
60. Honig, G.; Hirdes, U. A method for the numerical inversion of the Laplace transform. *J. Comp. Appl. Math.* **1984**, *10*, 113–132. [CrossRef]
61. Abbas, I.; Hobiny, A.; Alshehri, H.; Vlase, S.; Marin, M. Analysis of Thermoelastic Interaction in a Polymeric Orthotropic Medium Using the Finite Element Method. *Polymers* **2022**, *14*, 2112. [CrossRef]
62. Abbas, I.; Marin, M.; Hobiny, A.; Vlase, S. Thermal Conductivity Study of an Orthotropic Medium Containing a Cylindrical Cavity. *Symmetry* **2022**, *14*, 2387. [CrossRef]
63. Hobiny, A.; Abbas, I. Generalized Thermo-Diffusion Interaction in an Elastic Medium under Temperature Dependent Diffusivity and Thermal Conductivity. *Mathematics* **2022**, *10*, 2773. [CrossRef]
64. Abouelregal, A.E.; Marin, M. The size-dependent thermoelastic vibrations of nanobeams subjected to harmonic excitation and rectified sine wave heating. *Mathematics* **2020**, *8*, 1128. [CrossRef]
65. Abouelregal, A.E.; Marin, M. The response of nanobeams with temperature-dependent properties using state-space method via modified couple stress theory. *Symmetry* **2020**, *12*, 1276. [CrossRef]
66. Kaur, I.; Singh, K. Functionally graded nonlocal thermoelastic nanobeam with memory-dependent derivatives. *SN Appl. Sci.* **2022**, *4*, 329. [CrossRef]
67. Sene, N. Fractional diffusion equation described by the Atangana-Baleanu fractional derivative and its approximate solution. *J. Frac. Calc. Nonlinear Sys.* **2021**, *2*, 60–75. [CrossRef]
68. Mittal, G.; Kulkarni, V.S. Two temperature fractional order thermoelasticity theory in a spherical domain. *J. Therm. Stress.* **2019**, *42*, 1136–1152. [CrossRef]
69. Abouelregal, A.E. Mathematical modeling of functionally graded nanobeams via fractional heat Conduction model with non-singular kernels. *Arch. Appl. Mech.* **2022**. [CrossRef]

axioms

MDPI

Article

A Fractional-Order Improved Quantum Logistic Map: Chaos, 0-1 Testing, Complexity, and Control

Birong Xu [1,*], Ximei Ye [1], Guangyi Wang [2], Zhongxian Huang [3] and Changwu Zhang [1]

[1] College of Mechanic and Electronic Engineering, Wuyi University, Wuyishan 354300, China
[2] Institute of Modern Circuits and Intelligent Information, Hangzhou Dianzi University, Hangzhou 310018, China
[3] College of Mathematics and Computer Science, Wuyi University, Wuyishan 354300, China
* Correspondence: xubirong@wuyiu.edu.cn

Abstract: Based on a quantum logistic map and a Caputo-like delta difference operator, a fractional-order improved quantum logistic map, which has hidden attractors, was constructed. Its dynamical behaviors are investigated by employing phase portraits, bifurcation diagrams, Lyapunov spectra, dynamical mapping, and 0-1 testing. It is shown that the proposed fractional-order map is influenced by both the parameters and the fractional order. Then, the complexity of the map is explored through spectral entropy and approximate entropy. The results show that the fractional-order improved quantum logistic map has stronger robustness within chaos and higher complexity, so it is more suitable for engineering applications. In addition, the fractional-order chaotic map can be controlled for different periodic orbits by the improved nonlinear mapping on the wavelet function.

Keywords: improved quantum logistic map; discrete fractional calculus; hidden attractor; chaos control

MSC: 26A33; 34H10; 39A33

Citation: Xu, B.; Ye, X.; Wang, G.; Huang, Z.; Zhang, C. A Fractional-Order Improved Quantum Logistic Map: Chaos, 0-1 Testing, Complexity, and Control. *Axioms* **2023**, *12*, 94. https://doi.org/10.3390/axioms12010094

Academic Editors: António Lopes, Alireza Alfi, Liping Chen and Sergio Adriani David

Received: 4 December 2022
Revised: 7 January 2023
Accepted: 10 January 2023
Published: 16 January 2023

1. Introduction

Since May presented the logistic map in 1976, and as a well-known chaotic map, the logistic map and its generalizations have gained more and more attention in academic circles, especially regarding chaos and fractals [1–3]. A quantum logistic map that is associated with the logistic map is proposed in [4]. As a three-dimensional map, it was found that the quantum logistic map owns richer dynamical behaviors, and thus it has greater potential application in the field of information security. However, when compared to the logistic map, there has been relatively less research into quantum logistic maps. The generalization of quantum logistic maps has never been analyzed, so we have investigated it.

In recent years, the theory of the fractional differential equation has become a new research focus. The author of [5] introduced fractional LTI systems, and [6] investigated the existence of a mild-solution Hilfer fractional-neutral-integro-differential inclusion with almost sectorial operators. The authors of [7] studied the existence, uniqueness, Hyer–Ulam stability, and controllability of a fractional dynamic system using time scales, and [8] analyzed the existence, uniqueness, and stability of a nonlinear fractional differential equation with impulsive conditions on time scales. The dynamics of a fractional–order model with different strains of COVID-19 were explored in [9]. The new field of fractional differential equations emerged via the discretized definitions of continuous fractional derivatives and integrals [10–13]. With the rapid development of the fractional difference equations theory, the definition of fractional-order difference was introduced into discrete chaotic maps based on the Caputo operator, and the fractional standard map and the fractional logistic map were proposed [14,15]. Since then, researchers have diverted their interest to fractional-order chaotic maps. The authors of [16–18] presented fractional-order logistic maps and fractional-order delayed logistic maps and analyzed their nonlinear

behaviors by using phase portraits, bifurcation diagrams, and Lyapunov exponents. The authors of [19] designed an efficient image encryption scheme based on the fractional-order logistic map, while those of [20] put forward a fractional-order Hénon-Lozi map and then studied its dynamical properties. A two-dimensional fractional-order map was designed and applied to image encryption [21]. A fractional-order higher-dimensional multicavity chaotic map was studied in [22]. Fractional-order chaotic maps are sensitive to their fractional order apart from their initial values and parameters, thereby having richer nonlinear behaviors than the integer-order versions. Hence, a generalized quantum logistic map with fractional order is presented in the paper.

On the other hand, the chaotic system with hidden attractors is a new research hotspot. Some chaotic systems with hidden attractors were presented in the literature [23–25]. If a chaotic system possesses no equilibrium or stable equilibrium, i.e., its attraction basin does not connect with the neighborhood of the equilibrium, the chaotic system is regarded as a chaotic system with hidden attractors [26,27]. The hidden attractor is considerably important in science and engineering due to the occurrence of unexpected behaviors. The term "hidden attractors" originates from the research of continuous chaotic systems [28,29]. When compared with continuous chaotic systems, the investigation of chaotic maps with hidden attractors has seen a lack of investigation, especially for fractional-order maps with hidden attractors; they are rarely introduced in the literature. However, the fractional-order map owns more complex dynamical behaviors than the integer counterpart. In order to enrich the theory of hidden attractors, we propose a fractional-order improved quantum logistic map without equilibrium, i.e., a fractional-order map with hidden attractors. For future applications, its behaviors are explored by nonlinear tools, such as bifurcation diagrams and Lyapunov exponents. Moreover, the chaos control of this fractional-order map is also studied.

The remainder of this paper is outlined as follows. Section 2 gives a fractional-order improved quantum logistic map. Section 3 shows the dynamical analysis of the fractional-order map by exploiting bifurcation analysis, Lyapunov exponent spectrums, dynamical maps, and 0-1 tests. Section 4 focuses on the complexity of this map. Section 5 investigates the chaos control of the system. We draw conclusions in Section 6.

2. A Fractional-Order Improved Quantum Logistic Map

A quantum logistic map is a logistic map with quantum corrections [4]. In order to investigate the effects of these quantum corrections, researchers set $\hat{a} = \langle \hat{a} \rangle + \delta\hat{a}$, where $\delta\hat{a}$ is a quantum fluctuation about $\langle \hat{a} \rangle$, and $\langle \hat{a} \rangle$ is the mean value of $\hat{a}$. The quantum logistic map is described as

$$\begin{cases} x_n = r(x_{n-1} - |x_{n-1}|^2) - ry_{n-1}, \\ y_n = -y_{n-1}e^{-2\beta} + e^{-\beta}r[(2 - x_{n-1} - x^*_{n-1})y_{n-1} - x_{n-1}z^*_{n-1} - x^*_{n-1}z_{n-1}], \\ z_n = -z_{n-1}e^{-2\beta} + e^{-\beta}r[2(1 - x^*_{n-1})z_{n-1} - 2x_{n-1}y_{n-1} - x_{n-1}], \end{cases} \tag{1}$$

where $x = \langle \hat{a} \rangle$, $y = \langle \delta\hat{a}^+\delta\hat{a} \rangle$, $z = \langle \delta\hat{a}\delta\hat{a} \rangle$, and x^*, z^* are the complex conjugate of x, z, respectively. Besides, β and r denote the dissipation and control parameters, respectively. However, if we let the initial values x_0, y_0, and z_0 be real numbers, the successive values x_n, y_n, and z_n remain real. Therefore, Equation (1) is expressed as

$$\begin{cases} x_n = r(x_{n-1} - |x_{n-1}|^2) - ry_{n-1}, \\ y_n = -y_{n-1}e^{-2\beta} + e^{-\beta}r[(2 - 2x_{n-1})y_{n-1} - 2x_{n-1}z_{n-1}], \\ z_n = -z_{n-1}e^{-2\beta} + e^{-\beta}r[2(1 - x_{n-1})z_{n-1} - 2x_{n-1}y_{n-1} - x_{n-1}], \end{cases} \tag{2}$$

For the quantum logistic map, the map has one fixed-point: (0, 0, 0). In order to design a chaotic system with hidden attractors, Equation (2) is rewritten as

$$\begin{cases} x_n = f(x_{n-1}) - r_1 y_{n-1}, \\ y_n = -y_{n-1}e^{-2\beta} + e^{-\beta} r[(2 - 2x_{n-1})y_{n-1} - 2x_{n-1}z_{n-1}], \\ z_n = -z_{n-1}e^{-2\beta} + e^{-\beta} r[2(1 - x_{n-1})z_{n-1} - 2x_{n-1}y_{n-1} - x_{n-1}], \end{cases} \tag{3}$$

where r_1 is a parameter, and the function $f(x_{n-1})$ is defined as

$$f(x_{n-1}) = \begin{cases} 0.8 + r x_{n-1}(0.2 - x_{n-1}) \\ \quad if\ 0 < x_{n-1} < 0.2, \\ r(x_{n-1} - 0.8)(1 - x_{n-1}) \\ \quad if\ 0.8 < x_{n-1} < 1. \end{cases} \tag{4}$$

For solving the fixed-point of system (3), we have $x_n = x_{n-1}$, $y_n = y_{n-1}$, and $z_n = z_{n-1}$, that is

$$\begin{cases} x_n = f(x_n) - r_1 y_n, \\ y_n = -y_n e^{-2\beta} + e^{-\beta} r[(2 - 2x_n)y_n - 2x_n z_n], \\ z_n = -z_n e^{-2\beta} + e^{-\beta} r[2(1 - x_n)z_n - 2x_n y_n - x_n], \end{cases} \tag{5}$$

where the function $f(x)$ is described as

$$f(x_n) = \begin{cases} 0.8 + r x_n(0.2 - x_n)\ if\ 0 < x_n < 0.2, \\ r(x_n - 0.8)(1 - x_n)\ if\ 0.8 < x_n < 1. \end{cases} \tag{6}$$

The solution of Equation (5) has two cases. When $0 < 0.8 + r x_n(0.2 - x_n) - r_1 y_n < 0.2$ or $0.8 < r(x_n - 0.8)(1 - x_n) - r_1 y_n < 1$, the first equation can be solved, i.e., the fractional-order map has a fixed-point. If not, there is no solution to the first equation. In other words, the improved map is a system without equilibrium. The second case will be considered below.

Regarding the second and third equations as fractional order, we can obtain

$$\begin{cases} x_n = f(x_{n-1}) - r_1 y_{n-1}, \\ {}^{C}\Delta_a^{\nu} y(t) = -y(t + \nu - 1)e^{-2\beta} + e^{-\beta} r[(2 - 2x(t + \nu - 1))y(t + \nu - 1) \\ \qquad -2x(t + \nu - 1)z(t + \nu - 1)] - y(t + \nu - 1), \\ {}^{C}\Delta_a^{\nu} z(t) = -z(t + \nu - 1)e^{-2\beta} + e^{-\beta} r[2(1 - x(t + \nu - 1))z(t + \nu - 1) \\ \qquad -2x(t + \nu - 1)y(t + \nu - 1) - x(t + \nu - 1)] - z(t + \nu - 1), \end{cases} \tag{7}$$

where ${}^{C}\Delta_a^{\nu}$ is the ν-th Caputo-like delta difference operator, ν is the fractional order, and a is the starting point. Set N_a is the isolated time scale, $N_a = \{a, a + 1, a + 2, ...\}$ ($a \in R$ fixed). For $\nu > 0$, $\nu \notin N$, and $u(t)$ define on N_a, the Caputo-like delta difference [30] is defined by

$${}^{C}\Delta_a^{-\nu} u(t) = \Delta_a^{-(m-\nu)} \Delta^m u(t),\ t \in N_{a+m-\nu}, m = \lceil \nu \rceil + 1, \tag{8}$$

where ν is the difference order and $\Delta_a^{-(m-\nu)}$ is the fractional sum of m-ν order. Let u: $N_a \to R$ and $\nu > 0$, the fractional sum of ν order [10] is defined by

$$\Delta_a^{-\nu} u(t) = \frac{1}{\Gamma(\nu)} \sum_{s=a}^{t=\nu} (t - \sigma(s))^{(\nu-1)} u(s),\ t \in N_{a+\nu}, \tag{9}$$

where $\sigma(s) = s + 1$, $\Gamma(\nu)$ is the Gamma function, and $t(\nu)$ is the falling function defined by the Gamma function as

$$t^{(\nu)} = \frac{\Gamma(t + 1)}{\Gamma(t + 1 - \nu)}. \tag{10}$$

Therefore, the Caputo-like delta difference can be expressed as

$$ {}^{C}\Delta_{a}^{-\nu}u(t)=\frac{1}{\Gamma(m-\nu)}\sum_{s=a}^{t-(m-\nu)}(t-\sigma(s))^{(m-\nu-1)}\Delta^{m}u(s),t\in \mathrm{N}_{a+m-\nu},=\lceil\nu\rceil+1. \quad (11)$$

According to the theorem in [31], for the difference equation:

$$ C\Delta_{a}^{\nu}u(t)=f(t+\nu-1,u(t+\nu-1)),\Delta^{k}u(a)=u_{k},m=\lceil\nu\rceil+1,k=0,\ldots,m-1. \quad (12)$$

The equivalent discrete integral equation is described as

$$ u(n)=u_{0}(t)+\frac{1}{\Gamma(\nu)}\sum_{s=a+m-\nu}^{t-\nu}(t-\sigma(s))^{(\nu-1)}\times f(s+\nu-1,u(s+\nu-1)),\ t\in \mathrm{N}_{a+m}, \quad (13)$$

where the initial iteration is

$$ u_{0}(t)=\sum_{k=0}^{m-1}\frac{(t-a)^{(k)}}{k!}\Delta^{k}u(a). \quad (14)$$

By setting $m = 1$, $a = 0$, and substituting $\sigma(s) = s + 1$ into Equation (13), the following can be obtained as

$$ u(n)=u_{0}(t)+\frac{1}{\Gamma(\nu)}\sum_{s=1-\nu}^{t-\nu}(t-s-1)^{(\nu-1)}\times f(s+\nu-1,u(s+\nu-1)) \quad (15)$$

By using Equation (10), and setting $j = s + \nu$, Equation (15) is rewritten as

$$ u(n)=u_{0}(t)+\frac{1}{\Gamma(\nu)}\sum_{j=1}^{n}\frac{\Gamma(n-j+\nu)}{\Gamma(n-j+1)}\times f(j-1,u(j-1)) \quad (16)$$

According to Equation (16), the explicit numerical formula of Equation (7) is expressed as

$$ \begin{cases} x_{n}=f(x_{n-1})-r_{1}y_{n-1}, \\ y_{n}=y_{0}+\frac{1}{\Gamma(\nu)}\sum_{j=1}^{n}\frac{\Gamma(n-j-\nu)}{\Gamma(n-j-1)}\{-y_{j-1}e^{-2\beta}+e^{-\beta}r[(2-2x_{j-1})y_{j-1}-2x_{j-1}z_{j-1}]-y_{j-1}\}, \\ z_{n}=z_{0}+\frac{1}{\Gamma(\nu)}\sum_{j=1}^{n}\frac{\Gamma(n-j-\nu)}{\Gamma(n-j-1)}\{-z_{j-1}e^{-2\beta}+e^{-\beta}r[2(1-x_{j-1})z_{j-1}-2x_{j-1}y_{j-1}-x_{j-1}]-z_{j-1}\}, \end{cases} \quad (17)$$

where the function $f(x_{n-1})$ is the same as Equation (4).

For System (17), set the parameters as $r = 19.8$, $r_1 = 0.05$, $\beta = 4.5$, and $\nu = 0.90$, and the initial conditions as (0.05, 0.02, and 0.05); the chaotic attractors are depicted in Figure 1, which are hidden attractors (see Appendix A for the code of the simulation). In this case, we obtain the largest Lyapunov exponent LLE = 0.5426 via the wolf algorithm.

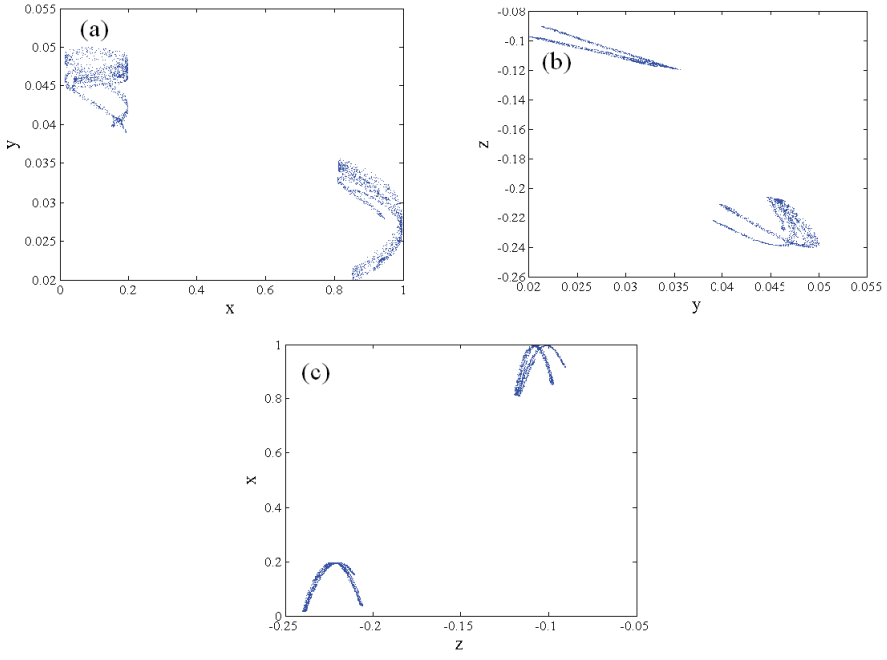

Figure 1. Chaotic attractors of the fractional-order improved quantum logistic map. (**a**) *x*-*y* phase portrait; (**b**) *y*-*z* phase portrait; (**c**) *z*-*x* phase portrait.

3. Dynamical Analysis

3.1. Bifurcation Analysis, Lyapunov Exponent Spectrum, and Dynamical Map

Chaotic maps have sensitivity to the parameters. In order to investigate the sensitivity of the parameters, we fixed the initial conditions as (0.05, 0.02, and 0.05). The bifurcation portrait with respect to the control parameter r and the corresponding largest Lyapunov spectrum is depicted in Figure 2, where the parameter r is in the interval [16,21], and the others are $r_1 = 0.05$, $\beta = 4.5$, and $\nu = 0.9$. It is clear to see that the bifurcation portrait is divided into two parts. With an increase in the parameter r, the system goes through period-2, period-4, a quasi-periodic, and a chaotic state. The system generates periodic windows of different sizes after the system appears in a chaotic state. In the region of $19.2 \leq r \leq 20$, the system keeps a chaotic state.

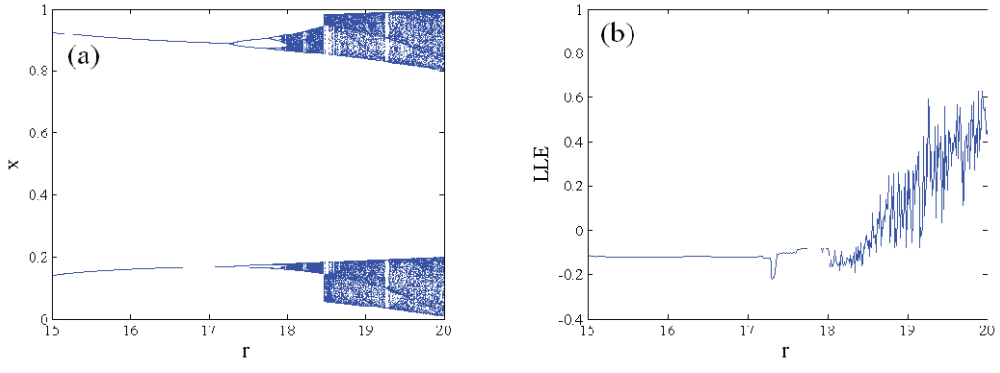

Figure 2. Bifurcation portrait and Lyapunov exponent spectrum with regard to r; (**a**) bifurcation portrait with regard to r; (**b**) Lyapunov exponent spectrum with regard to r.

For the dissipation parameter β, the bifurcation portrait and largest Lyapunov spectrum are plotted in Figure 3 with $r = 19.8$, $r_1 = 0.05$, and $\nu = 0.9$. Although the bifurcation portrait shows the phenomenon of bifurcation, the map is mainly in chaotic oscillation. Its chaotic regions are wider than those of the quantum logistic map. When the parameter β is greater than 3.75, the largest Lyapunov exponent is positive, which illustrates that the fractional-order map goes into chaos. When $\beta \in (3.75, 8.35]$, the largest Lyapunov roughly increases with the increasing parameter β. In the range of 8.35 to 15, the largest Lyapunov varies around 5.5. Some of the largest Lyapunov exponents exceed 6, indicating that the map has good nonlinearity and is suitable for information encryption.

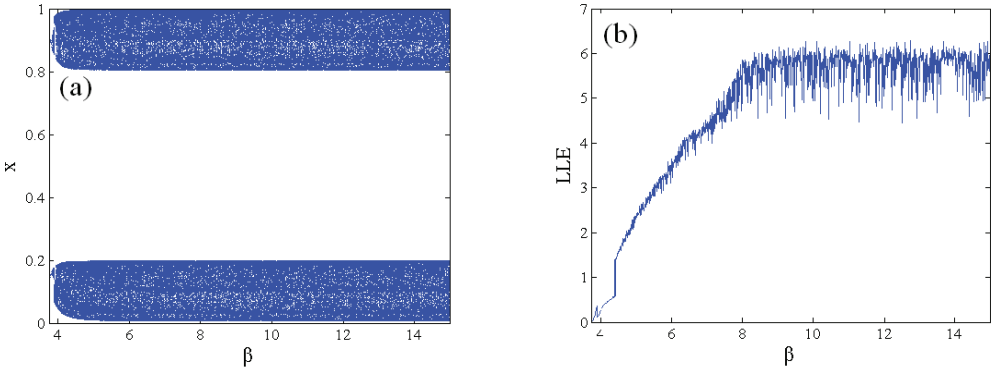

Figure 3. Bifurcation portrait and Lyapunov exponent spectrum with regard to β. (**a**) Bifurcation portrait with regard to β; (**b**) Lyapunov exponent spectrum with regard to β.

Next, we analyze how the fractional order ν influences the map. Figure 4 presents the bifurcation portrait and Lyapunov spectrum versus ν, where the parameters are set as $r_1 = 0.05$, $\beta = 4.5$, $r = 1.98$, and $0.326 \leq \nu \leq 1$. As can be seen from Figure 4, the largest Lyapunov exponent is always greater than zero, which means that the map remains chaotic. Unlike some other fractional-order chaotic maps [32,33], there are no periodic windows in the chaotic region. Further, the magnitude of the variable $x(n)$ hardly changes with the varying of the fractional order ν. This map demonstrates stronger robustness during chaos than the fractional-order logistic map, the fractional-order Hénon map, and the other fractional-order chaotic maps in [32,33]. When the fractional order is $\nu < 0.326$, the iteration value may not be in the domain of definition. If the iterative value is not in the domain of definition, the iteration will stop. In particular, the phase portrait shows finite points under the condition of $\nu = 0.2$, as shown in Figure 5a, which implies that the iteration stops. On the contrary, Figure 5b exhibits the chaotic attractors with $\nu = 0.5$. However, these chaotic attractors are different from the chaotic attractors shown in Figure 1. The analysis illustrates that the fractional-order map owns richer dynamical behaviors than the integer counterpart.

In order to investigate the influence of the parameters and fractional order on the fractional-order map simultaneously, the dynamical maps are depicted in Figure 6, where the color represents the value of the largest Lyapunov exponent. Figure 6a illustrates the impacts of the control parameters and fractional orders when $r_1 = 0.05$, $\beta = 10$, and $(x_0, y_0, z_0) = (0.05, 0.02, 0.05)$. It is clear to see that the fractional-order map undergoes a change from periodic oscillation to chaos with increasing fractional order. Figure 6b visualizes the influences of the dissipation parameters and fractional orders, where the parameters are set as $r = 5$ and $r_1 = 0.05$, and the initial condition is chosen as $(x_0, y_0, z_0) = (0.05, 0.02, 0.05)$. The effects of the dissipation parameters and fractional orders are different from those of the control parameters and fractional orders. The largest Lyapunov exponent in most of the areas is greater than zero, i.e., the system is mainly in a chaotic state.

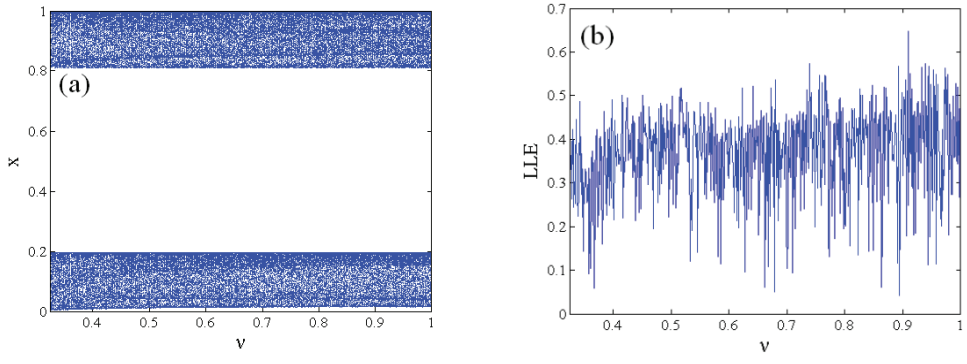

Figure 4. Bifurcation portrait and Lyapunov exponent spectrum with regard to ν. (**a**) Bifurcation portrait with regard to ν; (**b**) Lyapunov exponent spectrum with regard to ν.

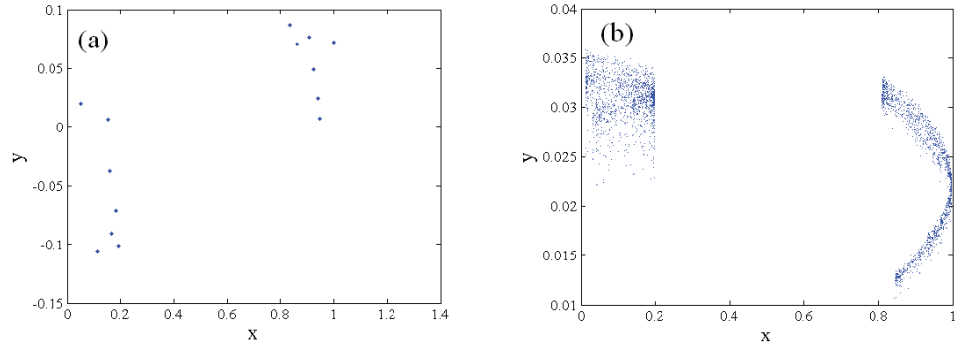

Figure 5. Phase portrait. (**a**) Phase portrait with $\nu = 0.2$; (**b**) phase portrait with $\nu = 0.5$.

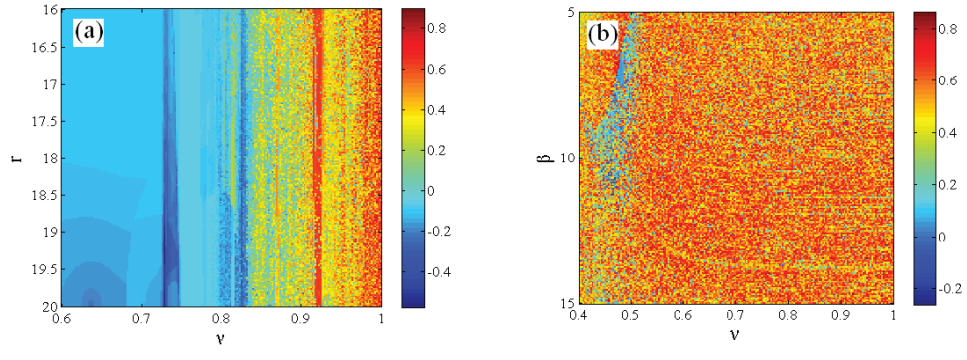

Figure 6. Dynamical maps. (**a**) Dynamical map with regard to ν and r; (**b**) dynamical map with regard to ν and β.

3.2. 0-1 Test

The 0-1 test is another approach to verify the existence of chaos, which can be utilized directly to a series of data without any phase space reconstruction [34]. Based on the state $\{x(j)\}$ of System (17), the translation components $p_c\ (n)$ and $q_c\ (n)$ are defined as

$$p_c(n) = \sum_{j=1}^{n} x(j)\cos(jc), \qquad q_c(n) = \sum_{j=1}^{n} x(j)\sin(jc) \tag{18}$$

where c is an arbitrary constant in the interval $(0, \pi)$. By plotting the dynamics of the translation components p_c–q_c, it is easy to determine the state of the system. If p–q trajectories are Brownian-like, the state of the system is chaotic, whereas if the trajectories are bounded, the state is periodic.

Next, the mean square displacement M_c on p_c (n) and q_c (n) is defined as

$$M_c = \lim_{N\to\infty} \frac{1}{N} \sum_{j=1}^{N} \{[p_c(j+n) - p_c(j)]^2 + [q_c(j+n) - q_c(j)]^2\}, \ n << N, \tag{19}$$

where N is the length of time sequences. In practice, n is chosen as $N/10$, and the superscript of $\sum$ is $N-n$.

Finally, the asymptotic growth rate K_c is calculated by

$$K_c = \lim_{n\to+\infty} \frac{\log M_c}{\log n}. \tag{20}$$

We get 100 values for K_c and then let K = median (K_c). When the value of K approaches 0, the system is in a periodic state, and when this value approaches 1, the system is chaotic.

The 0-1 test is performed, and the asymptotic growth rate, K, against r is depicted in Figure 7 under the conditions of $r_1 = 0.05$, $\beta = 4.5$, $\nu = 0.9$, and $(x_0, y_0, z_0) = (0.05, 0.02, 0.05)$. The asymptotic growth rate K is consistent with the bifurcation portrait and the largest Lyapunov spectrum shown in Figure 2. In order to further illustrate the nonlinear behaviors, the p–q trajectories are demonstrated in Figure 8. When $r = 17$, the bounded trajectory of the $p-q$ plane is shown in Figure 8a, and the asymptotic growth rate is $K = 0.0001$, implying that the system state is periodic. On the contrary, as $r = 19.8$, the Brownian-like trajectory is presented in Figure 8b, and the asymptotic growth rate is obtained as $K = 0.9958$, illustrating that the state is chaotic. Furthermore, the chaotic sequences of $r = 19.8$ are divided into two sequences according to the value of x_n. The trajectories of $0 < x_n < 0.2$ and $0.8 < x_n < 1$ are plotted in Figure 8c,d, respectively. The trajectories demonstrate that two sequences keep a chaotic state, so the map can produce multiple chaotic sequences.

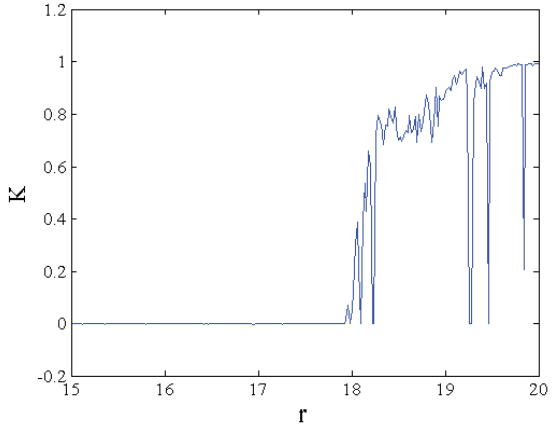

Figure 7. Asymptotic growth rate K of the fractional-order map with regard to r.

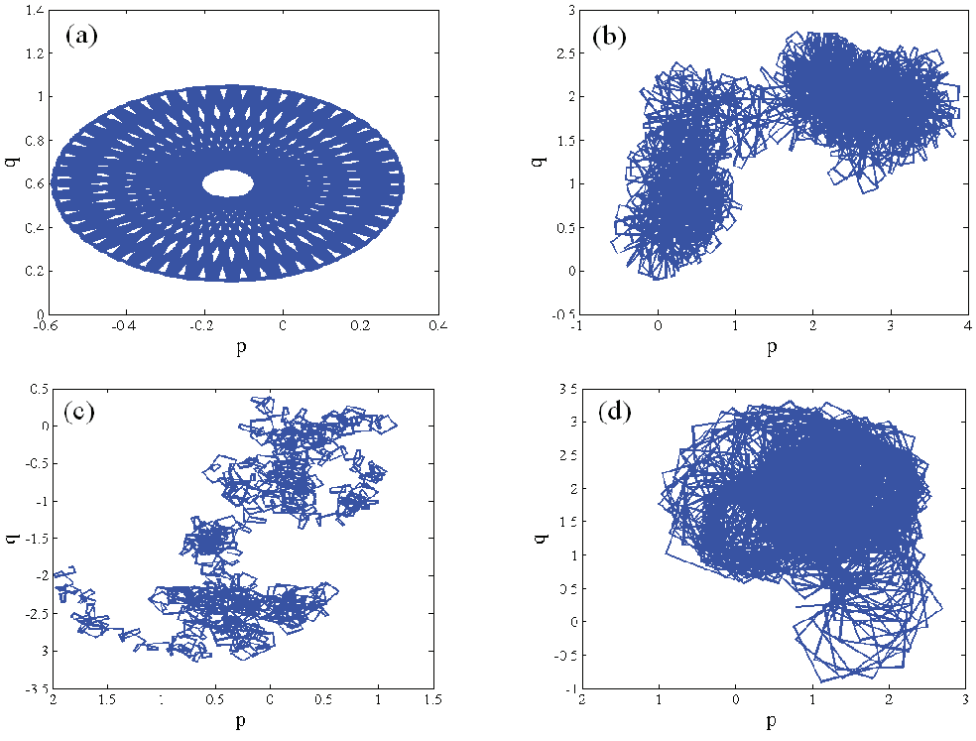

Figure 8. The p–q trajectories of the fractional-order map. (**a**) p–q trajectories of $r = 17$; (**b**) the p–q trajectories of $r = 19.8$; (**c**) p–q trajectories of $0 < x_n < 0.2$; (**d**) p–q trajectories of $0.8 < x_n < 1$.

4. Complexity and Entropy

4.1. Spectral Entropy

Complexity is an index that is used to measure how well a chaotic system generates random sequences, and larger complexity implies more randomness for the generated sequences. The complexity of the fractional-order map is evaluated by means of spectral entropy (SE). The spectral entropy algorithm [35] is defined as follows; consider a set of time sequences $\{x_n, n = 0, 1, 2, ..., N - 1\}$ with a length of N, and obtain a new discrete number of length N by subtracting the mean of this dataset, which is expressed as

$$x_n = x_n - \frac{\sum_{n=0}^{N-1} x_n}{N}, \tag{21}$$

The Fourier transformation is calculated by

$$X_k = \sum_{n=0}^{N-1} x_n e^{-j2n\pi k/N}, \tag{22}$$

where $k = 0, 1, 2, ..., N - 1$ and j is the unit imaginary. The probability of the power spectrum is given as

$$P_k = \frac{|X_k|^2}{\sum_{k=0}^{N/2-1} |X_k|^2}, \tag{23}$$

Then, the normalization spectral entropy is defined as

$$SE = \frac{\sum_{k=0}^{N/2-1} |P_k \ln(P_k)|}{\ln(N/2)} \tag{24}$$

We utilize spectral entropy to measure the complexity of the fractional-order map, and the result of SE complexity is presented in Figure 9. The SE complexity surpasses 0.85 in the highest range, so this fractional-order map can generate better random sequences.

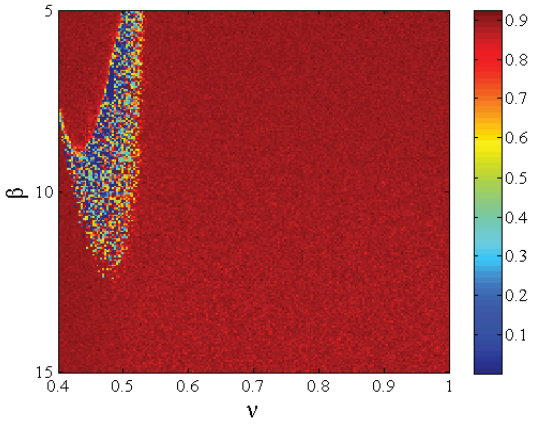

Figure 9. SE of the fractional-order map with regard to ν and β.

4.2. Approximate Entropy

The approximate entropy (ApEn) [36] is the other means to measure the complexity of the fractional-order map, which is described as follows. Consider a set of time sequences $x_1, x_2, \ldots, x_n$ obtained from System (17) and determine $n - m + 1$ vectors as follows:

$$X_i = [x_i, x_{i+1} \cdots \cdots x_{i+m-1}]. \tag{25}$$

These vectors denote m consecutive x values, which start from the ith data. Giving tolerance, r, and for each $i \in [1, n - m + 1]$, we define the following equation:

$$C_i^m(r) = \frac{K}{n - m + 1}, \tag{26}$$

in which K is the number of X_i with $d(X_i, X_j) \leq r$. In this case, $d(X_i, X_j)$ represents the largest absolute difference between X_i, and X_j. We calculate the approximate entropy by

$$APEn = \phi^m(r) - \phi^{m+1}(r), \tag{27}$$

where $\phi^m(r)$ is described as

$$\phi^m(r) = \frac{1}{n - m - 1} \sum_{i=1}^{n-m+1} \log C_i^m(r), \tag{28}$$

The result of ApEn complexity is shown in Figure 10, which agrees well with SE complexity. Therefore, this fractional-order map has a more complex structure. It has higher complexity than the fractional-order logistic map and the fractional-order Hénon map.

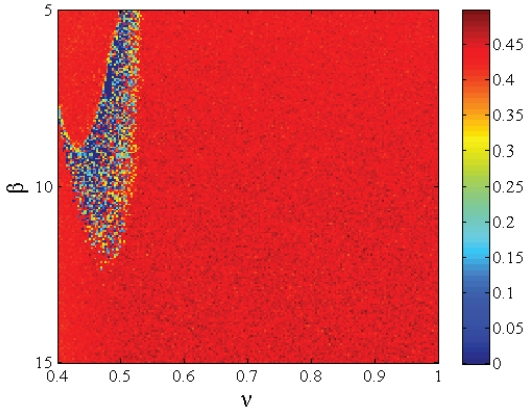

Figure 10. ApEn of the fractional-order map with regard to ν and β.

5. Chaos Control

As the fractional-order chaotic map is raised, the chaos control for the fractional-order map becomes a new topic. The occurrence of chaotic behaviors may cause instability in engineering applications, so chaos control has been widely studied. However, researchers have paid little attention to the topic of controlling fractional-order chaotic maps. In the section, the scheme of chaos control is proposed, which is based on improved nonlinear mapping on wavelet functions [37]. System (17) is controlled by it. This control method of fractional-order systems is of importance not only for control theory, but also for the application of fractional-order chaotic maps. A Marr wavelet function is employed to construct the improved nonlinear mapping. This chaos control algorithm is described as

$$\begin{cases} x_n = ke^{-\frac{x_{n-1}^2}{2}}(1-x_{n-1}^2)[f(x_{n-1}) - r_1 y_{n-1}], \\ {}^{C}\Delta_a^{\nu} y(t) = -y(t+\nu-1)e^{-2\beta} + e^{-\beta} r[(2-2x(t+\nu-1))y(t+\nu-1) \\ \qquad -2x(t+\nu-1)z(t+\nu-1)] - y(t+\nu-1), \\ {}^{C}\Delta_a^{\nu} z(t) = -z(t+\nu-1)e^{-2\beta} + e^{-\beta} r[2(1-x(t+\nu-1))z(t+\nu-1) \\ \qquad -2x(t+\nu-1)y(t+\nu-1) - x(t+\nu-1)] - z(t+\nu-1), \end{cases} \tag{29}$$

where k is a control parameter.

If System (17) is controlled when n = 1000, then the control results are presented in Figure 11. The fractional-order chaotic map is controlled to a period-1 orbit with k = 0.2; it is controlled to a period-2 orbit with k = 0.5, and it is controlled to period-4 orbit with k = 0.65, while it is controlled to quasiperiodic orbit with k = 0.7. As can be seen, the fractional-order chaotic map endures period-1, period-2, period-4, and quasiperiodic states with an increase in the control parameter k.

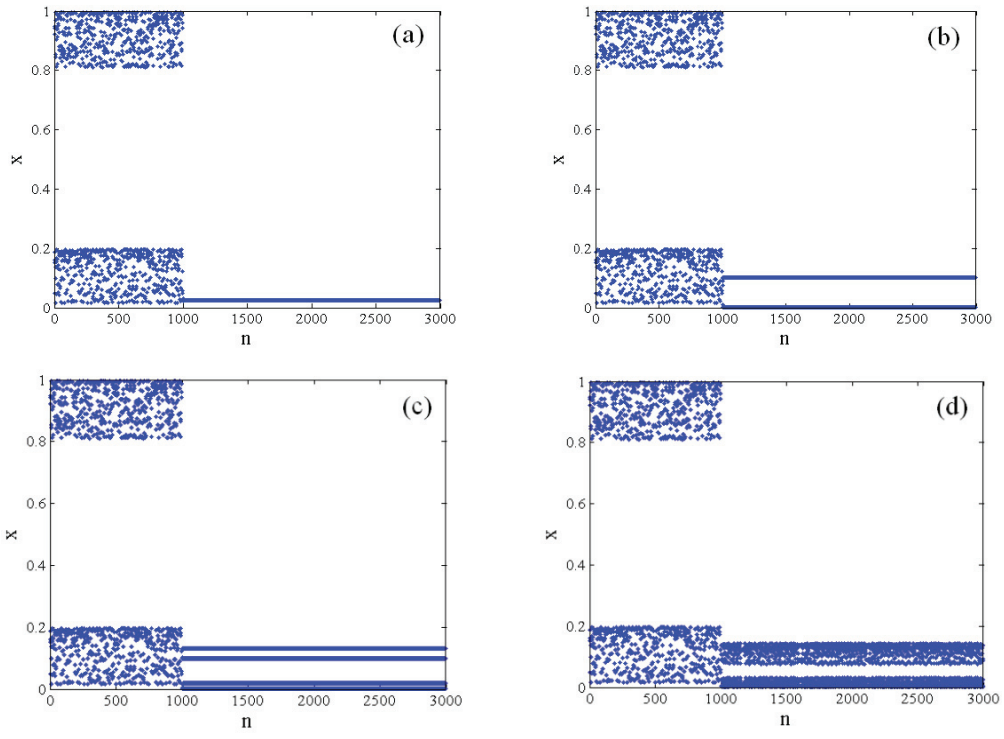

Figure 11. Chaotic controls. (**a**) Chaotic control with $k = 0.2$; (**b**) chaotic control with $k = 0.5$; (**c**) chaotic control with $k = 0.65$; (**d**) chaotic control with $k = 0.70$.

6. Conclusions

We build an improved quantum logistic map without equilibrium by reforming the classic quantum logistic map. The improved quantum logistic map with hidden attractors is generalized to the fractional case by introducing the Caputo-like delta difference operator. Through a phase portrait, the largest Lyapunov exponent, dynamical mapping, and 0-1 testing, the dynamical characteristics were studied. Both the parameters and fractional orders impact the system. With varying control parameters, the system shows periodic windows. However, for the dissipation parameter and the fractional order, there are no periodic windows in the chaotic region. This means that this chaotic map possesses stronger robustness in chaos, so the system could be applied to generate stable chaotic sequences for secure communication. The 0-1 test shows that this fractional-order map can generate several chaotic sequences. Then, the complexity of the fractional-order map was described by spectral entropy and approximate entropy, which shows that this fractional-order map can generate better random sequences. In addition, improved nonlinear mapping on a wavelet function for the fractional-order map was proposed. This map is controlled to different periodic orbits under different control parameters. The fractional-order map gains more degrees of freedom compared to the integer counterpart, so the fractional-order map has greater potential applications in the engineering field. Due to its higher complexity and stronger robustness in chaos, this fractional-order chaotic map can be employed in information encryptions, such as secret communications and image encryptions. In order to apply the fractional-order improved quantum logistic map, we will focus on designing the image encryption scheme based on this map in the future.

Author Contributions: Conceptualization, B.X. and G.W.; methodology, B.X. and G.W.; software, B.X., X.Y. and C.Z.; validation, B.X.; formal analysis, Z.H.; writing—original draft preparation, B.X. and C.Z.; writing—review and editing, X.Y., Z.H. and G.W.; supervision, G.W.; project administration, B.X.; funding acquisition, B.X., Z.H. and G.W. All authors have read and agreed to the published version of the manuscript.

Funding: This work is supported in part by the National Natural Science Foundation of China (Grant No. 61771176), the Natural Science Foundations of Fujian Province (Grant No. 2020J01395 and 2022J011203), and the innovation team of Wuyi University (Grant No. 2020-SSTD-005).

Data Availability Statement: Not applicable.

Conflicts of Interest: The authors declare that there is no conflict of interest.

Appendix A

The code generating chaotic attractors in MATLAB:

```
ν=0.9;β=4.5;r=19.8;r1=0.05;
x(1)=0.05;y(1)=0.02;z(1)=0.05;
for i=2:1:3000
temp4=0;temp7=0;
for j=2:1:i temp5=temp4+exp(gammaln(i−j+ν)−gammaln(i−j+1))*((−y(j−1)*exp(−2*β))+
exp(−β)*r*((2−2*x(j−1))*y(j−1)−2*x(j−1)*z(j−1))−y(j−1)); temp8=temp7+exp(gammaln
(i−j+ν)−gammaln(i−j+1))*((−z(j−1)*exp(−2*β))+exp(−β)*r*(2*(1−x(j−1))*z(j−1)−
(2*x(j−1)*y(j−1))−x(j−1))−z(j−1));
temp4=temp5;temp7=temp8;
temp6=(1/gamma(ν))*temp5; temp9=(1/gamma(ν))*temp8;
end
if (0<x(i−1))&&(x(i−1)<0.2)
x(i)=0.8+r*(x(i−1)−0)*(0.2−x(i−1))−r1*y(i−1);
elseif (0.8<x(i−1))&&(x(i−1)<1)
x(i)=0+r*(x(i−1)−0.8)*(1−x(i−1))−r1*y(i−1);
end
y(i)=y(1)+temp6; z(i)=z(1)+temp9;
end
figure;
plot(x(100:3000),y(100:3000),'b.','markersize',2);
xlabel('x');ylabel('y');
set(gca,'fontsize',12,'FontName','Times new Roman');
set(get(gca,'XLabel'),'FontName','Times new Roman','FontSize',16);
set(get(gca,'YLabel'),'FontName','Times new Roman','FontSize',16);
figure;
plot(y(100:3000),z(100:3000),'b.','markersize',2);
xlabel('y');ylabel('z');
set(gca,'fontsize',12,'FontName','Times new Roman');
set(get(gca,'XLabel'),'FontName','Times new Roman','FontSize',16);
set(get(gca,'YLabel'),'FontName','Times new Roman','FontSize',16);
figure;
plot(z(100:3000),x(100:3000),'b.','markersize',2);
xlabel('z');ylabel('x');
set(gca,'fontsize',12,'FontName','Times new Roman');
set(get(gca,'XLabel'),'FontName','Times new Roman','FontSize',16);
set(get(gca,'YLabel'),'FontName','Times new Roman','FontSize',16);
```

References

1. May, R.M. Simple mathematical models with very complicated dynamics. *Nature* **1976**, *261*, 459–467. [CrossRef] [PubMed]
2. Munir, F.A.; Zia, M.; Mahmood, H. Designing multi-dimensional logistic map with fixed-point finite precision. *Nonlinear Dyn.* **2019**, *97*, 2147–2158. [CrossRef]
3. Cánovas, J.; Muñoz-Guillermo, M. On the dynamics of the q-deformed logistic map. *Phys. Lett. A* **2019**, *383*, 1742–1754. [CrossRef]
4. Goggin, M.; Sundaram, B.; Milonni, P. Quantum logistic map. *Phys. Rev. A* **1990**, *41*, 5705. [CrossRef]
5. Petráš, I. Fractional-order systems. In *Fractional-Order Nonlinear Systems: Modeling, Analysis and Simulation*, 1st ed.; Springer: Berlin/Heidelberg, Germany, 2011; pp. 43–54.
6. Varun Bose, C.B.S.; Udhayakumar, R. Existence of mild solutions for hilfer fractional neutral integro-differential inclusions via almost sectorial operators. *Fractal Fract.* **2022**, *6*, 532. [CrossRef]
7. Kumar, V.; Malik, M. Existence, stability and controllability results of fractional dynamic system on time scales with application to population dynamics. *Int. J. Nonlin. Sci. Num.* **2021**, *22*, 741–766. [CrossRef]
8. Kumar, V.; Malik, M. Existence, uniqueness and stability of nonlinear implicit fractional dynamical equation with impulsive condition on time scales. *Nonauton. Dyn. Syst.* **2019**, *6*, 65–80. [CrossRef]
9. Baba, I.A.; Rihan, F.A. A fractional–order model with different strains of COVID-19. *Phys. A* **2022**, *603*, 127813. [CrossRef]
10. Atici, F.M.; Eloe, P.W. Initial value problems in discrete fractional calculus. *Proc. Am. Math. Soc.* **2009**, *137*, 981–989. [CrossRef]
11. Abu-Saris, R.; Al-Mdallal, Q. On the asymptotic stability of linear system of fractional-order difference equations. *Fract. Calc. Appl. Anal.* **2013**, *16*, 613–629. [CrossRef]
12. Mohan, J.J.; Deekshitulu, G.V.S.R. Fractional order difference equations. *Int. J. Differ. Equ.* **2012**, *2012*, 780619. [CrossRef]
13. Wyrwas, M.; Mozyrska, D.; Girejko, E. Stability of discrete fractional-order nonlinear systems with the nabla caputo difference. *IFAC Proc.* **2013**, *46*, 167–171. [CrossRef]
14. Edelman, M. Fractional maps and fractional attractors part I: α-families of maps. *Discontin. Nonlinearity Complex.* **2013**, *1*, 305–324. [CrossRef]
15. Edelman, M. Fractional maps and fractional attractors part II: Fractional difference α-families of maps. *Discont. Nonlinearity Complex.* **2015**, *4*, 391–402. [CrossRef]
16. Wu, G.C.; Baleanu, D. Discrete fractional logistic map and its chaos. *Nonlinear Dyn.* **2014**, *75*, 283–287. [CrossRef]
17. Wu, G.C.; Baleanu, D. Discrete chaos in fractional delayed logistic maps. *Nonlinear Dyn.* **2015**, *80*, 1697–1703. [CrossRef]
18. Wu, G.C.; Baleanu, D. Jacobian matrix algorithm for Lyapunov exponents of the discrete fractional maps. *Commun. Nonlinear Sci. Numer. Simulat.* **2015**, *22*, 95–100. [CrossRef]
19. Zhang, Y.Q.; Hao, J.L.; Wang, X.Y. An efficient image encryption scheme based on S-boxes and fractional-order differential logistic map. *IEEE Access* **2020**, *8*, 54175–54188. [CrossRef]
20. Ouannas, A.; Khennaoui, A.; Wang, X.; Pham, V.T.; Boulaaras, S.; Momani, S. Bifurcation and chaos in the fractional form of Hénon-Lozi type map. *Eur. Phys. J. Spec. Top.* **2020**, *229*, 2261–2273. [CrossRef]
21. Liu, Z.Y.; Xia, T.; Wang, Y.P. Image encryption technique based on new two-dimensional fractional-order discrete chaotic map and Menezes-Vanstone elliptic curve cryptosystem. *Chin. Phys. B* **2018**, *27*, 030502. [CrossRef]
22. Wang, L.; Sun, K.; Peng, Y.; He, S. Chaos and complexity in a fractional-order higher-dimensional multicavity chaotic map. *Chaos Soliton. Fract.* **2019**, *131*, 109488. [CrossRef]
23. Jafari, S.; Pham, V.T.; Golpayegani, S.M.R.H.; Moghtadaei, M.; Kingni, S.T. The relationship between chaotic maps and some chaotic systems with hidden attractors. *Int. J. Bifurcat. Chaos* **2016**, *26*, 1650211. [CrossRef]
24. Cui, L.; Luo, W.H.; Ou, Q.L. Analysis and implementation of new fractional-order multi-scroll hidden attractors. *Chin. Phys. B* **2021**, *30*, 020501. [CrossRef]
25. Chowdhury, S.N.; Ghosh, D. Hidden attractors: A new chaotic system without equilibria. *Eur. Phys. J. Spec. Top.* **2020**, *229*, 1299–1308. [CrossRef]
26. Jafari, S.; Sprott, J.C.; Nazarimehr, F. Recent new examples of hidden attractors. *Eur. Phys. J. Spec. Top.* **2015**, *224*, 1469–1475. [CrossRef]
27. Leonov, G.A.; Kuznetsov, N.V. Hidden attractors in dynamical systems: From hidden oscillation in Hilbert-Kolmogorov, Aizerman and Kalman problems to hidden chaotic attractor in Chua circuits. *Int. J. Bifurcat. Chaos* **2013**, *23*, 1330002. [CrossRef]
28. Leonov, G.A.; Kuznetsov, N.V.; Vagaitsev, V.I. Hidden attractor in smooth Chua systems. *Phys. D* **2012**, *241*, 1482–1486. [CrossRef]
29. Leonov, G.A.; Kuznetsov, N.V.; Vagaitsev, V.I. Localization of hidden Chua's attractors. *Phys. Lett. A* **2011**, *375*, 2230–2233. [CrossRef]
30. Abdeljawad, T. On Riemann and Caputo fractional differences. *Comput. Math. Appl.* **2011**, *62*, 1602–1611. [CrossRef]
31. Chen, F.; Luo, X.; Zhou, Y. Existence results for nonlinear fractional difference equation. *Adv. Differ. Equ.* **2011**, *2011*, 713201. [CrossRef]
32. Ouannas, A.; Khennaoui, A.A.; Momani, S.; Pham, V.T.; El-Khazali, R. Hidden attractors in a new fractional-order discrete system: Chaos, complexity, entropy, and control. *Chin. Phys. B* **2020**, *29*, 050504. [CrossRef]
33. Khennaoui, A.A.; Ouannas, A.; Boulaaras, S.; Pham, V.T.; Azar, A.T. A fractional map with hidden attractors: Chaos and control. *Eur. Phys. J. Spec. Top.* **2020**, *229*, 1083–1093. [CrossRef]
34. Sun, K.H.; Liu, X.; Zhu, C.X. The 0-1 test algorithm for chaos and its applications. *Chin. Phys. B* **2010**, *19*, 110510. [CrossRef]

35. Staniczenko, P.P.A.; Lee, C.F.; Jones, N.S. Rapidly detecting disorder in rhythmic biological signals: A spectral entropy measure to identify cardiac arrhythmias. *Phys. Rev. E* **2009**, *79*, 011915. [CrossRef]
36. Pincus, S.M. Approximate entropy as a measure of system complexity. *Proc. Natl. Acad. Sci. USA* **1991**, *88*, 2297–2301. [CrossRef] [PubMed]
37. Li, X.; Chu, Y.; Liu, X.; Zhang, J. Control discrete (hyper-)chaotic system using improved wavelet functions. *J. Huazhong Univ. Sci. Tech.* **2009**, *37*, 72–74.

symmetry

MDPI

Article

Analytical Investigation of the Heat Transfer Effects of Non-Newtonian Hybrid Nanofluid in MHD Flow Past an Upright Plate Using the Caputo Fractional Order Derivative

N. M. Lisha and A. G. Vijayakumar *

Department of Mathematics, School of Advanced Sciences, Vellore Institute of Technology, Vellore 632014, India
* Correspondence: vijayakumarag@vit.ac.in

Abstract: The objective of this paper is to examine the augmentation of the heat transfer rate utilizing graphene (Gr) and multi-walled carbon nanotubes (MWCNTs) as nanoparticles, and water as a host fluid in magnetohydrodynamics (MHD) flow through an upright plate using Caputo fractional derivatives with a Brinkman model on the convective Casson hybrid nanofluid flow. The performance of hybrid nanofluids is examined with various shapes of nanoparticles. The Caputo fractional derivative is utilized to describe the governing fractional partial differential equations with initial and boundary conditions on the flow model. Exact solutions are obtained for flow transport, temperature distribution besides that heat transfer rate and friction drag in terms of Mittag-Leffler function by using Fourier sine and Laplace techniques as hybrid methods. Further, we provided the limiting case solutions for classic partial differential equations on obtained governing fluid flow models. The influence of various physical parameters with different fractional orders are investigated on hybrid nanofluid's fractional momentum and energy by plotting velocity and energy curves. Few of the findings suggest that fractional parameters have significant effect on flow parameters and that blade-shaped nanoparticles have a high heat transfer rate. The graphical results reveal that the Grashof number shows a symmetry effect in the case of cooling and heating the plate. Furthermore, the performance of hybrid nanofluid is considerably more effective with the Caputo-fractional derivatives rather than in the classic derivative approach.

Keywords: Casson Fluid; Fourier Sine Transform; Laplace Transform; fractional heat equation; shape factor; Mittag-Leffler function

Citation: Lisha, N.M.; Vijayakumar, A.G. Analytical Investigation of the Heat Transfer Effects of Non-Newtonian Hybrid Nanofluid in MHD Flow Past an Upright Plate Using the Caputo Fractional Order Derivative. *Symmetry* **2023**, *15*, 399. https://doi.org/10.3390/sym15020399

Academic Editors: António Lopes, Alireza Alfi, Liping Chen and Sergio Adriani David

Received: 25 November 2022
Revised: 13 December 2022
Accepted: 19 December 2022
Published: 2 February 2023

1. Introduction

Nanotechnology has significantly advanced in heat transfer studies, which has enhanced the thermal characteristics of energy-transmitting fluids. Producing nanoparticles with great heat conductivity is one of the most trending uses of nanotechnology. To increase the thermal conductivity of fluids, nanofluids have great importance. They are prepared in laboratories by using nanoparticles with an average diameter of less than 100 nm which are suspended in typical heat transfer fluids such as oil, water, and ethylene glycol. First, Maxwell [1] proposed nanofluids after an attempt to optimize the heat transfer rate of regular fluids by suspending micro-sized particles failed owing to sedimentation and clogging of the flow patterns. Based on these issues, Choi [2] suggested in 1995 that the dispersion of nanoparticles into the host fluid might improve the thermal performance of the base fluid. Subsequently, a diverse range of devices have been developed for a variety of practical purposes and functions in various fields such as electrical engineering [3], helping to improve the thermal efficiency of horizontal spiral coils used in solar ponds [4], as a coolant in double pipe heat exchangers [5], stenotic artery [6] and drug agent [7]. Later research by Imran Siddique et al. [8], Maryam Aleem et al. [9], as well as Anum Shafiq et al. [10] broadened the literature on nanofluids. The discovery of nanofluids has achieved the major part of industry's requirements, but the suspension of single nanoparticles is inadequate

for the required thermal performance. Therefore, researchers have been attempting to develop a better and more efficient fluid. Yamada et al. [11] defined an upgraded kind of nanofluid in 1989 by combining two or more nanoparticles of distinct characteristics with common fluids. This advanced categorization of nanofluid, known as a hybrid nanofluid, shows potential improvements in heat transfer rate, which can be applied in many domains such as biomedicine [12–14], heat exchangers [15], solar energy [16] and so on. Some of the modern advances in the literature of hybrid nanofluids are observed in the studies carried by Hafeez et al. [17]; their study provides a numerical modelling of MHD rotational flow of hybrid nanomaterial by applying a bvp4c technique between two parallel porous sheets. Iskandar Waini et al. [18] examined the stable mixed convection flow along a vertical surface immersed in a porous medium using hybrid nanoparticles. Talha Anwar et al. [19] established two independent fractional models, Caputo–Fabrizio and Atangana–Baleanu, to analyze the flow patterns and thermal characteristics of a NaAlg/SA-based hybrid nanofluid. Their study revealed that the CF fractional operator improves the thermal rate more efficiently than the AB fractional operator.

Heat transmission is crucial for temperature controls in many industrial applications. Even with increased demand for energy-efficient equipment, achieving good heat transmission of a fluid remains a challenge. As a result, nanoparticles, nanofluids, and hybrid nanofluids exploration are some of the most significant topics of research. Consequently, heat transfer becomes more robust. Nepal T. Balaji et al. [20] investigated the micro channel heat sink, which is used to check the convective heat transfer properties of water-based hybrid nanofluids including graphene nanoplatelets and MWCNTs. Mumtaz Khan et al. [21] examined FDM combined with L1-technique utilization to perform the heat transfer of fractional transient MHD flow of viscoelastic hybrid nanofluids through an inclined surface fixed in a Darcy porous medium. Unsteady natural convection and heat transmission of hybrid nanofluid for two upright parallel plates were analyzed by Chandra Roy and Ioan Pop [22]. In the fields of biomechanics, aerospace, and chemical engineering, magnetohydrodynamics (MHD) free convection flow is extremely important. MHD primarily focuses on the study of the magnetic characteristics and behavior of electrically conducting fluids, including magneto fluids such as electrolytes, liquid metals, plasmas and salt water. Ndolane Sene [23] examined the heat transmission analysis of Brinkmantype fluid with Caputo derivative. Zar Ali Khan et al. [24] found the analytic solution of the transient flow of a generalized Brinkman-type fluid in a channel under the influences of MHD with Caputo–Fabrizio fractional derivative. Ridhwan Reyaz et al. [25] explored the effects of heat radiation on the MHD Casson Fluid as well as the Caputo fractional derivative on an oscillating upright plate.

The investigation of non-Newtonian materials is another intriguing research issue due to its interdisciplinary character and interesting rheological dynamics. Non-Newtonian fluids are flexible due to their applicability in numerous sectors and production processes. The relevance of non-Newtonian fluids may be seen in the oil packing, cooling/heating processes, hydraulics, lubricant industry and opto-electronics. In the literature, scientists have researched many non-Newtonian models, among which is included the Casson Fluid model [26], made known in 1959 by Casson, while inspecting the rheological data of pigment ink in a printer. Casson Fluid is a shear-thinning liquid with infinite viscosity at zero shear stress. When the yield stress is higher than the shear stress, the fluid acts like a solid. Toothpaste, slurries, blood, paint, molten polymers, honey, jelly, tomato sauce and chocolate are examples of Casson Fluid. This fluid model has been beneficial to polymer processing industries, food manufacturers, cosmetics, textiles, biomechanics, pharmaceuticals and many more. Ali Raza et al. [27] investigated the flow of Casson nanoparticles by applying Laplace Transform across a vertical moving plate using the Atangana–Baleanu time-fractional derivative and studies have shown that the fractional, ordinary velocity fields of Casson Fluid decreases when compared to viscous fluid. Muhammad Nazirul Shahrim et al. [28] were using the Laplace Transform to study the precise solution of fractional convective Casson Fluid over an accelerated plate. M. Veera Krishna et al. [29] explored the radiative

MHD flow of Casson hybrid nanofluid through an infinite exponentially accelerated vertical porous surface using the Laplace methodology, and the temperature of Casson hybrid nanofluid is considerably superior to that of Casson nanofluid.

In present times, fractional calculus [30] is essential in engineering and applied scientific disciplines such as physics, electronics, mechanics, population modelling, biosciences, economics and signal processing. Fractional calculus contains two categories singular operators and nonsingular operators. (1) Caputo derivative (2) Riemann–Liouville derivative are singular operators. The Caputo–Fabrizio derivative and the Atangana–Baleanu derivative are non-singular operators. They arose as a result of the application of conventional differentiation to the concept of non-local derivatives. As per several subject specialists, the findings obtained through the use of fractional operators are more precise and realistic than those obtained using classic differentiation. When it comes to understanding fluid performance, fractional operators are extremely important because of their self-similar qualities and memory-capturing capabilities. The Caputo derivative is the most commonly encountered derivative in the fractional calculus literature. The rationale stems from the fact that this derivative is consistent with the initial conditions utilized in modelling real-world issues. Michele Caputo proposed the Caputo fractional derivative in his study in the year 1967 [31]. Talha Anwar et al. [32] analyzed different shape effects of fractal fractional model for thermal analysis of hybrid nanofluid with a power-law kernel and noticed that the heat transfer rate was most effective for blade-shaped nanoparticles when graphene nanoparticles and graphite oxide were equally dispersed. Muhammad Saqib et al. [33] used the Atangana–Baleanu fractional derivative to examine the time fractional model of the convective flow of carboxy–methyl–cellulose (CMC)-based CNTs nanofluid through a porous media in a microchannel and observed that MWCNTs are more efficient than SWCNTs in improving the thermal conductivity of the nanofluids. Marjan Mohd Daud et al. [34] implemented the Caputo fractional derivative principle to Casson Fluid convective flow in a microchannel with radiant heat flux. M Ahmad et al. [35] described a generalization for natural convection flow of Maxwell nanofluid in two upright parallel plates adopting Caputo–Fabrizio utility of fractional order derivatives. Sidra Aman et al. [36] derived precise estimates for MHD flow of Casson nanofluid with hybrid nanoparticles using the Caputo time fractional derivatives.

Being motivated by Ndolane Sene [37], who analyzed the exact solution for a class of fluids model with the Caputo derivative by using Laplace and Fourier Sine Transform method, it is noticed that there has been no attempt in the prior literature to investigate MHD and hybrid nanofluids with Caputo fractional derivatives by using Fourier Sine Transform and Laplace Transform. Hence, the current study proposes to expand on the work of Ndolane Sene by adopting MHD with different shapes of hybrid nano fluid model using graphene (Gr), multiwall carbon nanotubes (MWCNTs) as nanoparticles and water as host fluid to analyze the heat transmission rate. The implementation of the Caputo derivative and its approach to obtaining the analytical results by employing the Laplace and Fourier transforms will be novel. The Caputo fractional derivative is used to fractionalize the MHD free convection Casson hybrid Brinkman-type fluid model. The Fourier sine and Laplace Transformation is used to transform non-linear governing PDEs into ordinary differential equations. These exact solutions are shown for temperature and flow fields of hybrid nanofluid. Eventually, by making $\alpha \to 1$, $\beta \to \infty$ the classic non-Newtonian solutions are recovered for velocity field. Further, the influence of several parameters on the fluid flow and thermal characteristics were discussed and shown in graphical and tabular form. The practical applications of employing these nanoparticles are in wastewater treatment, 3D printing, solar cell (dye-sensitized solar cells) industries.

The contents of the present paper are outlined as follows. Section 2 describes the fractional mathematical model using Caputo fractional derivatives. Section 3 gives the approaches to obtain analytical solutions using Fourier sine and Laplace Transform methods for temperature and velocity fields. Further discussed are the limiting cases, heat transmission rate and shearing stress. Discussion and the interpretations of the influences

of the parameters utilized in the modelling have been provided in Section 4. We conclude the paper with findings which are discussed in Section 5.

2. Fractional Mathematical Model with Caputo Derivative

Consider an unsteady MHD free convective Casson hybrid flow of water with graphene and MWCNTs nanoparticles over an infinite upright plate. The system rectilinear coordinate is implemented for the analysis, and the fluid flow is taken in the y-direction, whereas the x-axis is picked perpendicular to the plate. Magnetic field of strength B_0 is applied normal to the fluid flow direction. The fluid is viscous, incompressible, conducting and not electrified. The fluid is assumed to be gray, absorbing and emitting radiation but as a non-scattered medium. Different forms of nanoparticles (cylinder, blade, brick, platelet and spherical) are disseminated into the host fluid to obtain hybrid nanofluid. At time $\tau = 0$, the plate and hybrid nanofluid are both in equilibrium state with temperature T_∞. As time progresses, $\tau > 0$, the fluid is driven by the velocity U and at the same time, temperature of the fluid raised to T_W and then far away from the plate its ambient temperature is T_∞, causing free convection to occur, as presented in Figure 1. Body force emerges as buoyancy force in this circumstance because of the temperature difference. Further, for analyzing the flow phenomena of the hybrid nanofluid, the Brinkman-type fluid model is being used.

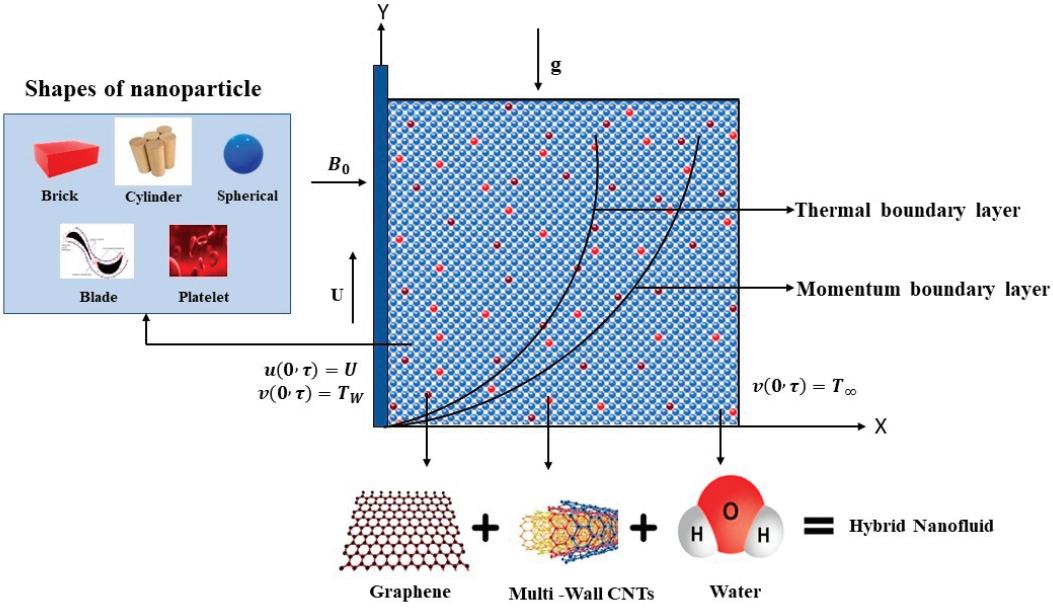

Figure 1. Flow geometry.

The following forms can be used to depict the rheological equation for an incompressible Casson Fluid (Nakamura et al. [38]).

$$\left.\begin{aligned} \pi_{i,j} &= 2(\mu_\gamma + \tfrac{p_y}{\sqrt{2\pi}})e_{ij} \quad when\ \pi > \pi_c \\ \pi_{i,j} &= 2(\mu_\gamma + \tfrac{p_y}{\sqrt{2\pi_c}})e_{ij} \quad when\ \pi < \pi_c \end{aligned}\right\} \tag{1}$$

Here, $\pi = e_{ij}e_{ij}$ where e_{ij} represents the $(i,j)^{th}$ component of the deformation rate, π is the product of the component of deformation rate with itself, π_c is the critical value of this product based on the non-Newtonian model, p_y symbolizes the yields stress, and μ_γ denotes the plastic dynamic viscosity of the non-Newtonian flow.

The mathematical structure of the corresponding conventional flow of Casson hybrid nanofluid (graphene–MWCNTs–H_2O) can be concise by Boussinesq's approximation (Nehad Ali Shah and Ilyas Khan [39]) with the following partial differential governing equations given under the aforementioned assumptions.

$$\frac{\partial u}{\partial x} + \frac{\partial v}{\partial y} = 0 \tag{2}$$

$$\rho_{hnf}\frac{\partial u}{\partial t} = \mu_{hnf}(1+\frac{1}{\beta})\frac{\partial^2 u}{\partial x^2} + \rho_{hnf}\gamma_{hnf}g(T-T_\infty) - \sigma_{hnf}B_0^2 u \tag{3}$$

$$(\rho C_p)_{hnf}\frac{\partial T}{\partial t} = \kappa_{hnf}\frac{\partial^2 T}{\partial x^2} \tag{4}$$

The dimensional initial and boundary conditions employed in this study are detailed below.

$$\begin{array}{ll} t \le 0: & u = 0, T = T_\infty \forall x \\ t > 0: & u = U,\ T = T_w : x = 0 \\ & u \to 0,\ T \to T_\infty : x \to \infty \end{array} \tag{5}$$

Table 1 lists the thermo-physical attributes of hybrid nanofluids and nanofluids. Table 2 portrays the thermophysical properties of the host fluid (H_2O) and nanoparticles (graphene and MWCNT). Table 3 displays the sphericity and shape factor for various shapes of nanoparticles.

Table 1. Hybrid nanofluid thermophysical description (Talha Anwar et al. [32]).

Properties	Hybrid Nanofluid
Viscosity, μ	$\mu_{hnf} = \frac{\mu_f}{(1-\phi_{Gr})^{2.5}(1-\phi_{MWCNT})^{2.5}}$ (Brinkman model)
Density, ρ	$\rho_{hnf} = \left[\rho_f(1-\phi_1) + \phi_1\rho_{p_1}\right](1-\phi_2) + \rho_{p_2}\phi_2$
Specific heat capacity, C_ρ	$(\rho C_p)_{hnf} = \left[\phi_{Gr}(\rho C_p)_{Gr} + (1-\phi_{Gr})(\rho C_p)_f\right](1-\phi_{MWCNT}) + (\rho C_p)_{MWCNT}\phi_{MWCNT}$
Thermal conductivity, κ	$\kappa_{hnf} = \kappa_{nf}\left[\frac{\kappa_{MWCNT}+(n-1)\kappa_{nf}-(n-1)(\kappa_{nf}-\kappa_{MWCNT})\phi_{MWCNT}}{\kappa_{MWCNT}+(n-1)\kappa_{nf}+(\kappa_{nf}-\kappa_{MWCNT})\phi_{MWCNT}}\right]$ (Maxwell model) where $\kappa_{nf} = \kappa_f\left[\frac{\kappa_{np_1}+\kappa_f(n-1)-(\kappa_f-\kappa_{np_1})(n-1)\phi_{np_1}}{\kappa_{np_1}+\kappa_f(n-1)+(\kappa_f-\kappa_{np_1})\phi_{np_1}}\right]$
Electrical conductivity, σ	$\sigma_{hnf} = \sigma_{nf}\left[\frac{\sigma_{p_2}+(n-1)\sigma_{nf}-(n-1)(\sigma_{nf}-\sigma_{p_2})\phi_2}{\sigma_{p_2}+(n-1)\sigma_{nf}+(\sigma_{nf}-\sigma_{p_2})\phi_2}\right]$ where $\sigma_{nf} = \sigma_f\left[\frac{\sigma_{p_1}+(n-1)\sigma_f-(n-1)(\sigma_f-\sigma_{p_1})\phi_1}{\sigma_{p_1}+(n-1)\sigma_f+(\sigma_f-\sigma_{p_1})\phi_1}\right]$
Thermal expansion coefficient, γ	$(\rho\gamma)_{hnf} = \left[(1-\phi_{Gr})(\rho\gamma)_f + \phi_{Gr}(\rho\gamma)_{Gr}\right](1-\phi_{MWCNT}) + (\rho\gamma)_{MWCNT}\phi_{MWCNT}$

Table 2. Thermophysical characteristics of the host fluid and nanoparticles (Mumtaz Khan et al. [21], Reddy SR and Reddy PB [40]).

Physical Properties	Water (H_2O)	Graphene (Gr)	Multiwall Carbon Nanotube (MWCNT)
$\rho/\mathrm{Kgm^{-3}}$	997.1	2250	1600
$C_\rho/\mathrm{JKg^{-1}K^{-1}}$	4179	2100	796
$\kappa/\mathrm{Wm^{-1}K^{-1}}$	0.613	2500	3000
$\sigma/\mathrm{Sm^{-1}}$	5.5×10^{-6}	10^7	10^7
$\gamma/\mathrm{K^{-1}}$	210×10^{-6}	-7×10^{-6}	2.1×10^{-5}

The following non-dimensional parameters are constructed using Buckingham's pi-theorem (W.D.Curtis [41]).

Table 3. Sphericity and shape factor of nanoparticles of various shapes (Muhammad Saqib et al. [33]).

Models	a	b	ψ	$p=\frac{3}{\psi}$
Blade	14.6	123.3	0.36	8.3
Brick	1.9	471.4	0.81	3.7
Platelet	37.1	612.6	0.52	5.7
Cylinder	13.5	909.4	0.62	4.9
Spherical	-	-	1	3

$$\begin{gathered} u^* = \frac{u}{U},\ x^* = x\frac{U}{v},\ \tau^* = \frac{U^2}{v}t,\ v = \frac{T-T_\infty}{T_w-T_\infty} \\ Pr = \frac{(\mu C_p)_f}{\kappa_f},\ Gr = \frac{g v_f \gamma_f (T_w-T_\infty)}{U^3},\ M = \frac{\sigma_f \nu_f B_0^2}{\rho_f U^2} \end{gathered} \tag{6}$$

When transforming the Equations (2)–(5) using the dimensionless variables specified in Equation (6) and further dropping * sign, a more simplified form of the non-dimensional fluid model is obtained as:

$$\frac{\partial u}{\partial \tau} = a_7\left(1+\frac{1}{\beta}\right)\frac{\partial^2 u}{\partial x^2} - a_{10}M + a_{12}Grv \tag{7}$$

$$\frac{\partial v}{\partial \tau} = \frac{a_4}{Pr}\frac{\partial^2 v}{\partial x^2} \tag{8}$$

Fractional calculus is an effective tool for describing real-world phenomena with the so-called memory effect. The Caputo derivative is used because the memory effect and a constant function's derivatives yield zero. Equations (9) and (10) are obtained by replacing the integer order derivative with the Caputo derivative in Equations (7) and (8) and generalizing the integer-order derivative to non-integer partial differential equations. They are:

$$D_\tau^\alpha u = a_7\left(1+\frac{1}{\beta}\right)\frac{\partial^2 u}{\partial x^2} - a_{10}M + a_{12}Grv \tag{9}$$

$$D_\tau^\alpha v = \frac{a_4}{Pr}\frac{\partial^2 v}{\partial x^2} \tag{10}$$

We treat the following relationships as dimensional initial and boundary conditions that momentum and temperature satisfy.

$$\begin{aligned} \tau \le 0: &\quad u = 0,\ v = 0 \forall x \\ \tau > 0: &\quad u = 1,\ v = 1 : x = 0 \\ &\quad u \to 0,\ v \to 0 : x \to \infty \end{aligned} \tag{11}$$

where

$$a_1 = \frac{\kappa_{p_2}+(n-1)\kappa_{nf}-(n-1)(\kappa_{nf}-\kappa_{p_2})\phi_2}{\kappa_{p_2}+(n-1)\kappa_{nf}+(\kappa_{nf}-\kappa_{p_2})\phi_2},$$

$$a_2 = \frac{k_{p_1}+(n-1)k_f-(n-1)(k_f-k_{p_1})\phi_1}{k_{p_1}+(n-1)k_f-(k_f-k_{p_1})\phi_1},$$

$$a_3 = (1-\phi_2)\left[(1-\phi_1)+\phi_1\frac{(\rho C_p)_{p_1}}{(\rho C_p)_f}\right]+\left[\frac{(\rho C_p)_{p_2}}{(\rho C_p)_f}\right]\phi_2,\ a_4 = \frac{a_1 a_2}{a_3},$$

$$a_5 = (1-\phi_1)^{2.5}(1-\phi_2)^{2.5},\ a_6 = (1-\phi_2)\left[(1-\phi_1)+\phi_1\frac{\rho_{p_1}}{\rho_f}\right]+\left[\frac{\rho_{p_2}}{\rho_f}\right]\phi_2,\ a_7 = \frac{1}{a_5 a_6},$$

$$a_8 = \frac{\sigma_{p_2}+(n-1)\sigma_{nf}-(n-1)(\sigma_{nf}-\sigma_{p_2})\phi_2}{\sigma_{p_2}+(n-1)\sigma_{nf}+(\sigma_{nf}-\sigma_{p_2})\phi_2},$$

$$a_9 = \frac{\sigma_{p_1}+(n-1)\sigma_f-(n-1)(\sigma_f-\sigma_{p_1})\phi_1}{\sigma_{p_1}+(n-1)\sigma_f+(\sigma_f-\sigma_{p_1})\phi_1},$$

$$a_{10} = \frac{a_8 a_9}{a_6},\ a_{11} = (1-\phi_2)\left[(1-\phi_1)+\phi_1\frac{(\rho\gamma)_{p_1}}{(\rho\gamma)_f}\right]+\frac{(\rho\gamma)_{p_2}}{(\rho\gamma)_f}\phi_2,\ a_{12} = \frac{a_{11}}{a_6}$$

3. Procedure for Solution

There are numerous approaches for solving the fractional differential equations provided in Equations (9) and (10). This section explains how to use analytical approaches to find solutions. In this work, Laplace and Fourier Sine Transformation are used to find exact results for our present model. This approach is mentioned in the following literatures [42,43]. The benefit of this method in this study is that it allows for the development of linear fractional differential equations. Figure 2 shows a flowchart that summarizes the solution method used in this study.

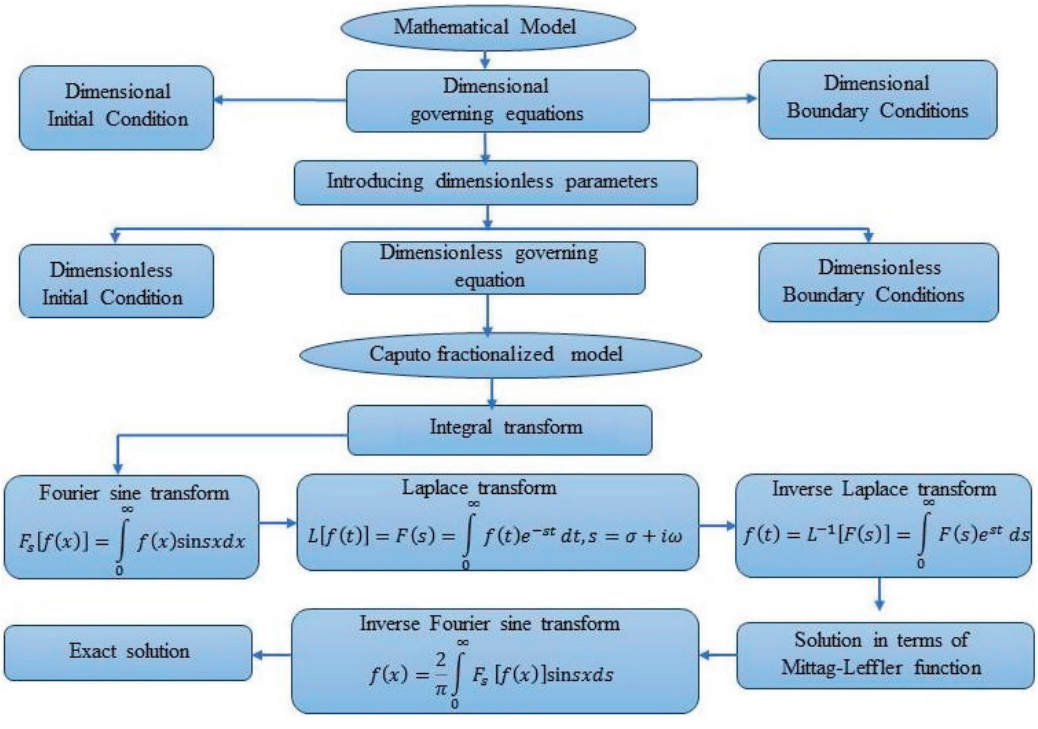

Figure 2. Flow chart for Fourier sine and Laplace Transform.

3.1. Integral Transform for Fractional Order Caputo Derivative

The Laplace Transform method is employed for obtaining accurate analytical solutions in this study, the Laplace Transformation of the Caputo derivative in the following lines are defined.

The Caputo fractional derivative of $f(t)$ is defined as:

$$D^{\alpha} f(t) = \frac{1}{\Gamma 1-\alpha}\int_0^t (t-s)^{-\alpha}\frac{df(s)}{ds};\ 0 < \alpha < 1 \tag{12}$$

where α is a fractional order, Γ is a gamma Euler function.

In Equation (12), the Laplace Transform and the Convolution theorem is utilized to obtain:

$$L\left[\int_0^t f'(u)(t-u)^{-\alpha}du\right] = \left(s\overline{f}(s) - f(0)\right)\frac{\Gamma 1-\alpha}{s^{1-\alpha}} \tag{13}$$

Then, using the Laplace Transform definition, the following is obtained:

$$L[D_c{}^{\alpha} f(t)] = s^{\alpha} L[f(t)] - s^{\alpha-1} f(0) \tag{14}$$

According to the present study Equation (15) is written as:

$$L[D_c{}^{\alpha} v(q,\tau)] = s^{\alpha} L[v(q,\tau)] - s^{\alpha-1} v(q,0) \tag{15}$$

The Laplace Transform in Equation (15) will be significant in the current investigation.

3.2. Hybrid Fractional Temperature Field Calculation

For solving the fractional temperature equation in Equation (10), initial and boundary conditions given in Equation (11) have been used.

Fourier Sine Transform is applied to Equation (10) as first step in this approach and the RHS and LHS are obtained as follows:

$$F_s[D_{\tau}^{\alpha} v(x,\tau)] = D_{\tau}^{\alpha} v(q,\tau) \tag{16}$$

$$F_s\left[\frac{\partial^2 v(x,\tau)}{\partial x^2}\right] = qv(0,\tau) - q^2 v(q,\tau) \tag{17}$$

where the Fourier Sine Transformation is denoted by F_s and the Fourier sine variable is q.

By replacing Equations (16) and (17) in the Fourier Sine Transform of Equation (10), the below Equation (18) is obtained,

$$D_{\tau}^{\alpha} v(q,\tau) = \frac{a_4}{Pr}[qv(0,\tau) - q^2 v(q,\tau)] \tag{18}$$

Now proceeding to the second part of the approach, which is to apply the Laplace Transformation to Equation (18) and use Equation (11) to obtain,

$$v(q,s) = \frac{qa_4}{sPr\left(s^{\alpha} + \frac{a_4 q^2}{Pr}\right)} \tag{19}$$

After some rearrangement, the Equation (20) is as below.

$$v(q,s) = \frac{a_4 q}{Pr}\left[\left(\frac{1}{s} - \frac{s^{\alpha-1}}{s^{\alpha} + \frac{a_4 q^2}{Pr}}\right)\frac{Pr}{a_4 q^2}\right] \tag{20}$$

To solve Equation (20), the inverse Laplace Transform is used, which generates the following relationship.

$$v(q,\tau) = \frac{1}{q}\left[1 - L^{-1}\left[\frac{s^{\alpha-1}}{s^{\alpha} + \frac{a_4 q^2}{Pr}}\right]\right] \tag{21}$$

In order to obtain the analytical solution for Equation (21), the Mittag-Leffler function [44] is used. That is:

Let $\alpha > 0$, $\beta \in \mathbb{R}$ and $z \in \mathbb{C}$. The Mittag-Leffler function is defined by the series:

$$E_{\alpha,\beta}(z) = \sum_{k=0}^{\infty} \frac{z^k}{\Gamma \alpha k + \beta} \text{ when } \alpha > 0 \text{ and } \beta > 0, \text{ the series is convergent.} \tag{22}$$

By doing so, $\beta = 1$, $z = -\lambda\tau^{\alpha}$ and $\lambda = \frac{a_4 q^2}{Pr}$ in Equation (22) and compare Equations (21) and (22), which after simplification acquire the following form:

$$E_{\alpha}(-\frac{a_4 q^2}{Pr}\tau^{\alpha}) = L^{-1}\left[\frac{s^{\alpha-1}}{s^{\alpha} + \frac{a_4 q^2}{Pr}}\right] \tag{23}$$

By replacing Equation (23) in Equation (21),

$$v(q,\tau) = \left[1 - E_\alpha\left(-\frac{q^2 a_4}{Pr}\tau^\alpha\right)\right]\frac{1}{q} \tag{24}$$

This technique is completed by employing the inverse Fourier Sine Transformation to Equation (24) and use the fact of integration $\int_0^\infty \frac{\sin qx}{q} dq = \frac{\pi}{2}$, resulting in:

$$v(x,\tau) = \frac{2}{\pi}\int_0^\infty v(q,\tau)\sin qx dq$$

$$v(x,\tau) = 1 - \frac{2}{\pi}\int_0^\infty \frac{\sin qx}{q} E_\alpha(-\frac{a_4 q^2 \tau^\alpha}{Pr})dq \tag{25}$$

3.3. Hybrid Fractional Velocity Field Calculation

For solving the fractional momentum equation, the Fourier Sine Transformation is applied to Equation (9) and considering $\mu = 1 + \frac{1}{\beta}$ the simplified equation is

$$D_\tau^\alpha u(q,\tau) = a_7\mu q u(0,\tau) - a_7\mu q^2 u(q,\tau) - a_{10}Mu(q,\tau) + a_{12}Grv(q,\tau) \tag{26}$$

and utilizing the Laplace Transform to Equation (26) with the use of Equation (11) yields that,

$$s^\alpha u(q,s) = a_7\mu q\frac{1}{s} - a_7\mu q^2 u(q,s) - a_{10}Mu(q,s) + a_{12}Grv(q,s) \tag{27}$$

With further simplifications Equation (27), reduces to:

$$u(q,s) = \frac{\mu q a_7}{s(s^\alpha + \mu q^2 a_7 + a_{10}M)} + \frac{Grq a_4 a_{12}}{sPr(s^\alpha + \mu q^2 a_7 + a_{10}M)(s^\alpha + \frac{a_4 q^2}{Pr})} \tag{28}$$

where,

$$a(q,s) = \frac{\mu q a_7}{s(s^\alpha + \mu q^2 a_7 + Ma_{10})},$$
$$b(q,s) = \frac{Grq a_4 a_{12}}{sPr(s^\alpha + \mu q^2 a_7 + a_{10}M)(s^\alpha + \frac{a_4 q^2}{Pr})}$$

The inverse of the function $b(q,s)$ is rewritten as below.

$$b(q,s) = \frac{Grq a_4 a_{12}}{Pr}\left[\frac{s^{\alpha-(1+\alpha)}}{s^\alpha + \frac{a_4 q^2}{Pr}} - \frac{s^{\alpha-(1+\alpha)}}{s^\alpha + \mu a_7 q^2 + Ma_{10}}\right] \tag{29}$$

$$b(q,s) = \frac{Gra_4 a_{12}}{Prq(\mu a_7 - \frac{a_4}{Pr} + \frac{Ma_{10}}{q^2})}\left[\frac{s^{\alpha-(1+\alpha)}}{s^\alpha + \frac{a_4 q^2}{Pr}} - \frac{s^{\alpha-(1+\alpha)}}{s^\alpha + \mu a_7 q^2 + Ma_{10}}\right] \tag{30}$$

The inverse of Laplace Transformation is used to Equation (30) to obtain:

$$b(q,\tau) = \frac{Gra_4 a_{12}}{Prq(\mu a_7 - \frac{a_4}{Pr} + \frac{Ma_{10}}{q^2})}\left[L^{-1}\left(\frac{s^{\alpha-\beta}}{s^\alpha + \frac{a_4 q^2}{Pr}}\right) - L^{-1}\left(\frac{s^{\alpha-\beta}}{s^\alpha + \mu a_7 q^2 + Ma_{10}}\right)\right] \tag{31}$$

where $\beta = 1 + \alpha$.

Using the Mittag-Leffler function as described in Equation (22) and further simplifying, it reduces to:

$$\tau^\alpha\left[E_{\alpha,\beta}(-\lambda t^\alpha)\right] = L^{-1}\left(\frac{s^{\alpha-\beta}}{s^\alpha + \lambda}\right) \tag{32}$$

By comparing Equations (31) and (32) and substituting $\lambda = \frac{a_4 q^2}{Pr}$, $\lambda = \mu a_7 q^2 + Ma_{10}$ the following form is obtained:

$$b(q,\tau) = \frac{Gra_4 a_{12}\tau^\alpha}{Prq(\mu a_7 - \frac{a_4}{Pr} + \frac{Ma_{10}}{q^2})}\left[E_{\alpha,\beta}(-\frac{q^2 a_4}{Pr}\tau^\alpha) - E_{\alpha,\beta}(-\mu q^2 a_7 - Ma_{10})\tau^\alpha\right] \tag{33}$$

Using the inverse Fourier Sine Transform formula:

$$b(x,\tau) = \frac{2}{\pi}\int_0^\infty b(q,\tau)\sin qx dq$$

$$b(x,\tau) = \frac{2Gra_4 a_{12}}{\pi Pr}\int_0^\infty \frac{\sin qx}{q(\mu a_7 - \frac{a_4}{Pr} + \frac{Ma_{10}}{q^2})}\left[E_{\alpha,\beta}(-\frac{q^2 a_4}{Pr})\tau^\alpha - E_{\alpha,\beta}(-\mu q^2 a_7 - Ma_{10})\tau^\alpha\right]dq \tag{34}$$

Again, the function $a(q,s)$ is rewritten as:

$$a(q,s) = \frac{\mu a_7}{q(\mu a_7 + \frac{Ma_{10}}{q^2})}\left[\frac{1}{s} - \frac{s^{\alpha-1}}{s^\alpha + \mu q^2 a_7 + Ma_{10}}\right]$$

and employing the inverse Laplace Transformation, solution is written in terms of Mittag-Leffler function as follows:

$$a(q,\tau) = \frac{\mu a_7}{q(\mu a_7 + \frac{Ma_{10}}{q^2})}\left[1 - L^{-1}\left[\frac{s^{a-1}}{s^\alpha + \mu q^2 a_7 + Ma_{10}}\right]\right] \tag{35}$$

$$E_{\alpha,1}(-\lambda\tau^\alpha) = L^{-1}\left[\frac{s^{a-1}}{s^\alpha + \lambda}\right] \tag{36}$$

Using the inverse Fourier Sine Transform, it implies that,

$$a(q,\tau) = \frac{\mu a_7}{q(\mu a_7 + \frac{Ma_{10}}{q^2})}\left[1 - E_\alpha(-q^2\mu a_7 - Ma_{10})\tau^\alpha\right]$$

where $\lambda = \mu a_7 q^2 + Ma_{10}$

$$a(x,\tau) = \frac{2}{\pi}\left[\int_0^\infty \frac{\mu a_7 \sin qx}{q(\mu a_7 + \frac{Ma_{10}}{q^2})}dq - \int_0^\infty \frac{\mu a_7 \sin qx}{q(\mu a_7 + \frac{Ma_{10}}{q^2})}E_\alpha(-q^2\mu a_7 - Ma_{10})\tau^\alpha dq\right] \tag{37}$$

The exact solution is,

$$u(x,\tau) = a(x,\tau) + b(x,\tau) \tag{38}$$

where,

$$a(x,\tau) = \frac{2}{\pi}\left[\int_0^\infty \frac{\mu a_7 \sin qx}{q(\mu a_7 + \frac{Ma_{10}}{q^2})}dq - \int_0^\infty \frac{\mu a_7 \sin qx}{q(\mu a_7 + \frac{Ma_{10}}{q^2})}E_\alpha(-q^2\mu a_7 - Ma_{10})\tau^\alpha dq\right]$$

$$b(x,\tau) = \frac{2Gra_4 a_{12}}{\pi Pr}\int_0^\infty \frac{\sin qx}{q(\mu a_7 - \frac{a_4}{Pr} + \frac{Ma_{10}}{q^2})}\left[E_{\alpha,\beta}(-\frac{q^2 a_4}{Pr})\tau^\alpha - E_{\alpha,\beta}(-\mu q^2 a_7 - Ma_{10})\tau^\alpha\right]dq$$

3.4. Limiting Cases

3.4.1. Temperature Field for Classic Case with Hybrid Nanoparticles

The temperature expression corresponding to $\alpha \to 1$ in Equation (10) reduces to the following expression,

$$v(x,\tau) = erfc(\frac{x\sqrt{Pr}}{2\sqrt{\tau a_4}})$$

where $erfc$ is a Gaussian error function.

3.4.2. Velocity Field for Classical Case with Hybrid Nanoparticles

The velocity expression corresponding to $\alpha \to 1$ in Equation (9) reduces to the following expression.

$$\begin{aligned}
u(x,\tau) &= \tfrac{1}{2}\left[e^{x\sqrt{a_{15}}}erfc\left(\tfrac{x}{2\sqrt{a_7\tau B}} + \sqrt{a_{15}a_7\tau B}\right) + e^{-x\sqrt{a_{15}}}erfc\left(\tfrac{x}{2\sqrt{a_7\tau B}} - \sqrt{a_{15}a_7\tau B}\right)\right] \\
&+ \tfrac{a_{13}}{2a_{14}}\left[e^{x\sqrt{a_{15}}}erfc\left(\tfrac{x}{2\sqrt{a_7\tau B}} + \sqrt{a_{15}a_7\tau B}\right) + e^{-x\sqrt{a_{15}}}erfc\left(\tfrac{x}{2\sqrt{a_7\tau B}} - \sqrt{a_{15}a_7\tau B}\right)\right] \\
&- \tfrac{a_{13}e^{\sqrt{a_{14}}\tau}}{2a_{14}}\left[e^{x\sqrt{a_{16}}}erfc\left(\tfrac{x}{2\sqrt{a_7\tau B}} + \sqrt{a_{16}a_7\tau B}\right) + e^{-x\sqrt{a_{16}}}erfc\left(\tfrac{x}{2\sqrt{a_7\tau B}} - \sqrt{a_{16}a_7\tau B}\right)\right] \\
&- \tfrac{a_{13}}{a_{14}}erfc(\tfrac{x\sqrt{Pr}}{2\sqrt{\tau a_4}}) \\
&+ \tfrac{a_{13}e^{\sqrt{a_{14}}\tau}}{2a_{14}}\left[e^{x\sqrt{\frac{a_{14}Pr}{a_4}}}erfc\left(\tfrac{x\sqrt{Pr}}{2\sqrt{a_4\tau}} + \sqrt{a_{14}\tau}\right) + e^{-x\sqrt{\frac{a_{14}Pr}{a_4}}}erfc\left(\tfrac{x\sqrt{Pr}}{2\sqrt{a_4\tau}} - \sqrt{a_{14}\tau}\right)\right]
\end{aligned}$$

where,

$$B = 1 + \frac{1}{\beta},\ a_{13} = -\frac{Gra_4a_{12}}{Pra_7B - a_4},\ a_{14} = \frac{Ma_4a_{10}}{a_7BPr - a_4},\ a_{15} = \frac{Ma_{10}}{a_7B}, a_{16} = \frac{a_{14}}{a_7B} + \frac{Ma_{10}}{a_7B}$$

3.4.3. Velocity Field for Classic Newtonian Fluid with Hybrid Nanoparticles

In the case of velocity for classical Newtonian fluid, the following expression is obtained by making $\beta \to \infty$, $\alpha \to 1$ in Equation (9):

$$\begin{aligned}
u(x,\tau) &= \tfrac{1}{2}\left[e^{x\sqrt{a_{19}}}erfc\left(\tfrac{x}{2\sqrt{a_7\tau}} + \sqrt{a_{19}a_7\tau}\right) + e^{-x\sqrt{a_{19}}}erfc\left(\tfrac{x}{2\sqrt{a_7\tau}} - \sqrt{a_{19}a_7\tau}\right)\right] \\
&+ \tfrac{a_{18}}{2a_{17}}\left[e^{x\sqrt{a_{19}}}erfc\left(\tfrac{x}{2\sqrt{a_7\tau}} + \sqrt{a_{19}a_7\tau}\right) + e^{-x\sqrt{a_{19}}}erfc\left(\tfrac{x}{2\sqrt{a_7\tau}} - \sqrt{a_{19}a_7\tau}\right)\right] \\
&- \tfrac{a_{18}e^{\tau a_{17}}}{2a_{17}}\left[e^{x\sqrt{a_{20}}}erfc\left(\tfrac{x}{2\sqrt{a_7\tau}} + \sqrt{a_{20}a_7\tau}\right) + e^{-x\sqrt{a_{20}}}erfc\left(\tfrac{x}{2\sqrt{a_7\tau}} - \sqrt{a_{20}a_7\tau}\right)\right] \\
&- \tfrac{a_{18}}{a_{17}}erfc(\tfrac{x\sqrt{Pr}}{2\sqrt{\tau a_4}}) \\
&+ \tfrac{a_{18}e^{\sqrt{a_{17}}\tau}}{2a_{17}}\left[e^{x\sqrt{\frac{a_{17}Pr}{a_4}}}erfc\left(\tfrac{x\sqrt{Pr}}{2\sqrt{a_4\tau}} + \sqrt{a_{17}\tau}\right) + e^{-x\sqrt{\frac{a_{17}Pr}{a_4}}}erfc\left(\tfrac{x\sqrt{Pr}}{2\sqrt{a_4\tau}} - \sqrt{a_{17}\tau}\right)\right]
\end{aligned}$$

where,

$$a_{17} = \frac{Ma_4a_{10}}{a_7Pr - a_4},\ a_{18} = -\frac{Gra_4a_{12}}{a_7Pr - a_4},\ a_{19} = \frac{Ma_{10}}{a_7},\ a_{20} = \frac{a_{17}}{a_7} + \frac{Ma_{10}}{a_7}$$

3.5. Analytical Expressions for the Heat Transfer and Shear Stress

Heat transmission rate along with shear stress are two important physical quantities that are analyzed to gain access to a wide range of information, such as efficacy of hybrid nanofluids, elements that improve or deteriorate hybrid nanofluid thermal efficiency, the role of accompanying development in deriving hybrid nanofluid flow patterns, and various others. Utilizing the importance of these values, the following mathematical relationships are predicted, which are mentioned as skin friction coefficient (C_f) and Nusselt number (Nu).

Nusselt number from Equation (25), an analytical expression of the dimensionless rate of heat transfer (Nu) is:

$$Nu = -\frac{\partial v}{\partial x}|_{x=0} = -L^{-1}\left[\lim_{x\to 0}\frac{\partial \overline{v}}{\partial x}\right]$$

$$Nu = \sqrt{\frac{Pr}{a_4}}\frac{\tau^{-\frac{\alpha}{2}}}{\Gamma 1-\frac{\alpha}{2}}$$

Skin friction from Equation (38), an analytical expression of the dimensionless skin friction is given by:

$$C_f = -\frac{\partial u}{\partial x}|_{x=0} = -L^{-1}\left[\lim_{x\to 0}\frac{\partial \overline{u}}{\partial x}\right]$$

$$\begin{aligned} C_f = \; & \frac{1}{\sqrt{Aa_7}}\left[\frac{t^{-\frac{\alpha}{2}}}{\Gamma-\frac{\alpha}{2}+1} - \sum_{k=1}^{\infty}\frac{(2k-2)!(-1)^k A_1{}^k t^{\alpha(k-\frac{1}{2})}}{2^{2k-1}(k)!(k-1)!\Gamma\alpha(k-\frac{1}{2})+1}\right] \\ & -\frac{A_4}{\sqrt{Aa_7}}\left[\frac{1}{\Gamma-\frac{\alpha}{2}+1}\int_0^t u^{\alpha-1}E_{\alpha,\alpha}(A_3u^{\alpha})(t-u)^{-\frac{\alpha}{2}}du\right] \\ & -\frac{A_4}{\sqrt{Aa_7}}\left[\sum_{k=1}^{\infty}\frac{(2k-2)!(-1)^k A_1{}^k}{2^{2k-1}(k)!(k-1)!\Gamma\alpha(k-\frac{1}{2})+1}\int_0^t u^{\alpha-1}E_{\alpha,\alpha}(A_3u^{\alpha})(t-u)^{\alpha(k-\frac{1}{2})}du\right] \\ & +\frac{A_4}{\sqrt{Aa_7}}\sqrt{\frac{Pr}{a_4}}\left[\frac{1}{\Gamma-\frac{\alpha}{2}+1}\int_0^t u^{\alpha-1}E_{\alpha,\alpha}(A_3u^{\alpha})(t-u)^{-\frac{\alpha}{2}}du\right] \end{aligned}$$

where,

$$A_1 = Ma_{10},\ A_2 = BPra_7,\ A_3 = \frac{A_1a_4}{A_2-a_4},\ A_4 = -\frac{Gra_4a_{12}}{A_1-a_4}$$

4. Graphical Findings and Outcomes

This section goes through graphical examination of temperature, flow field domains obtained for fractional order PDEs and flow parameters appearing in the problem. The fractional fluid model is determined analytically using the Laplace and Fourier Sine Transform methods. The Prandtl number, time, thermal Grashof number, Casson parameter, magnetic field, volume fraction parameters ϕ_1 and ϕ_2 are investigated and justified with a physical perspective. Recognizing the significance of shape effects, nanoparticles are thought to have five distinct shapes (brick, blade, cylinder, spherical and platelet). The impact of various flow characteristics is examined by using plotted curves in Figures 3–20 to illustrate various impacts on flow field, temperature, heat flow rate and friction drag, also illustrated with tables, bar graphs to analyze different elements of the topic under study. These graphical, tabular representations aid in understanding the effects of additional processes such as heat flow and energy fields. This section also includes a pictorial comparison of fractional and classical model-based solutions to emphasize their importance. A complete tabular analysis is also used to analyze the Nusselt number and skin friction.

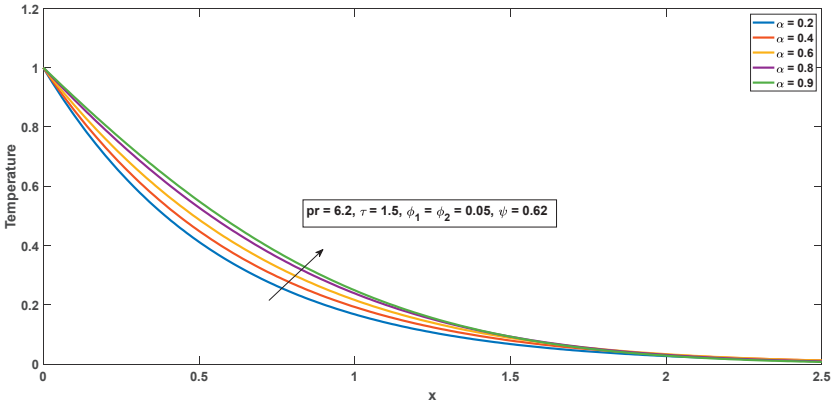

Figure 3. Fluid temperature for varied values of order α.

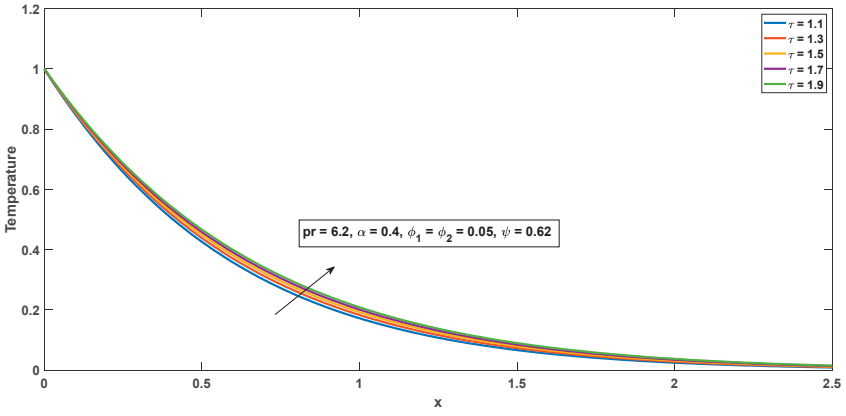

Figure 4. Fluid temperature for varied values of τ.

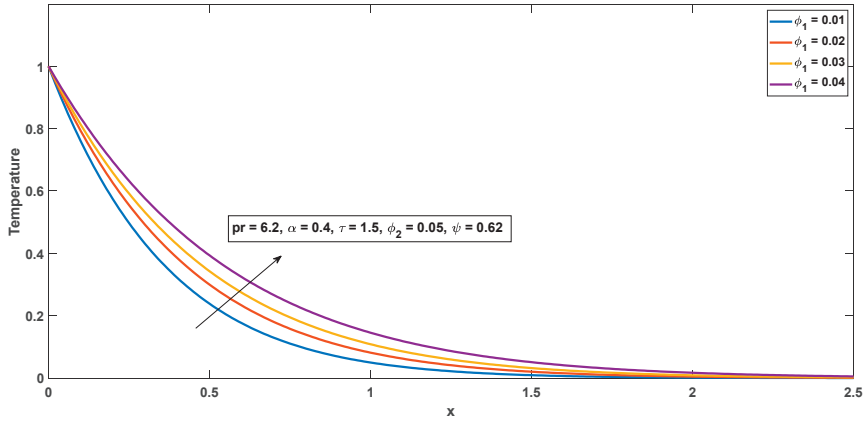

Figure 5. Fluid temperature for varied values of ϕ_1.

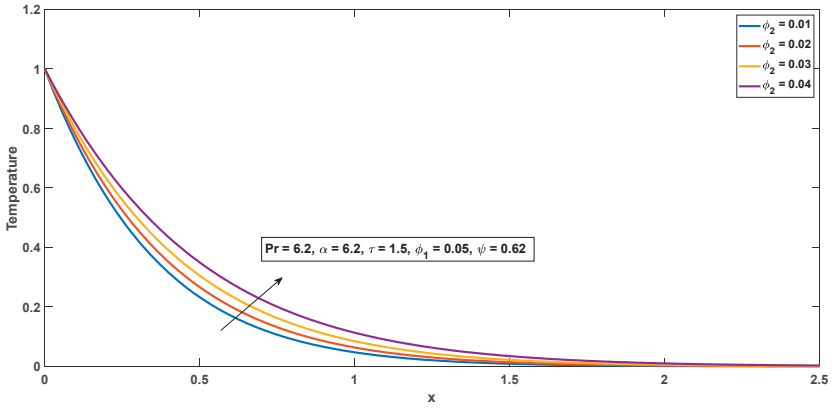

Figure 6. Fluid temperature for varied values of ϕ_2.

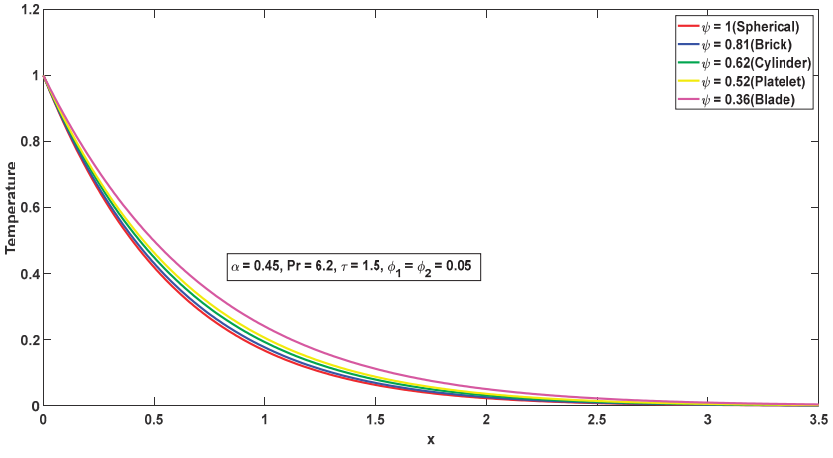

Figure 7. Fluid temperature for distinct shapes.

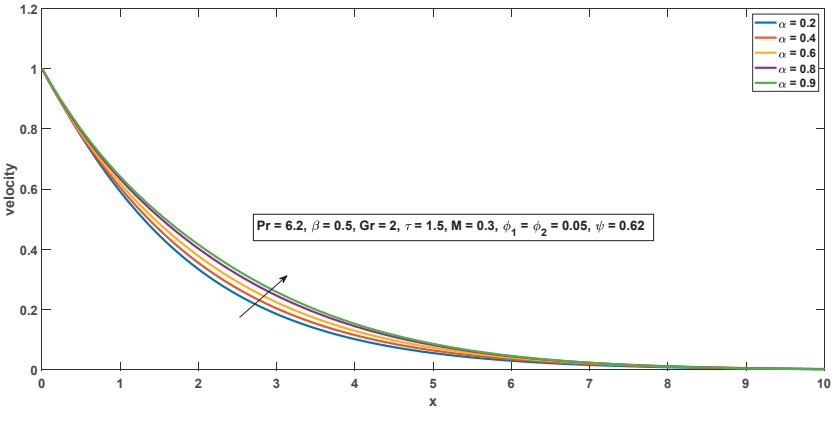

Figure 8. Fluid flow curve for varied values of fractional order α.

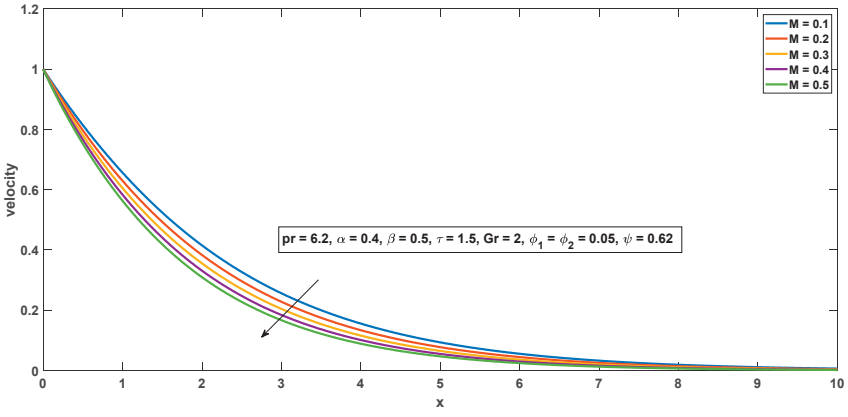

Figure 9. Fluid flow curve for varied values of M.

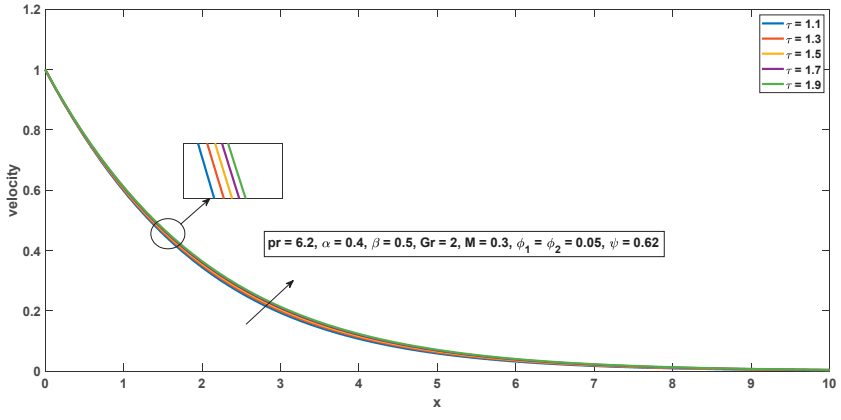

Figure 10. Fluid flow curve for varied values of τ.

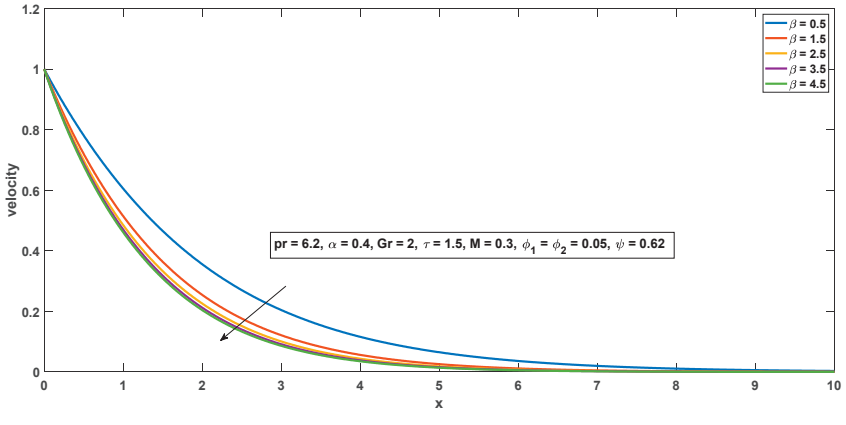

Figure 11. Fluid flow curve for varied values of β.

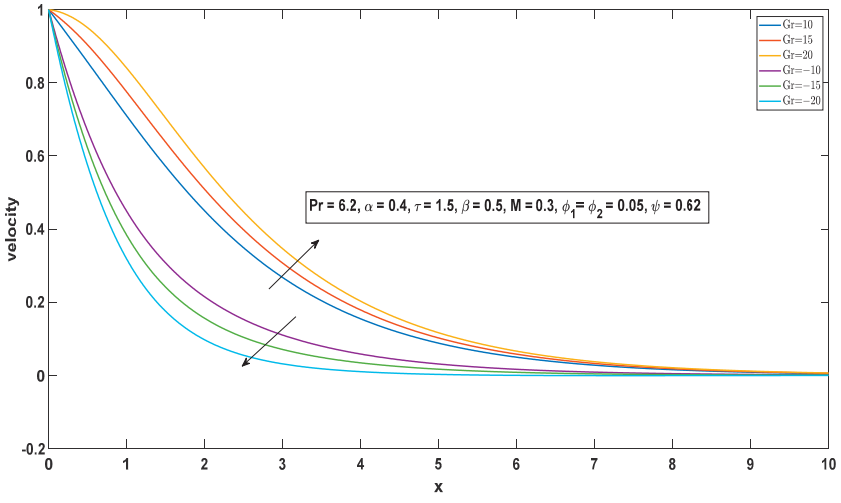

Figure 12. Fluid flow curve for varied values of Gr.

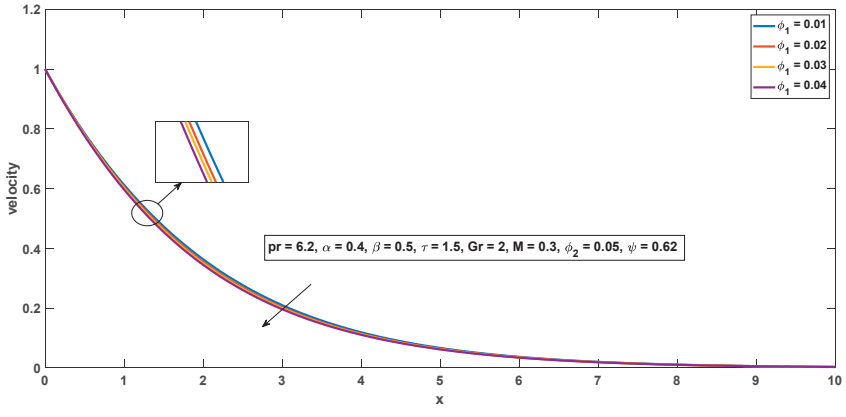

Figure 13. Fluid flow curve for varied values of ϕ_1.

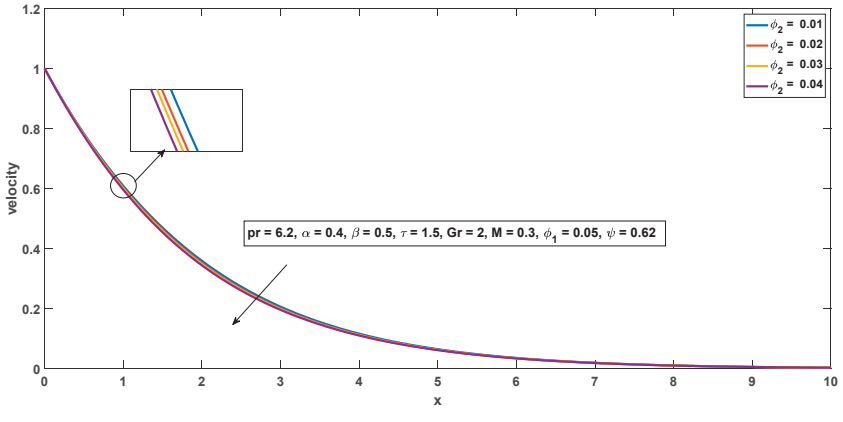

Figure 14. Fluid flow curve for varied values of ϕ_2.

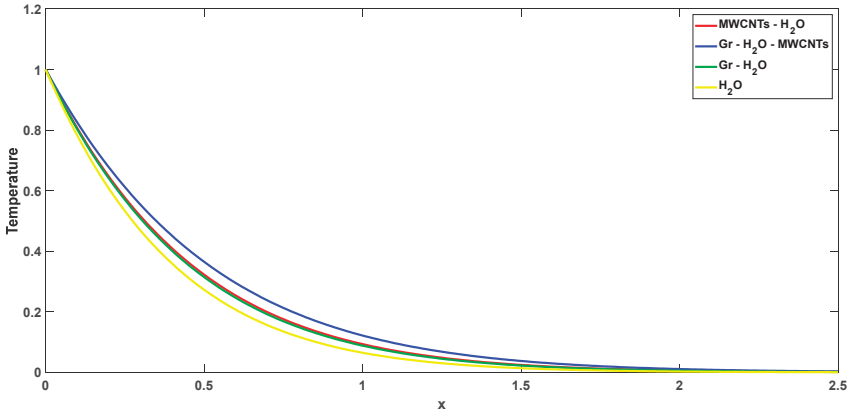

Figure 15. Fluid temperature for distinct nanofluids.

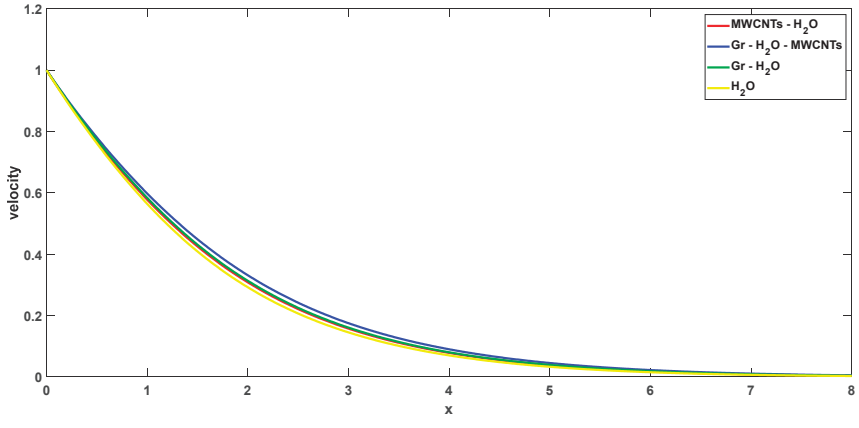

Figure 16. Fluid flow curve for distinct nanofluids.

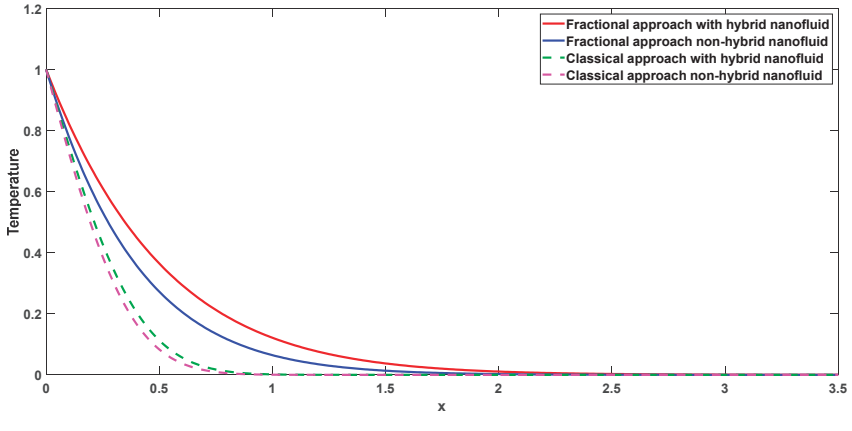

Figure 17. Fluid temperature for different fractional and classical approach.

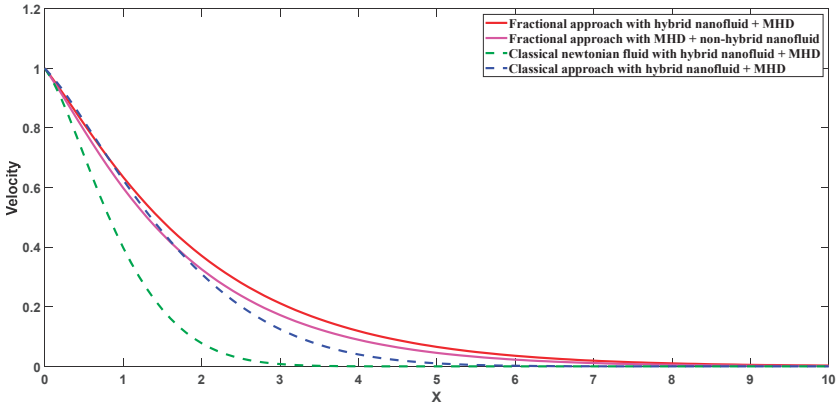

Figure 18. Fluid flow curve for different fractional and non-Newtonian approach.

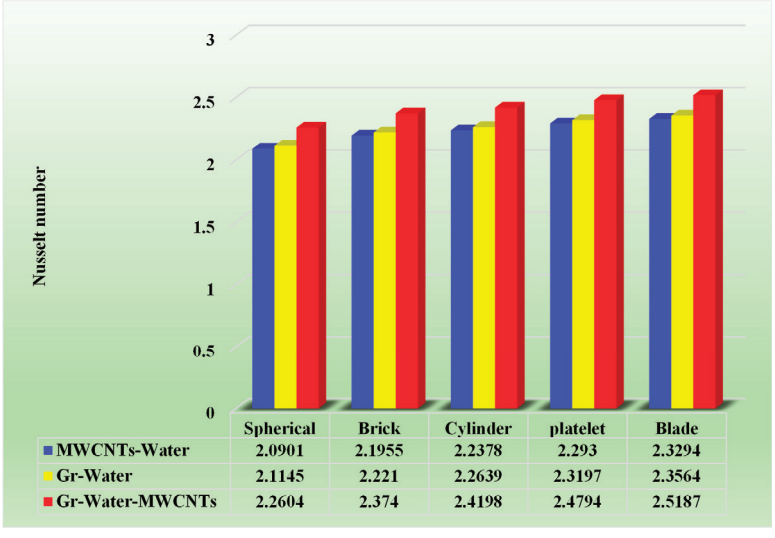

	Spherical	Brick	Cylinder	platelet	Blade
MWCNTs-Water	2.0901	2.1955	2.2378	2.293	2.3294
Gr-Water	2.1145	2.221	2.2639	2.3197	2.3564
Gr-Water-MWCNTs	2.2604	2.374	2.4198	2.4794	2.5187

Figure 19. Heat transfer enhancement in different nano particle shape.

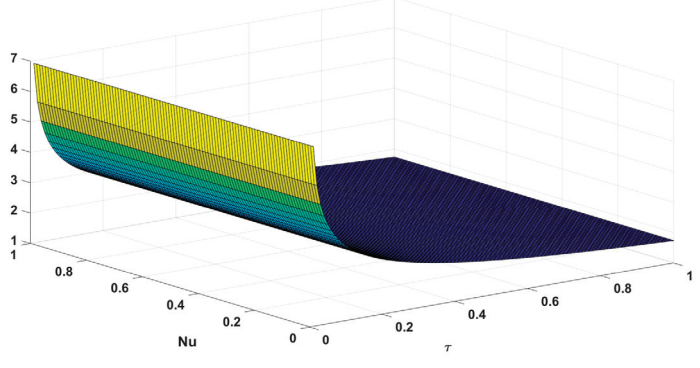

Figure 20. 3D graph for Nusselt number.

4.1. Impact of Physical Parameters on Temperature Field

The energy of Equation (11), whose solution is obtained as presented in Equation (25), has been used for the figures in this section. The temperature profile for fractional order, $\alpha = 0.4$ is considered for various flow parameters.

The impact of fractional parameters against temperature distribution is seen in Figure 3. When $\tau = 1.5$, the temperature field rises with a growing α. Physically, this is explained by the fact that as α increases, the thickness of the thermal boundary layer also increases, which becomes thickest as α approaches 1. The novelty arises from explaining how temperature rises as the order of the fractional operator advances. Because of the memory effect inherent in fractional operators, increases in order have a considerable impact on time value, resulting in a large accumulation. When the order of the fractional operator is raised, it is seen that an increase in time causes a rise in fluid temperature. A sub-diffusion in the range of (0, 1) is also noticed. When the order is modified, the literature's results corroborate Caputo's fractional derivative sub-diffusion (0, 1).

Figure 4 represents the impact of time on the temperature field. In the above fractional case, the temperature rises gradually as the value of time increases. This suggests that when the time under consideration exceeds one, the Caputo derivative has a slower impact on the diffusion process.

The temperature field is considerably impacted by the volume fraction of the hybrid nanofluid, as seen in Figures 5 and 6. The temperature field is noted to grow with increasing volume fraction values, i.e., ϕ_1 and ϕ_2. The physical factors of the hybrid nanofluid clearly show that a rise in ϕ_1 and ϕ_2 leads to an increase in the heat transfer of the hybrid nanofluid, thus resulting in the increase of temperature profile. This is due to the fact that when density of nanoparticles is enhanced, heat conductivity is improved.

The temperature field for different shapes of nanoparticles is represented in Figure 7. Due to the shape factor p included in Table 3, it is seen that the temperature of the blade-shaped nanoparticle is the highest, preceded by the platelet, cylinder, brick, and spherical. It is critical to remember that viscosity decreases as temperature rises. It is obvious that the shapes of platelets, cylinders, and bricks have more viscosity, resulting in lower temperatures, whereas blades and spherical ones have the greatest temperature due to the lowest viscosity. The figure also shows that the spherical form of the nanoparticle has a low viscosity. This is due to the temperature-dependent shear thinning behavior.

4.2. Impact of Physical Parameters on Flow Field

In this section Equation (10), whose solution is obtained as shown in Equation (39) has been taken into account to plot all the figures. Velocity dynamics for distinct flow parameters is illustrated for fractional order situation, $\alpha = 0.4$.

Figure 8 exhibits the impact of fractional order in relation to time. The velocity falls as the order of the Caputo derivative rises. Meaning to say, as order α accelerates the velocity decreases to zero, which also means increasing time causes an increase in the flow field, thus resulting in this outcome.

Figure 9 demonstrates the velocity curve of the magnetic field M parameter. The graph shows that as the magnetic field levels increased, the velocity decreased. This resulted from the application of the transverse magnetic field, which produces the resistive Lorentz force. The Lorentz force, which tends to oppose the flow of hybrid nanofluid, causes the velocity to decrease. When M is raised, the Lorentz force becomes more intense, enabling the hybrid nanofluid to gently come to a halt.

Figure 10 captures the time τ effect on the velocity field, the velocity increases gradually with time growth. This demonstrates that the Caputo derivative has a lesser influence on the diffusion process when the time under consideration reaches one.

Figure 11 shows the consequences of the Casson parameter when the other values are held constant. It illustrates that higher values of β tend to a reduction in fluid velocity. This is due to the physical impact of β, where a larger value of β will increase viscous forces while decreasing thermal forces. Thus, fluid velocity will tend to decrease.

Figure 12 represents the impact of the thermal Grashof number in cooling and heating scenarios. The Grashof number is defined as the ratio of buoyancy force to viscous force acting on a fluid, with fluid motion being linearly dependent on buoyancy force. In convection problems, the thermal Grashof number is responsible for heat transmission. This graph shows how the velocity field rises as the Grashof number increases in case of cooling of the plate $(Gr > 0)$ and the symmetry phenomenon is noted in the heating scenario $(Gr < 0)$. In addition, the symmetry effect is observed from the figure. The Grashof number represents the buoyancy force proportional strength to viscous force; hence, increase in Grashof number corresponds to increase in thermal buoyancy force. As a result, the velocity field tends to expand.

Figures 13 and 14 indicate the effect of hybrid nanofluid volume fraction on flow field. It is noted that the flow field of the hybrid nanofluid decelerates as the values of either ϕ_1 or ϕ_2 increases. The physical explanation for this phenomenon is that as the volume fraction ϕ_1 and ϕ_2 of the hybrid nanoparticle increases, fluid becomes more viscous, resulting in decrement of the nanofluid's flow field. Adding nanomaterials to a fluid raises its density, which decreases both boundary layer thickness and nanofluid velocity; velocity decelerates as time exceeds.

Figures 15 and 16 describe the comparison between the flow field and temperature distribution of the graphene–H_2O–MWCNT hybrid nanofluid to those of the equivalent nanofluids graphene–H_2O and MWCNT–H_2O and the base fluid H_2O. The profiles of the afore stated nanofluids are displayed by employing either $\phi_{Gr} = 0$ or $\phi_{MWCNT} = 0$ in the solutions obtained for hybrid nanofluids. Temperature has been found to be the highest for graphene–H_2O–MWCNT hybrid nanofluid, further observing the trend in temperature profiles followed by MWCNT–H_2O nanofluid, graphene–H_2O nanofluid and base fluid H_2O, in that order. MWCNT nanoparticles have a considerably superior heat-conduction capacity than graphene nanoparticles and water. When MWCNT nanoparticles are disseminated in the host fluid, the resulting MWCNTs–H_2O nanofluid has a higher temperature than graphene–H_2O nanofluid temperature, due to improved thermal and physical features such as heat capacitance and thermal conductivity. Moreover, the even dispersion of considered nanoparticles ($\phi_{Gr} = 0.05 = \phi_{MWCNT}$) improves the thermal conductivity of H_2O in such a way that the heat transfer capacity of the resulting hybrid nanofluid exceeds the heat transfer capacity of H_2O, graphene–H_2O nanofluid and MWCNT–H_2O nanofluid. The performance of the temperature curve is mostly determined by the thermal properties and volume percentage of the nanoparticles under consideration. This temperature fluctuation caused by various nanoparticles emphasizes the importance of nanofluids and hybrid nanofluids in heat control systems. Moreover, H_2O has the higher fluid flow velocity in comparison to other nanoparticles, which is followed by MWCNT–H_2O, graphene–H_2O and H_2O–graphene–MWCNT. The primary cause of these flow patterns is the disparity in nanoparticle density. According to Table 2, the density of host fluid is substantially lower than that of nanoparticles, making it less viscid for everyone. Greater the density of nanoparticles, the more viscid the resulting nanofluid. According to the figure, evenly spreading both nanoparticles in host fluid, results in an increase in the density of hybrid nanofluid.

In Figures 17 and 18, the curves are plotted in order to reveal a comparison between fractional and classical derivative calculus for both cases of hybrid and non-hybrid nanofluids. In the case of temperature, the figure reveals that the temperature of fractional hybrid nanofluid is faster followed by fractional non-hybrid than regular fluids. The fractional derivative model with hybrid nanofluid reveals a better heat transfer enhancement than the classical approach. In the velocity case the fractional hybrid fluid shows the high velocity followed by fractional non- hybrid, Newtonian fluid $(\alpha \to 1,\ \beta \to \infty)$ with hybrid while it has lower velocity for the classical fluid in limiting case.

Figure 19 was plotted to determine the applicability of fractional models for attaining a quicker temperature reduction. In the bar graph shown, numerical values of heat transmission rate (Nu) for fractional derivatives are in comparison with nanofluids and

hybrid nanofluids. Moreover, notable emphasis is given to the shape constituent, which resembles certain shapes of disseminated nanoparticles. Heat transmission from vertical plate to hybrid nanofluid happens faster when graphene and MWCNT nanoparticles have a blade form. When spherical-shaped nanoparticles are disseminated in water, the cooling rate of the plate is slower. This disparity in numerical results of Nusselt's number emphasizes the significance of the shape component. Based on these arguments, it is possible to conclude that the morphologies of nanoparticles play a critical part in improving the poor thermal properties of conventional fluids. As a result, evaluating shape factor qualities is an important aspect of such investigations.

The plotting shown in Figure 20 represents the 3D curves for the Nusselt number.

The impact of flow parameters on the Nusselt number is presented in Table 4. According to the table, increasing fractional parameter α, time τ, ϕ_{MWCNT} and ϕ_{Gr} leads to an decrement in the heat transfer rate, whereas increasing Prandtl number Pr, results in heat transfer increasing. The Nusselt number is defined as the ratio of convective heat transfer coefficient to fluid conduction heat transfer; a high Nusselt number value will almost certainly raise the fluid's temperature as heat is transferred at a faster pace, as seen in Figures 3–6.

Table 4. The influence of the various parameters on the Nusselt Number.

ϕ_{Gr}	ϕ_{MWCNT}	Pr	α	τ	Nu
0.02	0.02	6.2	0.6	1.5	1.591572294587753
0.03	-	-	-	-	1.569480227825062
0.04	-	-	-	-	1.547886513587993
-	0.03	-	-	-	1.562898376223181
-	0.04	-	-	-	1.534893820304120
-	-	8	-	-	1.807904639541740
-	-	9	-	-	1.917572445537878
-	-	-	0.8	-	1.332170104172774
-	-	-	0.9	-	1.202904460764115
-	-	-	-	1.7	1.532918522253240
-	-	-	-	1.8	1.506856850036236

Table 5 demonstrates the percent improvement in Nusselt number vs. different volume fraction values of ϕ_{Gr} and ϕ_{MWCNT}. The heat transmission rate of water-based hybrid nanofluid is shown in table for graphene and MWCNT utilized in this investigation, because they have a high heat transfer rate in the base fluid water. It is remarkable that for graphene and multiwall carbon nanotubes in water, the heat flow rate increases by 17.7 percent. This increase in heat transfer rate indicates that radiators used in engines or machines for cooling might be useful for mechanical engineers. Graphene and MWCNT are used as a photoanode and counter electrode in industries for manufacturing solar cells (dye-sensitized solar cells) to increase the efficiency.

Table 6 compares the heat transmission rates for distinct constituents of graphene and MWCNT nanoparticles as well as changes in their ratio in the base fluid. This table shows that, as the shape components values are increased from 3.0 to 8.3, Nu increases. In addition, it is recognized that, of all the investigated combinations, hybrid nanofluid achieves the best heat transmission rate when it is made of spherical-shaped graphene nanoparticles and blade-shaped MWCNT nanoparticles, as well as brick-shaped graphene nanoparticles and spherical-shaped MWCNTs.

Table 5. The effect of volume fraction on Nusselt number and increased percent.

ϕ_{Gr}	ϕ_{MWCNT}	Pr	α	τ	Nu	% Increased
0.00	0.00	6.2	0.4	1.5	1.9721	-
0.01	0.01	6.2	0.4	1.5	1.8751	4.9
0.02	0.02	6.2	0.4	1.5	1.7850	9.5
0.03	0.03	6.2	0.4	1.5	1.7011	13.7
0.04	0.04	6.2	0.4	1.5	1.6229	17.7

Table 6. Nusselt number varies for various combinations of shape components (p_1 and p_2).

ϕ_{Gr}	ϕ_{MWCNT}	$p_1 = 3.0$				$p_2 = 3.0$			
		$p_2 = 3.7$	$p_2 = 4.9$	$p_2 = 5.7$	$p_2 = 8.3$	$p_1 = 3.7$	$p_1 = 4.9$	$p_1 = 5.7$	$p_1 = 8.3$
0.01	0.01	1.9506	1.9545	1.9562	1.9594	1.9421	1.9341	1.9301	1.9139
0.02	0.02	1.9291	1.9368	1.9402	1.9467	1.9122	1.8965	1.8888	1.8577
0.03	0.03	1.9076	1.9190	1.9241	1.9338	1.8826	1.8596	1.8482	1.8034
0.04	0.04	1.8860	1.9012	1.9079	1.9208	1.8532	1.8231	1.8085	1.7509

Table 7 portrays the impact of flow parameters on skin friction near the vertical plate. As observed here, increasing Prandtl number, ϕ_{MWCNT}, M, α, β and time leads to increase in shear stress whereas increasing ϕ_{Gr} and Gr results in decrement of shear stress.

Table 7. The influence of the various parameters on the skin friction.

ϕ_{Gr}	ϕ_{MWCNT}	Pr	α	τ	β	Gr	M	C_f
0.03	0.03	6.2	0.45	0.5	1.5	2	2	0.959525615427890
0.04	-	-	-	-	-	-	-	0.952001945188767
0.05	-	-	-	-	-	-	-	0.944169083022009
-	0.04	-	-	-	-	-	-	0.966946221691135
-	0.05	-	-	-	-	-	-	0.974469891930258
-	-	12	-	-	-	-	-	0.942932315311468
-	-	15	-	-	-	-	-	0.944117551034069
-	-	-	0.65	-	-	-	-	1.094127167925078
-	-	-	0.9	-	-	-	-	1.246661852225108
-	-	-	-	0.7	-	-	-	1.091373887426613
-	-	-	-	0.9	-	-	-	1.206821899771669
-	-	-	-	-	2.5	-	-	1.061352823595748
-	-	-	-	-	4.5	-	-	1.151739930441103
-	-	-	-	-	-	4	-	0.877486690628685
-	-	-	-	-	-	6	-	0.796478405588264
-	-	-	-	-	-	-	3	1.131848583096572
-	-	-	-	-	-	-	5	1.422179803146021

Table 8 shows the comparison of the classic and fractional approaches for various values of the Prandtl number and t = 0.5 in the temperature field. The two approaches demonstrate a high level of agreement.

Table 8. Comparison of classic and fractional approach when $\phi = 0$.

Pr	Classic Approach ($\alpha = 1$) (Soundalgekar V.M [45])	Fractional Approach ($\alpha = 0.95$)	Difference
0.71	0.3994	0.4029	0.0035
1.0	0.0082	0.0117	0.0035
1.5	0.3173	0.3234	0.0061
7.0	0.2207	0.2295	0.0088

5. Conclusions

A model for the natural convection MHD flow of generalized non-Newtonian fluid containing graphene and MWCNT nanoparticles was derived using the Caputo fractional derivatives. The outcomes of the investigated flow characteristics exhibit several remarkable behaviours that allow for further research of the various flow models. The following conclusions are brought up:

- The order of fractional derivatives can induce an increment or decrement in flow field and temperature depending on the time factor.
- In the case of cooling the plate, the fluid flow trend accelerates as the value of the Grashof number rises, whereas in the scenario of heating the plate, the reverse trend is observed.
- Heat transmission rate of water-based hybrid nanofluid with cylindrical shaped nanoparticles are 4.9%, 9.5%, 13.7% and 17.7% greater as compared to regular fluid for volume fraction ϕ = 0.01 to 0.04, respectively.
- The blade-shaped hybrid nanoparticles are the most effective at increasing the heat transfer rate, whereas spherical nanoparticles perform at a lesser rate. These findings are significant in the long term because they help us plan for the improvement of heat transfer in cooling and heating applications.
- When compared to fluids with hybrid and non-hybrid nanofluids, fractional hybrid nanofluid shows the highest rate of heat transfer, whereas ordinary fluid shows minimum heat transmission rate. This demonstrates the fractional parameter improves fluid flow in a benchmark.

Author Contributions: Conceptualization, N.M.L. and A.G.V.; methodology, N.M.L.; software, N.M.L.; investigation, N.M.L.; writing—original draft preparation, N.M.L. and A.G.V.; writing—review and editing, N.M.L. and A.G.V. All authors have read and agreed to the published version of the manuscript.

Funding: The authors are gratefully acknowledge the Vellore Institute of Technology management for providing the necessary facilities and support to carry out this research work.

Institutional Review Board Statement: Not applicable.

Informed Consent Statement: Not applicable.

Data Availability Statement: Not applicable.

Conflicts of Interest: The authors declare no conflict of interest.

Nomenclature

u	Velocity
v	Temperature
a, b	Shape constants
Pr	Prandtl number
Gr	Grashof number
Gr	Graphene nanoparticle
$MWCNT$	Multi wall carbon nanotube

MHD	Magnetohydrodynamics
x, y	Cartesian coordinates
E_α	Mittag-Leffler function
Nu	Nusselt number
Cf	Skin friction coefficient
Greek symbols	
ρ_{nf}	Density of nanofluid (Kgm^{-3})
$(C_p)_{nf}$	Specific heat capacity of nanofluid $(\mathrm{JKg}^{-1}\mathrm{K}^{-1})$
$(\gamma)_{nf}$	Thermal expansion coefficient of nanofluid (K^{-1})
κ_{nf}	Thermal conductivity of nanofluid $(\mathrm{Wm}^{-1}\mathrm{K}^{-1})$
μ_{nf}	Dynamic viscosity of nanofluid $(\mathrm{Kgm}^{-1}\mathrm{s}^{-1})$
σ_{nf}	Electrical conductivity of nanofluid (Sm^{-1})
ρ_{hnf}	Density of hybrid nanofluid (Kgm^{-3})
$(C_p)_{hnf}$	Specific heat capacity of hybrid nanofluid $(\mathrm{JKg}^{-1}\mathrm{K}^{-1})$
$(\gamma)_{hnf}$	Thermal expansion coefficient of hybrid nanofluid (K^{-1})
κ_{hnf}	Thermal conductivity of hybrid nanofluid $(\mathrm{Wm}^{-1}\mathrm{K}^{-1})$
μ_{hnf}	Dynamic viscosity of hybrid nanofluid $(\mathrm{Kgm}^{-1}\mathrm{s}^{-1})$
σ_{hnf}	Electrical conductivity of hybrid nanofluid (Sm^{-1})
g	Specific gravity (Kgm^{-3})
B_0	Magnetic field strength (Wbm^{-1})
α	Fractional parameter
β	Casson parameter
τ	Time
γ	Volumetric coefficient of thermal expansion
ψ	Sphericity of nanoparticles
ϕ_1	Volume fraction of Graphene
ϕ_2	Volume fraction of MWCNTs
Subscripts	
f	Fluid
nf	Nanofluid
hnf	Hybrid nanofluid
np	Nanoparticle
w	Wall
∞	Ambient condition

References

1. Maxwell, J.C. *A Treatise on Electricity and Magnetism*; Clarendon Press: London, UK, 1873.
2. Choi, S.U.; Eastman, J.A. *Enhancing Thermal Conductivity of Fluids with Nanoparticles*; Argonne National Lab. (ANL): Argonne, IL, USA, 1995.
3. Pîslaru-Dănescu, L.; Morega, A.M.; Telipan, G.; Morega, M.; Dumitru, J.B.; Marinescu, V. Magnetic nanofluid applications in electrical engineering. *IEEE Trans. Magn.* **2013**, *49*, 5489–5497. [CrossRef]
4. Khodabandeh, E.; Safaei, M.R.; Akbari, S.; Akbari, O.A.; Alrashed, A.A. Application of nanofluid to improve the thermal performance of horizontal spiral coil utilized in solar ponds: Geometric study. *Renew. Energy* **2018**, *122*, 1–6. [CrossRef]
5. Bahiraei, M.; Hangi, M. Investigating the efficacy of magnetic nanofluid as a coolant in double-pipe heat exchanger in the presence of magnetic field. *Energy Convers. Manag.* **2013**, *76*, 1125–1133. [CrossRef]
6. Mekheimer, K.S.; Shahzadi, I.; Nadeem, S.; Moawad, A.M.; Zaher, A.Z. Reactivity of bifurcation angle and electroosmosis flow for hemodynamic flow through aortic bifurcation and stenotic wall with heat transfer. *Phys. Scr.* **2020**, *96*, 015216. [CrossRef]
7. Ayub, M.; Shahzadi, I.; Nadeem, S. A ballon model analysis with Cu-blood medicated nanoparticles as drug agent through overlapped curved stenotic artery having compliant walls. *Microsyst. Technol.* **2019**, *25*, 2949–2962. [CrossRef]
8. Siddique, I.; Sadiq, K.; Khan, I.; Nisar, K.S. Nanomaterials in convection flow of nanofluid in upright channel with gradients. *J. Mater. Res. Technol.* **2021**, *11*, 1411–1423. [CrossRef]
9. Aleem, M.; Asjad, M.I.; Shaheen, A.; Khan, I. MHD Influence on different water based nanofluids (TiO_2, Al_2O_3, CuO) in porous medium with chemical reaction and newtonian heating. *Chaos Solit. Fractals* **2020**, *130*, 109437. [CrossRef]
10. Shafiq, A.; Hammouch, Z.; Sindhu, T.N. Bioconvective MHD flow of tangent hyperbolic nanofluid with newtonian heating. *Int. J. Mech. Sci.* **2017**, *133*, 759–766. [CrossRef]
11. Yamada, A.; Sasabe, H.; Osada, Y.; Shiroda, Y.; Yamamoto, I. *Concepts of Hybrid Materials, Hybrid Materials—Concept and Case Studies*; ASM International: Novelty, OH, USA, 1989.

12. Shahzadi, I.; Bilal, S.A. Significant role of permeability on blood flow for hybrid nanofluid through bifurcated stenosed artery: Drug delivery application. *Comput. Methods Programs Biomed.* **2020**, *187*, 105248. [CrossRef]
13. Shahzadi, I.; Nadeem, S. Stimulation of metallic nanoparticles under the impact of radial magnetic field through eccentric cylinders: A useful application in biomedicine. *J. Mol. Liq.* **2017**, *225*, 365–381. [CrossRef]
14. Shahzadi, I.; Nadeem, S. A comparative study of Cu nanoparticles under slip effects through oblique eccentric tubes, a biomedical solicitation examination. *Can. J. Phys.* **2019**, *97*, 63–81. [CrossRef]
15. Javadi, H.; Urchueguia, J.F.; Mousavi Ajarostaghi, S.S.; Badenes, B. Impact of employing hybrid nanofluids as heat carrier fluid on the thermal performance of a borehole heat exchanger. *Energies* **2021**, *14*, 2892. [CrossRef]
16. Jamshed, W.; Alanazi, A.K.; Isa, S.S.; Banerjee, R.; Eid, M.R.; Nisar, K.S.; Alshahrei, H.; Goodarzi, M. Thermal efficiency enhancement of solar aircraft by utilizing unsteady hybrid nanofluid: A single-phase optimized entropy analysis. *Sustain. Energy Technol. Assess.* **2022**, *52*, 101898. [CrossRef]
17. Hafeez, M.U.; Hayat, T.; Alsaedi, A.; Khan, M.I. Numerical simulation for electrical conducting rotating flow of Au (Gold)-Zn (Zinc)/EG (Ethylene glycol) hybrid nanofluid. *Int. Commun. Heat Mass Transf.* **2021**, *124*, 105234. [CrossRef]
18. Waini, I.; Ishak, A.; Groşan, T.; Pop, I. Mixed convection of a hybrid nanofluid flow along a vertical surface embedded in a porous medium. *Int. Commun. Heat Mass Transf.* **2020**, *114*, 104565. [CrossRef]
19. Anwar, T.; Kumam, P.; Thounthong, P. A comparative fractional study to evaluate thermal performance of NaAlg–MoS_2–Co hybrid nanofluid subject to shape factor and dual ramped conditions. *Alex. Eng. J.* **2022**, *61*, 2166–2187. [CrossRef]
20. Balaji, T.; Rajendiran, S.; Selvam, C.; Lal, D.M. Enhanced heat transfer characteristics of water based hybrid nanofluids with graphene nanoplatelets and multi walled carbon nanotubes. *Powder Technol.* **2021**, *394*, 1141–1157. [CrossRef]
21. Khan, M.; Lone, S.A.; Rasheed, A.; Alam, M.N. Computational simulation of Scott-Blair model to fractional hybrid nanofluid with Darcy medium. *Int. Commun. Heat Mass Transf.* **2022**, *130*, 105784. [CrossRef]
22. Roy, N.C.; Pop, I. Analytical investigation of transient free convection and heat transfer of a hybrid nanofluid between two vertical parallel plates. *Phys. Fluids* **2022**, *34*, 072005. [CrossRef]
23. Sene, N. Analytical investigations of the fractional free convection flow of Brinkman type fluid described by the Caputo fractional derivative. *Results Phys.* **2022**, *37*, 105555. [CrossRef]
24. Khan, Z.A.; Haq, S.U.; Khan, T.S.; Khan, I.; Nisar, K.S. Fractional Brinkman type fluid in channel under the effect of MHD with Caputo-Fabrizio fractional derivative. *Alex. Eng. J.* **2020**, *59*, 2901–2910. [CrossRef]
25. Reyaz, R.; Lim, Y.J.; Mohamad, A.Q.; Saqib, M.; Shafie, S. Caputo fractional MHD Casson Fluid flow over an oscillating plate with thermal radiation. *J. Adv. Res. Fluid Mech. Therm. Sci.* **2021**, *85*, 145–158. [CrossRef]
26. Casson, N. A flow equation for pigment-oil suspensions of the printing ink type. *Rheol. Disperse Syst.* **1959**, 10021830093.
27. Raza, A.; Khan, S.U.; Farid, S.; Khan, M.I.; Sun, T.C.; Abbasi, A.; Khan, M.I.; Malik, M.Y. Thermal activity of conventional Casson nanoparticles with ramped temperature due to an infinite vertical plate via fractional derivative approach. *Case Stud. Therm. Eng.* **2021**, *27*, 101191. [CrossRef]
28. Shahrim, M.N.; Mohamad, A.Q.; Jiann, L.Y.; Zakaria, M.N.; Shafie, S.; Ismail, Z.; Kasim, A.R. Exact solution of fractional convective Casson Fluid through an accelerated plate. *CFD Lett.* **2021**, *13*, 15–25. [CrossRef]
29. Krishna, M.V.; Ahammad, N.A.; Chamkha, A.J. Radiative MHD flow of Casson hybrid nanofluid over an infinite exponentially accelerated vertical porous surface. *Case Stud. Therm. Eng.* **2021**, *27*, 101229. [CrossRef]
30. Kilbas, A.A.; Srivastava, H.M.; Trujillo, J.J. *Theory and Applications of Fractional Differential Equations*; North-Holland Mathematics Studies; Elsevier: Amsterdam, The Netherlands, 2006.
31. Caputo, M. Linear models of dissipation whose Q is almost frequency independent—II. *Geophys. J. Int.* **1967**, *13*, 529–539. [CrossRef]
32. Anwar, T.; Kumam, P. A fractal fractional model for thermal analysis of GO− NaAlg− Gr hybrid nanofluid flow in a channel considering shape effects. *Case Stud. Therm. Eng.* **2022**, *31*, 101828. [CrossRef]
33. Saqib, M.; Khan, I.; Shafie, S. Application of Atangana–Baleanu fractional derivative to MHD channel flow of CMC-based-CNT's nanofluid through a porous medium. *Chaos Solit. Fractals* **2018**, *116*, 79–85. [CrossRef]
34. Daud, M.M.; Jiann, L.Y.; Mahat, R.; Shafie, S. Application of Caputo Fractional Derivatives to the Convective Flow of Casson Fluids in a Microchannel with Thermal Radiation. *J. Adv. Res. Fluid Mech. Therm. Sci.* **2022**, *93*, 50–63. [CrossRef]
35. Ahmad, M.; Imran, M.A.; Nazar, M. Mathematical modeling of ($Cu-A l_2 O_3$) water based Maxwell hybrid nanofluids with Caputo-Fabrizio fractional derivative. *Adv. Mech. Eng.* **2020**, *12*, 1687814020958841. [CrossRef]
36. Aman, S.; Zokri, S.M.; Ismail, Z.; Salleh, M.Z.; Khan, I. Casson model of MHD flow of SA-based hybrid nanofluid using Caputo time-fractional models. *Defect Diffus.* **2019**, *390*, 83–90. [CrossRef]
37. Sene, N. Analytical solutions of a class of fluids models with the Caputo fractional derivative. *Fractal Fract.* **2022**, *6*, 35. [CrossRef]
38. Nakamura, M.; Sawada, T. Numerical study on the flow of a non-Newtonian fluid through an axisymmetric stenosis. *J. Biomech. Eng.* **1990**, *112*, 100–103. [CrossRef] [PubMed]
39. Shah, N.A.; Khan, I. Heat transfer analysis in a second grade fluid over and oscillating vertical plate using fractional Caputo–Fabrizio derivatives. *Eur. Phys. J. C* **2016**, *76*, 362. [CrossRef]
40. Reddy, S.R.; Reddy, P.B. Entropy generation analysis on MHD flow with a binary mixture of ethylene glycol and water based silver-graphene hybrid nanoparticles in automotive cooling systems. *Int. J. Heat Technol.* **2021**, *39*, 1781–1790. [CrossRef]

41. Curtis, W.D.; Logan, J.D.; Parker, W.A. Dimensional analysis and the pi theorem. *Linear Algebra Its Appl.* **1982**, *47*, 117–126. [CrossRef]
42. Sene, N. Stokes' first problem for heated flat plate with Atangana–Baleanu fractional derivative. *Chaos Solit. Fractals* **2018**, *117*, 68–75. [CrossRef]
43. Abro, K.A.; Khan, I.; Gómez-Aguilar, J.F. Thermal effects of magnetohydrodynamic micropolar fluid embedded in porous medium with Fourier Sine Transform technique. *J. Braz. Soc. Mech. Sci. Eng.* **2019**, *41*, 174. [CrossRef]
44. Podlubny, I. *Fractional Differential Equations, Mathematics in Science and Engineering*; Academic Press: New York, NY, USA, 1999.
45. Soundalgekar, V.M. Free convection effect on the stokes problem for a vertical plate in an elasto-viscous fluid. *Czechoslov. J. Phys.* **1978**, *28*, 721–727. [CrossRef]

fractal and fractional

MDPI

Article

Bifurcations and the Exact Solutions of the Time-Space Fractional Complex Ginzburg-Landau Equation with Parabolic Law Nonlinearity

Wenjing Zhu [1], Zijie Ling [1], Yonghui Xia [2,*] and Min Gao [1]

[1] School of Mathematics, China Jiliang University, Hangzhou 310018, China
[2] Department of Mathematics, Zhejiang Normal University, Jinhua 321004, China
* Correspondence: xiadoc@163.com or yhxia@zjnu.cn

Abstract: This paper studies the bifurcations of the exact solutions for the time–space fractional complex Ginzburg–Landau equation with parabolic law nonlinearity. Interestingly, for different parameters, there are different kinds of first integrals for the corresponding traveling wave systems. Using the method of dynamical systems, which is different from the previous works, we obtain the phase portraits of the the corresponding traveling wave systems. In addition, we derive the exact parametric representations of solitary wave solutions, periodic wave solutions, kink and anti-kink wave solutions, peakon solutions, periodic peakon solutions and compacton solutions under different parameter conditions.

Keywords: bifurcations; phase portraits; exact solutions

Citation: Zhu, W.; Ling, Z.; Xia, Y.; Gao, M. Bifurcations and the Exact Solutions of the Time-Space Fractional Complex Ginzburg-Landau Equation with Parabolic Law Nonlinearity. *Fractal Fract.* **2023**, *7*, 201. https://doi.org/10.3390/fractalfract7020201

Academic Editors: Carlo Cattani, António Lopes, Alireza Alfi, Liping Chen and Sergio Adriani David

Received: 4 January 2023
Revised: 3 February 2023
Accepted: 15 February 2023
Published: 18 February 2023

1. Introduction

The fractional complex Ginzburg–Landau (FCGL for short in the following) equation was first proposed by Weitzner and Zaslavsky [1]. It describes the dynamical processes in fractal media [2,3]. Various methods have been used to study the FCGL equation, including the semigroup method, the Galerkin method, the $\exp-\varphi(\chi)$-expansion method, Jacobian elliptic function expansion method, the improved $\tan(\psi(\xi/2))$-expansion method and so on [4–14]. For example, by employing the extended Jacobi's elliptic function expansion method, Abdou et al. [4] obtained the dark-singular combo optical solitons of the FCGL equation. Arshed [5] researched the soliton solutions of the FCGL equation with Kerr law and non-Kerr law nonlinearity. Using the modified Jacobian elliptic function expansion method, Fang et al. [6] derived the discrete fractional soliton solutions of the FCGL equation. Li et al. [7] establish the existence and uniqueness of weak solutions to the FCGL equation under the Galerkin method and a priori estimates. Lu et al. [8] studied the initial boundary value problem of the FCGL equation in three spatial dimensions. Milovanov and Rasmussen [9] discussed the fractional modifications of the free energy functional at criticality and of the widely known Ginzburg–Landau equation central to the classical Landau theory of second-type phase transitions. Mvogo et al. [10] proposed both the semi and the linearly implicit Riesz fractional finite-difference schemes to solve the FCGL equation efficiently. Pu and Guo [11] studied the global well-posedness and long-time dynamics of the FCGL equation. Qiu et al. [12] studied the soliton dynamics of an FCGL equation. Raza [13] investigated the exact periodic and explicit solutions of an FCGL equation. Sadaf et al. [14] considered the exact solutions of an FCGL equation by using the improved $\tan(\psi(\xi/2))$-expansion method.

Different from the above methods, we apply the theory of dynamical systems to research the exact solutions of the following FCGL equation with parabolic law nonlinearity:

$$i\frac{\partial^\delta u}{\partial t^\delta}+a\frac{\partial^{2\delta}u}{\partial x^{2\delta}}+b|u|^2u+c|u|^4u-\frac{1}{|u|^2u^*}\left(\alpha|u|^2\frac{\partial^{2\delta}|u|^2}{\partial x^{2\delta}}-\beta\left(\frac{\partial^\delta|u|^2}{\partial x^\delta}\right)^2\right)-\gamma u=0, \quad (1)$$

where x denotes distance along the fiber, $t>0$ denotes time in dimensionless form, a, b, c, α, β and γ are valued constants, and $0<\delta\leq 1$ denotes the order of the fractional derivative. The fractional derivative in Equation (1) is the conformable fractional derivative, defined as

$$\frac{\partial^\delta}{\partial t^\delta}f(t)=\lim_{\varepsilon\to 0}\frac{f(t+\varepsilon t^{1-\delta})-f(t)}{\varepsilon},\ 0<\delta\leq 1,$$

where $f:(0,\infty)\to R$, and $t>0$. For the conformable fractional derivative, we have following conclusions [15]:

$$\frac{\partial^\delta}{\partial t^\delta}t^k=kt^{k-\delta},\quad D_t^\delta u(t)=t^{1-\delta}\frac{du(t)}{dt},\ k\in R,\quad 0<\delta\leq 1.$$

The dynamical system theory is a useful tool to obtain the traveling wave solutions of the nonlinear partial differential equations. Via studying the number of zeros of Abelian, Chen et al. [16] obtained the periodic solutions of the Friedmann–Robertson–Walker model (also see [17,18]). Sun et al. [19] proved the existence of the periodic waves by constructing the Melnikov functions. Employing the geometric singular perturbation theory, Ge and Du [20] studied the solitary wave solutions of the perturbed shallow water wave model (also see [21–23]). Based on abstract bifurcation theory, Song and Tang [24] discussed the nonconstant solutions (also see [25]). Chen et al. [26] analyzed the global dynamics of a mechanical system (also, see [27–29]). Applying the first integral method, Deng [30] considered the solitary wave solutions of the generalized Burgers–Huxley equation. Li [31] introduced the "three-step" method to investigate the singular traveling wave equations (also see [32]). Under the "three-step" method, many results for exact solutions have been produced [15,33–43].

How do the traveling wave solutions of Equation (1) depend on the parameters of the system? Are there peakon solutions and periodic peakon solutions as well as compactons of Equation (1)? As far as we know, no one has considered these problems. In this paper, by using the method of dynamical systems, we shall consider the dynamical behavior of the bounded traveling wave solutions of Equation (1) in different parameter domains.

To achieve the research purpose, in Equation (1), we apply the traveling wave transform

$$u(x,t)=\phi(\xi)e^{i\eta(x,t)},\ \xi=\frac{x^\delta}{\delta}-v\frac{t^\delta}{\delta},\ \eta(x,t)=-\kappa\frac{x^\delta}{\delta}+\omega\frac{t^\delta}{\delta}+\theta, \quad (2)$$

where $\phi(\xi)$ represents the shape of the pulse, and v is the wave velocity. The function $\eta(x,t)$ is the phase component of the soliton, κ is the soliton frequency, ω is the wave number, and θ is the phase constant.

Then, separating the real part and the imaginary part, Equation (1) reduces to the following equations:

$$(v+2a\kappa)\phi_\xi=0, \quad (3)$$

which implies $v+2a\kappa=0$, and

$$(a-2\alpha)\phi_{\xi\xi}=(2\alpha-4\beta)\frac{\phi_\xi^2}{\phi}+(\omega+\gamma+a\kappa^2)\phi-b\phi^3-c\phi^5, \quad (4)$$

that is,

$$\frac{d\phi}{d\xi}=y,\quad \frac{dy}{d\xi}=\frac{(2\alpha-4\beta)y^2+(\omega+\gamma+a\kappa^2)\phi^2-b\phi^4-c\phi^6}{(a-2\alpha)\phi}. \quad (5)$$

As defined in Li's book [31], system (5) is the first class of the singular traveling wave system when $\alpha \neq 2\beta$, and its singular line is $\phi = 0$. However, when $\alpha = 2\beta$, system (5) is a regular system:

$$\frac{d\phi}{d\xi} = y, \quad \frac{dy}{d\xi} = \frac{1}{(a-2\alpha)}\Big((\omega+\gamma+a\kappa^2)\phi - b\phi^3 - c\phi^5\Big). \tag{6}$$

The first integral of system (5) is

$$H(\phi,y) = \phi^{\frac{4(2\beta-\alpha)}{(a-2\alpha)}}\left(y^2 - \frac{(\omega+\gamma+a\kappa^2)}{(a-4\alpha+4\beta)}\phi^2 + \frac{b}{(2a-6\alpha+4\beta)}\phi^4 + \frac{c}{(3a-8\alpha+4\beta)}\phi^6\right) = h, \tag{7}$$

if $a-4\alpha+4\beta \neq 0$, $a-3\alpha+2\beta \neq 0$ and $3a-8\alpha+4\beta \neq 0$;

$$H(\phi,y) = \frac{y^2}{\phi^2} - \frac{2(\omega+\gamma+a\kappa^2)}{(a-2\alpha)}\ln|\phi| + \frac{b}{(a-2\alpha)}\phi^2 + \frac{c}{2(a-2\alpha)}\phi^4 = h, \tag{8}$$

if $a-4\alpha+4\beta = 0$;

$$H(\phi,y) = \frac{y^2}{\phi^4} + \frac{(\omega+\gamma+a\kappa^2)}{(a-2\alpha)\phi^2} + \frac{2b}{(a-2\alpha)}\ln|\phi| + \frac{c}{(a-2\alpha)}\phi^2 = h, \tag{9}$$

if $a-3\alpha+2\beta = 0$;

$$H(\phi,y) = \frac{y^2}{\phi^6} + \frac{(\omega+\gamma+a\kappa^2)}{2(a-2\alpha)\phi^4} - \frac{b}{(a-2\alpha)\phi^2} + \frac{2c}{(a-2\alpha)}\ln|\phi| = h, \tag{10}$$

if $3a-8\alpha+4\beta = 0$.

In Section 2, through qualitative analysis, we give the phase portraits of system (5) in various parameter domains. In Sections 3–5, we figure out the exact solutions of Equation (1) in some special parameter domains. In Section 6, we give the main theory and the conclusion.

2. Bifurcations of Phase Portraits of System (5)

The associated regular system of (5) is

$$\frac{d\phi}{d\zeta} = (a-2\alpha)\phi y, \quad \frac{dy}{d\zeta} = (2\alpha-4\beta)y^2 + (\omega+\gamma+a\kappa^2)\phi^2 - b\phi^4 - c\phi^6, \tag{11}$$

where $d\xi = (a-2\alpha)\phi d\zeta$. Systems (5) and (11) have the same first integral. However, they have different time scales near the straight line $\phi = 0$ (see [31]).

Firstly, we analyze the number of equilibrium points and their parametric regions. Obviously, when $\Delta = b^2 + 4c(\omega+\gamma+a\kappa^2) > 0$, $\phi^2 = \frac{-b\pm\sqrt{\Delta}}{2c}$ make $c\phi^4 + b\phi^2 - (\omega+\gamma+a\kappa^2) = 0$. Then, we have the following conclusions:

1. System (11) has only one equilibrium point $E_0(0,0)$ in the ϕ-axis if $\Delta < 0$; or $\Delta > 0, c > 0, b > 0, \omega+\gamma+a\kappa^2 \leq 0$; or $\Delta > 0, c < 0, b < 0, \omega+\gamma+a\kappa^2 \geq 0$; or $\Delta = 0, bc > 0$.

2. System (11) has three equilibrium points $E_0(0,0)$, $E_1\left(\sqrt{\frac{-b+\sqrt{\Delta}}{2c}},0\right)$ and $E_2\left(-\sqrt{\frac{-b+\sqrt{\Delta}}{2c}},0\right)$ in the ϕ-axis if $\Delta > 0, c > 0, \omega+\gamma+a\kappa^2 > 0$; System (11) has three equilibrium points $E_0(0,0)$, $E_3\left(\sqrt{\frac{-b-\sqrt{\Delta}}{2c}},0\right)$ and $E_4\left(-\sqrt{\frac{-b-\sqrt{\Delta}}{2c}},0\right)$ in the ϕ-axis if $\Delta > 0, c < 0, \omega+\gamma+a\kappa^2 < 0$; System (11) has three equilibrium points $E_0(0,0)$, $E_5\left(\sqrt{-\frac{b}{2c}},0\right)$ and $E_6\left(-\sqrt{-\frac{b}{2c}},0\right)$ in the ϕ-axis if $\Delta = 0, bc < 0$.

3. System (11) has five equilibrium points $E_0(0,0)$, $E_1\left(\sqrt{\frac{-b+\sqrt{\Delta}}{2c}},0\right)$, $E_2\left(-\sqrt{\frac{-b+\sqrt{\Delta}}{2c}},0\right)$ $E_3\left(\sqrt{\frac{-b-\sqrt{\Delta}}{2c}},0\right)$ and $E_4\left(-\sqrt{\frac{-b-\sqrt{\Delta}}{2c}},0\right)$ in the ϕ-axis if $\Delta>0, c>0, b<0, \omega+\gamma+a\kappa^2<0$; or $\Delta>0, c<0, b>0, \omega+\gamma+a\kappa^2>0$.

Secondly, in order to judge the type of an equilibrium point $E_j(\phi_j, y_j)$, we should know the sign of $J(\phi_j, y_j) = \det M(\phi_j, y_j)$, where M is the coefficient matrix of the corresponding linear system of (11). When $\alpha = 2\beta$, we have

$$J(0,0) = -\frac{\omega+\gamma+a\kappa^2}{a-2\alpha},\ J\left(\pm\sqrt{\frac{-b+\sqrt{\Delta}}{2c}},0\right) = \frac{\sqrt{\Delta}(\sqrt{\Delta}-b)}{c(a-2\alpha)},$$

$$J\left(\pm\sqrt{\frac{-b-\sqrt{\Delta}}{2c}},0\right) = \frac{\sqrt{\Delta}(\sqrt{\Delta}+b)}{c(a-2\alpha)},\ J\left(\pm\sqrt{-\frac{b}{2c}},0\right) = 0.$$

when $\alpha \neq 2\beta$, we have

$$J(0,0) = 0,\ J\left(\pm\sqrt{\frac{-b+\sqrt{\Delta}}{2c}},0\right) = \frac{(a-2\alpha)\sqrt{\Delta}(\sqrt{\Delta}-b)^2}{2c^2},$$

$$J\left(\pm\sqrt{\frac{-b-\sqrt{\Delta}}{2c}},0\right) = -\frac{(a-2\alpha)\sqrt{\Delta}(\sqrt{\Delta}+b)^2}{2c^2},\ J\left(\pm\sqrt{-\frac{b}{2c}},0\right) = 0.$$

If $J<0$, then the equilibrium point $E_j(\phi_j, y_j)$ is a saddle; if $J>0$, then it is a center; if $J=0$ and the index of the equilibrium point is zero, then it is a cusp.

Next, we write that

$$h_0 = H(0,0) = 0(\infty) \text{ for } \frac{4(2\beta-\alpha)}{(a-2\alpha)} \geq 0(<0),$$

$$h_1 = H\left(\sqrt{\frac{-b+\sqrt{\Delta}}{2c}},0\right),\ h_2 = H\left(-\sqrt{\frac{-b+\sqrt{\Delta}}{2c}},0\right),\ h_3 = H\left(\sqrt{\frac{-b-\sqrt{\Delta}}{2c}},0\right),$$

$$h_4 = H\left(-\sqrt{\frac{-b-\sqrt{\Delta}}{2c}},0\right),\ h_5 = H\left(\sqrt{-\frac{b}{2c}},0\right),\ h_6 = H\left(-\sqrt{-\frac{b}{2c}},0\right),$$

where H is given by (7). We have $h_1 = h_2$, $h_3 = h_4$, $h_5 = h_6$, if $\frac{4(2\beta-\alpha)}{(a-2\alpha)} = 2n, n \in N$; and $h_1 = -h_2$, $h_3 = -h_4$, $h_5 = -h_6$, if $\frac{4(2\beta-\alpha)}{(a-2\alpha)} = 2n+1, n \in N$.

In the following, we only discuss the case of $c>0$, because there is a similar conclusion when $c<0$. Using the aforementioned data, the bifurcations of the phase portraits of (5) are given in Figures 1–6.

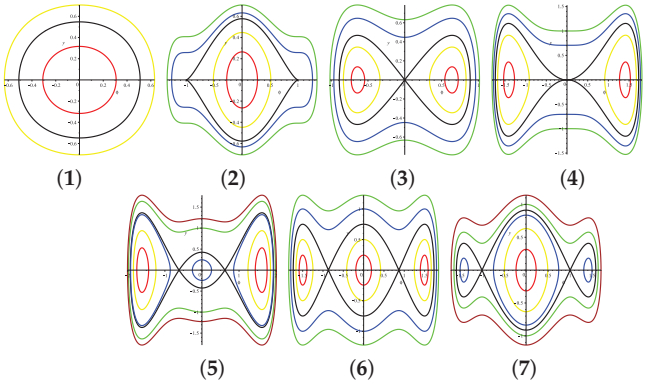

Figure 1. Phase portraits corresponding to system (5) under $c > 0, \alpha - 2\beta = 0, a - 2\alpha > 0$. (**1**) $\Delta < 0$ or $\Delta = 0, b > 0$ or $\Delta > 0, b > 0, \omega + \gamma + a\kappa^2 \geq 0$. (**2**) $\Delta = 0, b < 0$. (**3**) $\Delta > 0, \omega + \gamma + a\kappa^2 > 0$. (**4**) $\Delta > 0$, $b < 0, \omega + \gamma + a\kappa^2 = 0$. (**5**) $\Delta > 0$, $\frac{3b^2}{16c} < b < 0, \omega + \gamma + a\kappa^2 < 0$. (**6**) $\Delta > 0, b = \frac{3b^2}{16c}, \omega + \gamma + a\kappa^2 < 0$. (**7**) $\Delta > 0, b < \frac{3b^2}{16c}, \omega + \gamma + a\kappa^2 < 0$.

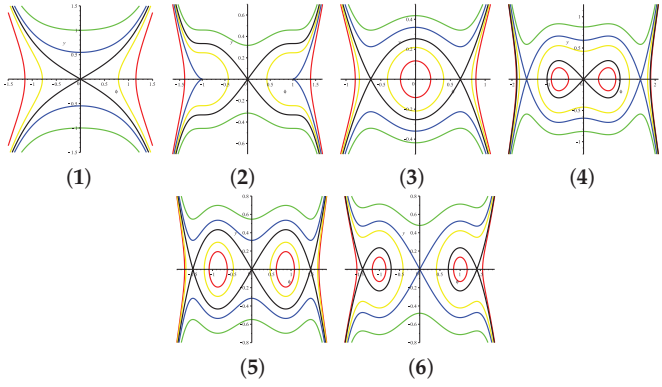

Figure 2. Phase portraits corresponding to system (5) under $c > 0, \alpha - 2\beta = 0, a - 2\alpha < 0$. (**1**) $\Delta < 0$ or $\Delta = 0, b > 0$ or $\Delta > 0, b > 0, \omega + \gamma + a\kappa^2 \geq 0$. (**2**) $\Delta = 0, b < 0$. (**3**) $\Delta > 0, \omega + \gamma + a\kappa^2 > 0$ or $\Delta > 0, b < 0, \omega + \gamma + a\kappa^2 = 0$. (**4**) $\Delta > 0$, $\frac{3b^2}{16c} < b < 0, \omega + \gamma + a\kappa^2 < 0$. (**5**) $\Delta > 0, b = \frac{3b^2}{16c}, \omega + \gamma + a\kappa^2 < 0$. (**6**) $\Delta > 0, b < \frac{3b^2}{16c}, \omega + \gamma + a\kappa^2 < 0$.

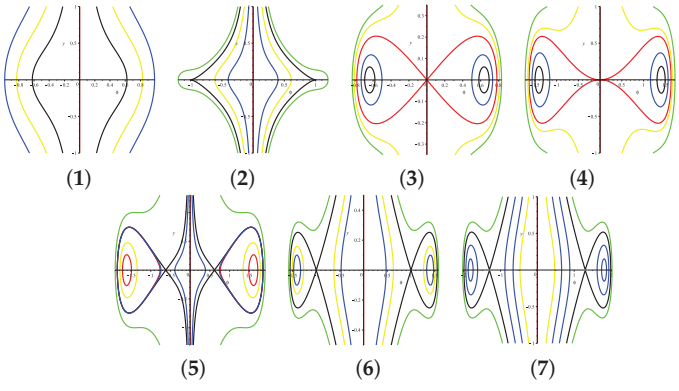

Figure 3. Phase portraits corresponding to system (5) under $c > 0, (2\beta-\alpha)(a-2\alpha) > 0, a-2\alpha > 0$. (**1**) $\Delta < 0$ or $\Delta = 0, b > 0$ or $\Delta > 0, b > 0, \omega+\gamma+a\kappa^2 \geq 0$. (**2**) $\Delta = 0, b < 0$. (**3**) $\Delta > 0$, $\omega+\gamma+a\kappa^2 > 0$. (**4**) $\Delta > 0, b < 0, \omega+\gamma+a\kappa^2 = 0$. (**5**) $\Delta > 0, b < 0, \omega+\gamma+a\kappa^2 < 0, h_1 = h_2 < h_0 < h_3 = h_4$. (**6**) $\Delta > 0, b < 0, \omega+\gamma+a\kappa^2 < 0, h_1 = h_2 = h_0 < h_3 = h_4$. (**7**) $\Delta > 0, b < 0, \omega+\gamma+a\kappa^2 < 0$, $h_0 < h_1 = h_2 < h_3 = h_4$.

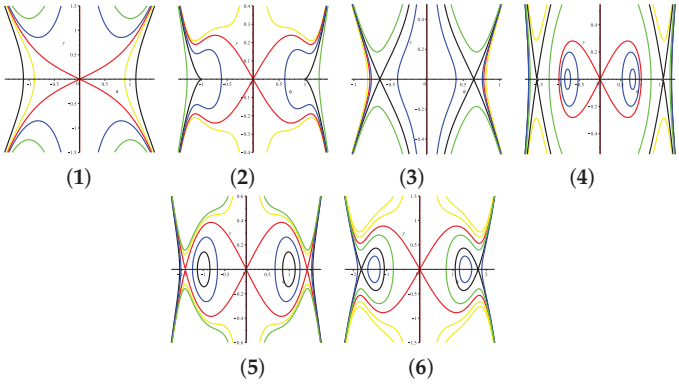

Figure 4. Phase portraits corresponding to system (5) under $c > 0, (2\beta-\alpha)(a-2\alpha) > 0, a-2\alpha < 0$. (**1**) $\Delta < 0$ or $\Delta = 0, b > 0$ or $\Delta > 0, b > 0, \omega+\gamma+a\kappa^2 \geq 0$. (**2**) $\Delta = 0, b < 0$. (**3**) $\Delta > 0$, $\omega+\gamma+a\kappa^2 > 0$ or $\Delta > 0, b < 0, \omega+\gamma+a\kappa^2 = 0$. (**4**) $\Delta > 0, b < 0, \omega+\gamma+a\kappa^2 < 0, h_3 = h_4 < h_0 < h_1 = h_2$. (**5**) $\Delta > 0, b < 0, \omega+\gamma+a\kappa^2 < 0, h_3 = h_4 < h_0 = h_1 = h_2$. (**6**) $\Delta > 0, b < 0$, $\omega+\gamma+a\kappa^2 < 0, h_3 = h_4 < h_1 = h_2 < h_0$.

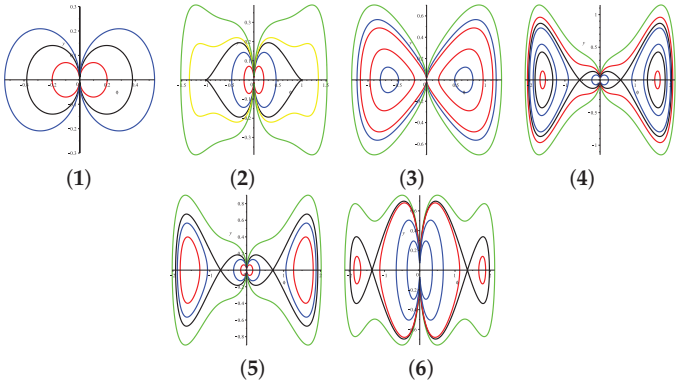

Figure 5. Phase portraits corresponding to system (5) under $c > 0, (2\beta-\alpha)(a-2\alpha) < 0, a-2\alpha > 0$. (**1**) $\Delta < 0$ or $\Delta = 0, b > 0$ or $\Delta > 0, b > 0, \omega+\gamma+a\kappa^2 \geq 0$. (**2**) $\Delta = 0, b < 0$. (**3**) $\Delta > 0$, $\omega+\gamma+a\kappa^2 > 0$ or $\Delta > 0, b < 0, \omega+\gamma+a\kappa^2 = 0$. (**4**) $\Delta > 0, b < 0, \omega+\gamma+a\kappa^2 < 0, h_1 = -h_2 < h_0 < h_3 = -h_4$. (**5**) $\Delta > 0, b < 0, \omega+\gamma+a\kappa^2 < 0, h_1 = h_2 = h_0 < h_3 = -h_4$. (**6**) $\Delta > 0$, $b < 0, \omega+\gamma+a\kappa^2 < 0, h_0 < h_1 = -h_2 < h_3 = -h_4$.

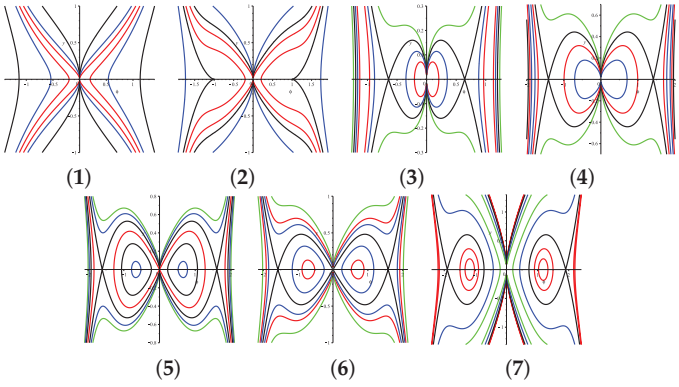

Figure 6. Phase portraits corresponding to system (5) under $c > 0, (2\beta-\alpha)(a-2\alpha) < 0, a-2\alpha < 0$. (**1**) $\Delta < 0$ or $\Delta = 0, b > 0$ or $\Delta > 0, b > 0, \omega+\gamma+a\kappa^2 \geq 0$.(**2**) $\Delta = 0, b < 0$. (**3**) $\Delta > 0, \omega+\gamma+a\kappa^2 > 0$. (**4**) $\Delta > 0, b < 0, \omega+\gamma+a\kappa^2 = 0$. (**5**) $\Delta > 0, b < 0, \omega+\gamma+a\kappa^2 < 0, h_3 = -h_4 < h_0 < h_1 = -h_2$. (**6**) $\Delta > 0, b < 0, \omega+\gamma+a\kappa^2 < 0, h_3 = -h_4 < h_0 = h_1 = h_2$. (**7**) $\Delta > 0$, $b < 0, \omega+\gamma+a\kappa^2 < 0, h_3 = -h_4 < h_1 = -h_2 < h_0$.

3. Expressions of the Traveling Wave Solutions of System (5) if $C > 0, \alpha = 2\beta$

Currently, through integral calculation, we compute the exact parametric expressions of the traveling wave solutions if $c > 0, \alpha = 2\beta$. According to Equation (7) and the first equation of system (5), we derive the following expression:

$$\xi = \int_{\phi_0}^{\phi} \frac{d\phi}{y(\phi)} = \int_{\phi_0}^{\phi} \frac{\pm d\phi}{\sqrt{\frac{c}{3(2\alpha-a)}\phi^6 + \frac{b}{2(2\alpha-a)}\phi^4 + \frac{\omega+\gamma+a\kappa^2}{a-2\alpha}\phi^2 + h}}. \tag{12}$$

3.1. The Parameter Condition of $A - 2\alpha > 0, \Delta = 0, B < 0$ (See Figure 1(2))

In formula (7), if $H(\phi, y) = h_5$, there are two heteroclinic orbits, which encircle the equilibrium point E_0 and link the saddle points E_5 and E_6. These two heteroclinic orbits correspond to kink and anti-kink wave solutions, respectively. Here, we have

$y^2 = \frac{c}{3(a-2\alpha)}\left(\sqrt{-\frac{b}{2c}} - \phi\right)^3\left(\phi + \sqrt{-\frac{b}{2c}}\right)^3$. Combined with the integral formula (12), we get the expressions of the kink wave solution as (see Figure 7a)

$$\phi(\xi) = \begin{cases} -\sqrt{\frac{b^3\xi^2}{24c^2(2\alpha-a)-2cb^2\xi^2}}, \xi \in (-\infty, 0], \\ \sqrt{\frac{b^3\xi^2}{24c^2(2\alpha-a)-2cb^2\xi^2}}, \xi \in [0, +\infty), \end{cases} \tag{13}$$

and the anti-kink wave solutions as (see Figure 7b):

$$\phi(\xi) = \begin{cases} \sqrt{\frac{b^3\xi^2}{24c^2(2\alpha-a)-2cb^2\xi^2}}, \xi \in (-\infty, 0], \\ -\sqrt{\frac{b^3\xi^2}{24c^2(2\alpha-a)-2cb^2\xi^2}}, \xi \in [0, +\infty). \end{cases} \tag{14}$$

From Equations (13) and (14), we deduce the expressions of two exact solutions of Equation (1) as

$$u(x,t) = \begin{cases} -\sqrt{\frac{b^3(x^\delta - vt^\delta)^2}{24c^2\delta^2(2\alpha-a)-2cb^2(x^\delta-vt^\delta)^2}}e^{i\eta(x,t)}, \frac{1}{\delta}(x^\delta - vt^\delta) \in (-\infty, 0], \\ \sqrt{\frac{b^3(x^\delta - vt^\delta)^2}{24c^2\delta^2(2\alpha-a)-2cb^2(x^\delta-vt^\delta)^2}}e^{i\eta(x,t)}, \frac{1}{\delta}(x^\delta - vt^\delta) \in [0, +\infty), \end{cases} \tag{15}$$

and

$$u(x,t) = \begin{cases} \sqrt{\frac{b^3(x^\delta - vt^\delta)^2}{24c^2\delta^2(2\alpha-a)-2cb^2(x^\delta-vt^\delta)^2}}e^{i\eta(x,t)}, \frac{1}{\delta}(x^\delta - vt^\delta) \in (-\infty, 0], \\ -\sqrt{\frac{b^3(x^\delta - vt^\delta)^2}{24c^2\delta^2(2\alpha-a)-2cb^2(x^\delta-vt^\delta)^2}}e^{i\eta(x,t)}, \frac{1}{\delta}(x^\delta - vt^\delta) \in [0, +\infty). \end{cases} \tag{16}$$

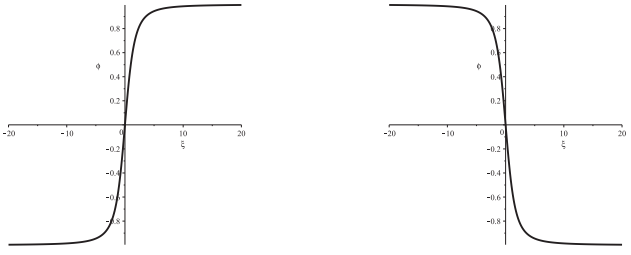

(**a**) (**b**)

Figure 7. Kink and anti-kink wave forms of system (5). (**a**) Kink wave. (**b**) Anti-kink wave.

3.2. The Parameter Condition of $A - 2\alpha > 0, \Delta > 0, \omega + \gamma + a\kappa^2 > 0$ (See Figure 1(3))

(i) In formula (7), if $H(\phi, y) = h, h \in (h_1, h_0)$, there are two families of periodic orbits, which respectively encircle the equilibrium points E_1 and E_2. These two families of periodic orbits correspond to two periodic wave solutions of system (5). At present, $y^2 = \frac{4c}{3(a-2\alpha)}(r_1 - \phi^2)(\phi^2 - r_2)(\phi^2 - r_3)$, where $r_1 > r_2 > 0 > r_3$. After calculation, we get the expressions of the two periodic wave solutions as (see Figure 8)

$$\phi(\xi) = \pm\sqrt{\frac{r_1(r_2 - r_3) + r_3(r_1 - r_2)\mathrm{sn}^2(g_1\xi, k_1)}{r_2 - r_3 + (r_1 - r_2)\mathrm{sn}^2(g_1\xi, k_1)}}, \tag{17}$$

where $g_1 = \sqrt{\frac{cr_1(r_2-r_3)}{3(a-2\alpha)}}$, $k_1^2 = \frac{r_3(r_2-r_1)}{r_1(r_2-r_3)}$.

Thus, the two exact solutions of Equation (1) are given as

$$u(x,t) = \pm\sqrt{\frac{r_1(r_2-r_3)+r_3(r_1-r_2)\mathrm{sn}^2(g_1\frac{1}{\delta}(x^\delta - vt^\delta),k_1)}{r_2-r_3+(r_1-r_2)\mathrm{sn}^2(g_1\frac{1}{\delta}(x^\delta - vt^\delta),k_1)}}e^{i\eta(x,t)}. \tag{18}$$

(ii) In formula (7), if $H(\phi,y) = h_0$, there are two homoclinic orbits, which respectively encircle the equilibrium points E_1 and E_2. The traveling wave solutions of the two homoclinic orbits are two solitary wave solutions of system (5). And, $y^2 = \frac{4c}{3(a-2\alpha)}(r_1 - \phi^2)\phi^2(\phi^2 - r_2)$, where $r_1 > 0 > r_2$.

Thus, we obtain the parametric representations of the solitary wave solutions (see Figure 9)

$$\phi(\xi) = \pm\sqrt{\frac{2r_1r_2}{r_1+r_2+(r_2-r_1)\cosh(g_2\xi)}}, \tag{19}$$

where $g_2 = \sqrt{\frac{4cr_1r_2}{3(2\alpha-a)}}$.

So, the two exact solutions of Equation (1) are given as

$$u(x,t) = \pm\sqrt{\frac{2r_1r_2}{r_1+r_2+(r_2-r_1)\cosh(g_2\frac{1}{\delta}(x^\delta - vt^\delta))}}e^{i\eta(x,t)}. \tag{20}$$

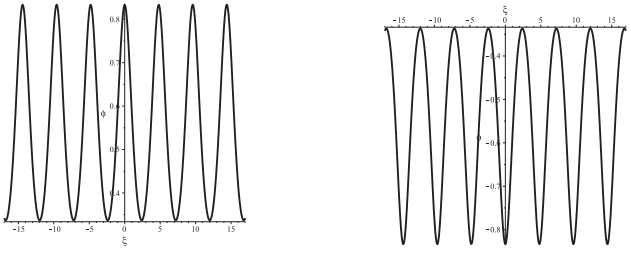

(**a**) (**b**)

Figure 8. Periodic wave forms of system (5). (**a**) Defined by $(17)_+$. (**b**) Defined by $(17)_-$.

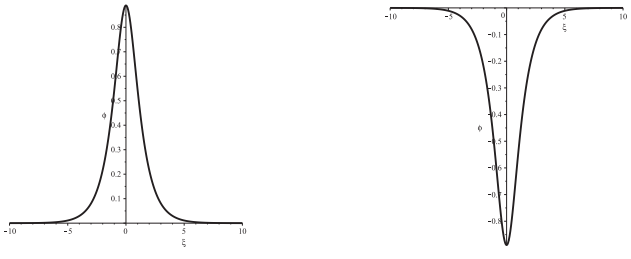

(**a**) (**b**)

Figure 9. Solitary wave forms of system (5). (**a**) Bright solitary wave derived by $(19)_+$. (**b**) Dark solitary wave derived by $(19)_-$.

3.3. The Parameter Condition of $A - 2\alpha > 0, \Delta > 0, B < 0, \omega + \gamma + a\kappa^2 = 0$ (*See Figure 1(4)*)

(i) There exist two families of periodic orbits when $H(\phi,y) = h, h \in (h_1,h_0)$, which correspond to two periodic wave solutions of system (5). They have the same expressions as Equation (17).

(ii) In formula (7), if $H(\phi,y) = h_0$, there are two homoclinic orbits, which respectively encircle the equilibrium points E_1 and E_2. The traveling wave solutions of the two homoclinic orbits are two solitary wave solutions of system (5). And, $y^2 = \frac{4c}{3(a-2\alpha)}(r_1 - \phi^2)\phi^4$,

where $r_1 > 0$. Thus, we obtain the parametric representations of the solitary wave solutions (see Figure 10):

$$\phi(\xi) = \pm\sqrt{\frac{3r_1(a-2\alpha)}{3(a-2\alpha)+cr_1^2\xi^2}}. \tag{21}$$

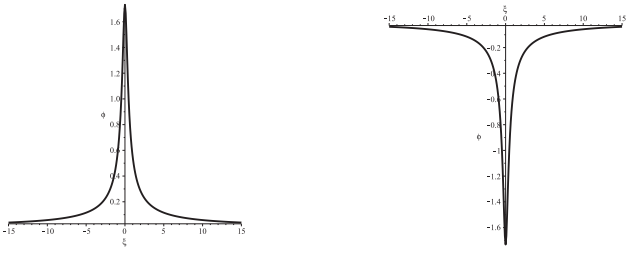

(**a**) (**b**)

Figure 10. Solitarywave forms of system (5). (**a**) Bright solitary wave derived by $(21)_+$. (**b**) Dark solitary wave derived by $(21)_-$.

So, the two exact solutions of Equation (1) are given as

$$u(x,t) = \pm\sqrt{\frac{3r_1(a-2\alpha)}{3(a-2\alpha)+cr_1^2\frac{1}{\delta^2}(x^\delta - vt^\delta)^2}}e^{i\eta(x,t)}. \tag{22}$$

3.4. The Parameter Condition of $A-2\alpha>0, \Delta>0, \frac{3b^2}{16c}<b<0, \omega+\gamma+a\kappa^2<0$ *(See Figure 1(5))*

(i) There exist two families of periodic orbits when $H(\phi, y) = h, h \in (h_1, h_0]$, which correspond to two periodic wave solutions of system (5). Their expressions are identical to Equation (17).

(ii) In formula (7), if $H(\phi, y) = h, h \in (h_0, h_3)$, there are three families of periodic orbits, which respectively encircle the equilibrium points E_0, E_1 and E_2. For the periodic orbits surrounding the equilibrium point E_0, we have $y^2 = \frac{4c}{3(a-2\alpha)}(r_1-\phi^2)(r_2-\phi^2)(r_3-\phi^2)$. Then, we compute the representation of the periodic wave solution of system (5) (see Figure 11a)

$$\phi(\xi) = \begin{cases} -\sqrt{\frac{r_2r_3-r_2r_3\mathrm{sn}^2(g_3\xi,k_2)}{r_2-r_3\mathrm{sn}^2(g_3\xi,k_2)}}, \xi \in \left[(4n+1)\xi_1, (4n+3)\xi_1\right], \\ \sqrt{\frac{r_2r_3-r_2r_3\mathrm{sn}^2(g_3\xi,k_2)}{r_2-r_3\mathrm{sn}^2(g_3\xi,k_2)}}, \xi \in \left[4n\xi_1, (4n+1)\xi_1\right] \cup \left[(4n+3)\xi_1, (4n+4)\xi_1\right], \end{cases} \tag{23}$$

where $g_3 = \sqrt{\frac{cr_2(r_1-r_3)}{3(a-2\alpha)}}$, $k_2^2 = \frac{r_3(r_1-r_2)}{r_2(r_1-r_3)}$, $\xi_1 = \frac{1}{g_3}\mathrm{sn}^{-1}(1,k_2)$, $n \in Z$.

For the periodic orbits surrounding the equilibrium points E_1 and E_2, we have $y^2 = \frac{4c}{3(a-2\alpha)}(r_1-\phi^2)(\phi^2-r_2)(\phi^2-r_3)$, where $r_1 > r_2 > r_3 > 0$. Then, the expressions of the two periodic wave solutions are derived as (see Figure 11b,c)

$$\phi(\xi) = \pm\sqrt{\frac{r_1r_2}{r_2+(r_1-r_2)\mathrm{sn}^2(g_3\xi,k_2)}}. \tag{24}$$

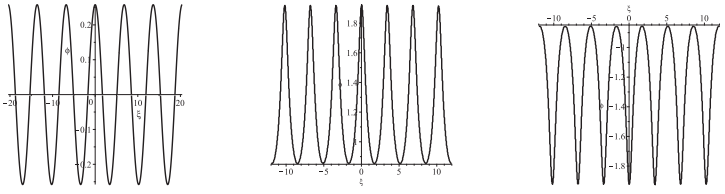

(**a**) (**b**) (**c**)

Figure 11. Periodic wave forms of system (5). (**a**) Defined by (23). (**b**) Defined by $(24)_+$. (**c**) Defined by $(24)_-$.

Subsequently, the three exact periodic wave solutions of Equation (1) are given as

$$u(x,t)=\begin{cases} -\sqrt{\frac{r_2r_3-r_2r_3\mathrm{sn}^2(g_3\frac{1}{\delta}(x^\delta-vt^\delta),k_2)}{r_2-r_3\mathrm{sn}^2(g_3\frac{1}{\delta}(x^\delta-vt^\delta),k_2)}}e^{i\eta(x,t)}, \frac{1}{\delta}(x^\delta-vt^\delta)\in\big[(4n+1)\xi_1,(4n+3)\xi_1\big], \\ \sqrt{\frac{r_2r_3-r_2r_3\mathrm{sn}^2(g_3\frac{1}{\delta}(x^\delta-vt^\delta),k_2)}{r_2-r_3\mathrm{sn}^2(g_3\frac{1}{\delta}(x^\delta-vt^\delta),k_2)}}e^{i\eta(x,t)}, \frac{1}{\delta}(x^\delta-vt^\delta)\in\big[4n\xi_1,(4n+1)\xi_1\big]\cup\big[(4n+3)\xi_1,(4n+4)\xi_1\big], \end{cases} \tag{25}$$

and

$$u(x,t)=\pm\sqrt{\frac{r_1r_2}{r_2+(r_1-r_2)\mathrm{sn}^2(g_3\frac{1}{\delta}(x^\delta-vt^\delta),k_2)}}e^{i\eta(x,t)}. \tag{26}$$

(iii) In formula (7), if $H(\phi,y)=h_3$, there are two homoclinic orbits encircling the equilibrium points E_1 and E_2, and two heteroclinic orbits linking two saddle points E_3 and E_4. For the two homoclinic orbits, we have $y^2=\frac{4c}{3(a-2\alpha)}(r_1-\phi^2)\Big(\phi^2-\frac{-b-\sqrt{\Delta}}{2c}\Big)^2$. Then, the expressions of the traveling wave solutions are derived as (see Figure 12)

$$\phi(\xi)=\pm\sqrt{\frac{r_1(b+\sqrt{\Delta})(1+\cosh(g_4\xi))}{2(b+\sqrt{\Delta})+2cr_1(1-\cosh(g_4\xi))}}, \tag{27}$$

where $g_4=\sqrt{\frac{(b+\sqrt{\Delta})(2cr_1+b+\sqrt{\Delta})}{3c(2\alpha-a)}}$.

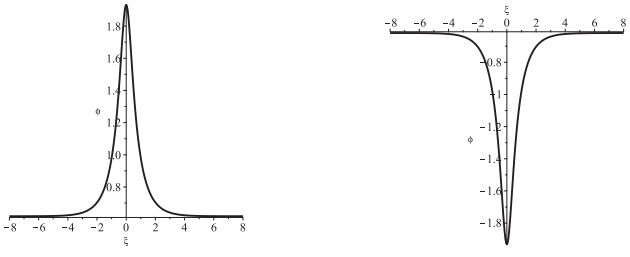

(**a**) (**b**)

Figure 12. Solitarywave forms of system (5). (**a**) Bright solitary wave derived by $(27)_+$. (**b**) Dark solitary wave derived by $(27)_-$.

For the two heteroclinic orbits, we have $y^2=\frac{4c}{3(a-2\alpha)}(r_1-\phi^2)\Big(\frac{-b-\sqrt{\Delta}}{2c}-\phi^2\Big)^2$, where $r_1>\frac{-b-\sqrt{\Delta}}{2c}>0$. Then, the the expression of the kink wave solution is given as (see Figure 13a)

$$\phi(\xi)=\begin{cases} -\sqrt{\frac{r_1(b+\sqrt{\Delta})(1-\cosh(g_4\xi))}{2(b+\sqrt{\Delta})+2cr_1(1+\cosh(g_4\xi))}}, \xi\in(-\infty,0], \\ \sqrt{\frac{r_1(b+\sqrt{\Delta})(1-\cosh(g_4\xi))}{2(b+\sqrt{\Delta})+2cr_1(1+\cosh(g_4\xi))}}, \xi\in[0,+\infty), \end{cases} \tag{28}$$

and the the expression of the anti-kink wave solution is given as (see Figure 13b)

$$\phi(\xi)=\begin{cases}\sqrt{\frac{r_1(b+\sqrt{\Delta})(1-\cosh(g_4\xi))}{2(b+\sqrt{\Delta})+2cr_1(1+\cosh(g_4\xi))}}, \xi\in(-\infty,0],\\ -\sqrt{\frac{r_1(b+\sqrt{\Delta})(1-\cosh(g_4\xi))}{2(b+\sqrt{\Delta})+2cr_1(1+\cosh(g_4\xi))}}, \xi\in[0,+\infty).\end{cases} \tag{29}$$

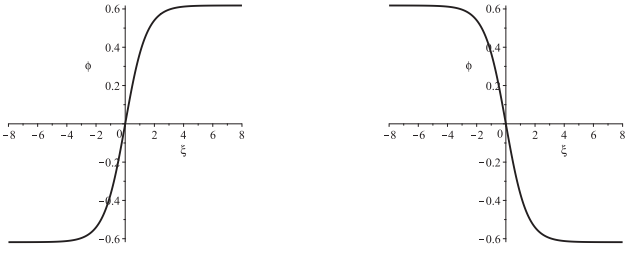

Figure 13. Kink and anti-kink wave forms of system (5). (**a**) Kink wave given by Equation (28). (**b**) Anti-kink wave given by Equation (29).

So, Equation (1) has the following four exact solutions:

$$u(x,t)=\pm\sqrt{\frac{r_1(b+\sqrt{\Delta})(1+\cosh(g_4\frac{1}{\delta}(x^\delta-vt^\delta)))}{2(b+\sqrt{\Delta})+2cr_1(1-\cosh(g_4\frac{1}{\delta}(x^\delta-vt^\delta)))}}e^{i\eta(x,t)}, \tag{30}$$

$$u(x,t)=\begin{cases}-\sqrt{\frac{r_1(b+\sqrt{\Delta})(1-\cosh(g_4\frac{1}{\delta}(x^\delta-vt^\delta)))}{2(b+\sqrt{\Delta})+2cr_1(1+\cosh(g_4\frac{1}{\delta}(x^\delta-vt^\delta)))}}e^{i\eta(x,t)}, \frac{1}{\delta}(x^\delta-vt^\delta)\in(-\infty,0],\\ \sqrt{\frac{r_1(b+\sqrt{\Delta})(1-\cosh(g_4\frac{1}{\delta}(x^\delta-vt^\delta)))}{2(b+\sqrt{\Delta})+2cr_1(1+\cosh(g_4\frac{1}{\delta}(x^\delta-vt^\delta)))}}e^{i\eta(x,t)}, \frac{1}{\delta}(x^\delta-vt^\delta)\in[0,+\infty),\end{cases} \tag{31}$$

and

$$u(x,t)=\begin{cases}\sqrt{\frac{r_1(b+\sqrt{\Delta})(1-\cosh(g_4\frac{1}{\delta}(x^\delta-vt^\delta)))}{2(b+\sqrt{\Delta})+2cr_1(1+\cosh(g_4\frac{1}{\delta}(x^\delta-vt^\delta)))}}e^{i\eta(x,t)}, \frac{1}{\delta}(x^\delta-vt^\delta)\in(-\infty,0],\\ -\sqrt{\frac{r_1(b+\sqrt{\Delta})(1-\cosh(g_4\frac{1}{\delta}(x^\delta-vt^\delta)))}{2(b+\sqrt{\Delta})+2cr_1(1+\cosh(g_4\frac{1}{\delta}(x^\delta-vt^\delta)))}}e^{i\eta(x,t)}, \frac{1}{\delta}(x^\delta-vt^\delta)\in[0,+\infty).\end{cases} \tag{32}$$

3.5. The Parameter Condition of $A-2\alpha>0,\Delta>0,B=\frac{3b^2}{16c},\omega+\gamma+a\kappa^2<0$ (*See Figure 1(6)*)

(i) In formula (7), if $H(\phi,y)=h, h\in(h_0,h_3)$, there are three families of periodic orbits. The expressions of the traveling wave solutions of these curves are identical to Equations (23) and (24).

(ii) In formula (7), if $H(\phi,y)=h_3$, there are two homoclinic orbits encircling the equilibrium points E_1 and E_2, and two heteroclinic orbits linking two saddle points E_3 and E_4. The expressions of the traveling wave solutions of these curves are identical to Equations (27)–(29).

3.6. The Parameter Condition of $A-2\alpha>0,\Delta>0,B<\frac{3b^2}{16c},\omega+\gamma+a\kappa^2<0$ (*See Figure 1(7)*)

(i) In formula (7), if $H(\phi,y)=h, h\in(h_1,h_3)$, there are three families of periodic orbits. The expressions of the traveling wave solutions of these curves are are identical to Equations (23) and (24).

(ii) In formula (7), if $H(\phi, y) = h_3$, there are two homoclinic orbits encircling the equilibrium points E_1 and E_2 and two heteroclinic orbits linking two saddle points E_3 and E_4. The expressions of the traveling wave solutions of these curves are identical to Equations (27)–(29).

3.7. The Parameter Condition of $\Delta > 0, \omega + \gamma + a\kappa^2 > 0$ *or* $\Delta > 0, B < 0, \omega + \gamma + a\kappa^2 = 0$ *(See Figure 2(3))*

(i) In formula (7), if $H(\phi, y) = h, h \in (h_0, h_1)$, there is a family of periodic orbits, which encircle the equilibrium point E_0. We have $y^2 = \frac{4c}{3(2\alpha - a)}(r_1 - \phi^2)(r_2 - \phi^2)(\phi^2 - r_3)$, where $r_1 > r_2 > 0 > r_3$. Then, the parametric representation of the periodic wave solution is given as follows (see Figure 14):

$$\phi(\xi) = \begin{cases} -\sqrt{\frac{r_1 r_2 - r_1 r_2 \mathrm{sn}^2(g_5\xi, k_3)}{r_1 - r_2 \mathrm{sn}^2(g_5\xi, k_3)}}, \xi \in \big[(4n+1)\xi_2, (4n+3)\xi_2\big], \\ \sqrt{\frac{r_1 r_2 - r_1 r_2 \mathrm{sn}^2(g_5\xi, k_3)}{r_1 - r_2 \mathrm{sn}^2(g_5\xi, k_3)}}, \xi \in \big[4n\xi_2, (4n+1)\xi_2\big] \cup \big[(4n+3)\xi_2, (4n+4)\xi_2\big], \end{cases} \tag{33}$$

where $g_5 = \sqrt{\frac{cr_1(r_3 - r_2)}{3(a - 2\alpha)}}$, $k_3^2 = \frac{r_2(r_1 - r_3)}{r_1(r_2 - r_3)}$, $\xi_2 = \frac{1}{g_5}\mathrm{sn}^{-1}(1, k_3)$, $n \in Z$.

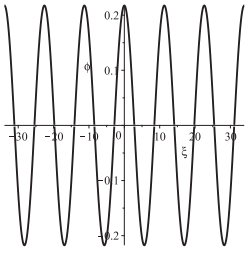

Figure 14. Periodicwave forms of system (5).

Therefore, the exact solution of Equation (1) is given as follows:

$$u(x,t) = \begin{cases} -\sqrt{\frac{r_1 r_2 - r_1 r_2 \mathrm{sn}^2(g_5 \frac{1}{\delta}(x^\delta - vt^\delta), k_3)}{r_1 - r_2 \mathrm{sn}^2(g_5 \frac{1}{\delta}(x^\delta - vt^\delta), k_3)}} e^{i\eta(x,t)}, \frac{1}{\delta}(x^\delta - vt^\delta) \in \big[(4n+1)\xi_2, (4n+3)\xi_2\big], \\ \sqrt{\frac{r_1 r_2 - r_1 r_2 \mathrm{sn}^2(g_5 \frac{1}{\delta}(x^\delta - vt^\delta), k_3)}{r_1 - r_2 \mathrm{sn}^2(g_5 \frac{1}{\delta}(x^\delta - vt^\delta), k_3)}} e^{i\eta(x,t)}, \frac{1}{\delta}(x^\delta - vt^\delta) \in \big[4n\xi_2, (4n+1)\xi_2\big] \cup \big[(4n+3)\xi_2, (4n+4)\xi_2\big]. \end{cases} \tag{34}$$

(ii) In formula (7), if $H(\phi, y) = h_1$, there are two heteroclinic orbits, which encircle the equilibrium point E_0 and link the saddle points E_1 and E_2. We have $y^2 = \frac{4c}{3(2\alpha - a)}\left(\frac{-b + \sqrt{\Delta}}{2c} - \phi^2\right)^2(\phi^2 - r_1)$, where $\frac{-b + \sqrt{\Delta}}{2c} > 0 > r_1$. Then, the parametric representations of the kink and anti-kink wave solutions are given as (see Figure 15)

$$\phi(\xi) = \begin{cases} -\sqrt{\frac{r_1(\sqrt{\Delta} - b)(1 - \cosh(g_6\xi))}{2(\sqrt{\Delta} - b) - 2cr_1(1 + \cosh(g_6\xi))}}, \xi \in (-\infty, 0], \\ \sqrt{\frac{r_1(\sqrt{\Delta} - b)(1 - \cosh(g_6\xi))}{2(\sqrt{\Delta} - b) - 2cr_1(1 + \cosh(g_6\xi))}}, \xi \in [0, +\infty), \end{cases} \tag{35}$$

and

$$\phi(\xi) = \begin{cases} \sqrt{\frac{r_1(\sqrt{\Delta} - b)(1 - \cosh(g_6\xi))}{2(\sqrt{\Delta} - b) - 2cr_1(1 + \cosh(g_6\xi))}}, \xi \in (-\infty, 0], \\ -\sqrt{\frac{r_1(\sqrt{\Delta} - b)(1 - \cosh(g_6\xi))}{2(\sqrt{\Delta} - b) - 2cr_1(1 + \cosh(g_6\xi))}}, \xi \in [0, +\infty), \end{cases} \tag{36}$$

where $g_6 = \sqrt{\frac{2(\sqrt{\Delta} - b)}{3(a - 2\alpha)}\left(r_1 - \frac{-b + \sqrt{\Delta}}{2c}\right)}$.

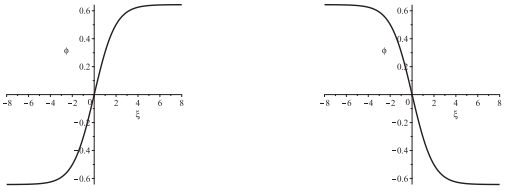

(**a**) (**b**)

Figure 15. Kinkand anti-kink wave forms of system (5). (**a**) Kink wave given by (35). (**b**) Anti-kink wave given by (36).

Thus, the exact expressions of solutions to Equation (1) are presented as

$$u(x,t)=\begin{cases} -\sqrt{\frac{r_1(\sqrt{\Delta}-b)(1-\cosh(g_6\frac{1}{\delta}(x^\delta-vt^\delta)))}{2(\sqrt{\Delta}-b)-2cr_1(1+\cosh(g_6\frac{1}{\delta}(x^\delta-vt^\delta)))}}e^{i\eta(x,t)}, \frac{1}{\delta}(x^\delta-vt^\delta)\in(-\infty,0], \\ \sqrt{\frac{r_1(\sqrt{\Delta}-b)(1-\cosh(g_6\frac{1}{\delta}(x^\delta-vt^\delta)))}{2(\sqrt{\Delta}-b)-2cr_1(1+\cosh(g_6\frac{1}{\delta}(x^\delta-vt^\delta)))}}e^{i\eta(x,t)}, \frac{1}{\delta}(x^\delta-vt^\delta)\in[0,+\infty), \end{cases} \tag{37}$$

and

$$u(x,t)=\begin{cases} \sqrt{\frac{r_1(\sqrt{\Delta}-b)(1-\cosh(g_6\frac{1}{\delta}(x^\delta-vt^\delta)))}{2(\sqrt{\Delta}-b)-2cr_1(1+\cosh(g_6\frac{1}{\delta}(x^\delta-vt^\delta)))}}e^{i\eta(x,t)}, \frac{1}{\delta}(x^\delta-vt^\delta)\in(-\infty,0], \\ -\sqrt{\frac{r_1(\sqrt{\Delta}-b)(1-\cosh(g_6\frac{1}{\delta}(x^\delta-vt^\delta)))}{2(\sqrt{\Delta}-b)-2cr_1(1+\cosh(g_6\frac{1}{\delta}(x^\delta-vt^\delta)))}}e^{i\eta(x,t)}, \frac{1}{\delta}(x^\delta-vt^\delta)\in[0,+\infty). \end{cases} \tag{38}$$

3.8. The Parameter Condition of $A-2\alpha<0, \Delta>0, \frac{3b^2}{16c}<b<0, \omega+\gamma+a\kappa^2<0$ (*See Figure 2(4)*)

(i) In formula (7), if $H(\phi,y)=h, h\in(h_3,h_0)$, there are two families of periodic orbits, which respectively encircle the equilibrium points E_3 and E_4. We have $y^2=\frac{4c}{3(2\alpha-a)}(r_3-\phi^2)(r_1-\phi^2)(\phi^2-r_2)$, where $r_3>r_1>r_2>0$. Then, we derive the parametric representations of the periodic wave solutions are given as (see Figure 16)

$$\phi(\xi)=\pm\sqrt{\frac{r_1(r_2-r_3)+r_3(r_1-r_2)\mathrm{sn}^2(g_7\xi,k_4)}{r_2-r_3+(r_1-r_2)\mathrm{sn}^2(g_7\xi,k_4)}}, \tag{39}$$

where $g_7=\sqrt{\frac{cr_1(r_2-r_3)}{3(a-2\alpha)}}$, $k_4^2=\frac{r_3(r_1-r_2)}{r_1(r_3-r_2)}$.

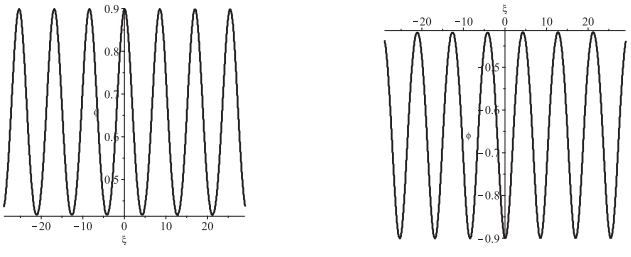

(**a**) (**b**)

Figure 16. Periodic wave forms of system (5). (**a**) Defined by $(39)_+$. (**b**) Defined by $(39)_-$.

Thus, the exact expressions of solutions to Equation (1) are presented as

$$u(x,t)=\pm\sqrt{\frac{r_1(r_2-r_3)+r_3(r_1-r_2)\mathrm{sn}^2(g_7\frac{1}{\delta}(x^\delta-vt^\delta),k_4)}{r_2-r_3+(r_1-r_2)\mathrm{sn}^2(g_7\frac{1}{\delta}(x^\delta-vt^\delta),k_4)}}e^{i\eta(x,t)}. \tag{40}$$

(ii) In formula (7), if $H(\phi, y) = h_0$, there are two homoclinic orbits, which respectively encircle the equilibrium points E_3 and E_4. We have $y^2 = \frac{4c}{3(2\alpha-a)}(r_1 - \phi^2)(r_2 - \phi^2)\phi^2$, where $r_1 > r_2 > 0$. Then, we derive the parametric expressions of the solitary wave solutions as (see Figure 17)

$$\phi(\xi) = \pm\sqrt{\frac{2r_1r_2}{r_1 + r_2 + (r_1 - r_2)\cosh(g_8\xi)}}, \tag{41}$$

where $g_8 = \sqrt{\frac{4cr_1r_2}{3(2\alpha-a)}}$.

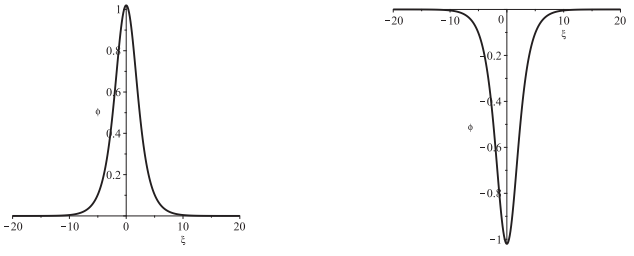

(**a**) (**b**)

Figure 17. Solitary wave forms of system (5). (**a**) Bright solitary wave derived by Equation $(41)_+$. (**b**) Dark solitary wave derived by Equation $(41)_-$.

Thus, the exact expressions of two solitary wave solutions to Equation (1) are presented as

$$u(x,t) = \pm\sqrt{\frac{2r_1r_2}{r_1 + r_2 + (r_1 - r_2)\cosh(g_8\frac{1}{\delta}(x^\delta - vt^\delta))}}e^{i\eta(x,t)}. \tag{42}$$

(iii) In formula (7), if $H(\phi, y) = h, h \in (h_0, h_1)$, there is a family of periodic orbits. The expressions of the traveling wave solutions of these curves are identical to Equation (33).

(iv) The curves $H(\phi, y) = h_1$ correspond to two heteroclinic orbits. The parametric expressions of the traveling wave solutions of these curves are the same as Equations (35) and (36).

3.9. The Parameter Condition of $A - 2\alpha < 0, \Delta > 0, B = \frac{3b^2}{16c}, \omega + \gamma + a\kappa^2 < 0$*(see Figure 2(5))*

(i) In formula (7), if $H(\phi, y) = h, h \in (h_3, h_0)$, there are two families of periodic orbits. The expressions of the traveling wave solutions of these curves are identical to Equation (39).

(ii) In formula (7), if $H(\phi, y) = h_0$, there are four heteroclinic orbits, which encircle the equilibrium points E_3 and E_4 and link the saddle points E_0, E_1 and E_2. We have $y^2 = \frac{4c}{3(2\alpha-a)}\left(\frac{-b+\sqrt{\Delta}}{2c} - \phi^2\right)^2\phi^2$. The heteroclinic orbit in the first quadrant corresponds to a kink wave solution, and the parametric expression of the kink wave solution is given as (see Figure 18a)

$$\phi(\xi) = \sqrt{\frac{-b+\sqrt{\Delta}}{4c} - \frac{-b+\sqrt{\Delta}}{4c}\tanh\left(\ln\sqrt{3} - \frac{-b+\sqrt{\Delta}}{4c}g_9\xi\right)}, \tag{43}$$

where $g_9 = \sqrt{\frac{4c}{3(2\alpha-a)}}$. The heteroclinic orbit in the forth quadrant corresponds to an

anti-kink wave solution, and the parametric representation of the anti-kink wave solution is given as (see Figure 18b)

$$\phi(\xi) = \sqrt{\frac{-b+\sqrt{\Delta}}{4c} - \frac{-b+\sqrt{\Delta}}{4c}\tanh\left(\ln\sqrt{3} + \frac{-b+\sqrt{\Delta}}{4c}g_9\xi\right)}. \tag{44}$$

The heteroclinic orbit in the second quadrant corresponds to a kink wave solution, and the parametric representation of the kink wave solution is given as (see Figure 18c)

$$\phi(\xi) = -\sqrt{\frac{-b+\sqrt{\Delta}}{4c} - \frac{-b+\sqrt{\Delta}}{4c}\tanh\left(\ln\sqrt{3} + \frac{-b+\sqrt{\Delta}}{4c}g_9\xi\right)}. \tag{45}$$

The heteroclinic orbit in the third quadrant corresponds to a anti-kink wave solution, and the parametric representation of the anti-kink wave solution is given as (see Figure 18d)

$$\phi(\xi) = -\sqrt{\frac{-b+\sqrt{\Delta}}{4c} - \frac{-b+\sqrt{\Delta}}{4c}\tanh\left(\ln\sqrt{3} - \frac{-b+\sqrt{\Delta}}{4c}g_9\xi\right)}. \tag{46}$$

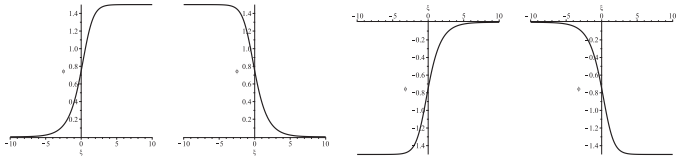

(**a**) (**b**) (**c**) (**d**)

Figure 18. Kink and anti-kink wave forms of system (5). (**a**) Kink wave given by (43). (**b**) Anti-kink wave given by (44). (**c**) Kink wave given by (45). (**d**) Anti-kink wave given by (46).

Thus, the exact expressions of solutions to Equation (1) are presented as

$$u(x,t) = \sqrt{\frac{-b+\sqrt{\Delta}}{4c} - \frac{-b+\sqrt{\Delta}}{4c}\tanh\left(\ln\sqrt{3} - \frac{-b+\sqrt{\Delta}}{4c}g_9\frac{1}{\delta}(x^\delta - vt^\delta)\right)}e^{i\eta(x,t)}, \tag{47}$$

$$u(x,t) = \sqrt{\frac{-b+\sqrt{\Delta}}{4c} - \frac{-b+\sqrt{\Delta}}{4c}\tanh\left(\ln\sqrt{3} + \frac{-b+\sqrt{\Delta}}{4c}g_9\frac{1}{\delta}(x^\delta - vt^\delta)\right)}e^{i\eta(x,t)}, \tag{48}$$

$$u(x,t) = -\sqrt{\frac{-b+\sqrt{\Delta}}{4c} - \frac{-b+\sqrt{\Delta}}{4c}\tanh\left(\ln\sqrt{3} + \frac{-b+\sqrt{\Delta}}{4c}g_9\frac{1}{\delta}(x^\delta - vt^\delta)\right)}e^{i\eta(x,t)}, \tag{49}$$

and

$$u(x,t) = -\sqrt{\frac{-b+\sqrt{\Delta}}{4c} - \frac{-b+\sqrt{\Delta}}{4c}\tanh\left(\ln\sqrt{3} - \frac{-b+\sqrt{\Delta}}{4c}g_9\frac{1}{\delta}(x^\delta - vt^\delta)\right)}e^{i\eta(x,t)}. \tag{50}$$

3.10. The Parameter Condition of
$A - 2\alpha < 0, \Delta > 0, B < \frac{3b^2}{16c}, \omega + \gamma + a\kappa^2 < 0$ (*see Figure 2(6)*)

(i) In formula (7), if $H(\phi, y) = h, h \in (h_3, h_1)$, there are two families of periodic orbits. The expressions of the traveling wave solutions of these curves are identical to Equation (39).

(ii) In formula (7), if $H(\phi, y) = h_1$, there are two homoclinic orbits, which respectively encircle the equilibrium points E_3 and E_4. We have $y^2 = \frac{4c}{3(2\alpha-a)}\left(\frac{-b+\sqrt{\Delta}}{2c} - \phi^2\right)^2(\phi^2 - r_1)$, where $\frac{-b+\sqrt{\Delta}}{2c} > r_1 > 0$. Then, the parametric representations of the solitary wave solutions are given as (see Figure 19)

$$\phi(\xi) = \pm\sqrt{\frac{r_1(\sqrt{\Delta}-b)(1+\cosh(g_{10}\xi))}{2(\sqrt{\Delta}-b)+2cr_1(\cosh(g_{10}\xi)-1)}}, \tag{51}$$

where $g_{10} = \sqrt{\frac{2(\sqrt{\Delta}-b)}{3(a-2\alpha)}\left(r_1 - \frac{-b+\sqrt{\Delta}}{2c}\right)}$.

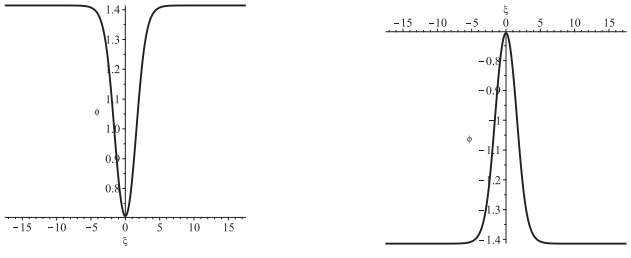

(**a**) (**b**)

Figure 19. Solitary waves forms of system (5). (**a**) Bright solitary wave derived by $(51)_+$. (**b**) Dark solitary wave derived by $(51)_-$.

Thus, the exact expressions of solutions to Equation (1) are presented as

$$u(x,t) = \pm\sqrt{\frac{r_1(\sqrt{\Delta}-b)(1+\cosh(g_{10}\frac{1}{\delta}(x^\delta - vt^\delta)))}{2(\sqrt{\Delta}-b)+2cr_1(\cosh(g_{10}\frac{1}{\delta}(x^\delta - vt^\delta))-1)}}e^{i\eta(x,t)}. \tag{52}$$

4. Expressions of the Traveling Wave Solutions of System Equation (5) under $C > 0, A = 4\beta$

Currently, through integral calculation, we compute the exact parametric expressions of the traveling wave solutions under $c > 0, a = 4\beta$. It follows from Equation (7) and the first equation of system (5) that

$$\xi = \int_{\phi_0}^{\phi} \frac{\pm|\phi|d\phi}{\sqrt{\frac{c}{4(2\alpha-a)}\phi^8 + \frac{b}{3(2\alpha-a)}\phi^6 + \frac{\omega+\gamma+a\kappa^2}{2(a-2\alpha)}\phi^4 + h}} \equiv \int_{\phi_0}^{\phi} \frac{\pm|\phi|d\phi}{\sqrt{G(\phi)}}. \tag{53}$$

4.1. The Parameter Condition of $A - 2\alpha > 0, \Delta > 0, \omega + \gamma + a\kappa^2 > 0$ (see Figure 3(3))

(i) In formula (7), if $H(\phi, y) = h, h \in (h_1, h_0)$, there are two families of periodic orbits, which respectively encircle the equilibrium points E_1 and E_2. We have $G(\phi) = \frac{c}{4(a-2\alpha)}(r_1 - \phi^2)(\phi^2 - r_2)(\phi^2 - r_3)(\phi^2 - r_4)$, where $r_1 > r_2 > 0 > r_3 > r_4$. Then, the expressions of the periodic wave solutions are derived as (see Figure 20)

$$\phi(\xi) = \pm\sqrt{\frac{r_1(r_2-r_4)+r_4(r_1-r_2)\mathrm{sn}^2(g_{11}\xi, k_5)}{r_2-r_4+(r_1-r_2)\mathrm{sn}^2(g_{11}\xi, k_5)}}, \tag{54}$$

where $g_{11} = \sqrt{\frac{c(r_1-r_3)(r_2-r_4)}{4(a-2\alpha)}}$, $k_5^2 = \frac{(r_1-r_2)(r_3-r_4)}{(r_1-r_3)(r_2-r_4)}$.

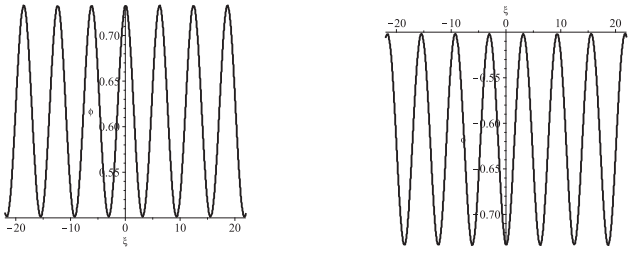

(**a**) (**b**)

Figure 20. Periodicwave forms of system (5). (**a**) Defined by $(54)_+$. (**b**) Defined by $(54)_-$.

Thus, the exact expressions of solutions to Equation (1) are presented as

$$u(x,t) = \pm\sqrt{\frac{r_1(r_2-r_4)+r_4(r_1-r_2)\mathrm{sn}^2(g_{11}\frac{1}{\delta}(x^\delta - vt^\delta), k_5)}{r_2-r_4+(r_1-r_2)\mathrm{sn}^2(g_{11}\frac{1}{\delta}(x^\delta - vt^\delta), k_5)}}e^{i\eta(x,t)}. \tag{55}$$

(ii) In formula (7), if $H(\phi, y) = h_0$, there are two homoclinic orbits, which respectively encircle the equilibrium points E_1 and E_2. We have $G(\phi) = \frac{c}{a-2\alpha}(r_1-\phi^2)\phi^4(\phi^2-r_2)$, where $r_1 > 0 > r_2$. Then, the parametric representations of the solitary wave solutions are given as (see Figure 21)

$$\phi(\xi) = \pm\sqrt{\frac{2r_1r_2}{r_1+r_2+(r_2-r_1)\cosh(g_{12}\xi)}}, \tag{56}$$

where $g_{12} = \sqrt{\frac{cr_1r_2}{2\alpha-a}}$.

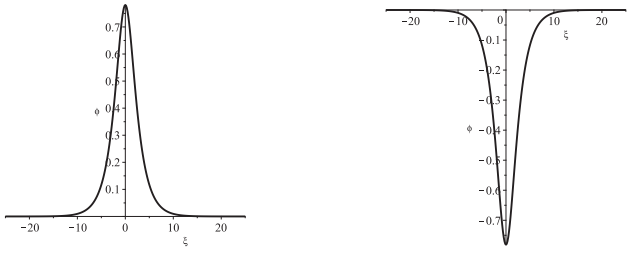

(**a**) (**b**)

Figure 21. Solitarywave forms of system (5). (**a**) Bright solitary wave derived by $(56)_+$. (**b**) Dark solitary wave derived by $(56)_-$.

Thus, the exact expressions of solutions to Equation (1) are presented as

$$u(x,t) = \pm\sqrt{\frac{2r_1r_2}{r_1+r_2+(r_2-r_1)\cosh(g_{12}\frac{1}{\delta}(x^\delta - vt^\delta))}}e^{i\eta(x,t)}. \tag{57}$$

4.2. The Parameter Condition of $A-2\alpha > 0, \Delta > 0, B < 0, \omega+\gamma+a\kappa^2 = 0$ (*See Figure 3(4)*)

(i) In formula (7), if $H(\phi, y) = h, h \in (h_1, h_0)$, there are two families of periodic orbits, which respectively encircle the equilibrium points E_1 and E_2. We have

$G(\phi) = \frac{c}{4(a-2\alpha)}(r_1 - \phi^2)(\phi^2 - r_2)(\phi^2 - r_3)(\phi^2 - \bar{r_3})$, where $r_1 > r_2$, r_3 and $\bar{r_3}$ are complex. Then, the parametric representation of the periodic wave solution are given as (see Figure 22)

$$\phi(\xi) = \pm\sqrt{\frac{r_1B_1 + r_2A_1 + (r_2A_1 - r_1B_1)\mathrm{cn}(g_{13}\xi, k_6)}{A_1 + B_1 + (A_1 - B_1)\mathrm{cn}(g_{13}\xi, k_6)}}, \tag{58}$$

where $A_1^2 = (r_1 - r_3)(r_1 - \bar{r_3})$, $B_1^2 = (r_2 - r_3)(r_2 - \bar{r_3})$, $g_{13} = \sqrt{\frac{cA_1B_1}{a-2\alpha}}$, $k_6^2 = \frac{(r_1-r_2)^2-(A_1-B_1)^2}{4A_1B_1}$.

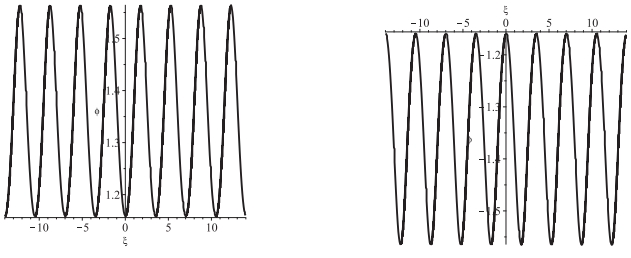

(**a**) (**b**)

Figure 22. Periodicwave forms of system (5). (**a**) Defined by $(58)_+$. (**b**) Defined by $(58)_-$.

Thus, the exact expressions of solutions to Equation (1) are presented as

$$u(x,t) = \pm\sqrt{\frac{r_1B_1 + r_2A_1 + (r_2A_1 - r_1B_1)\mathrm{cn}(g_{13}\frac{1}{\delta}(x^\delta - vt^\delta), k_6)}{A_1 + B_1 + (A_1 - B_1)\mathrm{cn}(g_{13}\frac{1}{\delta}(x^\delta - vt^\delta), k_6)}}e^{i\eta(x,t)}. \tag{59}$$

(ii) In formula (7), if $H(\phi, y) = h_0$, there are two homoclinic orbits, which respectively encircle the equilibrium points E_1 and E_2. We have $G(\phi) = \frac{c}{a-2\alpha}(r_1 - \phi^2)\phi^6$, where $r_1 > 0$. Then, the parametric representations of the solitary wave solutions are given as (see Figure 23)

$$\phi(\xi) = \pm\sqrt{\frac{4r_1(a-2\alpha)}{4(a-2\alpha) + cr_1^2\xi^2}}. \tag{60}$$

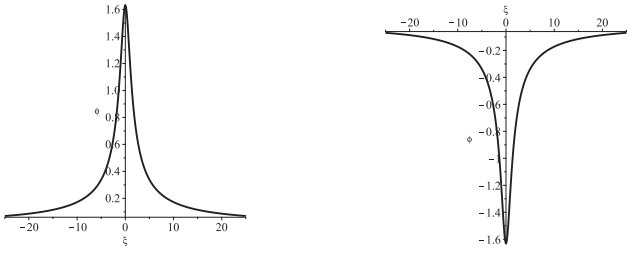

(**a**) (**b**)

Figure 23. Solitary wave forms of system (5). (**a**) Bright solitary wave derived by $(60)_+$. (**b**) Dark solitary wave derived by $(60)_-$.

Thus, the exact expressions of solutions to Equation (1) are presented as

$$u(x,t) = \pm\sqrt{\frac{4r_1(a-2\alpha)}{4(a-2\alpha) + cr_1^2\frac{1}{\delta^2}(x^\delta - vt^\delta)^2}}e^{i\eta(x,t)}. \tag{61}$$

4.3. The Parameter Condition of $A-2\alpha>0, \Delta>0, B<0, \omega+\gamma+a\kappa^2<0$, $H_1=h_2<h_0<h_3=h_4$ *(See Figure 3(5))*

(i) In formula (7), if $H(\phi,y)=h, h\in(h_1,h_0)$, there are two families of periodic orbits. The expressions of the traveling wave solutions of these curves are identical to Equations (56) and (58)

(ii) In formula (7), if $H(\phi,y)=h_0$, there are two families of periodic orbits, which respectively encircle the equilibrium points E_1 and E_2. We have $G(\phi)=\frac{c}{4(a-2\alpha)}(r_1-\phi^2)(\phi^2-r_2)\phi^4$, where $r_1>r_2>0$. Then, the expressions of the periodic wave solutions are derived as (see Figure 24)

$$\phi(\xi)=\pm\sqrt{\frac{2r_1r_2}{r_1+r_2-(r_1-r_2)\cos(g_{14}\xi)}}, \tag{62}$$

where $g_{14}=\sqrt{\frac{cr_1r_2}{a-2\alpha}}$.

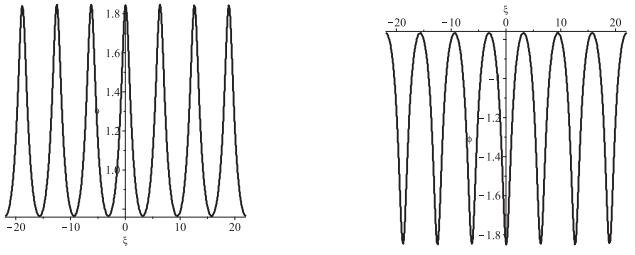

(**a**) (**b**)

Figure 24. Periodic wave forms of system (5). (**a**) Defined by $(62)_+$. (**b**) Defined by $(62)_-$.

Thus, the exact expressions of solutions to Equation (1) are presented as

$$u(x,t)=\pm\sqrt{\frac{2r_1r_2}{r_1+r_2-(r_1-r_2)\cos(g_{14}\frac{1}{\delta}(x^\delta-vt^\delta))}}e^{i\eta(x,t)}. \tag{63}$$

(iii) In formula (7), if $H(\phi,y)=h, h\in(h_0,h_3)$, there are two families of periodic orbits respectively surrounding the equilibrium points E_1 and E_2, and two families of open curves, which tend to the singular line $\phi=0$ under $|y|\to\infty$. $G(\phi)=\frac{c}{4(a-2\alpha)}(r_1-\phi^2)(\phi^2-r_2)(\phi^2-r_3)(\phi^2-r_4)$ applies to the two families of periodic orbits. Then, the expressions of the periodic wave solutions are derived as (see Figure 25)

$$\phi(\xi)=\pm\sqrt{\frac{r_1(r_2-r_4)+r_4(r_1-r_2)\mathrm{sn}^2(g_{15}\xi,k_7)}{r_2-r_4+(r_1-r_2)\mathrm{sn}^2(g_{15}\xi,k_7)}}, \tag{64}$$

where $g_{15}=\sqrt{\frac{c(r_1-r_3)(r_2-r_4)}{4(a-2\alpha)}}$, $k_7^2=\frac{(r_1-r_2)(r_3-r_4)}{(r_1-r_3)(r_2-r_4)}$.

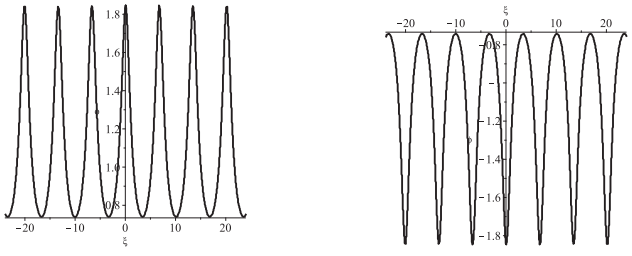

(**a**) (**b**)

Figure 25. Periodic wave forms of system (5). (**a**) Defined by $(64)_+$. (**b**) Defined by $(64)_-$.

$G(\phi) = \frac{c}{4(a-2\alpha)}(r_1-\phi^2)(r_2-\phi^2)(r_3-\phi^2)(\phi^2-r_4)$ applies to the two families of open curves, where $r_1 > r_2 > r_3 > 0 > r_4$. Then, the parametric representations of the compacton solutions are given as (see Figure 26)

$$\phi(\xi) = \pm\sqrt{\frac{r_3(r_4-r_2)+r_2(r_3-r_4)\mathrm{sn}^2(g_{15}\xi,k_7)}{r_4-r_2+(r_3-r_4)\mathrm{sn}^2(g_{15}\xi,k_7)}},\ \xi\in(-\xi_3,\xi_3), \tag{65}$$

where $\xi_3 = \frac{1}{g_{15}}\mathrm{sn}^{-1}\Big(\sqrt{\frac{r_3(r_2-r_4)}{r_2(r_3-r_4)}},k_7\Big)$.

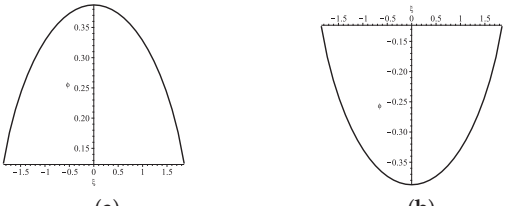

(**a**) (**b**)

Figure 26. Compactonsolution forms of system (5). (**a**) Compacton solution given by $(65)_+$. (**b**) Compacton solution given by $(65)_-$.

So, Equation (1) has the following four exact solutions:

$$u(x,t) = \pm\sqrt{\frac{r_1(r_2-r_4)+r_4(r_1-r_2)\mathrm{sn}^2(g_{15}\frac{1}{\delta}(x^\delta-vt^\delta),k_7)}{r_2-r_4+(r_1-r_2)\mathrm{sn}^2(g_{15}\frac{1}{\delta}(x^\delta-vt^\delta),k_7)}}e^{i\eta(x,t)}, \tag{66}$$

and

$$u(x,t) = \pm\sqrt{\frac{r_3(r_4-r_2)+r_2(r_3-r_4)\mathrm{sn}^2(g_{15}\frac{1}{\delta}(x^\delta-vt^\delta),k_7)}{r_4-r_2+(r_3-r_4)\mathrm{sn}^2(g_{15}\frac{1}{\delta}(x^\delta-vt^\delta),k_7)}}e^{i\eta(x,t)}, \frac{1}{\delta}(x^\delta-vt^\delta)\in(-\xi_3,\xi_3). \tag{67}$$

(iv) In formula (7), if $H(\phi,y) = h_3$, there are two homoclinic orbits, which respectively encircle the equilibrium points E_1 and E_2. We have $G(\phi) = \frac{c}{4(a-2\alpha)}(r_1-\phi^2)\Big(\phi^2-\frac{-b-\sqrt{\Delta}}{2c}\Big)^2(\phi^2-r_2)$, where $r_1 > \frac{-b-\sqrt{\Delta}}{2c} > 0 > r_2$. Then, the parametric representations of the solitary wave solutions are given as (see Figure 27)

$$\phi(\xi) = \pm\sqrt{\frac{4cr_1r_2+(r_1+r_2)(b+\sqrt{\Delta})+(r_1-r_2)(b+\sqrt{\Delta})\cosh(g_{16}\xi)}{2c(r_1+r_2)+2(b+\sqrt{\Delta})+2c(r_2-r_1)\cosh(g_{16}\xi)}}, \tag{68}$$

where $g_{16} = \sqrt{\frac{(2cr_1+b+\sqrt{\Delta})(2cr_2+b+\sqrt{\Delta})}{4c(2\alpha-a)}}$.

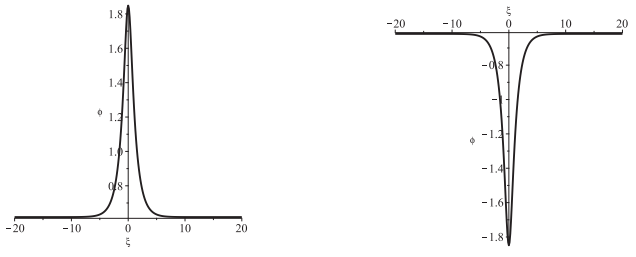

(**a**) (**b**)

Figure 27. Solitary wave forms of system (5). (**a**) Bright solitary wave derived by $(68)_+$. (**b**) Dark solitary wave derived by $(68)_-$.

Thus, the exact expressions of solutions to Equation (1) are presented as

$$u(x,t) = \pm\sqrt{\frac{4cr_1r_2 + (r_1+r_2)(b+\sqrt{\Delta}) + (r_1-r_2)(b+\sqrt{\Delta})\cosh(g_{16}\frac{1}{\delta}(x^\delta - vt^\delta))}{2c(r_1+r_2) + 2(b+\sqrt{\Delta}) + 2c(r_2-r_1)\cosh(g_{16}\frac{1}{\delta}(x^\delta - vt^\delta))}}e^{i\eta(x,t)}. \tag{69}$$

4.4. The Parameter Condition of $A-2\alpha>0, \Delta>0, B<0, \omega+\gamma+a\kappa^2<0$, $H_1=h_2=h_0<h_3=h_4$ *(See Figure 3(6))*

(i) In formula (7), if $H(\phi,y)=h, h\in(h_0,h_3)$, there are two families of periodic orbits and two families of open curves. The parametric representations of the traveling wave solutions of these curves are same as Equations (64) and (65).

(ii) The curves $H(\phi,y)=h_3$ correspond to two homoclinic orbits. The parametric expressions of the traveling wave solutions of these curves are the same as Equations (68).

4.5. the Parameter Condition of $A-2\alpha>0, \Delta>0, B<0, \omega+\gamma+a\kappa^2<0$, $H_0<h_1=h_2<h_3=h_4$ *(See Figure 3(7))*

(i) In formula (7), if $H(\phi,y)=h, h\in(h_2,h_3)$, there are two families of periodic orbits and two families of open curves. The parametric representations of the traveling wave solutions of these curves are the same as Equations (64) and (65).

(ii) The curves $H(\phi,y)=h_3$ correspond to two homoclinic orbits. The parametric expressions of the traveling wave solutions of these curves are the same as Equations (68).

4.6. The Parameter Condition of $A-2\alpha<0, \Delta>0, \omega+\gamma+a\kappa^2>0$ *or* $\Delta>0$, $B<0, \omega+\gamma+a\kappa^2=0$ *(See Figure 4(3))*

In formula (7), if $H(\phi,y)=h, h\in(h_0,h_1)$, there are two families of open curves, which tend to the singular line $\phi=0$ when $|y|\to\infty$. We have $G(\phi)=\frac{c}{4(2\alpha-a)}(r_1-\phi^2)(r_2-\phi^2)(\phi^2-r_3)(\phi^2-r_4)$, where $r_1>r_2>0>r_3>r_4$. Then, the parametric representations of the compacton solutions are given as (see Figure 28)

$$\phi(\xi) = \pm\sqrt{\frac{r_2(r_3-r_1)+r_1(r_2-r_3)\mathrm{sn}^2(g_{17}\xi,k_8)}{r_3-r_1+(r_2-r_3)\mathrm{sn}^2(g_{17}\xi,k_8)}},\ \xi\in(-\xi_4,\xi_4), \tag{70}$$

where $g_{17}=\sqrt{\frac{c(r_3-r_1)(r_2-r_4)}{4(a-2\alpha)}}$, $k_8^2=\frac{(r_2-r_3)(r_1-r_4)}{(r_1-r_3)(r_2-r_4)}$, $\xi_4=\frac{1}{g_{17}}\mathrm{sn}^{-1}\Big(\sqrt{\frac{r_2(r_1-r_3)}{r_1(r_2-r_3)}},k_8\Big)$.

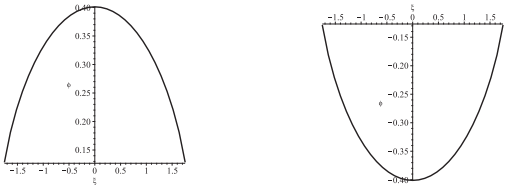

(**a**) (**b**)

Figure 28. Compactonsolution forms of system (5). (**a**) Compacton solution given by Equation $(70)_+$. (**b**) Compacton solution given by Equation $(70)_-$.

Thus, the exact expressions of solutions to Equation (1) are presented as

$$u(x,t)=\pm\sqrt{\frac{r_2(r_3-r_1)+r_1(r_2-r_3)\mathrm{sn}^2(g_{17}\frac{1}{\delta}(x^\delta-vt^\delta),k_8)}{r_3-r_1+(r_2-r_3)\mathrm{sn}^2(g_{17}\frac{1}{\delta}(x^\delta-vt^\delta),k_8)}}e^{i\eta(x,t)},\ \frac{1}{\delta}(x^\delta-vt^\delta)\in(-\xi_4,\xi_4). \tag{71}$$

4.7. The Parameter Condition of $A-2\alpha<0, \Delta>0, B<0, \omega+\gamma+a\kappa^2<0$, $H_3=h_4<h_0<h_1=h_2$ *(see Figure 4(4))*

(i) In formula (7), if $H(\phi,y)=h, h\in(h_3,h_0)$, there are two families of periodic orbits, which respectively encircle the equilibrium points E_3 and E_4. We have $G(\phi)=\frac{c}{4(2\alpha-a)}(r_1-\phi^2)(r_2-\phi^2)(\phi^2-r_3)(\phi^2-r_4)$, where $r_1>r_2>r_3>0>r_4$. Then, the expressions of the periodic wave solutions are derived as (see Figure 29)

$$\phi(\xi)=\pm\sqrt{\frac{r_2(r_3-r_1)+r_1(r_2-r_3)\mathrm{sn}^2(g_{18}\xi,k_9)}{r_3-r_1+(r_2-r_3)\mathrm{sn}^2(g_{18}\xi,k_9)}}, \tag{72}$$

where $g_{18}=\sqrt{\frac{c(r_3-r_1)(r_2-r_4)}{4(a-2\alpha)}}$, $k_9^2=\frac{(r_2-r_3)(r_1-r_4)}{(r_1-r_3)(r_2-r_4)}$.

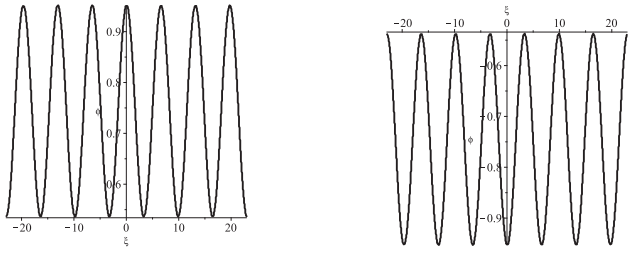

(**a**) (**b**)

Figure 29. Periodic wave forms of system (5). (**a**) Defined by $(72)_+$. (**b**) Defined by $(72)_-$.

Thus, the exact expressions of solutions to Equation (1) are presented as

$$u(x,t)=\pm\sqrt{\frac{r_2(r_3-r_1)+r_1(r_2-r_3)\mathrm{sn}^2(g_{18}\frac{1}{\delta}(x^\delta-vt^\delta),k_9)}{r_3-r_1+(r_2-r_3)\mathrm{sn}^2(g_{18}\frac{1}{\delta}(x^\delta-vt^\delta),k_9)}}e^{i\eta(x,t)}. \tag{73}$$

(ii) In formula (7), if $H(\phi,y)=h_0$, there are two homoclinic orbits, which respectively encircle the equilibrium points E_3 and E_4. We have $G(\phi)=\frac{c}{2\alpha-a}(r_1-\phi^2)(r_2-\phi^2)\phi^4$, where $r_1>r_2>0$. Then, the parametric representations of the solitary wave solutions are given as (see Figure 30)

$$\phi(\xi)=\pm\sqrt{\frac{2r_1r_2}{r_1+r_2+(r_1-r_2)\cosh(g_{19}\xi)}}, \tag{74}$$

where $g_{19} = \sqrt{\frac{cr_1r_2}{2\alpha - a}}$.

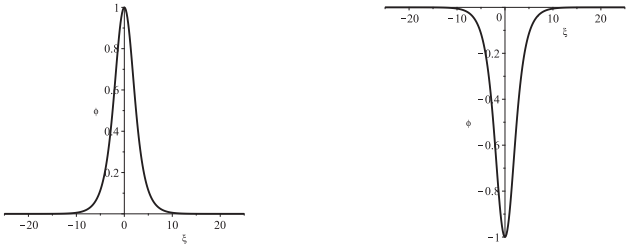

(**a**) (**b**)

Figure 30. Solitary wave forms of system (5). (**a**) Bright solitary wave derived by $(74)_+$. (**b**) Dark solitary wave derived by $(74)_-$.

Thus, the exact expressions of solutions to Equation (1) are presented as

$$u(x,t) = \pm\sqrt{\frac{2r_1r_2}{r_1 + r_2 + (r_1 - r_2)\cosh(g_{19}\frac{1}{\delta}(x^\delta - vt^\delta))}}e^{i\eta(x,t)}. \tag{75}$$

(iii) In formula (7), if $H(\phi, y) = h, h \in (h_0, h_1)$, there are two families of open curves, which tend to the singular line $\phi = 0$ under $|y| \to \infty$. The traveling wave solutions of these curves are as (70).

4.8. The Parameter Condition of $A - 2\alpha < 0, \Delta > 0, B < 0, \omega + \gamma + a\kappa^2 < 0$, $H_3 = h_4 < h_0 = h_1 = h_2$ *(See Figure 4(5))*

(i) In formula (7), if $H(\phi, y) = h, h \in (h_3, h_0)$, there are two families of periodic orbits. The expressions of the traveling wave solutions of these curves are identical to Equation (72).

(ii) In formula (7), if $H(\phi, y) = h_0$, there are four heteroclinic orbits, which encircle the equilibrium points E_3 and E_4 and link the saddle points E_0, E_1 and E_2. Now, we have $G(\phi) = \frac{c}{2\alpha - a}\left(\frac{-b+\sqrt{\Delta}}{2c} - \phi^2\right)^2\phi^4$. The heteroclinic orbit in the first quadrant corresponds to a kink wave solution, and the parametric expression of the kink wave solution is given as (see Figure 31a)

$$\phi(\xi) = \sqrt{\frac{-b+\sqrt{\Delta}}{4c} - \frac{-b+\sqrt{\Delta}}{4c}\tanh\left(\ln\sqrt{3} - \frac{-b+\sqrt{\Delta}}{4c}g_{20}\xi\right)}, \tag{76}$$

where $g_{20} = \sqrt{\frac{c}{2\alpha - a}}$.

The heteroclinic orbit in the forth quadrant corresponds to an anti-kink wave solution, and the parametric representation of the anti-kink wave solution is given as (see Figure 31b)

$$\phi(\xi) = \sqrt{\frac{-b+\sqrt{\Delta}}{4c} - \frac{-b+\sqrt{\Delta}}{4c}\tanh\left(\ln\sqrt{3} + \frac{-b+\sqrt{\Delta}}{4c}g_{20}\xi\right)}. \tag{77}$$

The heteroclinic orbit in the second quadrant corresponds to a kink wave solution, and the parametric representation of the kink wave solution is given as (see Figure 31c)

$$\phi(\xi) = -\sqrt{\frac{-b+\sqrt{\Delta}}{4c} - \frac{-b+\sqrt{\Delta}}{4c}\tanh\left(\ln\sqrt{3} + \frac{-b+\sqrt{\Delta}}{4c}g_{20}\xi\right)}. \tag{78}$$

The heteroclinic orbit in the third quadrant corresponds to an anti-kink wave solution, and the parametric representation of the anti-kink wave solution is given as (see Figure 31d)

$$\phi(\xi) = -\sqrt{\frac{-b+\sqrt{\Delta}}{4c} - \frac{-b+\sqrt{\Delta}}{4c}\tanh\left(\ln\sqrt{3} - \frac{-b+\sqrt{\Delta}}{4c}g_{20}\xi\right)}. \tag{79}$$

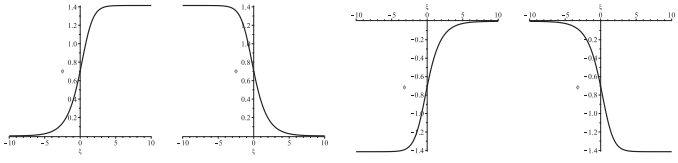

(**a**) (**b**) (**c**) (**d**)

Figure 31. Kink and anti-kink wave forms of system (5). (**a**) Kink wave given by (76). (**b**) Anti-kink wave given by (77). (**c**) Kink wave given by (78). (**d**) Anti-kink wave given by (79).

Thus, the exact expressions of solutions to Equation (1) are presented as

$$u(x,t) = \sqrt{\frac{-b+\sqrt{\Delta}}{4c} - \frac{-b+\sqrt{\Delta}}{4c}\tanh\left(\ln\sqrt{3} - \frac{-b+\sqrt{\Delta}}{4c}g_{20}\frac{1}{\delta}(x^\delta - vt^\delta)\right)}e^{i\eta(x,t)}, \tag{80}$$

$$u(x,t) = \sqrt{\frac{-b+\sqrt{\Delta}}{4c} - \frac{-b+\sqrt{\Delta}}{4c}\tanh\left(\ln\sqrt{3} + \frac{-b+\sqrt{\Delta}}{4c}g_{20}\frac{1}{\delta}(x^\delta - vt^\delta)\right)}e^{i\eta(x,t)}, \tag{81}$$

$$u(x,t) = -\sqrt{\frac{-b+\sqrt{\Delta}}{4c} - \frac{-b+\sqrt{\Delta}}{4c}\tanh\left(\ln\sqrt{3} + \frac{-b+\sqrt{\Delta}}{4c}g_{20}\frac{1}{\delta}(x^\delta - vt^\delta)\right)}e^{i\eta(x,t)}, \tag{82}$$

and

$$u(x,t) = -\sqrt{\frac{-b+\sqrt{\Delta}}{4c} - \frac{-b+\sqrt{\Delta}}{4c}\tanh\left(\ln\sqrt{3} - \frac{-b+\sqrt{\Delta}}{4c}g_{20}\frac{1}{\delta}(x^\delta - vt^\delta)\right)}e^{i\eta(x,t)}. \tag{83}$$

4.9. The Parameter Condition of $A-2\alpha<0, \Delta>0, B<0, \omega+\gamma+a\kappa^2<0$, $H_3=h_4<h_1=h_2<h_0$ *(See Figure 4(6))*

(i) In formula (7), if $H(\phi,y)=h, h\in(h_3,h_1)$, there are two families of periodic orbits. The expressions of the traveling wave solutions of these curves are identical to Equation (72).

(ii) In formula (7), if $H(\phi,y)=h_1$, there are two homoclinic orbits, which respectively encircle the equilibrium points E_3 and E_4. We have $G(\phi)=\frac{c}{4(2\alpha-a)}\left(\frac{-b+\sqrt{\Delta}}{2c}-\phi^2\right)^2(\phi^2-r_1)(\phi^2-r_2)$, where $\frac{-b+\sqrt{\Delta}}{2c}>r_1>0>r_2$. Then, the parametric representations of the solitary wave solutions are given as (see Figure 32)

$$\phi(\xi) = \pm\sqrt{\frac{(r_1+r_2)(\sqrt{\Delta}-b) - 4cr_1r_2 + (r_1-r_2)(\sqrt{\Delta}-b)\cosh(g_{21}\xi)}{2(\sqrt{\Delta}-b) - 2c(r_1+r_2) + 2c(r_1-r_2)\cosh(g_{21}\xi)}}, \tag{84}$$

where $g_{21}=\sqrt{\frac{(\sqrt{\Delta}-b-2cr_1)(\sqrt{\Delta}-b-2cr_2)}{4c(2\alpha-a)}}$.

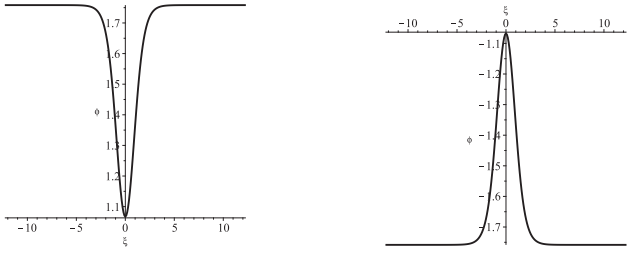

(**a**) (**b**)

Figure 32. Solitary wave forms of system (5). (**a**) Dark solitary wave derived by $(84)_+$. (**b**) Bright solitary wave derived by $(84)_-$.

Thus, the exact solutions of Equation (1) are

$$u(x,t)=\pm\sqrt{\frac{(r_1+r_2)(\sqrt{\Delta}-b)-4cr_1r_2+(r_1-r_2)(\sqrt{\Delta}-b)\cosh(g_{21}\frac{1}{\delta}(x^\delta-vt^\delta))}{2(\sqrt{\Delta}-b)-2c(r_1+r_2)+2c(r_1-r_2)\cosh(g_{21}\frac{1}{\delta}(x^\delta-vt^\delta))}}e^{i\eta(x,t)}. \tag{85}$$

5. Expressions of the Traveling Wave Solutions of System Equation (5) under $C>0, A=6\alpha-8\beta$

Currently, through integral calculation, we compute the exact parametric expressions of the traveling wave solutions under $c>0, a=6\alpha-8\beta$. However, in many cases, we cannot find the corresponding solution formulation; here, we only analyze the part where the solution formulation can be found. Because the solution of system (5) in this part is given in the form of a parametric expression, and the calculation process of the exact solution of Equation (1) obtained after the traveling wave transformation is substituted back is too complicated, the exact solution of Equation (1) is not given here. The solution follows from Equation (7) and the first equation of system (5):

$$\xi=\int_{\phi_0}^{\phi}\frac{d\phi}{y(\phi)}=\int_{\phi_0}^{\phi}\frac{\pm d\phi}{\sqrt{\frac{2c}{5(2\alpha-a)}\phi^6+\frac{2b}{3(2\alpha-a)}\phi^4+\frac{2(\omega+\gamma+a\kappa^2)}{a-2\alpha}\phi^2+h\phi}}. \tag{86}$$

5.1. The Parameter Condition of $A-2\alpha>0, \Delta>0, B<0, \omega+\gamma+a\kappa^2<0$, $H_1=-h_2<h_0<h_3=-h_4$ (See Figure 5(4))

(i) In formula (7), if $H(\phi,y)=h_4$, there are two homoclinic orbits and a periodic orbit. For one of the homoclinic orbits that tangents the singular line $\phi=0$ to $E_0(0,0)$, we have $y^2=\frac{2c}{5(a-2\alpha)}(r_1-\phi)(r_2-\phi)(0-\phi)\left(\phi+\sqrt{\frac{-b-\sqrt{\Delta}}{2c}}\right)^2(\phi-r_3)$. For the other homoclinic orbit, we have $y^2=\frac{2c}{5(a-2\alpha)}(r_1-\phi)(r_2-\phi)(0-\phi)\left(-\sqrt{\frac{-b-\sqrt{\Delta}}{2c}}-\phi\right)^2(\phi-r_3)$. For the periodic orbit, we have $y^2=\frac{2c}{5(a-2\alpha)}(r_1-\phi)(\phi-r_2)\phi\left(\phi+\sqrt{\frac{-b-\sqrt{\Delta}}{2c}}\right)^2(\phi-r_3)$, where $r_1>r_2>0>-\sqrt{\frac{-b-\sqrt{\Delta}}{2c}}>r_3$. Then, the parametric representations of the traveling wave solution for the homoclinic orbit that contacts the singular line $\phi=0$ at E_0 are given as

$$\begin{aligned}\phi(\chi)&=\frac{r_2r_3\mathrm{sn}^2(\chi,k_{10})}{r_2-r_3+r_3\mathrm{sn}^2(\chi,k_{10})},\\ \xi(\chi)&=\frac{\beta_1^2-\alpha_1^2}{g_{22}}\Pi(\chi,\beta_1^2)+\frac{\alpha_1^2}{g_{22}}\chi,\end{aligned} \tag{87}$$

where $\alpha_1^2 = \frac{r_3}{r_3 - r_2}$, $\beta_1^2 = \frac{r_3\left(r_2 + \sqrt{\frac{-b-\sqrt{\Delta}}{2c}}\right)}{(r_3 - r_2)\sqrt{\frac{-b-\sqrt{\Delta}}{2c}}}$, $k_{10}^2 = \frac{r_3(r_2 - r_1)}{r_1(r_2 - r_3)}$, $g_{22} = \frac{1}{2}\beta_1^2\sqrt{\frac{-b-\sqrt{\Delta}}{2c}}\sqrt{\frac{2cr_1(r_2 - r_3)}{5(a-2\alpha)}}$.

The parametric representations of the traveling wave solution for the other homoclinic orbit are given as

$$\begin{aligned} \phi(\chi) &= \frac{r_1 r_3(1 - \mathrm{sn}^2(\chi, k_{11}))}{r_1 - r_3\mathrm{sn}^2(\chi, k_{11})}, \\ \xi(\chi) &= \frac{\beta_2^2 - \alpha_2^2}{g_{23}}\Pi(\chi, \beta_2^2) + \frac{\alpha_2^2}{g_{23}}\chi, \end{aligned} \tag{88}$$

where $\beta_2^2 = \alpha_2^2\left(r_1 + \sqrt{\frac{-b-\sqrt{\Delta}}{2c}}\right)\left(r_3 + \sqrt{\frac{-b-\sqrt{\Delta}}{2c}}\right)$, $g_{23} = -\frac{1}{2}\beta_2^2\left(r_3 + \sqrt{\frac{-b-\sqrt{\Delta}}{2c}}\right)\sqrt{\frac{2cr_1(r_2 - r_3)}{5(a-2\alpha)}}$, $\alpha_2^2 = \frac{r_3}{r_1}$, $k_{11}^2 = \frac{r_3(r_2 - r_1)}{r_1(r_2 - r_3)}$.

The parametric expressions of the traveling wave solution for the periodic orbit are given as

$$\begin{aligned} \phi(\chi) &= \frac{r_1(r_2 - r_3) + r_3(r_1 - r_2)\mathrm{sn}^2(\chi, k_{12})}{r_2 - r_3 + (r_1 - r_2)\mathrm{sn}^2(\chi, k_{12})}, \\ \xi(\chi) &= \frac{\beta_3^2 - \alpha_3^2}{g_{24}}\Pi(\chi, \beta_3^2) + \frac{\alpha_3^2}{g_{24}}\chi, \end{aligned} \tag{89}$$

where $\beta_3^2 = \frac{(r_2 - r_1)\left(r_3 + \sqrt{\frac{-b-\sqrt{\Delta}}{2c}}\right)}{(r_2 - r_3)\left(r_1 + \sqrt{\frac{-b-\sqrt{\Delta}}{2c}}\right)}$, $g_{24} = \frac{1}{2}\beta_3^2\left(r_1 + \sqrt{\frac{-b-\sqrt{\Delta}}{2c}}\right)\sqrt{\frac{2cr_1(r_2 - r_3)}{5(a-2\alpha)}}$, $\alpha_3^2 = \frac{r_2 - r_1}{r_2 - r_3}$, $k_{12}^2 = \frac{r_3(r_2 - r_1)}{r_1(r_2 - r_3)}$.

(ii) For the curves $H(\phi, y) = h_3$, there exist a periodic orbit and two homoclinic orbits. For the periodic orbit, we have $y^2 = \frac{2c}{5(a-2\alpha)}(r_1 - \phi)\left(\sqrt{\frac{-b-\sqrt{\Delta}}{2c}} - \phi\right)^2(0 - \phi)(r_2 - \phi)(\phi - r_3)$. For one of the homoclinic orbits that contacts the singular line $\phi = 0$ at $E_0(0, 0)$, we have $y^2 = \frac{2c}{5(a-2\alpha)}(r_1 - \phi)\left(\sqrt{\frac{-b-\sqrt{\Delta}}{2c}} - \phi\right)^2\phi(\phi - r_2)(\phi - r_3)$. For the other homoclinic orbit, we have $y^2 = \frac{2c}{5(a-2\alpha)}(r_1 - \phi)\left(\phi - \sqrt{\frac{-b-\sqrt{\Delta}}{2c}}\right)^2\phi(\phi - r_2)(\phi - r_3)$, where $r_1 > \sqrt{\frac{-b-\sqrt{\Delta}}{2c}} > 0 > r_2 > r_3$. Then, the parametric representations of the traveling wave solution for the periodic orbit are given as

$$\begin{aligned} \phi(\chi) &= \frac{r_2 r_3}{r_3 + (r_2 - r_3)\mathrm{sn}^2(\chi, k_{13})}, \\ \xi(\chi) &= \frac{\beta_4^2 - \alpha_4^2}{g_{25}}\Pi(\chi, \beta_4^2) + \frac{\alpha_4^2}{g_{25}}\chi, \end{aligned} \tag{90}$$

where $\beta_4^2 = \frac{(r_2 - r_3)\sqrt{\frac{-b-\sqrt{\Delta}}{2c}}}{r_3\left(r_2 - \sqrt{\frac{-b-\sqrt{\Delta}}{2c}}\right)}$, $g_{25} = \frac{1}{2}\beta_4^2\left(\sqrt{\frac{-b-\sqrt{\Delta}}{2c}} - r_2\right)\sqrt{\frac{2cr_3(r_2 - r_1)}{5(a-2\alpha)}}$, $\alpha_4^2 = \frac{r_3 - r_2}{r_3}$, $k_{13}^2 = \frac{r_1(r_2 - r_3)}{r_3(r_2 - r_1)}$.

The parametric representations of the traveling wave solution for the homoclinic orbit that contacts the singular line $\phi = 0$ at E_0 are given as

$$\begin{aligned} \phi(\chi) &= \frac{r_1 r_2 \mathrm{sn}^2(\chi, k_{14})}{r_2 - r_1 + r_1\mathrm{sn}^2(\chi, k_{14})}, \\ \xi(\chi) &= \frac{\beta_5^2 - \alpha_5^2}{g_{26}}\Pi(\chi, \beta_5^2) + \frac{\alpha_5^2}{g_{26}}\chi, \end{aligned} \tag{91}$$

where $\alpha_5^2=\frac{r_1}{r_1-r_2}$, $\beta_5^2=\frac{r_1\left(\sqrt{\frac{-b-\sqrt{\Delta}}{2c}}-r_2\right)}{(r_1-r_2)\sqrt{\frac{-b-\sqrt{\Delta}}{2c}}}$, $k_{14}^2=\frac{r_1(r_2-r_3)}{r_3(r_2-r_1)}$, $g_{26}=\frac{1}{2}\beta_5^2\sqrt{\frac{-b-\sqrt{\Delta}}{2c}}\sqrt{\frac{2cr_3(r_2-r_1)}{5(a-2\alpha)}}$.

The parametric representations of the traveling wave solution for the other homoclinic orbit are given as

$$\begin{aligned}\phi(\chi)&=\frac{r_1r_3(\mathrm{sn}^2(\chi,k_{15})-1)}{r_1\mathrm{sn}^2(\chi,k_{15})-r_3},\\ \xi(\chi)&=\frac{\beta_6^2-\alpha_6^2}{g_{27}}\Pi(\chi,\beta_6^2)+\frac{\alpha_6^2}{g_{27}}\chi,\end{aligned}\tag{92}$$

where $\beta_6^2=\frac{r_1\left(\sqrt{\frac{-b-\sqrt{\Delta}}{2c}}-r_3\right)}{r_3\left(\sqrt{\frac{-b-\sqrt{\Delta}}{2c}}-r_1\right)}$, $g_{27}=\frac{1}{2}\beta_6^2\left(r_1-\sqrt{\frac{-b-\sqrt{\Delta}}{2c}}\right)\sqrt{\frac{2cr_3(r_2-r_1)}{5(a-2\alpha)}}$, $\alpha_6^2=\frac{r_1}{r_3}$, $k_{15}^2=\frac{r_1(r_2-r_3)}{r_3(r_2-r_1)}$.

5.2. The Parameter Condition of $A-2\alpha>0,\Delta>0,B<0,\omega+\gamma+a\kappa^2<0$, $H_1=h_2=h_0<h_3=-h_4$ (See Figure 5(5))

(i) In formula (7), if $H(\phi,y)=h_4$, there are two homoclinic orbits. For one of the homoclinic orbits that tangents the singular line $\phi=0$ to $E_0(0,0)$, we have $y^2=\frac{2c}{5(a-2\alpha)}(0-\phi)\left(\phi+\sqrt{\frac{-b-\sqrt{\Delta}}{2c}}\right)^2(\phi-r_1)(\phi-r_2)(\phi-\bar{r_2})$, but we do not find a corresponding formulation for solving it.

For the other homoclinic orbit, we have $y^2=\frac{2c}{5(a-2\alpha)}(0-\phi)\left(-\sqrt{\frac{-b-\sqrt{\Delta}}{2c}}-\phi\right)^2(\phi-r_1)(\phi-r_2)(\phi-\bar{r_2})$, where $-\sqrt{\frac{-b-\sqrt{\Delta}}{2c}}>r_1$, r_2 and $\bar{r_2}$ are complex. Then, we derive the parametric representations of the traveling wave solution for the homoclinic orbit as follows:

$$\begin{aligned}\phi(\chi)=&\frac{r_1A_2(1+\mathrm{cn}(\chi,k_{16}))}{A_2+B_2+(B_2-A_2)\mathrm{cn}(\chi,k_{16})},\\ \xi(\chi)=&g_{28}\left(\beta_7\chi+\frac{\alpha_7-\beta_7}{1-\alpha_7^2}\Pi\left(\chi,\frac{\alpha_7^2}{\alpha_7^2-1}\right)-\frac{\alpha_7(\alpha_7-\beta_7)}{2(1-\alpha_7^2)}\sqrt{\frac{\alpha_7^2-1}{k_{16}^2+(1-k_{16}^2)\alpha_7^2}}\right.\\ &\left.\ln\left(\frac{\sqrt{k_{16}^2+(1-k_{16}^2)\alpha_7^2}\mathrm{dn}\chi+\sqrt{\alpha_7^2-1}\mathrm{sn}\chi}{\sqrt{k_{16}^2+(1-k_{16}^2)\alpha_7^2}\mathrm{dn}\chi-\sqrt{\alpha_7^2-1}\mathrm{sn}\chi}\right)\right),\end{aligned}\tag{93}$$

where $A_2^2=r_2\bar{r_2}$, $B_2^2=(r_1-r_2)(r_1-\bar{r_2})$, $g_{28}=\frac{A_2+B_2}{\sqrt{A_2B_2}\left((B_2-A_2)\sqrt{\frac{-b-\sqrt{\Delta}}{2c}}-r_1A_2\right)}\sqrt{\frac{5(a-2\alpha)}{2c}}$, $k_{16}^2=\frac{r_1^2-(A_2-B_2)^2}{4A_2B_2}$, $\alpha_7=\frac{r_1A_2+(A_2-B_2)\sqrt{\frac{-b-\sqrt{\Delta}}{2c}}}{r_1A_2+(A_2+B_2)\sqrt{\frac{-b-\sqrt{\Delta}}{2c}}}$, $\beta_7=\frac{A_2-B_2}{A_2+B_2}$, $\frac{\alpha_7^2}{\alpha_7^2-1}>k_{16}^2$.

(ii) In formula (7), if $H(\phi,y)=h_3$, there are two homoclinic orbits. For one of the homoclinic orbits that tangents the singular line $\phi=0$ to $E_0(0,0)$, we have $y^2=\frac{2c}{5(a-2\alpha)}(r_1-\phi)\left(\sqrt{\frac{-b-\sqrt{\Delta}}{2c}}-\phi\right)^2\phi(\phi-r_2)(\phi-\bar{r_2})$, where $r_1>\sqrt{\frac{-b-\sqrt{\Delta}}{2c}}>0$, r_2 and $\bar{r_2}$ are complex. Then, we derive the expressions of the traveling wave solution for the homoclinic orbit as follows:

$$\begin{aligned}\phi(\chi) =&\frac{r_1B_3(1-\mathrm{cn}(\chi,k_{17}))}{A_3+B_3+(A_3-B_3)\mathrm{cn}(\chi,k_{17})},\\ \xi(\chi) =&g_{29}\left(\beta_8\chi+\frac{\alpha_8-\beta_8}{1-\alpha_8^2}\Pi\left(\chi,\frac{\alpha_8^2}{\alpha_8^2-1}\right)-\frac{\alpha_8(\alpha_8-\beta_8)}{2(1-\alpha_8^2)}\sqrt{\frac{\alpha_8^2-1}{k_{17}^2+(1-k_{17}^2)\alpha_8^2}}\right.\\ &\left.\ln\left(\frac{\sqrt{k_{17}^2+(1-k_{17}^2)\alpha_8^2}\mathrm{dn}\chi+\sqrt{\alpha_8^2-1}\mathrm{sn}\chi}{\sqrt{k_{17}^2+(1-k_{17}^2)\alpha_8^2}\mathrm{dn}\chi-\sqrt{\alpha_8^2-1}\mathrm{sn}\chi}\right)\right),\end{aligned}\tag{94}$$

where $A_3^2=(r_1-r_2)(r_1-\bar{r_2})$, $B_3^2=r_2\bar{r_2}$, $g_{29}=\frac{A_3+B_3}{\sqrt{A_3B_3}\left(r_1B_3+(A_3-B_3)\sqrt{\frac{-b-\sqrt{\Delta}}{2c}}\right)}\sqrt{\frac{5(a-2\alpha)}{2c}}$, $k_{17}^2=\frac{r_1^2-(A_3-B_3)^2}{4A_3B_3}$, $\alpha_8=\frac{(B_3-A_3)\sqrt{\frac{-b-\sqrt{\Delta}}{2c}}-r_1B_3}{r_1B_3-(A_3+B_3)\sqrt{\frac{-b-\sqrt{\Delta}}{2c}}}$, $\beta_8=\frac{A_3-B_3}{A_3+B_3}$, $\frac{\alpha_8^2}{\alpha_8^2-1}>k_{17}^2$.

For the other homoclinic orbit, we have $y^2=\frac{2c}{5(a-2\alpha)}(r_1-\phi)\left(\phi-\sqrt{\frac{-b-\sqrt{\Delta}}{2c}}\right)^2\phi(\phi-r_2)(\phi-\bar{r_2})$, but we do not find a corresponding formulation for solving it.

5.3. The Parameter Condition of $A-2\alpha>0,\Delta>0,B<0,\omega+\gamma+a\kappa^2<0$, $H_0<h_1=-h_2<h_3=-h_4$ (See Figure 5(6))

(i) In formula (7), if $H(\phi,y)=h_4$, there are one homoclinic orbit and two heteroclinic orbits that contact the singular line $\phi=0$ at $E_0(0,0)$. The traveling wave solutions of these curves are the same as (93).

(ii) In formula (7), if $H(\phi,y)=h_3$, there are one homoclinic orbit and two heteroclinic orbits that contact the singular line $\phi=0$ at $E_0(0,0)$. The traveling wave solutions of these curves are same as (94).

5.4. The Case of $\Delta>0,\omega+\gamma+a\kappa^2>0$ (See Figure 6(3))

For the curves $H(\phi,y)=h_1$, there exists a homoclinic orbit, which contacts the singular line $\phi=0$ at $E_0(0,0)$. We have $y^2=\frac{2c}{5(2\alpha-a)}\left(\sqrt{\frac{-b+\sqrt{\Delta}}{2c}}-\phi\right)^2\phi(\phi-r_1)(\phi-r_2)(\phi-\bar{r_2})$, where $\sqrt{\frac{-b+\sqrt{\Delta}}{2c}}>0>r_1$, r_2 and $\bar{r_2}$ are complex. Then, we derive the expressions of the traveling wave solution for the homoclinic orbit as follows:

$$\begin{aligned}\phi(\chi) =&\frac{r_1A_4(1-\mathrm{cn}(\chi,k_{18}))}{A_4-B_4-(A_4+B_4)\mathrm{cn}(\chi,k_{18})},\\ \xi(\chi) =&g_{30}\left(\beta_9\chi+\frac{\alpha_9-\beta_9}{1-\alpha_9^2}\Pi\left(\chi,\frac{\alpha_9^2}{\alpha_9^2-1}\right)-\frac{\alpha_9(\alpha_9-\beta_9)}{2(1-\alpha_9^2)}\sqrt{\frac{\alpha_9^2-1}{k_{18}^2+(1-k_{18}^2)\alpha_9^2}}\right.\\ &\left.\ln\left(\frac{\sqrt{k_{18}^2+(1-k_{18}^2)\alpha_9^2}\mathrm{dn}\chi+\sqrt{\alpha_9^2-1}\mathrm{sn}\chi}{\sqrt{k_{18}^2+(1-k_{18}^2)\alpha_9^2}\mathrm{dn}\chi-\sqrt{\alpha_9^2-1}\mathrm{sn}\chi}\right)\right),\end{aligned}\tag{95}$$

where $A_4^2=r_2\bar{r_2}$, $B_4^2=(r_1-r_2)(r_1-\bar{r_2})$, $g_{30}=\frac{A_4-B_4}{\sqrt{A_4B_4}\left(r_1A_4-(A_4+B_4)\sqrt{\frac{-b+\sqrt{\Delta}}{2c}}\right)}\sqrt{\frac{5(2\alpha-a)}{2c}}$, $k_{18}^2=\frac{(A_4+B_4)^2-r_1^2}{4A_4B_4}$, $\alpha_9=\frac{r_1A_4-(A_4+B_4)\sqrt{\frac{-b+\sqrt{\Delta}}{2c}}}{(A_4-B_4)\sqrt{\frac{-b+\sqrt{\Delta}}{2c}}-r_1A_4}$, $\beta_9=\frac{B_4+A_4}{B_4-A_4}$, $\frac{\alpha_9^2}{\alpha_9^2-1}>k_{18}^2$.

5.5. The Parameter Condition of $A-2\alpha<0,\Delta>0,B<0,\omega+\gamma+a\kappa^2<0$, $H_3=-h_4<h_0<h_1=-h_2$ (See Figure 6(5))

(i) For the curves $H(\phi,y)=h_2$, there exist a periodic orbit and a homoclinic orbit that contacts the singular line $\phi=0$ at E_0. For the periodic orbit, we have $y^2=\frac{2c}{5(2\alpha-a)}(r_1-$

$\phi)(r_2-\phi)(\phi-r_3)\phi\left(\phi+\sqrt{\frac{-b+\sqrt{\Delta}}{2c}}\right)^2$. For the homoclinic orbit, we have $y^2=\frac{2c}{5(2\alpha-a)}(r_1-\phi)(r_2-\phi)(r_3-\phi)(0-\phi)\left(\phi+\sqrt{\frac{-b+\sqrt{\Delta}}{2c}}\right)^2$, where $r_1>r_2>r_3>0>-\sqrt{\frac{-b+\sqrt{\Delta}}{2c}}$. Then, the parametric representations of the traveling wave solutions for the periodic orbit are given as

$$\begin{aligned}\phi(\chi)&=\frac{r_2(r_1-r_3)-r_1(r_2-r_3)\mathrm{sn}^2(\chi,k_{19})}{r_1-r_3-(r_2-r_3)\mathrm{sn}^2(\chi,k_{19})},\\ \xi(\chi)&=\frac{\beta_{10}^2-\alpha_{10}^2}{g_{31}}\Pi(\chi,\beta_{10}^2)+\frac{\alpha_{10}^2}{g_{31}}\chi,\end{aligned}\tag{96}$$

where $\beta_{10}^2=\frac{(r_2-r_3)\left(r_1+\sqrt{\frac{-b+\sqrt{\Delta}}{2c}}\right)}{(r_1-r_3)\left(r_2+\sqrt{\frac{-b+\sqrt{\Delta}}{2c}}\right)}$, $g_{31}=\frac{1}{2}\beta_{10}^2\left(r_2+\sqrt{\frac{-b+\sqrt{\Delta}}{2c}}\right)\sqrt{\frac{2cr_2(r_3-r_1)}{5(a-2\alpha)}}$, $\alpha_{10}^2=\frac{r_2-r_3}{r_1-r_3}$, $k_{19}^2=\frac{r_1(r_2-r_3)}{r_2(r_1-r_3)}$. The expressions of the traveling wave solution for the homoclinic orbit are presented as

$$\begin{aligned}\phi(\chi)&=\frac{r_1r_3\mathrm{sn}^2(\chi,k_{20})}{r_3-r_1+r_1\mathrm{sn}^2(\chi,k_{20})},\\ \xi(\chi)&=\frac{\beta_{11}^2-\alpha_{11}^2}{g_{32}}\Pi(\chi,\beta_{11}^2)+\frac{\alpha_{11}^2}{g_{32}}\chi,\end{aligned}\tag{97}$$

where $\alpha_{11}^2=\frac{r_1}{r_1-r_3}$, $\beta_{11}^2=\frac{r_1\left(r_3+\sqrt{\frac{-b+\sqrt{\Delta}}{2c}}\right)}{(r_1-r_3)\sqrt{\frac{-b+\sqrt{\Delta}}{2c}}}$, $k_{20}^2=\frac{r_1(r_2-r_3)}{r_2(r_1-r_3)}$, $g_{32}=\frac{1}{2}\beta_{11}^2\sqrt{\frac{-b+\sqrt{\Delta}}{2c}}\sqrt{\frac{2cr_2(r_3-r_1)}{5(a-2\alpha)}}$.

(ii) For the curves $H(\phi,y)=h_1$, there exist a periodic orbit and a homoclinic orbit that contacts the singular line $\phi=0$ at E_0. For the periodic orbit, we have $y^2=\frac{2c}{5(2\alpha-a)}\left(\sqrt{\frac{-b+\sqrt{\Delta}}{2c}}-\phi\right)^2(0-\phi)(r_1-\phi)(\phi-r_2)(\phi-r_3)$. For the homoclinic orbit, we have $y^2=\frac{2c}{5(2\alpha-a)}\left(\sqrt{\frac{-b+\sqrt{\Delta}}{2c}}-\phi\right)^2\phi(\phi-r_1)(\phi-r_2)(\phi-r_3)$, where $\sqrt{\frac{-b+\sqrt{\Delta}}{2c}}>0>r_1>r_2>r_3$. The parametric expressions of the traveling wave solution for the periodic orbit are given as

$$\begin{aligned}\phi(\chi)&=\frac{r_1r_2}{r_2+(r_1-r_2)\mathrm{sn}^2(\chi,k_{21})},\\ \xi(\chi)&=\frac{\beta_{12}^2-\alpha_{12}^2}{g_{33}}\Pi(\chi,\beta_{12}^2)+\frac{\alpha_{12}^2}{g_{33}}\chi,\end{aligned}\tag{98}$$

where $\beta_{12}^2=\frac{(r_1-r_2)\sqrt{\frac{-b+\sqrt{\Delta}}{2c}}}{r_2\left(r_1-\sqrt{\frac{-b+\sqrt{\Delta}}{2c}}\right)}$, $g_{33}=\frac{1}{2}\beta_{12}^2\left(\sqrt{\frac{-b+\sqrt{\Delta}}{2c}}-r_1\right)\sqrt{\frac{2cr_2(r_1-r_3)}{5(a-2\alpha)}}$, $\alpha_{12}^2=\frac{r_2-r_1}{r_2}$, $k_{21}^2=\frac{r_3(r_1-r_2)}{r_2(r_1-r_3)}$. The implicit parametric expression of the traveling wave solution for the homoclinic orbit is given as follows:

$$\begin{aligned}\phi(\chi)&=\frac{r_1r_3\mathrm{sn}^2(\chi,k_{22})}{r_1-r_3+r_3\mathrm{sn}^2(\chi,k_{22})},\\ \xi(\chi)&=\frac{\beta_{13}^2-\alpha_{13}^2}{g_{34}}\Pi(\chi,\beta_{13}^2)+\frac{\alpha_{13}^2}{g_{34}}\chi,\end{aligned}\tag{99}$$

where $\alpha_{13}^2=\frac{r_3}{r_3-r_1}$, $\beta_{13}^2=\frac{r_3\left(r_1-\sqrt{\frac{-b+\sqrt{\Delta}}{2c}}\right)}{(r_1-r_3)\sqrt{\frac{-b+\sqrt{\Delta}}{2c}}}$, $k_{22}^2=\frac{r_3(r_1-r_2)}{r_2(r_1-r_3)}$, $g_{34}=\frac{1}{2}\beta_{13}^2\sqrt{\frac{-b+\sqrt{\Delta}}{2c}}\sqrt{\frac{2cr_2(r_1-r_3)}{5(a-2\alpha)}}$.

5.6. The Parameter Condition of $A-2\alpha<0, \Delta>0, B<0, \omega+\gamma+a\kappa^2<0$, $H_3=-h_4<h_1=-h_2<h_0$ *(See Figure 6(7))*

For the level curves $H(\phi,y)=h_1$, there exists a homoclinic orbit to E_1. We have $y^2=\frac{2c}{5(2\alpha-a)}\left(\sqrt{\frac{-b+\sqrt{\Delta}}{2c}}-\phi\right)^2(\phi-r_1)\phi(\phi-r_2)(\phi-\bar{r_2})$, where $\sqrt{\frac{-b+\sqrt{\Delta}}{2c}}>r_1>0$, r_2 and $\bar{r_2}$ are complex. Then, the parametric representations of the traveling wave solution for the homoclinic orbit are given as

$$\begin{aligned}\phi(\chi)=&\frac{r_1B_5(1+\mathrm{cn}(\chi,k_{23}))}{B_5-A_5+(A_5+B_5)\mathrm{cn}(\chi,k_{23})},\\ \xi(\chi)=&g_{35}\left(\beta_{14}\chi+\frac{\alpha_{14}-\beta_{14}}{1-\alpha_{14}^2}\Pi\left(\chi,\frac{\alpha_{14}^2}{\alpha_{14}^2-1}\right)-\frac{\alpha_{14}(\alpha_{14}-\beta_{14})}{2(1-\alpha_{14}^2)}\sqrt{\frac{\alpha_{14}^2-1}{k_{23}^2+(1-k_{23}^2)\alpha_{14}^2}}\right.\\ &\left.\ln\left(\frac{\sqrt{k_{23}^2+(1-k_{23}^2)\alpha_{14}^2}\mathrm{dn}\chi+\sqrt{\alpha_{14}^2-1}\mathrm{sn}\chi}{\sqrt{k_{23}^2+(1-k_{23}^2)\alpha_{14}^2}\mathrm{dn}\chi-\sqrt{\alpha_{14}^2-1}\mathrm{sn}\chi}\right)\right),\end{aligned}\tag{100}$$

where $A_5^2=(r_1-r_2)(r_1-\bar{r_2})$, $B_5^2=r_2\bar{r_2}$, $g_{35}=\frac{A_5-B_5}{\sqrt{A_5B_5}\left(r_1B_5-(A_5+B_5)\sqrt{\frac{-b+\sqrt{\Delta}}{2c}}\right)}\sqrt{\frac{5(2\alpha-a)}{2c}}$, $k_{23}^2=\frac{(A_5+B_5)^2-r_1^2}{4A_5B_5}$, $\alpha_{14}=\frac{r_1B_5-(A_5+B_5)\sqrt{\frac{-b+\sqrt{\Delta}}{2c}}}{r_1B_5+(A_5-B_5)\sqrt{\frac{-b+\sqrt{\Delta}}{2c}}}$, $\beta_{14}=\frac{B_5+A_5}{B_5-A_5}$, $\frac{\alpha_{14}^2}{\alpha_{14}^2-1}>k_{23}^2$.

6. Main Results

Based on the above analysis and calculation, we obtain the exact expressions of wave solutions of the FCGL equation. We list them all in the following theorem.

Theorem 1. *The exact expressions of wave solutions of the FCGL equation are as below:*

(B1) *Corresponding to some periodic orbits, there exist exact periodic wave solutions determined by (17), (23), (24), (33), (39), (54), (58), (62), (64), (72), (89), (90), (96) and (98).*

(B2) *Corresponding to some homoclinic orbits, there exist exact solitary wave solutions determined by (19), (21), (27), (41), (51), (56), (60), (68), (74), (84), (87), (88), (91)–(95), (97), (99) and (100).*

(B3) *Corresponding to some heteroclinic orbits, there exist exact kink and anti-kink wave solutions determined by (13), (14), (28), (29), (35), (36), (43)–(46) and (76)–(79).*

(B4) *Corresponding to some open orbits, there exist exact compacton solutions determined by (65) and (70).*

7. Conclusions

In this paper, we investigate the bifurcations and the exact solutions of the time–space fractional complex Ginzburg–Landau equation with parabolic law nonlinearity ($F(|q|^2)=c_1|q|^2+c_2|q|^4$). All possible explicit representations of traveling wave solutions are given for the time-space FCGL equation under different parameter domains, including peakon solutions, periodic peakon solutions, compacton solutions, kink and anti-kink wave solutions, solitary wave solutions, periodic wave solutions and so on. Our method is different from the previous works on the exact solutions of the time-space FCGL equation and is based on the applying bifurcation theory of planar dynamical systems.

Author Contributions: Methodology, W.Z. and Y.X.; software, W.Z., Z.L. and M.G.; validation, W.Z., Z.L., Y.X. and M.G.; formal analysis, W.Z., Z.L. and Y.X.; investigation, W.Z., Z.L. and Y.X.; writing—original draft preparation, W.Z. and Z.L.; writing—review and editing, Y.X.; supervision, Y.X. All authors have read and agreed to the published version of the manuscript.

Funding: This work was jointly supported by the National Natural Science Foundation of China under Grant (No. 11901547), and Natural Science Foundation of Zhejiang Province under Grant (No. LQ19A040003).

Data Availability Statement: This manuscript has no associated data.

Acknowledgments: The authors are very grateful to the editors and anonymous reviewers for their constructive comments and suggestions.

Conflicts of Interest: The authors declare no conflict of interest.

References

1. Weitzner, H.; Zaslavsky, G.M. Some applications of fractional equations. *Commun. Nonlinear Sci. and Numer. Simul.* **2003**, *8*, 273–281. [CrossRef]
2. Tarasov, V.E. Fractional dynamics. In *Nonlinear Physical Science*; Springer: Berlin/Heidelberg, Germany, 2010.
3. Tarasov, V.E.; Zaslavsky, G.M. Fractional Ginzburg-Landau equation for fractal media. *Physica A* **2005**, *354*, 249–261. [CrossRef]
4. Abdou, M.A.; Soliman, A.A.; Biswas, A.; Ekici, M.; Zhou, Q.; Moshokoa, S.P. Dark-singular combo optical solitons with fractional complex Ginzburg-Landau equation. *Optik* **2018**, *171*, 463–467. [CrossRef]
5. Arshed, S. Soliton solutions of fractional complex Ginzburg-Landau equation with Kerr law and non-Kerr law media. *Optik* **2018**, *160*, 322–332. [CrossRef]
6. Fang, J.; Mou, D.; Wang, Y.; Zhang, H.; Dai, C.; Chen, Y. Soliton dynamics based on exact solutions of conformable fractional discrete complex cubic Ginzburg-Landau equation. *Results Phys.* **2021**, *20*, 103710. [CrossRef]
7. Li, L.; Jin, L.; Fang, S. Large time behavior for the fractional Ginzburg-Landau equations near the BCS-BEC crossover regime of Fermi gases. *Bound. Value Probl.* **2017**, *2017.1*, 1–16. [CrossRef]
8. Lu, H.; Bates, P.W.; Lü, S.; Zhang, M. Dynamics of the 3-D fractional complex Ginzburg-Landau equation. *Differ. Equ.* **2015**, *259*, 5276–5301. [CrossRef]
9. Milovanov, A.; Rasmussen, J. Fractional generalization of the Ginzburg-Landau equation: An unconventional approach to critical phenomena in complex media. *Phys. Lett. A* **2005**, *337*, 75–80. [CrossRef]
10. Mvogo, A.; Tambue, A.; Ben-Bolie, G.; Kofane, T. Localized numerical impulse solutions in diffuse neural networks modeled by the complex fractional Ginzburg-Landau equation. *Commun. Nonlinear Sci.* **2016**, *39*, 396–410. [CrossRef]
11. Pu, X.; Guo, B. Well-posedness and dynamics for the fractional Ginzburg-Landau equation. *Appl. Anal.* **2013**, *92*, 318–334. [CrossRef]
12. Qiu, Y.; Malomed, B.A.; Mihalache, D.; Zhu, X.; Zhang, L.; He, Y. Soliton dynamics in a fractional complex Ginzburg-Landau model. *Chaos Solitons Frcatals* **2020**, *131*, 109471. [CrossRef]
13. Raza, N. Exact periodic and explicit solutions of the conformable time fractional Ginzburg-Landau equation. *Opt. Quant. Electron.* **2018**, *50*, 154. [CrossRef]
14. Sadaf, M.; Akram, G.; Dawood, M. An investigation of fractional complex Ginzburg-Landau equation with Kerr law nonlinearity in the sense of conformable, beta and M-truncated derivatives. *Opt. Quantum Electron.* **2022**, *54*, 248. [CrossRef]
15. Zhu, W.; Xia, Y.; Zhang, B.; Bai, Y. Exact traveling wave solutions and bifurcations of the time fractional differential equations with applications. *Internat. J. Bifur. Chaos* **2019**, *29*, 1950041. [CrossRef]
16. Chen, A.; Tian, C.; Huang, W. Periodic solutions with equal period for the Friedmann-Robertson-Walker model. *Appl. Math. Lett.* **2018**, *77*, 101–107. [CrossRef]
17. Chen, A.; Guo, L.; Huang, W. Existence of kink waves and periodic waves for a perturbed defocusing mKdV equation. *Qual. Theory Dyn. Syst.* **2018**, *17*, 495–517. [CrossRef]
18. Sun, X.; Yu, P. Periodic traveling waves in a generalized BBM equation with weak backward diffusion and dissipation terms. *Discret. Contin. Dyn. Syst.* **2019**, *24*, 965–987. [CrossRef]
19. Sun, X.; Huang, W.; Cai, J. Coexistence of the solitary and periodic waves in convecting shallow water fluid. *Nonlinear Anal. Real World Appl.* **2020**, *53*, 103067. [CrossRef]
20. Ge, J.; Du, Z. The solitary wave solutions of the nonlinear perturbed shallow water wave model. *Appl. Math. Lett.* **2020**, *103*, 106202. [CrossRef]
21. Chen, A.; Guo, L.; Deng, X. Existence of solitary waves and periodic waves for a perturbed generalized BBM equation. *J. Differ. Equ.* **2016**, *261*, 5324–5349. [CrossRef]
22. Du, Z.; Li, J.; Li, X. The existence of solitary wave solutions of delayed Camassa-Holm equation via a geometric approach. *J. Funct. Anal.* **2018**, *275*, 988–1007. [CrossRef]
23. Zhu, K.; Shen, J. Smooth travelling wave solutions in a generalized Degasperis-Procesi equation. *Commun. Nonl. Sci. Numer. Simulat.* **2021**, *98*, 105763. [CrossRef]
24. Song, Y.; Tang, X. Stability, Steady-state bifurcations, and turing patterns in a predator-prey model with herd behavior and prey-taxis. *Stud. Appl. Math.* **2017**, *139*, 371–404. [CrossRef]
25. Song, Y.; Wu, S.; Wang, H. Spatiotemporal dynamics in the single population modelwith memory-based diffusion and nonlocal effect. *J. Differ. Equ.* **2019**, *267*, 6316–6351. [CrossRef]
26. Chen, H.; Duan, S.; Tang, Y.; Xie, J. Global dynamics of a mechanical system with dry friction. *J. Differ. Equ.* **2018**, *265*, 5490–5519. [CrossRef]
27. Chen H.; Li, Z.; Zhang, R. A sufficient and necessary condition of generalized polynomial Liénard systems with global centers. *arXiv* **2022**, arXiv:2208.06184

28. Chen, H.; Llibre, J.; Tang, Y. Global dynamics of a SD oscillator. *Nonlinear Dyn.* **2018**, *91*, 1755–1777. [CrossRef]
29. Chen, H.; Tang, Y. At most two limit cycles in a piecewise linear differential system with three zones and asymmetry. *Phys. D Nonlinear Phenom.* **2019**, *386*, 23–30. [CrossRef]
30. Deng, X. Travelling wave solutions for the generalized Burgers-Huxley equation. *Appl. Math. Comput.* **2008**, *204*, 733–737. [CrossRef]
31. Li, J. *Singular Nonlinear Travelling Wave Equations: Bifurcations and Exact Solutions*; Science Press: Beijing, China, 2013.
32. Li, J.; Chen, G. On a class of singular nonlinear traveling wave equations. *Int. J. Bifurcation Chaos* **2007**, *17*, 4049–4065. [CrossRef]
33. Li, J.; Qiao, Z. Peakon, pseudo-peakon, and cuspon solutions for two generalized Cammasa-Holm equations. *J. Math. Phys.* **2013**, *54*, 123501. [CrossRef]
34. He, B.; Meng, Q.; Long, Y.; Rui, W. New exact solutions of the double sine-Gordon equation using symbolic computations. *Appl. Math. Comput.* **2007**, *186*, 1334–1346.
35. Meng, Q.; He, B.; Long, Y.; Rui, W. Bifurcations of travelling wave solutions for a general sine-Gordon equation. *Chaos Solitons Fractals* **2006**, *29*, 483–489. [CrossRef]
36. Wen, Z. Bifurcations and exact traveling wave solutions of a new two-component system. *Nonlinear Dyn.* **2017**, *87*, 1917–1922. [CrossRef]
37. Wu, L.; He, G.; Geng, X. Quasi-periodic solutions to the two-component nonlinear Klein-Gordon equation. *J. Geom. Phys.* **2013**, *66*, 1–17. [CrossRef]
38. Xu, G.; Zhang, Y.; Li, J. Exact solitary wave and periodic-peakon solutions of the complex Ginzburg-Landau equation: Dynamical system approach. *Math. Comput. Simul.* **2022**, *191*, 157–167. [CrossRef]
39. Xu, Y.; Zhang, L. Bifurcations of traveling wave solutions for the nonlinear Schrödinger equation with fourth-order dispersion and cubic-quintic nonliearity. *J. Appl. Anal. Comput.* **2020**, *10*, 2722–2733.
40. Zhang, L.; Huang, W. Breaking wave solutions of a short wave model. *Results Phys.* **2019**, *15*, 102733. [CrossRef]
41. Zhang, L. Nilpotent singular points and smooth periodic wave solutions. *Proc. Rom. Acad. Ser. A* **2019**, *20*, 3–9.
42. Zhu, W.; Xia, Y.; Bai, Y. Traveling wave solutions of the complex Ginzburg-Landau equation with Kerr law nonlinearity. *Appl. Math. Comput.* **2020**, *382*, 125342. [CrossRef]
43. Feng, D.H.; Li, J.; Jiao, J. Dynamical behavior of singular traveling waves of (n+1)-dimensional nonlinear Klein-Gordon equation. *Qual. Theor. Dyn. Syst.* **2019**, *18*, 265–287. [CrossRef]

fractal and fractional

MDPI

Article

Instantaneous and Non-Instantaneous Impulsive Boundary Value Problem Involving the Generalized ψ-Caputo Fractional Derivative

Dongping Li [1], Yankai Li [2,*], Fangqi Chen [3] and Xiaozhou Feng [1]

[1] School of Sciences, Xi'an Technological University, Xi'an 710021, China
[2] School of Automation and Information Engineering, Xi'an University of Technology, Xi'an 710048, China
[3] Department of Mathematics, Nanjing University of Aeronautics and Astronautics, Nanjing 211106, China
* Correspondence: liyankai@xaut.edu.cn

Abstract: This paper studies a new class of instantaneous and non-instantaneous impulsive boundary value problem involving the generalized ψ-Caputo fractional derivative with a weight. Depending on critical point theorems and some properties of ψ-Caputo-type fractional integration and differentiation, the variational construction and multiplicity result of solutions are established.

Keywords: instantaneous impulse; non-instantaneous impulse; ψ-Caputo fractional operator; variational construction

MSC: 26A33; 34B15; 34A08

Citation: Li, D.; Li, Y.; Chen, F.; Feng, X. Instantaneous and Non-Instantaneous Impulsive Boundary Value Problem Involving the Generalized ψ-Caputo Fractional Derivative. *Fractal Fract.* **2023**, *7*, 206. https://doi.org/10.3390/fractalfract7030206

Academic Editors: António Lopes, Ricardo Almeida, Alireza Alfi, Liping Chen and Sergio Adriani David

Received: 26 December 2022
Revised: 8 February 2023
Accepted: 14 February 2023
Published: 21 February 2023

1. Introduction

Fractional calculus is an expansion of Newton Leibniz's integer order differential and integral. In recent decades, a large number of definitions of fractional calculus operators are generated with practical problem modeling requirements, such as the well known Riemann-Liouville, Caputo, Erdelyi-Kober, and Hadamard versions [1–3], and those forms play important roles in various interdisciplinary disciplines, like viscoelastic mechanics, anomalous diffusion, control theory, bioengineering, etc. [4–6]. However, many scholars discovered that some existing fractional operators may not well to describe many phenomena in the real world. Hence, a whole newly general definition is proposed recently, so-called ψ-Caputo-type fractional operator [7–9], which could combine the maximum number of definitions of fractional derivatives to a single one by depending upon a nonsingular kernel. The kernel function can provide free arguments to better calibrate a system [10–12]. Taking all these into account, we think that it is a promising topic for further investigation to study fractional differential equations (FDEs for short) with the generalized ψ-Caputo-type fractional operator.

Furthermore, the impulsive FDE can reflect the phenomenon that the state of a thing changes suddenly after being disturbed instantaneously, which is an effective means to depict the changing laws of objects. According to the duration of the change process, the impulse can be divided into the instantaneous (the definition of classical one) and non-instantaneous impulses. Most of the research on FDEs with instantaneous impulse are studied [13–15]. In 2013, Hernádez and O'Regan first proposed the non-instantaneous impulse concept based on pharmacokinetics [16], which refers to the behavior that the state is disturbed at a certain time and produces sudden changes, and it maintains the active state for a limited time interval. This work showed that the non-instantaneous impulse has more advantages in describing the human body's absorption, diffusion, and metabolism of drugs. Since then, non-instantaneous impulsive FDEs received great attention [17–20]. In [18], depending on the Weierstrass theorem, the existence of solutions was obtained for a class

of instantaneous and non-instantaneous impulsive fractional Dirichlet boundary value problems with perturbation. In view of the well known three critical points theorem due to B. Ricceri, the existence of at least three solutions for the non-instantaneous impulsive FDE was obtained in [19]. Because of the late development of non-instantaneous impulse comparing with the instantaneous impulse, many theoretical results need to be enriched and improved, so it has great potential research space and theoretical significance.

Motivated by above works, in this paper, we are concerned with a new class of instantaneous and non-instantaneous impulsive FDEs involving a ψ-Caputo fractional derivative

$$\begin{cases} {}^{C}D^{\alpha,\psi}_{T^-}({}^{C}D^{\alpha,\psi}_{0^+}x(t)) = \lambda f_i(t,x(t)), \ t \in (s_i,t_{i+1}], \ i=0,1,\ldots,n, \\ \Delta({}^{C}D^{\alpha,\psi}_{T^-}(I^{1-\alpha,\psi}_{0^+}x))(t_i) = I_i(x(t_i)), \ i=1,2,\ldots,n, \\ {}^{C}D^{\alpha,\psi}_{T^-}(I^{1-\alpha,\psi}_{0^+}x)(t) = {}^{C}D^{\alpha,\psi}_{T^-}(I^{1-\alpha,\psi}_{0^+}x)(t_i^+), \ t \in (t_i,s_i], \ i=1,2,\ldots,n, \\ {}^{C}D^{\alpha,\psi}_{T^-}(I^{1-\alpha,\psi}_{0^+}x)(s_i^-) = {}^{C}D^{\alpha,\psi}_{T^-}(I^{1-\alpha,\psi}_{0^+}x)(s_i^+), \ i=1,2,\ldots,n, \\ x(0)=x(T)=0, \end{cases} \tag{1}$$

where $\lambda > 0$, $0 < \alpha \le 1$, ${}^{C}D^{\alpha,\psi}_{T^-}$ and ${}^{C}D^{\alpha,\psi}_{0^+}$ denote the right and left ψ-Caputo fractional derivatives, $I^{1-\alpha,\psi}_{0^+}$ is the left ψ-Riemann-Liouville type fractional integral with order $1-\alpha$. $\psi(t) \in C^1[0,T]$ is an increasing function with $\psi'(t) \neq 0$ for all $t \in [0,T]$. $I_i \in C(\mathbb{R},\mathbb{R})$, $f_i \in C((s_i,t_{i+1}]\times\mathbb{R},\mathbb{R})$, $0 = s_0 < t_1 < s_1 < \cdots < s_n < t_{n+1} = T$, the instantaneous impulse begins suddenly at the point t_i, and the non-instantaneous impulse continues during a finite interval $(t_i, s_i]$,

$$\begin{aligned} \Delta({}^{C}D^{\alpha,\psi}_{T^-}(I^{1-\alpha,\psi}_{0^+}x))(t_i) &= {}^{C}D^{\alpha,\psi}_{T^-}(I^{1-\alpha,\psi}_{0^+}x)(t_i^+) - {}^{C}D^{\alpha,\psi}_{T^-}(I^{1-\alpha,\psi}_{0^+}x)(t_i^-), \\ {}^{C}D^{\alpha,\psi}_{T^-}(I^{1-\alpha,\psi}_{0^+}x)(t_i^+) &= \lim_{t\to t_i^+} {}^{C}D^{\alpha,\psi}_{T^-}(I^{1-\alpha,\psi}_{0^+}x)(t), \\ {}^{C}D^{\alpha,\psi}_{T^-}(I^{1-\alpha,\psi}_{0^+}x)(t_i^-) &= \lim_{t\to t_i^-} {}^{C}D^{\alpha,\psi}_{T^-}(I^{1-\alpha,\psi}_{0^+}x)(t). \end{aligned}$$

It is a new issue that has not been touched yet. Some existing results, which focus on the classical fractional operators, such as [19,21,22], are improved and supplemented by choosing special kernel functions in the derivative.

2. Fractional Integrals and Derivatives

This section introduces some essential definitions of fractional integrals and derivatives, as well as relevant lemmas and theorems, whose involvements assist us to establish variational construction and multiplicity results for impulsive FDE (1) successfully.

We deal mainly with the ψ-Riemann-Liouville and ψ-Caputo fractional integrals and derivatives in this paper, and the reader can refer to Res. [7–9] for more information. Let $\alpha > 0$, $-\infty \le a < b \le +\infty$, $f(t)$ is an integrable function and $\psi(t) \in C^1[0,T]$ is an increasing function, with $\psi'(t) \neq 0$ for all $t \in [a,b]$. The left ψ-Riemann-Liouville type fractional integral and derivative of a function f with respect to another function ψ are, respectively, defined as:

$$\begin{aligned} I^{\alpha,\psi}_{a^+}f(t) &= \frac{1}{\Gamma(\alpha)}\int_a^t \psi'(\xi)(\psi(t)-\psi(\xi))^{\alpha-1}f(\xi)d\xi, \\ D^{\alpha,\psi}_{a^+}f(t) &= \left(\frac{1}{\psi'(t)}\frac{d}{dt}\right)^n I^{n-\alpha,\psi}_{a^+}f(t) = \frac{1}{\Gamma(n-\alpha)}\left(\frac{1}{\psi'(t)}\frac{d}{dt}\right)^n \int_a^t \psi'(\xi)(\psi(t)-\psi(\xi))^{n-\alpha-1}f(\xi)d\xi, \end{aligned} \tag{2}$$

where $n = [\alpha]+1$ for $\alpha \notin \mathbb{N}$, $n = \alpha$ for $\alpha \in \mathbb{N}$.

Similar definitions can be given for the right ψ-Riemann-Liouville fractional integral and derivative:

$$I_{b^-}^{\alpha,\psi} f(t) = \frac{1}{\Gamma(\alpha)} \int_t^b \psi'(\xi)(\psi(\xi) - \psi(t))^{\alpha-1} f(\xi) d\xi, \tag{3}$$

$$D_{b^-}^{\alpha,\psi} f(t) = \left(\frac{-1}{\psi'(t)} \frac{d}{dt}\right)^n I_{b^-}^{n-\alpha,\psi} f(t) = \frac{1}{\Gamma(n-\alpha)} \left(-\frac{1}{\psi'(t)} \frac{d}{dt}\right)^n \int_t^b \psi'(\xi)(\psi(\xi) - \psi(t))^{n-\alpha-1} f(\xi) d\xi.$$

In particular, if $0 < \alpha < 1$, one has:

$$D_{a^+}^{\alpha,\psi} f(t) = \left(\frac{1}{\psi'(t)} \frac{d}{dt}\right) I_{a^+}^{1-\alpha,\psi} f(t) = \frac{1}{\Gamma(1-\alpha)} \left(\frac{1}{\psi'(t)} \frac{d}{dt}\right) \int_a^t \psi'(\xi)(\psi(t) - \psi(\xi))^{-\alpha} f(\xi) d\xi, \tag{4}$$

$$D_{b^-}^{\alpha,\psi} f(t) = \left(\frac{-1}{\psi'(t)} \frac{d}{dt}\right) I_{b^-}^{1-\alpha,\psi} f(t) = \frac{1}{\Gamma(1-\alpha)} \left(\frac{-1}{\psi'(t)} \frac{d}{dt}\right) \int_t^b \psi'(\xi)(\psi(\xi) - \psi(t))^{-\alpha} f(\xi) d\xi. \tag{5}$$

It is worth noting that, if we choose the kernel $\psi(t) = \ln t$ or $\psi(t) = t$, the ψ-Riemann-Liouville fractional integral and derivative can reduce into the well known Hadamard type or Riemann-Liouville type fractional integral and derivative.

Definition 1 ([9]). *Let $n \in \mathbb{N}$, $-\infty \le a < b \le +\infty$, $\alpha > 0$, $f(t), \psi(t) \in C^1[0,T]$ are two functions, such that $\psi(t)$ is an increasing function with $\psi'(t) \neq 0$ for all $t \in [a,b]$. Then, the left and right ψ-Caputo type fractional derivatives of f with respect to another function ψ are, respectively, defined as:*

$${}^C D_{a^+}^{\alpha,\psi} f(t) = I_{a^+}^{n-\alpha,\psi} \left(\frac{1}{\psi'(t)} \frac{d}{dt}\right)^n f(t) = \frac{1}{\Gamma(n-\alpha)} \int_a^t \psi'(\xi)(\psi(t) - \psi(\xi))^{n-\alpha-1} \left(\frac{1}{\psi'(\xi)} \frac{d}{d\xi}\right)^n f(\xi) d\xi,$$

$${}^C D_{b^-}^{\alpha,\psi} f(t) = I_{b^-}^{n-\alpha,\psi} \left(-\frac{1}{\psi'(t)} \frac{d}{dt}\right)^n f(t) = \frac{(-1)^n}{\Gamma(n-\alpha)} \int_t^b \psi'(\xi)(\psi(\xi) - \psi(t))^{n-\alpha-1} \left(\frac{1}{\psi'(\xi)} \frac{d}{d\xi}\right)^n f(\xi) d\xi.$$

In particular, if $0 < \alpha < 1$, one has:

$${}^C D_{a^+}^{\alpha,\psi} f(t) = I_{a^+}^{1-\alpha,\psi} \left(\frac{1}{\psi'(t)} \frac{d}{dt}\right) f(t) = \frac{1}{\Gamma(1-\alpha)} \int_a^t (\psi(t) - \psi(\xi))^{-\alpha} f'(\xi) d\xi, \tag{6}$$

$${}^C D_{b^-}^{\alpha,\psi} f(t) = I_{b^-}^{1-\alpha,\psi} \left(-\frac{1}{\psi'(t)} \frac{d}{dt}\right) f(t) = \frac{-1}{\Gamma(1-\alpha)} \int_t^b (\psi(\xi) - \psi(t))^{-\alpha} f'(\xi) d\xi. \tag{7}$$

Notice that the ψ-Caputo fractional derivative can reduce to the classical Caputo fractional derivative by choosing the kernel $\psi(t) = t$.

Definition 2 ([9]). *If $f(t) \in C^n[a,b]$, $-\infty \le a < b \le +\infty$, $\alpha > 0$, $n = [\alpha] + 1$ for $\alpha \notin \mathbb{N}$, $n = \alpha$ for $\alpha \in \mathbb{N}$, then*

$${}^C D_{a^+}^{\alpha,\psi} f(t) = D_{a^+}^{\alpha,\psi} \left[f(t) - \Sigma_{k=0}^{n-1} \frac{1}{k!} (\psi(t) - \psi(a))^k \left(\frac{1}{\psi'(t)} \frac{d}{dt}\right)^k f(a) \right],$$

$${}^C D_{b^-}^{\alpha,\psi} f(t) = D_{b^-}^{\alpha,\psi} \left[f(t) - \Sigma_{k=0}^{n-1} \frac{(-1)^k}{k!} (\psi(b) - \psi(t))^k \left(\frac{1}{\psi'(t)} \frac{d}{dt}\right)^k f(b) \right].$$

In what follows, we will begin the process of building an appropriate variational structure for the impulsive FDE (1). Before that, a fractional derivative space needs to be established.

Definition 3. *Define the ψ-Caputo fractional derivative space $E_0^{\alpha,\psi}$ by the closure of $C_0^\infty([0,T],\mathbb{R})$ with weighted norm:*

$$\|x\|_{\alpha,\psi} := \left(\int_0^T |\, x(t) \,|^2 \, dt + \int_0^T \psi'(t) \, |\, {}^C D_{0^+}^{\alpha,\psi} x(t) \,|^2 \, dt \right)^{\frac{1}{2}}. \tag{8}$$

Obviously, the space $E_0^{\alpha,\psi}$ *implies that* $x(t) \in L^2[0,T]$ *with* ${}^{C}D_{0^+}^{\alpha,\psi}x(t) \in L^2[0,T]$, *and* $x(0) = x(T) = 0$.

Lemma 1 ([11]). *The space* $E_0^{\alpha,\psi}$ *is a reflexive and separable Banach space.*

Lemma 2. *For any* $x(t) \in E_0^{\alpha,\psi}$, $\frac{1}{2} < \alpha \leq 1$, *we have*

$$\|x\|_\infty \leq M\bigg(\int_0^T \psi'(t) \mid D_{0^+}^{\alpha,\psi}x(t) \mid^2 dt\bigg)^{\frac{1}{2}}, \tag{9}$$

$$\|x\|_{L^2} \leq \widehat{M}\|D_{0^+}^{\alpha,\psi}x\|_{L^2}, \tag{10}$$

where

$$M = \frac{(\psi(T)-\psi(0))^{\alpha-\frac{1}{2}}}{\Gamma(\alpha)(2(\alpha-1)+1)^{\frac{1}{2}}},\ \widehat{M} = \frac{\max_{t\in[0,T]}\{\psi'(t)\}(\psi(T))^{\alpha}}{\Gamma(\alpha+1)}.$$

Proof. Based on Theorem 4 in [9] and the Hölder inequality, we deduce:

$$\begin{aligned}
|x(t)| =& |I_{0^+}^{\alpha,\psi}D_{0^+}^{\alpha,\psi}x(t)| = \frac{1}{\Gamma(\alpha)}\bigg|\int_0^t \psi'(\xi)(\psi(t)-\psi(\xi))^{\alpha-1}D_{0^+}^{\alpha,\psi}x(\xi)d\xi\bigg| \\
\leq& \frac{1}{\Gamma(\alpha)}\bigg(\int_0^T\bigg[(\psi'(\xi))^{\frac{1}{2}}(\psi(t)-\psi(\xi))^{\alpha-1}\bigg]^2 d\xi\bigg)^{\frac{1}{2}}\bigg(\int_0^T\bigg[(\psi'(\xi))^{\frac{1}{2}}D_{0^+}^{\alpha,\psi}x(\xi)\bigg]^2 d\xi\bigg)^{\frac{1}{2}} \\
\leq& \frac{(\psi(T)-\psi(0))^{\alpha-\frac{1}{2}}}{\Gamma(\alpha)(2(\alpha-1)+1)^{\frac{1}{2}}}\bigg(\int_0^T \psi'(t)|D_{0^+}^{\alpha,\psi}x(t)|^2 dt\bigg)^{\frac{1}{2}}.
\end{aligned}$$

The inequality (10) is immediately available according to [11]. The proof is completed. □

Lemma 3. *Based on Definition 2 and* $x(0) = x(T) = 0$, *one obtains:*

$${}^{C}D_{0^+}^{\alpha,\psi}x(t) = D_{0^+}^{\alpha,\psi}x(t),\ {}^{C}D_{T^-}^{\alpha,\psi}x(t) = D_{T^-}^{\alpha,\psi}x(t),\ \forall 0 < \alpha < 1.$$

From (10) and Lemma 3, we confirm that the norm defined by (8) is equivalent to:

$$\|x\|_{\alpha,\psi} := \bigg(\int_0^T \psi'(t) \mid {}^{C}D_{0^+}^{\alpha,\psi}x(t) \mid^2 dt\bigg)^{\frac{1}{2}},\ \forall\, x(t) \in E_0^{\alpha,\psi}. \tag{11}$$

Lemma 4 ([11]). *Let* $\frac{1}{2} < \alpha \leq 1$. *If any sequence* $\{x_k\}$ *converges to* x *in* $E_0^{\alpha,\psi}$ *weakly, then* $x_k \to x$ *in* $C[0,T]$ *as* $k \to \infty$, *i.e.,* $\|x_k - x\|_\infty \to 0$ *as* $k \to \infty$.

Based on the relevant definitions and lemmas introduced above, the definition of the weak solution of FDE (1) can be given as follows.

Lemma 5. *We say that* $x(t) \in E_0^{\alpha,\psi}$ *is a weak solution of FDE (1) if the following relationship holds:*

$$\int_0^T \psi'(t){}^{C}D_{0^+}^{\alpha,\psi}x(t){}^{C}D_{0^+}^{\alpha,\psi}y(t)dt - \sum_{i=1}^{n} I_i(x(t_i))y(t_i) = \lambda\sum_{i=0}^{n}\int_{s_i}^{t_{i+1}} f_i(t,x(t))\psi'(t)y(t)dt, \forall y(t) \in E_0^{\alpha,\psi}. \tag{12}$$

Proof. In view of (6), Dirichlet's formula and Lemma 3 yields:

$$\int_0^T \psi'(t)\,{}^C D_{0^+}^{\alpha,\psi} x(t)\,{}^C D_{0^+}^{\alpha,\psi} y(t)dt = \frac{1}{\Gamma(1-\alpha)} \int_0^T \int_0^t \psi'(t)\,{}^C D_{0^+}^{\alpha,\psi} x(t)(\psi(t)-\psi(\xi))^{-\alpha} y'(\xi)d\xi dt$$
$$= \frac{1}{\Gamma(1-\alpha)} \int_0^T \left[\int_t^T \psi'(\xi)\,{}^C D_{0^+}^{\alpha,\psi} x(\xi)(\psi(\xi)-\psi(t))^{-\alpha} d\xi \right] y'(t)dt$$
$$= \frac{1}{\Gamma(1-\alpha)} \sum_{i=0}^{n} \int_{s_i}^{t_{i+1}} \left[\int_t^T \psi'(\xi) D_{0^+}^{\alpha,\psi} x(\xi)(\psi(\xi)-\psi(t))^{-\alpha} d\xi \right] y'(t)dt$$
$$+ \frac{1}{\Gamma(1-\alpha)} \sum_{i=1}^{n} \int_{t_i}^{s_i} \left[\int_t^T \psi'(\xi) D_{0^+}^{\alpha,\psi} x(\xi)(\psi(\xi)-\psi(t))^{-\alpha} d\xi \right] y'(t)dt. \tag{13}$$

Due to (4), (5) and (7) yields

$$\frac{1}{\Gamma(1-\alpha)} \sum_{i=0}^{n} \int_{s_i}^{t_{i+1}} \left[\int_t^T \psi'(\xi) D_{0^+}^{\alpha,\psi} x(\xi)(\psi(\xi)-\psi(t))^{-\alpha} d\xi \right] y'(t)dt \tag{14}$$
$$= \frac{1}{\Gamma(1-\alpha)} \sum_{i=0}^{n} \left[\int_t^T \psi'(\xi) D_{0^+}^{\alpha,\psi} x(\xi)(\psi(\xi)-\psi(t))^{-\alpha} d\xi \right] y(t) \,|_{t=s_i^+}^{t=t_{i+1}^-}$$
$$- \frac{1}{\Gamma(1-\alpha)} \sum_{i=0}^{n} \int_{s_i}^{t_{i+1}} \frac{d}{dt} \left[\int_t^T \psi'(\xi) D_{0^+}^{\alpha,\psi} x(\xi)(\psi(\xi)-\psi(t))^{-\alpha} d\xi \right] \cdot y(t)dt$$
$$= \sum_{i=0}^{n} \frac{1}{\Gamma(1-\alpha)} \int_t^T \psi'(\xi)(\psi(\xi)-\psi(t))^{-\alpha} \left(\frac{1}{\psi'(\xi)} \frac{d}{d\xi} \right) I_{0^+}^{1-\alpha,\psi} x(\xi)d\xi \cdot y(t) \,|_{t=s_i^+}^{t=t_{i+1}^-}$$
$$+ \sum_{i=0}^{n} \int_{s_i}^{t_{i+1}} \frac{-1}{\Gamma(1-\alpha)} \left(\frac{1}{\psi'(t)} \frac{d}{dt} \right) \left[\int_t^T \psi'(\xi)(\psi(\xi)-\psi(t))^{-\alpha} D_{0^+}^{\alpha,\psi} x(\xi)d\xi \right] \cdot \psi'(t)y(t)dt$$
$$= \sum_{i=0}^{n} -{}^C D_{T^-}^{\alpha,\psi} (I_{0^+}^{1-\alpha,\psi} x(t))y(t) \,|_{t=s_i^+}^{t=t_{i+1}^-} + \sum_{i=0}^{n} \int_{s_i}^{t_{i+1}} D_{T^-}^{\alpha,\psi} (D_{0^+}^{\alpha,\psi} x(t))\psi'(t)y(t)dt,$$

and

$$\frac{1}{\Gamma(1-\alpha)} \sum_{i=1}^{n} \int_{t_i}^{s_i} \left[\int_t^T \psi'(\xi) D_{0^+}^{\alpha,\psi} x(\xi)(\psi(\xi)-\psi(t))^{-\alpha} d\xi \right] y'(t)dt \tag{15}$$
$$= \frac{1}{\Gamma(1-\alpha)} \sum_{i=1}^{n} \left[\int_t^T \psi'(\xi) D_{0^+}^{\alpha,\psi} x(\xi)(\psi(\xi)-\psi(t))^{-\alpha} d\xi \right] y(t) \,|_{t=t_i^+}^{t=s_i^-}$$
$$- \frac{1}{\Gamma(1-\alpha)} \sum_{i=1}^{n} \int_{t_i}^{s_i} \frac{d}{dt} \left[\int_t^T \psi'(\xi) D_{0^+}^{\alpha,\psi} x(\xi)(\psi(\xi)-\psi(t))^{-\alpha} d\xi \right] \cdot y(t)dt$$
$$= \sum_{i=1}^{n} \frac{1}{\Gamma(1-\alpha)} \int_t^T \psi'(\xi)(\psi(\xi)-\psi(t))^{-\alpha} \left(\frac{1}{\psi'(\xi)} \frac{d}{d\xi} \right) I_{0^+}^{1-\alpha,\psi} x(\xi)d\xi \cdot y(t) \,|_{t=t_i^+}^{t=s_i^-}$$
$$+ \sum_{i=1}^{n} \int_{t_i}^{s_i} \frac{d}{dt} \left[\frac{-1}{\Gamma(1-\alpha)} \int_t^T \psi'(\xi)(\psi(\xi)-\psi(t))^{-\alpha} \left(\frac{1}{\psi'(\xi)} \frac{d}{d\xi} \right) I_{0^+}^{1-\alpha,\psi} x(\xi)d\xi \right] \cdot y(t)dt$$
$$= \sum_{i=1}^{n} -{}^C D_{T^-}^{\alpha,\psi} (I_{0^+}^{1-\alpha,\psi} x(t))y(t) \,|_{t=t_i^+}^{t=s_i^-} + \sum_{i=1}^{n} \int_{t_i}^{s_i} \frac{d}{dt} \left[{}^C D_{T^-}^{\alpha,\psi} (I_{0^+}^{1-\alpha,\psi} x(t)) \right] \cdot y(t)dt.$$

Consequently, combining (13), (14), (15), and the impulsive conditions in FDE (1), one has:

$$
\begin{aligned}
&\int_0^T \psi'(t)\,{}^{C}D_{0^+}^{\alpha,\psi}x(t)\,{}^{C}D_{0^+}^{\alpha,\psi}y(t)dt\\
&=\sum_{i=0}^{n} -{}^{C}D_{T^-}^{\alpha,\psi}(I_{0^+}^{1-\alpha,\psi}x(t))y(t)\mid_{t=s_i^+}^{t=t_{i+1}^-}+\sum_{i=1}^{n} -{}^{C}D_{T^-}^{\alpha,\psi}(I_{0^+}^{1-\alpha,\psi}x(t))y(t)\mid_{t=t_i^+}^{t=s_i^-}+\sum_{i=0}^{n}\int_{s_i}^{t_{i+1}} D_{T^-}^{\alpha,\psi}(D_{0^+}^{\alpha,\psi}x(t))\psi'(t)y(t)dt\\
&=\sum_{i=1}^{n} {}^{C}D_{T^-}^{\alpha,\psi}(I_{0^+}^{1-\alpha,\psi}x(t_i^+))y(t_i^+)-{}^{C}D_{T^-}^{\alpha,\psi}(I_{0^+}^{1-\alpha,\psi}x(t_i^-))y(t_i^-)+\sum_{i=1}^{n} {}^{C}D_{T^-}^{\alpha,\psi}(I_{0^+}^{1-\alpha,\psi}x(s_i^+))y(s_i^+)-{}^{C}D_{T^-}^{\alpha,\psi}(I_{0^+}^{1-\alpha,\psi}x(s_i^-))y(s_i^-) \qquad (16)\\
&\quad+{}^{C}D_{T^-}^{\alpha,\psi}(I_{0^+}^{1-\alpha,\psi}x(0))y(0)-{}^{C}D_{T^-}^{\alpha,\psi}(I_{0^+}^{1-\alpha,\psi}x(T))y(T)+\sum_{i=0}^{n}\int_{s_i}^{t_{i+1}} D_{T^-}^{\alpha,\psi}(D_{0^+}^{\alpha,\psi}x(t))\psi'(t)y(t)dt\\
&=\sum_{i=1}^{n} I_i(x(t_i))y(t_i)+\sum_{i=0}^{n}\int_{s_i}^{t_{i+1}} D_{T^-}^{\alpha,\psi}(D_{0^+}^{\alpha,\psi}x(t))\psi'(t)y(t)dt.
\end{aligned}
$$

An equivalent form for FDE (1) can be derived by multiplying the first equation of (1) with $\psi'(t)y(t)$, and integrating on both sides from s_i to t_{i+1}, then summing from $i=0$ to $i=n$, according to (16), one has:

$$\int_0^T \psi'(t)\,{}^{C}D_{0^+}^{\alpha,\psi}x(t)\,{}^{C}D_{0^+}^{\alpha,\psi}y(t)dt-\sum_{i=1}^{n} I_i(x(t_i))y(t_i)=\lambda\sum_{i=0}^{n}\int_{s_i}^{t_{i+1}} f_i(t,x(t))\psi'(t)y(t)dt.$$

The proof is completed. □

Definition 4. *A function*

$$x\in\left\{x\in AC[0,T]:\int_{s_i}^{t_{i+1}}\mid x(t)\mid^2+\psi'(t)\mid {}^{C}D_{0^+}^{\alpha,\psi}x(t)\mid^2 dt<+\infty, i=1,2,\ldots,n\right\}$$

is called a classical solution of FDE (1) if x satisfies the first equation of FDE (1), the limits ${}^{C}D_{T^-}^{\alpha,\psi}(I_{0^+}^{1-\alpha,\psi}x)(t_i^{\pm})$ and ${}^{C}D_{T^-}^{\alpha,\psi}(I_{0^+}^{1-\alpha,\psi}x)(s_i^{\pm})$ exist and satisfy the impulsive conditions in (1), and boundary condition $x(0)=x(T)=0$ holds.

Lemma 6 ([23])**.** *Let E be a real reflexive Banach space, let $J_1: E\to\mathbb{R}$ be a sequentially weakly lower semi-continuous, coercive and continuously Gâteaux differentiable functional whose Gâteaux derivative admits a continuous inverse on E^*, and let $J_2: E\to\mathbb{R}$ be a sequentially weakly upper semi-continuous and continuously Gâteaux differentiable functional whose Gâteaux derivative is compact. Suppose that there exist $\rho\in\mathbb{R}$ and $x_1\in E$ with $0<\rho<J_1(x_1)$, such that*
(i) $\sup_{x\in J_1^{-1}(]-\infty,\rho])} J_2(x)<\rho\frac{J_2(x_1)}{J_1(x_1)}$.
(ii) For all $\lambda\in\mathcal{B}:=\left]\frac{J_1(x_1)}{J_2(x_1)},\frac{\rho}{\sup_{x\in J_1^{-1}(]-\infty,\rho])} J_2(x)}\right[$, *the functional $J_1-\lambda J_2$ is coercive.*

Then, for each $\lambda\in\mathcal{B}$, the functional $J_1-\lambda J_2$ possesses at least three distinct critical points on E.

3. Proof of Theorems

In this section, the multiplicity of at least three distinct classical solutions for impulsive FDE (1) is discussed depending on Lemma 6 and Definition 4.

For any $x(t)\in E_0^{\alpha,\psi}$, define the functional $J_\lambda:=J_1-\lambda J_2$, where

$$
\begin{aligned}
J_1(x)&=\frac{1}{2}\int_0^T \psi'(t)|{}^{C}D_{0^+}^{\alpha,\psi}x(t)|^2dt-\sum_{i=1}^{n}\int_0^{x(t_i)} I_i(\xi)d\xi,\\
J_2(x)&=\sum_{i=0}^{n}\int_{s_i}^{t_{i+1}} F_i(t,x(t))\psi'(t)dt,
\end{aligned}
\qquad (17)
$$

where $F_i(t,x)=\int_0^x f_i(t,\xi)d\xi$. Owing to the continuity of f_i and I_i, we can obtain $J_1, J_2 \in C^1(E_0^{\alpha,\psi},\mathbb{R})$ and

$$J_1'(x)(y)=\int_0^T \psi'(t)\,{}^{C}D_{0^+}^{\alpha,\psi}x(t)\,{}^{C}D_{0^+}^{\alpha,\psi}y(t)dt-\sum_{i=1}^{n}I_i(x(t_i))y(t_i),$$
$$J_2'(x)(y)=\sum_{i=0}^{n}\int_{s_i}^{t_{i+1}} f_i(t,x(t))\psi'(t)y(t)dt. \tag{18}$$

Apparently, the critical point of J_λ is the weak solution of impulsive FDE (1).

Theorem 1. *Assume that*
(A_1) $I_i(0)=0$ *and there exist* $d_i, L_i>0$ *with* $\max\{M^2\sum_{i=1}^n L_i, M^2\sum_{i=1}^n d_i\}<1$, *such that* $|I_i(\xi)|\le d_i|\xi|$ *and* $|\,I_i(\xi_1)-I_i(\xi_2)\,|\le L_i\,|\,\xi_1-\xi_2\,|$, $\forall \xi,\xi_1,\xi_2\in\mathbb{R}$.
(A_2) *There exist a constant* $\rho>0$ *and a function* $\varsigma(t)$, *such that* $\left(\frac{1}{2}-\frac{M^2\sum_{i=1}^n d_i}{2}\right)\|\varsigma\|_{\alpha,\psi}^2>\rho$, *and*

$$\frac{\sum_{i=0}^n\int_{s_i}^{t_{i+1}}\sup_{x\in\Omega_\rho}F_i(t,x(t))\psi'(t)dt}{\rho}<\frac{2\sum_{i=0}^n\int_{s_i}^{t_{i+1}}F_i(t,\varsigma(t))\psi'(t)dt}{\|\varsigma\|_{\alpha,\psi}^2-2\sum_{i=1}^n\int_0^{\varsigma(t_i)}I_i(\xi)d\xi}, \tag{19}$$

where $\Omega_\rho=\{x\in\mathbb{R}:\left(\frac{1}{2M^2}-\frac{\sum_{i=1}^n d_i}{2}\right)\,|\,x\,|^2\le\rho\}$.
(A_3) *there exist* $b_i,c_i>0$, $\theta_i\in[0,1)$, *such that* $|f_i(t,x)|\le b_i+c_i|x|^{\theta_i}$, $\forall t\in[0,T]$, $x\in\mathbb{R}$, $i=0,1,\ldots,n$.

Then, for each $\lambda\in\left]\frac{\|\varsigma\|_{\alpha,\psi}^2-2\sum_{i=1}^n\int_0^{\varsigma(t_i)}I_i(\xi)d\xi}{2\sum_{i=0}^n\int_{s_i}^{t_{i+1}}F_i(t,\varsigma(t))\psi'(t)dt},\frac{\rho}{\sum_{i=0}^n\int_{s_i}^{t_{i+1}}\sup_{x\in\Omega_\rho}F_i(t,x(t))\psi'(t)dt}\right[$, *the impulsive FDE (1) possesses at least three distinct weak solutions on* $E_0^{\alpha,\psi}$.

Proof. First, we are concerned with functionals J_1 and J_2. Let $\{x_k\}_{k=1}^\infty$ be a weakly convergent sequence to x in $E_0^{\alpha,\psi}$, then $\|x\|_{\alpha,\psi}\le\liminf_{k\to\infty}\|x_k\|_{\alpha,\psi}$. In view of Lemma 4 that $\{x_k\}$ converges to x in $C([0,T],\mathbb{R})$ uniformly. That is:

$$\begin{aligned}\liminf_{k\to\infty}J_1(x_k)&=\liminf_{k\to\infty}\left\{\frac{1}{2}\|x_k\|_{\alpha,\psi}^2-\sum_{i=1}^n\int_0^{x_k(t_i)}I_i(\xi)d\xi\right\}\\&\ge\frac{1}{2}\|x\|_{\alpha,\psi}^2-\sum_{i=1}^n\int_0^{x(t_i)}I_i(\xi)d\xi=J_1(x),\end{aligned}$$

which means that J_1 is weakly lower semi-continuous. In what follows, we assert that J_1 possesses a continuous inverse on $(E_0^{\alpha,\psi})^*$. By means of (18), (9) and (A_1) yield:

$$\begin{aligned}(J_1'(x)-J_1'(y))(x-y)&=\int_0^T\psi'(t)\,|\,{}^{C}D_{0^+}^{\alpha,\psi}(x(t)-y(t))\,|^2\,dt-\sum_{i=1}^n(I_i(x(t_i))-I_i(y(t_i)))(x(t_i)-y(t_i))\\&\ge\|x-y\|_{\alpha,\psi}^2-\sum_{i=1}^n|\,I_i(x(t_i))-I_i(y(t_i))\,|\,|\,x(t_i)-y(t_i)\,|\\&\ge\|x-y\|_{\alpha,\psi}^2-\sum_{i=1}^n L_i\,|\,x(t_i)-y(t_i)\,|^2\\&\ge\|x-y\|_{\alpha,\psi}^2-\|x-y\|_\infty^2\sum_{i=1}^n L_i\\&\ge(1-M^2\sum_{i=1}^n L_i)\|x-y\|_{\alpha,\psi}^2>0,\ \forall\, x\ne y,\end{aligned}$$

which shows that J_1' is strictly monotone. Based on the Theorem 26.A(d) in [24], we can obtain that there exists an inverse of J_1' on $(E_0^{\alpha,\psi})^*$, and the inverse is continuous. Obviously, J_1 is coercive. On the other hand, suppose that $\{x_k\} \subset E_0^{\alpha,\psi}$, $x_k \rightharpoonup x$ in $E_0^{\alpha,\psi}$ as $k \to \infty$. Then, $x_k \to x$ uniformly on $[0,T]$, and

$$\limsup_{k\to\infty} J_2(x_k) \le \sum_{i=0}^{n} \int_{s_i}^{t_{i+1}} \limsup_{k\to\infty} F_i(t, x_k(t))\psi'(t)dt = \sum_{i=0}^{n} \int_{s_i}^{t_{i+1}} F_i(t, x(t))\psi'(t)dt = J_2(x),$$

hence, J_2 is sequentially weakly upper semi-continuous. Considering $F_i \in C^1((s_i, t_{i+1}] \times \mathbb{R}, \mathbb{R})$, then $F_i(t, x_k(t)) \to F_i(t, x(t))$ as $k \to \infty$. According to the Lebesgue control convergence theorem, $J_2'(x_k) \to J_2'(x)$, i.e., J_2' is continuous strongly on $E_0^{\alpha,\psi}$. So, J_2' is a compact operator.

Take $x_0 = 0$, $x_1 = \varsigma$. Due to (A_1) and (A_2), we have $J_1(x_1) \ge \left(\frac{1}{2} - \frac{M^2\sum_{i=1}^{n} d_i}{2}\right)\|x_1\|_{\alpha,\psi}^2 > \rho > 0$ and $J_1(x_0) = 0$. In view of (17), (9), and (A_1), we have:

$$\begin{aligned} J_1^{-1}(]-\infty,\rho]) &= \{x \in E_0^{\alpha,\psi} : J_1(x) \le \rho\} = \{x \in E_0^{\alpha,\psi} : \frac{1}{2}\int_0^T \psi'(t)|{}^{C}D_{0^+}^{\alpha,\psi}x(t)|^2 dt - \sum_{i=1}^{n}\int_0^{x(t_i)} I_i(\xi))d\xi \le \rho\} \\ &\subseteq \{x \in E_0^{\alpha,\psi} : \frac{1}{2}\|x\|_{\alpha,\psi}^2 - \sum_{i=1}^{n}\int_0^{x(t_i)} d_i|\xi|d\xi \le \rho\} \\ &\subseteq \{x \in E_0^{\alpha,\psi} : \left(\frac{1}{2M^2} - \frac{\sum_{i=1}^{n} d_i}{2}\right) \mid x(t) \mid^2 \le \rho, t \in [0,T]\}, \end{aligned}$$

then

$$\sup_{x\in J_1^{-1}(]-\infty,\rho])} J_2(x) = \sup_{x\in J_1^{-1}(]-\infty,\rho])} \sum_{i=0}^{n}\int_{s_i}^{t_{i+1}} F_i(t,x(t))\psi'(t)dt \le \sum_{i=0}^{n}\int_{s_i}^{t_{i+1}} \sup_{x\in\Omega_\rho} F_i(t,x(t))\psi'(t)dt,$$

that is

$$\frac{\sup_{x\in J_1^{-1}(]-\infty,\rho])} J_2(x)}{\rho} \le \frac{\sum_{i=0}^{n}\int_{s_i}^{t_{i+1}} \sup_{x\in\Omega_\rho} F_i(t,x(t))\psi'(t)dt}{\rho} < \frac{2\sum_{i=0}^{n}\int_{s_i}^{t_{i+1}} F_i(t,\varsigma(t))\psi'(t)dt}{\|\varsigma\|_{\alpha,\psi}^2 - 2\sum_{i=1}^{n}\int_0^{\varsigma(t_i)} I_i(\xi)d\xi} = \frac{J_2(x_1)}{J_1(x_1)},$$

where (27) is used. Thus, the assumption (i) of Lemma 6 is satisfied.

In addition, for any fixed $\lambda \in \mathcal{B}$, by means of (17), (A_1), (A_3), and (9), we obtain:

$$\begin{aligned} J_1(x) - \lambda J_2(x) \ge& \frac{1}{2}\|x\|_{\alpha,\psi}^2 - \sum_{i=1}^{n}\left(\int_0^{x(t_i)} d_i|\xi|d\xi\right) - \lambda\sum_{i=0}^{n}\int_{s_i}^{t_{i+1}}\psi'(t)\int_0^x b_i + c_i|s|^{\theta_i}dsdt \\ \ge& \frac{1}{2}\|x\|_{\alpha,\psi}^2 - \left(\frac{1}{2}\|x\|_\infty^2\sum_{i=1}^{n} d_i\right) - \lambda(\psi(T)-\psi(0))\left(\sum_{i=0}^{n} b_i\|x\|_\infty + \frac{c_i}{\theta_i+1}\|x\|_\infty^{\theta_i+1}\right) \\ \ge& \left(\frac{1}{2} - \frac{M^2\sum_{i=1}^{n} d_i}{2}\right)\|x\|_{\alpha,\psi}^2 - \lambda(\psi(T)-\psi(0))M\|x\|_{\alpha,\psi}\left(\sum_{i=0}^{n} b_i\right) \\ & - \lambda(\psi(T)-\psi(0))\sum_{i=0}^{n}\frac{c_i M^{\theta_i+1}}{\theta_i+1}\|x\|_{\alpha,\psi}^{\theta_i+1}. \end{aligned}$$

Since $\theta_i \in [0,1)$ and $M^2\sum_{i=1}^{n} d_i < 1$, we assert that $\lim_{\|x\|_{\alpha,\psi}\to\infty} J_1(x) - \lambda J_2(x) = +\infty$, which implies that $J_1 - \lambda J_2$ is coercive. The condition (ii) in Lemma 6 holds. Consequently, the impulsive FDE (1) possesses at least three distinct weak solutions on $E_0^{\alpha,\psi}$ using Lemma 6. □

Theorem 2. *$x(t)$ is a weak solution of impulsive FDE (1), if and only if $x(t)$ is a classical solution of FDE (1).*

Proof. If $x(t)$ is a classical solution of impulsive FDE (1), then $x(t)$ also is a weak solution obviously. On the other hand, if $x(t) \in E_0^{\alpha,\psi}$ is a weak solution of FDE (1), then $x(0) = x(T) = 0$ and the Equation (12) holds. Without loss of generality, choose a test function $v_i(t) \in C_0^\infty(s_i, t_{i+1}]$ and $v_i(t) \equiv 0$ for $t \in [0, s_i] \bigcup (t_{i+1}, T]$, $i = 0, 2, \ldots, n$. Substituting $v_i(t)$ into (12), from (16), we have:

$$\int_{s_i}^{t_{i+1}} D_{T^-}^{\alpha,\psi}(D_{0^+}^{\alpha,\psi}x(t))\psi'(t)v_i(t)dt = \int_{s_i}^{t_{i+1}} \psi'(t)\,{}^C D_{0^+}^{\alpha,\psi}x(t)\,{}^C D_{0^+}^{\alpha,\psi}v_i(t)dt,$$
$$\int_{s_i}^{t_{i+1}} \psi'(t)\,{}^C D_{0^+}^{\alpha,\psi}x(t)\,{}^C D_{0^+}^{\alpha,\psi}v_i(t)dt = \lambda \int_{s_i}^{t_{i+1}} f_i(t, x(t))\psi'(t)v_i(t)dt,$$

which shows that

$${}^C D_{T^-}^{\alpha,\psi}({}^C D_{0^+}^{\alpha,\psi}x(t)) = \lambda f_i(t, x(t)), \forall t \in [s_i, t_{i+1}], i = 0, 1, \ldots, n. \tag{20}$$

Because $x \in E_0^{\alpha,\psi} \subset C[0, T]$ and $\psi(t) \in C^1[0, T]$, then

$$\int_{s_i}^{t_{i+1}} \mid x(t) \mid^2 + \psi'(t) \mid {}^C D_{0^+}^{\alpha,\psi}x(t) \mid^2 dt < +\infty.$$

Based on Lemma 3, (4) and (7) yield:

$$\begin{aligned} {}^C D_{T^-}^{\alpha,\psi}({}^C D_{0^+}^{\alpha,\psi}x(t)) =& D_{T^-}^{\alpha,\psi}(D_{0^+}^{\alpha,\psi}x(t)) = D_{T^-}^{\alpha,\psi}\left[\frac{1}{\psi'(t)}\frac{d}{dt}I_{0^+}^{1-\alpha,\psi}x(t)\right] \\ =& \frac{-1}{\Gamma(1-\alpha)}\left(\frac{1}{\psi'(t)}\frac{d}{dt}\right)\int_t^T \psi'(\xi)(\psi(\xi) - \psi(t))^{-\alpha}\left(\frac{1}{\psi'(\xi)}\frac{d}{d\xi}\right)I_{0^+}^{1-\alpha,\psi}x(\xi)d\xi \\ =& \frac{1}{\psi'(t)}\frac{d}{dt}\left[{}^C D_{T^-}^{\alpha,\psi}I_{0^+}^{1-\alpha,\psi}x(t)\right]. \end{aligned} \tag{21}$$

Since $\psi(t) \in C^1[0, T]$, $f_i \in C((s_i, t_{i+1}] \times \mathbb{R}, \mathbb{R})$, according to (20) and (21), one obtains ${}^C D_{T^-}^{\alpha,\psi}I_{0^+}^{1-\alpha,\psi}x(t) \in AC[s_i, t_{i+1}]$, which implies that the following limits exist:

$${}^C D_{T^-}^{\alpha,\psi}(I_{0^+}^{1-\alpha,\psi}x)(s_i^+) = \lim_{t \to s_i^+} {}^C D_{T^-}^{\alpha,\psi}(I_{0^+}^{1-\alpha,\psi}x)(t),$$
$${}^C D_{T^-}^{\alpha,\psi}(I_{0^+}^{1-\alpha,\psi}x)(t_{i+1}^-) = \lim_{t \to t_{i+1}^-} {}^C D_{T^-}^{\alpha,\psi}(I_{0^+}^{1-\alpha,\psi}x)(t).$$

Substituting (20) into (12), one obtains:

$$\int_0^T \psi'(t)\,{}^C D_{0^+}^{\alpha,\psi}x(t)\,{}^C D_{0^+}^{\alpha,\psi}y(t)dt - \sum_{i=1}^n I_i(x(t_i))y(t_i) - \sum_{i=0}^n \int_{s_i}^{t_{i+1}} {}^C D_{T^-}^{\alpha,\psi}({}^C D_{0^+}^{\alpha,\psi}x(t))\psi'(t)y(t)dt = 0. \tag{22}$$

Uniting (13) with (14), we have:

$$
\begin{aligned}
&\int_0^T \psi'(t)\,{}^{C}D_{0^+}^{\alpha,\psi}x(t)\,{}^{C}D_{0^+}^{\alpha,\psi}y(t)dt\\
&=\sum_{i=0}^{n}\int_{s_i}^{t_{i+1}} \psi'(t)\,{}^{C}D_{0^+}^{\alpha,\psi}x(t)\,{}^{C}D_{0^+}^{\alpha,\psi}y(t)dt+\sum_{i=1}^{n}\int_{t_i}^{s_i} \psi'(t)\,{}^{C}D_{0^+}^{\alpha,\psi}x(t)\,{}^{C}D_{0^+}^{\alpha,\psi}y(t)dt\\
&=\sum_{i=0}^{n}{}^{C}D_{T^-}^{\alpha,\psi}(I_{0^+}^{1-\alpha,\psi}x(s_i^+))y(s_i^+)-\sum_{i=0}^{n}{}^{C}D_{T^-}^{\alpha,\psi}(I_{0^+}^{1-\alpha,\psi}x(t_{i+1}^-))y(t_{i+1}^-) \qquad (23)\\
&\quad+\sum_{i=0}^{n}\int_{s_i}^{t_{i+1}} D_{T^-}^{\alpha,\psi}(D_{0^+}^{\alpha,\psi}x(t))\psi'(t)y(t)dt+\sum_{i=1}^{n}\int_{t_i}^{s_i} \psi'(t)\,{}^{C}D_{0^+}^{\alpha,\psi}x(t)\,{}^{C}D_{0^+}^{\alpha,\psi}y(t)dt.
\end{aligned}
$$

Then, from (22) and (23), we obtain:

$$
\begin{aligned}
&\sum_{i=0}^{n}{}^{C}D_{T^-}^{\alpha,\psi}(I_{0^+}^{1-\alpha,\psi}x(s_i^+))y(s_i^+)-\sum_{i=0}^{n}{}^{C}D_{T^-}^{\alpha,\psi}(I_{0^+}^{1-\alpha,\psi}x(t_{i+1}^-))y(t_{i+1}^-)\\
&+\sum_{i=1}^{n}\int_{t_i}^{s_i} \psi'(t)\,{}^{C}D_{0^+}^{\alpha,\psi}x(t)\,{}^{C}D_{0^+}^{\alpha,\psi}y(t)dt-\sum_{i=1}^{n}I_i(x(t_i))y(t_i)=0. \qquad (24)
\end{aligned}
$$

Without loss of generality, assume $v_i(t)\in C_0^{\infty}(t_i,s_i]$ and $v_i(t)\equiv 0$ for $t\in[0,t_i]\bigcup(s_i,T]$, $i=1,2,\ldots,n$. Substituting $v_i(t)$ into (24), from (15) we deduce:

$$
\sum_{i=1}^{n}\int_{t_i}^{s_i}\frac{d}{dt}\left[{}^{C}D_{T^-}^{\alpha,\psi}(I_{0^+}^{1-\alpha,\psi}x(t))\right]v_i(t)dt=0,
$$

because of the arbitrariness of $v_i(t)$, for $t\in(t_i,s_i]$, $i=1,2,\ldots,n$, we can obtain ${}^{C}D_{T^-}^{\alpha,\psi}(I_{0^+}^{1-\alpha,\psi}x(t))=Constant$. That is:

$$
{}^{C}D_{T^-}^{\alpha,\psi}(I_{0^+}^{1-\alpha,\psi}x)(t)={}^{C}D_{T^-}^{\alpha,\psi}(I_{0^+}^{1-\alpha,\psi}x)(t_i^+)={}^{C}D_{T^-}^{\alpha,\psi}(I_{0^+}^{1-\alpha,\psi}x)(s_i^-),\ \ t\in(t_i,s_i],\ i=1,2,\ldots,n. \qquad (25)
$$

Substituting (25) back into (24) yields:

$$
\begin{aligned}
&\sum_{i=0}^{n}{}^{C}D_{T^-}^{\alpha,\psi}(I_{0^+}^{1-\alpha,\psi}x(s_i^+))y(s_i^+)-\sum_{i=0}^{n}{}^{C}D_{T^-}^{\alpha,\psi}(I_{0^+}^{1-\alpha,\psi}x(t_{i+1}^-))y(t_{i+1}^-)-\sum_{i=1}^{n}I_i(x(t_i))y(t_i)\\
&+\sum_{i=1}^{n}{}^{C}D_{T^-}^{\alpha,\psi}(I_{0^+}^{1-\alpha,\psi}x(t_i^+))y(t_i)-\sum_{i=1}^{n}{}^{C}D_{T^-}^{\alpha,\psi}(I_{0^+}^{1-\alpha,\psi}x(t_i^+))y(s_i)=0,
\end{aligned}
$$

then

$$
\begin{aligned}
&\sum_{i=1}^{n}\left[{}^{C}D_{T^-}^{\alpha,\psi}(I_{0^+}^{1-\alpha,\psi}x(t_i^+))-{}^{C}D_{T^-}^{\alpha,\psi}(I_{0^+}^{1-\alpha,\psi}x(t_i^-))-I_i(x(t_i))\right]y(t_i)\\
&+\sum_{i=1}^{n}\left[{}^{C}D_{T^-}^{\alpha,\psi}(I_{0^+}^{1-\alpha,\psi}x(s_i^+))-{}^{C}D_{T^-}^{\alpha,\psi}(I_{0^+}^{1-\alpha,\psi}x(t_i^+))\right]y(s_i)=0,
\end{aligned}
$$

which implies that

$$
{}^{C}D_{T^-}^{\alpha,\psi}(I_{0^+}^{1-\alpha,\psi}x(t_i^+))-{}^{C}D_{T^-}^{\alpha,\psi}(I_{0^+}^{1-\alpha,\psi}x(t_i^-))=I_i(x(t_i)),\ {}^{C}D_{T^-}^{\alpha,\psi}(I_{0^+}^{1-\alpha,\psi}x(s_i^+))={}^{C}D_{T^-}^{\alpha,\psi}(I_{0^+}^{1-\alpha,\psi}x(t_i^+)).
$$

Combining with (25), we can obtain ${}^{C}D_{T^-}^{\alpha,\psi}(I_{0^+}^{1-\alpha,\psi}x(s_i^+))={}^{C}D_{T^-}^{\alpha,\psi}(I_{0^+}^{1-\alpha,\psi}x(s_i^-))$ for $i=1,2,\ldots,n$. Consequently, boundary conditions and impulsive conditions, as well as the first equation in FDE (1), are all satisfied by $x(t)$, which shows that $x(t)$ is a classical solution of FDE (1). □

Example 1. *Let $\alpha = 0.6$, $\psi(t) = e^t$, $t \in [0,1]$. Concern with the following system is as follows:*

$$\begin{cases} {}^{C}D_{1^-}^{0.6,e^t}({}^{C}D_{0^+}^{0.6,e^t}x(t)) = \lambda x^{\frac{1}{5}}(t),\ t \in (0,t_1]\bigcup(s_1,1], \\ \Delta({}^{C}D_{1^-}^{0.6,e^t}(I_{0^+}^{0.4,e^t}x))(t_1) = I_1(x(t_1)), \\ {}^{C}D_{1^-}^{0.6,e^t}(I_{0^+}^{0.4,e^t}x)(t) = {}^{C}D_{1^-}^{0.6,e^t}(I_{0^+}^{0.4,e^t}x)(t_1^+),\ \ t \in (t_1,s_1], \\ {}^{C}D_{1^-}^{0.6,e^t}(I_{0^+}^{0.4,e^t}x)(s_1^-) = {}^{C}D_{1^-}^{0.6,e^t}(I_{0^+}^{0.4,e^t}x)(s_1^+), \\ x(0) = x(1) = 0. \end{cases} \tag{26}$$

Put $I_1(x) = \frac{1}{100}x$. Clearly, $d_1 = L_1 = \frac{1}{100}$. By direct calculation, we have $M \approx 1.585$, $M^2L_1 = M^2d_1 \approx 0.025$, the condition (A_1) in Theorem 1 holds. Choose $\varsigma(t) = \Gamma(1.2)e^t$, $\rho = \frac{1}{10}$, a direct calculation yields

$${}^{C}D_{0^+}^{0.6,e^t}\varsigma(t) = \frac{\Gamma(1.2)}{\Gamma(0.4)}(-\frac{5}{2})(e^t-1)^{0.4},\ \|\varsigma\|_{\alpha,\psi}^2 \approx 1.576,\ \ \left(\frac{1}{2} - \frac{M^2d_1}{2}\right)\|\varsigma\|_{\alpha,\psi}^2 \approx 0.8 > \rho,$$

then

$$\frac{\sum_{i=0}^{n}\int_{s_i}^{t_{i+1}}\sup_{x\in\Omega(\rho)}F_i(t,x(t))\psi'(t)dt}{\rho} = \frac{(\int_0^{t_1}+\int_{s_1}^{1})\frac{5}{6}e^t\sup_{x\in\Omega(\rho)}x^{\frac{6}{5}}(t)dt}{0.1} \approx 0.55\left(\int_0^{t_1}+\int_{s_1}^{1}\right)e^t dt < 0.9,$$

and

$$\begin{aligned}\frac{2\sum_{i=0}^{n}\int_{s_i}^{t_{i+1}}F_i(t,\varsigma(t))\psi'(t)dt}{\|\varsigma\|_{\alpha,\psi}^2 - 2\sum_{i=1}^{n}\int_0^{\varsigma(t_i)}I_i(s))ds} &= \frac{\frac{5}{3}(\int_0^{t_1}+\int_{s_1}^{1})e^t(\Gamma(1.2)e^t)^{\frac{6}{5}}dt}{\|\varsigma\|_{\alpha,\psi}^2 - \frac{1}{100}(\varsigma(t_1))^2} \\ &> \frac{\frac{5}{3}(\int_0^{t_1}+\int_{s_1}^{1})e^t(\Gamma(1.2)e^t)^{\frac{6}{5}}dt}{\|\varsigma\|_{\alpha,\psi}^2 - \frac{1}{100}(\Gamma(1.2))^2} \approx 1.2\left(\int_0^{t_1}+\int_{s_1}^{1}\right)(e^t)^{\frac{11}{5}}dt > 1.2,\end{aligned}$$

which shows that the condition (A_2) holds. From Theorem 1, the system (26) possesses at least three distinct classical solutions for each $\lambda \in]0.8, 1.1[$.

Example 2. *Let $\alpha = 0.75$, $\psi(t) = ct^\sigma$ with $\sigma > 0$ and $c \geq 1$, $t \in [0,1]$. Concern with the following system is as follows:*

$$\begin{cases} {}^{C}D_{1^-}^{0.75,ct^\sigma}({}^{C}D_{0^+}^{0.75,ct^\sigma}x(t)) = \lambda f(t,x(t)),\ t \in (0,t_1]\bigcup(s_1,1], \\ \Delta({}^{C}D_{1^-}^{0.75,ct^\sigma}(I_{0^+}^{0.25,ct^\sigma}x))(t_1) = I_1(x(t_1)), \\ {}^{C}D_{1^-}^{0.75,ct^\sigma}(I_{0^+}^{0.25,ct^\sigma}x)(t) = {}^{C}D_{1^-}^{0.75,ct^\sigma}(I_{0^+}^{0.25,ct^\sigma}x)(t_1^+),\ \ t \in (t_1,s_1], \\ {}^{C}D_{1^-}^{0.75,ct^\sigma}(I_{0^+}^{0.25,ct^\sigma}x)(s_1^-) = {}^{C}D_{1^-}^{0.75,ct^\sigma}(I_{0^+}^{0.25,ct^\sigma}x)(s_1^+), \\ x(0) = x(1) = 0. \end{cases} \tag{27}$$

Obviously, if one chooses $c = 1$, i.e., $\psi(t) = t^\sigma$, the system (27) can reduce into the well known Caputo-Erdélyi-Kober type fractional differential system. Define $f(t,x) = \frac{5}{3^{\frac{11}{6}}}c^{-\frac{5}{4}}x^{\frac{2}{3}}\ln(t+1)$, $I_1(x) = \frac{1}{10}c^{-\frac{1}{2}}x$. Then $d_1 = L_1 = \frac{1}{10c^{\frac{1}{2}}}$. By direct calculation, we have $M \approx 1.15c^{\frac{1}{4}}$, $M^2L_1 = M^2d_1 \approx 0.132 < 1$. Choosing $\varsigma(t) = \Gamma(0.25)c^{\frac{3}{4}}t^\sigma$, $\rho = c$, a direct calculation yields:

$${}^{C}D_{0^+}^{0.75,ct^\sigma}\varsigma(t) = 4t^{\frac{1}{4}\sigma},\ \|\varsigma\|_{\alpha,\psi}^2 = \frac{32}{3}c,\ \ \left(\frac{1}{2} - \frac{M^2d_1}{2}\right)\|\varsigma\|_{\alpha,\psi}^2 \approx 4.6c > \rho,$$

then

$$\frac{\sum_{i=0}^{n}\int_{s_i}^{t_{i+1}}\sup_{x\in\Omega(\rho)}F_i(t,x(t))\psi'(t)dt}{\rho}=\frac{(\int_0^{t_1}+\int_{s_1}^{1})c\sigma t^{\sigma}\sup_{x\in\Omega(\rho)}3^{-\frac{5}{6}}c^{-\frac{5}{4}}x^{\frac{5}{3}}\ln(t+1)dt}{c}<\frac{1}{50\sigma},$$

and

$$\frac{2\sum_{i=0}^{n}\int_{s_i}^{t_{i+1}}F_i(t,\varsigma(t))\psi'(t)dt}{\|\varsigma\|^2_{\alpha,\psi}-2\sum_{i=1}^{n}\int_0^{\varsigma(t_i)}I_i(s))ds}=\frac{\frac{2}{3^{\frac{5}{6}}}\Gamma^2(0.25)c(\int_0^{t_1}+\int_{s_1}^{1})\sigma t^{2\sigma-1}\ln(t+1)dt}{\|\varsigma\|^2_{\alpha,\psi}-\frac{1}{10}c^{\frac{-1}{2}}(\varsigma(t_1))^2}>\frac{1}{10\sigma},$$

so that the condition (A_2) *holds. From Theorem 1, for each* $\lambda\in]10\sigma,50\sigma[$*, the system (27) possesses at least three distinct classical solutions.*

4. Conclusions

In this paper, we have investigated a new class of instantaneous and non-instantaneous impulsive boundary value problem involving the generalized ψ-Caputo fractional derivative. Based on properties of ψ-Caputo-type fractional operators and the three critical points theorem, the multiplicity results have been established. This problem is novel and hasn't been touched yet. By choosing special kernel functions in the ψ-Caputo fractional derivative, some existing results which focus on the classical fractional operators have been improved and supplemented.

Author Contributions: Formal analysis, D.L. and Y.L.; Investigation, D.L. and Y.L.; Methodology, D.L.; Writing—original draft, D.L. and Y.L.; Writing—review and editing, F.C. and X.F. All authors have read and agreed to the published version of the manuscript.

Funding: This research was funded by National Natural Science Foundation of China grant numbers 12101481, 62103327; Young Talent Fund of Association for Science and Technology in Shaanxi, China grant number 20220529; Young Talent Fund of Association for Science and Technology in Xi'an, China grant number 095920221344.

Data Availability Statement: Not applicable.

Acknowledgments: The authors would like to thank the editor and reviewers greatly for their precious comments and suggestions.

Conflicts of Interest: The authors declare no conflict of interest.

References

1. Kilbas, A.; Srivastava, H.; Trujillo, J. Theory and applications of fractional differential equations. In *North-Holland Mathematics Studies*; Elsevier Science B.V.: Amsterdam, The Netherland, 2006; pp. 2453–2461.
2. Teodoro, G.; Machado, J.; Oliveira, E. A review of definitions of fractional derivatives and other operators. *J. Comput. Phys.* **2019**, *388*, 195–208. [CrossRef]
3. Diethelm, K. *The Analysis of Fractional Differential Equations*; Springer: Berlin/Heidelberg, Germany, 2010.
4. Zeng, G.; Chen, J.; Dai, Y.; Li, L.; Zheng, C.; Chen, M. Design of fractional order PID controller for automatic regulator voltage system based on multi-objective extremal optimization. *Neurocomputing* **2015**, *160*, 173–184. [CrossRef]
5. Gómez-Aguilar, J.; López-López, M.; Alvarado-Martínez, V.; Reyes-Reyes, J.; Adam-Medina, M. Modeling diffusive transport with a fractional derivative without singular kernel. *Phys. A* **2016**, *447*, 467–481. [CrossRef]
6. Yu, Y.; Perdikaris, P.; Karniadakis, G. Fractional modeling of viscoelasticity in 3D cerebral arteries and aneurysms. *J. Comput. Phys.* **2016**, *323*, 219–242. [CrossRef]
7. Osler, T. Fractional derivatives of a composite function. *SIAM J. Math. Anal.* **1970**, *1*, 288–293. [CrossRef]
8. Jarad, F.; Abdeljawad, T. Generalized fractional derivatives and Laplace transform. *Discret. Contin. Dyn. Syst.* **2020**, *13*, 709–722. [CrossRef]
9. Almeida, R. A Caputo fractional derivative of a function with respect to another function. *Commun. Nonlinear Sci. Numer. Simul.* **2017**, *44*, 460–481. [CrossRef]
10. Almeida, R.; Malinowska, A.; Monteiro, M. Fractional differential equations with a Caputo derivative with respect to a Kernel function and their applications. *Math. Meth. Appl. Sci.* **2017**, *41*, 336–352. [CrossRef]
11. Khaliq, A.; Mujeeb, R. Existence of weak solutions for Ψ-Caputo fractional boundary value problem via variational methods. *J. Appl. Anal.Comput.* **2021**, *11*, 768–1778. [CrossRef]

12. Adjabi, Y.; Jarad, F.; Baleanu, D.; Abdeljawad, T. On Cauchy problems with Caputo Hadamard fractional derivatives. *J. Comput. Anal. Appl.* **2016**, *21*, 661–681.
13. Min, D.; Chen, F. Variational methods to the p-Laplacian type nonlinear fractional order impulsive differential equations with Sturm-Liouville boundary-value problem. *Fract. Calc. Appl. Anal.* **2021**, *24*, 1069–1093. [CrossRef]
14. Shah, K.; Abdalla, B.; Abdeljawad, T.; Gul, R. Analysis of multipoint impulsive problem of fractional-order differential equations. *Bound. Value Probl.* **2023**, *2023*, 1.. [CrossRef]
15. Lv, Z.; Ahmad, I.; Xu, J.; Zada, A. Analysis of a Hybrid coupled system of psi-Caputo fractional derivatives with generalized Slit-Strips-type integral boundary conditions and Impulses. *Fractal Fract.* **2022**, *10*, 618.. [CrossRef]
16. Hernádez, E.; O'Regan, D. On a new class of abstract implusive differential equations. *Proc. Am. Math. Soc.* **2013**, *141*, 1641–1649. [CrossRef]
17. Liu, J.; Wei, W.; Xu, W. Approximate controllability of non-Instantaneous impulsive stochastic evolution systems driven by fractional brownian motion with hurst parameter h is an element of $(0, \frac{1}{2})$. *Fractal Fract.* **2022**, *8*, 440.. [CrossRef]
18. Wang, Y.; Li, C.; Wu, H.; Deng, H. Existence of solutions for fractional instantaneous and non-Instantaneous impulsive differential equations with perturbation. *Discret. Cont. Dyn. Syst.* **2022**, *7*, 1767–1776. [CrossRef]
19. Li, D.; Chen, F.; Wu, Y.; An Y. Multiple solutions for a class of p-Laplacian type fractional boundary value problems with instantaneous and non-instantaneous impulses. *Appl. Math. Lett.* **2020**, *106*, 106352. [CrossRef]
20. Salem, A.; Abdullah, S. Non-instantaneous impulsive BVPs involving generalized Liouville-Caputo derivative. *Mathematics* **2022**, *3*, 291.. [CrossRef]
21. Tian, Y.; Zhang, M. Variational method to differential equations with instantaneous and non-instantaneous impulses. *Appl. Math. Lett.* **2019**, *94*, 160–165. [CrossRef]
22. Zhang, W.; Liu, W. Variational approach to fractional dirichlet problem with instantaneous and non-instantaneous impulses. *Appl. Math. Lett.* **2020**, *99*, 105993. [CrossRef]
23. Bonanno, G.; Marano, S. On the structure of the critical set of non-differentiable functions with a weak compactness condition. *Appl. Anal.* **2010**, *89*, 1–10. [CrossRef]
24. Zeidler, E. *Nonlinear Functional Analysis and Its Applications*; Springer: Berlin, Germany, 1990; Volume 2.

fractal and fractional

MDPI

Article

Refinable Trapezoidal Method on Riemann–Stieltjes Integral and Caputo Fractional Derivatives for Non-Smooth Functions

Gopalakrishnan Karnan [1] and Chien-Chang Yen [2,*]

[1] The Graduate Institute of Applied Science and Engineering, Fu-Jen Catholic University, New Taipei City 242062, Taiwan; 407068083@mail.fju.edu.tw
[2] Department of Mathematics, Fu-Jen Catholic University, New Taipei City 242062, Taiwan
* Correspondence: yen@math.fju.edu.tw

Abstract: The Caputo fractional α-derivative, $0 < \alpha < 1$, for non-smooth functions with $1+\alpha$ regularity is calculated by numerical computation. Let I be an interval and $\mathcal{D}_\alpha(I)$ be the set of all functions $f(x)$ which satisfy $f(x) = f(c) + f'(c)(x-a) + g_c(x)(x-c)|(x-c)|^\alpha$, where $x, c \in I$ and $g_c(x)$ is a continuous function for each c. We first extend the trapezoidal method on the set $\mathcal{D}_\alpha(I)$ and rewrite the integrand of the Caputo fractional integral as a product of two differentiable functions. In this approach, the non-smooth function and the singular kernel could have the same impact. The trapezoidal method using the Riemann–Stieltjes integral (TRSI) depends on the regularity of the two functions in the integrand. Numerical simulations demonstrated that the order of accuracy cannot be increased as the number of zones increases using the uniform discretization. However, for a fixed coarsest grid discretization, a refinable mesh approach was employed; the corresponding results show that the order of accuracy is $k\alpha$, where k is a refinable scale. Meanwhile, the application of the product of two differentiable functions can also be applied to some Riemann–Liouville fractional differential equations. Finally, the stable numerical scheme is shown.

Keywords: fractional derivative; Caputo derivative; trapezoidal method; Riemann–Stieltjes integral

Citation: Karnan, G.; Yen, C.-C. Refinable Trapezoidal Method on Riemann–Stieltjes Integral and Caputo Fractional Derivatives for Non-Smooth Functions. *Fractal Fract.* **2023**, *7*, 263. https://doi.org/10.3390/fractalfract7030263

Academic Editors: António Lopes, Alireza Alfi, Liping Chen and Sergio Adriani David

Received: 6 February 2023
Revised: 10 March 2023
Accepted: 12 March 2023
Published: 15 March 2023

1. Introduction

Fractional calculus [1–3] has attracted increased interest over the last decade and has been applied in several fields including finance, control theory, electronic circuit theory, mechanics, physics, and signal processing [4–11]. There are two popular definitions of the fractional differentiation: the Riemann–Liouville derivative and the Caputo derivative. Let $0 < \alpha < 1$, n be a positive integer with $n-1 \le \alpha < n$, and $a \in \mathbf{R}$.

Riemann–Liouville derivative: The Riemann–Liouville derivative of a function $f(x)$ starting at the point a is

$$ {}_aD_t^\alpha f(t) = \frac{1}{\Gamma(n-\alpha)} \frac{d^n}{dt^n} \int_a^t \frac{f(\tau)}{(t-\tau)^{\alpha-n+1}} d\tau.$$

Caputo derivative: The Caputo derivative of a function $f(x)$ starting at the point a is

$$ {}_a^C D_t^\alpha f(t) = \frac{1}{\Gamma(n-\alpha)} \int_a^t \frac{f^{(n)}(\tau)}{(t-\tau)^{\alpha-n+1}} d\tau. \quad (1)$$

The comparison of these two definitions can be found in [12] and the definitions of fractional derivatives are also revised in some studies [11–14].

The trapezoidal rule was used for integration or differential equations in the following papers [15–17]. However, the functions of the integrand are assumed to be regular. This paper is devoted to the computation of the Caputo fractional derivative on financial

derivatives [18–21]. In some of them, the functions of the stock or option prices are only of Lipschitz continuity. Our goal is to calculate the Caputo fractional integral for non-smooth functions. This calculation will also encounter the difficulty induced by the singular kernel. In [18], an implicit numerical discretization is used for the Riemann–Liouville integral to calculate the chaotic behavior for financial models. In [22], the treatment for a singular kernel involves the linear expansion of the smooth functions and direct integration of the product of the linear polynomial and the singular kernel. In our approach, we consider the function non-smooth. The function could be also singular, and the impact of the function for the integral is similar to the kernel.

Let n be a positive integer and $[a,b]$ be an interval. Define $h = (b-a)/n$ and $x_i = a + ih$, where $i = 0, 1, 2, \ldots, n$. To explore the niche of this research, let us explain the following examples. The set of $C^k([a,b])$ represents the collection of all functions whose domain on $[a,b]$ and they are of a continuous k-th derivative. If $f \in C^2([a,b])$, it is well known in the textbook of numerical analysis, and the approximation is

$$\int_a^b f(x)\,dx = \frac{h}{2}\left[f(a) + f(b) + 2\sum_{j=1}^{n-1} f(x_j)\right] - \frac{(b-a)}{12}h^2 f''(\xi),$$

where ξ is in (a,b). For the particular case, $f(x) = \sqrt{x-a}$, the order of accuracy of the trapezoidal rule method is reduced because the function $f(x)$ belongs exclusively to $C^0([a,b])$.

Definition 1. *Let I be an interval and the set*

$$\mathcal{D}_\alpha(I) \equiv \left\{f : f(x) = f(c) + f'(c)(x-c) + g_c(x)(x-c)|x-c|^\alpha\right\}, \tag{2}$$

where $g_c(x)$ is a continuous function for each $c \in I$.

For example, $I = [0,1]$, $\alpha = 1/2$, and $f(x) = x^{3/2}$. Then,

$$x^{3/2} = c^{3/2} + \frac{3}{2}c^{1/2}(x-c) + g_c(x)(x-c)|x-c|^{1/2}$$

with

$$g_c(x) = \begin{cases} \frac{x^{3/2} - c^{3/2} - \frac{3}{2}c^{1/2}(x-c)}{(x-c)|x-c|^{1/2}}, & x \neq c, \\ 0, & x = c \neq 0. \end{cases}$$

If $c = 0$, then $g_0(0) = 1$ and $g_c(x)$ is continuous on $[0,1]$ for each $c \in [0,1]$. Hence, $x^{3/2} \in \mathcal{D}_{1/2}([0,1])$. Moreover, for a fixed x, the function $h(c) = g_c(x)$ may not be continuous on c since $g_0(0) = 1$ and $g_c(0) = -1/2$ for all $c > 0$.

This paper is organized as follows. The order of accuracy for the trapezoidal method on the set $\mathcal{D}_\alpha(I)$ is derived in Section 2. The proposed method for calculation of Caputo fractional derivative is described in Section 3, using three examples. Smooth, regular and non-regular functions are used in numerical simulations in Section 4. Section 5 shows the analysis of the method to explain the obtained results and Section 6 demonstrates two applications of the proposed method. The conclusion is given in the last section.

2. Order of Accuracy for Trapezoidal Method on $\mathcal{D}_\alpha$

In this section, we extend the analysis of the order of accuracy for the trapezoidal method on the set $\mathcal{D}_\alpha(I)$. Let us begin to consider the interpolation on the set $\mathcal{D}_\alpha(I)$.

Lemma 1. *Let $f \in \mathcal{D}_\alpha(I)$. The linear interpolation of f on $[a,b] \subset I$ has the property*

$$f(x) = f(a)\frac{b-x}{b-a} + f(b)\frac{x-a}{b-a} + \frac{h(x)}{b-a}(x-a)(b-x),$$

where $h(x)$ is a continuous function and $x \in [a, b]$.

Proof. Since

$$\begin{aligned} f(x) &= f(a) + f'(a)(x-a) + g_a(x)(x-a)|x-a|^\alpha, \\ f(x) &= f(b) + f'(b)(x-b) + g_b(x)(x-b)|x-b|^\alpha, \end{aligned}$$

we obtain

$$\begin{aligned} f(x) &= f(a)\frac{b-x}{b-a} + f(b)\frac{x-a}{b-a} + \frac{1}{(b-a)}(f'(a) - f'(b))(x-a)(b-x) \\ &\quad + \frac{1}{b-a}(g_a(x)|x-a|^\alpha - g_b(x)|b-x|^\alpha)(x-a)(b-x) \\ &\equiv f(a)\frac{b-x}{b-a} + f(b)\frac{x-a}{b-a} + \frac{h(x)}{b-a}(x-a)(b-x). \end{aligned}$$

Here, $h(x) = f'(a) - f'(b) + g_a(x)|x-a|^\alpha - g_b(x)|b-x|^\alpha$. □

Lemma 2. *Let $f \in \mathcal{D}_\alpha(I)$ and $[a, b] \subset I$. Then,*

$$\int_a^b f(x)dx = \frac{1}{2}(f(a) + f(b))(b-a) + \frac{h(\xi)}{6}(b-a)^2,$$

where $h(\xi)$ is a continuous function.

Proof. This lemma holds. It is followed by Lemma 1 and

$$\begin{aligned} \int_a^b f(x)dx &= \int_a^b \left[f(a)\frac{b-x}{b-a} + f(b)\frac{x-a}{b-a} + \frac{h(x)}{b-a}(x-a)(b-x) \right] dx \\ &= \frac{1}{2}(f(a) + f(b))(b-a) + \frac{h(\xi)}{b-a}\int_a^b (x-a)(b-x)dx \\ &= \frac{1}{2}(f(a) + f(b))(b-a) + \frac{h(\xi)}{6}(b-a)^2, \end{aligned}$$

where ξ in (a, b), and the second equality is followed by the weighted mean value theorem. □

Lemma 3. *Let $f \in \mathcal{D}_\alpha(I)$ and $[a, b] \subset I$. Then,*

$$f'(b) - f'(a) = (g_b(a) - g_a(b))|b-a|^\alpha.$$

Proof. From the following,

$$\begin{aligned} \frac{f(b) - f(a)}{b-a} &= f'(a) + g_a(b)|b-a|^\alpha, \\ \frac{f(a) - f(b)}{a-b} &= f'(b) + g_b(a)|b-a|^\alpha, \end{aligned}$$

and taking the subtraction of the above two equations, it yields

$$f'(b) - f'(a) = (g_b(a) - g_a(b))|b-a|^\alpha. \tag{3}$$

□

Moreover, $|g_a(x)|x-a|^\alpha - g_b(x)|b-x|^\alpha| \leq (|g_a(x)| + |g_b(x)|)|b-a|^\alpha$ for $x \in [a, b]$ and $|h(x)| \leq (|g_b(a) - g_a(b)| + |g_a(x)| + |g_b(x)|)|b-a|^\alpha$. Since h is continuous and

bounded by the extremum theorem of continuous functions on a closed interval, Lemma 2 can be re-estimated to be Theorem 1 below.

Theorem 1. *Let $f \in \mathcal{D}_\alpha(I)$ and $[a,b] \subset I$. Then,*

$$\int_a^b f(x)dx = \frac{1}{2}(f(a)+f(b))(b-a) + O((b-a)^{2+\alpha}).$$

Remark. If $f \in C^2(I)$ then $g_c = \frac{1}{2}f''(\xi)$, where ξ between c and x, then $\alpha = 1$.

Theorem 2. *Let $f \in \mathcal{D}_\alpha(I)$ and $[a,b] \subset I$. If*

$$f(x) = f(c) + f'(c)(x-c) + g_c(x)(x-c)|x-c|^\alpha$$

and $|g_c(a)|$ is uniformly bounded for all $c \in [a,b]$, then

$$\int_a^b f'(x)dx = \frac{1}{2}(f'(a)+f'(b))(b-a) + O((b-a)^{1+\alpha}).$$

Proof. Using (3) as

$$f'(x) - f'(a) = (g_x(a) - g_a(x))|x-a|^\alpha,$$

taking the integration of the above equation on $[a,b]$, we have

$$\int_a^b [f'(x) - f'(a)]\,dx = \int_a^b (g_x(a) - g_a(x))|x-a|^\alpha\,dx.$$

Since $|g_x(a)|$ is uniformly bounded for all $x \in [a,b]$ and $g_a(x)$ is continuous on $x \in [a,b]$, it implies that $|g_x(a) - g_a(x)|$ is uniformly bounded for $x \in [a,b]$ and

$$\int_a^b (g_x(a) - g_a(x))|x-a|^\alpha\,dx = O(\int_a^b (x-a)^\alpha\,dx) = O((b-a)^{1+\alpha}). \tag{4}$$

Then,

$$\begin{aligned}\int_a^b f'(x)\,dx &= f'(a)(b-a) + \int_a^b [f'(x) - f'(a)]\,dx \\ &= \frac{1}{2}(f'(a)+f'(b))(b-a) - \frac{1}{2}(f'(b)-f'(a))(b-a) \\ &\quad + \int_a^b (g_x(a) - g_a(x))|x-a|^\alpha\,dx \\ &= \frac{1}{2}(f'(a)+f'(b))(b-a) + O((b-a)^{1+\alpha}).\end{aligned}$$

The last equality is followed by $\frac{1}{2}(f'(b)-f'(a))(b-a) = \frac{1}{2}(g_b(a)-g_a(b))(b-a)^{1+\alpha}$ and (4). Therefore, this theorem holds. □

3. Method

For the sake of simplicity and without loss generality, the case of $n = 1$ is considered in the whole paper. Equation (1) is equal to

$${}_a^C D_t^\alpha f(t) = \frac{1}{\Gamma(1-\alpha)} \int_a^t f'(\tau)(t-\tau)^{-\alpha}\,d\tau, \tag{5}$$

or

$$ {}_a^C D_t^\alpha f(t) = \frac{1}{\Gamma(1-\alpha)} \int_a^t f'(\tau)\varphi'(t-\tau)\, d\tau, \tag{6} $$

here, $\varphi(t) = -\frac{1}{1-\alpha} t^{1-\alpha}$.

Let the interval $I = [0,1]$ and N be a positive integer. The interval I is divided into N-subintervals $[t_{\ell-1}, t_\ell]$ with the sample points t_ℓ, $\ell = 1, 2, \ldots, N$.

$$ {}_0^C D_t^\alpha f(t_k) = \frac{1}{\Gamma(1-\alpha)} \sum_{\ell=1}^{k} \int_{t_{\ell-1}}^{t_\ell} f'(\tau)\varphi'(t_k-\tau) d\tau. $$

Since φ is monotonic whenever $0 < \alpha < 1$, the inverse of φ exists. Using the substitution rule, $y = \varphi(t-\tau)$ for fixed t, the integral

$$ \int_{t_{\ell-1}}^{t_\ell} f'(\tau)\varphi'(t_k-\tau) d\tau $$

can be rewritten into

$$ \int_{y_{\ell-1}}^{y_\ell} f'(t_k - \varphi^{-1}(y)) dy, \tag{7} $$

where $y_{\ell-1} = \varphi(t_k - t_{\ell-1})$ and $y_\ell = \varphi(t_k - t_\ell)$. The linear interpolation of $f'(y)$ on the interval I with the endpoints $\varphi(t_k - t_\ell)$ and $\varphi(t_k - t_{\ell-1})$ is

$$ f'(y) = f'(t_{\ell-1}) \frac{y_\ell - y}{y_\ell - y_{\ell-1}} + f'(t_\ell) \frac{y - y_{\ell-1}}{y_\ell - y_{\ell-1}}. \tag{8} $$

Substituting (8) into (7), it yields

$$ \begin{aligned} \int_{y_{\ell-1}}^{y_\ell} f'(t_k - \varphi^{-1}(y)) dy &\approx \frac{1}{2}(f'(t_{\ell-1}) + f'(t_\ell))(y_\ell - y_{\ell-1}) \\ &= \frac{1}{2}(f'(t_{\ell-1}) + f'(t_\ell))(\varphi(t_k - t_\ell) - \varphi(t_k - t_{\ell-1})). \end{aligned} \tag{9} $$

The approximation in the last equation listed above represents the trapezoidal method but uses the Riemann–Stieltjes integral. The roles of f and g may be interchanged. Equation (9) is modified to

$$ \begin{aligned} \int_{y_{\ell-1}}^{y_\ell} f'(t_k - \varphi^{-1}(y)) dy &\approx H \frac{1}{2}(f'(t_{\ell-1}) + f'(t_\ell))(\varphi(t_k - t_\ell) - \varphi(t_k - t_{\ell-1})) \\ &\quad + (1-H)\frac{1}{2}(f(t_\ell) - f(t_{\ell-1}))(\varphi'(t_k - t_\ell) + \varphi'(t_k - t_{\ell-1})), \end{aligned} \tag{10} $$

where $H = H(|\varphi(t_k - t_\ell) - \varphi(t_k - t_{\ell-1})| - |f(t_\ell) - f(t_\ell)|)$ is the Heaviside step function. We refer to the approach in (10) as the TRSI method. If the function f is smooth and φ is non-smooth, then TRSI in (10) may only use $H = 1$. On the other hand, the function φ is smooth and f is non-smooth, then TRSI in (10) may only use $H = 0$. For Caputo fractional derivatives, φ is described as the form $-\frac{1}{1-\alpha} t^{1-\alpha}$ and its derivative is singular at its origin. Therefore, if the function f is smooth, then $H = 0$ only occurs at the singularity of φ'.

The stability of the TRSI method to use Equation (6) is to estimate the following:

$$\begin{aligned} |{}_a^C D_t^\alpha f(t_k)| &\leq \left| \frac{1}{\Gamma(1-\alpha)} \sum_{\ell=1}^{k} \int_{t_{\ell-1}}^{t_\ell} f'(\tau)\varphi'(t_k-\tau)\, d\tau \right| \\ &\leq \left| \frac{1}{\Gamma(1-\alpha)} \sum_{\ell=1}^{k} \min\{|\varphi(t_k-t_\ell)-\varphi(t_k-t_{\ell-1}))|, |f(t_\ell)-f(t_{\ell-1})|\} \times \right. \\ &\quad \left. \frac{1}{2}(|f'(t_{\ell-1})+f'(t_\ell)|+|\varphi'(t_k-t_\ell)+\varphi'(t_k-t_{\ell-1})|) \right|. \end{aligned}$$

If $\frac{1}{\Delta t}\min\{|\varphi(t_k-t_\ell)-\varphi(t_k-t_{\ell-1}))|, |f(t_\ell)-f(t_{\ell-1})|\}$ is uniformly bounded for Δt, $\int_0^t |f'(s)|ds$ and $\int_0^t |\varphi'(s)|ds$ are bounded, $\mathcal{M}$, then

$$|{}_a^C D_t^\alpha f(t_k)| \leq \frac{\mathcal{M}}{\Gamma(1-\alpha)} \left(\int_0^{t_k} |f'(s)|\, ds + \int_0^{t_k} |\varphi'(s)| ds \right)$$

and it follows that TRSI is stable. The condition $\frac{1}{\Delta t}\min\{|\varphi(t_k-t_\ell)-\varphi(t_k-t_{\ell-1}))|, |f(t_\ell)-f(t_{\ell-1})|\}$ is uniformly bounded. It also indicates the existence of the Riemann–Stieltjes integral. It is identical to the existence of the Riemann–Stieltjes integral

$$\int_a^b f'(s) d\varphi(s),$$

requires the condition that the discontinuity of f' and φ cannot occur coincidentally, and vice versa. Therefore, the stability theorem of the TRSI method is stated in the following theorem.

Theorem 3. *The TRSI method is stable if the condition that the discontinuity of f' and φ cannot occur coincidentally is held.*

4. Simulations

Let us consider the interval $I = [0,1]$ and there are N uniform cells; that is, each subinterval $[t_{\ell-1}, t_\ell]$ has the length $\Delta t = \frac{1}{N}$ with the sample points $t_\ell = \frac{\ell}{N}$. We will vary $N = 2^K$ from $K = 5$ to $K = 12$. To probe the behavior of the TRSI method, let us define the 1-norm, 2-norm and ∞-norm in vectors of numerical solutions by

$$\|f(\cdot)\|_1 = \sum_{\ell=1}^{N} |f(t_\ell)|\Delta t, \quad \|f(\cdot)\|_2 = (\sum_{\ell=1}^{N} |f(t_\ell)|^2)^{1/2}\Delta t, \quad \|f(\cdot)\|_\infty = \max_{1\leq \ell \leq N} |f(t_\ell)|.$$

Furthermore, the order of accuracy is defined as

$$O_{q,K} = \log_2\left(\frac{\|e_K\|_q}{\|e_{K+1}\|_q}\right),$$

where $q = 1, 2, \infty$ and e_K is the error between the numerical and exact solutions at the size of zones 2^K. In the following subsection, we adopt three examples as model examples which represent the smooth, regular and non-smooth functions from Example 1 to Example 3 below, respectively.

4.1. Model Examples

Example 1 . Let us consider $f(t) = \frac{1}{4}t^4$ and $g(t) = 2t^{\frac{1}{2}}$. The polynomial is smooth because $f^{(n)}$ exists for any n, which is a non-negative integer. The Caputo fractional derivative of $f(t)$ for $\alpha = \frac{1}{2}$ is

$$ {}_0^C D_t^{\alpha} f(t) = \frac{1}{\Gamma(1-\alpha)} \int_0^t f'(\tau)(t-\tau)^{-\alpha}\, d\tau = \frac{1}{\Gamma(\frac{1}{2})} \int_0^t \tau^3 (t-\tau)^{-\frac{1}{2}}\, d\tau. \tag{11} $$

The analytic solution is ${}_0^C D_t^{\alpha} f(t) = \frac{32}{35\sqrt{\pi}} t^{\frac{7}{2}}$. The errors between the exact and numerical solutions are shown in Table 1, which demonstrates that the order of accuracy is near 1.5 for 1-norm, 2-norm and ∞-norm.

Table 1. The errors between numerical and analytic solutions for $f(t) = \frac{1}{4}t^4$ and the order of accuracy. The order of accuracy is near 1.5 for 1-norm, 2-norm and ∞-norm.

N_ℓ	E_1	E_2	E_∞	$N_\ell/N_{\ell+1}$	O_1	O_2	O_∞
32	1.038×10^{-3}	1.415×10^{-3}	3.124×10^{-3}	32/64	1.41	1.41	1.40
64	3.915×10^{-4}	5.312×10^{-4}	1.186×10^{-3}	64/128	1.43	1.44	1.43
128	1.449×10^{-4}	1.960×10^{-4}	4.391×10^{-4}	128/256	1.45	1.46	1.46
256	5.291×10^{-5}	7.140×10^{-5}	1.602×10^{-4}	256/512	1.47	1.47	1.47
512	1.914×10^{-5}	2.579×10^{-5}	5.784×10^{-5}	512/1024	1.48	1.48	1.48
1024	6.880×10^{-6}	9.256×10^{-6}	2.075×10^{-5}	1024/2048	1.48	1.48	1.49
2048	2.461×10^{-6}	3.308×10^{-6}	7.413×10^{-6}	2048/4096	1.49	1.49	1.49
4096	8.771×10^{-7}	1.179×10^{-6}	2.639×10^{-6}	-	-	-	-

Example 2. Let us consider $f(t) = \frac{3}{2}t^{3/2}$ and $g(t) = 2t^{\frac{1}{2}}$. The power function f' only can take the first derivate because f'' is singular at the origin. The Caputo fractional derivative of $f(t)$ for $\alpha = \frac{1}{2}$ is

$$ {}_0^C D_t^{\alpha} f(t) = \frac{1}{\Gamma(1-\alpha)} \int_0^t f'(\tau)(t-\tau)^{-\alpha}\, d\tau = \frac{1}{\Gamma(\frac{1}{2})}, \int_0^t \tau^{\frac{1}{2}} (t-\tau)^{-\frac{1}{2}}\, d\tau. \tag{12} $$

The analytic solution is ${}_0^C D_t^{\alpha} f(t) = \frac{\sqrt{\pi}}{2} t$. The errors are shown in Table 2. The results demonstrate that the order of accuracy is near 1.5, 1.45 and 1 for 1-norm, 2-norm and ∞-norm, respectively.

Table 2. The errors between numerical and analytic solutions for $f(t) = \frac{2}{3}t^{3/2}$ and the order of accuracy. The order of accuracy is near 0.52, 0.54 and 0.16 for 1-norm, 2-norm and ∞-norm, respectively.

N_ℓ	E_1	E_2	E_∞	$N_\ell/N_{\ell+1}$	O_1	O_2	O_∞
32	2.390×10^{-3}	2.920×10^{-3}	1.006×10^{-2}	32/64	1.47	1.41	1.00
64	8.649×10^{-4}	1.100×10^{-3}	5.032×10^{-3}	64/128	1.48	1.42	1.00
128	3.109×10^{-4}	4.115×10^{-4}	2.516×10^{-3}	128/256	1.48	1.42	1.00
256	1.112×10^{-4}	1.531×10^{-4}	1.258×10^{-3}	256/512	1.49	1.43	1.00
512	3.967×10^{-5}	5.668×10^{-5}	6.290×10^{-4}	512/1024	1.49	1.44	1.00
1024	1.411×10^{-5}	2.091×10^{-5}	3.145×10^{-4}	1024/2048	1.49	1.44	1.00
2048	5.001×10^{-6}	7.686×10^{-6}	1.572×10^{-4}	2048/4096	1.50	1.45	1.00
4096	1.777×10^{-6}	2.818×10^{-6}	7.862×10^{-4}	-	-	-	-

Example 3. Let us consider $f(t) = 2t^{1/2}$ and $g(t) = \frac{3}{2}t^{\frac{2}{3}}$. The power function f does not have the first derivative because $f'(0)$ does not exist. The Caputo fractional derivative of $f(t)$ for $\alpha = \frac{1}{3}$ is

$$ {}_0^C D_t^\alpha f(t) = \frac{1}{\Gamma(1-\alpha)} \int_0^t f'(\tau)(t-\tau)^{-\alpha}\, d\tau = \frac{1}{\Gamma(\frac{2}{3})} \int_0^t \tau^{-\frac{1}{2}}(t-\tau)^{-\frac{1}{3}}\, d\tau. \tag{13} $$

The analytic solution is ${}_0^C D_t^\alpha f(t) = \frac{\Gamma(\frac{1}{2})}{\Gamma(\frac{7}{6})} t^{\frac{1}{6}}$. The errors are shown in Table 3. The order of accuracy is near 0.52, 0.54 and 0.16 for 1-norm, 2-norm and ∞-norm, respectively. In Figure 1, the top-left panel shows the exact solution (red dot line) and the numerical solution (blue solid line). The errors between the numerical and exact solutions are shown in the top-right panel. The zoom-in profiles on $[0, 0.2]$ are shown in the corresponding panels below.

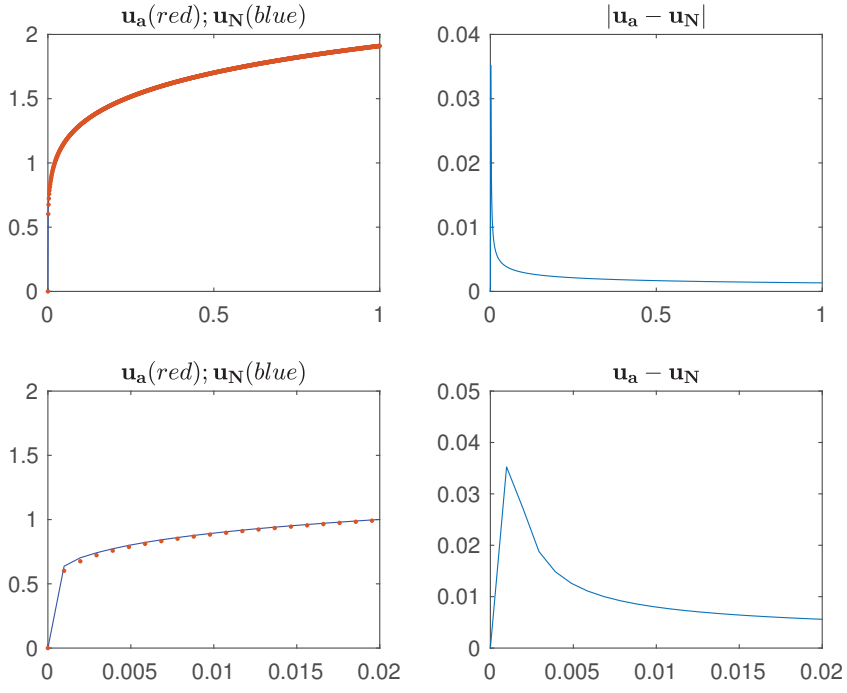

Figure 1. The profiles of the simulations of Example 3. The analytic (u_a) and the numerical u_N solutions are shown in the top-left panel. The absolute value of the error $|u_a - u_N|$ is shown in the top-right panel. The zoom-in profiles on $[0, 0.2]$ are shown in the corresponding panels below.

The approximation of the non-smooth or continuous function may improve the accuracy by refining the meshes. However, it is not equivalent to a finer mesh refinement in this case, as the kernel function $\varphi(t_k - s)$ is not only non-smooth, but it is singular for fixed t_k. Therefore, we divide the subinterval by $\mathcal{K}$-zones again. More precisely,

$$ \int_{t_{\ell-1}}^{t_\ell} f'(s)(t_k - s)^{-\alpha}\, ds = \sum_{m=1}^{\mathcal{K}} \int_{t_{\ell,m-1}}^{t_{\ell,m}} f'(s)\varphi'(t_k - s)\, ds, $$

where $t_{\ell,m} = t_{\ell-1} + m\Delta\mathcal{K}$, $m = 0, 1, 2, \ldots, \mathcal{K}$, with $\Delta\mathcal{K} = \frac{t_\ell - t_{\ell-1}}{\mathcal{K}}$. The results of fixed $N = 128$ for $\mathcal{K} = 2^p$, $p = 2, 3, \ldots, 6$ are shown in Table 4 and the corresponding pro-

files are shown in Figure 2. The errors were reduced from 2.8×10^{-2} to 4.7×10^{-5}; see Tables 3 and 4, respectively.

Table 3. The errors between numerical and analytic solutions for $f(t) = 2t^{1/2}$ and the order of accuracy. It shows that the order of accuracy is near 0.52, 0.54 and 0.16 for 1-norm, 2-norm and ∞-norm, respectively.

N_ℓ	E_1	E_2	E_∞	$N_\ell/N_{\ell+1}$	O_1	O_2	O_∞
32	1.565×10^{-2}	1.967×10^{-2}	6.281×10^{-2}	32/64	0.63	0.58	0.16
64	1.009×10^{-2}	1.315×10^{-2}	5.596×10^{-2}	64/128	0.61	0.58	0.16
128	6.635×10^{-3}	8.825×10^{-3}	4.985×10^{-2}	128/256	0.58	0.57	0.16
256	4.445×10^{-3}	5.948×10^{-3}	4.441×10^{-2}	256/512	0.55	0.56	0.16
512	3.029×10^{-3}	4.031×10^{-3}	3.957×10^{-2}	512/1024	0.54	0.55	0.16
1024	2.087×10^{-3}	2.746×10^{-3}	3.525×10^{-2}	1024/2048	0.52	0.55	0.16
2048	1.451×10^{-3}	1.881×10^{-3}	3.140×10^{-2}	2048/4096	0.52	0.54	0.16
4096	1.014×10^{-3}	1.294×10^{-3}	2.780×10^{-2}	-	-	-	-

Table 4. The errors between numerical and analytic solutions for $f(t) = 2t^{1/2}$ and the order of accuracy using TRSI with refining mesh. The order of accuracy is near 1.76, 1.61 and 1.59 for 1-norm, 2-norm and ∞-norm, respectively.

$\mathcal{K}(N = 128)$	E_1	E_2	E_∞	$\mathcal{K}_{p-1}/\mathcal{K}_p$	O_1	O_2	O_∞
4	9.393×10^{-4}	1.651×10^{-3}	1.399×10^{-2}	4/8	1.88	1.76	1.72
8	2.548×10^{-4}	4.860×10^{-4}	4.260×10^{-3}	8/16	1.86	1.72	1.67
16	7.013×10^{-5}	1.480×10^{-4}	1.343×10^{-3}	16/32	1.83	1.67	1.63
32	1.973×10^{-5}	4.636×10^{-5}	4.328×10^{-4}	32/64	1.80	1.64	1.60
64	5.690×10^{-6}	1.487×10^{-5}	1.418×10^{-4}	64/128	1.76	1.61	1.59
128	1.685×10^{-6}	4.861×10^{-6}	4.708×10^{-5}	-	-	-	-

4.2. A Comparison Study

The modified trapezoidal rule (MTR) [22] uses the linear interpolation on $f'(s)$ rather than $f'(s)(t_k - s)^{-\alpha}$ in the traditional sense for the following integral, and we rewrite it as shown below. The integral can be approximated by

$$\int_{t_{\ell-1}}^{t_\ell} f'(s)(t_k - s)^{-\alpha}\, ds \approx \frac{f'(t_{\ell-1})}{t_\ell - t_{\ell-1}} W_{L,\ell}^k + \frac{f'(t_\ell)}{t_\ell - t_{\ell-1}} W_{R,\ell}^k,$$

where

$$\begin{aligned} W_{L,\ell}^k &= \frac{(t_k - t_\ell)^{2-\alpha}}{1-\alpha} - \frac{(t_k - t_\ell)(t_k - t_{\ell-1})^{1-\alpha}}{1-\alpha} - \frac{(t_k - t_\ell)^{2-\alpha}}{2-\alpha} + \frac{(t_k - t_{\ell-1})^{2-\alpha}}{2-\alpha}, \\ W_{R,\ell}^k &= \frac{(t_k - t_\ell)^{2-\alpha}}{2-\alpha} - \frac{(t_k - t_{\ell-1})^{2-\alpha}}{2-\alpha} - \frac{(t_k - t_{\ell-1})(t_k - t_\ell)^{1-\alpha}}{1-\alpha} + \frac{(t_k - t_{\ell-1})(t_k - t_{\ell-1})^{1-\alpha}}{1-\alpha}. \end{aligned}$$

The errors are shown in Tables 5 and **??** for model example 1 and 2, respectively. However, Example 3 cannot be simulated by the MTR method because the derivative of the exact function does not exist at the origin.

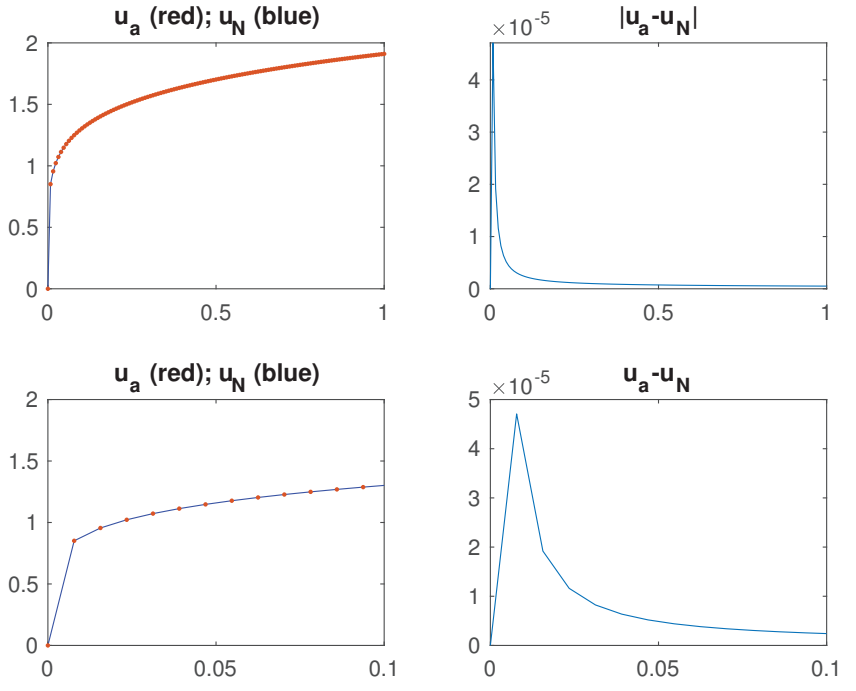

Figure 2. The profiles of the simulations of Example 3 with a refinable approach. The analytic (u_a) and the numerical u_N solutions are in the top-left panel. The absolute value of the error $|u_a - u_N|$ is in the top-right panel. The zoom-in profiles on $[0, 0.2]$ are shown in the corresponding panels below.

Table 5. The errors between numerical and analytic solutions for $f(t) = \frac{1}{4}t^4$ and the order of accuracy using the MTR method. It shows that the order of accuracy is 2.0 for 1-norm, 2-norm and ∞-norm.

N_ℓ	E_1	E_2	E_∞	$N_\ell/N_{\ell+1}$	O_1	O_2	O_∞
32	1.423×10^{-4}	1.776×10^{-4}	3.473×10^{-4}	32/64	2.00	1.99	1.98
64	3.565×10^{-5}	4.459×10^{-5}	8.830×10^{-5}	64/128	1.99	1.99	1.98
128	8.958×10^{-6}	1.121×10^{-5}	2.233×10^{-5}	128/256	1.99	1.99	1.98
256	2.252×10^{-6}	2.818×10^{-6}	5.629×10^{-6}	256/512	1.99	1.99	1.99
512	5.656×10^{-7}	7.077×10^{-7}	1.415×10^{-6}	512/1024	1.99	1.99	1.99
1024	1.419×10^{-7}	1.776×10^{-7}	3.553×10^{-7}	1024/2048	2.00	2.00	2.00
2048	3.559×10^{-8}	4.451×10^{-8}	8.907×10^{-8}	2048/4096	2.00	2.00	2.00
4096	8.917×10^{-9}	1.115×10^{-8}	2.231×10^{-8}	-	-	-	-

Table 6. The errors between numerical and analytic solutions for $f(t) = \frac{2}{3}t^{3/2}$ and the order of accuracy. It shows that the order of accuracy is near 1.49, 1.44 and 1.0 for 1-norm, 2-norm and ∞-norm, respectively.

N_ℓ	E_1	E_2	E_∞	$N_\ell/N_{\ell+1}$	O_1	O_2	O_∞
32	1.161×10^{-3}	1.362×10^{-3}	4.187×10^{-3}	32/64	1.45	1.40	1.00
64	4.237×10^{-4}	5.176×10^{-4}	2.093×10^{-3}	64/128	1.47	1.41	1.00
128	1.533×10^{-4}	1.950×10^{-4}	1.047×10^{-3}	128/256	1.48	1.42	1.00

Table 6. *Cont.*

N_ℓ	E_1	E_2	E_∞	$N_\ell/N_{\ell+1}$	O_1	O_2	O_∞
256	5.507×10^{-5}	7.293×10^{-5}	5.233×10^{-4}	256/512	1.48	1.43	1.00
512	1.969×10^{-5}	2.713×10^{-5}	2.617×10^{-4}	512/1024	1.49	1.43	1.00
1024	7.019×10^{-6}	1.004×10^{-5}	1.308×10^{-4}	1024/2048	1.49	1.44	1.00
2048	2.496×10^{-6}	3.703×10^{-6}	6.542×10^{-5}	2048/4096	1.49	1.44	1.00
4096	8.861×10^{-6}	1.361×10^{-6}	3.271×10^{-5}	-	-	-	-

5. Error Analysis

Let us start to observe the approximation of the function $y = \sqrt{t}$ by the linear interpolation $\mathcal{L}(t)$ on $[t_{\ell-1}, t_\ell]$,

$$\mathcal{L}(t) = \frac{\sqrt{t_\ell} - \sqrt{t_{\ell-1}}}{t_\ell - t_{\ell-1}}(t - t_{\ell-1}) + \sqrt{t_{\ell-1}}.$$

The error $e(t) = y(t) - \mathcal{L}(t)$ on $[t_{\ell-1} - t_\ell]$ has the maximum error

$$|e(t^*)| = |\frac{(t_\ell - t_{\ell-1})^2}{4(\sqrt{t_\ell} + \sqrt{t_{\ell-1}})^2}|,$$

where $t^* = \frac{1}{4}(\sqrt{t_\ell} + \sqrt{t_{\ell-1}})^2$. Let $t_\ell = \ell\Delta t$, $\ell = 0, 1, \ldots, N$; the error for $\ell = 1$ is $\frac{1}{4}\Delta t$. This explains that the reason for Example 2 using the trapezoidal method is only of first-order accuracy.

Theorem 4. *Let the function $\mathcal{L}_\ell(t)$ be the linear interpolation of the function $f'(t)$ on each subinterval $[t_{\ell-1}, t_\ell]$, $\ell = 1, 2, \ldots, N$ and $\int_0^t |\varphi'(t-\tau)|\, d\tau$ is uniformly bounded for $0 \le t \le 1$. The modified trapezoidal rule for calculation*

$${}_0^C D_t^\alpha f(t) = \frac{1}{\Gamma(1-\alpha)} \int_0^t f'(\tau)(t-\tau)^{-\alpha}\, d\tau$$

has the error bounded by $C \max_\ell\{|\mathcal{L}_\ell(t) - f'(t)|\}$ and

$$C = \frac{1}{\Gamma(1-\alpha)} \int_0^t |t-\tau|\, d\tau.$$

Proof. The error is given by

$$|\frac{1}{\Gamma(1-\alpha)} \int_0^t f'(\tau)(t-\tau)^{-\alpha}\, d\tau - \frac{1}{\Gamma(1-\alpha)} \int_0^t \mathcal{L}_\ell(\tau)(t-\tau)^{-\alpha}\, d\tau|.$$

It follows that the error is less than

$$\begin{aligned} \frac{1}{\Gamma(1-\alpha)} \int_0^t |f'(\tau) - \mathcal{L}_\ell(\tau)|(t-\tau)^{-\alpha}\, d\tau &\le \frac{1}{\Gamma(1-\alpha)} \int_0^t \max_\ell |f'(\tau) - \mathcal{L}_\ell(\tau)(t-\tau)|^{-\alpha}\, d\tau \\ &= \max_\ell |f'(\tau) - \mathcal{L}_\ell(\tau)| \frac{1}{\Gamma(1-\alpha)} \int_0^t |t-\tau|^{-\alpha}\, d\tau \end{aligned}$$

□

Theorem 4 can be applied to explain the results (Tables 5 and **??**) for Example 1 and Example 2 obtained using MTR. Next, we will analyze the TRSI method. Let us first recall the error analysis for smooth functions as Theorem 5 below for the trapezoidal method in comparison with the estimation of the errors for the functions in $\mathcal{D}_\alpha(I)$ shown in Theorem 6 below.

Let

$$\mathcal{H}(t) = \int_{t_{\ell-1}}^{t} f'(s)g'(t_k - s)\,ds$$

and $\Delta t = (t_\ell - t_{\ell-1})$. Then,

$$\mathcal{H}(t_\ell) = \mathcal{H}(t_{\ell-1}) + \mathcal{H}'(t_{\ell-1})(\Delta t) + \frac{1}{2}\mathcal{H}''(t_{\ell-1})(\Delta t)^2 + O((\Delta t)^3)$$

if $\mathcal{H}$ has the third continuous derivative. Furthermore, if f'''' and g'''' are continuous whenever $\ell < N$, then

$$\begin{aligned} f'(t_\ell) &= f'(t_{\ell-1}) + \frac{1}{2}f''(t_{\ell-1})(\Delta t) + O((\Delta t)^2), \\ g'(t_k - t_\ell) &= g'(t_k - t_{\ell-1}) - \frac{1}{2}g''(t_k - t_{\ell-1})(\Delta t) + O((\Delta t)^2). \end{aligned}$$

It follows that

$$\int_{t_{\ell-1}}^{t_\ell} f'(s)g'(t_k - s)\,ds = \frac{1}{2}(f'(t_{\ell-1}) + f'(t_\ell))(g(t_k - t_\ell) - g(t_k - t_{\ell-1})) + O((\Delta t)^3).$$

The above approximation leads to the theorem below.

Theorem 5. *If f'''' exists and is continuous and $g(t) = -\frac{t^{1-\alpha}}{1-\alpha}$, $0 < \alpha < 1$ then*

$$\int_{t_{\ell-1}}^{t_\ell} f'(s)g'(t_k - s)\,ds = \frac{1}{2}(f'(t_{\ell-1}) + f'(t_\ell))(g(t_k - t_\ell) - g(t_k - t_{\ell-1})) + O((\Delta t)^3)$$

for $\ell < k$. Furthermore,

$$\sum_{\ell=1}^{k-1}\int_{t_{\ell-1}}^{t_\ell} f'(s)g'(t_k - s)\,ds = \sum_{\ell=1}^{k-1}\frac{1}{2}(f'(t_{\ell-1}) + f'(t_\ell))(g(t_k - t_\ell) - g(t_k - t_{\ell-1})) + O((\Delta t)^2)$$

and for $\ell = k$, the following approximation is reduced to

$$\int_{t_{k-1}}^{t_k} f'(s)g'(t_k - s)\,ds = \frac{1}{2}(f'(t_k) + f'(t_{k-1}))(g(t_k - t_k) - g(t_k - t_{k-1})) + O(\Delta t).$$

From (7) and Theorem 2, if $f \in \mathcal{D}_\alpha(I)$, then we have

$$\int_{y_{\ell-1}}^{y_\ell} f'(t_k - \varphi^{-1}(y))dy = \frac{1}{2}\big(f'(t_{\ell-1}) + f'(t_\ell)\big)(y_\ell - y_{\ell-1}) + O((y_\ell - y_{\ell-1})^{1+\alpha})$$

for $\ell < k$ and for $\ell = k$, it is reduced to

$$\int_{y_{\ell-1}}^{y_\ell} f'(t_k - \varphi^{-1}(y))dy = \frac{1}{2}\big(f'(t_{\ell-1}) + f'(t_\ell)\big)(y_\ell - y_{\ell-1}) + O((y_\ell - y_{\ell-1})^{\alpha}).$$

Furthermore, the term $O((y_\ell - y_{\ell-1})^{1+\alpha}) = O((t_\ell - t_{\ell-1})^{1+\alpha})$. On the other hand,

$$\begin{aligned} \int_{y_{\ell-1}}^{y_\ell} f'(t_k - \varphi^{-1}(y))dy &= \frac{1}{2}(f(t_\ell) - f(t_{\ell-1}))(\varphi'(t_k - t_\ell) + \varphi'(t_k - t_{\ell-1})) \\ &\quad + O((f(t_\ell) - f(t_{\ell-1}))^3) \\ &= \frac{1}{2}(f(t_\ell) - f(t_{\ell-1}))(\varphi'(t_k - t_\ell) + \varphi'(t_k - t_{\ell-1})) + O((t_\ell - t_{\ell-1})^3) \end{aligned}$$

Theorem 6. *If $f \in \mathcal{D}_\alpha(I)$ and $g(t) = -\frac{t^{1-\alpha}}{1-\alpha}$, $0 < \alpha < 1$ then*

$$\int_{t_{\ell-1}}^{t_\ell} f'(s)g'(t_k - s)\,ds = \frac{1}{2}(f'(t_{\ell-1}) + f'(t_\ell))(g(t_k - t_\ell) - g(t_k - t_{\ell-1})) + O((\Delta t)^{1+\alpha})$$

for $\ell < k$. Furthermore,

$$\sum_{\ell=1}^{k-1}\int_{t_{\ell-1}}^{t_\ell} f'(s)g'(t_k - s)\,ds = \sum_{\ell=1}^{k-1}\frac{1}{2}(f'(t_{\ell-1}) + f'(t_\ell))(g(t_k - t_\ell) - g(t_k - t_{\ell-1})) + O((\Delta t)^{\alpha})$$

and for $\ell = k$, the following approximation is reduced to

$$\int_{t_{k-1}}^{t_k} f'(s)g'(t_k - s)\,ds = \frac{1}{2}(f'(t_k) + f'(t_{k-1}))(g(t_k - t_k) - g(t_k - t_{k-1})) + O((\Delta t)^{\alpha}).$$

Let k be a positive integer and $0 < \alpha < 1$. If an integration scheme has the order of accuracy α,

$$\int_a^b f'(s)g'(b - s)\,ds = \mathcal{N}(h_j) + O(h_j^\alpha),$$

where $h_j = (b-a)/2^j$ and $\mathcal{N}$ for some numerical method, then the refinable approach using the mesh h_{j+k} is read as

$$\int_a^b f'(s)g'(b - s)\,ds = \mathcal{N}(h_{j+k}) + O(h_{k+j}^\alpha).$$

This implies that the order of accuracy is $\log_2(h_j^\alpha / h_{k+j}^\alpha) = \log_2(2^{k\alpha}) = k\alpha$.

6. Applications

We are going to demonstrate the applications of the integrand in (10) rewritten as a product of two derivatives of functions on fractional differential equations with Caputo and Riemann–Liouville derivatives.

6.1. Fractional Differential Equation with Caputo Derivatives

We first solve the fractional differential equation to evaluate the TRSI method

$$\text{IVP: } \begin{cases} {}_0^C D_t^\alpha y + y & = \frac{3}{4}t\sqrt{\pi} + t^{3/2} \\ y(0) & = y'(0) = 0 \end{cases}$$

The exact solution for (14) is $y(t) = t^{3/2}$.

The discretization approach at the zone $[t_{\ell-1}, t_\ell]$ is

$$\frac{1}{\Gamma(1-\alpha)}\sum_{m=1}^{\ell}\int_{t_{m-1}}^{t_m} y'(s)(t_\ell - s)^{-\alpha}ds + y(t_\ell) = \frac{3}{4}t_\ell\sqrt{\pi} + (t_\ell)^{3/2}. \tag{14}$$

If $y(t_m)$ and $y'(t_m)$ for $m = 0, 1, \ldots, \ell - 1$ are given, then we have to solve $y(t_\ell)$ and $y'(t_\ell)$. There are two unknowns, $y(t_\ell)$ and $y'(t_\ell)$, in Equation (14) but only one equation. We further impose the condition

$$\frac{y(t_\ell) - y(t_{\ell-1})}{\Delta t} = \frac{y'(t_\ell) + y'(t_{\ell-1})}{2},$$

which means that the central difference at the midpoint of t_ℓ and t_ℓ approximation. It gives us

$$\frac{\Delta t}{2}y'(t_\ell) - y(t_\ell) = \frac{\Delta t}{2}y'(t_{\ell-1}) - y(t_{\ell-1}). \tag{15}$$

Coupling (14) and (15), the linear system for $y'(t_\ell)$ and $y(t_\ell)$ is obtained

$$\begin{bmatrix} a_{11} & a_{12} \\ a_{21} & a_{22} \end{bmatrix} \begin{bmatrix} y'(t_\ell) \\ y(t_\ell) \end{bmatrix} = \begin{bmatrix} b_1 \\ b_2 \end{bmatrix},$$

where $a_{12} = 1$, $a_{22} = -1$, $a_{21} = \frac{\Delta t}{2}$,

$$\begin{aligned} a_{11} &= \frac{1}{\Gamma(1-\alpha)}(-\varphi(\Delta t)), \\ b_1 &= \frac{3}{4}t_\ell\sqrt{\pi} + (t_\ell)^{3/2} + \frac{\varphi(\Delta t)}{2\Gamma(1-\alpha)} \\ &\quad - \frac{1}{\Gamma(1-\alpha)}\sum_{m=1}^{\ell-1}\frac{1}{2}(y'(t_m) + y'(t_{m-1}))(\varphi(t_\ell - t_m) - \varphi(t_\ell - t_{m-1})). \end{aligned}$$

The errors between the analytic and numerical solutions for the IVP problem are shown in Table 7. It shows the order of accuracy is 1.49 for the 1-norm and 2-norm and 1.46 for the ∞-norm.

Table 7. The errors between the analytic and numerical solutions for the IVP problem are shown in this table. The order of accuracy is 1.49 for 1-norm and 2-norm and 1.46 for ∞-norm.

N_ℓ	E_1	E_2	E_∞	$N_\ell/N_{\ell+1}$	O_1	O_2	O_∞
32	8.440×10^{-4}	8.490×10^{-4}	1.000×10^{-3}	32/64	1.45	1.44	1.38
64	3.094×10^{-4}	3.121×10^{-4}	3.847×10^{-4}	64/128	1.46	1.46	1.40
128	1.123×10^{-4}	1.135×10^{-4}	1.461×10^{-4}	128/256	1.47	1.47	1.41
256	4.045×10^{-5}	4.097×10^{-5}	5.486×10^{-5}	256/512	1.48	1.48	1.43
512	1.449×10^{-5}	1.470×10^{-5}	2.041×10^{-5}	512/1024	1.49	1.48	1.44
1024	5.172×10^{-6}	5.254×10^{-6}	7.536×10^{-6}	1024/2048	1.49	1.49	1.45
2048	1.841×10^{-6}	1.872×10^{-6}	2.764×10^{-6}	2048/4096	1.49	1.49	1.46
4096	6.538×10^{-7}	6.656×10^{-7}	1.008×10^{-6}	-	-	-	-

6.2. Fractional Differential Equation with Riemann–Liouville Derivatives

In this subsection, we consider the fractional ordinary equation [23]:

$$\text{IVP2: } \begin{cases} \frac{d}{dt}\frac{1}{\Gamma(1-\alpha)}\int_0^t y'(s)(t-s)^{-\alpha} + y(t) & = \frac{3}{4}\sqrt{\pi} + t^{3/2} \\ y(0) & = y'(0) = 0 \end{cases}$$

The exact solution is the same as the previous case, $y(t) = t^{3/2}$. Taking the integration from $t_0 = 0$ to t_ℓ, we obtain

$$\frac{1}{\Gamma(1-\alpha)}\int_0^{t_\ell} y'(s)(t_\ell - s)^{-\alpha}ds + \int_0^{t_\ell} y(t)\,dt = \frac{3}{4}t_\ell\sqrt{\pi} + \frac{2}{5}(t_\ell)^{5/2}$$

or

$$\frac{1}{\Gamma(1-\alpha)}\sum_{m=1}^{\ell}\int_{t_{m-1}}^{t_m} y'(s)(t_\ell - s)^{-\alpha}ds + \int_0^{t_\ell} y(t)\,dt = \frac{3}{4}t_\ell\sqrt{\pi} + \frac{2}{5}(t_\ell)^{5/2}.$$

We use the traditional trapezoidal method for the second integral on the left-hand side as the same approach in [23]. Meanwhile, people can define the coefficients $\tilde{a}_{11} = a_{11}$, $\tilde{a}_{21} = a_{21}$, $\tilde{b}_2 = b_2$ and

$$\tilde{a}_{12} = \frac{1}{2}\Delta t, \quad \tilde{b}_1 = b_1 - \frac{1}{2}\sum_{m=1}^{\ell-1}(y(t_m) + y(t_{m-1}))\Delta t,$$

where a_{11}, a_{12}, a_{21}, a_{22}, b_1, and b_2 are defined in the (6.1). The numerical solution is obtained by solving the following linear system:

$$\begin{bmatrix} \tilde{a}_{11} & \tilde{a}_{12} \\ \tilde{a}_{21} & \tilde{a}_{22} \end{bmatrix} \begin{bmatrix} y'(t_\ell) \\ y(t_\ell) \end{bmatrix} = \begin{bmatrix} \tilde{b}_1 \\ \tilde{b}_2 \end{bmatrix}.$$

The errors between the exact and numerical solutions are shown in Table 8, which demonstrates that the order of accuracy is near 1.49 for 1-norm and 2-norm and 1.48 for ∞-norm.

Table 8. The errors between the analytic and numerical solutions for the IVP2 problem are shown in this table. It shows the order of accuracy is 1.49 for 1-norm and 2-norm and 1.48 for ∞-norm.

N_ℓ	E_1	E_2	E_∞	$N_\ell/N_{\ell+1}$	O_1	O_2	O_∞
32	1.082×10^{-3}	1.105×10^{-3}	1.349×10^{-3}	32/64	1.43	1.43	1.41
64	4.015×10^{-4}	4.107×10^{-4}	5.069×10^{-4}	64/128	1.45	1.45	1.44
128	1.468×10^{-4}	1.504×10^{-4}	1.873×10^{-4}	128/256	1.47	1.46	1.45
256	5.311×10^{-5}	5.449×10^{-5}	6.846×10^{-5}	256/512	1.48	1.47	1.46
512	1.909×10^{-5}	1.961×10^{-5}	2.482×10^{-5}	512/1024	1.48	1.48	1.47
1024	6.826×10^{-6}	7.018×10^{-6}	8.942×10^{-6}	1024/2048	1.49	1.49	1.48
2048	2.433×10^{-6}	2.503×10^{-6}	3.207×10^{-6}	2048/4096	1.49	1.49	1.48
4096	8.652×10^{-7}	8.907×10^{-7}	1.147×10^{-6}	-	-	-	-

7. Conclusions

The analysis of the trapezoidal method was extended from C^2 to $\mathcal{D}_\alpha(I)$ and, for each $f \in \mathcal{D}_\alpha(I)$, has the order of accuracy $1 + \alpha$. The trapezoidal method using the Riemann–Stieltjes integral on Caputo fractional derivatives for non-smooth functions was proposed, and the approximation ability was also investigated using three models of examples of smoothness, regularity and non-smoothness. The product of the integrand reveals that, if $f \in \mathcal{D}_\alpha(I)$ and the integration is approximated by using the differential df, then the trapezoidal method has the second order of accuracy compared to the traditional one. On the other hand, if the integration is approximated by using the differential $d\varphi$, $\varphi(x) = -\frac{1}{1-\alpha}x^{1-\alpha}$, then the order of accuracy for the trapezoidal method is of the α fractional order of accuracy. The novelty of this method can be addressed to automatically choose the non-smooth functions or the singular kernel for linear interpolation.

The errors in Table 3 show that increasing the number of zones cannot significantly improve the accuracy, and the order of accuracy is 0.16 for ∞-norm. Therefore, a refining mesh shown in Table 4 demonstrated that the order of accuracy is 1.59 for the ∞-norm. To confirm this point, we further apply the refinable approach to MTR. The result for the MTR method using a refinable approach is shown in Table 9; the order of accuracy improves from 1.0 to 1.50 for the ∞-norm, see Tables **??** and 9.

Table 9. The errors between numerical and analytic solutions for $f(t) = 2t^{1/2}$ and the order of accuracy using MTR with refining mesh. The order of accuracy is near 1.5 for 1-norm, 2-norm and ∞-norm.

$\mathcal{K}(N = 128)$	E_1	E_2	E_∞	$\mathcal{K}_{p-1}/\mathcal{K}_p$	O_1	O_2	O_∞
4	1.900×10^{-5}	2.366×10^{-5}	1.156×10^{-4}	4/8	1.50	1.50	1.51
8	6.713×10^{-6}	8.352×10^{-6}	4.064×10^{-5}	8/16	1.50	1.51	1.50
16	2.373×10^{-6}	2.951×10^{-6}	1.434×10^{-5}	16/32	1.50	1.50	1.50
32	8.389×10^{-7}	1.043×10^{-6}	5.066×10^{-6}	32/64	1.50	1.50	1.50
64	2.966×10^{-7}	3.688×10^{-7}	1.790×10^{-6}	64/128	1.50	1.50	1.50
128	1.049×10^{-7}	1.304×10^{-7}	6.328×10^{-7}	-	-	-	-

Author Contributions: Conceptualization, G.K. and C.-C.Y.; methodology, C.-C.Y.; formal analysis, C.-C.Y.; investigation, G.K.; writing—original draft preparation, G.K.; writing—review and editing, C.-C.Y. All authors have read and agreed to the published version of the manuscript.

Funding: C.C. Yen acknowledges the grant support from the Ministry of Science and Technology (MoST) under 109-2115-M-030-004-MY2 and National Science and Technology Council (NSC) under 111-2115-M-030 -002.

Informed Consent Statement: Not applicable.

Data Availability Statement: Not applicable.

Acknowledgments: We sincerely appreciate the reviewers for all valuable comments and suggestions that helped us to improve the quality and the better presentation of the results in the manuscript.

Conflicts of Interest: The authors declare no conflicts of interest.

References

1. Kilbas, A.A.; Srivastava, H.M.; Trujillo, J.J. *Theory and Applications of Fractional Differential Equations*; Series North-Holland Mathematics Studies; North-Holland: New York, NY, USA, 2006.
2. Oldham, K.; Spanier, J. *The Fractional Calculus, Theory and Applications of Differentiation and Integration of Arbitrary Order*; Academic Press: Cambridge, MA, USA, 1974.
3. Podlubny, I. *Fractional Differential Equations*; Academic Press: Cambridge, MA, USA, 1999.
4. Burrage, K.; Hale, N.; Kay, D. An efficient implicit FEM scheme for fractional-in-space reaction-diffusion equations. *SIAM J. Sci. Comput.* **2012**, *34*, A2145–A2172. [CrossRef]
5. Cafagna, D.; Grassi, G. Observe-based projective synchronization of fractional systems via a scalar signal: Application to hyperchaotic Rössler systems. *Nonlinear Dyn.* **2012**, *68*, 117–128. [CrossRef]
6. Caponetto, R.; Maione, G.; Pisano, A.; Rapaić, M.M.R.; Usai, E. Analysis and shaping of the self-sustained oscillations in relay controlled fractional-order systems. *Fract. Calc. Appl. Anal.* **2013**, *16*, 93–108. [CrossRef]
7. Diethelm, K. An investigation of some nonclassical methods for the numerical approximation of Caputo-type fractional Derivatives. *Numer. Algorithms* **2008**, *47*, 361–390. [CrossRef]
8. Garrappa, R.; Poplizio, M. On accurate product integration rules for linear fractional differential equations. *J. Comput. Appl. Math.* **2011**, *235*, 1085–1097. [CrossRef]
9. Miller, K.S. *An Introduction to Fractional Calculus and Fractional Differential Equations*; John Wiley and Sons: New York, NY, USA, 1993.
10. Moret, I.; Novati, P. On the convergence of Krylov subspace methods for matrix Mittag-Leffler functions. *SIAM. J. Numer. Anal.* **2011**, *49*, 2144–2164. [CrossRef]
11. Rahimy, M. Applications of fractional differential equations. *Appl. Math. Sci.* **2010**, *4*, 2453–2461.
12. Khalil, R.; Horani, M.A.I.; Yousef, A.; Sabaheh, M. A new definition of fractional derivative. *J. Comput. Appl. Math.* **2014**, *264*, 65–70. [CrossRef]
13. Garrappa, R. Trapezoidal methods for fractional differential equations: Theoretical and computational aspects. *Math. Comput. Simul.* **2015**, *10*, 96–112. [CrossRef]
14. Pandiangan, N.; Johar, D.; Purwani, S. Fractional integral approximation and Caputo derivatives with modification of trapezoidal rule. *World Sci. News* **2021**, *153*, 169–180.
15. Arashad, S.; Huang, J.; Khaliq, A.Q.M.; Tang, Y. Trapezoid scheme for time-space fractional diffusion equation with Riesz derivative. *J. Comput. Phys.* **2017**, *350*, 1–15. [CrossRef]

16. Odibat, Z. Approximations of fractional integrals and Caputo fractional derivatives. *Appl. Math. Comput.* **2006**, *178*, 527–533. [CrossRef]
17. Rapaić, M.R.; Pisano, A.; Jeličić, Z.D.J. Trapezoidal rule for numerical evaluation of fractional order integrals with applications to simulation and identification of fractional order system. In Proceedings of the 2012 IEEE International Conference on Control Applications (CCA), Part of 2012 IEEE Multi-Conference on Systems and Control, Dubrovnik, Croatia, 3–5 October 2012.
18. Diouf, M.; Sene, N. Analysis of the financial chaotic model with the fractional derivative operator. *Complexity* **2020**, *2020*, 9845031. [CrossRef]
19. Fall, A.N.; Ndiaye, S.N.; Sene, N. Black-Scholes option pricing equations described by the Caputo generalized fractional derivative. *Chaos Solitons Fractals* **2019**, *125*, 108–118. [CrossRef]
20. Jumaric, G. New stochastic fractional models of the Malthusian growth the poissonian birth process and optimal management of population. *Math. Comput. Model* **2006**, *44*, 231–254. [CrossRef]
21. Ma, S.; Xu, Y.; Yue, W. Numerical solutions of a variable-order fractional financial system. *J. Appl. Math.* **2012**, *2012*, 417942. [CrossRef]
22. Jahanshahi, S.; Babolian, E.; Torres, D.F.M.; Vahidi, A. A fractional Gauss-Jacobi quadrature rule for approximating fractional integrals and derivatives. *Chaos Solitons Fractals* **2017**, *102*, 295–304. [CrossRef]
23. Li, B.; Wang, T.; Xie, X. Analysis of the L1 scheme for fractional wave equations with nonsmooth data. *Comput. Math. Appl.* **2021**, *90*, 1–12. [CrossRef]

axioms

MDPI

Article

Lyapunov Inequalities for Two Dimensional Fractional Boundary-Value Problems with Mixed Fractional Derivatives

Tatiana Odzijewicz

Institute of Mathematics and Mathematical Economics, SGH Warsaw School of Economics, 02-554 Warszawa, Poland; tatiana.odzijewicz@sgh.waw.pl

Abstract: We consider two types of partial fractional differential equations in two dimensions with mixed fractional derivatives. Appropriate Lyapunov-type inequalities are proved, and applications to the certain eigenvalue problems are presented. Moreover, some connections with the fractional variational problems are highlighted.

Keywords: Lyapunov-type inequality; mixed fractional derivatives; fractional partial differential equations; eigenvalue problems

MSC: 35P15; 26D20; 26B99

Citation: Odzijewicz, O. Lyapunov Inequalities for Two Dimensional Fractional Boundary-Value Problems with Mixed Fractional Derivatives. *Axioms* **2023**, *12*, 301. https://doi.org/10.3390/axioms12030301

Academic Editors: António Lopes, Alireza Alfi, Liping Chen, Sergio Adriani David and Chris Goodrich

Received: 28 December 2022
Revised: 28 February 2023
Accepted: 8 March 2023
Published: 15 March 2023

1. Introduction

The Lyapunov inequality provides a necessary condition for the existence of a non-trivial positive solution to the certain ordinary second-order differential equation. Since it was proved in 1907 by A. M. Lyapunov, it has been generalized in many ways and found to play a remarkable role in the analysis of differential equations- available results concern, e.g., bounds for eigenvalues [1], estimates for intervals of disconjugacy [2], or criteria for stability of periodic differential equations [3]. Most results, however, refer to the single time case. Results for multitime are scarce and are considered, e.g., in [4], where the partial differential equation involving Grushin operator was investigated, or in [5,6], where problems with Laplace and p-Laplace operators were studied, respectively. For more details of Lyapunov and other type inequalities, we refer to the papers [7–11].

In the references cited above, the authors consider integer order derivatives. Nevertheless, in recent years, a lot of papers studied Lyapunov inequalities for the boundary-value problems involving fractional differential operators [12]. In contrary to the classical approach, fractional derivatives are operators with memory, i.e., they are defined non-locally and because of that they model time-dependent processes more accurately [13–18]. The first work on Lyapunov inequality for fractional boundary-value problems has been written by R. Ferreira and concerns a problem with a derivative of order in the interval $(1,2]$ [19]. In this paper, however, we find a class of fractional differential equations with mixed right and left fractional derivatives to be more interesting [15,20]. Mixed fractional differential operators have a significant property, specifically, they are symmetric in agreement with the fractional integration by parts formulas and because of that they naturally arise in the theory of fractional calculus of variations [13,15,16,21]. The following theorems, concerning Lyapunov inequality for boundary-value problems with mixed fractional derivatives, can be found in the literature and will be used further in the work.

Theorem 1 (Theorem 4 in [22]). *If the following boundary-value problem:*

$$
\begin{aligned}
{}^{c}D^{\alpha}_{b-}\left(D^{\beta}_{a+}v(t)\right) + f(t)v(t) = 0, \;\; t \in (a,b),\; \alpha,\beta \in (0,1],\; \alpha+\beta \in (1,2],\\
v(a) = D^{\beta}_{a+}v(b) = 0,
\end{aligned}
$$

where $f : [a,b] \to \mathbb{R}_+$, $f \in C[a,b]$ has a continuous solution, which is nontrivial, then

$$\int_a^b |f(s)|ds \geq \frac{(\alpha+\beta-1)\Gamma(\alpha)\Gamma(\beta)}{(b-a)^{\alpha+\beta-1}}. \tag{1}$$

Theorem 2 ([23]). *Suppose that $\alpha \in \left(\frac{1}{2}, 1\right)$ and $v \in C^1[0,1]$ is such that $I_{0+}^{1-\alpha c} D_{1-}^{\alpha} v \in AC[0,1]$. If v is a nonzero solution to the following boundary-value problem:*

$$\begin{gathered} D_{0+}^{\alpha}\left({}^{c}D_{1-}^{\alpha} v(t)\right) - f(t)v(t) = 0, \ \ t \in (0,1), \\ v(0) = v(1) = 0, \end{gathered}$$

where $f : [0,1] \to \mathbb{R}$ is continuous. Then,

$$\int_0^1 |f(s)|ds > \frac{(2\alpha-1)\Gamma^2(\alpha)}{h}, \tag{2}$$

where

$$h = \sup_{0<x<1}\left[(1-x)^{2\alpha-1} - (1-x^{2\alpha-1})^2\right].$$

The interest of this article lies in the derivation of the Lyapunov-type inequalities for two different types of fractional partial differential equations involving mixed fractional derivatives. Like in [4,24], our method is based first on reducing the analysis of considered fractional partial differential equations to the study of fractional ordinary differential equations and next to applying above theorems in the proofs of the Lyapunov–type inequalities. Summing up, the contributions of this paper are as follows:

- We obtain the Lyapunov-type inequalities, which provide the necessary conditions for the existence of nonzero positive solutions. Thanks to this, we can indicate when the nontrivial positive solution to the problem does not exist.
- Mixed fractional derivatives are considered, and because of that we can establish a connection to the fractional calculus of variations.

The rest of the paper is organized as follows. In Section 2, we present preliminary definitions and properties of fractional calculus. Then, in Sections 3 and 4, we analyze two different types of problems involving mixed fractional derivatives—we prove Lyapunov-type inequalities in two dimensions and illustrate our results through some examples.

2. Preliminaries

In this section, we recall definitions and some elementary properties of the Riemann–Liouville and the Caputo fractional oprators. Throughout the work, we suppose that $a, b \in \mathbb{R}$, $a < b$ and by Γ we understand the Euler's gamma function.

Definition 1. *Let $\alpha \in \mathbb{R}$ ($\alpha > 0$) and $f \in L^1[a,b]$. The left Riemann–Liouville fractional integral I_{a+}^{α} of order α of function f is defined by*

$$I_{a+}^{\alpha} f(x) := \frac{1}{\Gamma(\alpha)} \int_a^x \frac{f(t)dt}{(x-t)^{1-\alpha}}, \ \ x \in (a,b],$$

while the right Riemann–Liouville fractional integral I_{b-}^{α} of order α ($\alpha > 0$) of function f is given by

$$I_{b-}^{\alpha} f(x) := \frac{1}{\Gamma(\alpha)} \int_x^b \frac{f(x)dt}{(t-x)^{1-\alpha}}, \ \ x \in [a,b).$$

With definitions of fractional integrals in hand, we are able to formulate the notions of the Riemann–Liouville and the Caputo fractional differential operators.

Definition 2. *Let $\alpha \in \mathbb{R}_+$ $(n-1 < \alpha \leq n,\ n \in \mathbb{N})$ and function $f \in L^1[a,b]$ be such that functions $I_{a+}^{n-\alpha} f$ and $I_{b-}^{n-\alpha} f$ are in $AC^n[a,b]$. The left Riemann–Liouville fractional derivative of order α of function f is given by*

$$\forall x \in (a,b],\ \ D_{a+}^{\alpha} f(x) := \left(\frac{d}{dx}\right)^n I_{a+}^{n-\alpha} f(x),$$

while the right Riemann–Liouville fractional derivative of order α of function f is defined by

$$\forall x \in [a,b),\ \ D_{b-}^{\alpha} f(x) := \left(-\frac{d}{dx}\right)^n I_{b-}^{n-\alpha} f(x).$$

Definition 3. *Suppose that $\alpha \in \mathbb{R}_+$ $(n-1 < \alpha \leq n,\ n \in \mathbb{N})$ and $f \in C^n[a,b]$. The left Caputo fractional derivative of order α of function f is given by*

$$\forall x \in (a,b],\ \ {}^{c}D_{a+}^{\alpha} f(x) := D_{a+}^{\alpha}\left[f(x) - \sum_{k=0}^{n-1} \frac{f^{(k)}(a)}{k!}(x-a)^k\right],$$

while the right Caputo fractional derivative of order α of function f is defined by

$$\forall x \in [a,b),\ \ {}^{c}D_{b-}^{\alpha} f(x) := D_{b-}^{\alpha}\left[f(x) - \sum_{k=0}^{n-1} \frac{f^{(k)}(b)}{k!}(b-x)^k\right].$$

The next theorem presents a fractional counterpart of the integration by parts formula for the Riemann–Liouville-type and the Caputo-type differential operators.

Theorem 3 (cf. Lemma 2.19 [15])**.** *Let $\alpha \in (0,1)$, $f \in AC[a,b]$ and $g \in L^p[a,b]$, $(1 \leq p \leq \infty)$. Then, the following integration by parts formulas are satisfied*

$$\int_a^b f(x) D_{a+}^{\alpha} g(x)\, dx = \int_a^b g(x)\, {}^{c}D_{b-}^{\alpha} f(x)\, dx + f(x) I_{a+}^{1-\alpha} g(x)\Big|_{x=a}^{x=b}, \tag{3}$$

$$\int_a^b f(x) D_{b-}^{\alpha} g(x)\, dx = \int_a^b g(x)\, {}^{c}D_{a+}^{\alpha} f(x)\, dx - f(x) I_{b-}^{1-\alpha} g(x)\Big|_{x=a}^{x=b}. \tag{4}$$

Remark 1. *In the Formula* (3)*, through integration by parts, left-sided Riemann–Liouville fractional derivative is changed to the right-sided Caputo fractional derivative, while in the Formula* (4) *we do the opposite. Observe that, in both Formulas* (3) *and* (4)*, we apply Riemmann–Liouville-type differentiation to the function g and the Caputo-type differentation to the function f. Assumptions on functions f and g correspond to the type of differentiation (not the side of the derivative) and because of that they can be the same for* (3) *and* (4)*. In the book [15], only Formula* (3) *is given; however, the derivation of* (4) *is analogous.*

Note that definitions of the partial fractional integrals and derivatives, for functions of many variables, can be formulated in the similar manner when the order is integer. Precisely, we bring derivation of the partial fractional derivatives and integrals to the computation of a single-variable fractional operators (for more details see e.g., Section 24 of the book [17]).

3. Partial Differential Equation of the First Type

In this section, our goal is to prove the Lyapunov-type inequality for problems involving partial fractional derivatives. In contrast to the work [24], the derivative with respect to time is a composition of the right Caputo and the left Riemann–Liouville differential operators.

Suppose that $\alpha, \beta \in (0,1]$, $\alpha + \beta \in (1,2]$, $\gamma = \delta/2 \in (0,1]$, $\delta \in (0,2]$, $K \in \mathbb{R}_+$ and $w \in C[a,b]$. We are concerned with the following equation:

$$ {}^cD^{\alpha}_{b-,t}\left(D^{\beta}_{a+,t}u(t,x)\right) - (1-x)^{\gamma}(1+x)^{\gamma}D^{\gamma}_{1-,x}(K^cD^{\gamma}_{-1+,x}u(t,x)) = w(t)u(t,x) \text{ for } (t,x) \in (a,b)\times(-1,1), \quad (5) $$

under the boundary conditions

$$ u(t,-1) = 0, \quad I^{1-\gamma}_{1-,x}(K^cD^{\gamma}_{-1+,x}u(t,x))\Big|_{x=1} = 0, t \in (a,b), \quad (6) $$

$$ u(a,x) = D^{\beta}_{a+,t}u(b,x) = 0, x \in (-1,1). \quad (7) $$

By solution to the problem (5)–(7), we understand function $u \in C([a,b]\times[-1,1])$ satisfying conditions (5)–(7) such that the derivative $D^{\beta}_{a+,t}$ of u exists and is continuously differentiable for any $x \in [-1,1]$.

Lemma 1. *Let us consider the following boundary-value problem with mixed fractional derivatives:*

$$ {}^cD^{\alpha}_{b-}\left(D^{\beta}_{a+}v(t)\right) + f(t)v(t) = 0 \ \ for \ \ t \in (a,b),\ \alpha,\beta \in (0,1),\ \alpha+\beta \in (1,2], \quad (8) $$

$$ v(a) = D^{\beta}_{a+}v(b) = 0, \quad (9) $$

where

$$ f(t) = -\left(w(t) + \frac{K\Gamma(1+\gamma)}{\Gamma(1-\gamma)}\right), \ \ t \in [a,b]. \quad (10) $$

If u is a positive solution to (5)–(7)*, which is not identically equal to zero, then function*

$$ v(t) = \int_{-1}^{1}(1-x)^{-\gamma}u(t,x)\,dx, \ \ t \in [a,b] \quad (11) $$

is a nonzero solution to the problem (8) *and* (9)*.*

Proof. Let u be a positive solution to (5)–(7) such that $u \not\equiv 0$. If we multiply (5) by $y(x) = \dfrac{1}{(1-x)^{\gamma}}$ and integrate over (−1,1), then

$$ \int_{-1}^{1}(1-x)^{-\gamma}{}^cD^{\alpha}_{b-,t}\left(D^{\beta}_{a+,t}u(t,x)\right)dx - \int_{-1}^{1}(1+x)^{\gamma}D^{\gamma}_{1-,x}(K^cD^{\gamma}_{-1+,x}u(t,x))\,dx = \int_{-1}^{1}(1-x)^{-\gamma}w(t)u(t,x)\,dx, \ \ t \in (a,b). $$

Since we integrate over x, we can exclude partial fractional derivatives with respect to t and obtain

$$ {}^cD^{\alpha}_{b-,t}\left(D^{\beta}_{a+,t}\int_{-1}^{1}(1-x)^{-\gamma}u(t,x)\,dx\right) - \int_{-1}^{1}(1+x)^{\gamma}D^{\gamma}_{1-,x}(K^cD^{\gamma}_{-1+,x}u(t,x))\,dx = w(t)\int_{-1}^{1}(1-x)^{-\gamma}u(t,x)\,dx, \ \ t \in (a,b). $$

Now, by applying (3) and (4) as well as the boundary conditions (6), we obtain

$$\int_{-1}^{1}(1+x)^{\gamma}D_{1-,x}^{\gamma}(K^{c}D_{-1+,x}^{\gamma}u(t,x))\,dx=\int_{-1}^{1}D_{1-,x}^{\gamma}(K^{c}D_{-1+,x}^{\gamma}(1+x)^{\gamma})u(t,x)\,dx$$

Moreover, applying Theorem 3.4 from [20], because $y(x)=(1+x)^{\gamma}$ is an eigenfunction that corresponds to the eigenvalue $\lambda=\frac{K\Gamma(1+\gamma)}{\Gamma(1-\gamma)}$, we obtain

$$\int_{-1}^{1}D_{1-,x}^{\gamma}(K^{c}D_{-1+,x}^{\gamma}(1+x)^{\gamma})u(t,x)\,dx=\frac{K\Gamma(1+\gamma)}{\Gamma(1-\gamma)}\int_{-1}^{1}(1-x)^{-\gamma}u(t,x)\,dx.$$

Therefore, for v being given by (11) and f being defined by (10), we have

$${}^{c}D_{b-}^{\alpha}\left(D_{a+}^{\beta}v(t)\right)+f(t)v(t)=0\ \text{ for } t\in(a,b),\ \alpha,\beta\in(0,1],\ \alpha+\beta\in(1,2].$$

Note that, because of the boundary conditions (7), we have $v(a)=v(b)=0$. Consequently, v is a solution to (8). Finally, since $u(t,x)>0$ for all $(t,x)\in(a,b)\times(-1,1)$ is a solution to (5)–(7) and because $(1-x)^{-\gamma}$ is positive for all $x\in(-1,1)$, we conclude that v is nonzero. □

Theorem 4. *If u is a positive solution to* (5)–(7)*, which is not identically equal to zero, then the following Lyapunov-type inequality is satisfied*

$$\int_{a}^{b}\left|w(s)+\frac{K\Gamma(1+\gamma)}{\Gamma(1-\gamma)}\right|ds\geq\frac{(\alpha+\beta-1)\Gamma(\alpha)\Gamma(\beta)}{(b-a)^{\alpha+\beta-1}}.\tag{12}$$

Proof. If u is positive solution to (5)–(7), which is not identically equal to zero, then by Lemma 1, the function v given by (11) is a nontrivial solution to (8). Consequently, Theorem 1 implies (12). □

Example 1. *Now, let us analyze problem* (5)–(7) *with $a=0$, $b=1$, $K\in\mathbb{R}_{+}$, and $w(t)\equiv 0$. Precisely, we consider the following homogeneous partial differential equation:*

$${}^{c}D_{1-,t}^{\alpha}\left(D_{0+,t}^{\beta}u(t,x)\right)-(1-x)^{\gamma}(1+x)^{\gamma}D_{1-,x}^{\gamma}(K^{c}D_{-1+,x}^{\gamma}u(t,x))=0,\ \ (t,x)\in(0,1)\times(-1,1),\tag{13}$$

with given boundary conditions

$$u(t,-1)=0,\ \ I_{1-,x}^{1-\gamma}(K^{c}D_{-1+,x}^{\gamma}u(t,x))\Big|_{x=1}=0\ \text{ for } t\in(0,1),\tag{14}$$

$$u(0,x)=D_{0+,t}^{\beta}u(1,x)=0\ \text{ for } x\in(-1,1).\tag{15}$$

Observe that, in this case, we deal with the finite-time fractional superdiffusion equation, where both the derivative with respect to time and the derivative with respect to space are compositions of the left-sided and the right-sided fractional derivatives.

The Lyapunov–type inequality for problem (13)–(15) *is given by*

$$\frac{K\Gamma(1+\gamma)}{\Gamma(1-\gamma)}\geq(\alpha+\beta-1)\Gamma(\alpha)\Gamma(\beta).\tag{16}$$

Moreover, if we take $\alpha=\frac{1}{2}$, $\beta=\frac{3}{4}$ and $\gamma=\frac{1}{2}$, then (16) *is satisfied if and only if $K>\frac{1}{2}\sqrt{\pi}\Gamma\left(\frac{3}{4}\right)$, which means that for $K\leq\frac{1}{2}\sqrt{\pi}\Gamma\left(\frac{3}{4}\right)$ nonzero positive solution to* (5)–(7) *does not exist.*

4. Partial Differential Equation of the Second Type

This section is dedicated to the following partial differential equation with mixed partial fractional derivatives defined on the set $(0,1)\times(-1,1)$

$$D^{\alpha}_{0+,t}\left({}^{c}D^{\alpha}_{1-,t}u(t,x)\right)-(1-x)^{\beta}(1+x)^{\beta}D^{\beta}_{1-,x}(K^{c}D^{\beta}_{-1+,x}u(t,x))=w(t)u(t,x), \tag{17}$$

with boundary conditions

$$u(t,-1)=0,\ \ I^{1-\beta}_{1-,x}(K^{c}D^{\beta}_{-1+,x}u(t,x))\Big|_{x=1}=0,\ \ t\in(0,1), \tag{18}$$

$$u(0,x)=u(1,x)=0,\ \ x\in(-1,1), \tag{19}$$

where $\alpha\in(\frac{1}{2},1)$, $\beta=\delta/2\in(0,1]$, $\delta\in(0,2]$, $K\in\mathbb{R}_{+}$, and $w\in C[0,1]$.

By solution to the problem (17)–(19) we mean function $u\in C^{1}([0,1]\times[-1,1])$ such that $I^{1-\alpha c}_{0+}D^{\alpha}_{1-}u(\cdot,x)\in AC[0,1]$ for any $x\in[-1,1]$.

Note that, using a similar method as in Theorem 4 proved in the work [25], we can deduce that Equation (17) is an Euler–Lagrange equation associated with some fractional variational problem. Precisely, let us note that Euler–Lagrange equation for the problem of minimizing the functional

$$J(u)=\iint\limits_{(a,b)\times(c,d)}F(t,x,u(t,x),{}^{c}D^{\alpha}_{b-,t}u(t,x),{}^{c}D^{\beta}_{c+,x}u(t,x))\,dt\,dx,$$

where $F\in C^{1}([a,b]\times[c,d]\times\mathbb{R}^{3})$, $(t,x,u,v,z)\mapsto F(t,x,u,v,z)$, subject to the boundary conditions

$$u(t,c)=0,\ \ I^{1-\beta}_{d-,x}\left(\frac{\partial F}{\partial z}\right)\Big|_{x=d}=0,\ \ t\in(a,b),$$

$$u(a,x)=u(b,x)=0,\ \ x\in(c,d),$$

is given by

$$\frac{\partial F}{\partial u}+D^{\alpha}_{a+,t}\left(\frac{\partial F}{\partial v}\right)-D^{\beta}_{d-,x}\left(\frac{\partial F}{\partial z}\right)=0. \tag{20}$$

In particular, for problem of minimizing the functional

$$J(u)=\iint\limits_{(0,1)\times(-1,1)}\left(\left({}^{c}D^{\alpha}_{1-,t}u(t,x)\right)^{2}+K\left({}^{c}D^{\beta}_{-1+,x}u(t,x)\right)^{2}-(1-x)^{-\beta}(1+x)^{-\beta}w(t)(u(t,x))^{2}\right)dt\,dx$$

subject to

$$u(t,-1)=0,\ \ I^{1-\beta}_{d-,x}(K^{c}D^{\beta}_{c+,x}u(t,x))\Big|_{x=1}=0,\ \ t\in(0,1),$$

$$u(1,x)=u(1,x)=0,\ \ x\in(-1,1),$$

We have $F(t,x,u,v,z)=v^{2}+Kz^{2}-(1-x)^{-\beta}(1+x)^{-\beta}w(t)u^{2}$, and from Equation (20) we deduce (17).

Lemma 2. *Let us consider the following boundary-value problem with mixed fractional derivatives:*

$$D^{\alpha}_{0+}\left({}^{c}D^{\alpha}_{1-}v(t)\right)-f(t)v(t)=0,\ \ t\in(0,1), \tag{21}$$

$$v(0)=v(1)=0, \tag{22}$$

where

$$f(t)=-\left(w(t)+\frac{K\Gamma(1+\beta)}{\Gamma(1-\beta)}\right),\ \ t\in[0,1]. \tag{23}$$

If u is a positive solution to (17)–(19), *such that $u \neq 0$, then function*

$$v(t) = \int_{-1}^{1} (1-x)^{-\beta} u(t,x)\, dx, \quad t \in [0,1] \tag{24}$$

is a nontrivial solution to (21)–(22).

Proof. Let u be a positive solution to (17)–(19) such that $u \neq 0$. If we multiply (17) by $y(x) = (1-x)^{-\beta}$ and integrate with respect to x over $(-1,1)$, then we obtain

$$D^{\alpha}_{0+,t}\left({}^{c}D^{\alpha}_{1-,t} \int_{-1}^{1} (1-x)^{-\beta} u(t,x)\, dx \right) - \int_{-1}^{1} (1+x)^{\beta} D^{\beta}_{1-,x}(K\, {}^{c}D^{\beta}_{-1+,x} u(t,x))\, dx = w(t) \int_{-1}^{1} (1-x)^{-\beta} u(t,x)\, dx,$$

for all $t \in (0,1)$. Following arguments analogous to the ones used in the proof of Lemma 1, for v being given by (24) and f being given by (23), applying integration by parts formula stated in Theorem 3, and boundary conditions (18) and Theorem 3.4 from [20], we have

$$D^{\alpha}_{0+}\left({}^{c}D^{\alpha}_{1-} v(t) \right) - f(t) v(t) = 0, \quad t \in (0,1).$$

In addition, bearing in mind boundary conditions (19), we have $v(a) = v(b) = 0$. Therefore, we deduce that v is a solution to (21)–(22). Finally, because u is a positive solution to (17)–(19) such that $u \neq 0$ and

$$(1-x)^{-\beta} > 0, \quad x \in (-1,1),$$

We see that v is nontrivial. □

The following theorem provides the Lyapunov–type inequality to problem (17)–(19).

Theorem 5. *Let $\alpha \in (\frac{1}{2}, 1)$, $\beta = \delta/2 \in (0,1]$, $\delta \in (0,2]$ and w be continuous on $[0,1]$. If u is a positive solution to* (17)–(19) *such that $u \neq 0$, then*

$$\int_{0}^{1} \left| w(s) + \frac{K\Gamma(1+\beta)}{\Gamma(1-\beta)} \right| ds > \frac{(2\alpha-1)\Gamma^2(\alpha)}{h}, \tag{25}$$

where

$$h = \sup_{0<x<1} \left[(1-x)^{2\alpha-1} - (1-x^{2\alpha-1})^2 \right].$$

Proof. Inequality (25) can be easily proved using Lemma 2 and Theorem 2. □

Example 2. *In this example, we analyze* (17)–(19) *with $w(t) = \mu$, $\mu \in \mathbb{R}$, $K = 1$. Precisely, we study the following eigenvalue problem:*

$$D^{\alpha}_{0+,t}\left({}^{c}D^{\alpha}_{1-,t} u(t,x) \right) - (1-x)^{\beta}(1+x)^{\beta} D^{\beta}_{1-,x}({}^{c}D^{\beta}_{-1+,x} u(t,x)) = \mu u(t,x), \quad (t,x) \in (0,1) \times (-1,1), \tag{26}$$

$$u(t,-1) = 0, \quad I^{1-\beta}_{1-,x}({}^{c}D^{\beta}_{-1+,x} u(t,x))\Big|_{x=1} = 0, \quad t \in (0,1), \tag{27}$$

$$u(0,x) = u(1,x) = 0, \quad x \in (-1,1). \tag{28}$$

Theorem 5 implies that, if $\mu \in \mathbb{R}$ is an eigenvalue of problem (26)–(28)*, then*

$$\left|\mu + \frac{\Gamma(1+\beta)}{\Gamma(1-\beta)}\right| > \frac{(2\alpha-1)\Gamma^2(\alpha)}{h},$$

where

$$h = \sup_{0<x<1}\left[(1-x)^{2\alpha-1} - (1-x^{2\alpha-1})^2\right].$$

Note that, using similar method as in the proof of Theorem 3.4 from [26], one can deduce that Equation (26) *is an Euler–Lagrange equation for the following fractional isoperimetric problem:*

$$J(u) = \iint\limits_{(0,1)\times(-1,1)} \left(\left({}^cD^{\alpha}_{1-,t}u(t,x)\right)^2 + \left({}^cD^{\beta}_{-1+,x}u(t,x)\right)^2 \right) dt\, dx$$

subject to the boundary conditions

$$u(t,-1) = 0, \;\; I^{1-\beta}_{1-,x}({}^cD^{\beta}_{-1+,x}u(t,x))\Big|_{x=1} = 0, \;\; t \in (0,1),$$
$$u(0,x) = u(1,x) = 0, \;\; x \in (-1,1),$$

and an isoperimetric constraint

$$I(u) = \iint\limits_{(0,1)\times(-1,1)} (u(t,x))^2(1-x)^{-\beta}(1+x)^{-\beta}\, dt\, dx = 1.$$

5. Conclusions

In this work, two types of partial differential equations involving mixed fractional derivatives are studied. We provide simple conditions (Lyapunov-type inequlities) to allow one to check whether these highly complicated nonlocal problems possess positive nontrivial solutions. Furthermore, contrary to the previous works, we link our boundary-value problems with the fractional calculus of variations theory. Our results are illustrated through two examples: in Example 1, we study the equation that could be interpreted as the fractional counterpart of the finite-time superdiffusion equation, while in Example 2, our results allow us to give bounds on eigenvalues for some eigenvalue problems. Note that, unfortunately, the Lyapunov-type inequalities are necessary conditions, which means that if they fail we can say that the solution does not exist, but if they are satisfied, the solution may or may not exist. This is an important issue, and in the forthcoming works we will study this problem.

Funding: This research received no external funding.

Data Availability Statement: Not applicable.

Acknowledgments: Research supported by the SGH Warsaw School of Economics grant KAE/S22:1.11.

Conflicts of Interest: The author declares that she has no conflict of interest.

References

1. Ha, C.-W. Eigenvalues of a Sturm–Liouville problem and inequalities of Lyapunov-type. *Proc. AMS* **1998**, *126*, 3507–3511. [CrossRef]
2. Brown, R.C.; Hinton, D.B. Lyapunov inequalities and their applications. In *Survey on Mathematical Inequalities, Mathematics and Its Applications*; Rassias, T.M., Ed.; Springer: Berlin/Heidelberg, Germany, 2000; pp. 1–25.
3. Medriveci, A.F.; Guseinov, G.S.; Kaymakcalan, B. On Lyapunov inequality in stability theory for Hill's equation on time scales. *J. Inequal. Appl.* **2000**, 5, 603–620.
4. Jleli, M.; Kirane, M.; Samet, B. On Lyapunov–type inequalities for a certain class of partial differential equations. *Appl. Anal.* **2020**, *99*, 40–49. [CrossRef]

5. Canada, A.C.; Monteiro, J.A.; Villegas, S. Lyapunov inequalitites for partial differential equations. *J. Funct. Anal.* **2006**, *237*, 176–193. [CrossRef]
6. de Nápoli, P.L.; Pinasco, J.P. Lyapunov–type inequalities for partial differential equations. *J. Funct. Anal.* **2016**, *270*, 1995–2018. [CrossRef]
7. Agarwal, R.P.; Bohner, M.; Özbekler, A. *Lyapunov Inequalities and Applications*; Springer: Cham, Switzerland, 2021.
8. Agarwal, R.P.; Jleli, M.; Samet, B. On De La Vallée Poussin–type inequalities in higher dimension and applications. *Appl. Math. Lett.* **2018**, *86*, 264–269. [CrossRef]
9. Bohner, M.; Clark, S.; Ridenhour, J. Lyapunov inequalities for time scales. *J. Inequal. Appl.* **2002**, *7*, 61–67. [CrossRef]
10. De La Vallée Poussin, C. Sur l'équation différentielle linéqire du second order. Détermination d'une intégrale par deux valuers assignés. Extension aux équasions d'ordre n. *J. Math. Pures Appl.* **1929**, *8*, 125–144.
11. Saker, S.H.; Tunç, C.; Mahmoud, R.R. New Carlson–Bellman and Hardy–Littlewood dynamic inequalities. *Math. Inequal. Appl.* **2018**, *21*, 967–983. [CrossRef]
12. Ntouyas, S.K.; Ahmad, B.; Horikis, T.P. Recent developments of Lyapunov-type inequalities for fractional differential equations. In *Differential and Integral Inequalities*; Springer Optimization and Its Applications; Andrica, D., Rassias, T.M., Eds.; Springer: Berlin/Heidelberg, Germany, 2019; pp. 619–686.
13. Almeida, R.; Pooseh, S.; Torres, D.F.M. *Computational Methods in the Fractional Calculus of Variations*; Imperial College Press: Singapure, 2015.
14. Bohner, M.; Hristova, S. Stability for generalized Caputo proportional fractional delay integro–differential equations. *Bound. Value Probl.* **2022**, *14*, 1–15. [CrossRef]
15. Klimek, M. *On Solutions of Linear Fractional Differential Equations of a Variational Type*; The Publishing Office of Czestochowa University of Technology: Czestochowa, Poland, 2009.
16. Malinowska, A.B.; Odzijewicz, T.; Torres, D.F.M. *Advanced Methods in the Fractional Calculus of Variations*; Springer Briefs in Applied Sciences and Technology; Springer International Publishing: Cham, Switzerland, 2015.
17. Samko, S.G.; Kilbas A.A.; Marichev, Ȯ.I. *Fractional Integrals and Derivatives*; Translated from the 1987 Russian original; Gordon and Breach: Yverdon, Switzerland, 1993.
18. Tunç, O.; Tunxcx, C. Solution estimates to Caputo proportional fractional derivative delay integro—Differential equations. *Rev. Real Acad. Cienc. Exactas Fis. Nat. Ser. A-Mat.* **2023**, *12*, 117. [CrossRef]
19. Ferreira, R.A.C. A Lyapunov-type inequality for a fractional boundary-value problem. *Fract. Calc. Appl. Anal.* **2013**, *16*, 978–984. [CrossRef]
20. Zayernouri, M.; Karniadakis, G.E. Fractional Sturm–Liouville eigen–problems: Theory and numerical approximation. *J. Comput. Phys.* **2013**, *252*, 495–517. [CrossRef]
21. Klimek, M.; Odzijewicz, T.; Malinowska, A.B. Variational methods for the fractional Sturm–Liouville problem. *J. Math. Anal. Appl.* **2014**, *416*, 402–426. [CrossRef]
22. Guezane-Lakoud, A.; Khaldi, R.; Torres, D.F.M. Lyapunov–type inequality for a fractional boundary-value problem with natural conditions. *SeMA J.* **2018**, *75*, 157–162. [CrossRef]
23. Eneeva, L.M. Lyapunov inequality for an equation with fractional derivatives with different origins. *Vestnik KRAUNC. Fiz.-Mat. Nauki* **2019**, *28*, 32–39.
24. Odzijewicz, T. Inequality criteria for existence of solutions to some fractional partial differential equations. *Appl. Math. Lett.* **2020**, *101*, 106075. [CrossRef]
25. Odzijewicz, T.; Malinowska, A.B.; Torres, D.F.M. Fractional calculus of variations of several independent variables. *Eur. Phys. J.* **2013**, *222*, 1813–1826. [CrossRef]
26. Odzijewicz, T. *Variable o Fractional Isoperimetric Problem of Several Variables, Advances in the Theory and Applications of Non-integer Order Systems*; Springer: Berlin/Heidelberg, Germany, 2013; Volume 257, pp. 133–139.

mathematics

MDPI

Article

A Second-Order Accurate Numerical Approximation for a Two-Sided Space-Fractional Diffusion Equation

Taohua Liu [1], Xiucao Yin [1], Yinghao Chen [2,3] and Muzhou Hou [2,*]

[1] School of Science, Shaoyang University, Shaoyang 422000, China
[2] School of Mathematics and Statistics, Central South University, Changsha 410083, China
[3] Eastern Institute for Advanced Study, Yongriver Institute of Technology, Ningbo 315201, China
* Correspondence: houmuzhou@sina.com

Abstract: In this paper, we investigate a practical numerical method for solving a one-dimensional two-sided space-fractional diffusion equation with variable coefficients in a finite domain, which is based on the classical Crank-Nicolson (CN) method combined with Richardson extrapolation. Second-order exact numerical estimates in time and space are obtained. The unconditional stability and convergence of the method are tested. Two numerical examples are also presented and compared with the exact solution.

Keywords: variable coefficients; crank-nicolson method; stability and convergence; richardson extrapolation

MSC: 65M60; 65N12

Citation: Liu, T.; Yin, X.; Chen, Y.; Hou, M. A Second-Order Accurate Numerical Approximation for a Two-Sided Space-Fractional Diffusion Equation. *Mathematics* **2023**, *11*, 1838. https://doi.org/10.3390/math11081838

Academic Editors: António Lopes, Hovik Matevossian, Alireza Alfi, Liping Chen and Sergio Adriani David

Received: 13 February 2023
Revised: 10 March 2023
Accepted: 10 April 2023
Published: 12 April 2023

1. Introduction

In recent years, fractional differential equations have been of great interest for their use in modelling problems in physics (for an excellent review, see [1]), biology [2], chemistry [3] and even finance [4]. Numerical methods have become the main way to solve fractional-order equations, since we cannot easily obtain explicit analytical solutions to fractional-order equations. Several authors have proposed some effective numerical methods. Liu et al. [5] proposed a novel spatial second-order exact semi-implicit alternating direction method for the two-dimensional fractional FitzHugh-Nagumo single-domain model. Li et al. [6] proposed a spectral method for solving a fractional diffusion-absorption-reaction equation. She et al. [7] studied and analysed the Crank-Nicolson time discretisation of one- and two-dimensional spatial fractional diffusion equations. Hao et al. [8] studied the regularity of two-sided fractional diffusion equations with reaction terms and spectral methods. Li et al. [9] studied the fractional spectral localisation discretization of optimal control problems governed by spatial fractional diffusion equations. Gunzburger et al. [10] proposed a stable finite volume element method to approximate the coupled Stokes-Darcy problem. Ozbilge et al. [11] considered a finite difference scheme for the inverse problem of time-fractional parabolic partial differential equations with non-local boundary conditions. Feng et al. [12] developed a new fractional finite volume method based on the nodal basis functions for a two-sided space-fractional diffusion equation. Liu et al. [13] considered the problem of minimising a non-convex integral function in control, which is a solution to a control system described by fractional differential equations with mixed non-convex constraints on the control. Jia et al. [14] considered a fast finite difference method for a spatial fractional diffusion equation with fractional derivative boundary conditions. Lai et al. [15] considered the numerical solution of a Riesz spatial fractional partial differential equation with second order time derivatives. Chen et al. [16] considered a compact difference scheme for a second-order backward differential formulation of the fractional-order Volterra equation with a truncation error of order 4 in time and order 4

in space. Ma et al. [17] proposed a new signal smoothing equations, and they introduced generalized filters by use of memory effects of fractional derivatives. Shiri et al. [18] proposed an interesting Neural Network method for solving diffusion equations. Qu et al. [19] proposed a weight finite difference scheme for space fractional diffusion equations. There are some new papers in the fractional differential equations (see [20,21]). Based on the fractional-order Fick's law, a fractional-order diffusion model is derived for the space of variable coefficients with two-sided derivatives in the conserved form. The continuum equation in one-dimensional form can be written according to the mass conservation law as

$$\frac{\partial p(x,t)}{\partial t} + \frac{\partial Q(x,t)}{\partial x} = f(x,t), \tag{1}$$

where $p(x,t)$ is the distribution function of the diffusing quantity, $Q(x,t)$ is the diffusion flux and $f(x,t)$ is the source term. The classical Fick's law can be extended as follows:

$$Q(x,t) = -C(x)\frac{\partial}{\partial x}\int_a^x K_+(x,\xi)p(\xi,t)d\xi - D(x)\frac{\partial}{\partial x}\int_x^b K_-(x,\xi)p(\xi,t)d\xi, \tag{2}$$

where $C(x)$ and $D(x)$ are non-negative diffusion coefficients. On the interval $[a,b]$, $C(x)$ is a monotonically decreasing function of x and $D(x)$ is a monotonically increasing function of x. The kernel functions $K_+(x,\xi)$ and $K_-(x,\xi)$ are defined as follows

$$\begin{cases} K_+(x,\xi) = \frac{1}{\Gamma(1-\alpha)}(x-\xi)^{-\alpha} & a \le \xi \le x, \\ K_-(x,\xi) = \frac{1}{\Gamma(1-\alpha)}(\xi-x)^{-\alpha} & x \le \xi \le b, \end{cases} \tag{3}$$

where $0 < \alpha < 1$. Combination of Equations (1) and (2), Chen et al. [22] have derived the following nonlinear two-sided space fractional diffusion equation with variable coefficients.

$$\begin{gathered} \frac{\partial p(x,t)}{\partial t} = \frac{\partial}{\partial x}(C(x)\frac{\partial^\alpha p(x,t)}{\partial x^\alpha} - D(x)\frac{\partial^\alpha p(x,t)}{\partial(-x)^\alpha}) + f(x,t), \\ a \le x \le b, 0 < \alpha < 1, 0 < t \le T, \end{gathered} \tag{4}$$

where $\frac{\partial^\alpha p(x,t)}{\partial^\alpha(-x)}$ is the right Riemman-Liouville fractional derivatives, $\frac{\partial^\alpha p(x,t)}{\partial^\alpha x}$ is the left Riemman-Liouville fractional derivatives (see [23,24] for details) defined by

$$\frac{\partial^\alpha p(x,t)}{\partial(-x)^\alpha} = \frac{-1}{\Gamma(1-\alpha)}\frac{\partial}{\partial x}\int_x^b \frac{p(s,t)}{(s-x)^\alpha}ds, \tag{5}$$

$$\frac{\partial^\alpha p(x,t)}{\partial x^\alpha} = \frac{1}{\Gamma(1-\alpha)}\frac{\partial}{\partial x}\int_a^x \frac{p(s,t)}{(x-s)^\alpha}ds. \tag{6}$$

In this paper, we consider the above one-dimensional fractional two-sided space-fractional diffusion Equation (4) with the following initial value conditions and Dirichlet boundary conditions:

$$p(x,0) = \phi(x), a \le x \le b, \tag{7}$$

$$p(a,t) = p(b,t) = 0, 0 \le t \le T. \tag{8}$$

For this new one-dimensional two-sided spatial fractional diffusion equation, Chen et al. [22] gave a fast semi-implicit difference method. However, the method is only first order accuracy. To the best of our knowledge, there is limited research on the numerical computation of this equation with high accuracy based on the classical Crank-Nicolson scheme. This motivates us to propose in this paper an approach to this equation based on the classical Crank-Nicolson scheme and combined with a Richard space extrapolation. Our method is second order accuracy in time and space.

The remaining work is structured as follows. In Section 2, we present the classical Crank-Nicolson difference method for the one-dimensional two-sided spatial fractional diffusion equation and analyse its consistency. In Section 3, we prove the stability and convergence of the method. The method is then combined with spatial extrapolation. The convergence accuracy is improved to second order accuracy in time and space. In Section 4, two numerical experiments are given in order to verify the theoretical analysis of the method.

2. The Classical CN Difference Scheme for the One-Dimensional Two-Sided Space-Fractional Diffusion Equation and Its Consistency

For the numerical approximation, define $t_n = n\triangle t$, $0 \le t_n \le T$, for $n = 0, 1, 2, \ldots, N$ and $x_i = a + ih$ for $i = 0, 1, \ldots, M$, where $\triangle t, h$ are the mesh-width in the time and space respectively, $\triangle t = T/N$, $h = (b-a)/M$, $C_i = C(x_i)$, $D_i = D(x_i)$, and $f_i^n = f(x_i, t_n)$. Let P_i^n, p_i^n denote the exact and numerical solutions at the grid point (x_i, t_n) respectively. The initial conditions are given by $p_i^0 = \phi_i = \phi(x_i)$. Similarly, the Dirichlet zero boundary conditions are given by $p_0^n = p_M^n = 0$, for $n = 0, 1, \ldots, N$.

To approximate $\frac{\partial^\alpha p(x,t)}{\partial^\alpha (-x)}$ and $\frac{\partial^\alpha p(x,t)}{\partial^\alpha x}$, we use shifted left and standard right Grünwald formulas [25], respectively, at time $t_{n+1/2} = \frac{1}{2}(t_n + t_{n+1})$. The formulas are as follows:

$$\frac{\partial^\alpha p(x_i, t_{n+1/2})}{\partial^\alpha (-x)} = \frac{1}{(h)^\alpha} \sum_{s=0}^{M-i} g_s^{(\alpha)} P_{i+s}^{n+1/2} + O(h),$$

$$\frac{\partial^\alpha p(x_i, t_{n+1/2})}{\partial^\alpha x} = \frac{1}{(h)^\alpha} \sum_{s=0}^{i+1} g_s^{(\alpha)} P_{i+1-s}^{n+1/2} + O(h),$$

where $g_s^{(\alpha)} = (-1)^s \binom{\alpha}{s}$ is the normalized Grünwald weights. Its properties meet the following Lemma 1.

Lemma 1 (see [26]). *Let $0 < \alpha < 1$, the Grünwald weights $g_s^{(\alpha)}$ satisfy the properties:*
(i) $\sum_{s=0}^{\infty} g_0^{(\alpha)} = 0$.
(ii) $g_0^{(\alpha)} = 1$, $g_s^{(\alpha)} < 0$ *for* $s \ge 1$.
(iii) $\sum_{s=0}^{n} g_s^{(\alpha)} > 0$ *for any* $n \ge 1$.
(iv) $g_{s+1}^{(\alpha)} - g_s^{(\alpha)} = g_{s+1}^{(\alpha+1)}$, *for* $s \ge 1$.
(v) $\sum_{s=0}^{n} g_s^{(\alpha+1)} < 0$ *for any* $n \ge 1$.

Thus, we obtain a CN difference scheme for the one-dimensional two-sided space-fractional diffusion equation at the point $(x_i, t_{n+1/2})$.

$$
\begin{aligned}
\frac{p_i^{n+1}-p_i^n}{\triangle t} &\approx \frac{1}{h}(C(x)\frac{\partial^\alpha p(x,t_{n+1/2})}{\partial x^\alpha} - D(x)\frac{\partial^\alpha p(x,t_{n+1/2})}{\partial(-x)^\alpha})|_{x_{i-1}}^{x_i} + f_i^{n+1/2} \\
&= \frac{1}{h}(C_i\frac{\partial^\alpha p(x_i,t_{n+1/2})}{\partial x^\alpha} - D_i\frac{\partial^\alpha p(x_i,t_{n+1/2})}{\partial(-x)^\alpha}) \\
&- \frac{1}{h}(C_{i-1}\frac{\partial^\alpha p(x_{i-1},t_{n+1/2})}{\partial x^\alpha} - D_{i-1}\frac{\partial^\alpha p(x_{i-1},t_{n+1/2})}{\partial(-x)^\alpha}) + f_i^{n+1/2} \\
&\approx \frac{1}{2h^{\alpha+1}}[(C_i\sum_{s=0}^{i+1} g_s^{(\alpha)} p_{i+1-s}^{n+1} + C_i\sum_{s=0}^{i+1} g_s^{(\alpha)} p_{i+1-s}^{n}) - (C_{i-1}\sum_{s=0}^{i} g_s^{(\alpha)} p_{i-s}^{n+1} + C_{i-1}\sum_{s=0}^{i} g_s^{(\alpha)} p_{i-s}^{n})] \\
&- \frac{1}{2h^{\alpha+1}}[(D_i\sum_{s=0}^{M-i} g_s^{(\alpha)} p_{i+s}^{n+1} + D_i\sum_{s=0}^{M-i} g_s^{(\alpha)} p_{i+s}^{n}) \\
&- (D_{i-1}\sum_{s=0}^{M-i+1} g_s^{(\alpha)} p_{i+s-1}^{n+1} + D_{i-1}\sum_{s=0}^{M-i+1} g_s^{(\alpha)} p_{i+s-1}^{n})] \\
&= \frac{1}{2h^{\alpha+1}}[(\sum_{s=0}^{i+1}(C_i g_{i+1-s}^{(\alpha+1)} - C_{i-1} g_{i-s}^{(\alpha+1)}) p_s^{n+1} + C_i g_0^{(\alpha)} p_{i+1}^{n+1}) \\
&+ (\sum_{s=0}^{i+1}(C_i g_{i+1-s}^{(\alpha+1)} - C_{i-1} g_{i-s}^{(\alpha+1)}) p_s^{n} + C_i g_0^{(\alpha)} p_{i+1}^{n})] + p_{i+1}^n \\
&- \frac{1}{2h^{\alpha+1}}[\sum_{s=i}^{M}(D_{i-1} g_{s+1-i}^{(\alpha)} - D_i g_{s-i}^{(\alpha)}) p_s^{n+1} + D_{i-1} g_0^{(\alpha)} p_s^{n+1}) \\
&+ (\sum_{s=i}^{M}(D_{i-1} g_{s+1-i}^{(\alpha)} - D_i g_{s-i}^{(\alpha)}) p_s^{n} + D_{i-1} g_0^{(\alpha)} p_s^{i-1})].
\end{aligned}
$$

After some rearrangements, we can get CN scheme

$$
\begin{aligned}
\frac{p_i^{n+1}-p_i^n}{\triangle t} &= \frac{1}{2h^{\alpha+1}}[(\sum_{s=0}^{i+1} C_i g_{i+1-s}^{(\alpha+1)} p_s^{n+1} + \sum_{s=0}^{i+1} C_i g_{i-s}^{(\alpha)} p_s^{n}) \\
&+ (\sum_{s=0}^{i}(C_i - C_{i-1}) g_{i-s}^{(\alpha)} p_s^{n+1} + \sum_{s=0}^{i}(C_i - C_{i-1}) g_{i-s}^{(\alpha)} p_s^{n})] \\
&- \frac{1}{2h^{\alpha+1}}[(\sum_{s=i-1}^{M} D_{i-1} g_{s+1-i}^{(\alpha+1)} p_s^{n+1} + \sum_{s=i-1}^{M} D_{i-1} g_{s+1-i}^{(\alpha+1)} p_s^{n}) \\
&+ (\sum_{s=i}^{M}(D_{i-1} - D_i) g_{s-i}^{(\alpha)} p_s^{n+1} + \sum_{s=i}^{M}(D_{i-1} - D_i) g_{s-i}^{(\alpha)} p_s^{n})].
\end{aligned} \tag{9}
$$

Organize the above equation and write it in the following operators form

$$
(1-\delta_{\alpha,x}) p_i^{n+1} = (1+\delta_{\alpha,x}) p_i^n + \triangle t f_i^{n+1/2}, \tag{10}
$$

where the difference operators as

$$
\begin{aligned}
\delta_{\alpha,x} p_i^n &= \frac{\Delta t}{2h^{\alpha+1}}[(\sum_{s=0}^{i}(C_i g_{i+1-s}^{(\alpha)} - C_{i-1} g_{i-s}^{(\alpha)}) p_s^n) + C_i g_0^{(\alpha)} p_{i+1}^n] \\
&+ \frac{\Delta t}{2h^{\alpha+1}}[(\sum_{s=i}^{M}(D_{i-1} g_{s+1-i}^{(\alpha)} - D_i g_{s-i}^{(\alpha)}) p_s^n) + D_{i-1} g_0^{(\alpha)} p_{i-1}^n].
\end{aligned}
$$

It can be further written in the matrix form as follows:

$$
(I-A)P^{n+1} = (I+A)P^n + \triangle t F^{n+1/2}, \tag{11}
$$

where I is $(M-1)\times(M-1)$ *identity matrix;* $P^n=(p_1^n,p_2^n,...,p_{M-1}^n)$ *;* $F^{n+1/2}=(f_1^{n+1/2},$ $f_2^{n+1/2},...,f_{M-1}^{n+1/2})$*; and the matric* $A=(A_{i,s})$*,* $i,s=1,2,\ldots,M-1$*, is defined by*

$$A_{i,s}=\begin{cases}\eta(D_{i-1}g_{s-i+1}^{(\alpha)}-D_ig_{s-i}^{(\alpha)}) & \text{when } s>i+1,\\ \eta(C_ig_0^{(\alpha)}+D_{i-1}g_2^{(\alpha)}-D_ig_1^{(\alpha)}) & \text{when } s=i+1,\\ \eta(C_ig_1^{(\alpha)}-C_{i-1}g_0^{(\alpha)}+D_{i-1}g_1^{(\alpha)}-D_ig_0^{(\alpha)}) & \text{when } s=i,\\ \eta(C_ig_2^{(\alpha)}-C_{i-1}g_0^{(\alpha)}+D_{i-1}g_0^{(\alpha)}) & \text{when } s=i-1,\\ \eta(C_ig_{i+1-s}^{(\alpha)}-C_{i-1}g_{i-s}^{(\alpha)}) & \text{when } s<i-1,\end{cases}\tag{12}$$

where $\eta=\frac{\Delta t}{2h^{\alpha+1}}$.

Theorem 1. *The classical CN method defined by Equation (9) is consistent with Equation (4) of order* $O((\Delta t)^2+h)$.

Proof. The Equation (4) can be rewritten as

$$\begin{aligned}\frac{\partial p(x,t)}{\partial t}&=\frac{dC(x)}{dx}\frac{\partial^\alpha p(x,t)}{\partial x^\alpha}+C(x)\frac{\partial^{\alpha+1}p(x,t)}{\partial x^{\alpha+1}}\\&\quad-\frac{dD(x)}{dx}\frac{\partial^\alpha p(x,t)}{\partial(-x)^\alpha}+D(x)\frac{\partial^{\alpha+1}p(x,t)}{\partial(-x)^{\alpha+1}}+f(x,t).\end{aligned}\tag{13}$$

We define the local truncation error term as R_i^n, using Equations (9) and (13), we get

$$\begin{aligned}R_i^n&=\frac{P_i^{n+1}-P_i^n}{\Delta t}-\frac{1}{2h^{\alpha+1}}[(\sum_{s=0}^{i+1}C_ig_{i+1-s}^{(\alpha+1)}P_s^{n+1}+\sum_{s=0}^{i+1}C_ig_{i-s}^{(\alpha)}P_s^n)\\&\quad+(\sum_{s=0}^{i}(C_i-C_{i-1})g_{i-s}^{(\alpha)}P_s^{n+1}+\sum_{s=0}^{i}(C_i-C_{i-1})g_{i-s}^{(\alpha)}P_s^n)]\\&\quad-\frac{1}{2h^{\alpha+1}}[(\sum_{s=i-1}^{M}D_{i-1}g_{s+1-i}^{(\alpha+1)}P_s^{n+1}+\sum_{s=i-1}^{M}D_{i-1}g_{s+1-i}^{(\alpha+1)}P_s^n)\\&\quad+(\sum_{s=i}^{M}(D_{i-1}-D_i)g_{s-i}^{(\alpha)}P_s^{n+1}+\sum_{s=i}^{M}(D_{i-1}-D_i)g_{s-i}^{(\alpha)}P_s^n)]-f_i^{n+1/2}\\&=\frac{P_i^{n+1}-P_i^n}{\Delta t}-\frac{\partial p(x,t)}{\partial t}|_i^{n+1/2}\\&\quad-\frac{1}{2h^\alpha}[\sum_{s=0}^{i}\frac{(C_i-C_{i-1})}{h}g_{i-s}^{(\alpha)}(P_s^{n+1}+P_s^n)-\frac{dC(x)}{dx}\frac{\partial^\alpha p(x,t)}{\partial x^\alpha}|_i^{n+1/2}]\\&\quad-[\frac{1}{2h^{\alpha+1}}\sum_{s=0}^{i+1}C_ig_{i+1-s}^{(\alpha+1)}(P_s^{n+1}+P_s^n)-(C(x)\frac{\partial^{\alpha+1}p(x,t)}{\partial x^{\alpha+1}})|_i^{n+1/2}]\\&\quad+\frac{1}{2h^\alpha}[\sum_{s=i}^{M}\frac{(D_i-D_{i-1})}{h}g_{s-i}^{(\alpha)}(P_s^{n+1}+P_s^n)-\frac{dD(x)}{dx}\frac{\partial^\alpha p(x,t)}{\partial(-x)^\alpha}|_i^{n+1/2}]\\&\quad-[\frac{1}{2h^{\alpha+1}}\sum_{s=i-1}^{M}D_{i-1}g_{i+1-s}^{(\alpha+1)}(P_s^{n+1}+P_s^n)-(D(x)\frac{\partial^{\alpha+1}p(x,t)}{\partial(-x)^{\alpha+1}})|_i^{n+1/2}]\\&=O((\Delta t)^2+h).\end{aligned}$$

Thus, the classical CN method is consistent. □

3. Stability and Convergence of the Classical Fractional CN Method

Let $\tilde{p}_i^n$ $(i = 1, 2, \ldots, M-1)$ be an approximate solution of p_i^n with initial conditions $\tilde{p}_i^0$ in order to discuss the stability and convergence of the numerical method. Let $\varepsilon_i^n = p_i^n - \tilde{p}_i^n$, $e_i^n = P_i^n - p_i^n$ be defined with the corresponding vectors

$$\varepsilon^n = (\varepsilon_1^n, \varepsilon_2^n, \ldots, \varepsilon_{M-1}^n), \tag{14}$$

$$e^n = (e_1^n, e_2^n, \ldots, e_{M-1}^n). \tag{15}$$

Theorem 2. *On the interval $[a, b]$, if $C(x) \geq 0$ monotonically decreases, and $D(x) \geq 0$ monotonically increases, the CN difference scheme defined by Equation (10) is uniquely solvable.*

Proof. Since $C(x)$ and $D(x)$ are both non-negative, $C(x)$ is monotonically decreasing, and $D(x)$ is monotonically increasing, we have $C_{i-1} \geq C_i \geq 0$, $D_i \geq D_{i-1} \geq 0$, $i = 1, 2, \ldots, M-1$.

According to Lemma 1, then we have $C_i g_{j+1}^{\alpha} \geq C_i g_j^{(\alpha)} \geq C_{i-1} g_j^{(\alpha)}$, $D_{i-1} g_{j+1}^{(\alpha)} \geq D_{i-1} g_j^{(\alpha)} \geq D_i g_j^{(\alpha)}$, for $j \geq 2$. Let r_i be the sum of the absolute values of all the elements of row i of the matrix A excluding the diagonal elements, then we have

$$\begin{aligned}
r_i &= \sum_{s=1, s\neq i}^{M-1} |A_{i,s}| \\
&= \eta[\sum_{s=1}^{i-2} |C_i g_{i+1-s}^{(\alpha)} - C_{i-1} g_{i-s}^{(\alpha)}| + |C_i g_2^{(\alpha)} - C_{i-1} g_0^{(\alpha)} + D_{i-1} g_0^{(\alpha)}| \\
&+ |C_i g_0^{(\alpha)} + D_{i-1} g_2^{(\alpha)} + D_i g_1^{(\alpha)}| + \sum_{s=i+2}^{M-1} |D_{i-1} g_{s-i+1}^{(\alpha)} - D_i g_{s-i}^{(\alpha)}|] \\
&= \eta[\sum_{s=1}^{i-2} (C_i g_{i+1-s}^{(\alpha)} - C_{i-1} g_{i-s}^{(\alpha)}) + (C_i g_2^{(\alpha)} - C_{i-1} g_0^{(\alpha)} + D_{i-1} g_0^{(\alpha)}) \\
&+ (C_i g_0^{(\alpha)} + D_{i-1} g_2^{(\alpha)} + D_i g_1^{(\alpha)}) + \sum_{s=i+2}^{M-1} (D_{i-1} g_{s-i+1}^{(\alpha)} - D_i g_{s-i}^{(\alpha)})] \\
&= \eta[C_i (\sum_{s=0}^{i} g_s^{(\alpha)} - g_1^{(\alpha)}) - C_{i-1} (\sum_{s=0}^{i-1} g_s^{(\alpha)} - g_0^{(\alpha)}) \\
&+ D_{i-1} (\sum_{s=0}^{M-i} g_s^{(\alpha)} - g_1^{(\alpha)}) - D_i (\sum_{s=0}^{M-i} g_s^{(\alpha)} - g_0^{(\alpha)})] \\
&= \eta[(C_i - C_{i-1}) \sum_{s=0}^{i-1} g_s^{(\alpha)} + C_i g_i^{(\alpha)} - C_i g_i^{(\alpha)} + C_{i-1} g_i^{(\alpha)} \\
&- (D_i - D_{i-1}) \sum_{s=0}^{M-1} g_s^{(\alpha)} + D_{i-1} g_{M-i}^{(\alpha)} - D_{i-1} g_1^{(\alpha)} + D_i g_0^{(\alpha)} \\
&- C_i g_i^{(\alpha)} + C_{i-1} g_i^{(\alpha)} - D_{i-1} g_1^{(\alpha)} + D_i g_0^{(\alpha)}] = -A_{i,i}.
\end{aligned} \tag{16}$$

It follows from the above that the eigenvalues of a matrix A have negative real parts according to Gerschgorin's theorem [27], when λ is an eigenvalue of A only when $1 - \lambda$ is an eigenvalue of the matrix $I - A$. Thus, the eigenvalue of the matrix A all contain negative real parts, which implicitly means that every eigenvalue of the matrix $I - A$ has a modulus large than 1. In addition, we can see that the spectral radius of the matrix $I - A$ is large than 1, so the matrix $I - A$ is reversible [28]. The difference scheme is unique and solvable. □

Theorem 3. *On the interval $[a, b]$, if $C(x) \geq 0$ monotonically decreases, and $D(x) \geq 0$ monotonically increases, then the CN difference scheme defined by Equation (10) is unconditionally stable and convergent and exists in a positive constant $C > 0$ such that $\|e^n\|_\infty \leq C((\triangle t)^2 + h)$.*

Proof. λ is an eigenvalue of the matrix A, if and only if $1 - \lambda$ is an eigenvalue of the matrix $I - A$, if and only if $(1 + \lambda)/(1 - \lambda)$ is an eigenvalue of the matrix $(I - A)^{-1}(I + A)$. We know that the eigenvalues of the matrix A all have negative real parts from Theorem 2, This implicity means that $|(1 + \lambda)/(1 - \lambda)| < 1$, and therefore the spectral radius of the matrix $(I - A)^{-1}(I + A)$ can be obtained to be less than 1. In addition, according to the relationship between the two-norm of the matrix and the spectral radius of the matrix, we obtain

$$\|(I - A)^{-1}(I - A)\|_2 = \rho((I - A)^{-1}(I - A)) < 1. \tag{17}$$

By Equation (10) and the definition of ε^n, $I - A$ is invertible, we have

$$\varepsilon^{n+1} = (I - A)^{-1}(I - A)\varepsilon^n, \tag{18}$$

Further, we obtain

$$\|\varepsilon^{n+1}\|_2 = \|(I - A)^{-1}(I - A)\varepsilon^n\|_2 \leq \|(I - A)^{-1}(I + A)\|_2\|\varepsilon^n\|_2 < \|\varepsilon^n\|_2. \tag{19}$$

If we repeat the above equation $n + 1$ times, we obtain the following equation

$$\|\varepsilon^{n+1}\|_2 < \|\varepsilon^0\|_2. \tag{20}$$

Thus, the CN difference scheme defined by Equation (10) is unconditionally stable.

We then consider the convergence of the CN difference scheme. From Equation (10) and the definition of e^n, we have

$$(I - A)e^{n+1} = (I + A)e^n + \Delta t R^n, \tag{21}$$

and

$$e^0 = 0, \tag{22}$$

where $R^n = (R_1^n, R_2^n, \ldots, R_{M-1}^n)^T$, $\|R^n\|_2 \leq C_1((\Delta t)^2 + h)$ and C_1 is a positive constant.

Similarly, we have also developed

$$\|e^{n+1}\|_2 < \|e^n\|_2 + \|\Delta t R^n\|_2. \tag{23}$$

Repeating the above equation $n + 1$ times, we have $\|e^n\|_2 < n(\Delta t)C_1((\Delta t)^2 + h)$. Since $n(\Delta t) \leq T$, $\|e^n\|_\infty \leq C((\Delta t)^2 + h)$. □

Remark 1. *$p_x^{t_n}$ is the Richardson extrapolated solution (see [27,28]), then can be computed from $p_x^{t_n} = 2p_{x,h/2}^{t_n} - p_{x,h}^{t_n}$, where x is a common grid point on both the fine and the coarse meshes, and $p_{x,h}^{t_n}, p_{x,h/2}^{t_n}$ are the CN solutions at the point x using the coarse grid (grid with h) and the fine grid (grid size $h/2$), respectively. In this way, we can obtain second-order accuracy both in space and time.*

Proof. The error in the right-shifted and left standard Grunwald formulas are $K_1 h + K_2(h)^2 + O((h)^3)$ (see [25]), where K_1 and K_2 are positive constant independent of h. According to Richardson extrapolation method (see [27]), at a grid size h and $h/2$,we apply the CN method, we can get the Richardson extrapolated solution $p_x^{t_n} = 2p_{x,h/2}^{t_n} - p_{x,h}^{t_n}$, and Richardson extrapolated solution has local truncation error $C((\Delta t)^2 + h^2)$, according to Lax's Equivalence Theorem (see [29]), we obtain second-order accuracy both in time and space. The detailed steps to get Richardson's extrapolated solution are as follows:

Step 1: On the spatially coarse grid h, solve using this CN difference format method to obtain the numerical solution $p_{x,h}^{t_n}$ on the coarse grid.

Step 2: On the spatially fine grid $h/2$ with the same Δt, solve again using this CN difference format method to obtain the numerical solution $p_{x,h/2}^{t_n}$ on the fine grid.

Step 3: The Richard extrapolation solution, which can be written in the following form $p_x^{t_n} = 2p_{x,h/2}^{t_n} - p_{x,h}^{t_n}$.

□

4. Numerical Example

In this section, we carry out two numerical experiments to demonstrate the effectiveness of the second-order accurate finite difference method. $\|e_h^N\|_\infty$ the maximum error of the Crank-Nicolson numerical solution, $\|e_h^{N-ex}\|_\infty$ the maximum error of the corresponding extrapolated Crank-Nicolson numerical solution.

Example 1 (Parabolic case [22])**.** *The following two-sided space-fractional diffusion equation was considered*

$$\begin{aligned} \frac{\partial p(x,t)}{\partial t} &= \frac{\partial}{\partial x}(C(x)\frac{\partial^\alpha p(x,t)}{\partial x^\alpha} - D(x)\frac{\partial^\alpha p(x,t)}{\partial(-x)^\alpha}) + f(x,t), \\ & a \le x \le b, 0 < \alpha < 1, 0 \le t \le T. \end{aligned} \tag{24}$$

The finite domain is $[0,1]$*. The nonnegative diffusion coefficient* $C(x) = \frac{1-x^2}{2}$, $D(x) = \frac{1+x^2}{2}$*. The source term* $f(x,t)$ *is given by*

$$f(x,t) = -e^{-t}[x^2(1-x)^2 - xq(x,\alpha) + \frac{1-x^2}{2}q(x,1+\alpha) - xq(1-x,\alpha) + \frac{1+x^2}{2}q(1-x,1+\alpha)], \tag{25}$$

here

$$q(x,t) = \frac{\Gamma(5)}{\Gamma(5-\alpha)}x^{4-\alpha} - \frac{2\Gamma(4)}{\Gamma(4-\alpha)}x^{3-\alpha} + \frac{\Gamma(3)}{\Gamma(3-\alpha)}x^{2-\alpha}. \tag{26}$$

The exact solution to this problem is

$$p(x,t) = e^{-t}x^2(1-x)^2, \tag{27}$$

which satisfies the initial function

$$\phi(x) = x^2(1-x)^2, \tag{28}$$

and the Dirichlet boundary conditions are

$$p(0,t) = p(1,t) = 0. \tag{29}$$

In the numerical experiments, we consider four different α *in the case, respectively.*

Table 1 shows the convergence rates of the numerical solutions of Example 1 with $\alpha = 0.2, 0.4, 0.6$ at the time $T = 1$. The numerical solution matches the exact analytical solution of the fractional differential equation. It shows stability and a convergence order of $O((\Delta t)^2 + h)$. Figure 1 shows the numerical solution in Crank-Nicolson format and the exact solution of Example 1, where $\alpha = 0.2$, $\Delta t = h = 2^{-7}$ at time $T = 1$. Figure 2 shows the numerical solution in Crank-Nicolson format and the exact solution of Example 1, where $\alpha = 0.4$, $\Delta t = h = 2^{-7}$ at time $T = 1$. Figure 3 shows the numerical solution in Crank-Nicolson format and the exact solution of Example 1, where $\alpha = 0.6$, $\Delta t = h = 2^{-7}$ at time $T = 1$. The numerical solution compares well with the exact analytic solution to the fractional partial differential equation in this test case.

Table 1. Error behaviors and rate with $\alpha = 0.2, 0.4, 0.6$ at time $T = 1$ for Example 1.

	$\alpha = 0.2$		$\alpha = 0.4$		$\alpha = 0.6$	
$\Delta t = h$	$\|e_h^N\|_\infty$	*Rate*	$\|e_h^N\|_\infty$	*Rate*	$\|e_h^N\|_\infty$	*Rate*
2^{-3}	7.5340×10^{-3}	-	4.2000×10^{-3}	-	1.9000×10^{-3}	-
2^{-4}	4.2214×10^{-3}	1.78	2.4000×10^{-3}	1.75	1.2000×10^{-3}	1.83
2^{-5}	2.2199×10^{-3}	1.90	1.3000×10^{-3}	1.85	6.565×10^{-4}	1.58
2^{-6}	1.1356×10^{-3}	1.95	6.4325×10^{-4}	2.02	3.4039×10^{-4}	1.93
2^{-7}	5.7351×10^{-4}	1.98	3.2425×10^{-4}	1.98	1.7301×10^{-4}	1.97

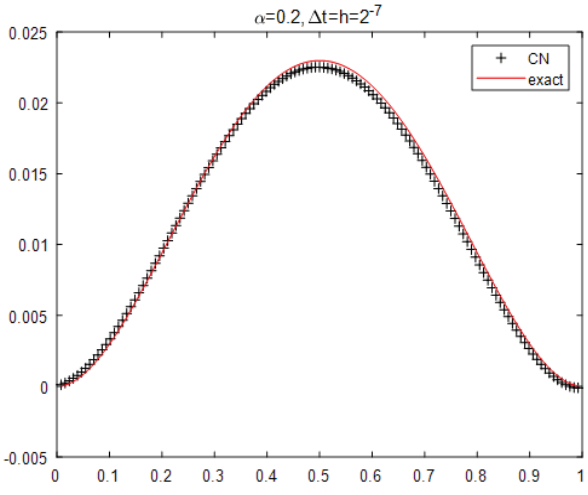

Figure 1. The numerical solution for the Crank-Nicolson scheme and exact solution for Example 1 with $\alpha = 0.2$, $\Delta t = h = 2^{-7}$ at time $T = 1$.

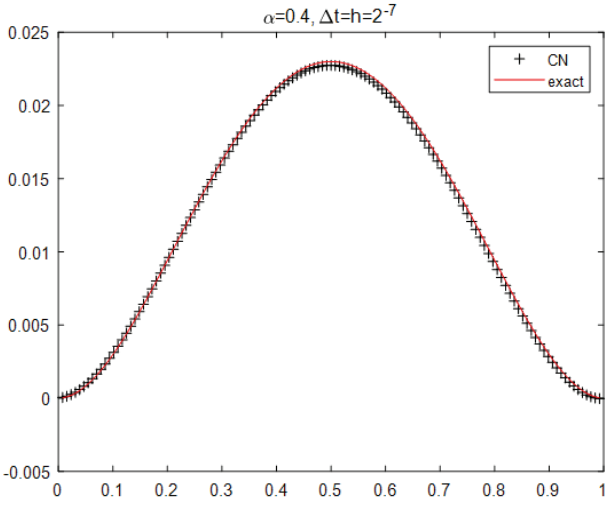

Figure 2. The numerical solution for the Crank-Nicolson scheme and exact solution for Example 1 with $\alpha = 0.4$, $\Delta t = h = 2^{-7}$ at time $T = 1$.

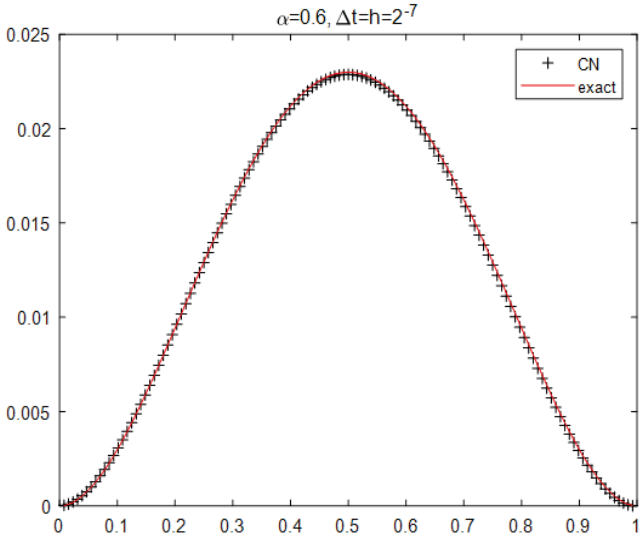

Figure 3. The numerical solution for the Crank-Nicolson scheme and exact solution for Example 1 with $\alpha = 0.6$, $\Delta t = h = 2^{-7}$ at time $T = 1$.

To check the speed of convergence of this method, we start with $\Delta t = h = 2^{-3}$. To obtain an extrapolated CN solution on this grid size, in the first step the problem is solved numerically $p^{t_n}_{x,h}$ on a coarse grid with $\Delta t = h = 2^{-3}$ and in the second step a finer grid size is created using the same and in the second step a finer grid size is created using the same Δt but halving h ($\Delta t = 2^{-3}$,$h = 2^{-4}$). The third step is to calculate the extrapolation solution for the points on the coarse grid as $p^{t_n}_{x} = 2p^{t_n}_{x,h/2} - p^{t_n}_{x,h}$.

For Example 1 with $T = 1$ and $\alpha = 0.8$, Table 2 shows the absolute error in the numerical solution. The second column shows the absolute value of the maximum error in the numerical solution. The third column shows the rate of reduction of the error as the mesh is refined. It shows the order of convergence as $O((\Delta t)^2 + h)$. The fourth column shows the maximum absolute error for the Crank-Nicholson extrapolation. The last column shows the error rate of these extrapolated solutions. We note that the order of convergence is second order $O((\Delta t)^2 + h^2)$. Figure 4 shows the numerical solution for the Crank-Nicolson scheme and the extrapolated Crank-Nicolson scheme and rate for Example 1 with $\alpha = 0.8$, $\Delta t = h = 2^{-6}$ at time $T = 1$.

Table 2. Error behaviors and rate for the Crank-Nicolson scheme and exact solution for Example 1 with $\alpha = 0.8$ at time $T = 1$.

$\Delta t = h$	$\|e^N_h\|_\infty$	*Rate*	$\|e^{N-ex}_h\|_\infty$	*Rate*
2^{-3}	7.7198×10^{-4}	-	7.4596×10^{-4}	-
2^{-4}	4.0338×10^{-4}	1.91	1.7406×10^{-4}	4.29
2^{-5}	2.4992×10^{-4}	1.61	4.1151×10^{-5}	4.23
2^{-6}	1.3734×10^{-4}	1.82	9.7767×10^{-6}	4.21

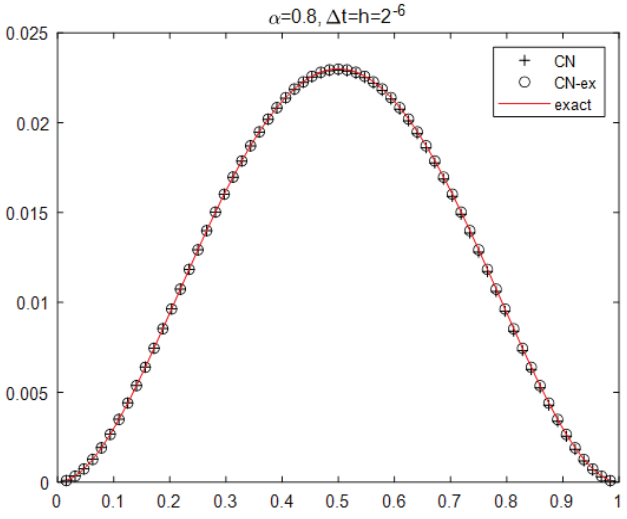

Figure 4. The numerical solution for the Crank-Nicolson scheme and the extrapolated Crank-Nicolson scheme and rate for Example 1 with $\alpha = 0.8$, $\Delta t = h = 2^{-6}$ at time $T = 1$.

Example 2 (Linear case [22]). *The following two-sided space-fractional diffusion equation was considered*

$$\frac{\partial p(x,t)}{\partial t} = \frac{\partial}{\partial x}(C(x)\frac{\partial^{\alpha} p(x,t)}{\partial x^{\alpha}} - D(x)\frac{\partial^{\alpha} p(x,t)}{\partial(-x)^{\alpha}}) + f(x,t), \quad a \le x \le b, 0 < \alpha < 1, 0 \le t \le T. \tag{30}$$

The finite domain is $[0,1]$. *The nonnegative diffusion coefficient* $C(x) = 2 - x$, $D(x) = 2 + x$. *The source term* $f(x,t)$ *is given by*

$$f(x,t) = -e^{-t}[x^2(1-x)^2 - q(x,\alpha) + (2-x)q(x,1+\alpha) - q(1-x,\alpha) + (2+x)q(1-x,1+\alpha)], \tag{31}$$

here

$$q(x,t) = \frac{\Gamma(5)}{\Gamma(5-\alpha)}x^{4-\alpha} - \frac{2\Gamma(4)}{\Gamma(4-\alpha)}x^{3-\alpha} + \frac{\Gamma(3)}{\Gamma(3-\alpha)}x^{2-\alpha}. \tag{32}$$

The exact solution to this problem is

$$p(x,t) = e^{-t}x^2(1-x)^2, \tag{33}$$

which satisfies the initial function

$$\phi(x) = x^2(1-x)^2, \tag{34}$$

and the Dirichlet boundary conditions are

$$p(0,t) = p(1,t) = 0. \tag{35}$$

In the numerical experiments, we consider four different α *values in the case, respectively.*

Table 3 shows the convergence rates for the numerical solutions of Example 2 with $\alpha = 0.2, 0.4, 0.6$ at the time $T = 1$. In this test case the numerical solution agrees well with the exact analytical solution of the fractional order partial differential equation. It shows stability and a convergence order of $O((\Delta t)^2 + h)$. Figure 5 shows the numerical solution in Crank-Nicolson format and the exact solution of Example 2 with $\alpha = 0.2$, $\Delta t = h = 2^{-7}$ at time $T = 1$. Figure 6 shows the numerical solution in Crank-Nicolson format and the exact solution of Example 4.2 with $\alpha = 0.4$, $\Delta t = h = 2^{-7}$ at time $T = 1$. Figure 7 shows

the numerical solution in Crank-Nicolson format and the exact solution of Example 2 with $\alpha = 0.6$, $\Delta t = h = 2^{-7}$ at time $T = 1$. The numerical solution compares well with the exact analytic solution to the fractional partial differential equation in this test case.

Table 4 shows the absolute error in the numerical solution for Example 2 at time $T = 1$ and $\alpha = 0.8$. The second column shows the absolute value of the maximum error in the numerical solution. The third column shows the rate of reduction of the error as the mesh is refined. It shows the order of convergence as $O((\Delta t)^2 + h)$. The fourth column shows the maximum absolute error for the Crank-Nicholson extrapolation. The last column shows the error rate of these extrapolated solutions. We note that the order of convergence is second order $O((\Delta t)^2 + h^2)$. Figure 8 shows the numerical solution for the Crank-Nicolson scheme and the extrapolated Crank-Nicolson scheme and rate for Example 2 with $\alpha = 0.8$, $\Delta t = h = 2^{-6}$ at time $T = 1$.

Table 3. Error behaviors and rate with $\alpha = 0.2, 0.4, 0.6$ at time $T = 1$ for Example 2.

	$\alpha = 0.2$		$\alpha = 0.4$		$\alpha = 0.6$	
$\Delta t = h$	$\|e_h^N\|_\infty$	*Rate*	$\|e_h^N\|_\infty$	*Rate*	$\|e_h^N\|_\infty$	*Rate*
2^{-3}	8.3000×10^{-3}	-	3.8000×10^{-3}	-	1.3000×10^{-3}	-
2^{-4}	5.0000×10^{-3}	1.66	2.3000×10^{-3}	1.75	9.1101×10^{-4}	1.43
2^{-5}	2.7000×10^{-3}	1.85	1.2000×10^{-3}	1.85	5.1674×10^{-4}	1.76
2^{-6}	1.4000×10^{-3}	1.93	6.4069×10^{-4}	2.02	2.7250×10^{-4}	1.90
2^{-7}	7.1602×10^{-4}	1.96	3.2564×10^{-4}	1.98	1.3953×10^{-4}	1.95

Table 4. Error behaviors and rate for the Crank-Nicolson scheme and exact solution for Example 2 with $\alpha = 0.8$ at time $T = 1$.

$\Delta t = h$	$\|e_h^N\|_\infty$	*Rate*	$\|e_h^{N-ex}\|_\infty$	*Rate*
2^{-3}	7.1922×10^{-4}	-	6.5386×10^{-4}	-
2^{-4}	1.8018×10^{-4}	3.99	1.5769×10^{-4}	4.15
2^{-5}	1.3921×10^{-4}	1.29	3.7662×10^{-5}	4.19
2^{-6}	8.2345×10^{-5}	1.69	8.2345×10^{-5}	4.57

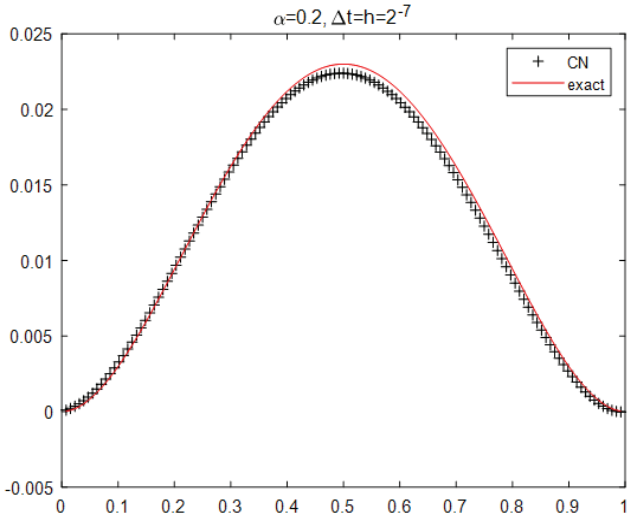

Figure 5. The numerical solution for the Crank-Nicolson scheme and exact solution for Example 2 with $\alpha = 0.2$, $\Delta t = h = 2^{-7}$ at time $T = 1$.

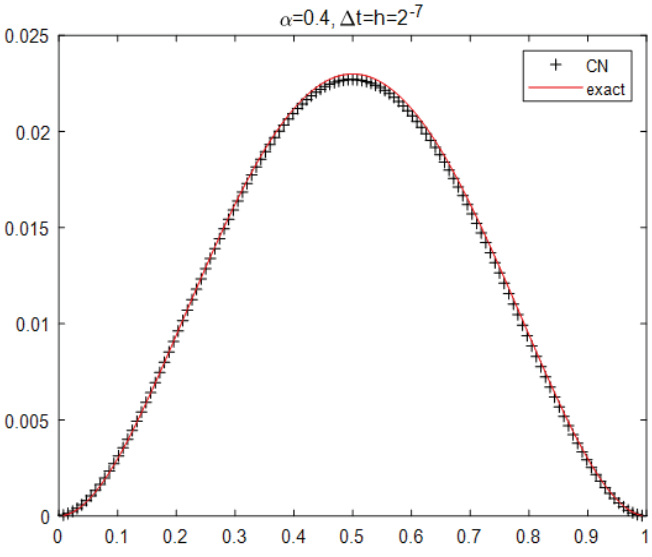

Figure 6. The numerical solution for the Crank-Nicolson scheme and exact solution for Example 2 with $\alpha = 0.4$, $\Delta t = h = 2^{-7}$ at time $T = 1$.

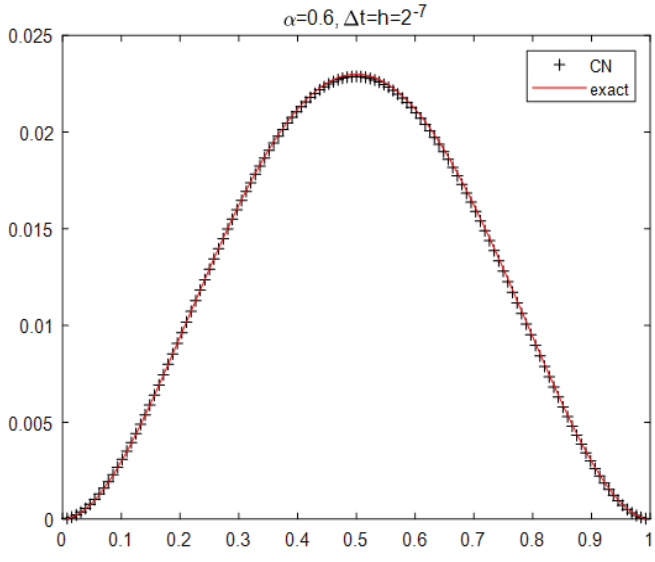

Figure 7. The numerical solution for the Crank-Nicolson scheme and exact solution for Example 2 with $\alpha = 0.6$, $\Delta t = h = 2^{-7}$ at time $T = 1$.

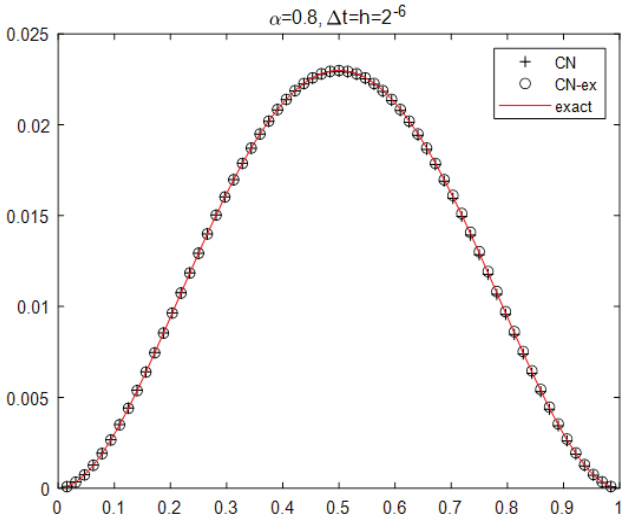

Figure 8. The numerical solution for the Crank-Nicolson scheme and the extrapolated Crank-Nicolson scheme and exact solution for Example 2 with $\alpha = 0.8$, $\Delta t = h = 2^{-6}$ at time $T = 1$.

5. Conclusions

In this paper, we have considered a two-sided spatial fractional order diffusion equation with variable diffusion coefficients from a fractional Fick's law. Although finite difference estimates for the fractional order derivatives have been elusive, a high precision convergence method for the superdiffusion equation is feasible by applying the extrapolation to the Crank-Nicolson method and the Richardson method, in combination with the Grünwald estimates using shifts. We can obtain second-order accurate numerical estimates in time and space using the CN and Richardson extrapolation methods. We then consider more general cases, such as the case where $C(x)$ and $D(x)$ are not monotonic, or higher accuracy differential methods. We also look at numerical solutions of this equation for different boundary conditions, such as fractional boundary conditions.

Author Contributions: Conceptualization, T.L.; Investigation, T.L., X.Y. and M.H.; Methodology, T.L.; Software, T.L. and Y.C.; Formal analysis, T.L. and X.Y.; Writing-original draft, T.L. and X.Y.; Writing-review & editing, T.L., X.Y. and Y.C.; Visualization, X.Y.; Supervision, M.H. All authors have read and agreed to the published version of the manuscript.

Funding: This work was supported by the Natural Science Foundation of Hunan Province (Grant No.2022*JJ*50229 and No.2022*JJ*30673), the Fundamental Research Funds for Central University of Central South University (Grant No.2022*zyts*0611), the Key Program of National Social Science Foundation of China (Grant No.22*ATJ*008), the Shaoyang Science and Technology Innovation Guidance Project (Grant No.2022*GZ*4060), and the General projects of Shaoyang Federation of Social Sciences (Grant No.22*YBB*22).

Data Availability Statement: Data sharing is not applicable.

Acknowledgments: This work was supported by High Performance Computing Center at Eastern Institute for Advanced Study. The authors are grateful to four reviewers for their constructive comments and suggestions.

Conflicts of Interest: The authors declare no conflict of interest.

References

1. Sokolov, L.M.; Klafer, J.; Blumen, A. Fractional kinetics. *Phys. Today* **2002**, *55*, 48–54. [CrossRef]
2. Magin, R.L. *Fractional Calculus in Bioengineering, Bioengineering*; Begell House Publishers: Danbury, CT, USA, 2006.

3. Kirchner, J.W.; Feng, X.; Neal, C. Fractal stream chemistry and its implications for contaminant transport in catchments. *Nature* **2000**, *403*, 524–527. [CrossRef] [PubMed]
4. Raberto, M.; Scalas, E.; Mainardi, F. Waiting-times and returns in high-frequency financial data: An empirical study. *Phys. Stat. Mech. Its Appl.* **2002**, *314*, 749–755. [CrossRef]
5. Liu, F.; Zhuang, P.; Turner, I.; Anh, V.; Burrage, K. A semi-alternating direction method for a 2-D fractional FitzHugh-Nagumo monodomain model on an approximate irregular domain. *J. Comput. Phys.* **2015**, *293*, 252–263. [CrossRef]
6. Li, S.; Cao, W.; Wang, Y. On spectral Petrov-Galerkin method for solving optimal control problem governed by a two-sided fractional diffusion equation. *Comput. Math. Appl.* **2022**, *107*, 104–116. [CrossRef]
7. She, Z.H.; Qu, H.D.; Liu, X. Stability and convergence of finite difference method for two-sided space-fractional diffusion equations. *Comput. Math. Appl.* **2021**, *89*, 78–86. [CrossRef]
8. Hao, Z.P.; Lin, G.; Zhang, Z.Q. Error estimates of a spectral Petrov-Galerkin method for two-sided fractional reaction-diffusion equations. *Appl. Math. Comput.* **2020**, *374*, 125045. [CrossRef]
9. Li, S.; Zhou, Z. Fractional spectral collocation method for optimal control problem governed by space fractional diffusion equation. *Appl. Math. Comput.* **2019**, *350*, 331–347. [CrossRef]
10. Gunzburger, M.; Wang, J. Error analysis of fully discrete finite element approximations to an optimal control problem governed by a time-fractional PDE. *SIAM J. Control. Optim.* **2019**, *57*, 241–263. [CrossRef]
11. Ozbilge, E.; Kanca, F.; Zbilge, E. Inverse Problem for a Time Fractional Parabolic Equation with Nonlocal Boundary Conditions. *Mathematics* **2022**, *10*, 1479. [CrossRef]
12. Feng, L.B.; Zhuang, P.; Liu, F.; Turner, I. Stability and convergence of a new finite volume method for a two-sided space-fractional diffusion equation. *Appl. Math. Comput.* **2015**, *257*, 52–65. [CrossRef]
13. Liu, X.Y.; Liu, Z.H.; Fu, X. Relaxation in nonconvex optimal control problems described by fractional differential equations. *J. Math. Anal. Appl.* **2014**, *409*, 446–458. [CrossRef]
14. Jia, J.; Wang, H. Fast finite difference methods for space-fractional diffusion equations with fractional derivative boundary conditions. *J. Comput. Phys.* **2015**, *293*, 359–369. [CrossRef]
15. Lai, J.J.; Liu, H.Y. On a Novel Numerical Scheme for Riesz Fractional Partial Differential Equations. *Mathematics* **2021**, *9*, 1–14. [CrossRef]
16. Chen, H.B.; Gan, S.Q.; Xu, D.; Liu, Q.W. A second-order BDF compact difference scheme for fractional-order Volterra equation. *Int. J. Comput. Math.* **2016**, *93*, 1140–1154. [CrossRef]
17. Ma, C.Y.; Shiri, B.; Wu, G.C.; Baleanu, D. New fractional signal smoothing equations with short memory and variable order. *Optik* **2020**, *218*, 164507. [CrossRef]
18. Shiri, B.; Kong, H.; Wu, G.C. Adaptive Learning Neural Network Method for Solving Time-Fractional Diffusion Equations. *Neural Comput.* **2022**, *34*, 971–990. [CrossRef]
19. Qu, W.; Lei, S.L.; Vong, S.W. A note on the stability of a second order finite difference scheme for space fractional diffusion equations, Numerical Algebra. *Control. Optim.* **2014**, *4*, 317–325.
20. Sitho, S.; Ntouyas, S.K.; Sudprasert, C.; Tariboon, J. Integro-Differential Boundary Conditions to the Sequential -Hilfer and -Caputo Fractional Differential Equations. *Mathematics* **2023**, *11*, 867. [CrossRef]
21. Hakkar, N.; Dhayal, R.; Debbouche, A.; Torres, D.F.M. Approximate Controllability of Delayed Fractional Stochastic Differential Systems with Mixed Noise and Impulsive Effects. *Fractal Fract.* **2023**, *7*, 104. [CrossRef]
22. Chen, S.; Liu, F.; Jiang, X.; Turner, I.; Anh, V. A fast semi-implicit difference method for a nonlinear two-sided space-fractional diffusion equation with variable diffusivity coefficient. *Appl. Math. Comput.* **2015**, *257*, 591–601. [CrossRef]
23. Podlubny, I. *Fractional Differential Equations*; Academic Press: New York, NY, USA, 1999.
24. Meerschaert, M.M.; Sikorskii, A. *Stochastic Models for Fractional Calculus*; De Gruyter: Berlin, Germany, 2012.
25. Tadjeran, C.; Meerschaert, M.M. Finite difference approximations for two-sided space-fractional partial differential equations. *Appl. Numer. Math.* **2006**, *56*, 80–90.
26. Samko, S.G.; Kilbas, A.A.; Marichev, O.I. *Fractional Integrals and Derivatives, Theory and Applications*; Gordon Breach: London, UK, 1993.
27. Isaacson, E.; Keller, H.B.; Weiss, G.H. *Analysis of Numerical Methods*; Wiley: New York, NY, USA, 1966.
28. Tadjeran, C.; Meerschaert, M.M.; Scheffler, P. A second-order accurate numerical approximation for the fractional diffusion equation. *J. Comput. Phys.* **2006**, *213*, 205–213. [CrossRef]
29. Richtmyer, R.D.; Morton, K.W. *Difference Methods for Initial-Value Problems*; Krieger Publishing: Malabar, FL, USA, 1994.

MDPI
St. Alban-Anlage 66
4052 Basel
Switzerland
www.mdpi.com

MDPI Books Editorial Office
E-mail: books@mdpi.com
www.mdpi.com/books

Academic Open
Access Publishing

mdpi.com

ISBN 978-3-7258-1148-9